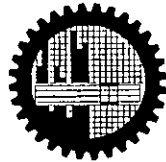
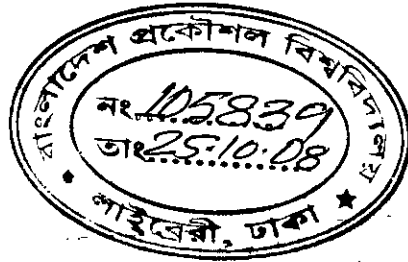


# Investigation of Strength and Deformation Characteristics of Cement and Lime Treated Soft Clays

by

Md. Mokhlesur Rahman

A Thesis in Partial Fulfillment of the Requirement for the Degree of  
DOCTOR OF PHILOSOPHY

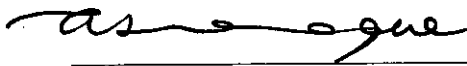


DEPARTMENT OF CIVIL ENGINEERING  
BANGLADESH UNIVERSITY OF ENGINEERING AND TECHNOLOGY DHAKA

2008

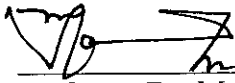
The thesis entitled "Investigation of Strength and Deformation Characteristics of Cement and Lime Treated Soft Clays" by Md. Mokhlesur Rahman, Roll No-P-10010404F, Registration No.- 9504223, Session: October, 2001, has been accepted as satisfactory in partial fulfillment of the requirement for the degree of Doctor of Philosophy on 6th May, 2008.

### BOARD OF EXAMINERS



Professor Dr. Abu Siddique  
Department of Civil Engineering  
BUET, Dhaka

Chairman  
(Supervisor)



Professor Dr. Md. Kamal Uddin  
Institute of Appropriate Technology  
BUET, Dhaka

Member  
(Co-Supervisor)



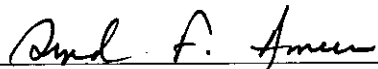
Professor Dr. Muhamamad Zakaria  
Head, Department of Civil Engineering  
BUET, Dhaka

Member  
(Ex-Officio)



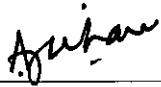
Professor Dr. A. M. M. Safiullah  
Vice-Chancellor  
BUET, Dhaka

Member



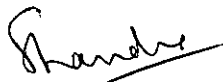
Professor Dr. Syed Fakhrul Ameen  
Department of Civil Engineering  
BUET, Dhaka

Member



Dr. Ahsanul Jalil Khan  
Director, Construction and Development Co.  
55, North Road, Dhanmondi, Dhaka

Member



Professor Dr. Sarvesh Chandra  
Department of Civil Engineering  
I.I.T. Kanpur 208016 India.

Member  
(External)

## CANDIDATE'S DECLARATION

It is hereby declared that this thesis or any part of it has not been submitted elsewhere for the award of any degree or diploma but papers have been submitted in various journal for publications.



---

**Md. Mokhlesur Rahman**

*Affectionately dedicated  
To  
My Parents, Wife and Children*

for their sacrifice and bearable during this research

# TABLE OF CONTENTS

	Page
<b>CHAPTER 1 INTRODUCTION</b>	
1.1 General Background	1
1.2 The Current Issues	3
1.3 Objectives of the Study	5
1.4 Organization of the Thesis	7
<b>CHAPTER 2 LITERATURE REVIEW</b>	
2.1 General	9
2.2 Deep Mixing	10
2.2.1 Previous History	10
2.2.2 Treated Soil Characteristics	11
2.2.3 Construction Methods and Equipment	11
2.2.4 Quality Control and Testing	12
2.3 Fundamental Concepts of Cement Stabilization	13
2.3.1 Mechanism of Soil-Cement Stabilization	13
2.3.2 Schematic Illustrations of Clay-Cement Interactions and Improved Soil	14
2.4 Predominant Factors that Controls Hardening Characteristics of Cement Treated Clays	15
2.4.1 Type of Admixtures and Amount of Cement	15
2.4.2 Curing Time	16
2.4.3 Soil Type	17
2.4.4 Initial Mixing Water Content and Clay-Water/Cement Ratio	18
2.4.5 Soil pH	18
2.4.6 Soil Minerals	18
2.5 Fundamental Concepts of Lime Stabilization	19
2.5.1 Types and Properties of Limes	19
2.5.2 Mechanism of Lime Stabilization	19
2.5.2.1 Hydration	20
2.5.2.2 Ion Exchange and Flocculation	20
2.5.2.3 Pozzolanic Reaction	21
2.5.2.4 Carbonation	21
2.6 Predominant Factors that Control Hardening Characteristics of Lime Treated Clay	22
2.6.1 Type and Amount of Lime	22
2.6.2 Curing Time	23
2.6.3 Type of soil	23
2.6.4 Clay Minerals	24
2.6.5 Soil pH	25
2.6.6 Curing Temperature	25
2.6.7 Compaction Delay Time	26

2.7 Comparison on the Mechanisms of Cement and Lime Stabilization	27
2.8 Modification of Clay Mineralogy Due to Cementation	27
2.9 Modification of Micro-structure Due to Cementation	27
2.10 Modification of Chemical Properties of Treated Clays	28
2.10.1 pH Value	28
2.10.2 Organic Matter and Organic Carbon	28
2.10.3 Electrical Conductivity	29
2.10.4 Cation Exchange Capacity	29
2.10.5 Exchangeable Cations	30
2.11 Modification of Physical Properties for Treated Clays	31
2.11.1 Grain Size Distribution	31
2.11.2 Water Content	32
2.11.3 Unit Weight	32
2.11.4 Specific Gravity	33
2.11.5 Atterberg Limits	33
2.11.6 Degree of Saturation	34
2.12 Modifications of Engineering Properties due to Chemical Stabilization	34
2.12.1 Compressibility Characteristics	34
2.12.1.1 Pre-consolidation Pressure, Void Ratio and Volumetric Strain	35
2.12.1.2 Compression Index and Swell Index	35
2.12.1.3 Coefficient of Consolidation	36
2.12.1.4 Intrinsic Compression Line and Generalized Compression Line	36
2.12.2 Permeability Characteristics	37
2.12.2.1 Permeability and Vertical Stress	37
2.12.2.2 Permeability and Void Ratio	37
2.12.3 Stress-Strain, Strength and Stiffness Characteristics	38
2.12.3.1 Deviator Stress-Strain Relationship from CIU Test	38
2.12.3.2 Deviator Stress-Shear Strain Relationship from CID Test	38
2.12.3.3 Volumetric Strain and Shear Strain	38
2.12.4 Pore Pressure Characteristics	38
2.12.5 Failure Envelopes Characteristics	39
2.12.6 Stress Ratio and Volumetric Strain	39
2.12.7 Effective Stress Paths Characteristics	39
2.12.8 Shear Stress, Vertical and Horizontal Displacement Characteristics	39
2.12.9 Shear Strength Parameters	40
2.12.10 Failure Strain Characteristics	40
2.12.11 Strength Development Index	40
2.12.12 Normalized Strength	41
2.12.13 Flexural Strength	41
2.12.14 Stiffness Characteristics	41
2.12.15 Interrelationship among Strength, Curing Time and $w_c/c$ Ratio	41
2.12.16 Direct Shear Test and Unconfined Compression Test Results Relationship	42
2.13 Critical State Models for Prediction of Soil Behaviour	43
2.13.1 State Boundary Surface	45

2.13.2	Cam Clay Model	47
2.13.3	Modified Cam Clay (MCC) Model	49
2.13.3.1	The Critical State	49
2.13.3.2	Yield Function	49
2.13.3.3	Strain Hardening	50
2.13.3.4	Plastic Potential Function	50
2.13.3.5	Elastic Behaviour	51
2.13.4	Modified Modified Cam Clay (MMCC) model	51
2.13.4.1	The MMCC Yield Locus and Plastic Flow Rule	52
2.13.4.2	Tensile Strength and Unconfined Compression Strength	53
2.13.5	Extended Modified Modified Cam Clay (EMMCC) Model	54
2.13.5.1	Tensile Strength Breakdown Parameter	54
2.13.5.2	Consolidation Strength Breakdown Parameter	54
2.13.5.3	Yield Locus and Flow Rule	55
2.13.6	Prediction and Comparison Results by Developed MCC Model	55
2.14	Cap Model	56
2.14.1	Fixed Yield Surface	57
2.14.2	Yield Caps	57
2.14.3	Prediction and Comparison Results by Cap Model	58

### **CHAPTER 3 LABORATORY INVESTIGATIONS, EQUIPMENT AND INSTRUMENTATION**

3.1	General	100
3.2	Geology and Sub-soil Conditions of the Project Sites	100
3.3	Properties of Soft Base Clays Used	102
3.4	Sampling Procedure	102
3.5	Admixtures Used	103
3.5.1	Type of Cement Used	103
3.5.2	Type of Lime Used	103
3.5.3	Admixture Content	103
3.6	Methodology Used for Sample Preparation	103
3.7	Preparation of Specimens for Testing	104
3.8	Scope of Experimental Investigation	104
3.8.1	Test Variables	104
3.8.2	Characteristics of the Base Clay	105
3.8.3	Characteristics of Treated Clays	105
3.8.4	Number of Treated Samples depending on Test Variables	106
3.9	Chemical, Mineralogical, Micro-structural and Physical Properties	106
3.9.1	Chemical Property Tests and Test Programme	106
3.9.1.1	pH Test	107
3.9.1.2	Loss on Ignition Test	107
3.9.1.3	Organic Content Test	107
3.9.1.4	Electrical Conductivity Test	108

3.9.1.5 Cation Exchange Capacity Test	108
3.9.1.6 Exchangeable Cations Test	109
3.9.2 Mineralogy Tests and Test Programme	109
3.9.3 Microstructure Tests	109
3.9.4 Physical Property Tests and Test Programme	111
3.10 Determination of Engineering Properties and Test Programme	111
3.10.1 Unconfined Compression Test	111
3.10.1.1 Testing Programme	111
3.10.1.2 Test Apparatus	112
3.10.1.3 Specimen Preparation and Set-up	112
3.10.1.4 Testing Procedure	112
3.10.2 One Dimensional Consolidation Test	113
3.10.2.1 Testing Programme	113
3.10.2.2 Test Apparatus and Accessories	113
3.10.2.3 Specimen Preparation and Set-up	113
3.10.2.4 Testing Procedure	114
3.10.3 Direct Shear Test	115
3.10.3.1 Testing Programme	115
3.10.3.2 Test Apparatus and Accessories	115
3.10.3.3 Specimen Preparation and Set-up	115
3.10.3.4 Testing Procedure	116
3.10.4 Triaxial Test	116
3.10.4.1 Testing Programme	116
3.10.4.2 Triaxial Cell	117
3.10.4.3 Loading Device	117
3.10.4.4 Measurement of Strains and Pore Pressure	118
3.10.4.5 Calibration of Pressure Transducer	118
3.10.4.6 Calibration of Displacement Strain Gauge	118
3.10.4.7 Calibration of Proving Ring for Measuring Load	118
3.10.4.8 Triaxial Testing Sample Preparation	118
3.10.4.9 Setting-up of Specimen	119
3.10.4.10 Saturation of Specimen	119
3.10.4.11 Consolidation of Specimen	120
3.10.4.12 Shearing of Specimen	120
3.10.4.13 Unconsolidated Undrained Triaxial Compression Test	120
3.10.4.14 Consolidated Undrained Triaxial Compression Test	120
3.10.4.15 Consolidated Drained Triaxial Compression Test	121
3.10.4.16 Isotropic Compression Test	121
3.10.4.17 End of Testing of Triaxial Test	121
3.11 Extra Precaution Measures During Triaxial Test	121
3.12 Processing and Analysis of Triaxial Test Data	122
3.12.1 Calculation of Stress	122
3.12.2 Calculation of Strains	122



## **CHAPTER 4 CHEMICAL, MINERALOGICAL AND PHYSICAL PROPERTIES OF CEMENT TREATED CLAYS**

4.1 General	131
4.2 Chemical Properties of Untreated Base and Cement Treated Clays	131
4.2.1 Soil pH Value	131
4.2.2 Loss on Ignition	132
4.2.3 Organic Matter and Organic Carbon	133
4.2.4 Electrical Conductivity	134
4.2.5 Cation Exchange Capacity	134
4.2.6 Exchangeable Cations	135
4.2.7 Nitrogen and Phosphorus	136
4.2.8 Chemical Effect for Potential Acidity or Buffering Capacity	137
4.2.9 Summary for Effect of Cement Treatment on Chemical Properties	137
4.3 Mineralogical Properties of Treated and Untreated Clays	138
4.4 Micro-structural Properties of Treated and Untreated Clays	140
4.5 Physical Properties of Treated and Untreated Clays	142
4.5.1 Colour	142
4.5.2 Grain Size Distribution and Surface Area Distribution	142
4.5.3 Water Content	143
4.5.4 Unit Weight	145
4.5.5 Specific Gravity	146
4.5.6 Atterberg Limits	147
4.5.7 Void Ratio	149
4.5.8 Degree of Saturation	150
4.5.9 Summary for the Effect of Cement Treatment on Basic Properties	150

## **CHAPTER 5 STRENGTH, STIFFNESS AND DEFORMATION CHARACTERISTICS OF TREATED CLAYS**

5.1 General	183
5.2 Compressibility Characteristics of Cement and Lime Treated Clays	184
5.2.1 Effect of Clay-Water/ Admixture Ratio on Compressibility Characteristics	185
5.2.1.1 Void Ratio Versus Effective Vertical Pressure Curve	185
5.2.1.2 Volumetric Strain Versus Effective Vertical Pressure Curve	186
5.2.1.3 Compression Index and Swell Index	186
5.2.1.4 Coefficient of Consolidation	187
5.2.1.5 Coefficient of Volume Compressibility	187
5.2.2 Effect of Curing Time on Compressibility Characteristics	187
5.2.2.1 Void Ratio Versus Effective Vertical Pressure Curve	187
5.2.2.2 Volumetric Strain Versus Effective Vertical Pressure Curves	188
5.2.2.3 Compression Index and Swell Index	188
5.2.2.4 Coefficient of Consolidation	189
5.2.2.5 Coefficient of Volume Compressibility	189
5.2.3 Effect of Clay Type on Compressibility Characteristics	189

5.2.3.1	Void Ratio Versus Effective Vertical Pressure Curves	189
5.2.3.2	Volumetric Strain Versus Effective Vertical Pressure Curve	189
5.2.3.3	Compression Index and Swell Index	190
5.2.3.4	Coefficient of Consolidation	190
5.2.3.5	Coefficient of Volume Compressibility	190
5.2.4	Effect of Mixing Clay-Water Content on Compressibility Characteristics	191
5.2.4.1	Void Ratio Versus Effective Vertical Pressure Curve	191
5.2.4.2	Volumetric Strain Versus Effective Vertical Pressure Curve	191
5.2.4.3	Compression Index and Swell Index	191
5.2.4.4	Coefficient of Consolidation	192
5.2.4.5	Coefficient of Volume Compressibility	192
5.2.5	Compressibility Effects on SEM Images	192
5.2.6	Intrinsic Compression Line and Generalized Compression Line	193
5.3	Permeability Characteristics of Cement and Lime Treated Clays	195
5.3.1	Effect of Clay-Water/ Admixture Ratio on Permeability Characteristics	195
5.3.2	Effect of Curing Time on Permeability Characteristics	195
5.3.3	Effect of Clay Type on Permeability Characteristics	196
5.3.4	Effect of Mixing Clay-Water Content on Permeability Characteristics	196
5.3.5	Permeability and Void Ratio Relationships of Cement and Lime Treated Clays	197
5.4	Stress-Strain, Strength and Stiffness Characteristics from UC Test	197
5.4.1	Stress-Strain Behaviour for Cement and Lime Treated Clays	197
5.4.2	Strength Characteristics for Cement and Lime Treated Clays	198
5.4.2.1	Strength Activeness	198
5.4.2.2	Strength Development Index (SDI)	199
5.4.2.3	Normalized Strength	200
5.4.2.4	Effect of Plasticity of Clay on Unconfined Compressive Strength	200
5.4.2.5	Strength Relationship Based on Yield and Ultimate Conditions	201
5.4.2.6	Strength Prediction Based on Clay-water/Cement Ratio's Concept	202
5.4.3	Failure Strain Behaviour of Cement and Lime Treated Clays	204
5.4.3.1	Effect of Mixing Ratio, Curing Time and Clay Type on Strain at Failure	204
5.4.3.2	Failure Strain Prediction of Cement Treated Clays	204
5.4.4	Stiffness Characteristics of Cement and Lime Treated Clays	205
5.4.4.1	Effect of Mixing Ratio, Curing Time and Clay-Type on Initial Stiffness	205
5.4.4.2	Initial Stiffness Prediction of Cement Treated Clays	206
5.4.4.3	Effect of Mixing Ratio, Curing Time and Clay-Type on Secant Stiffness	206
5.4.4.4	Secant Stiffness Prediction of Cement Treated Clays	207
5.4.5	Failure Mode and Brittleness Characteristics of Cement Treated Clays	207
5.5	Stress-Strain Behaviour and Strength Parameters from Direct Shear Test	208
5.5.1	Shear Stress and Shear Displacement Relationship of Cement Treated Clays	208
5.5.2	Vertical and Horizontal Displacement Relationship of Cement Treated Clays	208
5.5.3	Effect of Clay-Type, Cement and Curing Time on Shear Strength Parameters	209
5.5.4	Effect of Clay-water Content on Strength Parameters	210
5.5.5	Relation between Strength from Direct Shear and Unconfined Compression Tests	210
5.6	Stress-Strain Characteristics of Cement Treated Clays from UU Triaxial Test	210

5.7	Stress Path, Stress-Strain, Pore Pressure and Failure Envelopes from CIU Triaxial Tests	211
5.7.1	Effective Stress Paths for Untreated and Cement Treated Clays	211
5.7.1.1	Effective Stress Paths for Untreated Samples	211
5.7.1.2	Effects of Clay-water/Cement Ratio on Effective Stress Paths	212
5.7.1.3	Effects of Curing Time on Effective Stress Paths	213
5.7.1.4	Effects of Mixing Water Content on Effective Stress Paths	214
5.7.1.5	Effects of Pre-Shear Consolidation Pressure on Effective Stress Paths	214
5.7.1.6	Pertinent Features of Undrained Stress Path	216
5.7.2	Stress-Strain Behaviour of Untreated and Cement Treated Clays	216
5.7.2.1	Deviator Stress-Axial strain Relationships for Untreated Samples	216
5.7.2.2	Effects of wc/c Ratio on Deviator Stress-Axial strain Relationships	217
5.7.2.3	Effects of Curing Time and Clay-type on Stress-Strain Relationships	217
5.7.2.4	Effects of Mixing Water Content on Stress-Strain Relationships	218
5.7.2.5	Effects of Pre-Shear Consolidation Pressure on Stress-Strain Relationships	218
5.7.2.6	Normalized Deviator Stress - Axial strain Relationships	219
5.7.3	Pore Pressure Characteristics of Untreated and Cement Treated Clays	220
5.7.3.1	Pore Pressure-Axial strain Relationships for Untreated Samples	220
5.7.3.2	Effects of wc/c Ratio on Pore Pressure Change-Axial Strain Relationships	220
5.7.3.3	Effects of Curing and Clay Type on Pore Pressure Change-Strain Relationships	220
5.7.3.4	Effects of Water on Pore Pressure Change-Axial strain Relationships	221
5.7.3.5	Effects of Pre-shear Stress on Pore Pressure Change-Strain Relationships	221
5.7.3.6	Normalized Pore Pressure Change - Axial strain Relationships	222
5.7.4	Peak and Destructured Envelopes of Cement Treated Clays	222
5.7.4.1	Peak Deviator Stress Conditions and Undrained Failure Envelopes	223
5.7.4.2	Residual State and End-of-Test Destructured Envelope Behaviour	223
5.7.5	SEM Images at Shear Stage	225
5.8	Stress-Strain and Volumetric Strain Characteristics from CID Triaxial Compression Tests	225
5.8.1	Stress-Strain Behaviour of Untreated and Cement Treated Clays	225
5.8.1.1	Deviator Stress- Axial Strain Relationships of Untreated Clays	225
5.8.1.2	Effect of wc/c Ratio on Deviator Stress-Axial strain Relationships	226
5.8.1.3	Effects of Curing and Clay Type on Deviator Stress-Strain Relationships	226
5.8.1.4	Effect of Mixing Water on Deviator Stress - Axial strain Relationships	227
5.8.1.5	Effect of Pre-Shear Pressure on Deviator Stress-Axial strain Relationships	227
5.8.1.6	Normalized Deviator Stress - Axial strain Relationships	228
5.8.2	Volumetric Strain Characteristic of Untreated and Cement Treated Clays	228
5.8.2.1	Volumetric Strain-Shear Strain relationships of Untreated Samples	228
5.8.2.2	Effect of wc/c Ratio on Volumetric Strain-Axial Strain Relationships	229
5.8.2.3	Effect of Curing and Clay Type on Volumetric Strain-Axial Strain Curves	229
5.8.2.4	Effect of Mixing Water on Volumetric Strain-Axial Strain Relationships	229
5.8.2.5	Effect of Pre-shear Pressure on Volumetric Strain-Axial Strain Relations	230
5.8.1.6	Normalized Volumetric Strain - Axial strain Relationships	230
5.8.3	Stress Ratio Versus Volumetric Strain, $(\eta-\epsilon_v)$ Relationships	231
5.8.4	Peak and Destructured Envelopes Characteristics of Cement Treated Clays	232

5.8.4.1 Peak Deviator Stress Conditions and Drained Failure Envelopes	232
5.8.4.2 Residual Stress States and End-of-Test Destructured Envelope	232
<b>CHAPTER 6 NUMERICAL ANALYSIS OF TREATED CLAYS USING DIFFERENT MODELS</b>	
6.1 General	333
6.2 Soil Constants and Critical State Parameters Analysis of Untreated and Treated Clays	333
6.3 Critical State Lines of the Untreated and Treated Clays	334
6.4 State Boundary Surfaces of the Untreated and Treated Clays	335
6.5 Correlation of Soil Constants with Plasticity Index	335
6.6 Prediction of Drained Response Using MCC, MMCC and EMMCC Models	338
6.6.1 Model Parameters	338
6.6.2 Drained Stress-Strain Behaviour	339
6.6.3 Volume Change Responses	340
6.7 Prediction of Undrained Response Using MCC, MMCC and EMMCC	341
6.7.1 Model Parameters	341
6.7.2 Undrained Stress-Strain Behaviour	342
6.7.3 Pore Pressure Change Responses	343
6.7.4 Undrained Stress Paths	344
6.8 Prediction of Drained and Undrained Responses using Cap Model	344
6.8.1 Drained Stress-Strain Behaviour	345
6.8.2 Volume Change Response	345
6.9 Prediction of Undrained Response using Cap Model	345
6.9.1 Undrained Stress-Strain Behaviour	346
6.9.2 Pore Pressure Change Response	346
6.9.3 Stress Path in the $I_1 - \sqrt{J_2}$ Space	346
<b>CHAPTER 7 CONSLUSIONS AND RECOMMENDATIONS</b>	
7.1 Conclusions	389
7.1.1 Investigation of Physicochemical and Micro-Structural Behaviour of Cement Treated Clays	390
7.1.2 Investigation of Compressibility and Permeability Properties of Cement and Lime Treated Clays	392
7.1.3 Investigation of Stress-Strain, Strength, Stiffness Characteristics of Cement and Lime Treated Clays	393
7.1.4 Evaluation of Soil Constants and Applicability of Constitutive Models and Cap Models for the Prediction of Drained and Undrained Behaviour of Clays	397
7.2 Recommendation for Future Study	399
<b>REFERENCES</b>	400

## NOTATIONS

$p_{to}$ (PTO)	Tensile Strength Parameter for Cementation
$\rho_m$ (RHO)	Cementation Breakdown Parameter
$\eta$	Stress Ratio = $q/p_o'$
$\kappa$	Gradient of Swelling Line
$\lambda$	Gradient of Normal Consolidation Line
$v$	Specific Volume
$\tau$	Shear Stress at Zero Normal Stress
$\phi'$	Effective Friction Angle
$v_k$	Specific Volume (OC clay)
$\sigma_1', \sigma_2', \sigma_3'$	Effective Principal Stresses
$\sigma_p'$	Pre-Consolidation Pressure / Stress
$\sigma_v'$	Effective Vertical Stress / Pressure
$\sigma_y'$	Yield Stress
$\epsilon_a$	Axial Strain
$\epsilon_s$	Shear Strain
$\epsilon_v$	Volumetric Strain
$\phi_c'$	Critical Effective Friction Angle
$\gamma_d$	Dry Unit Weight
$\gamma_w$	Wet Unit Weight
$\mu$	Poisson's Ratio
$A_c$	Activity of Clay
AERC	Atomic Energy Research Centre
$A_w$	Admixture Content
B (BWRAT)	Ratio of Bulk Modulus of Pore Water to Bulk Modulus of Soil
BUET	Bangladesh University of Engineering and Technology
$c$	Cement Content
$c'$	Effective Cohesion
$Ca^{2+}, Ca^{++}$	Calcium Ion
CaO	Calcium Oxide (lime)

CASH	Calcium Aluminum Silicate Hydrate
$C_c$	Compression Index
CC	Cam Clay
CEC	Cation Exchange Capacity
CID	Isotropically Consolidated Drained Triaxial Compression Test
CIU	Isotropically Consolidated Unconsolidated Triaxial Compression Test
$C_s$	Swell Index
CSH	Calcium Silicate Hydrate
CSL	Critical State Line
$c_v$	Coefficient of Consolidation
DUET	Dhaka University of Engineering and Technology
$e$	Void Ratio
$e_{100}$	Void Ratio at Vertical Effective Stress, 100 kPa
$E_{50}$	Secant Modulus of Elasticity = E at 50% of Peak Strength
EC	Electrical Conductivity
$E_i$	Initial Elastic Modulus of Elasticity
EMMCC	Extended Modified Modified Cam Clay
GCL	Generalized Compression Line
$G_s$	Specific Gravity
H	Slope of Hvorslev Surface
$H^+$	Hydrogen Ion
ICL	Intrinsic Compression Line
$I_v$	Void Index
$k$	Coefficient of Permeability
$Ka^+$	Pottasium Ion
LI	Liquidity Index
LL	Liquid Limit
M	Slope of Critical State Line
MCC	Modified Cam Clay
$Mg^{2+}, Mg^{++}$	Magnesium Ion
MMCC	Modified Modified Cam Clay
$m_v$	Coefficient of Volume Compressibility
N	Specific Volume (NC clay)
$Na^+$	Sodium Ion
NCL	Normal Consolidation Line
OCR	Over-consolidation Ratio

OH <sup>-</sup>	Hydroxyl Ion
OPC	Ordinary Portland Cement
p'	Mean Normal Effective Stress = $(\sigma_1' + 2\sigma_2')/3$ , $\sigma_2' = \sigma_3'$
p'/p <sub>o</sub> '	Normalized Mean Effective Stress
Pc'	Apparent Pre-consolidation Pressure
p <sub>co</sub> (PCO)	Preeconsolidation Pressure
pH	pH Value
PI	Plasticity Index
PL	Plastic Limit
p <sub>o</sub> '	Pre-shear Effective Confining Pressure
q	Deviator Stress = $\sigma_1' - \sigma_3'$
q/p <sub>o</sub> '	Normalized Deviator Stresses
q <sub>max</sub>	Maximum Deviator Stress
q <sub>u</sub>	Unconfined Compressive Strength
R <sup>2</sup>	Correlation Coefficient
SEM	Scanning Electron Microscope
SEM	Scanning Electron Microscope
S <sub>r</sub>	Degree of Saturation
SRDI	Soil Resource Development Institute
S <sub>u</sub>	Undrained Shear Strength
u	Excess Pore Water Pressure
u/p <sub>o</sub> '	Normalized Pore Water Pressure
UC	Unconfined Compression Test
UU	Unconfined Unconsolidated Triaxial Compression Test
w	Week
wc/A <sub>w</sub>	Clay-Water/Admixture Ratio
wc/c	Clay-Water/Cement Ratio
wc/l	Clay-Water/Lime Ratio
w <sub>f</sub>	Final Water Content
w <sub>i</sub>	Initial Water Content of the Clay Slurry
w <sub>n</sub>	Natural Water Content
XRD	X-ray Diffraction

## ACKNOWLEDGMENT

Thanks to ALMIGHTY ALLAH for His unbound graciousness and unlimited kindness in all the endeavors author has been taken up throughout his life.

The author wishes to express his profound gratitude and indebtedness to his Supervisors Prof. Dr. Abu Siddique and Prof. Dr. Md. Kamal Uddin for their unfailing guidance constant supervision, invaluable suggestions, helpful criticisms and encouragement given throughout the course of this research work. Without their unstinted help in both academic and personal concerns throughout the years of the author's graduate studies at the Bangladesh University of Engineering and Technology (BUET) Dhaka, this dissertation work could not have been completed.

Author is also very grateful to Prof. Dr. A. M. M. Safiullah, Prof. Dr. Muhammad Zakaria, Prof. Dr. Syed Fakhurul Ameen and Dr. Ahsanul Jalil Khan for their valuable suggestions, guidance and encouragement. Fervent debt of deep gratitude, sincere thanks, and extreme respects are due to them for their valuable help throughout the study. The author is grateful to Prof. Dr. Sarvesh Chandra for his comments on this study as an external examiner. A note of appreciation and regards is extended for his valuable suggestion, encouragement and interest in this study.

The author express his gratefulness to the Head of the Civil Engineering Department, BUET, Dhaka, for providing laboratory facilities and co-operation during the period of the research. Sincere gratitude is due to the BUET, Dhaka for providing financial support and rendering an excellent learning environment. The author expresses sincere thanks to Prof. Dr. Md. Kabirul Islam, BUET and Asstt. Prof. Mr. Md. Abu Taiyab, DUET for helping in this study. The author expresses thanks to Mr. Md. Sharafat Ali, Mr. Muhammad Habibur Rahman and Mr. Md. Alimuddin in the Department of Civil Engineering, BUET, for providing necessary facilities and help needed for conducting research.

A very special debt of deep gratitude is offered to his parents and all members of his family. The author dedicates this piece of work to his loving parents and all family members, religions, and this work related future researcher, who are always a constant source of inspiration throughout his whole life.



## ABSTRACT

This thesis presents experimental and numerical investigations for the effects of cement and lime treatment on compressibility, permeability, stress-strain, strength and stiffness behaviour of three soft clays. Effects of cement treatment on physiochemical and micro-structural properties have also been investigated. X-ray Diffraction, Scanning Electron Microscopy, particle size distribution, pH measurement, organic content, electrical conductivity, cation exchange capacity, exchangeable cation, water content, unit weight, specific gravity, and Atterberg limits tests were conducted to examine physiochemical and micro-structural properties. Compressibility and permeability properties of untreated and, cement and lime treated clays were investigated by performing one-dimensional consolidation tests. Stress-strain, strength and stiffness behaviour of untreated and, cement and lime treated clays were evaluated by performing unconfined compression (UC) tests. Consolidated drained direct shear (DS), unconsolidated undrained (UU), isotropically consolidated undrained (CIU) and isotropically consolidated drained (CID) triaxial compression tests were also carried out to assess the stress, deformation and strength properties of cement treated clays. Sets of variables considered in the testing program include a wide range for type of clay (PI = 13% to 47%), type of admixture, clay-water/cement ratio (2 to 30), curing time (1 to 104 weeks), mixing water content (120% to 250%) and effective confining pressure (50 kPa to 400 kPa). Finally, applicability of different constitutive models and Cap models were assessed for the predictions of drained and undrained behaviour.

It has been observed that pH value, electrical conductivity (EC), cation exchange capacity (CEC), increases with decreasing clay-water/cement ratio. pH value, however, decreases while EC and CEC value increases with increasing curing time. Loss on ignition and organic matter decreases due to increasing cement content and with increasing curing time. The relative amount of cementitious product (CSH + CASH) was identified by the XRD analysis and found to increase with the increase of cement content and curing time. Due to the formation of cementitious product, the fabric of the treated clays changed to flocculated type, comprising of clay-cement clusters separated by large inter-cluster voids with smaller intra-cluster pores as seen from the SEM images of treated clays. These changes were more pronounced with higher cement content and longer curing time.

The significant increase in yield stress and reduction in compression index ( $C_c$ ) and swell index ( $C_s$ ) were observed with increasing admixture (cement/lime) content and increasing curing time.  $C_c$  and  $C_s$  for lime treated clays were found to be greater than those of cement treated clays.  $C_c$  and  $C_s$  values increase significantly with the increase of mixing clay-water content. The lime-treated clays gained comparatively higher void ratio and volumetric strains and lower yield stress than those of cement-treated clays. The effect of cementation is to increase the values of coefficient of consolidation ( $c_v$ ) and coefficient of volume compressibility ( $m_v$ ). The higher the admixture content and curing time, the lower is the values of  $c_v$  and  $m_v$ .  $c_v$  and  $m_v$  values for lime treated clay were found to be higher than those of cement treated clay. A substantial increase in the value of  $c_v$  and  $m_v$  was found to have occurred within higher mixing water content.

At higher stress level, progressive destructuration of the treated clay particles occurred, which has been verified from the SEM images of cement treated clay compressed at different consolidation pressure. Addition of admixture to the clay increases the permeability and void of the soils, due to flocculation of the soil particles, which has been seen from SEM images. The Intrinsic Compression Line (ICL) and Generalized Compression Line (GCL) have been proposed for the untreated and treated clays. Coefficient of permeability ( $k$ ) and void ratio relationships have also been proposed for cement and lime treated clays. The values of  $k$  of cement and lime treated clays have been found to reduce with increasing cement or lime content and curing period. Values of  $k$  for lime treated clays were found to be higher than those of cement treated clays.

Based on the rate of strength development with time, the unconfined compressive strength and cement content relationships have been divided into 3 zones: Inactive Zone, Active Zone and Inert Zone. Since the behaviour of cement treated clays was remarkably governed by  $w/c$ , the strength prediction in terms of  $w/c$  as well as the interrelationship involving strength, curing time and clay-water content/cement content ratio ( $w/c$ ) have been proposed.

From stress-strain relationships, the overall behaviour has been categorized into brittle, quasi-brittle and ductile. Comparatively, brittle, quasi-brittle and ductile types for the cement treated clays, while quasi-brittle and ductile types for the lime treated clays have been found. The correlation between yield stress, ( $\sigma_y'$ ) and unconfined compressive strength ( $q_u$ ),  $\tau_{10}$  and  $q_u$ , axial strain at failure ( $\epsilon_f$ ) and  $q_u$ , and stiffness ( $E_i$  and  $E_{50}$ ) and  $q_u$  have also been proposed.

In direct shear test, for cement treated clays, vertical expansion (dilation) was observed at low normal stress and experienced vertical contractions or settlement throughout the shearing stage at higher normal stress. The cohesion and friction angle have been increased with increasing cement content and curing time.

The undrained effective stress paths of the cement treated clays obtained from CIU triaxial compression tests indicate that the stress paths belong to different category of states such as normally consolidated, lightly, moderately and heavily over-consolidated state. The degree of alteration have been found different for different samples depending on the amount of cement content, curing time and pre-shear effective consolidation pressure. Upon reaching the peak deviator stress in CIU triaxial test, the progressive destructuration takes place and thus the stress path tends to move either on the Hvorslev envelope or envelope of strain softening behaviour.

SEM results have been suggested that complete destructuration takes place only on the shear plane at which the clay-cement cluster crushes. The prevalent role of pre-shear effective consolidation pressure was manifested to annihilate the cementation effect attributing ductility to the treated matrix. The main effect of cement treatment was to modify the behaviour of the soft clay form normally consolidated to over-consolidated state.

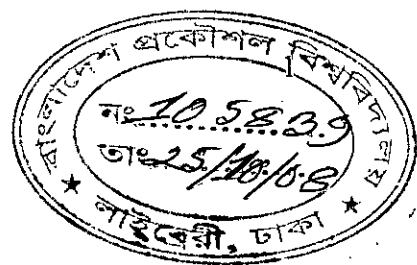
Similar natures of deviator stress-axial strain and volumetric strain-axial strain relationships were observed for all samples having the identical  $w/c$  ratio in CID triaxial tests. So, the  $w/c$  is a prime parameter governing the engineering behaviour of cement treated samples having different mixing water content. For cement treated clays, peak deviator stress ( $q_{max}$ ) criterion of failure envelopes can be used as obtained from CIU and CID triaxial compression tests. The degree of overall curvature of the failure envelope for each type of clay depends on the range of consolidation stresses and hence increases with increasing cement content and curing time.

The values of soil constants  $\lambda$  and  $\kappa$  for the treated clays have been found to be less than those for the untreated clays while the values of the constant  $N$  and  $M$  are greater for the cement treated clays than those of untreated clays. At a particular curing time, the soil constants  $\lambda$  and  $\kappa$  decreased, while the constant  $N$  and  $M$  increased with increasing cement content. Correlations between the soil constants  $\lambda$ ,  $\kappa$  and  $N$  with plasticity index have been proposed. Hvorslev surface was established for the cemented clays. No definite Roscoe surface could be found for cemented clays.

For the untreated clay, it has been observed that the predicted stress paths, deviator stresses, volumetric strains and excess pore pressure responses at small strain levels using the MCC model appear to be significantly close to experimental curves. It appears from the present study that MCC, MMCC, EMMCC and Cap models (Plane Cap and Elliptic Cap) cannot be applied for predictions of drained and undrained behaviour of cemented clays at high water content.

# CHAPTER 1

## INTRODUCTION



### 1.1 General Background

Soft clay deposits are widespread in Southeast Asia, and they present very special problems of arise at soft clay formations in low land of Bangladesh, which have large potential engineering design and construction, many of which are not common to other earth materials. Similar problems for settlement with low inherent shear strength of soft clays have been studied in Bangladesh (Safiullah, 1991; Molla, 1993; Siddique et al., 2002). Foundation failures in soft clay are comparatively common, high surface loading in the form of embankments and shallow foundations inevitably results in large settlements which must be accommodated for in design, and which invariably necessitate long-term maintenance of engineered facilities. The construction of buildings, roads, embankments, bridges, canals, harbours and railways in soft soils has always been associated with stability and settlement problems. Methods and applications of ground improvement techniques in Bangladesh have been summarized by Ansary and Doulah (1993). Typical methods were used to increase the bearing capacity of soft soils of Bangladesh include preloading (or precompression) and vertical drainage in conjunction with precompression. Loading berms, or pressure berms, are being used as counter weights to increase the stability of road and railway embankments in Bangladesh. Fabric-reinforced soil, where woven or non-woven fibre materials are placed in road and railway embankments to improve their overall stability. Vertical drainage methods using three types of drains, namely, sand drain, wick drain and prefabricated vertical drain are being used. Due to lack of mechanical skills and equipment, other ground improvement techniques like dynamic compaction, admixture stabilization, stone columns, electro-osmosis and lime piles and columns are yet to gain popularity in Bangladesh. An alternative technique for short time is the chemical stabilization to enhance the level of cementation bond with soft clays by the use of supplementary cementing agents. In such a cemented state for soft clays, the resistance to compressibility and consequent strength development increase with increasing curing time. But, it is not practicable to mix a cementing agent with a large area or volume of in-situ soft clays. To overcome this problem, in-situ deep mixing methods (DMM) have been developed during the last two decades primarily to effect columnar inclusions into the soft ground to transform such whole the ground to composite grounds (Miura et al., 1986).

The increase in the strength of soft clay arising from the mixing of cement has been well established (Mitchell, 1981; Kamaluddin et al., 1997; Horpibulsuk et al., 2000; Kamruzzaman, 2002, Chew et al., 2004). This strength increase is often accompanied by an increase in stiffness (Porbaha et al., 2000; Ghee et al., 2004) and a decrease in the ductility of the soil, which is manifested as a large post-peak reduction in the strength of the treated soil

(Kamaluddin et al., 1997; Balasubramaniam et al., 1999). All these features are characteristic of natural structured soils (Ameen and Safiullah, 1986; Islam et al., 2004) and indicate that the mixing of cement into the soil leads to the formation of structure within the soil grain assemblage. Miura et al., (2001) also examined the improvement for engineering behaviour of cement stabilized clay at high water content. Horpibulsuk (2002) found that the compressibility of the soil is similarly altered due to the cementation, with a much higher pre-consolidation pressure (yield stress) than the untreated soil. Exceeding of the pre-consolidation pressure leads to sharp decrease in void ratio (Balasubramaniam et al., 1998; Bergado et al., 2003), which has also been observed in natural structured soil (Amin et al., 1987; Ansary et al., 1999). Other basic soil property that can be significantly altered by the addition of cement, is its permeability (Chew et al., 2004). In regions where problems of groundwater intrusion exist, alteration of the permeability is often an important factor in the use of cement stabilization to construct cut-off walls (Porbaha et al., 2000; Takahashi and Kitazume, 2004). The physicochemical and engineering behaviour of cement treated clay are studied by Chew et al., (2004) while the micro-structural behaviour of cement treated clay are studied by Kamruzzaman et al. (2004). A number of researchers compared the constitutive model predictions with the experimental results for untreated and cement treated soil (Siddique et al. 2007; Islam et al. 2007; Khalilulah 2007; Siddiquee 2006; Youwai and Bergado 2003; Siddique et al. 2003; Bashar, 2002). Desai and Siriwardane (1984); Chen and Mizuno (1990) explained the Cap model applications for soft rocks.

The interactions of cement or lime and clay minerals are responsible for a drastic parametric alteration (Mitchell, 1981). In soft clay, hydration of cement creates rather strong bonds between the various mineral substances and forms a matrix which efficiently encloses the non-bonded soil particles. The matrix develops a cellular structure. Since the matrix penetrates the particles, the cement reduces the plasticity on one hand, and increases the shear strength on the other hand. The effect of chemical surface of the cement reduces the water affinity of the clay and, thereby, the clay's water retention capacity. The products of these reactions are amorphous but consider a crystalline form. First of all, a primary and secondary process may be distinguished on consolidation of the clay cement mixture according to the hypothesis of clay-cement interaction. The primary process includes hydrolysis and hydration of cement, in the course of which the usual hydration products appear, and the pH value of the water increases. The improvement of the properties of cement treated soil has been attributed to the soil cement reaction (Mitchell, 1981), which produces primary and secondary cementing materials in the soil-cement matrix (Kamruzzaman, 2002; Chew et al., 2004). The primary cementing materials are formed by hydration and comprise of hydrated calcium silicates ( $C_2SH_x$ ,  $C_3S_2H_x$ ), calcium aluminates ( $C_3AH_x$ ,  $C_4AH_x$ ) and hydrated lime  $Ca(OH)_2$ . Secondary pozzolanic reaction between the hydrated lime and the silica and alumina from the clay minerals leads to the formation of further calcium silicate hydrates (CSH) and calcium aluminate hydrates (CAH). The soil-cement reaction provides a clear basis to explain the

observed engineering behaviour of treated clay. What is, however, not so clear is the type of structure that is induced into the soil-cement mixture by the soil-cement reaction. Many processes of introducing cement into soft ground, such as jet grouting and deep mixing, involve a large amount of mixing and remoulding of the in-situ soil. It can, therefore, be understood that the original in-situ structure of the soil would have been totally destroyed during the improvement process and yet, the engineering behaviour of cement treated soil outlined above appears to indicate that apart from an increase in strength and pre-consolidation pressure some from the "structure" has been induced of in-situ soil.

The chemical admixture stabilization of soft clay by lime or cement is one kind of the most economical and desirable improved techniques in low land at high water content. Winterkorn (1975) defined chemical admixture stabilization as the collective term for any physical, chemical or biological method used to improve the engineering properties of a natural soil to make it serve adequately for an intended engineering purpose. The main goals of the stabilization include an increment in strength, a reduction in compressibility, an improvement of the swelling or squeezing characteristics and increasing the durability of soil with time. So, the improvement of soft clays with lime or cement can easily be achieved to beneficial effects on the strength, compressibility, plasticity, permeability and workability of soil. Chemical admixture stabilization has been broadly applied in both shallow and deep stabilization. It is used for construction purposes such as in the field of highways, rail roads and airport constructions in order to improve mechanical properties of the bearing layers. The modern applications include the use of cement or lime column act as a type of soil reinforcement and to improve the stability of slopes, trenches and deep excavations; to prevent sliding failure of embankments; to reduce the vibrations from traffic loads and to accelerate the consolidation settlements under embankments. The stabilization generally is used to increase the bearing capacity and reduce the total and differential settlements below lightly loaded structures. It is used as an alternative measure of costly pile foundation to reduce the negative skin friction on structural piles, blasting and pile driving.

## **1.2 The Current Issues**

The deep stabilization technique has been used in many countries to treat the soft clay layers, and knowledge is limited to the global performance of the treated ground. So far, very few studies have been carried out to understand the fundamental physicochemical and micro-structural behaviour of such treated clays at high water content and their influence on the observed engineering behaviour.

Natural soil structures are often formed by solute deposition at inter-particle contacts, charge deficiencies and Van der Waal's forces (Mitchell, 1981), rather than by hydration and pozzolanic reactions. Hence, there may be some differences between the naturally structured soil and the cement treated structured soil. The microstructure of lime-treated soil has been

studied by Locat et al. (1990) amongst others. However, the absence of the primary hydration reaction in lime treatment may lead to a different microstructure from that produced by cement treatment. The physicochemical and micro-structural behaviour of cement treated Singapore marine clays were studied by Kamruzzaman (2002), Chew et al., (2004) and Kamruzzaman et al. (2004). So far no such research is carried out on Bangladesh clays. Previous studies on regional soils of Bangladesh basically focused on physical and engineering properties of compacted soil treated with admixtures, like cement, lime, fly ash and ricehusk (Ahmed, 1984; Hossain, 1986; Serajuddin and Azmal, 1991; Serajuddin, 1992; Rajbongshi 1997; Molla, 1997; Shahjahan, 2001; Hasan, 2002; Siddique and Rajbongshi, 2001, 2002; Siddique and Hossain, 2003; Ansary et al., 2003; Toyeb, 2006).

Chew et al. (1997) and Kamruzzaman (2002) studied the strength and stiffness behaviour of cement treated soft clays of Singapore based on unconfined compression test data. Rajbongshi (1997), Hasan (2002) and Toyeb (2006) have done some works on strength and stiffness properties of lime and cement treated clays of Bangladesh by conducting unconfined compression test. However, proper interpretation of the strength and stiffness of the treated soil with the observed micro-structural behaviour remains unclear. The unconfined compression test is widely and frequently used as an index of the strength of treated clays. However, there are number of factors that contribute significantly to the strength and stiffness of cement treated clay that cannot be understood through unconfined compression test. The two main factors are (i) the effect of lateral restraint and (ii) the effect of internal soil conditions (e.g. the degree of saturation, volume and pore water pressure changes, and drainage condition under loading). Hence, extensive triaxial tests (unconsolidated undrained, isotropically consolidated undrained and drained) could be conducted for the proper interpretations of strength and stiffness of treated clays.

A few researches have been carried out focusing on global performance of cemented clays to understand the strength and compressibility behaviour (Kamaluddin, 1995; Balasubramaniam et al., 1999; Horpibulsuk et al., 2000, 2001; and Miura et al., 2001). Kabir et al. (2007) studied on the constitutive model prediction for stabilized local clay of Bangladesh. However, the relationship between the observed microstructure of such treated clays and the changes of their strength and compressibility characteristics yet have not been completely clarified. In addition, the strength and compressibility characteristics of cement treated clays might be related to the structuration (creating of cementation bond) and destructuration (breaking of cementation bond) phenomenon as found in the natural structured soil (Kamruzzaman, 2002). Hence, it is important to have fundamental understanding of the improvement of strength and compressibility behaviour of treated Bangladesh clays that involves structuration and destructuration processes.

In the case of deep excavation projects, the soil improvement is carried out before start of excavation that provides an improved soil layer and helps in limiting the movement of soil

below the final excavation level. In this application, the stiffness behaviour of stabilized clay layer is more critical than its shear strength. Until now the research concentrated either on the initial elastic or secant stiffness where the cementation bond of treated soil governs the stiffness behaviour. To date, what remains unclear is the effect of destructuration (breaking of cementation bond) on the stiffness of treated clay.

The permeability of cemented clay is often an important factor to construct cut-off walls (Yu et al., 1999; Porbaha et al., 2000 and Kamruzzaman, 2002). So far no study has been conducted to integrate the permeability behaviour for treated regional clays of Bangladesh.

The model prediction of untreated and cement treated clays is an important issue (Bashar, 2002; Siddique et al., 2003; Siddique et al., 2007; Islam et al., 2007 and Khalilullah, 2007). So far no study has been conducted to predict the drained and undrained behaviour by constitutive models for treated clays at high water content.

Considering the above issues, it can be concluded that there is a need to study the physicochemical as well as micro-structural behaviour of cemented soft Bangladesh clays at high water content and use them to explain some aspects of the observed engineering behaviour for deep mixing method in a well-controlled laboratory condition first, before extending it to the field condition. The engineering properties have also been simulated and implemented by constitutive models for soil-cementation analysis. Attempts may also be made to compare the experimental test results with those predicted using different constitutive models.

### 1.3 Objectives of the Study

The major objectives of this research are as follows:

- To study how the engineering behaviour (i.e. strength as well as stiffness, compressibility and permeability) are altered when cement and lime are added to the soft clays at high water content;
- To study the influence of physicochemical as well as micro-structural behaviour of cement treated clays on the observed engineering behaviour; and
- To study the applicability of Modified Cam Clay (MCC) model, Modified Modified Cam Clay (MMCC) model, Extended Modified Modified Cam Clay (EMMCC) model and Cap model to predict the behaviour of cement treated clays.

A schematic outline of the scope and objectives of the present study is shown in Fig. 1.1. To understand the physicochemical and micro-structural behaviour of cement treated clays; pH and determination of  $\text{Ca}^{++}$  ion concentration, grain sizes analyses, X-ray diffraction (XRD) analyses and Scanning Electron Microscopic (SEM) analyses were carried out. While for

engineering behaviour; basic index properties (Atterberg's limits and water content), one-dimensional consolidation, consolidated drained direct shear (DS), unconfined compression (UC), unconsolidated undrained (UU), isotropically consolidated undrained (CIU) and isotropically consolidated drained (CID) triaxial compression tests have been conducted. Sets of variables have been considered in the testing programme which include a wide range of type of clay, clay-water/cement ratio, curing time, initial water content of the clay slurry and effective confining pressures.

The microstructure of cement treated clays in Bangladesh has been first examined using X-ray diffraction (XRD) and scanning electron microscopic (SEM) analyses. The grain sizes, basic index properties,  $\text{Ca}^{++}$  ion concentration and pH of the treated clay have been examined and explained in terms of the soil-cement reactions and induced microstructures. For the evaluation of the presence of  $\text{Ca}^{++}$  ion concentration on the clay surface, lime has been used as an index in the evaluation of the strength of cement treated clay versus lime treated clay.

The changes to the strength, stiffness, compressibility and permeability characteristics of the treated clay have been evaluated and explained in the light of the soil-cement reaction and induced microstructure. Apart from clarifying the underlying mechanisms leading to the changes in compressibility and strength characteristics of treated clays, structuration (existing of cementation bond) and destructuration (breaking of cementation bond) phenomenon have been studied and explained from the SEM and XRD analyses of the consolidation, UC and UU, CIU, CID triaxial samples.

The compressibility of the treated clays has been investigated by conducting the one-dimensional consolidation test. The coefficients of permeability have been calculated from the one-dimensional consolidation tests. The stress-strain as well as stiffness characteristics of treated clays have been studied from the DS, UC and UU, CIU, CID triaxial compression tests. The effects of destructuration on the stiffness of treated clays are also studied from the CIU and CID triaxial tests.

The present research has been carried out in the laboratory to assess the strength and deformation for cemented clays at high water contents so that the state of water contents will simulate the condition realized in deep mixing method. In the present investigation, an attempt has been made to identify the critical factors governing the engineering behaviour of cement treated clays, which helps not only to control the input of cementing agent to attain strength development with curing time, microstructure and clay-water content, but also to understand the subsequent engineering behaviour.



#### **1.4 Organization of the Thesis**

This is the first introductory chapter, which deals with the aim and scope of the work in relation to the general background and the current issues of its importance. Chapter 2 presents a literature review on deep mixing and the behaviour of soils treated with lime and cement. In this chapter, the basic concepts, mechanisms, properties, crucial parametric behaviour, various key factors controlling the parameters and results of past researchers are reviewed. Concluding remarks are also presented at the end of the chapter as a way of establishing the present state-of-art in the evaluation of physicochemical and micro-structural behaviour of treated clays at high water content and integrate them with the observed engineering behaviour.

Chapter 3 describes the experimental investigations, presents details of test apparatus, test programme, sample preparation and testing procedure. The test results and discussions of the testing programme are presented in Chapter 4 and 5. Chapter 4 explains the chemical, mineralogical and physical properties and integrates them with the basic engineering properties of treated clays at high water content. In Chapter 5, the compressibility, permeability, stress-strain, strength and stiffness behaviour in terms of structuration and destructuration processes involved in the treated clays at high water content are discussed and clarified with the knowledge of the induced physicochemical and microstructure. Chapter 6 presents the applicability of Critical State Soil Models and Cap Model to predict engineering properties of cemented clay. The conclusions and the main findings related to major areas of the present study are summarized in Chapter 7. Recommendations for future research are also presented in this Chapter.

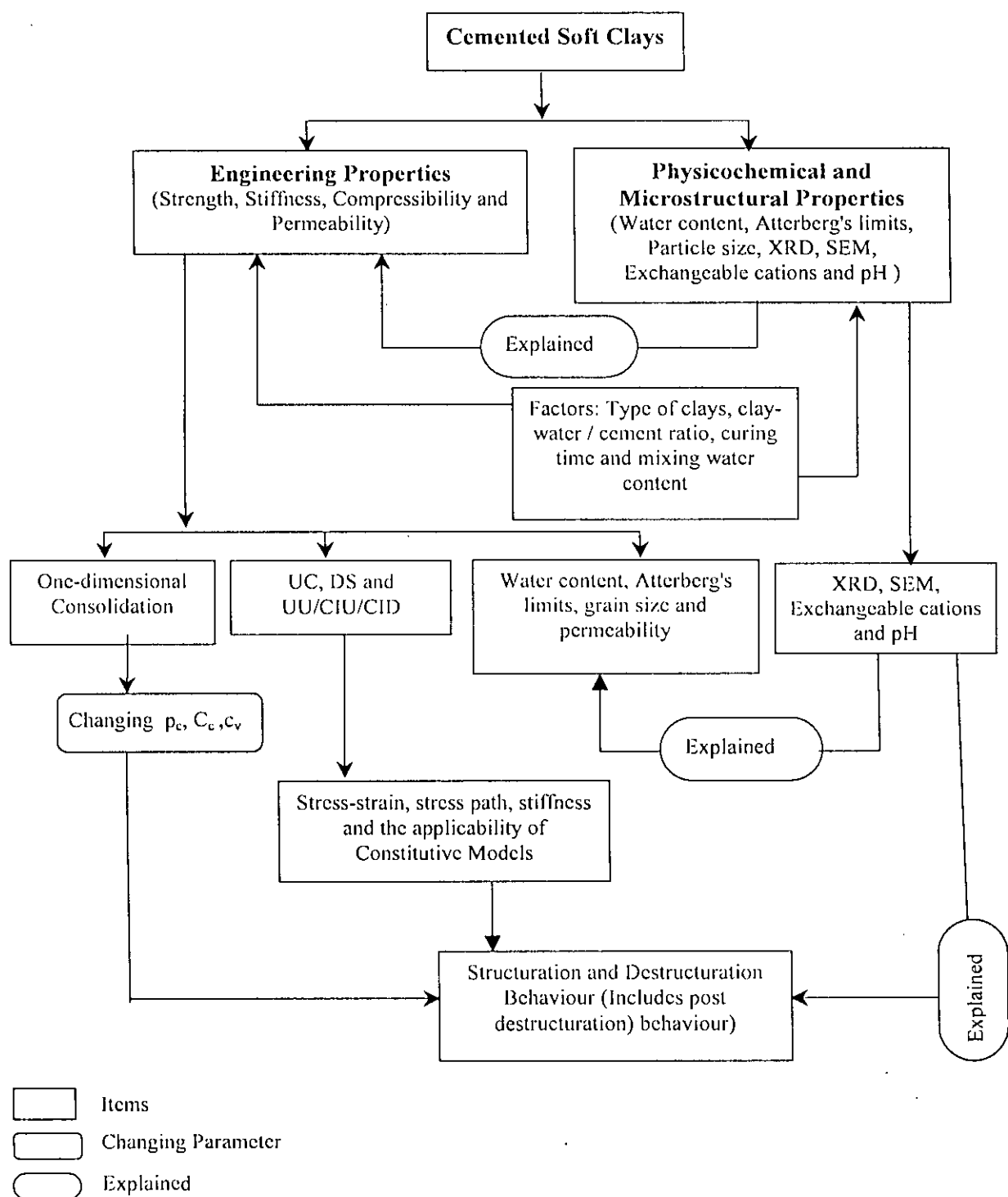


Fig. 1.1 Schematic Outline of the Scope and Objectives of the Present Research Highlighting the Relationship of Various Components

## CHAPTER 2

### LITERATURE REVIEW

#### 2.1 General

Major geotechnical problems often arise in construction at Bangladesh involving soft clays at low land with high water content owing to its low shear strength and high compressibility (Siddique et al., 2002). Thus, suitable ground improvement techniques are needed for deep excavation projects in soft clay for stability and deformation control. Chemical deep mixing stabilization is one of the commonly used methods. Chemical stabilization has been extensively used in the past recent years, both in deep and shallow foundations in order to improve inherent properties of soil such as strength and deformation behaviour. The resistance to compression and consequent strength development in such a cemented state increase with increasing curing time. It is not practicable to admix a cementing agent with a large volume of in-situ soft clay. Hence in-situ deep mixing methods (DMM) have been developed during the last two decades primarily to effect columnar inclusions of cementing admixture into the soft ground to transform such whole soft ground to composite grounds. Moreover, the new geo-material of waste clays being added in the construction works can be made by mixing with cement. It is of interest to understand the chemical situation and be able to predict the strength development of stabilized materials. The outcome of the chemical reactions is such that the strength of the clay multiplies immediately on mixing and continues to increase for several years. Parallel to the practical use of the methods, together follow-ups of projects continued, a continuous development has been made on various researches. Such research works, which are criticised in the chapter.

The subjects contained in this chapter deals with literature review on the fundamental ideas for deep mixing methods (DMM), mechanisms of cement and lime stabilization. The discussions on the basic concepts and mechanisms of reactions between hardening agent and soft soil by modifying of soil parameters, have been mainly drawn from a number of published works that dealt with shallow and deep stabilizations. The present knowledge on the stress-strain-strength behaviour of the treated clay is very limited. The strength property of the treated clay was mostly evaluated by the past researchers by unconfined compression tests specially in Bangladesh. The limitation of those studies is that the effects of initial consolidation stress and drained condition on the strength can not be properly evaluated by only unconfined compression tests. In this chapter, those phenomena have been reviewed.

A boundary has been made on some strength and deformation characteristic of lime and cement treated clay explaining the mechanism of compression, particle breakage, the time-dependent consolidation characteristics and the load-compression behaviour. To comprehend

the compression behaviour of cemented clay, it is necessary to understand the controlling mechanisms of un-cemented clay to form the model framework demonstrating the behaviour of deep mixing cement admixed clay. The model factors affecting the parameters providing to stress-strain and compressibility behaviour of the stabilized clays have been critically reconsidered. The critical soil model parameters with their previous deep mixing analysis are discussed. Prediction for the stress-strain, volumetric strain response and excess pore pressure of treated soils tested using the constitutive critical state models and comparison the predictions with experimental results are also reviewed.

## **2.2 Deep Mixing**

The deep mixing or ground modification technique, has been used many diverse applications including building and bridge foundation retaining structures, liquefaction mitigation, temporary support of excavation and water control. Names such as Jet Grouting soil deep mixing, Cement Deep Mixing (CDM), Soil Mixed Wall (SMW), Geo Jet, Deep Soil Mixing (DSM), Hydra-Mech, Dry Jet Mixing (DJM), and Lime Columns are known to many. Each of these methods has the same basic root, finding the most efficient and economical method to mix cement (or in some cases fly ash or lime) with soil and cause the properties of the soil to become more like the properties of a soft rock.

### **2.2.1 Previous History**

Various methods of soil deep mixing, mechanical, hydraulic, with and without air, and combinations of both types have been used widely in Japan for about 20 years and more recently have gained wide acceptance in the United States. At the present time, the total volume of soil deep mixing work performed annually in Japan is about 5,000,000 million cubic meters. This includes CDM, SMW, DJM, and Jet Grouting. Total Yen (Dollar) volume annually is on the order of \$2 Billion performed by over 500 rigs in all categories operating throughout the country. In contrast, in the United States, currently there are about 10 traditional soil deep mixing rigs operating, plus about another 10 jet grouting rigs, and total of soil treated in any one year has not exceeded approximately 30,000 cubic meters. Japan has a population of about  $\frac{1}{2}$  that of the United States and a land area smaller than the state of California. Therefore, their need to utilize all available space has made reclamation of soft soils along their coastline critical to providing the needs their populations. Much of their soil deep mixing has been to treat soft bay muds in coastal areas, developing strength of 5-20 kg/cm<sup>2</sup>.

At about the same time as the use of soil deep mixing was expanding in Japan (mid 1970's), independent progress was being made in Scandanavia with a lime column technique for the stabilization and reinforcement of very soft, cohesive soils. This technology has evolved in Sweden and Finland to the present time where production of what is now lime-cement columns ranges between 3 and 4 million lineal meters per year. This production is mainly for

new reduction of settlements and improvement of stability for the construction of new roads and railroads. Almost all this production is construction using dry reagents that are introduced by compressed air and mixed mechanically with the soft soils.

Several representative deep mix design have been reported for construction of large-scale project in many countries, including Japan, Singapore, Thailand and US, in recent years, which could be used as a database for new project. The most distinctive project in the under water tunnel in Tokyo Bay, namely the trans-Tokyo Bay highway project in which DM (deep mixing) technology was used for seabed stabilization and for facilitating driving of the shield tunnel in soft clay (Uchida et al., 1996; Wasa et al., 1991). Uchida et al. (1996) presented the mechanical properties of four types of mixtures with different target strengths, and the mixing conditions for that project. Another representative project is the central Artery/Tunnel project in Boston, in which DM technology was used for different purposes, including a deep excavation in soft clay. This project has been well documented (e.g. Lambrechts and Roy, 1997; O'Rourke et al., 1998; Das et al, 1998). The projects reported for rehabilitation of dams in the US reported mix design for cut-off wall and foundation stabilization, for instance, the Lockington dam in Ohio (walker, 1994), and the Jackson Lake dam in Wyoming (Taki and Yang, 1991). Carlsten (1995) presented some experience gained in Sweden; similarly, Harnan and Lagolnitzer (1992) in France. The increase in the strength of soft clay arising from the introduction of cement has been well established in various countries (Chew et al., 1998, Porbaha et al., 2000; Horpibulsuk et al., 2000; Kamaluddin et al., 2004; Ghee et al., 2004). Some typical applications for which soil deep mixing has been used in the United States, Scandinavia and in Japan are shown in Fig. 2.1.

### **2.2.2 Treated Soil Characteristics**

The most deep mixing is to modify the soil so the it's properties become similar to that of a soft rock such as a clay shale or lightly cemented sandstone. The modulus of elasticity and unconfined compressive strengths are typically 1/5 to 1/10 that of normal concrete. Almost all soil types are amenable to treatment, however, soils containing more than 10% peat must be thoroughly prior to treatment. Deep mixing of soft, clay soils must be carefully controlled to avoid significant pockets of untreated soils. However, there are methods available to insure competent mixing and methods of insure that adequate mixing and treatment has been achieved.

### **2.2.3 Construction Methods and Equipment**

Mechanical deep mixing is typically performed using single or multiple shafts of augers and mixing paddles. The auger is slowly rotated into the soft ground, typically 10-20 rpm, and advanced at 0.5-1.5 meters per minute. As the auger advances, cement slurry is pumped through the hollow steem of the shafts feeding out at the tip of the auger. Mixing paddles are arrayed along the shaft above the auger to provide mixing and blending of the slurry and soil.

The slurry helps to lubricate the tool and assists in the breaking up of the soil into smaller pieces. Since fluid volume is being introduced into the soft ground, spoils must come to the surface. These spoils are a combination of the cement slurry and soil particles, typically with a similar cement content as what remains in the soft ground. After final depth is reached, the tools remain on the hole, rotating for about 0.5 to 2 minutes for complete mixing. At this point, the tools are raised while continuing to pump at a reduced rate. Withdrawal is typically at twice the speed of penetration, 1-3 meters per minute.

Other methods of deep mixing cement with soil consist of jet grouting. Here, high-pressure cement slurry (4000-7000 psi) is pumped through horizontal ports in a drill string above the drill bit. The high velocity and pressure of the cement jets cuts and mixes the soil insitu. This is termed single fluid jet grouting. In double fluid jet grouting, a shroud of compressed air (10-15 bar pressure) is pumped to surround the slurry jet thus enhancing the penetrating ability of the jet. In triple jet grouting, the cement is pumped at low pressure at the bottom of the hole while high pressure water, surrounded by a shroud of compressed air, cuts and removes the soil during the withdrawal of the tools. Other methods of introducing and deep mixing cement with soil involve such methods as Hdra-Mech. Utilizing both hydraulic (jet) and mechanical energy to cut and mix the soil and cement. A different method not utilizing slurry is the DJM (Dry Jet Mixing) method. Here, compressed air carries lime and/or cement powder to the bottom of the hole where mixing paddles blend the dry reagent with the soil. This method can only be used in high water content, soft soils.

#### **2.2.4 Quality Control and Testing**

Since the aggregate being used in producing the engineered "low strength" concrete insitu is the native soils, pre-construction soil borings, testing of the mix design with the in-situ soil is a must. One to two cubic feet of the treated soils is sufficient to run the required laboratory, pre-production tests on the soil cement mix. Various water cement ratios are considered, usually between 1:1 and 1.5:1 (by weight) the amount of cement, again by weight, is typically 5-15% of the weight of the soft soil to be treated. Test results for soil deep mixed gravity wall applications are shown in Table 2.1.

Proper injection of slurry, deep mixing and blending of the cement slurry and soil is verified by several means. Initially, during installation, wet grab samples are taken from different elevations in the mixed columns after the tools are withdrawn. Remote closing tubes are inserted, filled with the wet, deep mixed soil and slurry, a closure lid secured and the sample brought to the surface. The slurry is poured into cylinders for later laboratory testing. In addition, core cutter sampling of the completed columns may be performed. It is wise to wait at least until 28 days after installation to perform coring, and the only with triple tube coring equipment, as the sample may be difficult to retrieve intact because of its low strength.

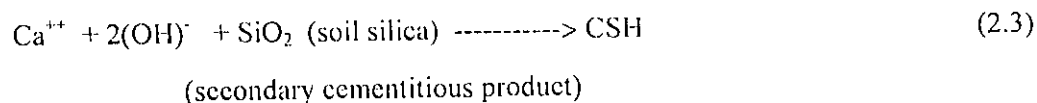
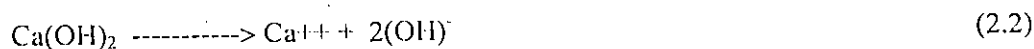
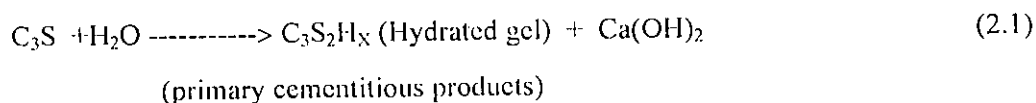
The improvement and applications of deep mixing are continued more or less in various countries according to their demand on construction. A lot of cost is needed for conducting and operating the deep mixing technique. Cost and demand facilities are balanced the deep mixing technique. There is a lack of facilities in many countries such as Bangladesh, the deep mixing technique cannot be developed and established smoothly now-a-day.

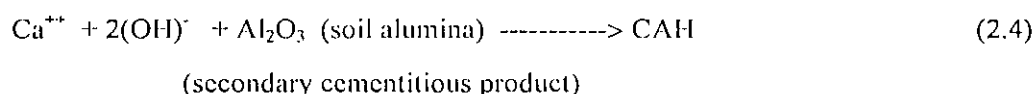
## 2.3 Fundamental Concepts of Cement Stabilization

### 2.3.1 Mechanism of Soil-Cement Stabilization

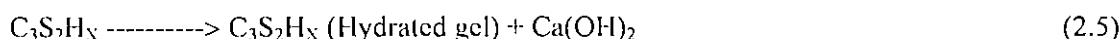
The fundamental mechanism of soil cement stabilization for physicochemical changes has been outlined by Chew et. al. (2004), Schaefer et al. (1997), amongst others. The components of Portland cement are tricalcium silicate ( $C_3S$ ), dicalcium silicate ( $C_2S$ ), tricalcium aluminate ( $C_3A$ ) is a solid solution known as tetracalcium alumino-ferrite ( $C_4AF$ ). Lea (1956) stated that these four main constituents are major strength producing compounds of Portland cement. The major hydration products are called primary cementitious products, which are combination of hydrated calcium silicates ( $C_2SH_x$ ,  $C_3S_2H_x$ ), hydrated calcium aluminates ( $C_3AH_x$ ,  $C_4AH_x$ ) and hydrated lime  $Ca(OH)_2$ , when the clay-water of the soil encounters with cement, hydration if the cement occurs rapidly. The first two of the hydration products listed above are the main cementitious products formed and the hydrated lime is deposited as a separate crystalline solid phase. These cement particles bind the adjacent cement grains together during hardening and form a hardened skeleton matrix, which encloses unaltered soil particles. In addition, the hydration of cement leads to a rise of pH value of the pore water, which is caused by the dissociation if the hydrated lime. The strong bases dissolve the soil silica and alumina (which are inherently acidic) from both the clay minerals and amorphous materials on the clay particle surfaces, in a manner similar to the reaction between a weak acid and strong base. The hydrous silica and alumina will then gradually react with the calcium ions liberated from the hydrolysis of cement to form insoluble compounds are called secondary cementitious products, which are combination of calcium silicate hydrate (CSH) and calcium aluminum hydrate (CAH) and hardens when cured to stabilize the soil. This secondary reaction is called as pozzolanic reaction.

The reactions which take place in soil-cement stabilization can be represented in the following qualitative equations; the reactions given here are for tricalcium silicate ( $C_3S$ ) only, because it is most important constituent of cement for strength development.





When  $\text{pH} < 12.6$ , then the following reaction occurs:



The silicates and aluminates in the material must be soluble and they have additional bonding forces produced in cement-clay mixture. The solubility of the clay minerals is equally affected by the impurities present, the crystalline degree of the materials involved, the grain size, etc. The cementation strength of the primary cementitious products is much stronger than that of the secondary products in the above equations.

At low pH values ( $\text{pH} < 12.6$ ), the Equation 2.5 will occur. However, the pH drops during pozzolanic reaction and a drop in the pH trends to promote the hydrolysis of  $\text{C}_3\text{S}_2\text{H}_x$ , to form CSH. The formation of CSH is beneficial only if it is formed by the pozzolanic reaction of lime and soil particles, but it is detrimental when CSH is formed at the expense of the formation of the  $\text{C}_3\text{S}_2\text{H}_x$ , whose strength generating characteristics are superior to those of CSH. Bergado et al. (2003) found that the strength of cement treated clay is increased with time for the reason of cement hydration and pozzolanic reaction which continues for months, or even years, after the mixing.

### 2.3.2 Schematic Illustrations of Clay-Cement Interactions and Improved Soil

Fig. 2.2 presents the chemical reactions between a cohesive soil, ordinary Portland cement (OPC) and blast-furnace slag and their reaction products in generally. The effect of adding OPC and blast furnace slag to several types clay and other soils was proposed by Saitoh et al. (1985), who identified the required reactions between soil, cement and slag in this figure diagrammatically such as: (i) Hydration of Ordinary Portland Cement producing  $\text{Ca}(\text{OH})_2$ , (the calcium hydroxide generated equals up to 25% of the weight of the cement), (ii) Adsorption of  $\text{Ca}(\text{OH})_2$  by the clay and (iii) If and when the clay is saturated with  $\text{Ca}(\text{OH})_2$ , a pozzolanic reaction between these two components occurs. The finalization of deep mixing varies with the type of soil being treated, more specifically on their calcium hydroxide adsorption capacity and their pozzolanic reactivity. Some soils show a marked increase in strength once enough  $\text{Ca}(\text{OH})_2$  is available to cause a pozzolanic reaction. Saitoh et al. (1985) also concluded that from the point of view of its wide applicability is more advantageous with respect to soil types, deep mixing with OPC, blended with blast furnace slag.

Saitoh et al. (1985) illustrated the conditions of hardening with schematic diagrams as shown in Fig. 2.3. The condition immediately after mixing a cohesive soil and a hardening agent slurry are shown in Fig. 2.3(a). If the cohesive soil and hardening agent slurry are thoroughly mixed, clay particles will form to a cluster, which will be surrounded by the slurry. The condition of the cohesive soil and hardening agent slurry that have formed a hardened body



are shown in Fig. 2.3(b). The hardening agent slurry produces hydrated calcium silicates, hydrated calcium aluminates,  $\text{Ca(OH)}_2$ , etc., and forms hardened cement bodies. The cement hydration reaction produces hardened soil bodies by the pozzolanic reaction between the clay and the  $\text{Ca(OH)}_2$ . It is concluded by Saitoh et al. (1985) that the strength of the improved soil depends upon the strength characteristics of both types of hardened bodies as shown in Fig. 2.3.

## **2.4 Predominant Factors that Controls Hardening Characteristics of Cement Treated Clays**

Fig. 2.4 represents an outline of some superficial hardening factors exerting an influence on the properties of cement treated soils, which was proposed by Kezdi (1979). Owing to the large number of alternatives and combinations, it is impossible to tabulate the various mechanical properties as function of these factors, so the experimental determination is indispensable in some cases. There are, nevertheless, some predominant factors presented in the following sections, but they only provide information outlining order-of-dominance value, and illustrating the effect of these factors on the stress-strain-strength and stiffness of the cement treated clay.

### **2.4.1 Type of Admixtures and Amount of Cement**

Some investigators (Balasubramaniam et al, 1999, Porbaha et al, 2000, Bergado et al, 2003) found the different results for improvement of soft clays by using different types of admixtures (lime, cement, fly ash, rice husk ash, slag cement, slaked lime etc) and they reported that cement is the best one. Balasubramaniam et al (1999) reported that the stress-strain behaviour for the binding materials fly ash (FA), lime, cement, rice husk ash (RHA) as shown in Fig. 2.5. They found that different admixtures have different stress-strain behaviour and cemented products are gained higher strength and lower failure strain than those of other admixtures.

Felt (1955) made experiments on three different types of soils to find out the effect of cement type on cement-treated soil mixtures. Felt (1955) compared the results of compaction test, compressive strength tests and the wet-dry tests made on soils treated by normal Portland cement (Type-I) and air-entraining Portland cement (Type-IA). It was found that moisture-density relationships, compressive strengths and the soil-cement losses in the wet-dry tests were almost the same. This indicates that these two types of cement can be used interchangeably in soil-cement construction. It was further observed on experimentation with Type-III cement that the optimum moisture contents and maximum densities obtained are approximately the same for Type-I and Type-III cements. Felt (1955) also found that influence of Type-III cement on strength of different soils varies. For loamy sand, the 7 and 28-day strength for Type-III cement were about 2 and 1.4 times those for Type-I cement respectively. For a silty-clay loam, the strength for Type-III was only slightly higher than that for Type-I cement.

Ahmed (1984), Hossain (1986), Rajbongshi (1997), Hasan (2002), and Siddique and Rajbongshi (2002) investigated the effect of cement stabilization on unconfined compressive strength (1.4 in. diameter by 2.8 in. high samples) of a number of regional soils of Bangladesh. Ahmed (1984) and Hossain (1986) found that compared with the untreated soil, unconfined compressive strength of the cement-treated samples increased markedly, depending on the cement content and curing age. The effect of cement content and age on compressive strength, and the rate of gain in strength with cement content for coastal soils reported from Siddique and Rajbongshi (2002) are shown in Figs. 2.6.

#### 2.4.2 Curing Time

It was well established that the strength of the cement treated clay increases with the increase of curing time (Kawasaki et al., 1981; Nagaraj et al., 1997; Kamruzzaman et al., 2004). Porbaha et al. (2000) reported that the rate of increase of strength is generally rapid in the early stages of curing period and thereafter decreases with time. The rate of reduction also depends on the amount of cement added. Kamruzzaman et al. (2004) found that beyond a certain curing period (>1 year) the rate of increase of unconfined compressive strength is almost negligible as can be seen in Fig. 2.7. Saitoh et al. (1996) found that the strength ratio at 28 days to 7 days was between 1.2 to 2.1. Mitchell (1981) established the following relationship among  $q_u$ , curing time ( $t$ ) and cement content ( $c$ ):

$$q_u(t) = q_u(t_0) + K \log(t/t_0) \quad (2.6)$$

Where,  $q_u(t)$  = Unconfined compressive strength at  $t$  days, in kPa.

$q_u(t_0)$  = Unconfined compressive strength at  $t_0$  days, in kPa.

$K = 480c$  for granular soils and  $70c$  for fine grained soil.

$c$  = Cement content, % by mass.

Similarly, Kawasaki et al. (1981) suggested the following correlation based on the Tokyo Bay marine clay:

$$q_{u60} = 1.17q_{u28} \quad (2.7)$$

Where,  $q_{u60}$  and  $q_{u28}$  are the unconfined compressive strength at 60 days and 28 days curing periods, respectively.

Serajuddin and Azmal (1991) and Serajuddin (1992) reported the effect of curing age on unconfined compressive strength (50 mm diameter and 100 mm high samples) of regional alluvial soils of Bangladesh. Typical results are presented in Fig. 2.8. Fig. 2.8 shows that compressive strength of samples stabilized with cement increases with the increase in curing age.

### 2.4.3 Soil Type

The physicochemical properties of the untreated soil (such as grain size, water content, Atterberg limits, clay minerals, cation exchange capacity, soluble silica and alumina, pH of pore water and organic matter content) affect the properties of the treated soil (Wissa et al. 1965; Ahnberg et al., 1995; Porbaha et al., 2000; Chew et al., 2004). Ahnberg et al. (1995) established that the relationship for improvement of fine grained soils depend on generally type of clays with different plasticity index for cement and lime stabilization as shown in Fig. 2.9. Porbaha et al. (2000) suggested for fine grained soils that special considerations are needed in the case of soil with a high organic content and soils with an excessive salt content (especially sulphates), which may retard the hydration reaction of the cement. The rate of increase of strength in cement treated organic soil is very low as reported by Miura et al. (1986).

There are three types of clay on the basis of soil plasticity, namely high plastic clay ( $LL > 50\%$ ), medium plastic clay ( $LL = 35-50\%$ ) and low plastic clay ( $LL < 35\%$ ), reported by Singh (1998). Yamadera et al. (1997) analyzed the strength data with the water content as one of the variables from three different clays at the liquid limit water content, since they are considered that the fabric pattern of all soils at such a state is the same. With the liquid limit of clay as a variable parameter, the previous analysis (Yamadera et al., 1997) indicated that as the liquid limit water content of the clay increases; the spacing between clusters as well as that between particles increases; hence strength developed for the same cement content decreases. To enhance the strength to the same level, the cement content has to be decreased. The effects of cement content gradually decrease with increasing clay content and increasing plasticity index. In general, when the activity of a soil is very high, the increase of the shear strength of the soil treated with cement is low. However, these are in the reversed order in the case of lime, since the strength of the lime treated clay depends mainly on the participation of the clay particles in the pozzolanic reactions. The increase of the shear strength due to the flocculation is often relatively small for marine clays deposited in salt water, since these clays already have a flocculated structure (Broms, 1986). But for cement treated clay, it depends mainly on the cementation from the cement hydration.

Taki and Yang (1991) reported that the effect of different soil types on unconfined compressive strength of cement treatment as shown in Fig. 2.10. As can be seen, the coarse grained soil shows the largest increase in strength as compared to the fine grained soil for a given cement content. Bergado et al. (1996) reported that the rate of increase in strength of treated soil decreases with the increase of percentage clay content and plasticity index. It was also reported that in general when the activity of the soil is very high, the rate of increase in strength of treated soil is low. Similarly, Bell (1993) found that as the clay content increases, higher quantity of stabilizing agent is required to increase the strength, perhaps owing to the increase in surface area and contact between the clay particles.

#### 2.4.4 Initial Mixing Water Content and Clay-Water/Cement Ratio

The strength and deformation are changed effectively for cement treated clays at different initial mixing water content were reported by a number of investigators (Chew et al., 1997, Porbaha et al., 2000, Miura et al., 2001). Effect of initial mixing content on unconfined compressive strength is shown in Fig. 2.11. Fig. 2.11 shows at same cement content, the unconfined compressive strength decreases with increasing initial mixing water content (Porbaha et al., 2000). It is observed that strength varies about linearly with cement content in each case of mixing water content increment. The above results are also supported by Chew et al. (1997). Chew et al. (1997) found that the unconfined compressive strength and cement content relationship is a function of initial mixing water content of the untreated soil as shown in Fig. 2.12. They stated that for the same amount of cement content, the lower mixing water/soil ratio, the higher strength gained for final products.

Miura et al. (2001) reported that stress-strain characteristics of Ariake clay at different mixing water contents and different levels of cementing agent but at the same clay-water/cement (wc/c) ratio, 7.5, 10 and 15. Fig. 2.13 shows the stress-strain relationship of cement stabilized Ariake clay at high water content. The experimental model study for Ariake clay (test samples are prepared without compaction blows) indicated that it would be advantageous to deep mixing include the cement content in the same parameter since it would take care of the bonding component of the state represented by initial water content ( $w_i$ ). Miura et al. (2001) found that the initial clay-water/cement ratio (wc/c) is expressed as an integrated parameter of the structural state of the soft clay in its induced cemented state. It was a convenient parameter to adjust cement content in water to get the same level of strength with the same curing time. It has been observed that as the clay-water/cement ratio increases, which mean that cement content is decreased, the yield stress reduces. As the curing time increases for the same input condition, the yield stress further increases. The Ariake clay and cement were mixed with four levels of water content i.e., 120%, 150%, 180% and 250%, the change in physical and consolidation parameters are summarized in Table 2.2.

#### 2.4.5 Soil pH

The pH value rises rapidly at lower cement content but the rate of the rise moderated at higher cement content. The long term pozzolanic reactions are favored by high pH values, since the reactions are accelerated due to the increased solubility of the silicates and the aluminates of the clay particles. Furthermore, the cement content at which the pH values moderate also agree closely with that at which the water content reduction moderates.

#### 2.4.6 Soil Minerals

Saitoh et al. (1985) suggested that the improvement conditions are equal, greater strength is obtained from the soil with higher pozzolanic reactivity. At higher pozzolanic reactivity, the

strength characteristic of the treated soil is governed by the strength behaviour of the hardened cement bodies. But at lower pozzolanic reactivity, the strength characteristics of the treated soils are governed by the strength characteristics of the hardened soil bodies (Saitoh, 1985). Grim (1981) observed that montmorillonitic and kaolinitic clayey soils were found to be effective pozzolanic agents, as compared to clays which contain illite, chlorite or vermiculite. The montmorillonite clay mineral will probably react more readily than the illites and kaolins because of their defined crystallinity. Grim (1981) also explained that the amount of secondary cementitious materials that are produced during pozzolanic reaction of the clay particle and hydrated lime,  $\text{Ca}(\text{OH})_2$  is dependent on the amount and mineral composition of the clay fraction as well as the amorphous silica and the alumina present in the soil. Wissa et al. (1965) reported that for clay containing illite, the improvement of effective cohesion intercept ( $c'$ ) from the untreated clay is very high, while the improvement of angle of shearing resistance is moderate.

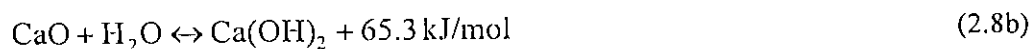
## 2.5 Fundamental Concepts of Lime Stabilization

### 2.5.1 Types and Properties of Limes

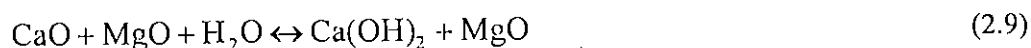
Most commonly, lime is the calcination products of calcitic and dolomitic lime stones and hence it is classified into two groups, calcitic lime and dolomitic lime. The formation of calcitic lime involves the following chemical processes:



Heat is required for the dissolution of  $\text{CaCO}_3$  (Kczdi, 1979), since the process is called endothermic in nature. The oxide of  $\text{Ca}^{2+}$  (bivalent calcium) is the burnt or quicklime. Oxides can be produced from dolomitic or calcium magnesium carbonate,  $\text{CaMg}(\text{CO})_2$  in the form of dolomitic lime or  $(\text{CaO} + \text{MgO})$ . Lime can exist in two forms, either as quicklime,  $\text{CaO}$  and hydrated lime,  $\text{Ca}(\text{OH})_2$ . But calcitic quicklime can easily be hydrated according to the following equation.



Hydration of dolomitic lime follows the reactions under normal conditions:



The properties of the quicklime and hydrated lime are presented in Table 2.3 while Table 2.4 presents the specifications of pure lime.

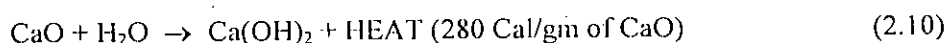
### 2.5.2 Mechanism of Lime Stabilization

Three reactions namely, dehydration of soil, ion exchange and pozzolanic reaction are guided the major strength gain of lime treated clay. Carbonation is also other mechanisms causes

minor strength increase and can be neglected. Short term reactions include hydration (for quicklime) and flocculation (ion exchange). Longer term reactions are cementation and carbonation. The natural stabilizing agent for cohesive soils is calcium hydroxide, hydrated lime or slaked lime. Calcium hydroxide is not itself a binder, but will produce a binder (consisting mainly of calcium silicate) by slow chemical reactions principally with the silicates in the clay mineral of cohesive soils (Assarson et al., 1974). The use of lime as a stabilizing additive is mainly due to its well-known effects when mixed with soils.

### 2.5.2.1 Hydration

The hydration of quicklime is started with the pore water of the soil and a large amount of heat is released. The increase in temperature can, at times, be so high that the pore water start to boil (Broms, 1986). An immediate reduction of natural water contents occurs when quicklime with cohesive soil as water is consumed in the hydration process. Assarson et al. (1974) reported that at the slacking of the lime, a part of the soil water, about 0.3 kg/kg CaO is consumed. Moreover, a considerably larger amount of the pore water evaporates of the heavy heat release, i. e., as the hydration of the quicklime proceeds and the temperature increases, the amount of pore water is reduced. This drying action is particularly beneficial in the treatment of the moist clays. Thus if a reduction of the natural water content in a cohesive soil is desirable, quicklime (or unslaked lime) instead of calcium hydroxide is used. It is important that the water content of the base clay must be sufficient for the complete slacking of the quicklime. Furthermore, to make the ion exchange possible between calcium ions of hydrated and the alkali ions of the clay minerals, there must be enough water after the evaporation caused by the heat release at the slacking of the quicklime. During the placement of lime columns and layers, the heat generation and the expansion of lime further affect the consolidation phenomena.



$\text{Ca(OH)}_2$  form the hydration of quicklime or when using calcium hydroxide as the stabilizer, dissociates in to the water, increasing the electrolytic concentration and the pH of the pore water, and dissolve the  $\text{SiO}_2$  and  $\text{Al}_2\text{O}_3$  from the clay particles.



The reaction outputs will result of ion exchange and flocculation and pozzolanic reactions.

### 2.5.2.2 Ion Exchange and Flocculation

Sodium and other cations adsorbed to the clay mineral surfaces are exchanged with calcium when the lime is mixed with clay. This change in cation complex affects the structural component of the clay mineral. Within a period of a couple of minutes up to some hours mixing the calcium hydroxide is transformed again due to the presence of carbonic acid ( $\text{H}_2\text{CO}_3$ ) in the soil (Kezdi, 1979). The presence of carbonic acid in the soil is due to the

reaction of carbon dioxide of the air in the soil and the free water. The reaction results in the dissociation of the lime into  $\text{Ca}^{++}$  (or  $\text{Mg}^{++}$ ) and  $(\text{OH})^-$  which modifies the electrical surface forces of the clay minerals. A transformation of the soil structure begins, i.e., flocculation and coagulation of soil particles into larger sized aggregates or grains and an associated increase in the plastic limit. Lime causes the clay to coagulate, aggregate or flocculate. The clay plasticity (measured in terms of Atterberg Limits) is reduced making it more easy workable and potentially increasing its strength and stiffness. The change in the soil structure is a consequence of cation exchange caused by dissociated bivalent calcium ions in the pore water replacing such univalent alkali ions that normally are attracted to the negatively charged clay particles (Assarson et al., 1974). This is the outputs in the flocculation of the clay particles.



Replace ability of common cations associated with soils follows the general order of the Hofmeister series:  $\text{Na}^+ < \text{K}^+ < \text{Ca}^{++} < \text{Mg}^{++}$ , with highly metallic ions replacing the weaker one on the surface of clay particles. The crowding of  $\text{Ca}^{++}$  ions onto the surface of the clay particles. The crowding of  $\text{Ca}^{++}$  ions onto the surface of the clay particles (adsorption) brings about flocculation (Herrin and Mitchell, 1961). The cation exchange capacity highly depends on the pH of the soil water and on the type of clay mineral in the soil. Among the types of clay mineral, Montmorillonites have the highest and Kaolinites have the lowest cation exchange capacities (Assaron et al., 1974).

### 2.5.2.3 Pozzolanic Reaction

Calcium hydroxide in the soil water reacts with the silicates and aluminates which are called pozzolans in the form cementing materials or binders, consisting of calcium silicates and aluminate hydrate, they are principally dihydrates (Diamond and Kinter, 1965). The dissolved dissociated  $\text{Ca}^{++}$  ions react with the dissolved  $\text{SiO}_2$  and  $\text{Al}_2\text{O}_3$  from the clay particle's surface and form hydrated gels, resulting in the combination of the soil particles (Diamond and Kinter, 1965). Thus, the shear strength of the stabilized soil gradually increases with time only due to pozzolanic reactions.



### 2.5.2.4 Carbonation

Carbonation may be defined as a process that the lime reacts with carbon dioxide in the atmosphere or in the soil to form relatively weak cementing agent, such as calcium carbonate or magnesium carbonate (Ingles and Metcalf, 1972). The strength calcium carbonate which formed by this process can be discounted, and its significance on the soil lime stabilization can be dismissed (Broms, 1986). Eades and Grim (1960) found that although carbonation does take place, the strength gain that is said to occur by virtue of cementation of soil grains

by calcium carbonate has yet to be conclusively demonstrated. Diamond and Kinter (1965) even suggested that carbonation is probably a delirious rather than helpful phenomenon in the soil stabilization.

## 2.6 Predominant Factors that Control Hardening Characteristics of Lime Treated Clay

### 2.6.1 Type and Amount of Lime

Unslaked lime or quicklime is generally more effective than slaked lime or hydrated lime, but generally it needs care in handling for soils with moisture contents (Kezdi, 1979). Thus the efficiency of soil stabilization depends in part on the type of lime material used and the effect of lime are compared with other binding materials as shown in the previous Fig. 2.5 (Balasubramaniam et. al., 1999). Quicklime is more effective and important since water to be absorbed from the soil, the hydration will cause an increase in temperature which is favorable to strength gain during soil stabilization.

Lime contents equal to the lime fixation point for a soil will generally contribute to the improvement in soil workability, but may not result in sufficient strength increases. Handy et al., (1965) referred this point as the 'Lime retention point'. This is because the plastic limit is indicative only of the lime fixation capacity in clayey soils, and that it is necessary to use additional amounts of lime above the lime fixation capacity to permit the formation of cementing materials within clayey soils to increase strength. Thus the lime fixation point is defined as the point at which the percentage of lime is such that additional increments of lime produce no appreciable increase in the plastic limit.

Eades and Grim (1960) suggested that the amount of lime consumed by a soil after one hour affords by a quick method of determining the percentage of lime required for stabilization, i.e., the lowest percentage of lime required to maintain a pH of 12.6 is the percentage required to stabilize the soil. However, a strength test is still necessary to show the percentage of strength increase. He gave correlation which showed that the amount of lime is proportion to the type and amount of clay present and is independent of the absorbed cation present in the clays. The relationship is established as follows:

$$\text{Optimum Lime Content} = \% \text{ of clay} / 35 + 1.25 \quad (2.15)$$

In Bangladesh, a number of research works was carried out on lime treated samples (Ahmed, 1984; Serajuddin and Azmal, 1991; Serajuddin, 1992; Rajbongshi, 1997; Molla, 1997; Shahjahan, 2001; Hasan, 2002; Siddique and Rajbongshi, 2001, 2002; Siddique and Hossain, 2003; Ansary et al., 2003; Toyeb, 2006). These works reported the effects of lime stabilization on geotechnical properties and strength characteristics of regional alluvial soils and coastal soils, where test model samples were prepared by compaction. Ahmed (1984) reported the effect of lime content and curing age on unconfined compression strength for sandy silt and silty clay samples (1.4 in. diameter by 2.8 in. high) treated with various lime contents (0.5% to 5%) and



found that unconfined compressive strength increases with the increase in lime content and curing age. Serajuddin and Azmal (1991) and Serajuddin (1992) also reported the effect of lime content and curing age on unconfined compressive strength of samples (50 mm diameter and 100 mm high) of regional alluvial soils of Bangladesh. Samples were treated with 5%, 7.5% and 10% slaked lime. Typical results showed that unconfined compressive strength of lime-treated samples increase with the increase in curing age and lime content. Hossain (1991) also found an increase in unconfined compressive strength with the increase in lime content and curing age lime for two regional soils of Bangladesh. Molla (1997) also found that the same effect for lime-treated samples.

Rajbongshi (1997) investigated the effect of lime content and curing age on unconfined compressive strength of large diameter samples (2.8 in. diameter by 5.6 in. high) of a coastal soil. Siddique and Rajbongshi (2001) reported that unconfined compressive strength of lime-treated samples increase with the increase in lime content and curing age as shown in Fig. 2.14. Shahjahan (2001) also found that unconfined compressive strength of lime-treated samples increased with the increase in lime content and curing age for three regional soils of Bangladesh. Similar effects were reported by Siddique and Hossain (2003) and Ansary et al. (2003).

### **2.6.2 Curing Time**

The shear strength of lime stabilized soils increase with time in a manner similar to concrete. The rate of increase is generally rapid at the early stage of curing time; thereafter, the rate of increase in strength decreases with time. Lime has an initial reaction with soil taking place during the first 2-3 days after mixing, and a secondary reaction which starts after this period and continues indefinitely (Taylor and Arman, 1960). The subsequent increase in strength which continue for years is mainly due to pozzolanic reactions. Broms (1986) reported that approximately one third of the increase in shear strength after one year is usually gained after a month and approximately three-quarters after three month.

Shahjahan (2001) also reported that unconfined compressive strength of lime-treated samples increased with increasing curing time at different lime content for three regional clays of Bangladesh as shown in Fig. 2.15. Similar effects were also reported by a number of investigators (Molla, 1997; Siddique and Rajbongshi, 2001; Siddique and Hossain, 2003; Ansary et al. 2003).

### **2.6.3 Type of soil**

For lime to be effective, there must be within the soil, clay particles or other pozzolanic materials that are reactive with the lime. Thompson (1966a) stated that the extent of improvement of the engineering characteristics of soil depends largely upon the soil type. The gain in strength of a soil lime system is mainly due to the pozzolanic reaction i.e. the long-term reaction between lime and certain clay minerals (silicate and aluminates) in the presence of water. He also noted that

soils having larger amount of clay fraction and less amount of organic matter are very effective to lime stabilization.

In general the more plastic the clay fines and the higher the clay content, the larger will be the lime content to produce a specific strength gain or other effect. On the other hand, the amount of bonding achievable with lime can be limited by the amount of reactive material. For lime stabilization to be successful, the clay content of the soil should not be less than 20% and the sum of the silt and clay fractions should preferably exceed 35%, which is normally the case when the plasticity index of the soil is greater than 10 (Broms, 1986). Ingles and Metcalf (1972) did not recommend crushed rock and sands for use in lime stabilization.

NASSRA (1970) stated that highly plastic soils are more effective to gain strength. NASSRA (1970) pointed out that soil having plasticity index in the range of 10 to over 50 are suitable for lime stabilization. Soils with plasticity index lower than 10 do not react readily with lime, although there are some few exceptions. Ingles and Metcalf (1972) studied the effect of the unconfined compressive strength on different types of soil stabilized using lime. It was found that the strength of lime stabilized silty clay is higher than the other types of soil.

Yu Kuen (1975) stated that in general, highly plastic soils are more effective than other types of soil when stabilized with lime. Compendium (1987) stated that lime is very effective in stabilizing the clay soils with a substantial portion of the coarse grained soil. Rodriguez et al. (1988) noted that the maximum effect of lime is on clayey gravel soil. Sometimes, the strength increase due to lime stabilization on these types of soil is such that the stabilized soil becomes stronger than those that would be obtained with cement. Rodriguez et al. (1988) also reported that lime has been more frequently used with plastic clays, which become more workable and easy to compact. Lime also provides volumetric stability of the soil in the presence of changing water.

Locat et al. (1990) studied the effect of four types of soil of Canada stabilized with lime. He observed that the unconfined compressive strength of the silty clay soil is higher than the other types of soil. He reported that the variation of unconfined compressive strength with lime content for four types of soil. It has been found that the maximum strength is gained by the soil with higher clay content.

Serajuddin (1992) reported that the results of three types of lime treated soil of the South West region of Bangladesh. Silt and clay types of soil were used in the investigation. It has been found that silty soil has much lower unconfined compressive strength than the clay types of soil.

#### **2.6.4 Clay Minerals**

Clay minerals are classified into three main groups, namely the Kaolinite minerals, the Montmorillonite groups, and the Illites. Eades and Grim (1960) observed that although Kaolinites, Illites, Montmorillonites and other mixed-layered clays all react with lime to give

greater strengths, the quantity of lime needed to treat a clay is dependent on the type of mineral present. For Kaolinite clay, the increase in strength begins with the addition of the first increment of lime. The strength begins to increase as some of the calcium attacks the edges of the Kaolinite particles and a new phase of calcium silicate hydrates formed. In contrast, Illite, Montmorillonite and some mixed layered clays required in excess of 4% to 6% before any strength developed. It is found that unconfined compression test results suggested that Kaolinitic and Montmorillonitic clayey soils are effectively stabilized with lime alone, where as Illitic clays require addition of fly-ash to obtain a significant strength gain. Lee et al., (1982) found that in terms of strength increase, lime treatment has greater effect in montmorillonites than kaolinitic soils. Wissa et al. (1965) reported that for lime stabilization, clay that contained montmorillonite showed higher improvement of angle of shearing resistance as compared to cohesion of the clay that contained illite.

### 2.6.5 Soil pH

The base exchange of soil is low when the pH-value is less than 7. Lime addition will increase the pH of the water content in the soil, and give rise to increased solubility. The long term chemical reactions in lime stabilized soils are favored by a high pH-value ( $\text{pH} > 12$ ) since the reactions are accelerated due to the increased solubility of the silicates and aluminates which are called pozzolans present in the clays (Broms, 1986). Davidson et al., (1965) suggested that a minimum pH of approximately 10.5 is necessary for pozzolanic reaction to take place, while Eades and Grim (1960); Rao and Rajasekaran (1996) suggested that the lowest percentage of lime required to maintain a pH of 12.40 is the percentage required to stabilize a soil. Broms (1986) pointed out that the pH of the treated soil will normally exceed 12 even when only a few percent of lime has been added to the soil.

### 2.6.6 Curing Temperature

Broms (1986) attributed that the favorable effects of high curing temperature to the increased the chemical reactions and solubility of the silicates and aluminates (pozzolans) in the clay at high temperatures. For lime-soil mixture at the same age, the effect of increasing the curing temperature is to increase strength as shown in Fig. 2.16. Bell (1988) expressed from Fig. 2.16 that for a particular curing age unconfined compressive strength increases considerably with curing temperature and that at a particular temperature strength increases with increasing curing age. For lime stabilized clays, it is found in Fig. 2.16 that the curves (UC strength versus temperature) were different for different curing time and that there was an abrupt change in the slope in the vicinity of 45°C, although he gave no explanation for this phenomenon. The different reaction products are formed at different curing temperatures and that the cut-off strength-temperature slope is different from 15°C to 25°C. Furthermore, it was found that there was increase of strength with time at all temperatures, with greater rate of increase at the

higher temperature. The curing temperature has found to affect the long term reactions between lime and clay.

### 2.6.7 Compaction Delay Time

Compaction delay time is the time interval between mixing of lime with soil and compaction. Mitchell and Hooper (1961) from their experiments on an expansive clay reported that a delay between mixing and compaction is definitely detrimental in terms of density, swell and strength for samples under the same compactive effort. Croft (1964) also concluded that compaction should proceed immediately. The sooner the particles are brought into contact with one another, the greater will be the final strength achieved and prolonged delays will certainly be detrimental. The IRC (1973) stipulates a maximum time lag of 3 hours between mixing and compaction for the construction of roads and runways.

NAASRA (1986) suggests that if high strengths are required, then this can best be obtained by early compaction as these results in high densities. Delayed compaction lowers density but the rate of reduction in maximum density is nowhere near as rapid as with cement. If soils are wet, a delay can be used to improve handling and compactability. Conversely, with dry soils a delay in compaction will increase the moisture requirements.

Townsend et al. (1970) observed that the compaction delay time of 24 hours can reduce the strength of the specimen up to 30% as compared to the specimen prepared by compacting immediately after mixing.

Sastry et al. (1987) observed that for a delay period of time for two hours between mixing and compaction, there is practically no reduction in strength. But for further delay the strength of soil lime mixture continues to fall. By an independent study Sastry et al. (1987) observed the delay for 96 hours between mixing and compaction, strength of the soil lime mixture continuous to fall in the same trend.

Compendium (1987) stated that granular soil-lime mixture should be compacted as soon as possible after mixing, although delays up to two days are not detrimental, especially if the soil is not allowed to dry out. Fine grain soils can also be compacted, soon after final mixing, although delays of up to 4 days are not detrimental.

Boominathan and Prasad (1992) stated that compaction delay of 24 hours can decrease the strength from 30% to 70%. Boominathan and Prasad (1992) reported that the reduction in strength and density are attributed to granulation of loose soil particles by weak cementation, as the soil mellows.

Molla (1997) and Shahjahan (2001) also investigated the effect of compaction delay time on unconfined compressive strength for regional soils of Bangladesh. Shahjahan (2001) reported

that unconfined compressive strength decreases with the increase in compaction delay time as shown in Fig. 2.15.

### **2.7 Comparison on the Mechanisms of Cement and Lime Stabilization**

The mechanism of the cement stabilization is composed of cement hydration and the pozzolanic reaction but lime stabilization is mainly composed of the hydration of the soil, the ion exchange and the pozzolanic reaction (Siddique and Hossain, 2003; Ansary et al., 2003). The rate of the strength gain of cement treated soils is very rapid in the early stages but decreases very rapidly with increasing curing periods, which is similar to that of concrete. The rate of strength gain of lime treated soils is slower compared to cement treated soils, but last longer. At low concentrations, lime treated clays have higher strengths than the cement treated clays do. However, after certain values of concentration, cement treated clays have higher strengths than the lime treated clays do during chemical stabilization.

### **2.8 Modification of Clay Mineralogy Due to Cementation**

Figures 2.18(a) and 2.18(b) show the X-ray diffraction pattern of untreated and cement-treated Singapore marine clay respectively as reported by Chew et al., (2004). They found that the combined mass of CSH and CASH cementitious product increased with increasing cement contents for cement treated Singapore marine clay as shown in Fig. 2.18. The relative amounts of constituents in the soil samples were determined using the semi quantitative procedure suggested by Pierce and Siegel (1969). Chew et al., (2004) reported that kaolinite appears to have vanished in all three of the cement-treated soil specimens as listed in Table 2.5. This is suggested by Eades and Grim (1960) that kaolinite is rapidly exhausted by the pozzolanic reaction and is consistent with the highly pozzolanic behaviour of kaolinite. It is also consistent with the rapid increase in cementitious product content at low cement content as shown in Fig. 2.19. They found that at low cement content, cementitious products are formed by the hydration and pozzolanic reaction, with the latter using up the kaolinite and at higher cement content, exhaustion of the kaolinite leads to cessation of the pozzolanic reaction and additional cementitious products are formed only by the hydration reaction.

### **2.9 Modification of Micro-structure Due to Cementation**

Kamruzzaman et al. (2004) reported the microstructure of untreated and treated Singapore marine clay. As shown in Fig. 2.20(a), untreated Singapore marine clay exhibits a fairly open type of microstructure with the platy clay particles assembled in a dispersed arrangement. Figure 2.20(b) shows the micrograph of cement-treated marine clay specimens after 28 days curing. Kamruzzaman et al. (2004) observed that the cement content of 20% results in an open fabric, with some sign of reticulation and as the cement content increases to 30-50% the flocculated nature of the fabric becomes more evident, with soil particle clusters interspersed by large openings. At the same time, the platiness of the fabric becomes less evident and the

degree of reticulation appears to increase. At 50% cement content fine networks of reticulation become quite evident. The increase in the degree of reticulation can be attributed to an increase in the amount of CSH, which is reticular in nature, which is also reported by Locate et al. (1990). This is consistent with the results of the X-ray diffraction analysis, as well as with SEM results for lime-treated clay (Locate et al., 1990; Onitsuka et al., 2001). The flocculated nature of the fabric has been attributed to the cation exchange process, which results in  $\text{Ca}^{2+}$  ions replacing  $\text{K}^+$  cations (Locate et al. 1990; Shen 1998). The adsorption of  $\text{Ca}^{2+}$  ions onto the illite particle surface leads to a decrease in repulsion between successive diffused double layers and results in more edge-to-face contacts between successive illite sheets. Thus, clay particles flocculate into larger size clusters.

## **2.10 Modification of Chemical Properties of Treated Clays**

### **2.10.1 pH Value**

Kamaluddin, (1995) reported that the pH value of the Bangkok clay was found to be 6.1, which indicates that the clay is acidic and the low pH reveals that the clay contains a significant amount of  $\text{H}^+$  ions. According to the criteria of pH that the neutral soil solution is expressed by numerical pH value 7 and if pH value exists above 7, soil solution is alkaline and pH value exists below 7, soil solution is acidic in nature. Chew et al. (2004) reported that the pH value rises rapidly at lower cement content but the rate of the rise moderated at higher cement content and at very high cement content, the pH value approaches 12.5, which corresponds to that of  $\text{Ca}(\text{OH})_2$  as shown in Fig. 2.21. The increase of pH with an increase of cement content is due to crowding of the  $\text{Ca}^{2+}$  ion concentration on the clay surface, leading to changes in fabric of the cement-treated clay (i.e., the formation of a flocculated clay-cement matrix). A similar effect of pH on fabric changes of a clay-water-electrolyte system has been reported by Santamarina et al., (2001).

### **2.10.2 Organic Matter and Organic Carbon**

Organic matter in soil is derived from a wide variety of animal and plant remains so there can be a great variety of organic compounds. Organic matter has undesirable effects on the engineering behaviour of soils. Arora (2000) reported that the effect organic content on engineering properties of soil layer are as follows:

- (i) Bearing capacity / strength of soil layer is reduced.
- (ii) Compressibility of soil layer is increased.
- (iii) Swelling and shrinkage potential due to changes in moisture content is increased.
- (iv) The presence of gas in the voids can lead to large immediate settlements and can affect the derivation of consolidation coefficients from laboratory tests.
- (v) The gas can also give misleading shear strength values derived from total stress.

- (vi) The presence of organic matter (e.g. in peat) is usually associated with acidity (low pH) and sometimes with the presence of sulphates. Detrimental effects on foundations could result if precautions are not taken.
- (vii) Organic matter is harmful in soils used for stabilization roads.

A measure of the organic content of soils is necessary in order to make the soil for allowable properties. These effects on the engineering behaviour of soils are minimized and improved by cement and lime stabilization. The organic matter and organic carbon of the treated and untreated clays are determined by wet oxidation methods. Kamaluddin (1995) reported that the organic matter content and organic carbon content for Bangkok clay were found to be 5.6% and 2.87% respectively. Arman and Muhfakh (1972) reported that the undesirable effects of organic content on the strength for lime treated clays as shown in Fig. 2.22. It is concluded that the strength decreases with increasing organic matter. Generally, the effect of cement / lime decreases with increasing organic content. Some other accelerating agent (e.g., gypsum) has often been used together to stabilize organic soil when cement / lime alone is not effective. At the present of organic matter and organic carbon for cement / lime treated clays, strength increases slowly with increasing curing time.

### 2.10.3 Electrical Conductivity

Kamaluddin (1995) reported that the electrical conductivity for Bangkok clay was determined to be 2.29 mmho/cm, signifying that the clay is saline. The range of values indicates that the pore water contains a moderate amount of soluble cations. The salinity of clay is measured by the electrical conductivity (EC) test. The amount of salts are dissolved in the pore water which are responsible for amount of soluble cations.

During chemical stabilization, electrical conductivity of soil is increased by reactions with increasing cement. The EC values increases with increasing curing time because chemical reactions proceed on and flocculated structures are formed. Stabilized soils with a flocculent structure are light in weight and have a high void ratio (Arora, 2000). However, these soils are quite strong and can resist external forces because of strong bond due to attraction between particles. The stabilized soils are insensitive to vibration. In general, the stabilized soils in a flocculated structure have a low compressibility, a high permeability and a high shear strength (Arora, 2000).

### 2.10.4 Cation Exchange Capacity

Das (1999) defined that the phenomenon of replacement of cations is called cation exchange or base exchange. The net negative charge on mineral which can be satisfied by exchangeable cations is termed cation exchange capacity (CEC) or base-exchange capacity. In other words, base exchange capacity is the capacity of the clay particles to change the cation adsorbed on the surface. Base-exchange capacity is expressed in terms of the total number of positive

charges adsorbed per 100 gm of dry soil. It is measured in milliequivalent (meq), which is equal to  $6 \times 10^{20}$  electronic charges. Thus one meq per 100 gm that 100 gm of material can exchange  $6 \times 10^{20}$  electronic charges if the exchangeable ions are univalent, such as  $\text{Na}^+$ . However, if the exchangeable ions are divalent, such as  $\text{Ca}^{2+}$ , 100 gm material will replace  $3 \times 10^{20}$  electronic charges of calcium ions.

Kamaluddin, (1995) reported that the cation exchange capacity (CEC) of the Bangkok clay was found to be 28.2 meq/100g, that means the clay tends to absorb cations and it's 28.2 numbers of chemical equivalents per hundred grams of oven dry soil. While Chew et. al., (2004) reported that the cation exchange capacity (CEC) of the Singapore marine clay was found to be 33.30 meq/100g, that means the clay tends to absorb cations and it's 33.30 numbers of chemical equivalents per hundred grams of oven dry soil. The base-exchange capacity of clay mineral depends upon the pH value of the water in the environment. If the water is acidic ( $\text{pH} < 7$ ), the cations exchange capacity is reduced.

Das (1999) reported that the base exchange capacity of the kaolinite, illite and montmorillonite mineral are about 3-8 meq per 100 gm, 10-40 meq per 100 gm and 70-100 meq per 100 gm respectively. CEC is the sum of the exchangeable cations that a mineral can absorb at a specific pH, i.e., a measurement of the negative charges carried by the mineral. One of the fundamental properties of the clays is the electrical charge on their unit particles which means that clays will absorb cations and/or anions that neutralize the layer charge, but which are exchangeable. This means that they can be readily replaced by another anion or cation when brought into contact with these ions in aqueous solution during chemical stabilization. Except under extremely acidic conditions, the layer charge is predominantly negative.

#### 2.10.5 Exchangeable Cations

A soil particle carries either a negative charge or positive charge. However, by the actual tests, only negative charges have been measured, when clay particles mixed with water and cement. Arora (1998) reported that the net negative charge on clay particles may be due to one of the following reasons:

- (i) Isomorphous substitution of one atom ( $\text{Ca}^{2+}$ ) by another ( $\text{Na}^+$ ) of lower valence.
- (ii) Dissociation of hydroxyl ion ( $\text{OH}^-$ ) into hydrogen ions.
- (iii) Adsorption of anions (negative ions) on clay surface.
- (iv) Absence of cations (positive ions) in the lattice of the crystal.
- (v) Presence of organic matter and salt concentration.

Kamaluddin, (1995) reported that the cation exchange capacity (CEC) of the Bangkok clay was found to be 28.2 meq/100g, with the exchangeable cations identified as  $\text{Na}^+ = 3.26$



meq/100g,  $K^+ = 1.99$  meq/100g,  $Ca^{++} = 26.78$  meq/100g and  $Mg^{++} = 6.1$  meq/100g and cations in the pore water were found to consist of  $K^+ = 0.34$  meq/l,  $Mg^{++} = 9.9$  meq/l,  $Na^+ = 3.22$  meq/l,  $Ca^{++} = 6.98$  meq/l. It is compared that the cation exchange capacities for treated samples are higher than that of untreated sample.

Eades and Grims (1960) indicated to the formation of new crystalline phases in the soil lime electrolyte system due to the addition of lime to the soil in presence of water, which are tentatively identified as calcium silicate hydrate. The reaction of lime with three layers material, which are montmorillonite, kaolinite, and illite begin by the replacement of existing cations between the silicate sheets with  $Ca^{++}$ . Following the saturation of inter layer positions with  $Ca^{++}$ , the whole clay minerals deteriorate without the formation of substantial new crystalline phases.

Rao and Rajashekar (1996) reported that the effect of curing time on exchangeable calcium ion ( $Ca^{2+}$ ) concentration of lime treated clay, which depend on quality of water as shown in Fig. 2.23. It is found that  $Ca^{2+}$  ions are increased rapidly within short time about 5 days and afterward rate of rise moderated to be asymptotic. The exchangeable cations ( $Ca^{2+}$ ) that a mineral can absorb at a specific pH value. As increasing cement content, the pH value approaches 12.5, which corresponds to that of  $Ca(OH)_2$ . The increase of pH with an increase of cement content is due to crowding of the  $Ca^{2+}$  ion concentration on the clay surface, leading to changes in fabric of the cement-treated clay (i.e., the formation of a flocculated clay-cement matrix). The flocculated nature of the fabric has been attributed to the cation exchange process, which results in  $Ca^{2+}$  ions replacing  $Mg^{2+}$ ,  $K^+$  and  $Na^+$  cations (Locate et al. 1990).

Kamruzzaman (2002) and Chew et al. (2004) reported that the cations behaviour of cement treated and untreated clays. The adsorption of  $Ca^{2+}$  ions onto the clay particle surface leads to a decrease in repulsion between successive diffused double layers and results in more edge-to-face contacts between successive clay sheets. Thus, clay particles flocculate into larger size clusters. As the silicates and aluminates from the mineral component go into solution, they react with the adsorbed  $Ca^{2+}$  ions on the mineral particle surface and form CSH (Calcium silicate hydrate) and CASH (Calcium aluminium silicate hydrate), which induces cementation of the flocculated clay particles and forms clay-cement clusters.

## 2.11 Modification of Physical Properties for Treated Clays

### 2.11.1 Grain Size Distribution

The reactions which occur when cement is mixed with clay, will result in changes in the grain size distribution of the soil. Chew et al. (2004) reported that the dissociation of hydrated lime  $Ca(OH)_2$  into  $Ca^{2+}$  and  $OH^-$  ions causes the cement to lose most of its crystalline structure and assumed an amorphous form, i.e., it creates a transition to gel phase. The finest soil particles

agglomerate which brings about a change in grain size distribution. The extent of agglomeration is influenced by factors such as the type of soil, the amount of cement added and the curing time. The gel phase is an important stage from the aspect of strength, as the gel substance will connect and cement the mineral grains, thus changing the pore structure. Assarson et al. (1974) concluded that the dissolved bivalent calcium ions ( $\text{Ca}^{2+}$ ) replace the monovalent ions ( $\text{Na}^+$  and  $\text{K}^+$ ) which are normally attracted to the surface of the negatively charged clay particles. The crowding of ( $\text{Ca}^{2+}$ ) ions onto the surface of the clay particles brings about the flocculation of the clay (Herrin and Mitchell, 1961). Thus, the soluble products of cement hydration cause the electrolytic concentration of pore pressure and pH value to increase. The flocculation can also be brought about by the hydration of cement, resulting in a change of (coarser) grain size distribution of the soil particles.

Changes in the grain size distribution by chemical stabilization are rather difficult to determine as the usual analysis by hydrometer, does not render a true picture. Kezdi (1979) suggested that the changes in the grain size should instead of to be expressed numerically on the basis of another characteristic property such as specific surface area, pore size, permeability or plasticity.

### **2.11.2 Water Content**

Chew et al. (2004) reported that the immediate reduction of the water content from that of the clay slurry is due to the addition of dry cement, so it should therefore be regarded as the initial water content as shown in Fig. 2.24. They found that much of the decrease in water content takes place within the first 7 days of curing, and the magnitude of the reduction increases with the cement content. This is not surprising since water is absorbed and transformed into hydrated CSH and CASH during the hydration and pozzolanic reactions, and would not be expelled by reheating the cementitious products to  $105^\circ\text{C}$ . Both the 7-day and 28-day water contents show in Fig. 2.24, a very rapid decrease at cement content of less than 10%, which then moderated substantially at higher cement contents. At higher cement content, the exhaustion of the kaolinite further inhibits pozzolanic reaction, leaving only the hydration reaction. Bergado et al. (2003) concluded that the hydration of the cement treated clays generally continues with time, leading to the reduction of the water content until the completion of the reactions. Bergado et al. (2003) reported that the water content immediately decreases after mixing soil-cement and significantly reduces with increasing cement content and curing time.

### **2.11.3 Unit Weight**

General effect for unit weight of cement treated clay in comparison to untreated clay can be reviewed that at low mixing water content with compaction by blows is increased in nature as reported by Bergado et al. (2003) while at high mixing water content without compaction by blows is decreased in nature as reported by Miura et al. (2001). The unit weight increases with

increasing cement content and curing time. The unit weight of cement treated clay is also affected by the soil type and the water-cement ratio. Kamaluddin, (1995) reported that the influence of curing time on unit weight at different cement content are shown in Fig. 2.25. It is found that and the longer curing time produces treated clay of higher unit weight. The curvilinear variation can be observed up to 8 weeks curing period and then turns into a linear pattern. It is also found that higher the cement content, higher the unit weight.

#### 2.11.4 Specific Gravity

General effect for specific gravity of cement treated clay in comparison to untreated clay can be reconsidered that at low mixing water content with compaction by blows is decreased in nature as reported by Bergado et al. (2003) and at high mixing water content without compaction by blows is also decreased in nature significantly as reported by Miura et al. (2001). The specific gravity decreases with increasing cement content and curing time. Kamaluddin (1995) stated that cement causes significant reduction in specific gravity and this change is dependent on cement content and curing time as shown in Fig. 2.26. The figure shows that the reduction process of specific gravity follows a pattern; the lowest curing time possesses a curvilinear type of variation and the curvature reduces gradually with increasing curing time. It is also found that lower the cement content, higher the specific gravity.

#### 2.11.5 Atterberg Limits

In general, liquid limit and plastic limit of the soil generally increases with increasing cement, while the plasticity index reduces with the increase in cement content. Felt (1955) showed that the plasticity index for a plastic granular soil reduced considerably when treated with cement. Willis (1947), however, showed that the cement admixture reduces slightly the liquid limit of mixtures made from soils having liquid limit greater than 40. Willis (1947) also showed that liquid limit increases for soils having liquid limits less than 40 when treated with cement.

Ahmed (1984) showed that for sandy silt (LL = 40, PI = 10) and silty clay (LL = 43, PI = 21), plastic limits increased while plasticity indices reduced as cement content increased. Rajbongshi (1997) found that with the increase in cement content, for coastal soil (Type: A-4, LL=41, PI=7) liquid limit and plastic limit increased while plasticity index reduced while for coastal soil (Type: A-7-6, LL = 44, PI = 19) liquid limit reduced.

Ahmed (1984) investigated that the effect of increasing lime content on the liquid limit, plastic limit and plasticity index of regional soils of Bangladesh. Ahmed (1984) found that an increase in plastic limit while liquid limit and the plasticity index reduced with increasing addition of lime. Hossain (1991), however, found that an increase in liquid limit and plastic limit while plasticity index reduced (became non-plastic) with increasing addition of lime for two regional soils (LL = 25 and 42, PI = 12 and 20) of Bangladesh. Rajbongshi (1997) also investigated that the effect of increasing lime content on the liquid limit, plastic limit, plasticity index and shrinkage limit of a

coastal soil ( $LL = 44$ ,  $PI = 19$ ) of Bangladesh. Rajbongshi (1997) found that an increase in plastic limit and shrinkage limit while liquid limit and the plasticity index reduced with increasing addition of lime. Molla (1997) and Hasan (2002) also found the same effect for lime treated clays. The linear shrinkage of a clayey soil is also affected by addition of lime. Linear shrinkage reduces as the lime content increases, while the reduction in linear shrinkage with the increase in lime content in the heavy clay is much higher (IRC, 1976).

Bergado et al. (2003) found that for treated clays, the plastic limit of the soil increases with increasing cement content, while the plasticity index reduces. Chew et al. (2004) reported that the rates of increase in the liquid and plastic limits with respect to the cement content are almost equal at low cement content as shown in Fig. 2.27. This is consistent with the notion of water trapped with intra-aggregate pores. However, the rates of change of these two Atterberg limits at higher cement content are not the same. This suggests that the entrapped water hypothesis explains much, but not all, of the observed changes in the plastic and liquid limits. One possible reason for this is the deposition of cementitious products onto the surfaces of the flocculated clay clusters, which would lower the surface activity of these clusters. This also explains the slight decrease in liquid limit between 7-day curing and 28-day curing periods.

#### **2.11.6 Degree of Saturation**

General effect for degree of saturation of cement treated clay in comparison to untreated clay can be reviewed that at low mixing water content with compaction by blows is increase in nature (Bergado et al., 2003) and at high mixing water content without compaction by blows is also increase in nature significantly (Miura et al. 2001). The degree of saturation increases with increasing cement content. The degree of saturation of cement treated clay is affected by the soil type and the clay-water/cement ratio. A summary of the general effects of cementation on various physical properties of soft Bangkok clay is presented in Table 2.6.

### **2.12 Modifications of Engineering Properties due to Chemical Stabilization**

Essential engineering properties such as compressibility, permeability, stress-strain, strength and stiffness were studied from the one-dimensional consolidation, triaxial compression, direct shear and unconfined compression tests.

#### **2.12.1 Compressibility Characteristics**

The influences of  $w/c$  ratio (clay-water content/cement content) and curing time on different compressibility parameters including pre-consolidation pressure ( $\sigma_p'$ ), void ratio ( $e$ ), volumetric strain ( $\epsilon_v$ ), compression index ( $C_c$ ), swell index ( $C_s$ ) and coefficient of consolidation ( $c_v$ ) were investigated by a number of researchers (Kamaluddin, 1995; Miura et al., 2001; Horpibulsuk, 2002; and Chew et al., 2004). These are presented in the following sections.

### 2.12.1.1 Pre-consolidation Pressure, Void Ratio and Volumetric Strain

The increase in apparent pre-consolidation pressure (yield stress) and reduction in compression indices of soft clay arising from the inclusion of cement have been well established by Miura et al. (2001) and Bergado et al. (2003). Miura et al. (2001) investigated the  $(e-\log\sigma'_v)$  and  $(\epsilon_v-\log\sigma'_v)$  relationships of clay-cement mixtures at  $w/c$  ratios of 10 with clay-water contents of 120%, 150%, 180% and 250% and cured for after 28 days for cement treated Ariake clay. The test model samples were prepared without compaction blows for deep mixing. The  $(\epsilon_v-\log\sigma'_v)$  relationship is plotted so as to take care of the effect of the difference in void ratio for the vertical stresses less than the yield stress. The  $e-\log\sigma'_v$  and  $\epsilon_v-\log\sigma'_v$  relationships are shown in Fig. 2.28. Miura et al. (2001) found that the yield stress and the deformation behaviour at pre-yield stress of all samples having identical  $w/c$  are practically the same. They showed that the higher the cement content and curing time, the lower is the volumetric strain incurred by the treated sample. Miura et al. (2001) suggested that the resistance to compression of the treated clay is markedly enhanced until the consolidation pressure reaches the apparent pre-consolidation pressure (yield stress), which is due to the induced cementation bond created by the inclusion of cement. It was also suggested that beyond the yield stress, drastic compression occurs at which the cementation bond breaks down. Takahashi and Kitazume (2004) concluded that the well defined consolidation yield stress ( $\sigma'_y$ ) and the unconfined compressive strength ( $q_u$ ) were correlated as  $\sigma'_y = (1.27 \text{ to } 2.55) q_u$ .

### 2.12.1.2 Compression Index and Swell Index

The compression indices of treated clays in terms of  $C_c$  (compression index) and  $C_s$  (swell index) for Singapore Marine clay at different cement content and curing periods were reported by Chew et al. (2001). The test model samples are prepared without compaction blows for deep mixing. The effect of cement content on  $C_c$  and  $C_s$  is shown in Fig. 2.29. It was found that  $C_c$  value decreases significantly with the increase for cement content. For cement content up to 20%, the reduction of  $C_c$  is more pronounced. However, at cement content 30% or more almost no change of  $C_c$  is noticed. For cement content 30% or more, the reduction of  $C_s$  values is very marginal and approaching almost zero. This observation is consistent with the findings of Liu and Carter (1999) who showed that during virgin yielding, the structured soil is more compressible than the reconstituted soil. Chew et al. (2004) suggested that at higher stresses (beyond the apparent pre-consolidation pressure), the treated samples exhibit normally consolidated behaviour with larger  $C_c$ . The effect of curing time on compression indices is also significant.  $C_c$  and  $C_s$  decrease with increasing curing time.

### 2.12.1.3 Coefficient of Consolidation

Bergado et al. (2003) reported that the effect of cement treatment is to increase the values of coefficient of consolidation ( $c_v$ ) as shown in Fig. 2.30. The  $c_v$  value generally decrease approximately linearly with increasing consolidation pressure. Bergado et al. (2003) found that the higher the cement content, the greater the value of  $c_v$ . The highest enhancement of  $c_v$  value with cement content occurs in the vicinity of 15% cement content.

### 2.12.1.4 Intrinsic Compression Line and Generalized Compression Line

The compressibility and strength characteristics of reconstituted clays are used as a basic frame of reference for interpreting the corresponding of natural sedimentary clays (Burland, 1990). The intrinsic properties provide a frame of reference for assessing the in-situ state of a natural clay and the influence of structure on its in-situ properties. For overconsolidated natural clays, the Intrinsic Compression Line (ICL) provides a useful means of assessing the degree of overconsolidation.

Kamaluddin (1995) reported for cement treated Bangkok clay that the intrinsic properties for ( $I_v$ - $\log \sigma_v'$ ) plot renders excellent confirmation of the over-consolidation effect and assessing the degree of over-consolidation of the treated clays as shown in Fig. 2.31. The untreated clay proceeds with Intrinsic Compression Line (ICL) as the cement content increases, the curve is displaced with an increasing value of  $\sigma_v'$ . Kamaluddin (1995) showed that the curves are shifted with an increasing value of  $\sigma_v'$  as shown by the bands of higher cement content.

Burland (1990) introduced a new normalizing parameter called the void index to aid in correlating the compression characteristics of various clays. One-dimensional compression curve for reconstituted natural clays is normalized by assigning fixed values to  $e_{100}$  and  $e_{1000}$ . The quantities  $e_{100}$  and  $e_{1000}$  are the intrinsic void ratio corresponding to the consolidation pressure,  $\sigma_v' = 100$  kPa and  $\sigma_v' = 1000$  kPa respectively. The normalizing parameter chosen has been defined as the void index,  $I_v$  such that,

$$\frac{e - e_{100}}{e - e_{1000}} = \frac{e - e_{100}}{C_c} \quad (2.17)$$

The intrinsic compression index,  $C_c$ , is defined as  $e_{100} - e_{1000}$ . According to Burland (1990), the parameters  $e_{100}$  and  $C_c$  are called as the constant of intrinsic compressibility. The compression curves may be transformed to the normalized curve by using void index  $I_v$ . Clearly there is a close analogy between void index,  $I_v = (e - e_{100})/C_c$  and liquidity index. It is of utmost importance to be clear about the difference between these two indices. The void index is defined in terms of two directly measured mechanical properties ( $e_{100}$  and  $C_c$ ) derived from a one-dimensional compression test. There are two unknown parameters required to obtain ICL, which are compression index and  $e_{100}$ . Since the  $e_{100}$  can be written in terms of  $C_c$ , the modification of the Intrinsic Compression Line has been obtained by plotting normalized

void ratio,  $e/e_{100}$  versus vertical pressure,  $\sigma_v'$ . This line is designated as Generalized Compression Line (GCL). Thus, Horpibulsuk et al. (2002) reported that ICL and GCL by the equation nos. 2.18a and 2.18b respectively as below:

$$I_v = 2.45 - 1.285 \log \sigma_v' + 0.015 (\log \sigma_v')^3 \quad (2.18a)$$

$$e/e_{100} = 2.025 - 0.504 \log \sigma_v' \quad (2.18b)$$

## 2.12.2 Permeability Characteristics

### 2.12.2.1 Permeability and Vertical Stress

Chew et al. (2004) reported that permeability is increased due to cementation, which was explained by the permeability and vertical stress ( $\log k - \log \sigma_v'$ ) relationship of treated and untreated Singapore Marine clay as shown in Fig. 2.32. Test results reveal that at the same effective vertical stress, the treated clay has higher permeability than the untreated clay. Furthermore, it can be seen that the 7-day permeability is much higher than the 28-day permeability. Locat et al. (1996) and Takahashi and Kitazume (2004) also the similar trend of change in permeability.

### 2.12.2.2 Permeability and Void Ratio

As a pozzolanic reaction occurs, cementitious products gradually in fill the intracluster voids and strengthen the contacts between soil particles, thereby rendering the soil less compressible. As shown in Fig. 2.33, the increase in permeability  $k$  is closely correlated to the increase in void ratio ( $e$ ) by the following relations (Chew et al., 2004):

$$e = 0.26 \ln(k) + 6.86 \text{ with } R^2 = 0.80 \quad \text{for treated clays} \quad (2.19)$$

$$e = 0.21 \ln(k) + 5.14 \text{ with } R^2 = 0.87 \quad \text{for untreated clay} \quad (2.20)$$

The regression equation for treated clay appears to be independent of the curing time and cement content, being almost entirely dependent on the void ratio. Furthermore, Chew et al. (2004) reported that at the same void ratio, the treated clay would have higher permeability than the untreated soft clay. At the time of soil treatment, the addition of cement to the clay increases the permeability of the soils, due to flocculation of the soil particles. This phenomenon was consistent with Takahashi and Kitazume, (2004) for treated clay that has rather large intra-cluster voids which are enclosed by layers of cementations products with much smaller entrance pore diameters. The coefficient of permeability of the soil-cement mixtures was ranges from  $10^{-5}$  and  $10^{-9}$  cm/sec based on laboratory testing found by Takahashi and Kitazume (2004). Siddque and Safiullah (1995) reported that the same natured void ratio and permeability relationship for untreated Dhaka clay of Bangladesh.

### 2.12.3 Stress-Strain, Strength and Stiffness Characteristics

The influences of  $w_c/c$  ratio (clay-water content/cement content), pre-consolidation pressure and curing time on stress-strain behaviour of cement treated clay over that of the untreated clay were investigated by Miura et al. (2001), Bergado et al. (2003), Ghee et al. (2004).

#### 2.12.3.1 Deviator Stress-Strain Relationship from CIU Test

Ghee et al., 2004 reported that the specimen consolidated to higher pre-shear consolidation pressure attains higher values of maximum deviator stress. Bergado et al. (2003) reported deviator stress, shear strain relationship for time treated Bangkok clay. The characteristic shape of the  $(q-\epsilon_s)$  curves shows that the deviator stress increases to a peak value, then strain-softens to a lower value of  $q$ . The improvement of the sample with low lime content was found for treated Bangkok clays, to be much smaller than those for the samples of high lime content and lie close to the untreated clay as shown in Fig. 2.34. A general trend exists in these figures that the maximum deviator stress increases with the increasing value of lime content. It is also found that generally shear strain at the maximum deviator stress is reduced when lime content is increased.

#### 2.12.3.2 Deviator Stress-Shear Strain Relationship from CID Test

Miura et al., (2001) investigated the strain softening drained behaviour for the samples with same clay-water/cement ratio ( $w_c/c$ ) and subjected to low and high effective cell pressures,  $p_o'$  as shown in Fig. 2.35. The samples consolidated to a higher  $p_o'$  sustain higher failure strain accompanied by greater deviator stress. They found that the characteristics before their peak deviator stresses of clay-cement mixtures with a  $w_c/c$  value of 10 are the same for all effective cell pressures, and slightly diverse approaching the peak deviator stresses.

#### 2.12.3.3 Volumetric Strain and Shear Strain

Miura et al. (2001) investigated the volumetric strain and shear strain relationships as shown in Fig. 2.35. For the same  $w_c/c$  of 10, similar relationships up to their peak deviator stresses was obtained, but their peak and ultimate volumetric strains are different and dependent on  $p_o'$ . They found that the higher  $p_o'$  is generally associated with larger volumetric and shear strains. The lower the value of effective cell pressure, the greater the degree of dilation with showing negative volumetric strain (Kamaluddin, 1995). The dilation starts at lower levels of strain for samples, which are consolidated to a lower  $p_o'$ .

### 2.12.4 Pore Pressure Characteristics

Chew et al. (2004) investigated the pore pressure responses of cement treated Bangkok clay. Cement treated samples with pre-shear consolidation pressure modifies pore pressure response behaviour by reducing the strain at peak pore pressure. For low  $p_o'$  values, the maximum pore pressure attains prior to the failure of the sample, whereas for higher values of



$p_o'$ , the maximum pore pressure occurs after the failure of the sample (Fig. 2.36). Chew et al. (2001) found that at low consolidation pressures, excess pore pressure during shearing of stabilized soil increased slightly and then dropped and became negative at larger strain. This behaviour was similar to that of overconsolidated clay.

### 2.12.5 Failure Envelopes Characteristics

Bergado et al. (2003) reported the failure envelopes derived from the points of peak deviator stress ( $q_{max}$ ) obtained from triaxial tests which are shown in Fig. 2.37. Based on their results, they found that the failure envelope of the treated soil could not be characterized by a single straight line over the range of confining pressures investigated but for untreated soil by a single straight line. The authors are of the opinion that it fits well into a model of bilinear failure envelope for treated soil. On the other hand, Porbaha et al. (2000) found that both peak and residual failure state of cement treated soil was represented by a best fit straight line.

### 2.12.6 Stress Ratio and Volumetric Strain

Miura et al. (2001) reported that for cement treated samples subjected to high effective cell pressures, their ( $q$ - $e_s$ ) and ( $\epsilon_v$ - $e_s$ ) relationships are the same at the initial state up to a certain stress ratio,  $\eta$  ( $q/p$ ) and that samples with higher clay-water content exhibit higher volumetric and axial strains at the same stress ratio,  $\eta$ . This is attributed to the yield stress being the same. Kamaluddin (1995) also reported similar observations. The elastic behaviour is recognized for these treated samples. They found that samples with higher clay-water content undergo higher volumetric deformation when the states of stress are on the state boundary surfaces due to the break up of the cementation bond. It is shown that the transformation of the small strain zone into the large strain zone occurs at a smaller stress ratio,  $\eta$  for samples with a higher clay water content, as illustrated in Fig.2.38.

### 2.12.7 Effective Stress Paths Characteristics

Ghee et al. (2004) reported that the undrained stress paths at various pre-shear consolidation pressure for treated and untreated Singapore clays samples as shown in 2.39. They found indicated that these stress paths, corresponds to different category of states such as normally consolidated, lightly and heavily over-consolidated state; though all of the samples originated from the same untreated samples possessing normally consolidated state. Bergado (2003) also found that the stress paths evidently, belong to different category ranging from a low OCR value to a high OCR value depending on amount of cement content, curing period and pre-shear consolidation pressure.

### 2.12.8 Shear Stress, Vertical and Horizontal Displacement Characteristics

Fig. 2.40 shows the relation between shearing stress and horizontal displacement for consolidated drained test of the undisturbed Vertical (V)-specimens in soaked and unsoaked

conditions, which was investigated by Taha et al. (1998). Generally, there were no distinct peak points in stress displacement curves and the curves for soaked condition located well below that of unsoaked specimens. For unsoaked condition, vertical expansion (dilation) was observed at low normal stress and contractions or settlements at higher normal stress. Vertical settlements dominated for specimens in soaked condition at all normal stress levels.

### 2.12.9 Shear Strength Parameters

Kamruzzaman et al. (2004) reported the effect of cement content and curing age on effective shear strength parameters ( $c'$  and  $\phi'$ ) of cement treated clays as shown in Fig. 2.41. As can be seen, from Fig. 2.41 that at 7 days curing periods, both  $c'$  and  $\phi'$  increases with the increase of cement content but 28 days curing periods,  $c'$  increased and  $\phi'$  dropped. It was explained that the strength behaviour of the samples cured at lower time was mainly govern from the hydration reaction, hence  $c'$  and  $\phi'$  increases almost linearly with the increase of cement content. On the other hand, at higher curing periods, the strength behaviour mostly depends upon the pozzolanic reaction than the hydration reaction. Thus, the strength parameter  $c'$  increases significantly with the increase of cement content, while  $\phi'$  almost stabilizes at higher cement content, Shibuya and Ozawa (1992) reported similar results.

### 2.12.10 Failure Strain Characteristics

Kamaluddin (1995) introduced from unconfined compression test that the relationship ( $\epsilon_f - q_u$ ) is an arithmetic plot as shown in Fig. 2.42. Such a figure is wrathful to delineate the ductile and brittle behaviour of the samples. The relationship has produced a definite trend of reduction failure strain with incremental values of cement content and curing time. Ductile behaviour is associated with low strength and higher failure strain. The brittle characteristics was seen at higher values of  $q_u$ , where samples cluster along the best fit line and Kamaluddin (1995) expressed the value of  $\epsilon_f$  by the following equation:

$$\epsilon_f = 3.3 - 19.0 \times q_u / 10^4 \quad (2.21)$$

### 2.12.11 Strength Development Index

Rajbongshi (1997) and Hasan (2002) investigated the rate of strength gain with curing time in terms of the parameter termed as strength development index (SDI) for lime and cement treated clays respectively as proposed by Kamaluddin (1995). SDI is defined by the following expression (Kamaluddin, 1995):

$$SDI = \frac{\text{Strength of treated soil} - \text{Strength of untreated soil}}{\text{Strength of untreated soil}} \quad (2.22)$$

Plotting of SDI with curing age of samples of lime-treated clays of Bangladesh is shown in Fig. 2.43. It can be seen from Fig. 2.43 show that the values of SDI increases with increasing curing time and admixture content as well. Fig. 2.44 also the relative degree of strength gain resulted

due to increasing cement content and curing age. As can be seen from Fig. 2.44 that the strength gain for samples treated with 7% lime are relatively much higher than those of samples treated with 3% and 5% lime.

#### 2.12.12 Normalized Strength

Kamaluddin (1995) explained from unconfined compression test the strength normalization for Bangkok clay as shown in Fig. 2.45, where the different strengths were normalized by the unconfined compressive strength at 24 weeks,  $q_{u(T24)}$  that has been found to produce the most stable and ultimate value of  $q_u$  that a sample can experience in the course of various curing time. Kamaluddin (1995) proposed that the parameter, cement content was independent variable in a manner that it produces similar effects for samples with different ratio. It was explained that the methodology produces an overall narrow band with more close values ranging from low and high levels of curing time. Two polynomial equations of third order were found that bound the narrow band.

#### 2.12.13 Flexural Strength

The flexural strength of lime and cement treated regional soils in Bangladesh were investigated by Rajbongshi (1997), Hasan (2002), and Siddique and Rajbongshi (2002). It has been found that compared with the untreated sample, flexural strength of the cement treated samples cured at 7 and 28 days increased significantly. The effect of cement content on flexural strength is shown in Fig. 2.46. The figure shows that flexural strength increases with increasing cement content. It is evident from the figure that curing time has got insignificant effect on increase in flexural strength.

#### 2.12.14 Stiffness Characteristics

Brandl (1981) reported that the relative improvement of deformation resistance after adding lime is much more significant than the increase in strength, with common increase of modulus from 20 to 40 times. Balasubramaniam et al. (1999) observed that the initial tangent moduli of treated soil increase with increase in confining pressure and curing time. Kamaluddin (1995) reported the relationship between initial tangent modulus, ( $E_i$ ) and  $q_u$  for cement treated Bangkok clay (where test model samples are prepared with compaction) as shown in Fig. 2.47. Kamaluddin (1995) found that higher strength corresponds to high values of modulus. It has been shown that data points of these relations lie closely on a straight narrow band in such a way that the relationship between  $E_i$  and  $q_u$  can be approximated to linearity. Kamaluddin (1995) proposed that the relation for  $E_i$  and  $E_{50}$  (secant stiffness) with  $q_u$  by the equation 2.23 and 2.24 respectively as follows:

$$E_i = 6.2 \times (q_u^{1.5}) / 10^3 \quad (2.23)$$

$$E_{50} = 5.8 \times (q_u^{1.5}) / 10^3 \quad (2.24)$$

The flexural modulus of untreated and treated samples of Bangladesh were investigated by Rajbongshi (1997), Hasan (2002) and Siddique and Rajbongshi (2002) for lime and cement treated clays. It has been found that compared with the untreated sample, flexural modulus of cement treated samples cured at 7 and 28 days are increased significantly as shown in Fig. 2.48. The figure shows that flexural modulus increases with increasing cement content. It is evident from the figure that curing time has got insignificant effect on increase in flexural modulus.

### 2.12.15 Interrelationship among Strength, Curing Time and wc/c Ratio

The interrelationship was developed by Horpibulsuk et al. (2000) based on the unconfined compression test result of Ariake clay(3) and Island clays in Japan, where the test model samples are prepared without compaction blows for deep mixing. The relations referred to the clay water content/cement ratio's concept was proposed by Horpibulsuk et al. (2000) as follows:

"..... for given clay-cement mixtures, the strength at any curing time depends on one factor clay-water/cement ratio, wc/c". The observed relationship between unconfined compressive strength after a certain period of curing was expressed by a formula having the following equation:

$$\left( \frac{q_{(wc/c)1}}{q_{(wc/c)2}} \right) = 1.24^{\{(wc/c)_2 - (wc/c)_1\}} \quad (2.25)$$

where  $q_{(wc/c)1}$  is the strength to be estimated at clay-water/cement ratio of  $(wc/c)_1$  and  $q_{(wc/c)2}$  is the strength value at clay-water/cement ratio of  $(wc/c)_2$ .

Again, they suggested that the wc/c does not play any significant role on the strength development with time from Figures 2.49 through 2.50. As a result, the strength normalization of the cement admixed clay by 28 day-strength was performed by them in terms of curing time only.

$$\frac{q_D}{q_{28}} = [0.116 + 0.247] \ln D \quad (2.26)$$

where  $q_D$  is the strength after D days,  $q_{28}$  is the 28 day-strength as the reference value.

The normalization was made so as to account for the effect of clay-type, clay-water and cement contents. Finally, Horpibulsuk et al. (2000) developed that the interrelationship among strength, curing time and wc/c for predicting strength development of cement admixed clays was expressed by combination of equations (2.25) and (2.26) as follows:

$$\left( \frac{q_{(wc/c)1.D}}{q_{(wc/c)28}} \right) = 1.24^{\{(wc/c)_28 - (wc/c)_1.D\}} (0.116 + 0.247 \ln D) \quad (2.27)$$

where  $q_{(wc/c)_t,D}$  is the strength of cement admixed clay to be estimated at clay-water /cement ratio of  $(wc/c)_t$  after  $D$  days of curing and  $q_{(wc/c),28}$  is the strength of cement admixed clay at clay-water/cement ratio of  $(wc/c)$  after 28 days of curing.

#### 2.12.16 Direct Shear and Unconfined Compression Tests Results Relationship

Porbaha et al. (2000) reported that the relationship between the DS and UC results for marine clay treated with 10-20<sup>0</sup>/<sub>0</sub> cement and cured for 28 days as shown in Fig.2.51. They found that for low-strength cement treated clay, the shear strength can be roughly represented by half of the unconfined compressive strength. However, when the cement content is increased, the shear strength may reach only about one-third of the unconfined compressive strength. Broms (1986) reported for lime treated clay that the shear strength determined by fall cone / laboratory vane test was about 2 to 3 times higher than unconfined compressive strength. From the regression analysis, the following relationship was proposed by Porbaha et al. (2000):

$$\tau_{10} = 0.53 + 0.37q_u - 0.0014q_u^2 \quad (2.28)$$

where  $\tau_{10}$  is the shear strength ( $\text{kg/cm}^2$ ) from a direct shear (DS) test without normal stress and  $q_u$  is the unconfined compressive strength ( $\text{kg/cm}^2$ ) from a unconfined compression (UC) test for specimens cured for 28 days.

#### 2.13 Critical State Models for Prediction of Soil Behaviour

Atkinson and Bransby (1978) stated that generally the critical state is the condition in which the clay continues to deform at constant volume under constant effective stress. The critical state concept represents idealized behaviour clays, but it is assumed to apply also to undisturbed clays in triaxial compression test. The critical state soil parameters were studied by a number of investigators (Hvorslev, 1949; Schofield and Wroth, 1968; Allman and Atkinson, 1992; Bashar, 2002; Siddique et al. 2003; Khaliullah, 2007; Siddique et al., 2007; Islam et al. 2007).

The single and unique line of failure points of both drained and undrained tests are defined as the critical state line. Figure 2.52 shows a schematic representation of the behaviour of a soil as a function of the shear stress  $q$ , normal stress,  $p$  and void ratio,  $e$ . The material can sustain and pass through any state ( $p$ - $q$ - $e$ ) below the surface formed by two surfaces that intersect at the critical state. The surfaces ABCD is referred to as the state boundary surfaces of Roscoe surfaces and B' B' C' C is referred to as the Hvorslev surface. States of wet, normally consolidated soil lie below the state boundary surface. on the hand, dry and over consolidated soil exhibit behaviour on the right side of the CSL, A' B' C' D' is indicated as the Tension failure zone. Before the material reaches the critical state, it passes through successive state of yielding; during this yielding, the material hardens. This continuous yielding state can lead to

the critical state of ultimate yield state, at which the material flows without changes in volume and in shear stress.

Atkinson and Bransby (1978) reported that the critical state model in its original form is described by reference to a three dimensional space as shown in Fig. 2.52, whose three axes define the magnitudes of the variables  $p'$ ,  $q'$  and  $v$ , where

$$p' = \sigma'_{oct} = \frac{\sigma'_1 + \sigma'_2 + \sigma'_3}{3} \quad (2.29a)$$

$$q' = \frac{3}{\sqrt{2}} \tau_{oct} \quad (2.29b)$$

$$\tau_{oct} = \frac{1}{3} \sqrt{(\sigma'_1 - \sigma'_2)^2 + (\sigma'_2 - \sigma'_3)^2 + (\sigma'_1 - \sigma'_3)^2} \quad (2.30a)$$

$$v = 1 + e \quad (2.30b)$$

The specific volume ( $v$ ) is the total volume of soil containing unit volume of solid particles. In case of triaxial compression test in hydrostatic state, then the stress parameters are defined as

$$p' = (\sigma'_1 + 2\sigma'_3)/3 \quad (2.31a)$$

$$q' = \sigma'_1 - \sigma'_3 \quad (2.31b)$$

in which  $\sigma'_1$ ,  $\sigma'_2$  and  $\sigma'_3$  are the principal effective compressive stresses,  $p'$  and  $q'$  are referred to as the mean normal stress and deviator stress respectively. The slope of CSL,  $q'/p'$  is denoted by  $M$ . The stress parameter,  $p_e$ , is called the mean equivalent pressure and defined as

$$p_e = p'_o \exp [(e_o - e)/\lambda] \quad (2.31c)$$

in which  $p'_o$  and  $e_o$  correspond to the pre-shear consolidation pressure and void ratio on the isotropic consolidation line; and  $\lambda$  is the slope of the isotropic consolidation line in the  $(e, \ln p')$  plot. During untrained tests, there is no change in voids ratio and, therefore,  $p_e$  remains constant during shear at a value of  $p'_o$ . However, during a drained test in which the voids ratio,  $e$ , decreases, the mean equivalent pressure,  $p_e$ , increases from its initial value of  $p'_o$ .

Atkinson and Bransby (1978) also reported that for one-dimensional consolidation, there is a nearly linear relationship between specific volume ( $v$ ) and the logarithm of mean effective stress. This relationship may be expressed as

$$v = N - \lambda \log_e p' \quad (2.31d)$$

Where  $N$  (capital nu) is defined as the specific volume corresponding to  $p' = 1.0 \text{ kN/m}^2$ . Then,

$$p' = \exp [(N - v)/\lambda] \quad (2.31e)$$

Since the curves for one dimensional and spherical are nearly parallel,

$$C_c = 2.303 \lambda \quad (2.31f)$$

For over-consolidated soil, relationship between specific volume ( $v$ ) and the logarithm of mean effective stress can be expressed as follows:

$$v = v_k - \kappa \log_e p' \quad (2.31g)$$

Where  $v_k$  is defined as the value of  $v$  of an over-consolidated soil corresponding to on swelling line.

Since, however, the slopes of the lines for one dimensional and spherical consolidation are not exactly the same,  $C_s$  is only approximately equal to  $2.303\kappa$ .

$$C_s = 2.303 \kappa \quad (2.31h)$$

The equivalent consolidation pressure,  $p_e$  as the value of  $p_o'$  on the normal consolidation line corresponding to any value of  $c$ . Then for any value of  $v$ ,

$$v = N - \lambda \log_e p_e' \quad (2.31i)$$

$$\text{So that, } p_e' = \exp [(N - v)/\lambda] \quad (2.31j)$$

For over-consolidated soils, where  $p' < p_e'$ , the over-consolidation ratio (for spherical consolidation) will be defined as

$$\text{OCR} = p_o'/p' \quad (2.31k)$$

Siddique et al. (2003) proposed a number of constitutive models showing the correlations of above critical parameters with plasticity index (PI) of three coastal soils in Bangladesh as follows:

$$\lambda = 0.094 + 0.0021 \text{ PI}, (R^2 = 1.0) \quad (2.32a)$$

$$\kappa = 0.0076 + 0.0011 \text{ PI}, (R^2 = 0.97) \quad (2.32b)$$

$$N = 2.128 + 0.0158 \text{ PI}, (R^2 = 0.99) \quad (2.32c)$$

$$M = 1.37(1 - 0.0022 \text{ PI}) \text{ PI}, (R^2 = 1.0) \quad (2.32d)$$

$$H = 1.219(1 - 0.0068 \text{ PI}), (R^2 = 1.0) \quad (2.32e)$$

Typical values of the constants  $M$ ,  $N$ ,  $\lambda$  and  $\kappa$  for some clays are in Table 2.7 for regional clay in Bangladesh.

### 2.13.1 State Boundary Surface

The State Boundary Surface (SBS) has been defined as a unique surface as shown in Figs. 2.53, which separates the states of an element of the soil from those that are not admissible as

reported, by Atkinson and Bransby (1978). This surface is formed by two distinct surfaces, namely the Roscoe surface, on which volumetric yielding takes place, and the Hvorslev failure surface. Roscoe surface has been defined by undrained stress paths of normally consolidated clay while the Hvorslev surface is the locus of failure points for heavily over-consolidated samples.

When a state of sample reaches the Critical State, it experiences unlimited distortion while the effective stress and the volume of the soil remains unchanged. The area between the Critical State Line (CSL) and the Normal Consolidation Line (NCL) in the water content-log mean normal stress plot is called 'wet of critical' while the area to the left of the Critical State Line is called 'dry of critical'. The soil when sheared in the 'wet' zone would generate a positive pore pressure response under undrained condition or decrease in volume under drained conditions. On the other hand, a soil in the 'dry' zone would show an increase in volume under drained conditions or tend to develop a negative pore pressure. In its simplified form, the SBS is accepted to be symmetrical about the hydrostatic p-axis provided there is no substantial time effects and anisotropy either from the depositional mode or from the applied stress conditions. Much of the challenge and arguments on SBS and the Critical State Concept seem to be on these aspects, but nevertheless their effects can be incorporated in a primary SBS with appropriate deviations as per the perturbations. Atkinson and Bransby (1978) defined that the State Boundary Surface (SBS) parameters for triaxial compression (isotropic) were expressed as follows:

$$(a) \text{ Critical State Line (CSL): } q' = Mp' \text{ and } M = \frac{6 \sin \phi'_c}{3 - \sin \phi'_c} \quad (2.33a)$$

$$(b) \text{ Normal Consolidation Line (NCL): } v = N - \lambda \ln p' \quad (2.33b)$$

$$(c) \text{ Elastic Walls: } v = v_k - \kappa \ln p' \quad (2.33c)$$

$$(d) \text{ Roscoe Surface: } \frac{q'}{Mp'} + \left( \frac{\lambda}{\lambda - \kappa} \right) \ln p' - \left( \frac{N - v}{\lambda - \kappa} \right) = 1 \quad (2.33d)$$

$$(e) \text{ Hvorslev Surface: } \frac{q}{Hp} - \left( \frac{M - H}{Hp} \right) \exp \left( \frac{N - v}{\lambda} \right) = 1 \quad (2.33e)$$

$$(f) \text{ Tension Cutoff: } q' = 3p' \quad (2.33f)$$

For one dimensional compression:

$$(a) \text{ Normal Consolidation Line (NCL): } v = N_0 - \lambda \ln p' \quad (2.34a)$$

$$(b) \text{ Elastic Walls (or over-consolidated clay): } v = v_{k0} - \kappa \ln p' \quad (2.34b)$$

Siddique et al. (2003) established the complete state boundary surface (Roscoe surface and Hvorslev surface) of three coastal soils in Bangladesh from undrained stress paths of normally



consolidated and overconsolidated samples of the soils and it has been found that these surfaces vary with the type of soil. Fig. 2.54 shows the complete state boundary surface for one of the coastal soils.

### 2.13.2 Cam Clay Model

Atkinson and Bransby, (1978) explained that stress-strain models to describe the soil behaviour are developed based on several assumptions and hypothesis in conjunction with well-known concepts of plasticity theory. These theories assume that the soil is isotropic, follow the Critical State Concept, and that there is no recoverable axial strain. The state of the sample inside the State Boundary Surface must remain on the elastic wall which is a vertical plane above an isotropic swelling line. The plastic deformation is assumed to occur only when the state of the sample changes on the State Boundary Surface. These theories appeal to only a few well-known soil parameters instead of depending on a large number of empirical constants.

The Cam Clay model was developed for normally consolidated and lightly over consolidated clay. The author assumed that the energy dissipated at any infinitesimal increment of plastic work is only a function of the plastic axial strain. The proposed expression for energy dissipation with an assumption that the principal axes of stress and plastic strain increment coincide, is,

$$dW = pd\varepsilon_{vp} + qd\varepsilon_{sp} \quad (2.35a)$$

where,  $dW$  : energy dissipated per unit volume of soil

$p, q$  : mean effective principal stress, deviator stress

$d\varepsilon_{vp}, d\varepsilon_{sp}$  : increments of plastic strains

Equation (2.35a) can be expressed as,

$$dW = pd\varepsilon_{vp} + qd\varepsilon_{sp} = M pd\varepsilon_{sp} \quad (2.35b)$$

where  $M$  is the slope of the Critical State Line in  $(q', p')$  plot. Eqn. (2.35b) leads to the following flow rule,

$$\left( \frac{pd\varepsilon_{vp}}{pd\varepsilon_{sp}} \right) = M - \eta \quad (2.35c)$$

where  $\eta$  is the stress ratio,  $q'/p'$ . The normality rule is applied such that the equation of the yield locus is,

$$q' = Mp' \ln \left( \frac{p_0}{p'} \right) \quad (2.35d)$$

where  $p_0$  is the preconsolidation stress. In this theory, the shear and volumetric strain increments for states on the State Boundary Surface are given as,

$$d\varepsilon_s = \left( \frac{\lambda - \kappa}{\nu} \right) \left( \frac{1}{M - \eta} \right) \left[ \frac{d\eta}{M} + \frac{dp'}{p'} \right] = d\varepsilon_s^p, \quad \text{As } [d\varepsilon_s^e \rightarrow 0] \quad (2.35e)$$

$$d\varepsilon_v = \frac{1}{\nu} \left[ \frac{(\lambda - \kappa)d\eta}{M} + \lambda \frac{dp'}{p'} \right] \quad (2.35f)$$

The State Boundary Surface can be derived as,

$$\eta = \frac{\lambda M}{(\lambda - \kappa)} \ln \left( \frac{p_0}{p'} \right) \quad (2.35g)$$

The volumetric yield loci as described by Eqn. (2.35d) is bullet shaped at the p-axis and seems to be more applicable for volumetric yielding inside the SBS when the associated plastic volumetric strain is smaller than the value when the state paths lie on the SBS as shown in Fig. 2.53.

In an attempt to improve the limitations of the Cam Clay model, Burland (1965) proposed that a modified equation which considers the work dissipated in plastic volume change. The energy dissipated in the Modified Cam Clay (MCC) Model is given by,

$$dW = p[(d\varepsilon_{vp})^2 + (Md\varepsilon_{sp})^2]^{1/2} \quad (2.36)$$

The flow rule and yield locus are given by the following equations (2.37) and (2.38),

respectively:

$$\frac{d\varepsilon_{sp}}{d\varepsilon_{vp}} = \frac{M^2 - \eta^2}{2\eta} \quad (2.37)$$

$$p' = \frac{p_0 M^2}{M^2 + \eta^2} \quad (2.38)$$

Hence, the shape of the volumetric yield locus was changed from the earlier log spiral to an elliptic form. The incremental shear and volumetric strains (plastic potential function) are as follows:

$$d\varepsilon_s = \left( \frac{\lambda - \kappa}{\nu} \right) \left( \frac{2\eta}{M^2 - \eta^2} \right) \left[ \frac{2\eta d\eta}{M^2 + \eta^2} + \frac{dp'}{p'} \right] \quad (2.39a)$$

$$d\varepsilon_v = \frac{1}{\nu} \left[ \frac{2\eta(\lambda - \kappa)d\eta}{M^2 + \eta^2} + \lambda \frac{dp'}{p'} \right] \quad (2.39b)$$

The State Boundary Surface described in this theory is,

$$\frac{p_0}{p'} = \left( \frac{M^2 + \eta^2}{M^2} \right)^{\left(1 - \frac{\lambda}{\lambda'}\right)} \quad (2.40)$$

Thus 'Cam Clay (CC) Model' is developed to 'Modified Cam Clay (MCC) Model', 'Modified Modified Cam Clay (MMCC) Model' and 'Extended Modified Modified Cam Clay (EMMCC) Model'.

### 2.13.3 Modified Cam Clay (MCC) Model

Atkinson and Bransby (1978) defined that the model originally devised in Cambridge and termed as the "Modified Cam Clay Model", is generally used to simulate the stress-strain response for clays. The Modified Cam Clay (MCC) Model is a critical state model incorporating volumetric strain hardening assumptions in Cam Clay (CC) Model. The model has been generally observed to predict, with reasonable accuracy, the stress-strain response of cement treated and untreated clays. Finally, conclusions were drawn regarding the capabilities of the MCC model to predict the undrained and drained response of cement treated and untreated clays at various preconsolidation effective cell pressures. The significant aspects of the MCC model are described below:

#### 2.13.3.1 The Critical State

The MCC model is based on the critical state concept. The critical state is defined to be that condition of the soil at which the soil shears continuously at constant stress and at constant volume. Such a condition is observed at failure of the soil at its ultimate state. Atkinson and Bransby (1978) stated that the critical state occurs at a certain ratio of the mean effective stress  $p'$  and the shear or deviator stress  $q$ . The critical states may be defined by a straight line in  $(p' - q)$  space. This straight line is termed as the critical state line. The slope of this line is termed as the critical state ratio generally identified by the parameter  $M$ . The mean effective pressure  $p'$  and the deviator or shear stress  $q$  at the octahedral plane is given in terms of the effective principal stresses  $\sigma'_1, \sigma'_2, \sigma'_3$  as below:

$$p' = (\sigma'_1 + \sigma'_2 + \sigma'_3) / 3 \quad (2.41)$$

$$q = \sqrt{\frac{(\sigma'_1 - \sigma'_2)^2 + (\sigma'_2 - \sigma'_3)^2 + (\sigma'_1 - \sigma'_3)^2}{2}} \quad (2.42)$$

$$M = \frac{q'}{p'} \quad (2.43)$$

In the above equations  $\sigma'_1$  is the major principal effective stress and  $\sigma'_2, \sigma'_3$  are minor principal effective stresses.  $M$  is the critical stress ratio.  $p'_f$  and  $q'_f$  are respectively the mean effective stress and deviator stress at the ultimate or failure state. The ultimate stress state is the condition, at which soil shears at constant stress and constant excess pore pressure (undrained case) or constant volume strain (drained case). The locus of ultimate stress states is generally a straight line passing through the origin in  $(p', q)$  space. This line is termed as the critical state line. The critical state parameter  $M$  was then indirectly determined from the drained friction angle using the following relation:

$$M = \frac{6 \sin \varphi}{3 - \sin \varphi} \quad (2.44)$$

### 2.13.3.2 Yield Function

Atkinson and Bransby (1978) found that the combination of mean and effective stresses  $(p', q)$  at which the soil starts to have irrecoverable or plastic deformations may be represented by a convex function in  $(p' - q)$  space. This function may be represented as follows:

$$f(p', q, p'_o) = 0 \quad (2.45)$$

Equation (2.45) is called the yield function, where  $p'_o$  is the preconsolidation effective cell pressure of the soil. In the Modified Cam Clay model, preconsolidation effective cell pressure  $p'_o$  is the soil parameter which determines the size of the yield locus in the effective stress space. Once the stress state touches the yield locus, the stress-strain response becomes elasto-plastic.  $p'_o$  is also termed as the hardening parameter in elasto-plasticity. For stress states within the yield function, the stress-strain response of the soil is assumed to be elastic.

### 2.13.3.3 Strain Hardening

At stress states on the yield function, an increment of stress applied outside of the yield function, results in incremental plastic strains. At the same time the value of the hardening parameter  $p'_o$  increases. Consequently the yield function expands and the current stress state lies on the new expanded yield surface. The elastic region is permanently expanded. This is observed as an apparent hardening effect if the soil is unloaded and then reloaded. The hardening parameter  $p'_o$  is related to the plastic volumetric deformation of the soil. This may be derived from the  $e - \log p'$  or void ratio by log of mean effective stress relation of a soil. It is given as follows:

$$\frac{dp'_o}{d\varepsilon_v^p} = \frac{p'_o(1+e)}{(\lambda - \kappa)} \quad (2.46)$$

In equation (2.46),  $p'_o$  is the preconsolidation effective cell pressure,  $dp'_o$  is the increment of this pressure,  $e$  is the void ratio, and  $\lambda$  and  $\kappa$  are respectively the slope of the normal consolidation line and elastic rebound line of the  $e - \log p'$  line.

#### 2.13.3.4 Plastic Potential Function

Atkinson and Bransby (1978) defined that at the yield or plastic condition, the Modified Cam Clay model assumes the ratio of incremental plastic volumetric strains to incremental plastic deviator or axial strains to be related to the stress ratio  $\eta$  as follows:

$$\frac{d\varepsilon_q^p}{d\varepsilon_v^p} = \frac{M^2 - \eta^2}{2n} \quad (2.47)$$

where  $\eta = \frac{q}{p'}$

In equation (6.20),  $M$  is the critical stress ratio. At stress ratios  $\eta > M$ , the soils undergo expansive volume strain and soften. At stress ratios  $\eta < M$ , the soil goes compressive plastic volume strain and hardens. At the critical state ratio  $M$ , the incremental plastic volumetric strain is zero and the soil becomes perfectly plastic.

Assuming associated flow rule and integrating equation (2.47), the yield and the plastic potential function for the Modified Cam Clay model may be obtained as below:

$$\left( \frac{q}{Mp'} \right)^2 = \frac{p'}{p'_o} - 1 \quad (2.48)$$

#### 2.13.3.5 Elastic Behaviour

The MCC model assumes elastic stress-strain response for stress states within the yield locus. The MCC model defines a pressure dependent non-linear stress-strain response defined by the elastic bulk modulus and elastic shear modulus. The elastic bulk modulus of the MCC model is given as below:

$$\frac{dp'}{d\varepsilon_v^e} = \frac{p'(1+e)}{\kappa} \quad (2.49)$$

Generally, a constant value of the Poisson's ratio  $\mu$  is assumed in the MCC model. The elastic shear modulus  $G$  is then obtained as below:

$$G = \frac{K}{3(1+2\mu)} \quad (2.50)$$

From the theory of elasticity it can be shown that a value of elastic Poisson's ratio,  $\mu$  0.40 to 0.50 implies volume incompressibility. This is the basic assumption for undrained condition. In this research, an elastic Poisson's ratio,  $\mu$  0.41 to 0.49 was assumed for numerical stability for undrained triaxial tests. For clays, the value of the drained elastic Poisson's ratio,  $\mu$  is generally assumed to be between 0.2 to 0.3. In this study, an elastic Poisson's ratio,  $\mu$  0.21 to 0.29 was assumed for numerical stability for drained triaxial tests.

The MCC model is a mathematical model giving the response of clays to applied loads. In the undrained analysis, the bulk modulus of pore water pressure is generally given a very high value compared to the bulk modulus of soil particles and in this case, it is considered 1 to 50. As a result an incompressibility condition is simulated. On the other hand, in drained conditions, the bulk modulus of pore water pressure is set equal to zero. Volume change of the soil skeleton is then predicted. No excess pore water pressures are predicted under these circumstances. Islam et al. (2007) and Khalilulah (2007) verified the applicability of the MCC model for reconstituted cemented Savar clays, while Siddique et al. (2007), Siddique (2006), Siddique et al. (2003) and Bashar (2002) verified the applicability of the MCC model for reconstituted uncemented coastal clays in Bangladesh.

#### 2.13.4 Modified Modified Cam Clay (MMCC) model

Using the finite element programme AFENA, Carter and Balaam (1995) developed the MCC model in which incorporated tensile strength parameter as a model parameter, is discussed here as the Modified Modified Cam Clay (MMCC) model for cemented clays. The various aspects of the MMCC model are discussed as given below.

##### 2.13.4.1 The MMCC Yield Locus and Plastic Flow Rule

Cement treatment of clays gives it the ability to resist tensile forces. This is termed as tensile or cementation strength. The tensile strength is explicitly incorporated in the MMCC yield locus as follows:

$$\left\{ \frac{q}{M(p' + p'_t)} \right\}^2 = \frac{p'_o + p'_t}{p' + p'_t} - 1 \quad (2.51)$$

Where

$$M = \frac{q}{p' + p'_t} \quad (2.52)$$

In the above equations, mean effective pressure  $p'$  and the deviator or shear stress  $q$  as above equations (2.41) and (2.42) respectively,  $p'_t$  is the tensile strength and  $p'_o$  is the preconsolidation effective cell pressure of the soil.

The MMCC model is assumed to obey the associated flow rule. Thus the MMCC model plastic potential function is identical to its yield locus equation given by equation (2.51). The plastic flow rule of the MMCC model is identical to that of the plastic flow rule of the MCC model and is given as below:

$$\frac{d\varepsilon_v^p}{d\varepsilon_q^p} = \frac{M^2 - \eta^2}{2\eta} \quad (2.53)$$

However, the  $\eta$  term in the above equation is defined in the MMCC model as follows:

$$\eta = \frac{q}{p' + p'_i} \quad (2.54)$$

#### 2.13.4.2 Tensile Strength and Unconfined Compression Strength

When tensile strength is explicitly incorporated in the MCC model, it is termed as the MMCC model. Islam et al. (2007) and Khalilullah (2007) verified the applicability of the MMCC model for reconstituted cemented Savar clays in Bangladesh. The tensile strength of clay may be obtained from its unconfined compression strength by following procedure.

The undrained shear strength of the soil at zero cell pressure or zero mean effective pressure may be termed as the unconfined compression strength of the soil. Thus substituting  $p' = 0$  and  $q = q_u$  in equation (2.51), the MMCC yield equation may be rewritten as below:

$$\left\{ \frac{q_u}{M(0 + p'_i)} \right\}^2 = \frac{p'_o + p'_i}{0 + p'_i} - 1 \quad (2.55)$$

From equation (2.55) the relationship between tensile strength and unconfined compression strength may be obtained as below:

$$\frac{q_u^2}{M^2 p_i'^2} = \frac{p_o'}{p_i'} \quad (2.56)$$

$$p_i' = \frac{q_u^2}{M^2 p_o'} \quad (2.57)$$

Equation (2.56) relates the tensile strength  $p_i'$  cemented clay with its unconfined compression strength  $q_u$ ,  $M$  and  $p_o'$  are the critical state ratio and preconsolidation effective cell pressure of the cemented soil, which were proposed by Carter and Balaam (1995).

### 2.13.5 Extended Modified Modified Cam Clay (EMMCC) Model

As a result of cementation of clays, both the consolidation and tensile strength of the clay increases. Both these components of cementation components may be distinctly incorporated in the MCC model, along with separate breakdown effects for each of these components. Only tensile strength component of cementation was incorporated in the MCC model. This was termed as the MMCC model. The resulting model is termed here as the EMMCC model with incorporating cementation breakdown parameters in MMCC model, which was developed and established for cemented clays by Carter and Balaam (1995) using the finite element programme AFENA. The aspects of the EMMCC model are discussed as below.

#### 2.13.5.1 Tensile Strength Breakdown Parameter

It is assumed in the EMMCC model that the tensile strength degrades with the accumulation of the absolute value of plastic volumetric strain. The equation used to simulate the breakdown of tensile strength with plastic volumetric strain is given as below:

$$p'_t = p'_{m0} \exp[-\rho_t (\varepsilon^d)] \quad (2.58)$$

$$\text{Where } \varepsilon^d = \int |d\varepsilon_v^p| \quad (2.59)$$

In the above equation,  $\rho_t$  is the degradation parameter for tensile strength,  $p'_{m0}$  is the tensile strength of reconstituted cemented Bangladesh clays. Generally a large positive number greater than 1.0 is used to effectively simulate a realistic cementation breakdown effect. Zero value is assumed for  $\rho_t$  in the case of no break down assumption.

#### 2.13.5.2 Consolidation Strength Breakdown Parameter

It is assumed in the EMMCC model that the increment of consolidation strength as a result of cementation degrades with the accumulation of the absolute value of plastic volumetric strain. The equation that is used to simulate the breakdown of increment of consolidation strength (as a result of cementation) with volumetric strain is as given below:

$$p_m = p_{m0} \exp[-\rho_m (\varepsilon^d)^3] \quad (2.60)$$

$$\text{Where, } \varepsilon^d = \int |d\varepsilon_v^p| \quad (2.61)$$

In the above equation,  $\rho_m$  is the degradation parameter for the increment of consolidation strength  $p_{m0}$  of reconstituted cemented clays. As discussed before, generally a large positive number greater than 1.0 is used for  $\rho_m$  to realistically simulate the breakdown effects. Zero value is assumed for  $\rho_m$  for no break down assumption. It is to be noted that in the numerical



predictions presented in this chapter using the EMMCC model. Carter and Balaam (1995) was proposed that there is no breakdown of the increment of consolidation strength component occurring as a result of cementation. Islam et al. (2007) and Khalilulah (2007) also verified the applicability of the EMMCC model for reconstituted cemented Savar clays of Bangladesh.

### 2.13.5.3 Yield Locus and Flow Rule

The yield locus of the EMMCC model is given as follows:

$$\left\{ \frac{q}{M(p' + p'_i)} \right\}^2 = \frac{p'_o + p'_i + p'_m}{p' + p'_i} - 1 \quad (2.62)$$

$$\text{Where } M = \frac{q}{p' + p'_i} \quad (2.63)$$

In the above equations, mean effective pressure  $p'$  and the deviator or shear stress  $q$  as the equations (2.41) and (2.42) respectively,  $p'_i$  is the tensile strength due to cementation or cohesion,  $p'_m$  is the increment of consolidation strength due to cementation and  $p'_o$  is the pre-consolidation pressure of the untreated clays without any cementation effects.

The EMMCC model is assumed to obey the associated flow rule. Thus the EMMCC model plastic potential function is identical to its yield locus equation. The plastic flow rule for the EMMCC model in its incremental form is identical to that of the plastic flow rule of MCC model as given below:

$$\frac{d\varepsilon_v^p}{d\varepsilon_q^p} = \frac{M^2 - \eta^2}{2\eta} \quad (2.64)$$

However, the  $\eta$  term in the above equation is defined in the EMMCC model as follows:

$$\eta = \frac{q}{p + p_i} \quad (2.65)$$

The remaining aspects of the EMMCC model are identical to the MCC and MMCC model, which are described previously.

### 2.13.6 Prediction and Comparison Results by Developed MCC Model

Siddique et al. (2007), Islam et al. (2007), Khalilulah (2007), Siddiquee (2006), Youwai and Bergado (2003), Siddique et al. (2003), Bashar (2002) and Desai and Siriwardane (1984) reported that the prediction using cam clay and cap models and the comparison with test data for untreated and treated clays. Youwai and Bergado (2003) compared the constitutive model prediction with the test results from drained test for stabilized soil as shown in Fig. 2.55. It

was found that the model simulations broadly matched the experimental results at different confining pressures and mix ratios. The effectiveness of the critical state framework in conjunction with state- dependent dilatancy can simulate the deformation and strength characteristics for stabilized soil. The constitutive model can better capture overall the dilatancy characteristics, including both negative and positive values.

Islam et al. (2007) compared the MCC (Modified Cam Clay) model and MMCC (Modified Modified Cam Clay) model predictions as shown in Fig. 2.56 from undrained test for cemented Savar clay of Bangladesh. It was observed that the predicted initial shear stiffness and initial pore pressure are higher for cemented soil using MMCC model compared to the prediction of the MCC model. The predicted deviator stress becomes constant with continuous shearing. This indicated that the critical state condition has been reached.

The EMMCC (Extended Modified Modified Cam Clay) model with different values for including the tensile strength breakdown parameter,  $RHO$  (values of 1, 10 and 100) was used to predict the stress-strain response for cemented Savar clays as shown in Fig. 2.57. Khalilullah (2007) found that a higher value of the cementation break down parameter ( $RHO$ ), predicted a relatively lower increase of deviator stress and volumetric strain with axial strain.

Siddique et al. (2007) reported that the predicted and observed behaviour regarding undrained stress-strain and pore pressure response of reconstituted coastal clays at different over consolidation ratio in triaxial shear by Modified Cam Clay model, which predicts non-linear strain hardening response before the ultimate stress state is reached as shown in Fig. 2.58. This happens as the Modified Cam Clay model simulates elastic behaviour prior to yielding in case of high OCR clays. Thus the Modified cam Clay model is a rational predictor of excess pore pressure response of coastal clays, at least qualitatively.

## 2.14 Cap Model

In developing models for various soils based on the critical state concept, the Cambridge group expressed the behaviour by using quantities relevant to the conventional (cylindrical) triaxial and conventional consolidation tests (Desai and Siriwardane, 1984). The using parameters were  $q = (\sigma_1' - \sigma_3')$  and  $p' = (\sigma_1' + 2\sigma_3')/3$  and the void ratio  $e$ . The cap models are also based on the concept of continuous yielding of soils but they are expressed in terms of three-dimensional state of stress and are formulated on the basis of consistent mechanics principles. The name cap models derives from the shape of the elliptical yield surfaces which look like "caps" as shown in Fig. 2.59.

There are certain other differences between the cap and Cam clay models. In the cap models, the portion of the cap above the fixed yield or failure surface (Fig 2.59) is omitted and only the surface marked ABC is considered. In the Cam clay models, the moving cap play the main

role in defining yielding, and the fixed yield surface is used essentially to define the critical state. On the other hand, in the cap model both fixed and moving surfaces are used to define the yielding process.

### 2.14.1 Fixed Yield Surface

The fixed yield surface (Fig 2.60), which can be considered to be an ultimate yield surface, is expressed as

$$f_1(J_1, \sqrt{J_{2D}}) = 0 \quad (2.66)$$

In the initial Cap model, the fixed surface was assumed to be composed of an initial portion of the Drucker-Prager envelope joined smoothly to the subsequent von Mises surface (Fig. 2.59). The logic for adopting the von Mises surface at higher stresses was based on the observation that at higher stresses the material behaves like a "liquid". This was adopted particularly to simulate behaviour of cohesionless materials subjected to high stresses caused by dynamic (blast) loads.

The expression for  $f_1$  in Eq. 2.66 adopted by DiMaggio and Sandler is given by

$$f_1 = \sqrt{J_{2D}} + Y e^{-\beta J_1} - \alpha = 0 \quad (2.67)$$

where  $\alpha$ ,  $\beta$  and  $Y$  are materials parameters.

### 2.14.2 Yield Caps

The yield surfaces (Fig 2.60) are expressed as

$$f_2(J_1, \sqrt{J_{2D}}, k_1) = 0 \quad (2.68)$$

where  $k_1$  defines the deformation history, and usually is taken as the volumetric plastic strain.  $\epsilon_v^p = \epsilon_{ij}^p = I_p / 3$ . Consequently, a yield surface represents the locus of the points with the same volumetric plastic strain. The fixed and moving yield surfaces are assumed to intersect such that the tangents to the yield surfaces at the intersection are parallel to the  $J_1$ -axis. As a result, with the associated plasticity, the increment of plastic strain vector is parallel to the  $\sqrt{J_{2D}}$ -axis implying no volume change once the fixed surface is reached. This is similar to the critical state concept in which the material does not change in volume at the critical state.

The yield surfaces intersect the  $J_1$ -axis at right angles, implying that under isotropic compression there are no shear deformations. This assumption removes the anomaly that can arise due to non-orthogonal yield surfaces to the  $J_1$ -axis.

The cap model has been applied successfully to simulate behaviour of various geological materials such as McCormick Ranch Sand and an artificial soil (Desai and Siriwardane,

1984). Subsequent developments have considered anisotropic and kinematic hardening in the study of the cap model. Dimaggio and Sandler (1984) adopted an elliptic cap for representing yield surfaces for the cohesionless material considered by them. Hence the expression for  $f_2$  in Equation 2.68 used was

$$f_2 = R^2 J_{2D} + (J_1 - C)^2 = R^2 b^2 \quad (2.69)$$

where  $Rb = (X - C)$  (Fig.2.60),  $R$  is the ratio of the major to minor axis of the ellipse,  $X$  the value of  $J_1$  at the intersection of the cap with the  $J_1$ -axis,  $C$  the value of  $J_1$  at the center of the ellipse and  $b$  the value of  $\sqrt{J_{2D}}$  when  $J_1 = C$ . The value of  $X$ , which is the hardening parameter similar to  $p_0$  in the Cam clay models, depends on the plastic volumetric strain  $\varepsilon_v^p$  and is expressed as

$$X = -\frac{1}{D} \ln \left( 1 - \frac{\varepsilon_v^p}{W} \right) + Z \quad (2.70)$$

where  $D$ ,  $Z$ , and  $W$  are materials parameters to be determined. On the basis of the above variables, Cap Model has been developed by Chen and Mizuno (1990). A flow chart for the implementation of Coulomb and Prager Models in Cap Model is shown in Fig. 2.61.

### 2.14.3 Prediction and Comparison of Results by Cap Model

Desai and Siriwardane (1984) reported the behaviour regarding drained stress-strain and volumetric strain response of clays in triaxial shear by Cap model, which predicts non-linear strain hardening response before the ultimate stress state is reached as shown in Fig. 2.62. It can be seen that the predicted and observed results for the drained test are satisfactory.

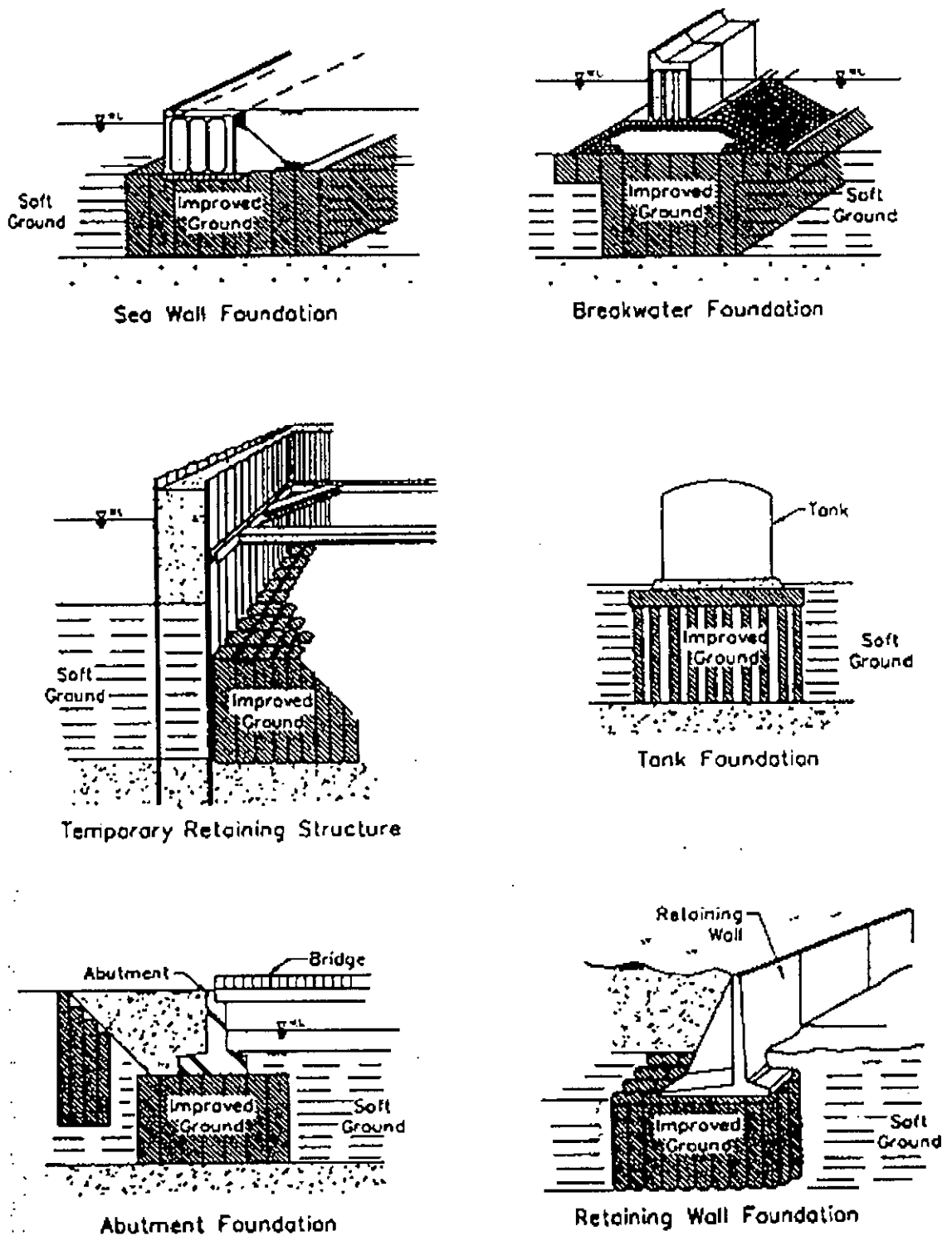
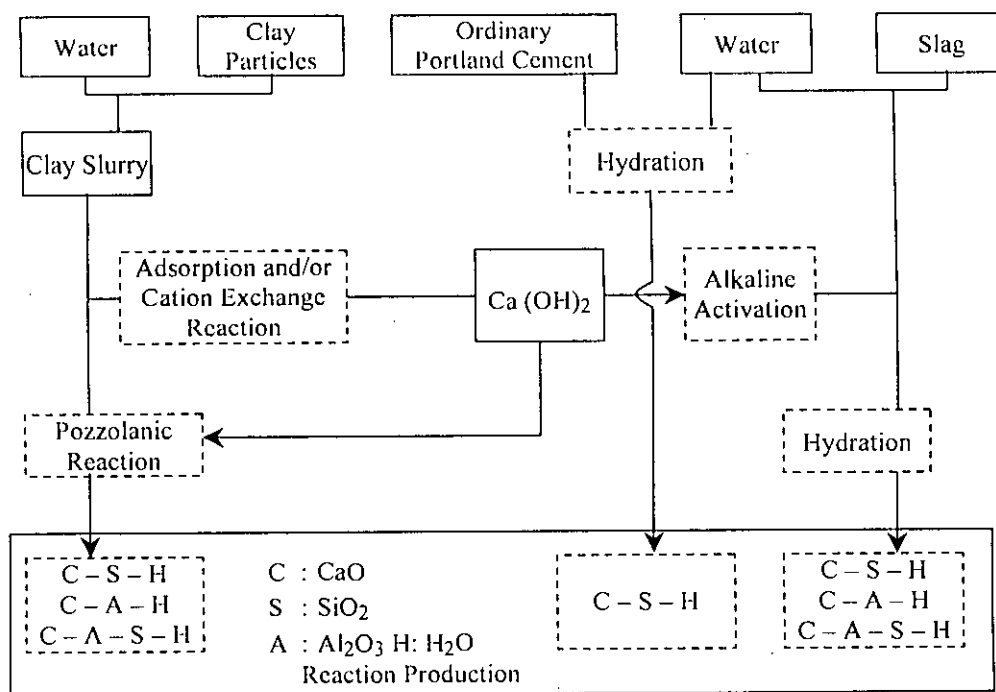


Fig. 2.1 Deep mixing for ground stabilization (after CDM 1994)

**Table 2.1 Test Results for Soil Deep Mixed Gravity Wall Applications (after CDM 1994)**

Soil Type	Cement Usage (kg/m <sup>3</sup> )	Unconfined Compression Strength (kPa)	Permeability (m/sec)
Sludge	240 to 400	70-350	$10 \times 10^{-9}$
Organic silts and clay	150 to 260	350-1400	$5 \times 10^{-9}$
Cohesive silts and clay	120 to 240	700-2100	$5 \times 10^{-9}$
Silty sands and sands	120 to 240	1400-3500	$50 \times 10^{-9}$
Sands and gravels	120 to 240	3000-7000	$100 \times 10^{-9}$



**Fig. 2.2 Chemical Reaction between Soil and Hardening Agents (after Saitoh et al., 1985)**

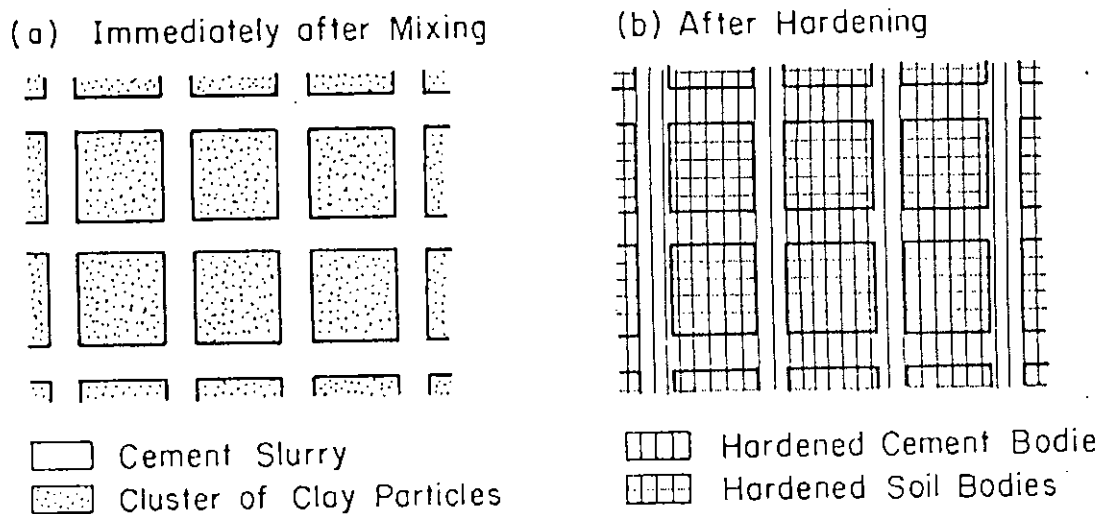


Fig. 2.3 Schematic Illustrations of Improved Soil (after Saitoh et al., 1985)

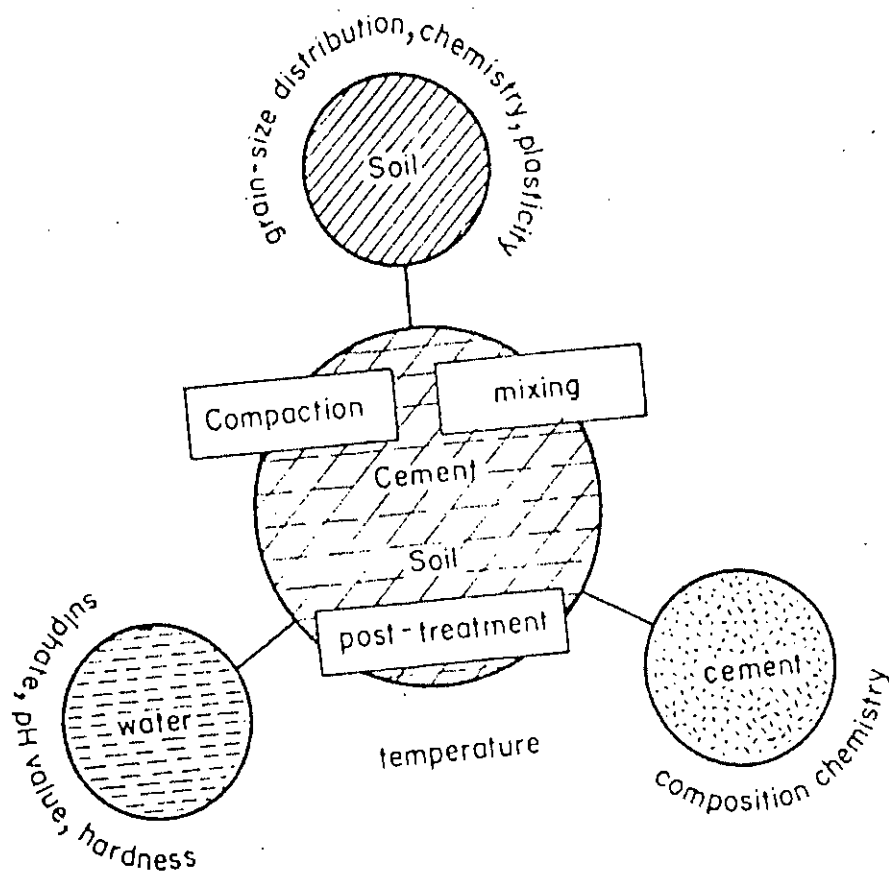


Fig. 2.4 Factors Affecting the Properties for Cement Treated Soils (after Kezdi, 1979).

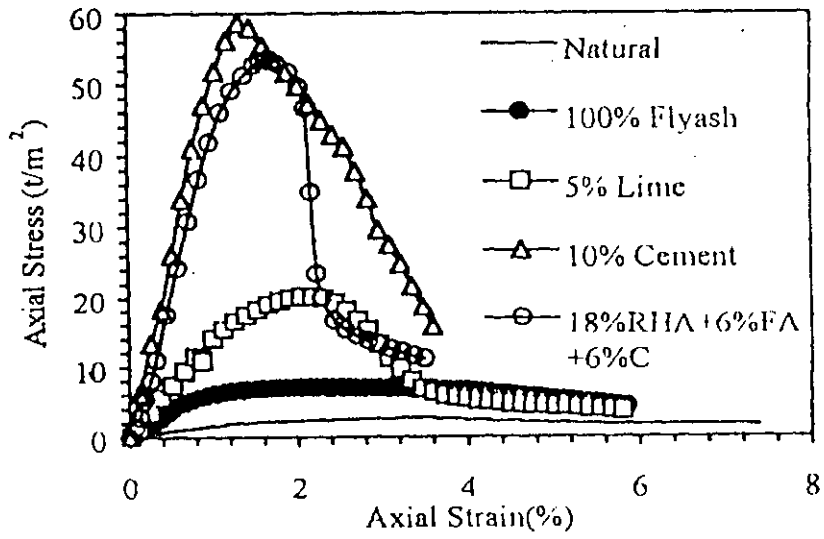


Fig. 2.5 Strength improvement of soft clays by using different types of admixture (after Balasubramaniam et al, 1999)

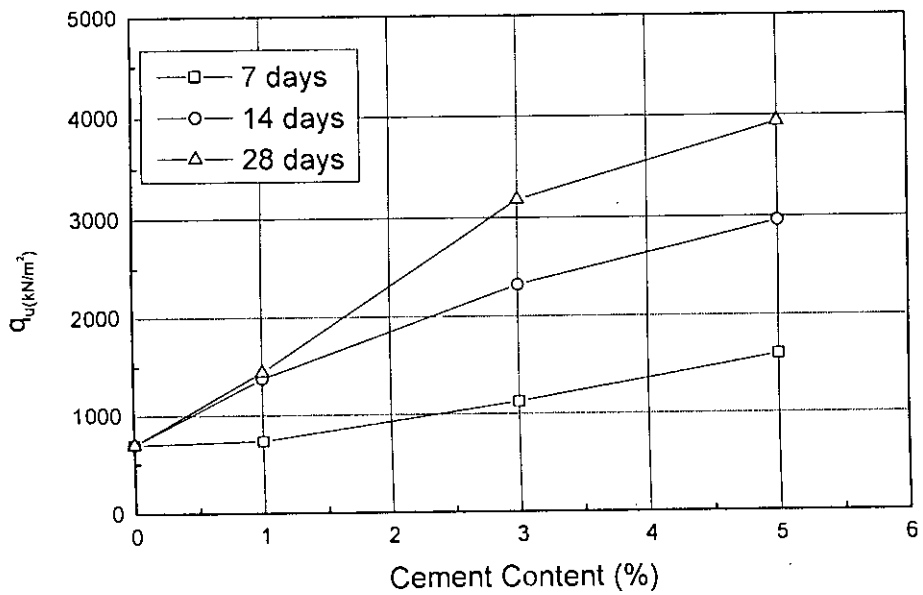


Fig. 2.6 Effect of Cement Content on Unconfined Compressive Strength for Coastal Soil of Bangladesh (after Siddique and Rajbongshi, 2002)



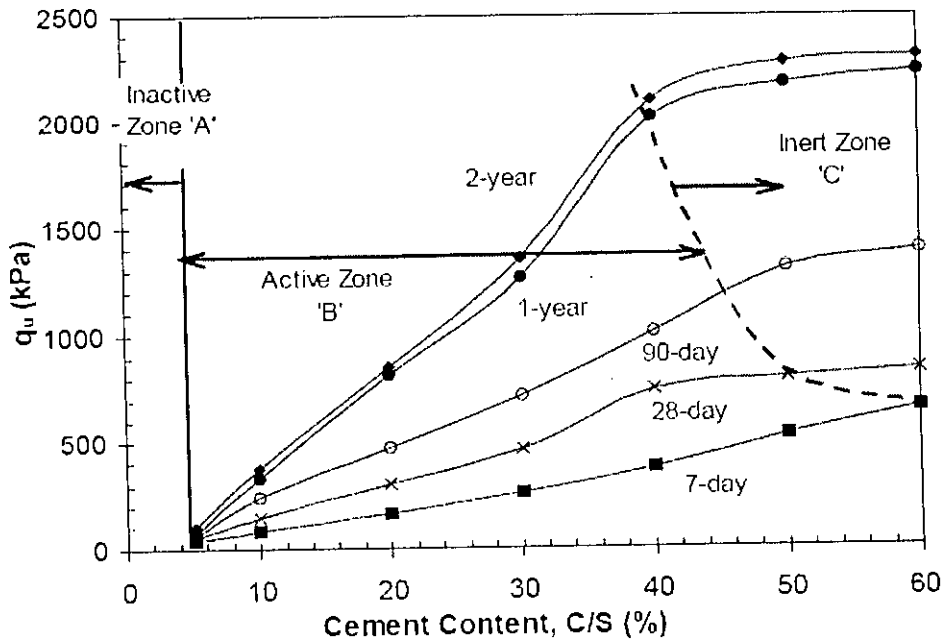


Fig. 2.7 Unconfined Compressive Strength and Cement Content Relationship (120% water) at different Curing Periods for Cement Treated clays (after Kamruzzaman et al., 2004)

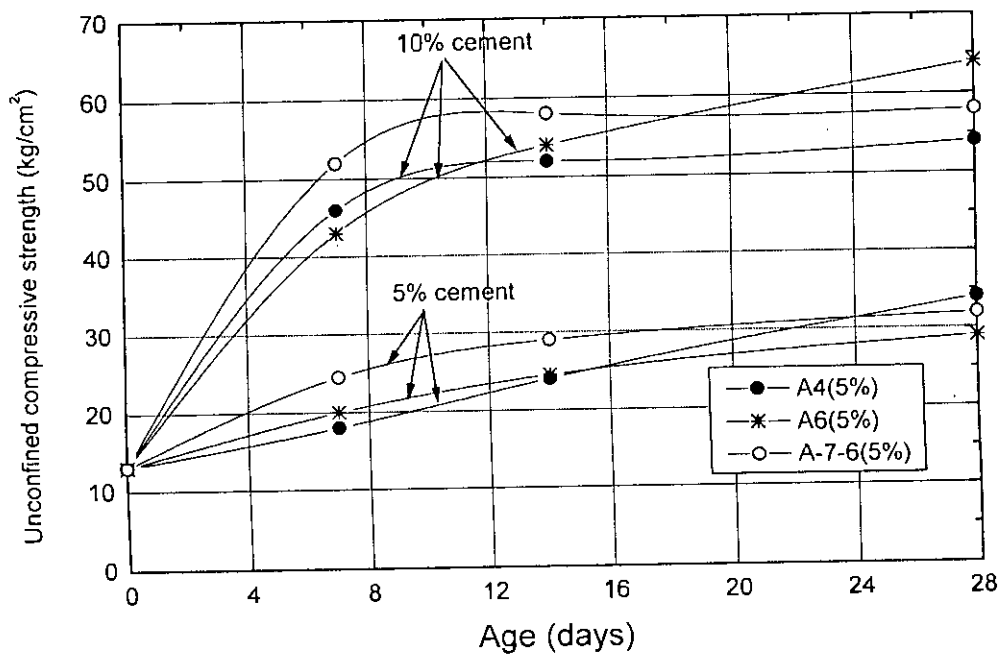


Fig. 2.8 Effect of Curing Age on Unconfined Compressive Strength for Soil-Cement Mix Specimens of Three Soils in Bangladesh (after Serajuddin and Azmal, 1991)

105699

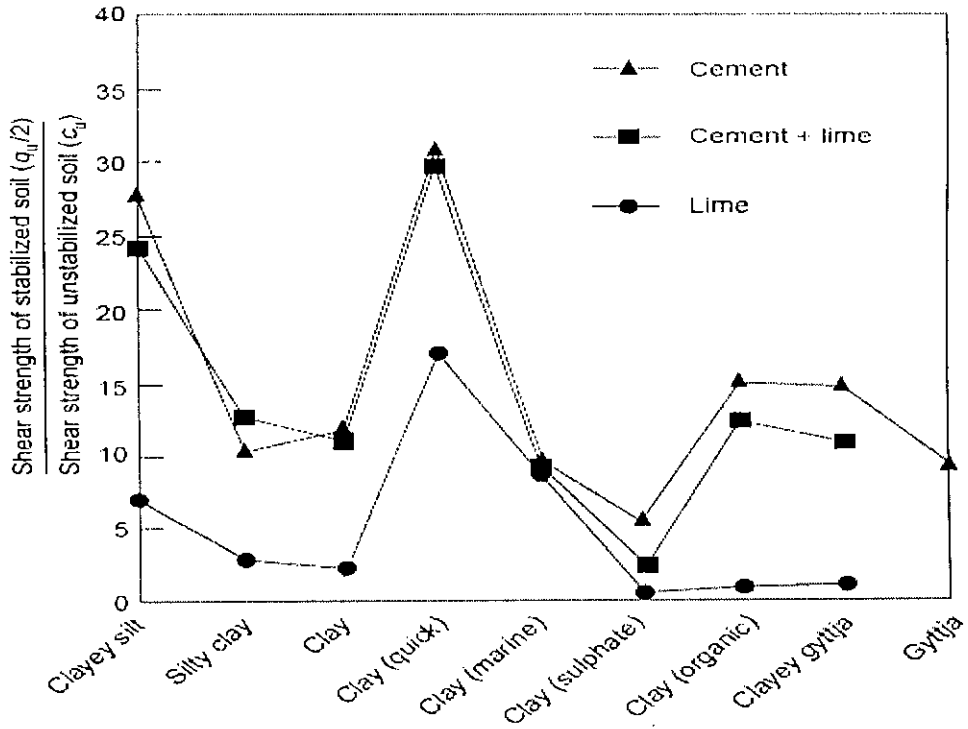


Fig. 2.9 Effect of Stabilizing Agents and Type of Clay on Unconfined Strength for Cement Treated clays (after Ahnberg et al.,1995)

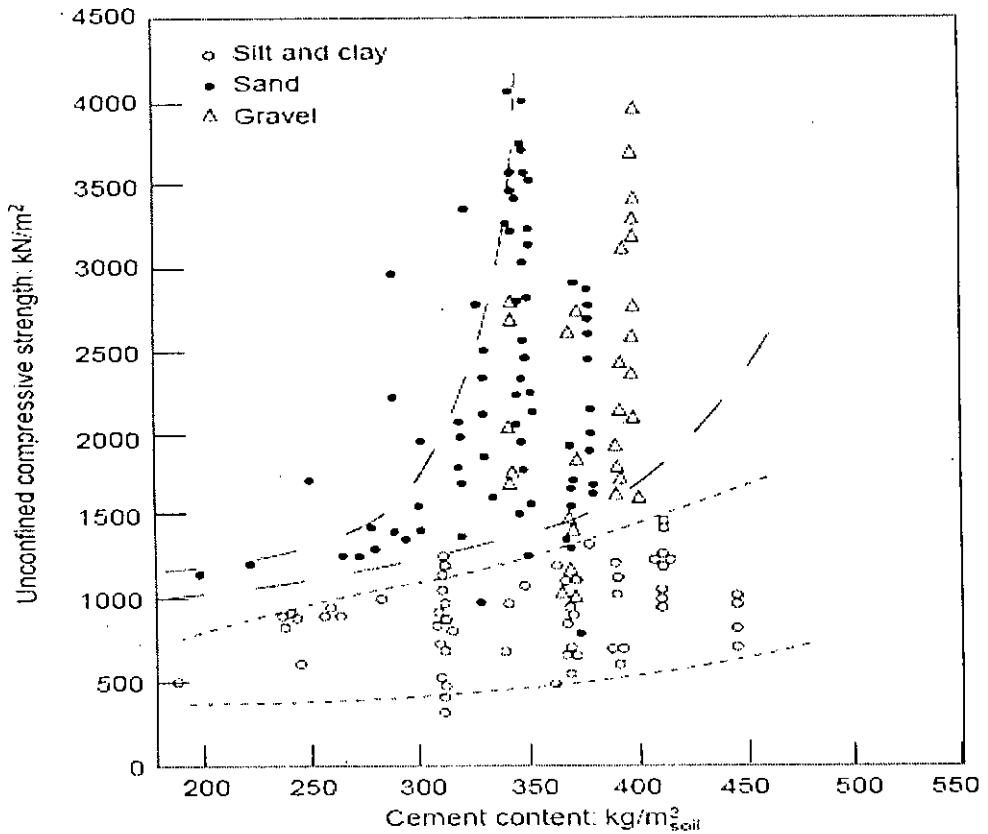


Fig. 2.10 Effect of Soil Type on Unconfined Compressive Strength for Cement Treated clays (after Taki and Yang, 1991)

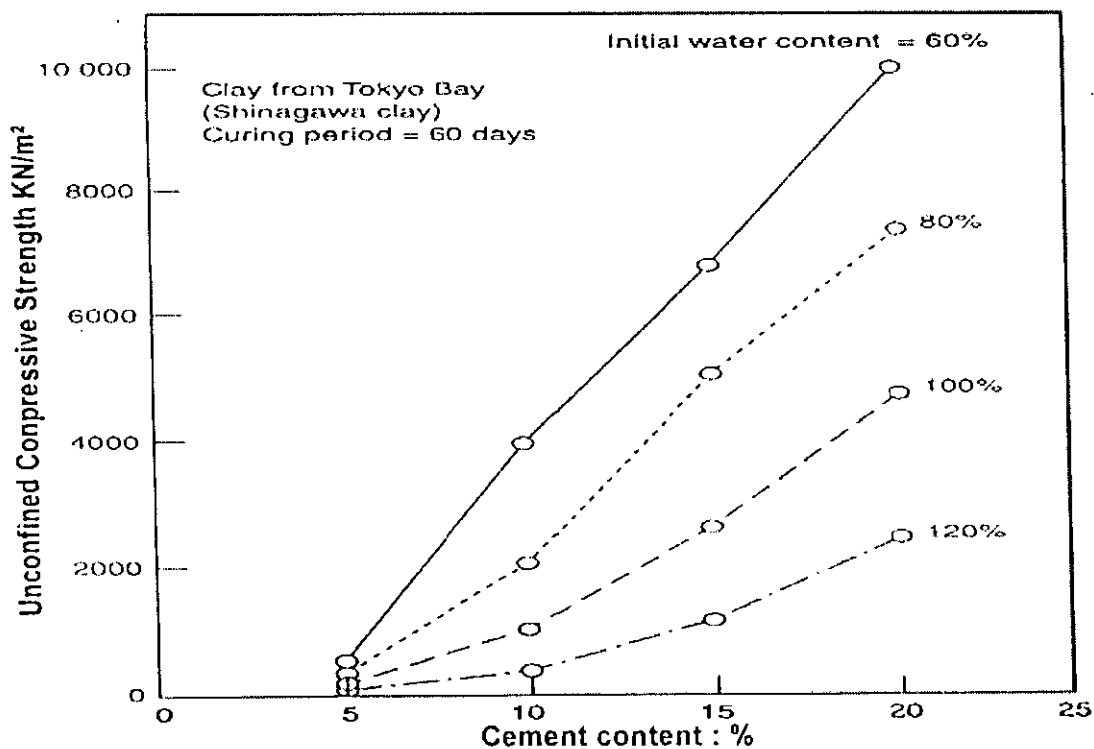
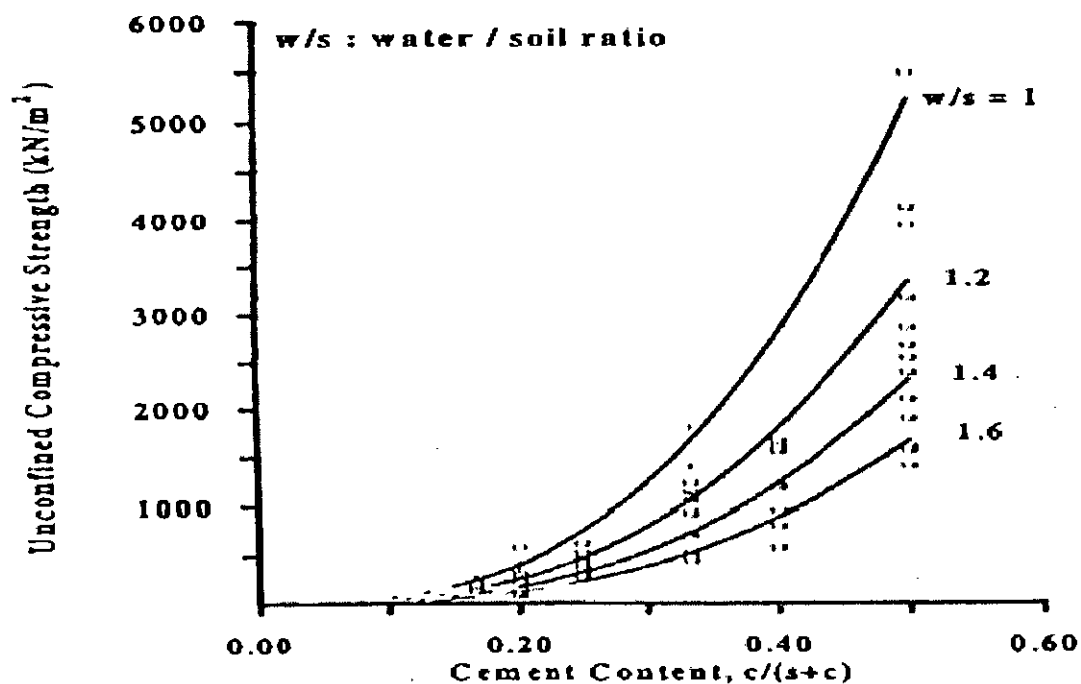


Fig. 2.11 Effect of Initial Water Content on Unconfined Compressive Strength of Cement Treated clays (after Porbaha et al., 2000)



\*\*Cement Content,  $c/(s+c)$  = wt of dry cement/wt of dry cement + wt of dry soil solid.

Fig. 2.12 Effect of Water/Soil Ratio on Unconfined Compressive Strength of Cement Treated Singapore marine clays (after Chew et al., 1997)

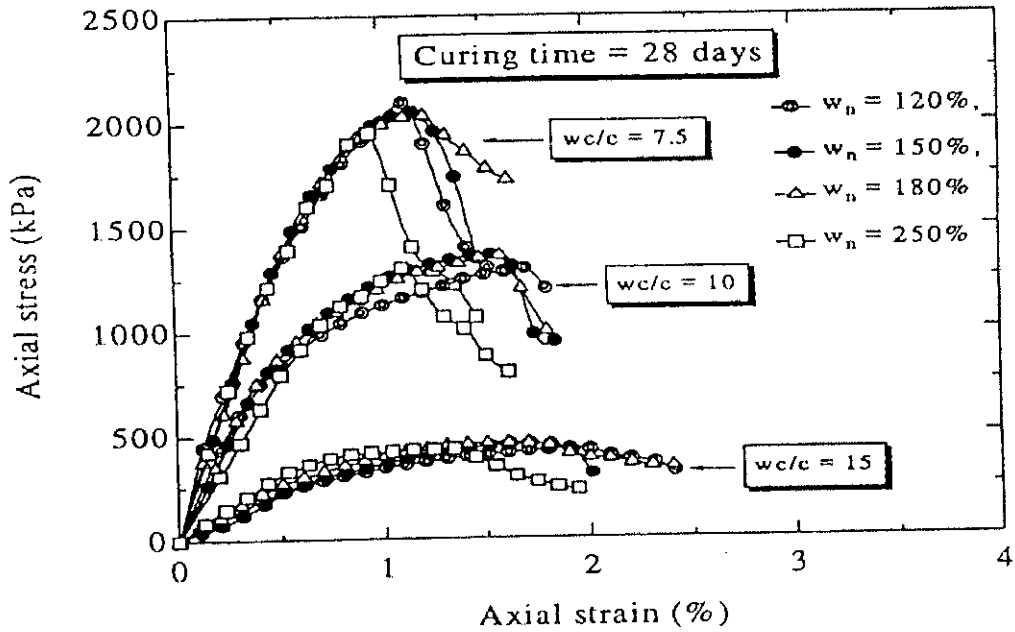


Fig. 2.13 Stress-Strain Relationships of Cement Stabilized Ariake clays at High Water Content (after Miura et al., 2001)

Table 2.2 Properties of Cement Treated Ariake Clay (after Miura et al., 2001)

Curing (days)	$w_i$ (%)	wc/c ratio	$w_r$ (%)	$\gamma_d$ ( $\text{kN/m}^3$ )	$S_r$ (%)	$C_s$	$C_c$	$\sigma_y$ (kPa)
28	120	15	111	6.54	98	0.018	0.807	820
		10	103	6.95	97	0.010	0.850	2100
		7.5	100	7.05	96	0.014	-	3500
	150	15	131	5.71	98	0.011	1.122	810
		10	120	6.09	96	0.020	1.011	2300
		7.5	113	6.34	95	0.013	-	3600
	180	15	143	5.43	99	0.023	1.226	850
		10	138	5.55	98	0.021	1.431	2150
		7.5	125	5.95	98	-	-	-
	250	15	193	4.27	100	0.031	1.492	900
		10	168	4.85	100	0.025	1.559	200
		7.5	159	5.23	100	0.014	1.407	3400

**Table 2.3 Properties for Pure Lime (after Kamaluddin, 1995)**

Property	Quicklime		Hydrated Lime	
	Calcium Oxide	Magnesium Oxide	Calcium Hydroxide	Magnesium Hydroxide
Chemical Name	CaO	MgO	Ca(OH) <sub>2</sub>	Mg(OH) <sub>2</sub>
Chemical Formula	Cubic	Cubic	Hexagonal	Hexagonal
Melting Point	2570°C	2800°C	-	-
Decomposition Point	-	-	580°C	745°C
Boiling Point	2850°C	3600°C	-	-
Molecular Weight	56.09	40.32	74.10	58.34
Specific Gravity	3.40	3.65	2.34	2.40

\*(Specification provided by May and Baker Ltd., England)

**Table 2.4 Specification for Pure Lime (after Kamaluddin, 1995)**

	Specification of Quicklime
CaO Content	Not less than 95% CaO
Loss Ignition	Not more than 10%
Al, Fe and Acid Insoluble	Not more than 1%
Chloride	Not more than 0.02%
Sulphate	Not more than 0.2%
Arsenic	Not more than 0.0004%

\*(Specification provided by May and Baker Ltd., England)

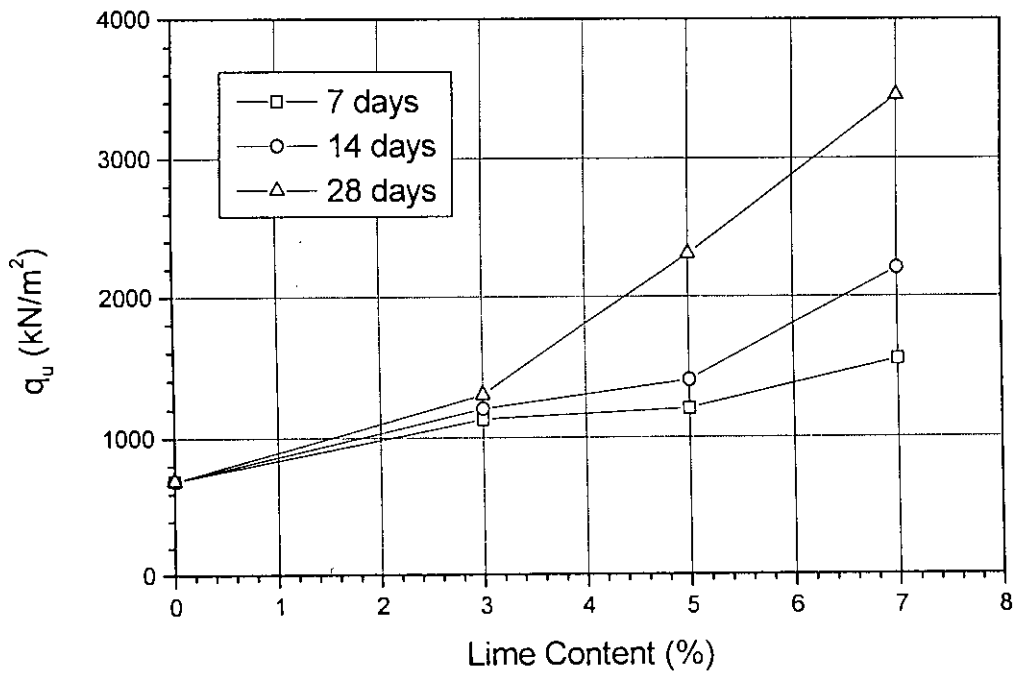


Fig. 2.14 Effect of Lime Contents on Unconfined Compressive Strength ( $q_u$ ) of Coastal Clay (PI = 19%) in Bangladesh (after Rajbongshi, 1997)

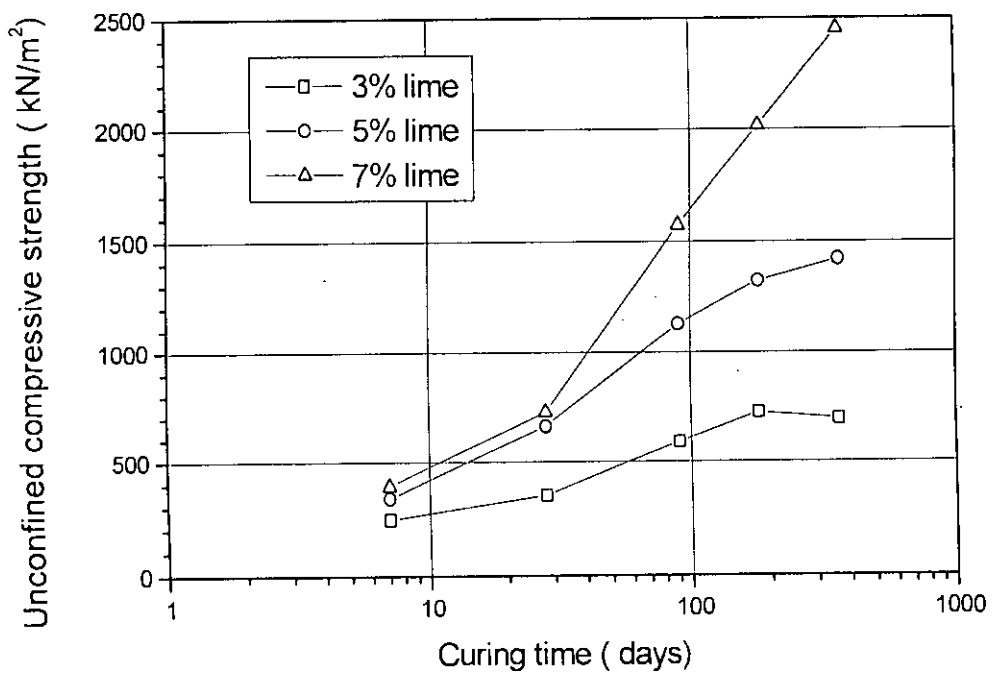


Fig. 2.15 Effect of Curing Age on Unconfined Compressive Strength ( $q_u$ ) for Lime Treated Regional Clays (Type-CL, PI = 20%) in Bangladesh (after Shahjahan, 2001)

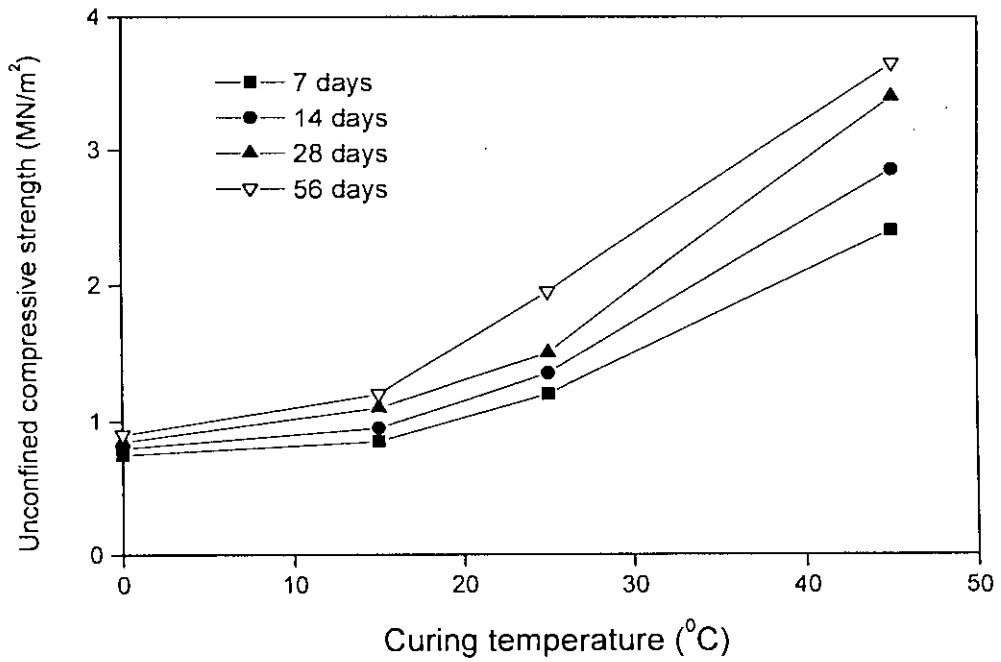


Fig. 2.16 Effect of Curing Temperature and Curing Age on Unconfined Compressive Strength of High Plastic Stabilized Clay with 5% lime (after Bell, 1988)

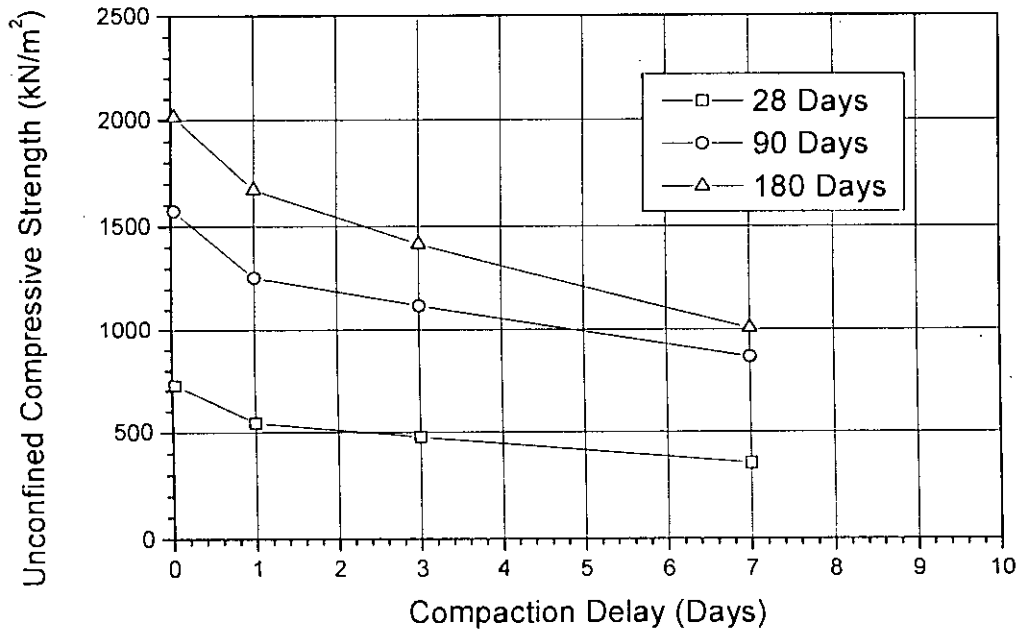
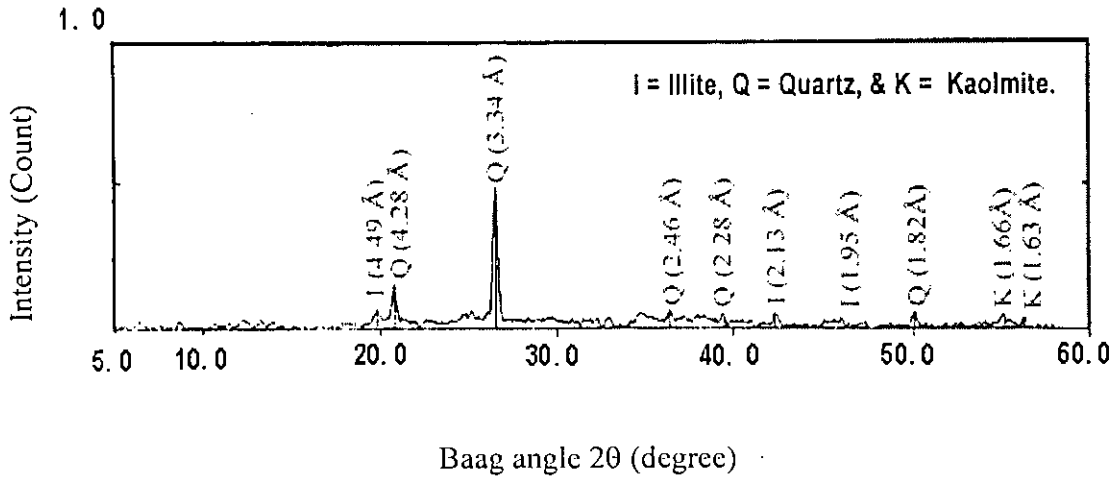
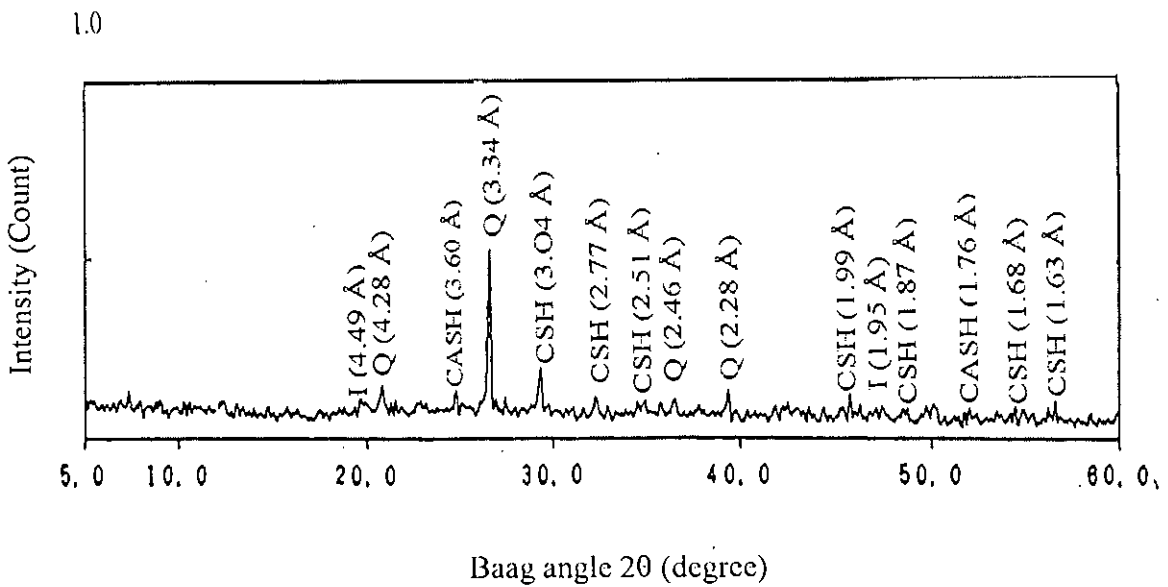


Fig. 2.17 Variation of Unconfined Compressive Strength with Compaction Delay Time for Soil type- CL (PI = 20%) in Bangladesh (after Shahjahan, 2001)



(a)



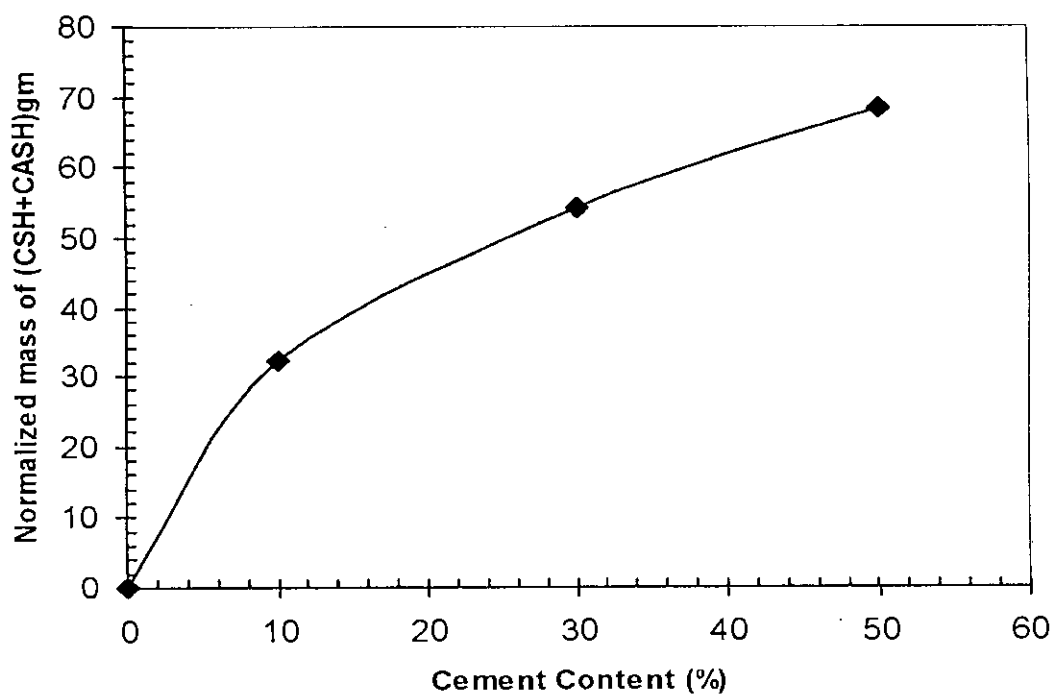
(b)

Fig. 2.18 X-ray Diffraction Patterns of (a) Untreated and (b) 30% Cement Treated Singapore Clays at  $w_1 = 120\%$  and Curing = 28 days (after Chew et al., 2004)

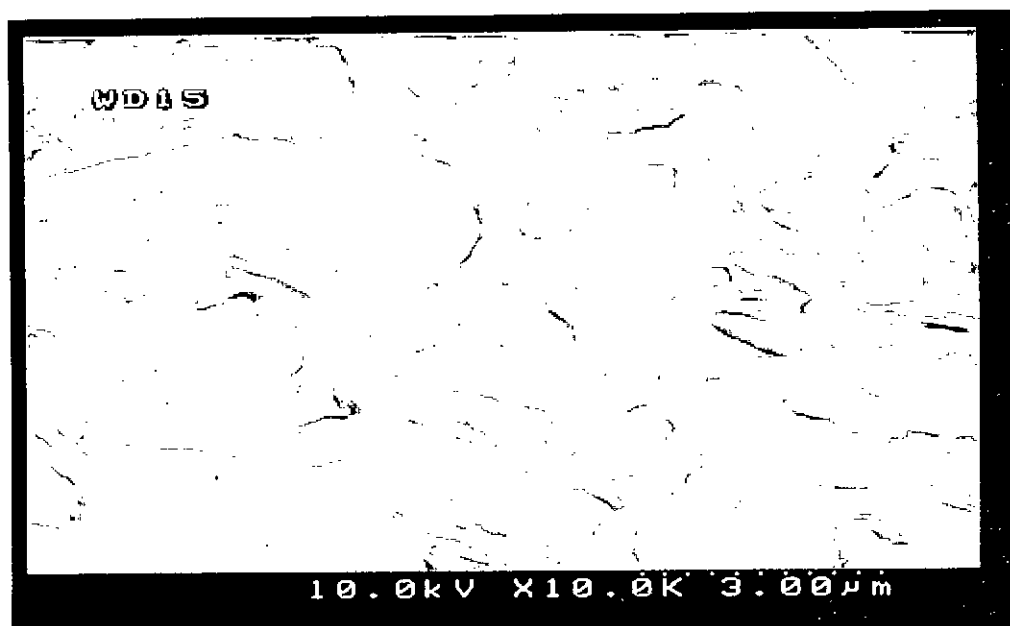


**Table 2.5 Clay Minerals Cementitious Compounds of Treated Singapore Clays at 120% water and 28 days curing (after Chew et al., 2004)**

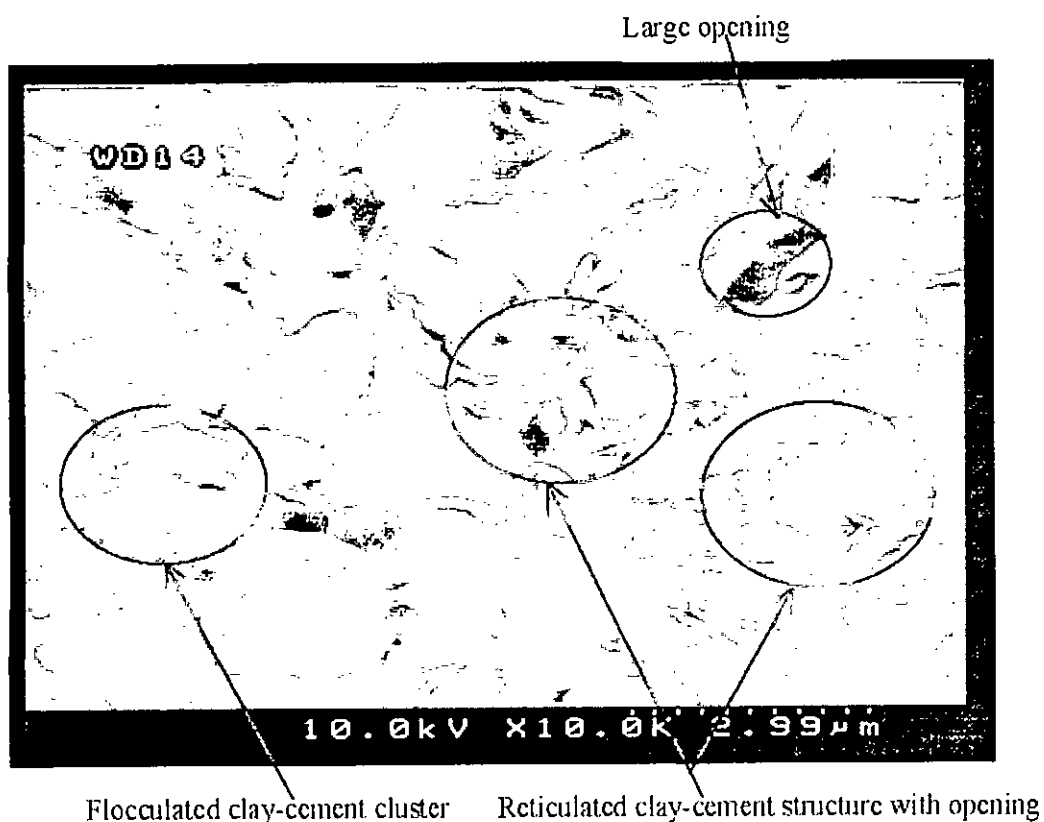
Normalized mass of mineral (% by weight)	Untreated clay	10% cement treated clay	30% cement treated clay	50% cement treated clay
Total mass (% by wt.)	100	110	130	150
Illite (% by wt.)	18	6	11	11
Quartz (% by wt.)	71	72	65	71
Kaolinite (% by wt.)	11	0	0	0
CSH+ CASH (% by wt.)	0	32	54	68



**Fig. 2.19 Cementitious Products (CSH + CASH) Versus Cement Content Relationship of Cement Treated Clays at  $w_i = 120\%$  and Curing = 28 days (after Chew et al., 2004)**



(a)



(b)

Fig. 2.20 SEM Image of (a) Untreated and (b) 30% Cement Treated Singapore Clays at 120% Water and 28 days Curing (after Kamruzzaman et al., 2004)

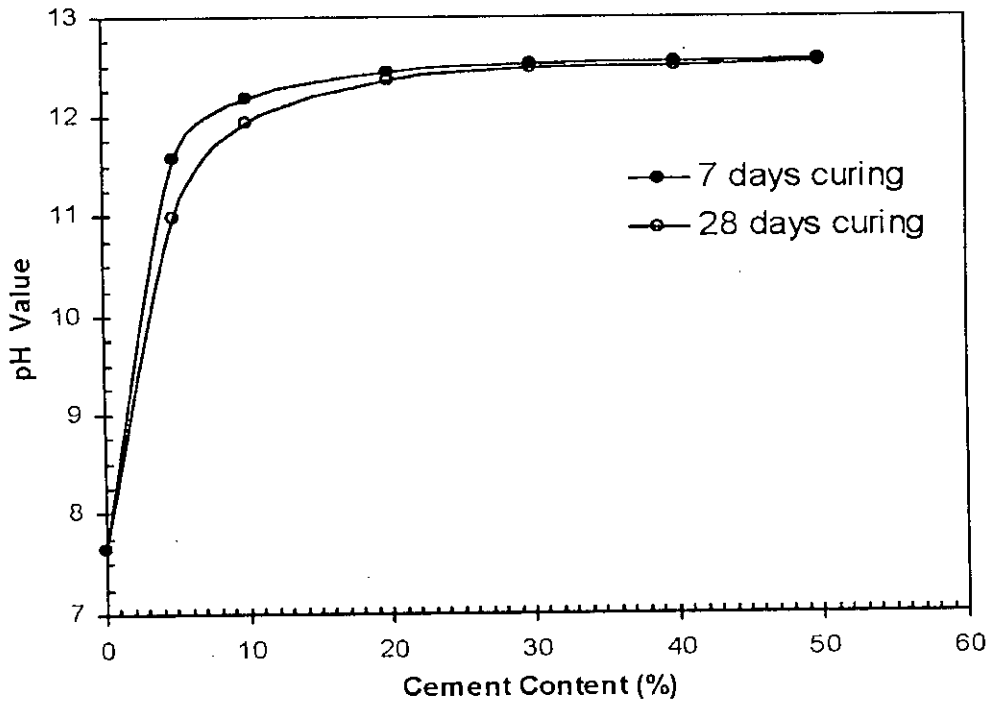


Fig. 2.21 Effect of Cement Content and Curing Time on pH Values of Cement Treated Soil at Soil : Water = 1 : 2.5 and  $w_i = 120\%$  (after Chew et al. 2004)

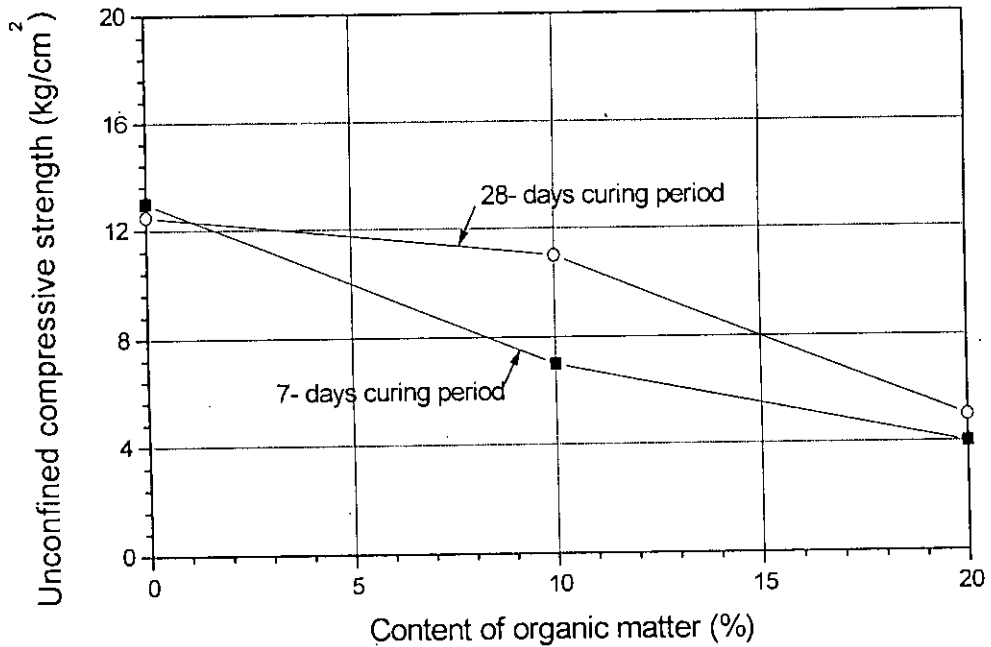


Fig. 2.22 Effects of Organic Matter on the Strength for Lime Treated Clays (after Arman and Muhfakh, 1972)

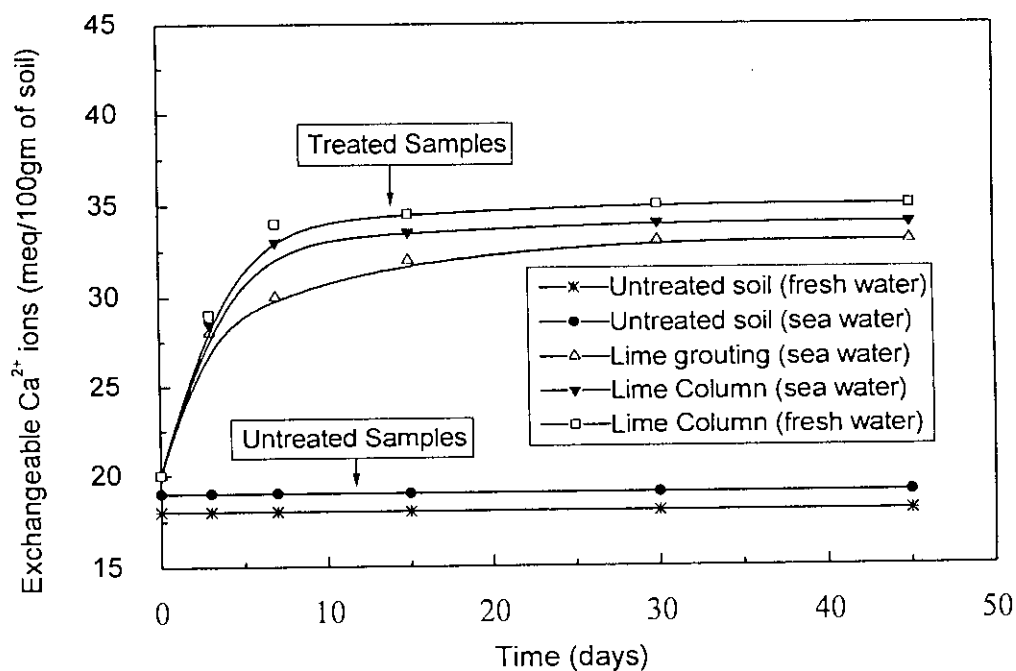


Fig. 2.23 Effect of Curing Time on Exchangeable Calcium ion Concentration of Lime Treated Clays (Reproduced after Rao and Rajashekar, 1996)

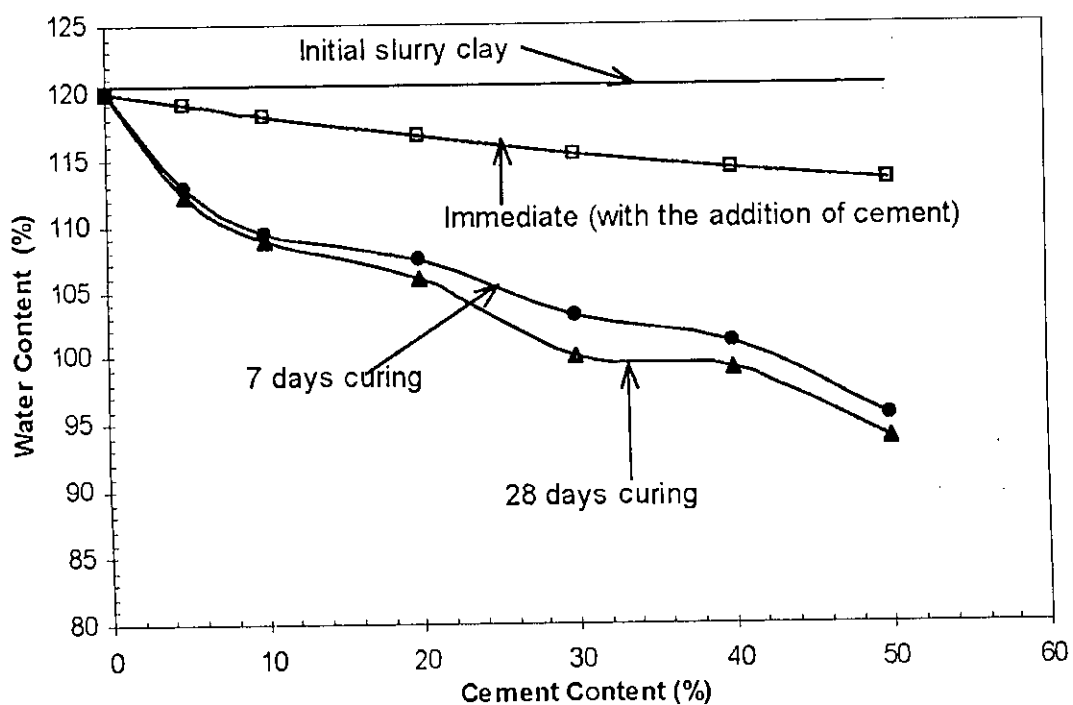


Fig. 2.24 Effect of Cement Content and Curing Time on Final Water Content at Mixing Water Content, 120% for Cement Treated Clays (after Chew et al., 2004)

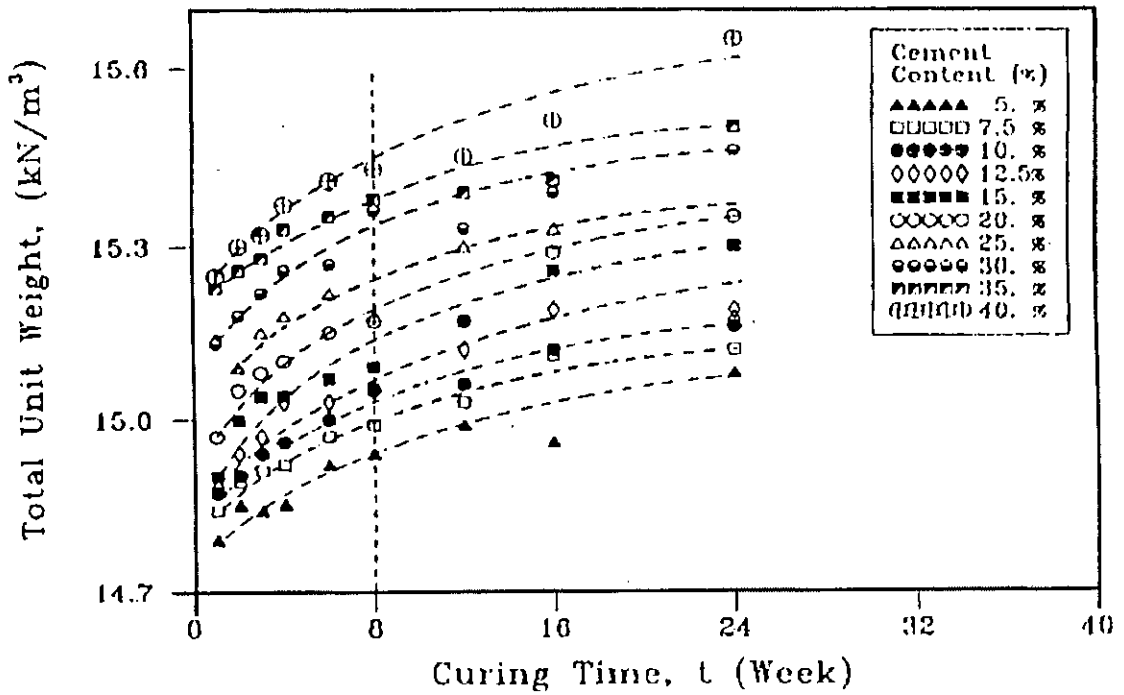


Fig. 2.25 Effect of Cement Content and Curing Time on Total Unit Weight for Cement Treated Clays (after Kamaluddin, 1995)

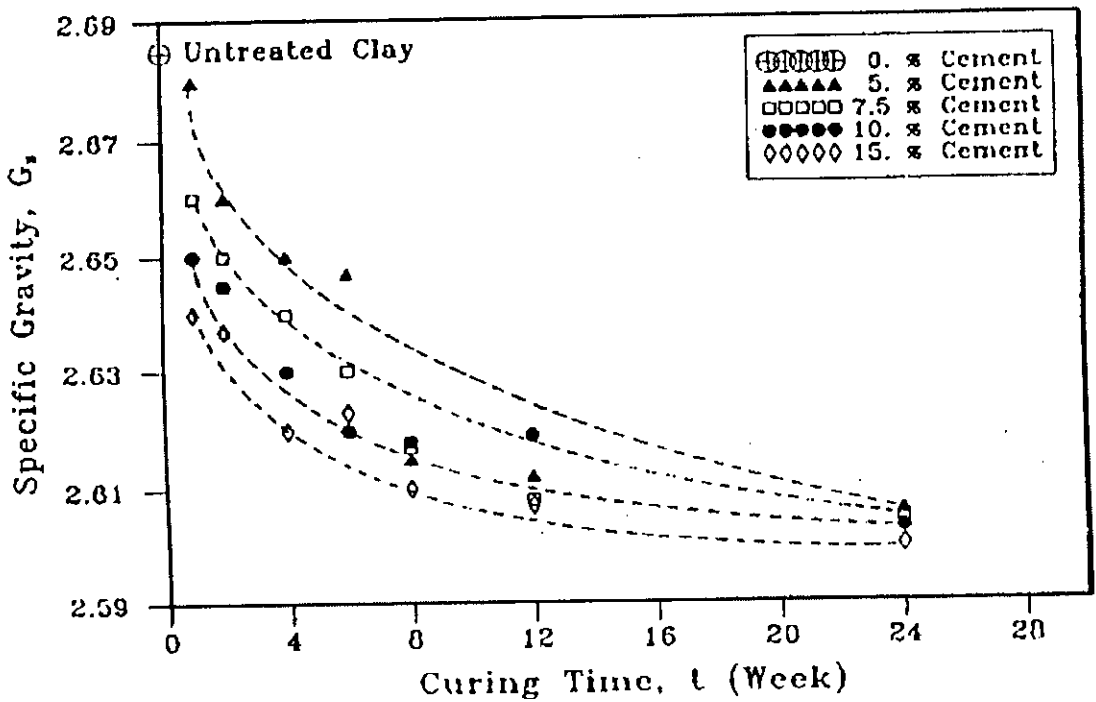


Fig. 2.26 Effect of Cement Content and Curing Time on Specific Gravity for Cement Treated Clays (after Kamaluddin, 1995)

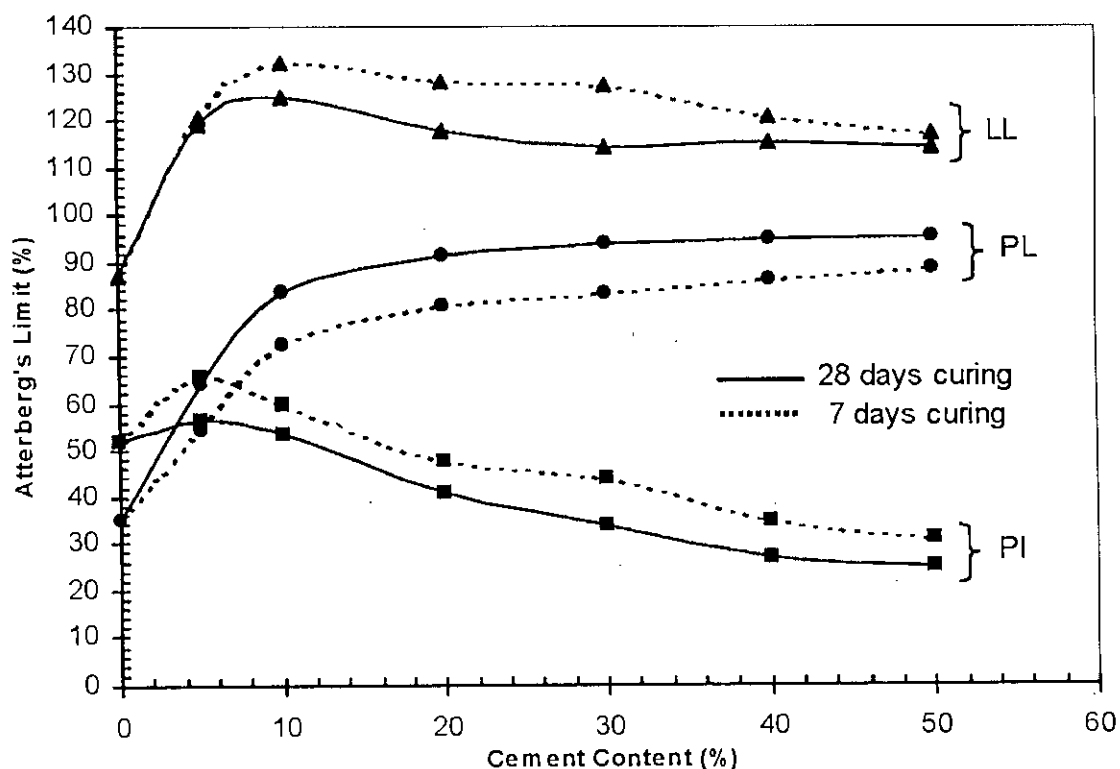


Fig. 2.27 Effect of Cement Content and Curing Time on Atterberg Limit for Cement Treated Clays (after Chew et al., 2004)

Table 2.6 Effect of Cimentation on Engineering Properties of the Soft Bangkok Clays (after, Bergado et al., 2003)

Properties	General effect in comparison to untreated clay	Effect of increasing cement / lime content	Effect increasing curing time
Specific gravity	Decreases significantly	Reduces significantly	Decreases with time
Water content	Immediate decrease about 5% to 10%.	Reduces significantly	Reduces substantially
Plastic limit	Increases	Increases at higher cement content	Increases with time increasing
Liquid limit	Small reduction	Insignificant change	Reduces with time increasing
Plasticity index	Reduces	Reduces at higher cement content	Decreases at longer time
Unit weight	Increases	Increases at higher cement content	Increases at longer time
Void ratio	Decreases	Reduces at higher cement content	Reduces with time increasing
Degree of saturation	Increases	Increases at higher cement content	Decreases at longer time

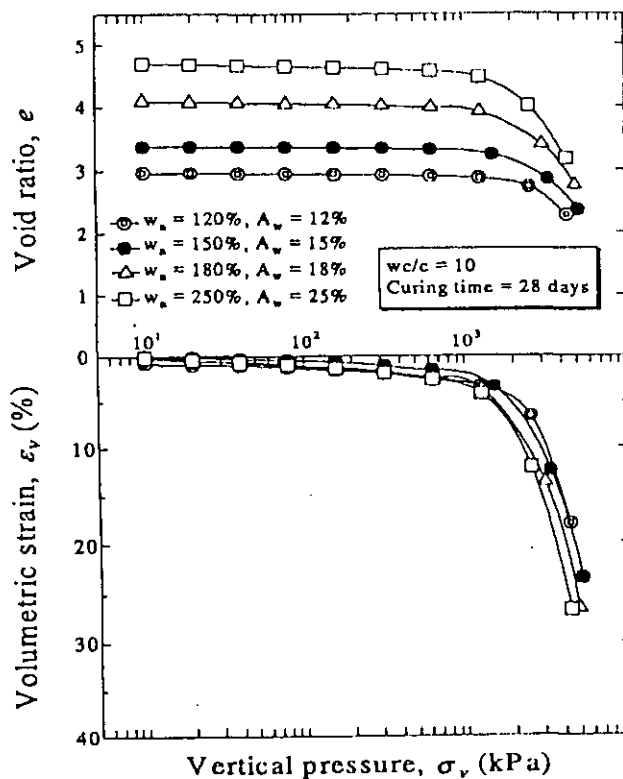


Fig. 2.28  $e$ - $\log \sigma'_v$  and  $\varepsilon_v$ - $\log \sigma'_v$  Relationships of Cement Treated Ariake Clay with same  $w_c/c$  Ratio, 10 (after Miura et al., 2001)

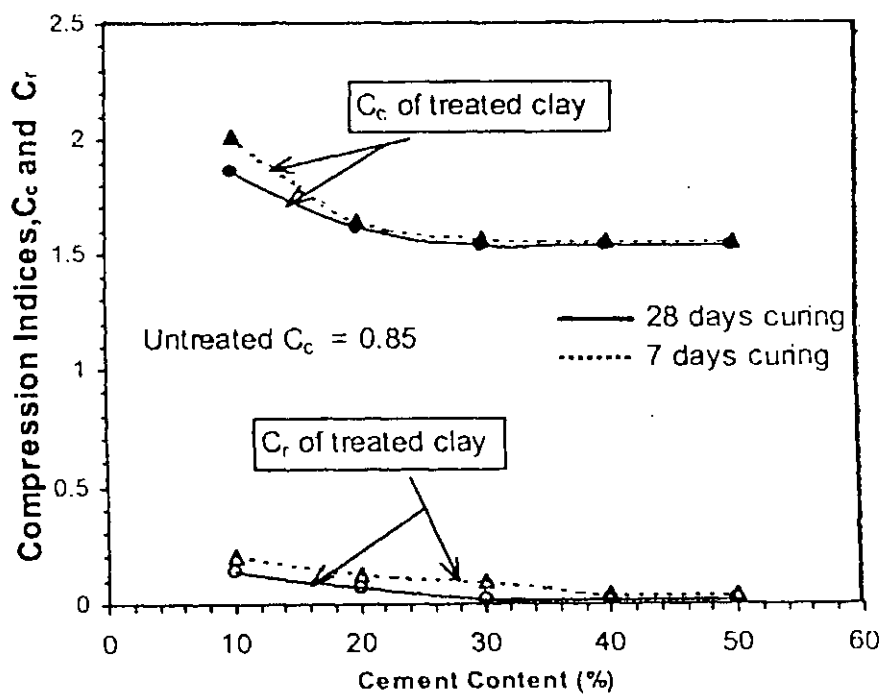


Fig. 2.29 Effect of Cement Content and Curing Time on Compression Indices of Cemented Singapore Clay with 120% water (after Chew et al., 2001)

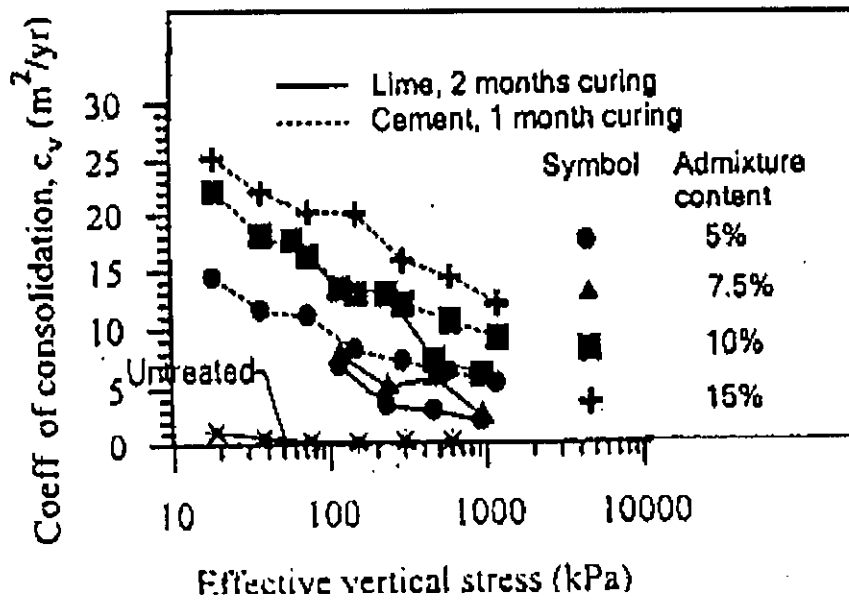


Fig. 2.30 Effect of Cement Content and Curing Time on Coefficient of Consolidation for Cement Treated Bangkok Clays (after Bergado et al., 2003)



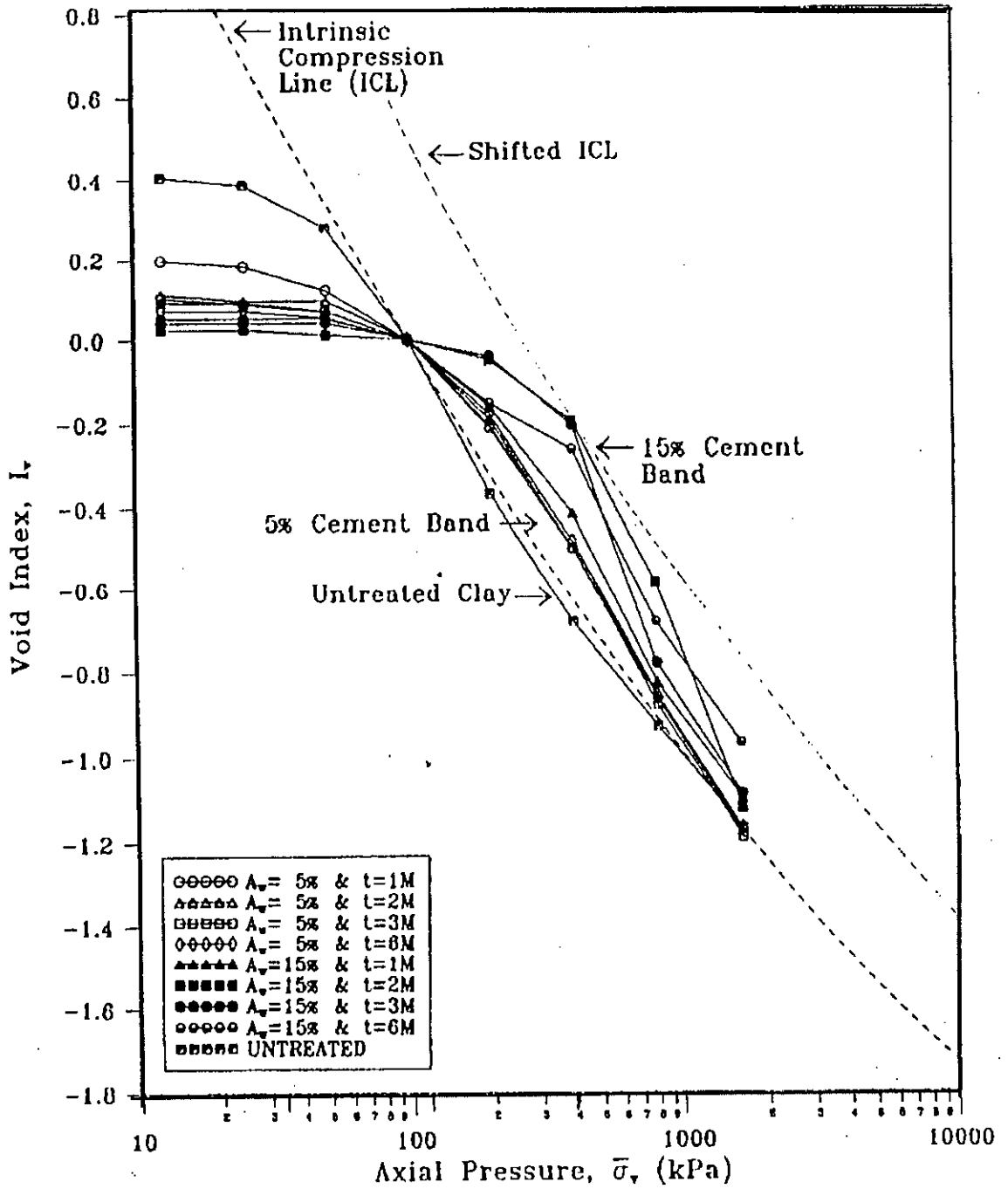


Fig. 2.31 Effect of Cement on Intrinsic Compression Line for Cement Treated clays (after, Kamaluddin, 1995)

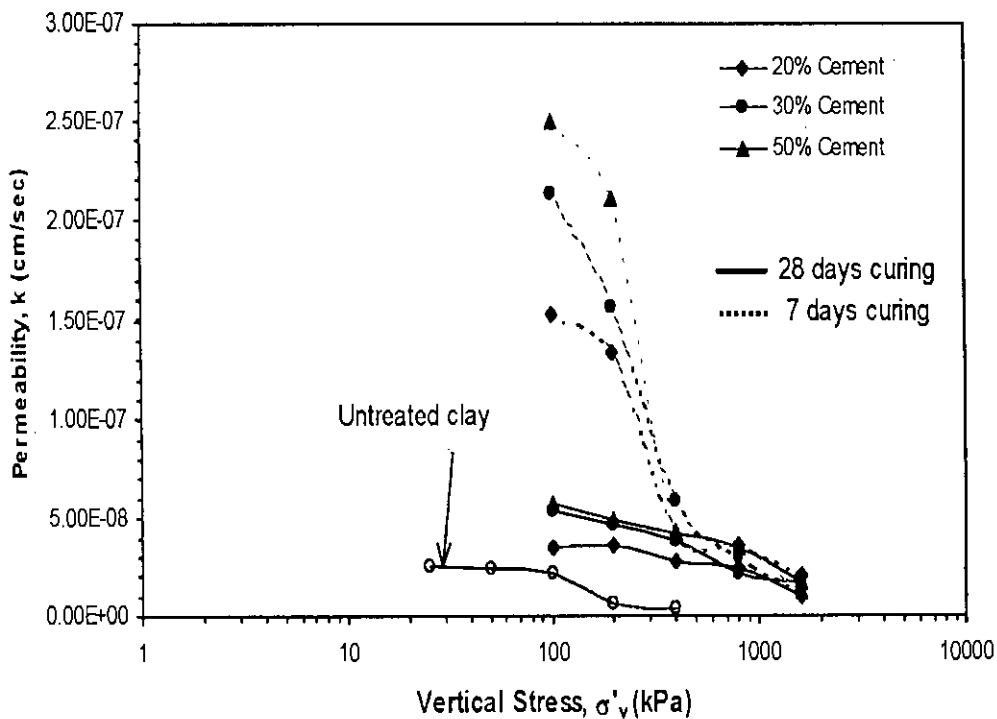


Fig. 2.32 Effect of Cement and Curing Time on  $k$ - $\log\sigma'_v$  Relationships of Treated Singapore Marine Clays at  $w_i$ , 120% (after Chew et al., 2004)

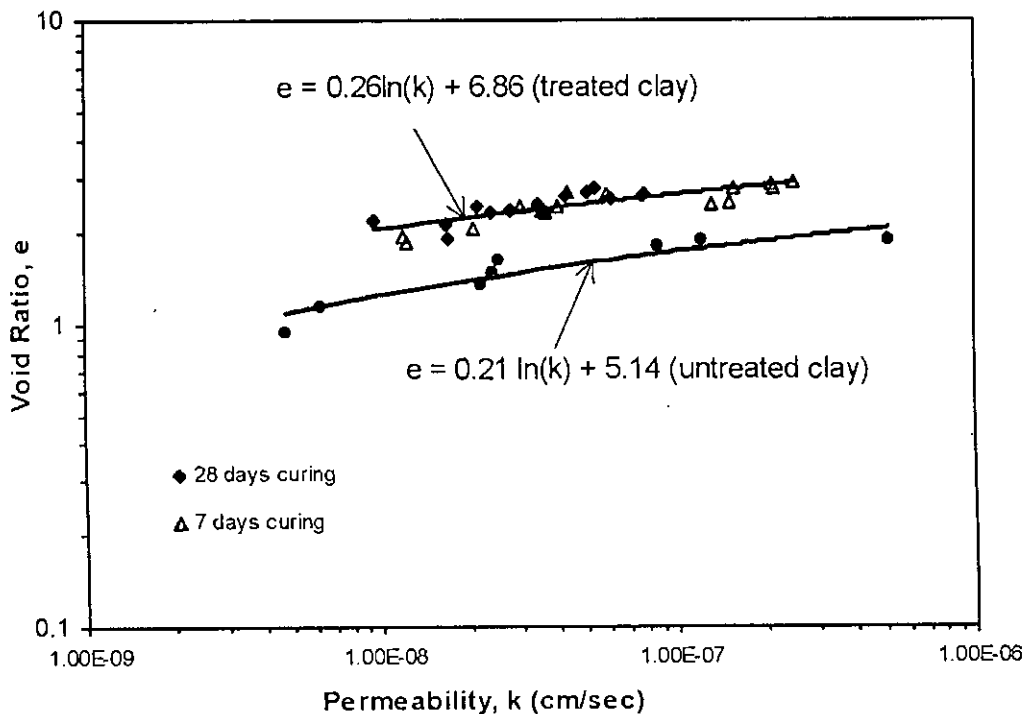


Fig. 2.33 Void ratio and Permeability ( $\log$ - $\log k$ ) Relationships of Cement Treated Singapore Clays at  $w_i$ , 120% (after Chew et al., 2004)

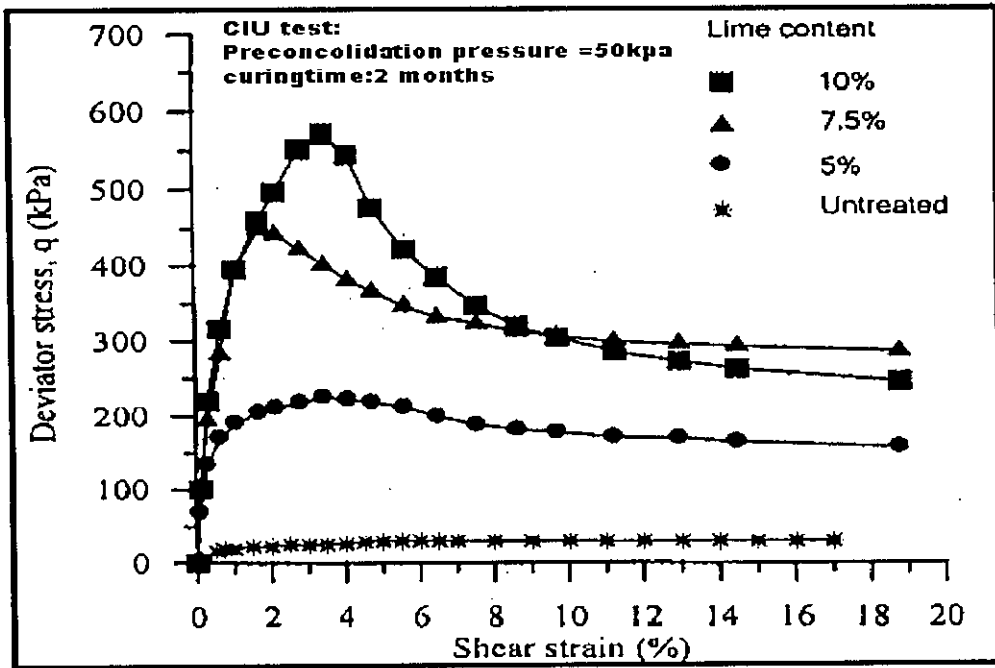


Fig. 2.34 Effect of Lime Content on (q- $\epsilon_s$ ) Relationships for Lime Treated Clays (after Bergado et al., 2003)

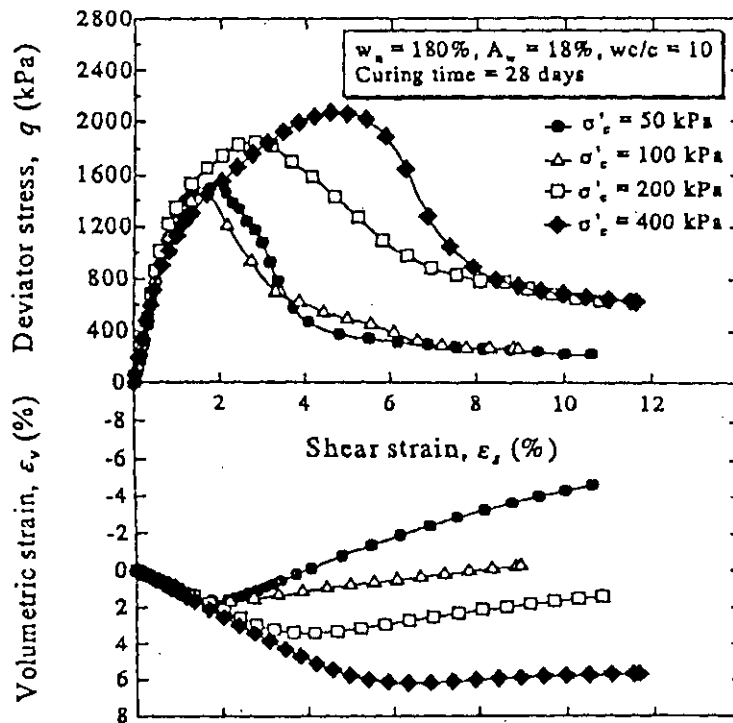


Fig. 2.35 Effect of Pre-Shear Consolidation Pressure on (q- $\epsilon_s$ ) and ( $\epsilon_v$ - $\epsilon_s$ ) Relationships for Cement Treated Clays (after Miura et al., 2001)

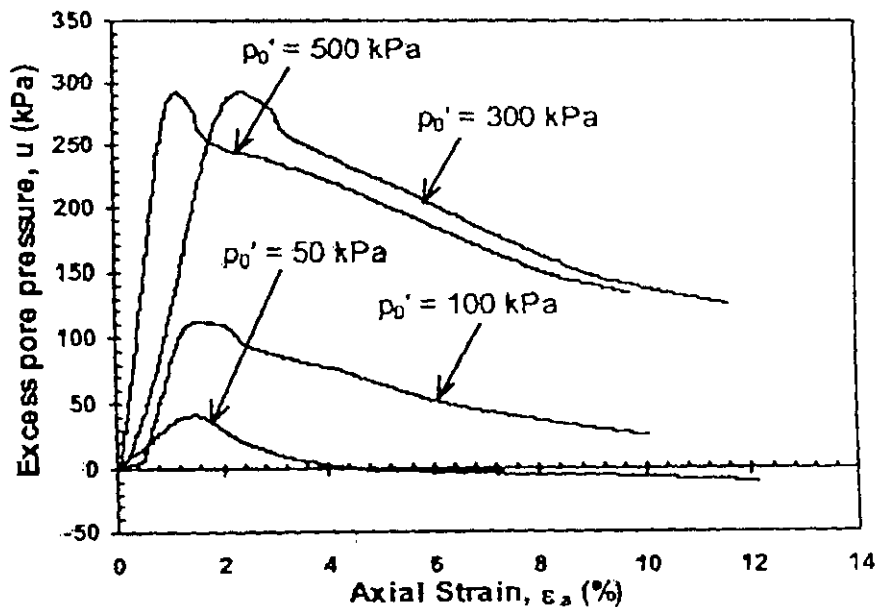


Fig. 2.36 Effect of Pre-Shear Consolidation Pressure on Pore Pressure Versus Axial Strain ( $u-\epsilon_s$ ) Relationships for Cement Treated Clays (after Chew et al., 2001)

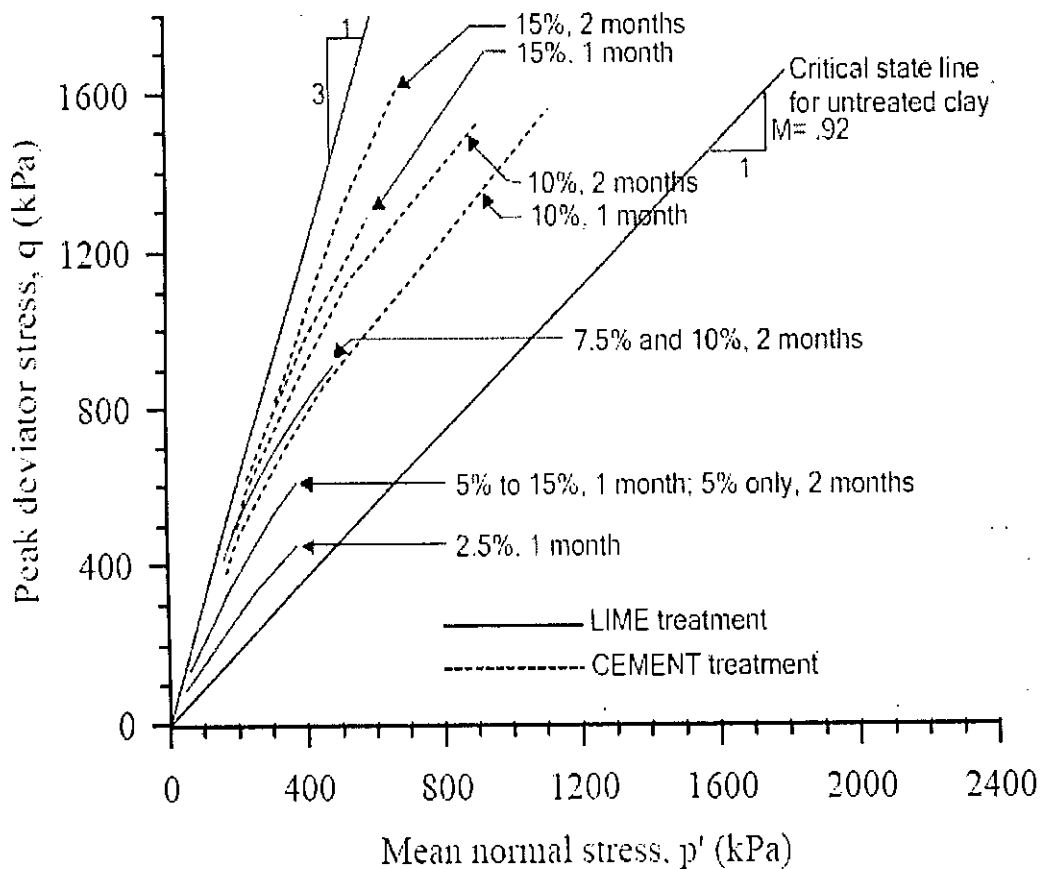


Fig. 2.37  $q_{max} - p'$  Relationships for Cement Treated Clays from CIU Tests (after Bergado et al., 2003)

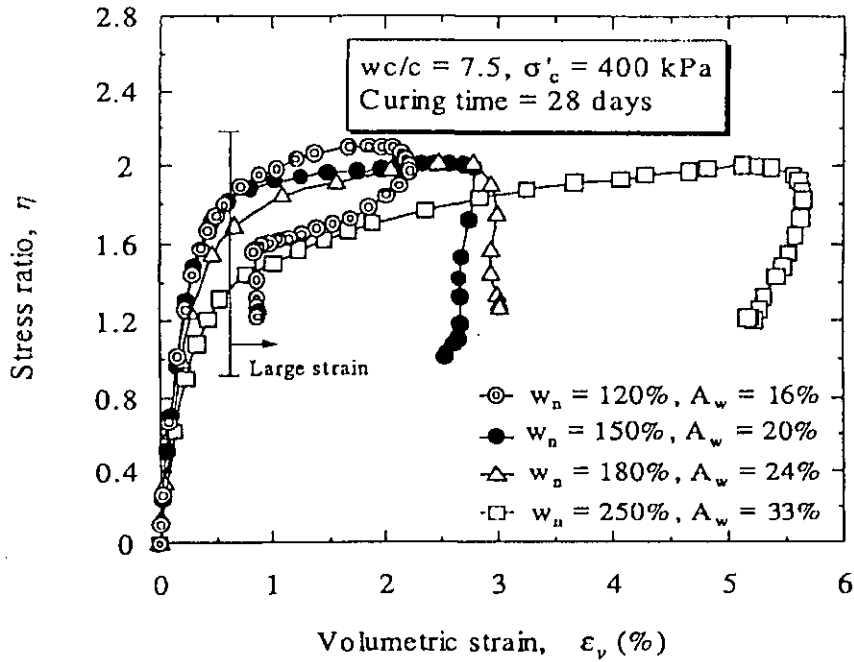


Fig. 2.38 Effect of Mixing Water Content on  $(\eta, \epsilon_v)$  Relationships for  $w_c/c$  Ratio = 7.5 and  $p'_0 = 400$  kPa for Cement Treated Clays (after Miura et al., 2001)

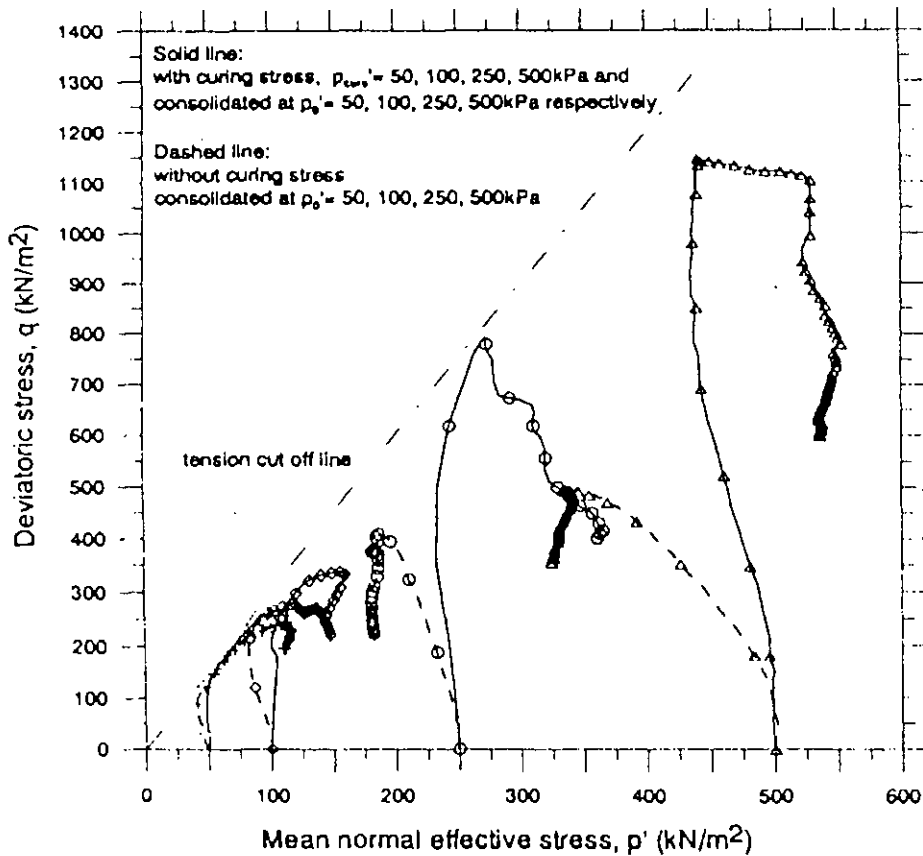


Fig. 2.39 Effect of Pre-Shear Consolidation Pressure on Undrained Stress Paths for Cement Treated and Untreated Clay (after Ghee et al., 2004)

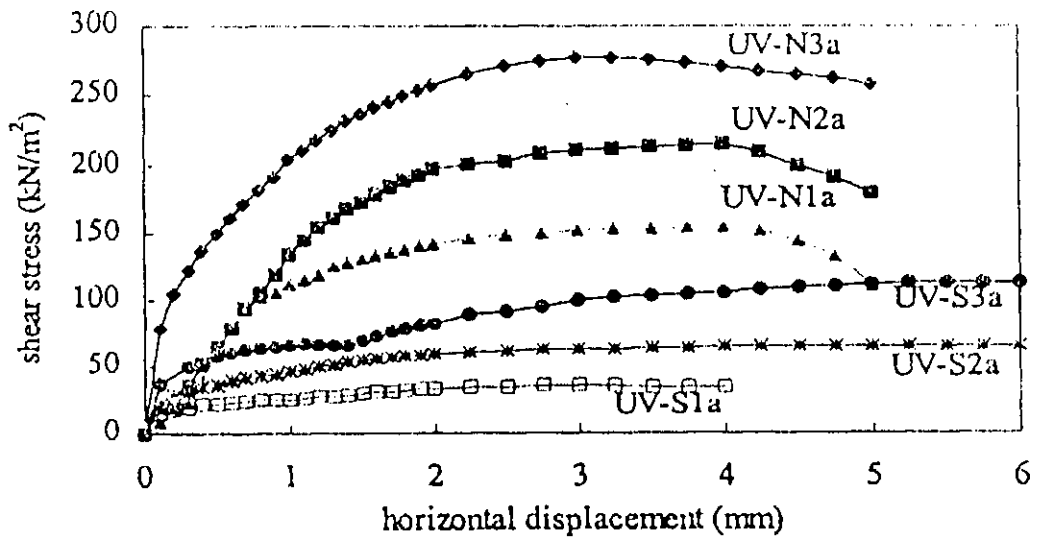


Fig. 2.40 Relationships between Shearing Stress and Horizontal Displacement from Direct Shear Test for Untreated Clays (after Taha et al., 1998)

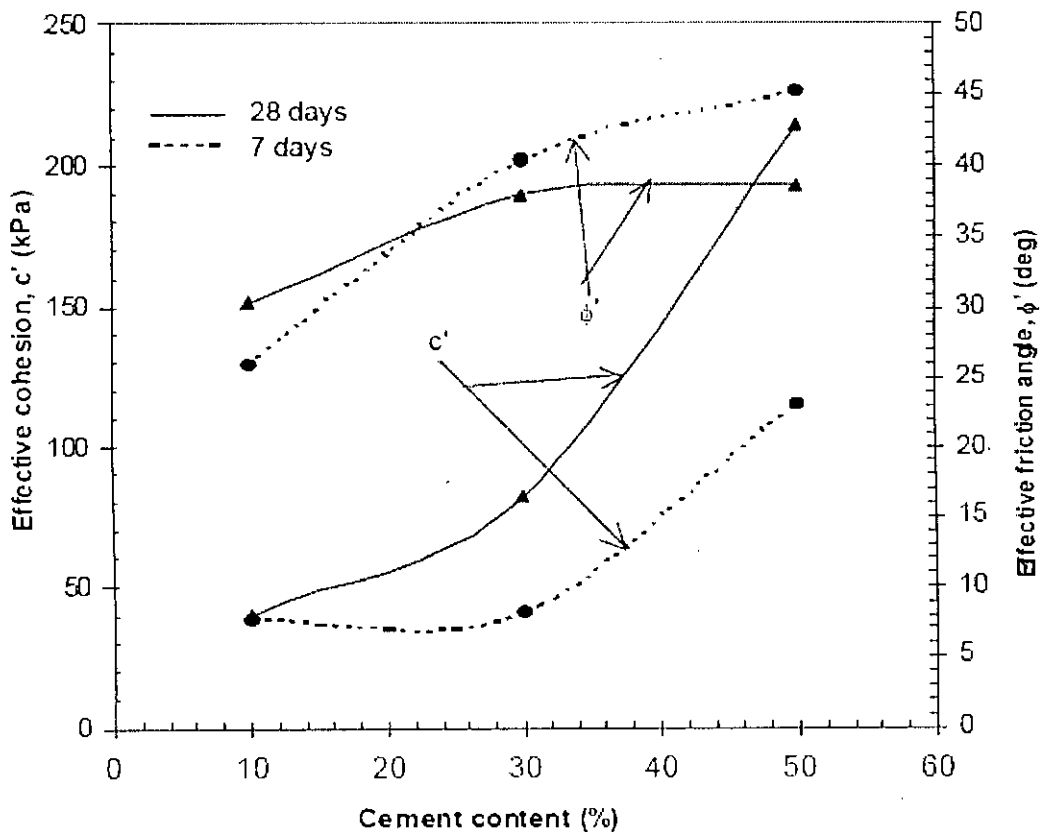


Fig. 2.41 Effect of Cement and Curing Time on Effective Shear Strength Parameters for Cement Treated Clays (after Kamruzzaman et al., 2004)

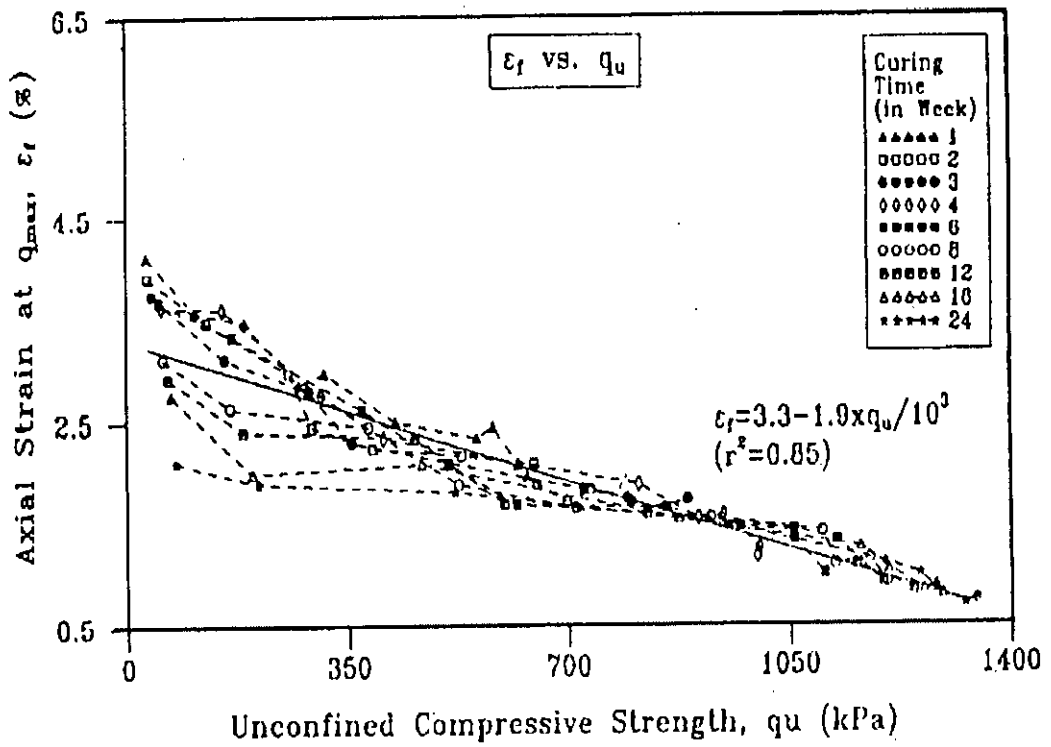


Fig. 2.42 Relationship between  $q_u$  and Axial Strain at  $q_{max}$  Shown in Terms of Curing Time for Cement Treated Clays (after Kamaluddin, 1995)

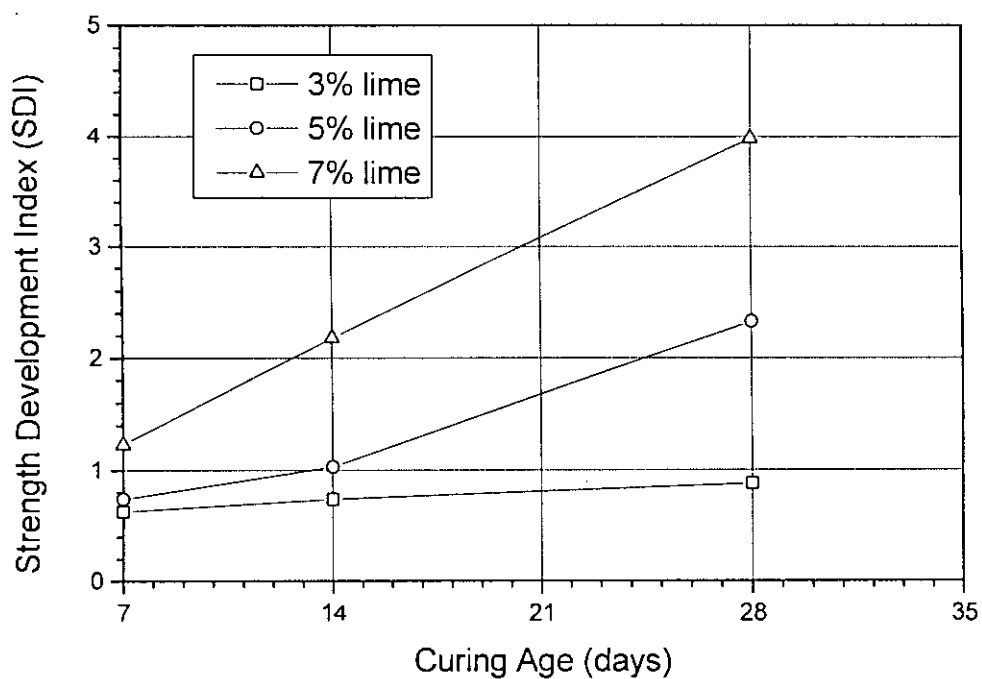


Fig. 2.43 SDI Versus Curing Age Curves for Samples of a Lime Treated Coastal Clays in Bangladesh (after Rajbongshi, 1997)

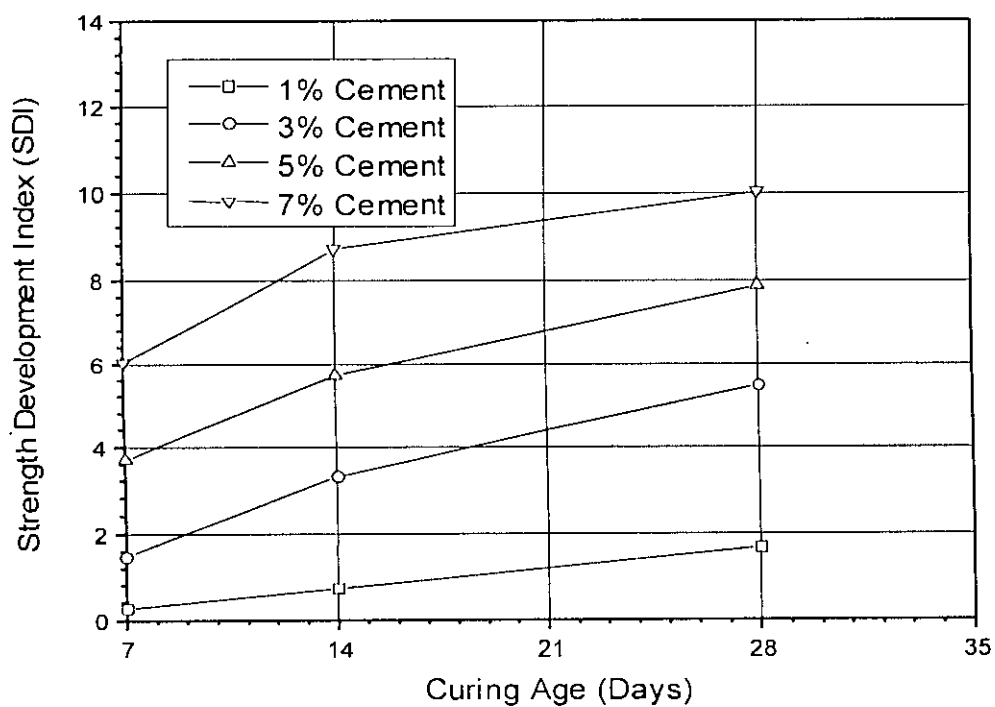


Fig. 2.44 SDI Versus Curing Age Curves for Samples of a Cement Treated Regional Clays in Bangladesh (after Hasan, 2002)



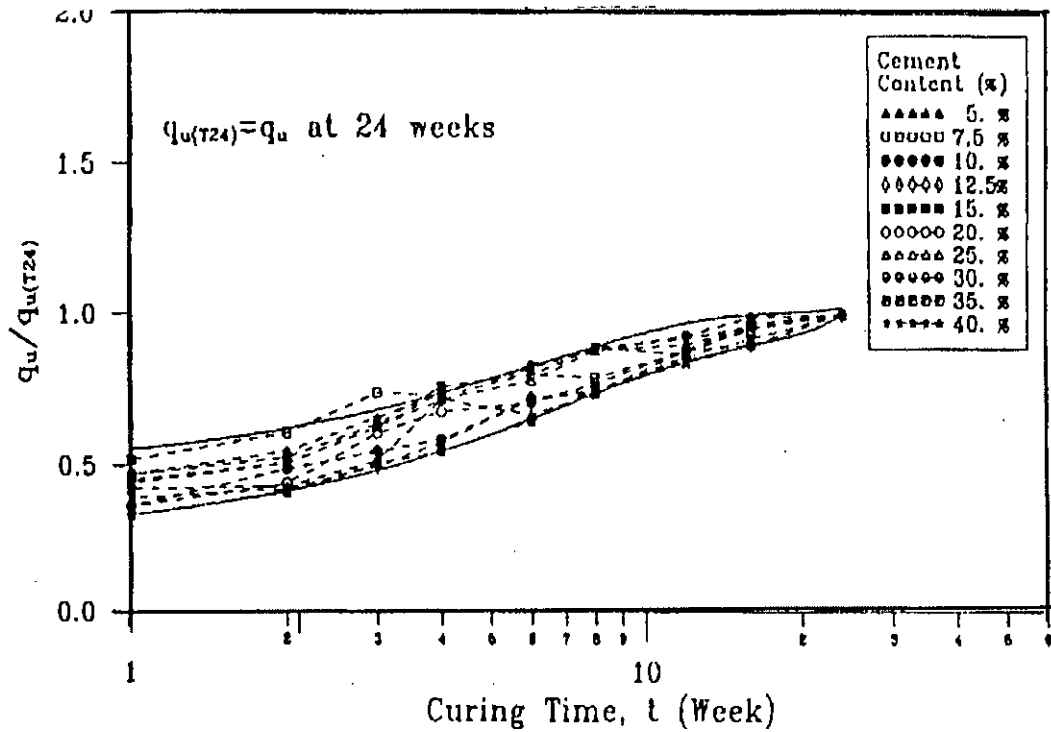


Fig. 2.45 Normalized Behavior of Unconfined Compressive Strength with Curing Time for Cement Treated Clays (after Kamaluddin, 1995)

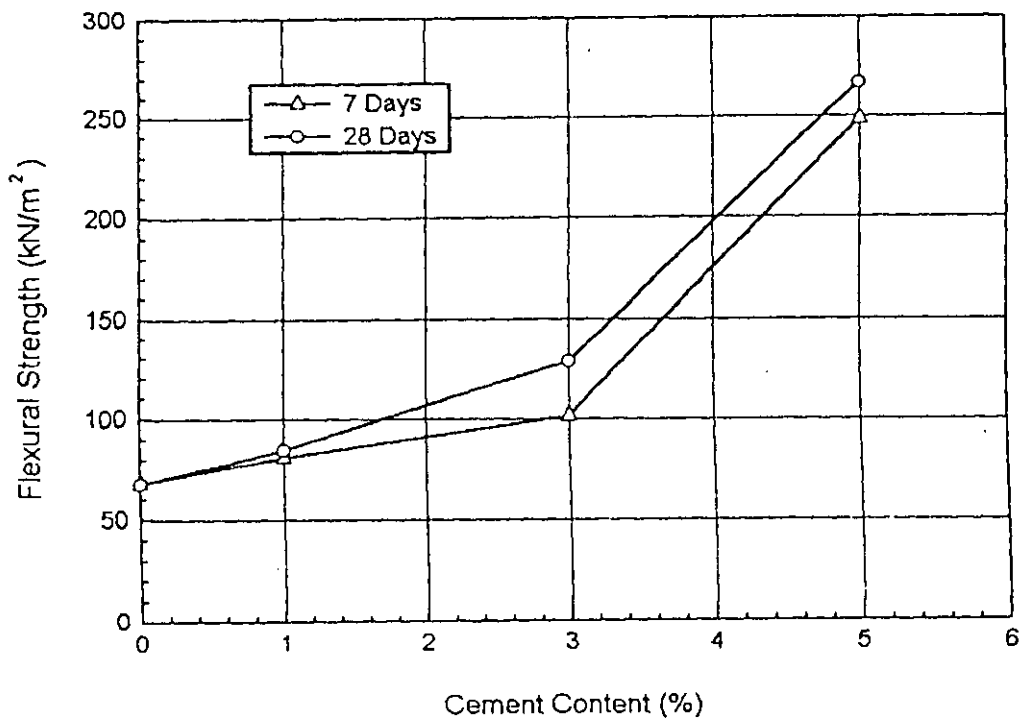


Fig. 2.46 Effect of Cement Content and Curing Time on Flexural Strength for Cement Treated Coastal Clays in Bangladesh (after Siddique and Rajbongshi, 2002)

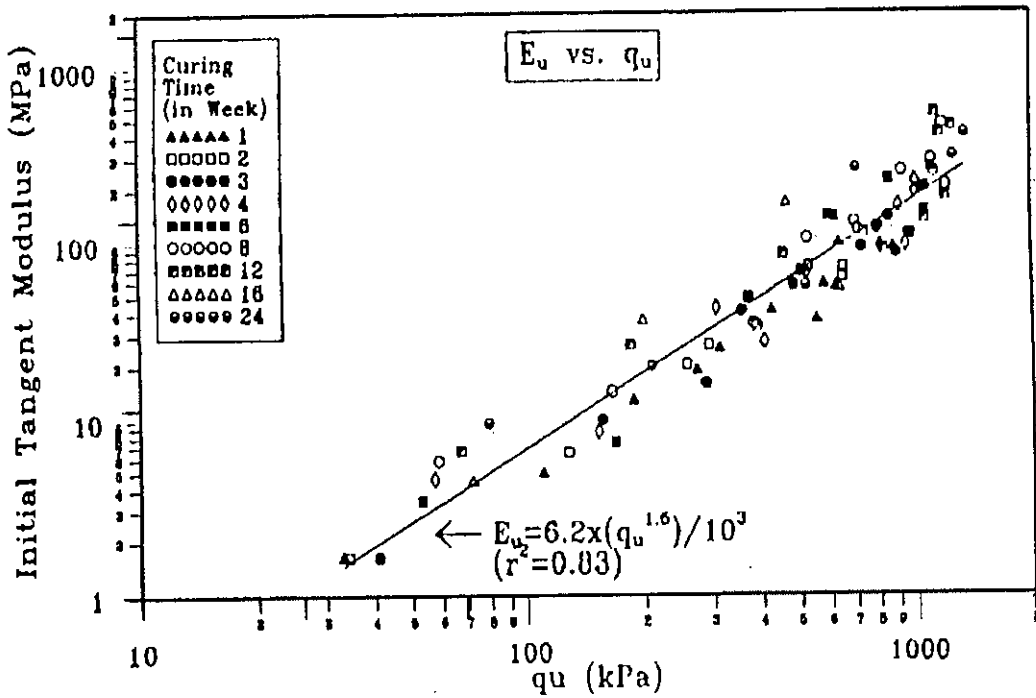


Fig. 2.47 Relationship between Initial Tangent Modulus and  $q_u$  in Terms of Curing Time for Cement Treated Clays (after Kamaluddin, 1995)

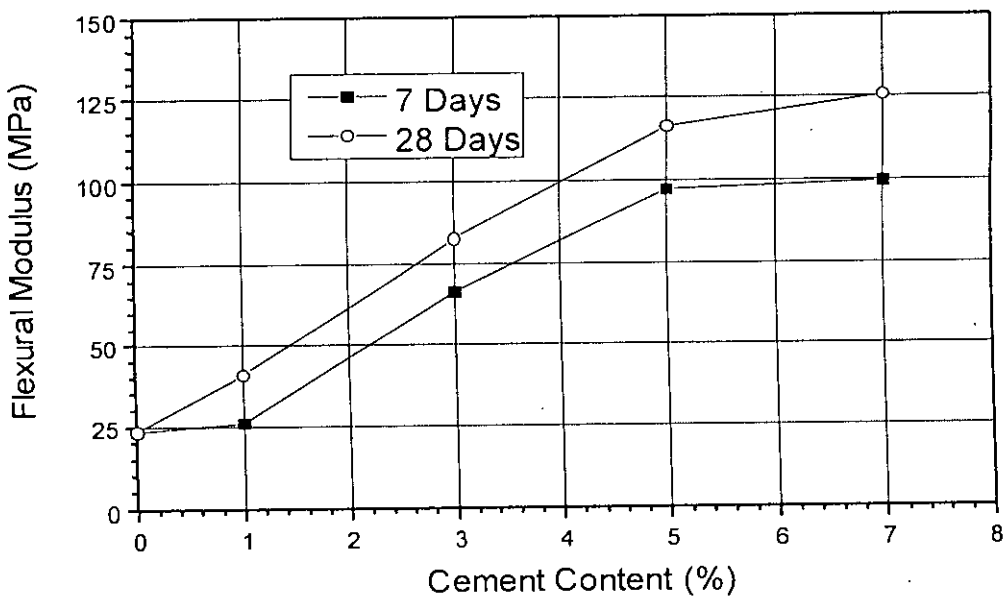


Fig. 2.48 Effect of Cement Content and Curing Time on Flexural Modulus for Cement Treated Coastal Clays in Bangladesh (after Hasan, 2002)

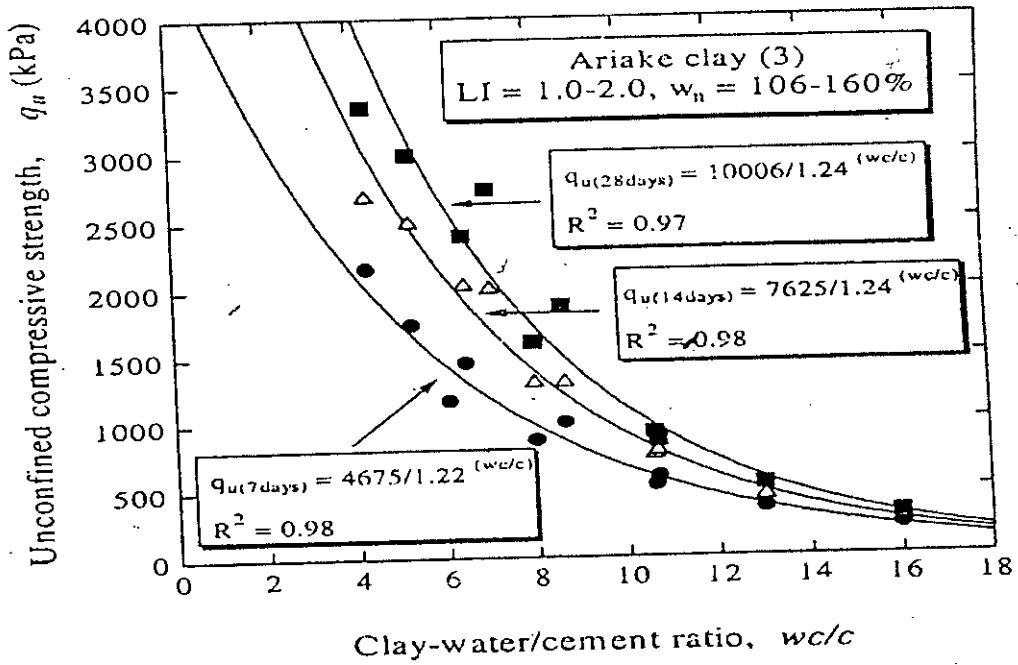


Fig. 2.49 Influence of  $w/c$  on the Strength Development of Cement Admixed Ariake Clay<sup>(3)</sup> with its Various Fabric Pattern (after Horpibulsuk et al. 2000)

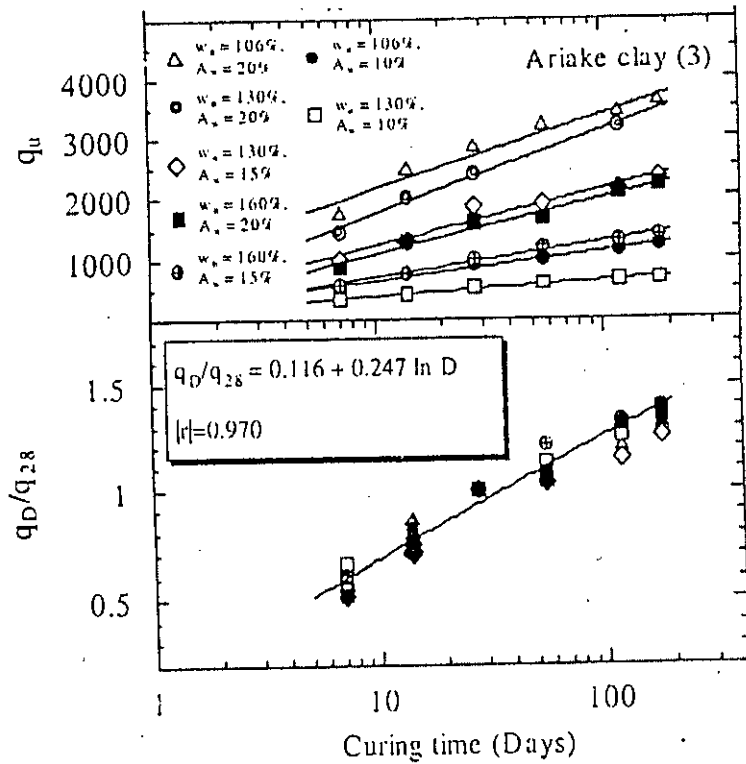


Fig. 2.50 Strength Development with Time and its Generalization of Cement Admixed Ariake Clay<sup>(3)</sup> (after Horpibulsuk et al. 2000)

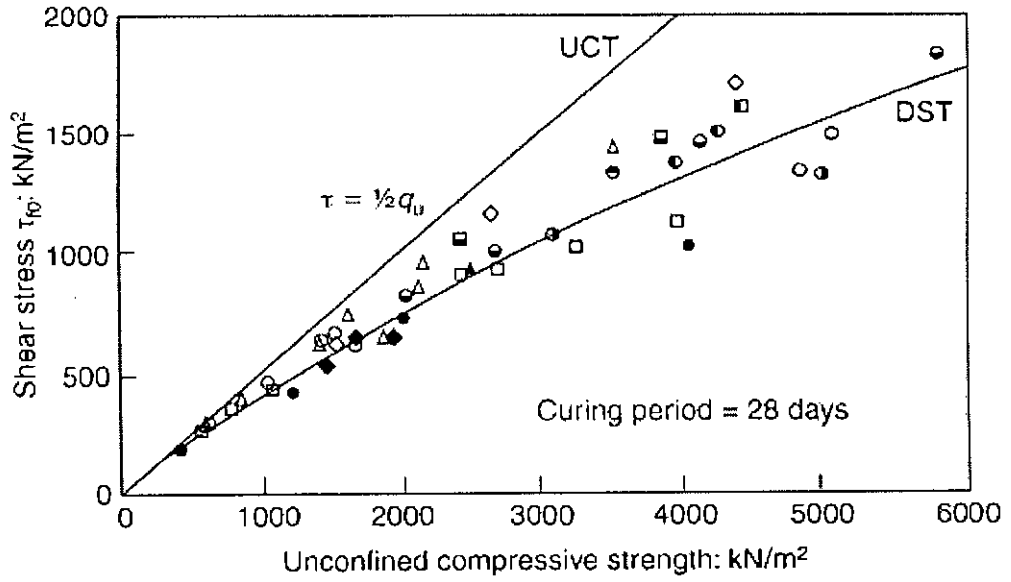


Fig. 2.51 Relation between DS and UC Test Results for Cement Treated Clays (after Porbaha et al., 2000)

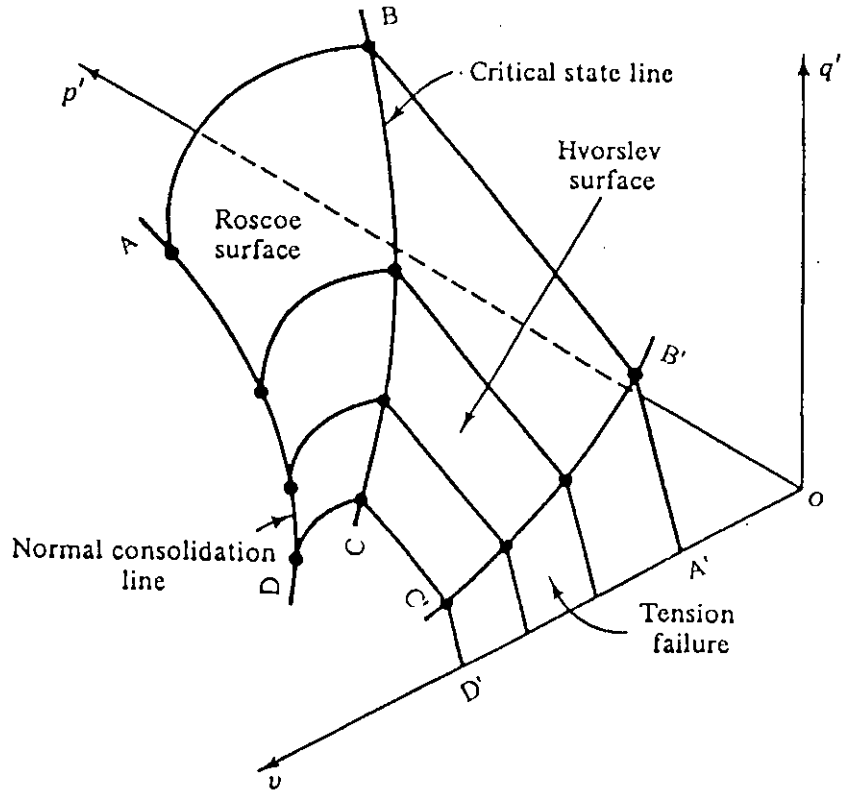


Fig. 2.52 Three Dimensional presentation for State Boundary Surface and Critical State Line (Atkinson and Bransby, 1978)

**Table 2.7 Values of Critical State Soil Parameters for Regional Clays of Bangladesh (Uncemented and Cemented State)**

Properties	Banskhali clay	Anwara Clay	Chandanaish Clay	Savar clay uncemented	Savar clay 7% cemented	Savar clay 14% cemented
$\lambda$	0.115	0.128	0.136	0.290	0.197	0.100
$\kappa$	0.019	0.023	0.03	0.033	0.03	0.01
N	2.29	2.37	2.45	1.603	1.75	1.80
M	1.34	1.32	1.31	1.16	1.25	1.30
$\phi'_c$	33.21°	32.75°	32.50°	29.08°	31.15°	32.29°
$\Lambda = (\lambda - \kappa) / \lambda$	0.835	0.820	0.783	0.886	0.848	0.900
LL (%)	34	40	45	43	43	42
PI (%)	10	16	20	26	21	18
$G_s$	2.69	2.70	2.72	2.68	2.64	2.60
Source of Data	after Siddique et al. (2003)			after Khaliullah (2007)		

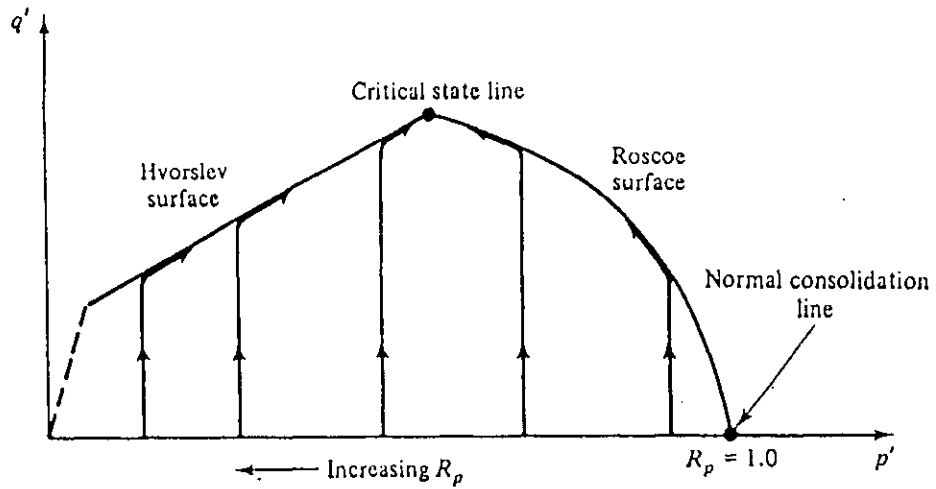


Fig. 2.53 Definitions of Hvorslev Surface, Roscoe Surface and Critical State Line (after Atkinson and Bransby, 1978)

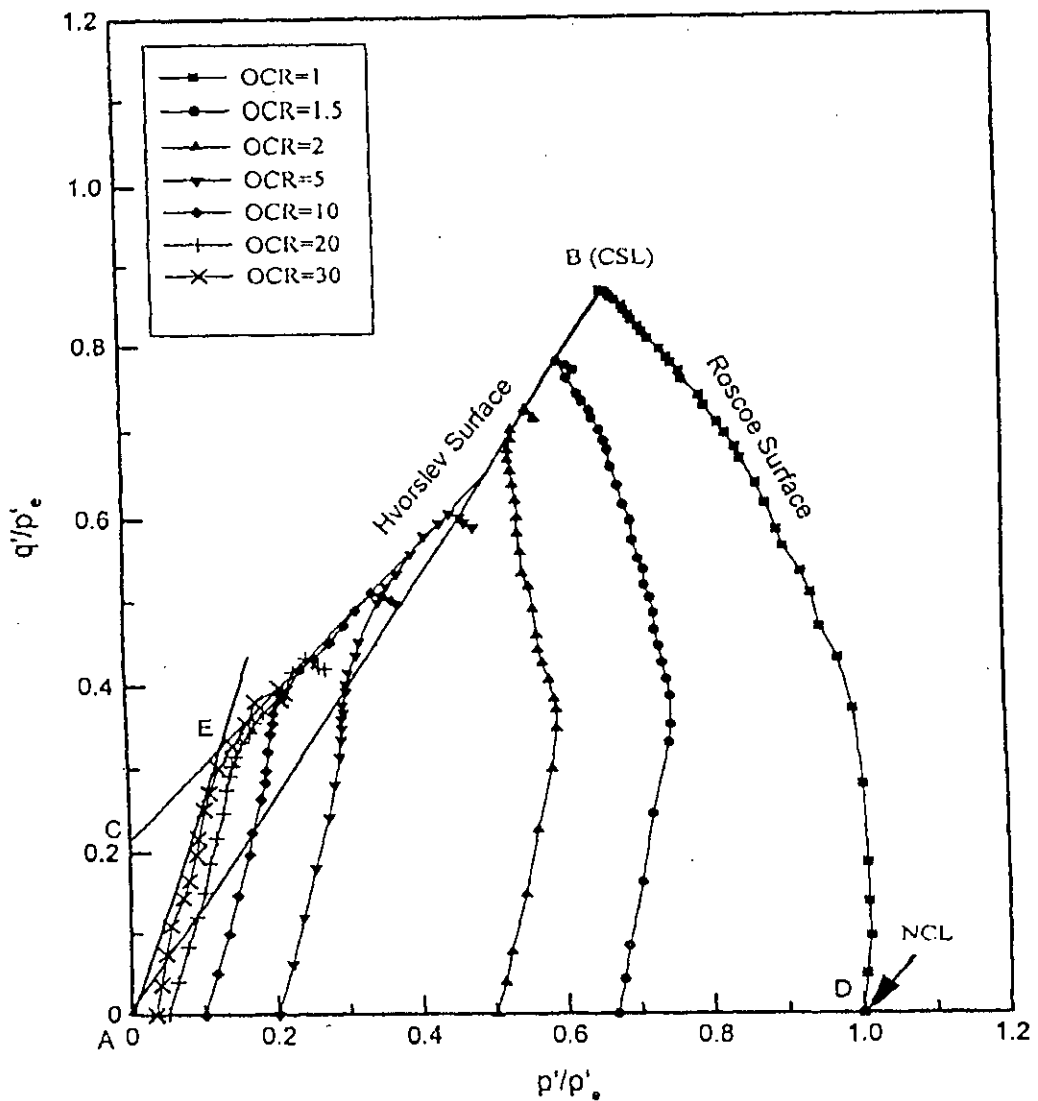


Fig. 2.54 Stress Paths, Roscoe Surface and Hvorslev Surface for Undrained Tests on Coastal Soil in Bangladesh (Siddique et al., 2003)

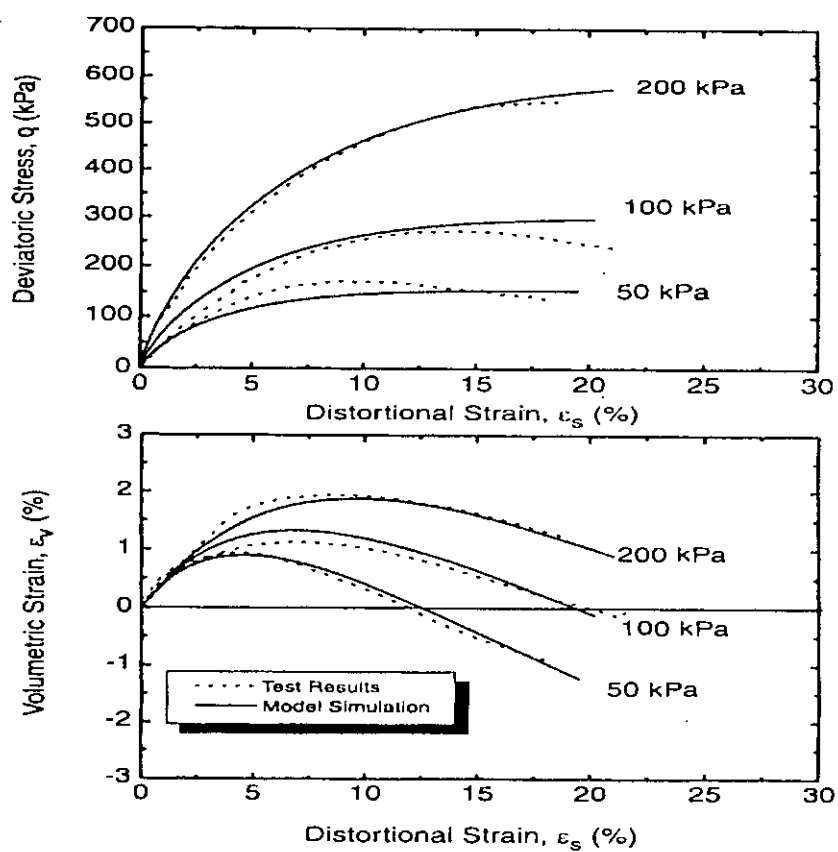
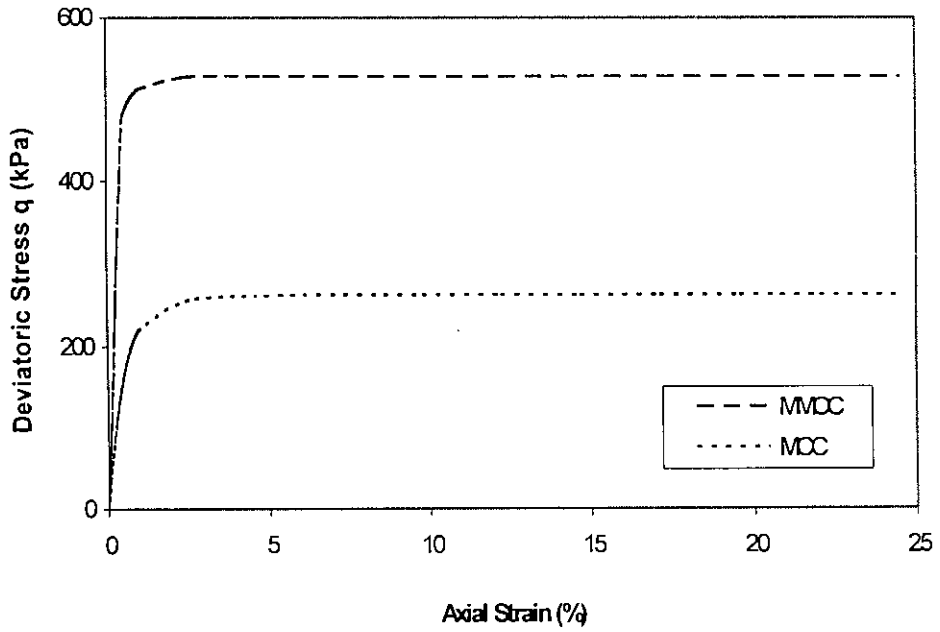
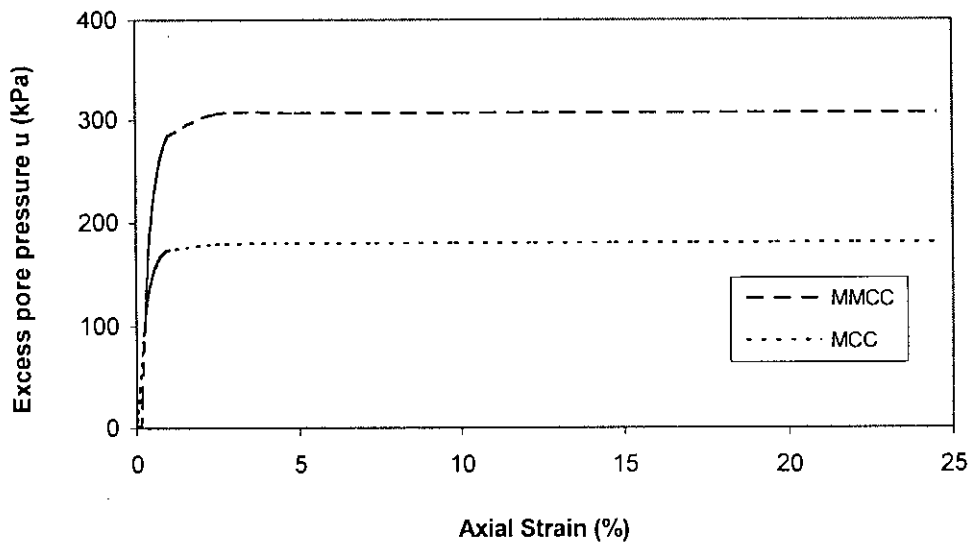


Fig. 2.55 Comparison of Constitutive Model prediction and Test results from Drained Test for Stabilized Soil (after Youwai and Bergado, 2003)



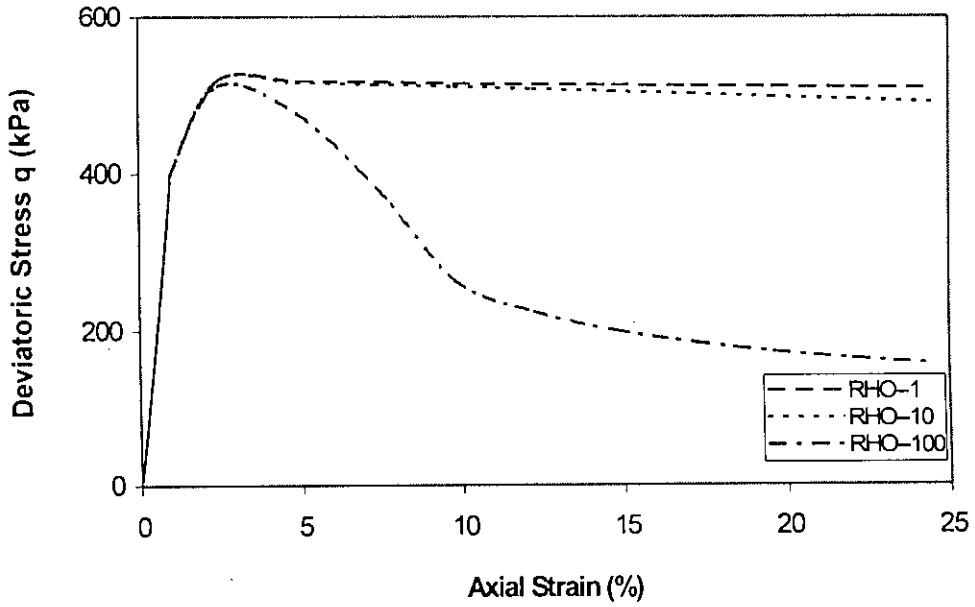
(a)



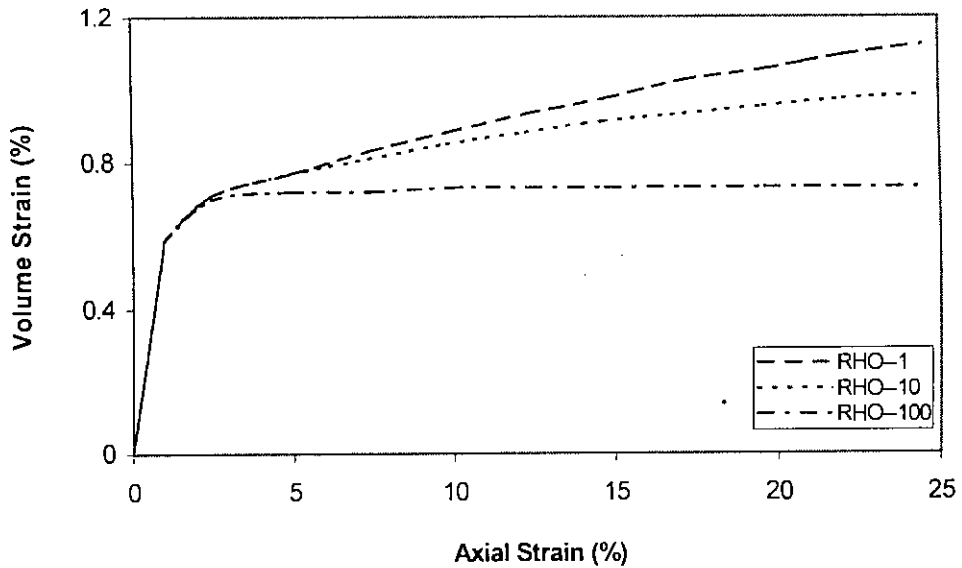
(b)

Fig. 2.56 Comparison of MCC and MMCC Model Prediction from Undrained Test for 7% Cemented Soil in Bangladesh (after Islam et al., 2007)



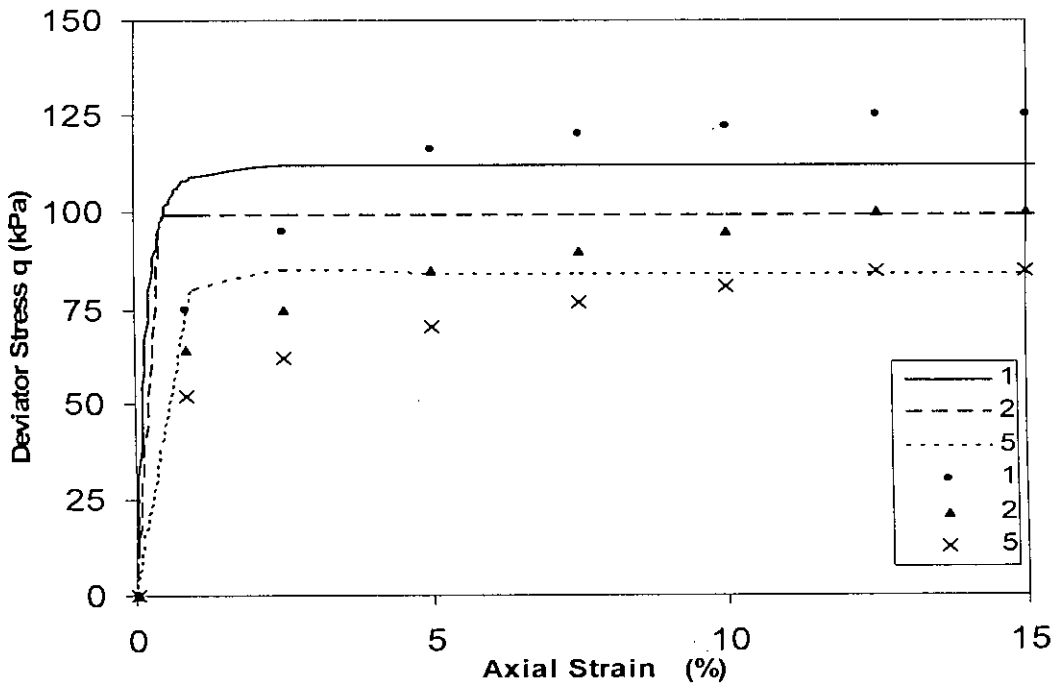


(a)

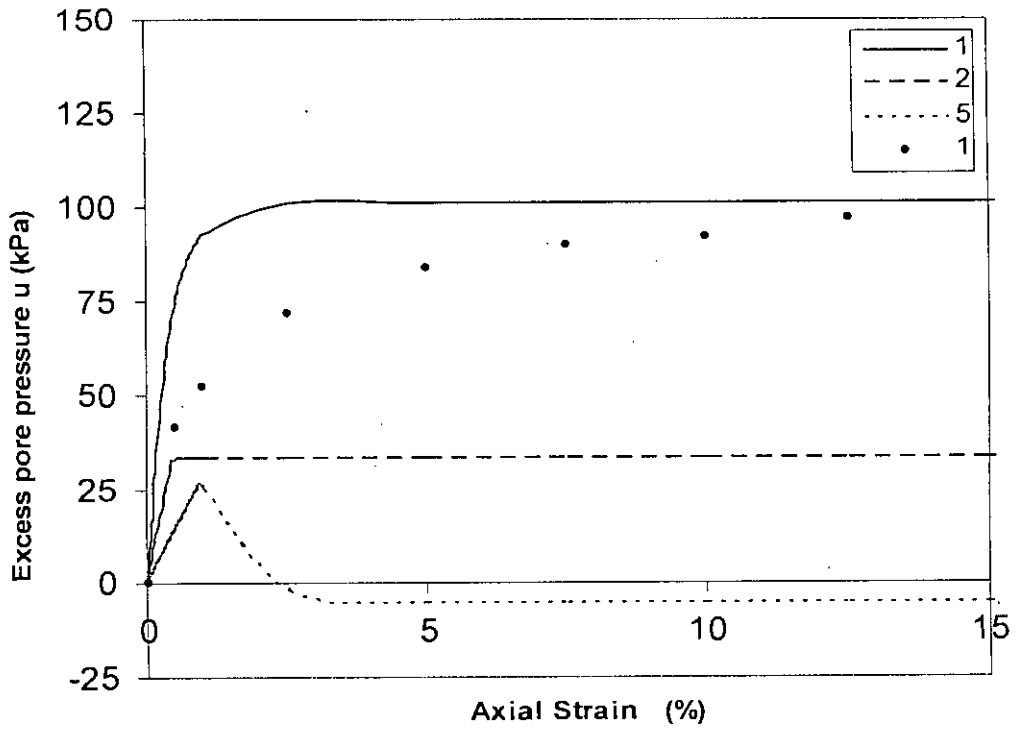


(b)

Fig. 2.57 Comparison of EMMCC Model Prediction at Different Cementation Breakdown Factors for 7% Cemented Soil in Bangladesh from Drained Test (after Khaliullah, 2007)



(a)



(b)

Fig. 2.58 Comparison of MCC and MMCC Model Prediction from Undrained Test for Uncemented Coastal Soils (OCR = 1, 2, 5) in Bangladesh (after Siddique et al., 2007)

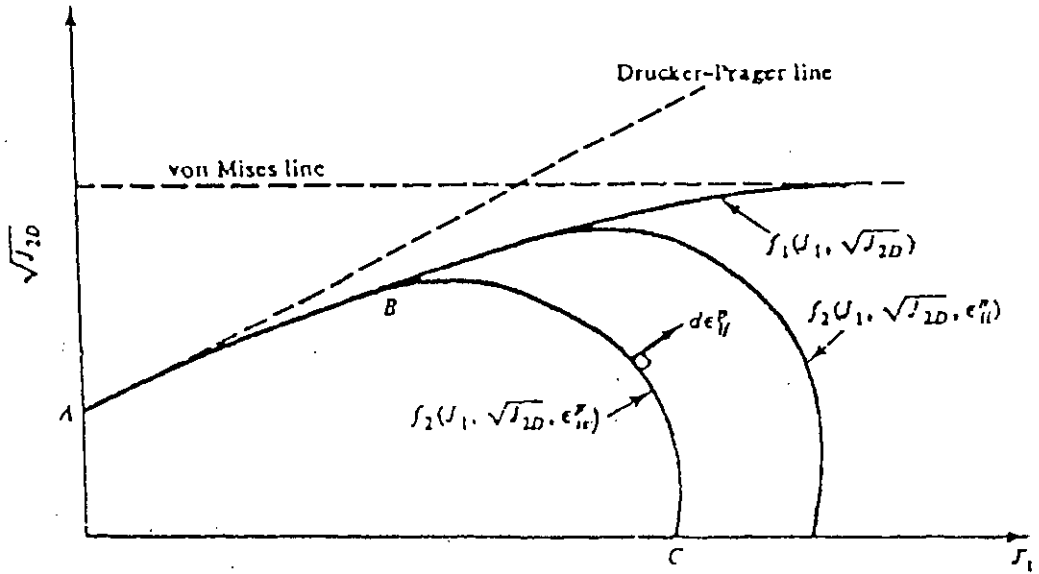


Fig. 2.59 CAP model for Soft Rock (after Desai and Siriwardane, 1984)

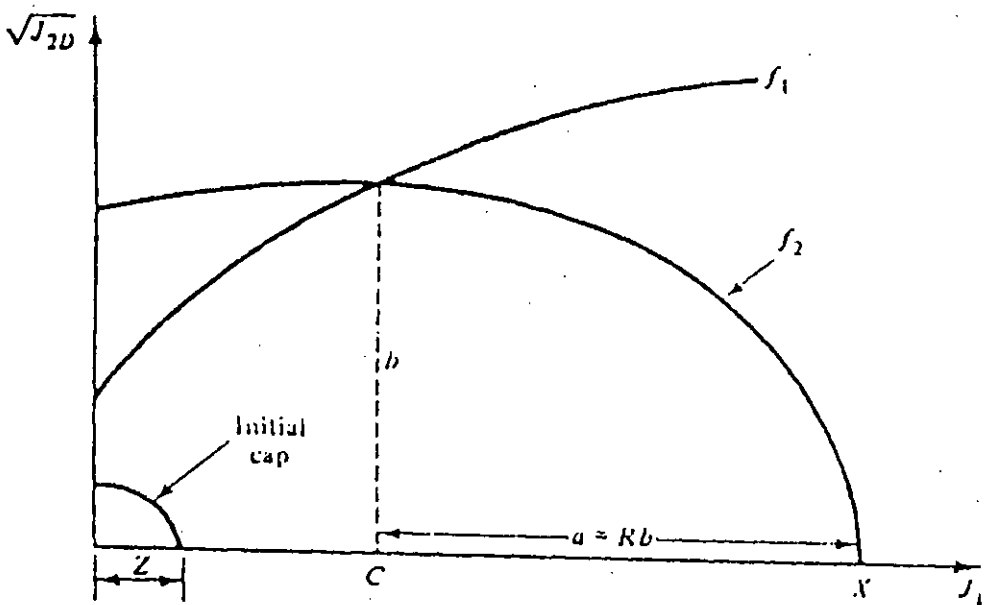


Fig. 2.60 Fixed and Yield Surface for CAP model for Uncemented Soils (after Desai and Siriwardane, 1984)

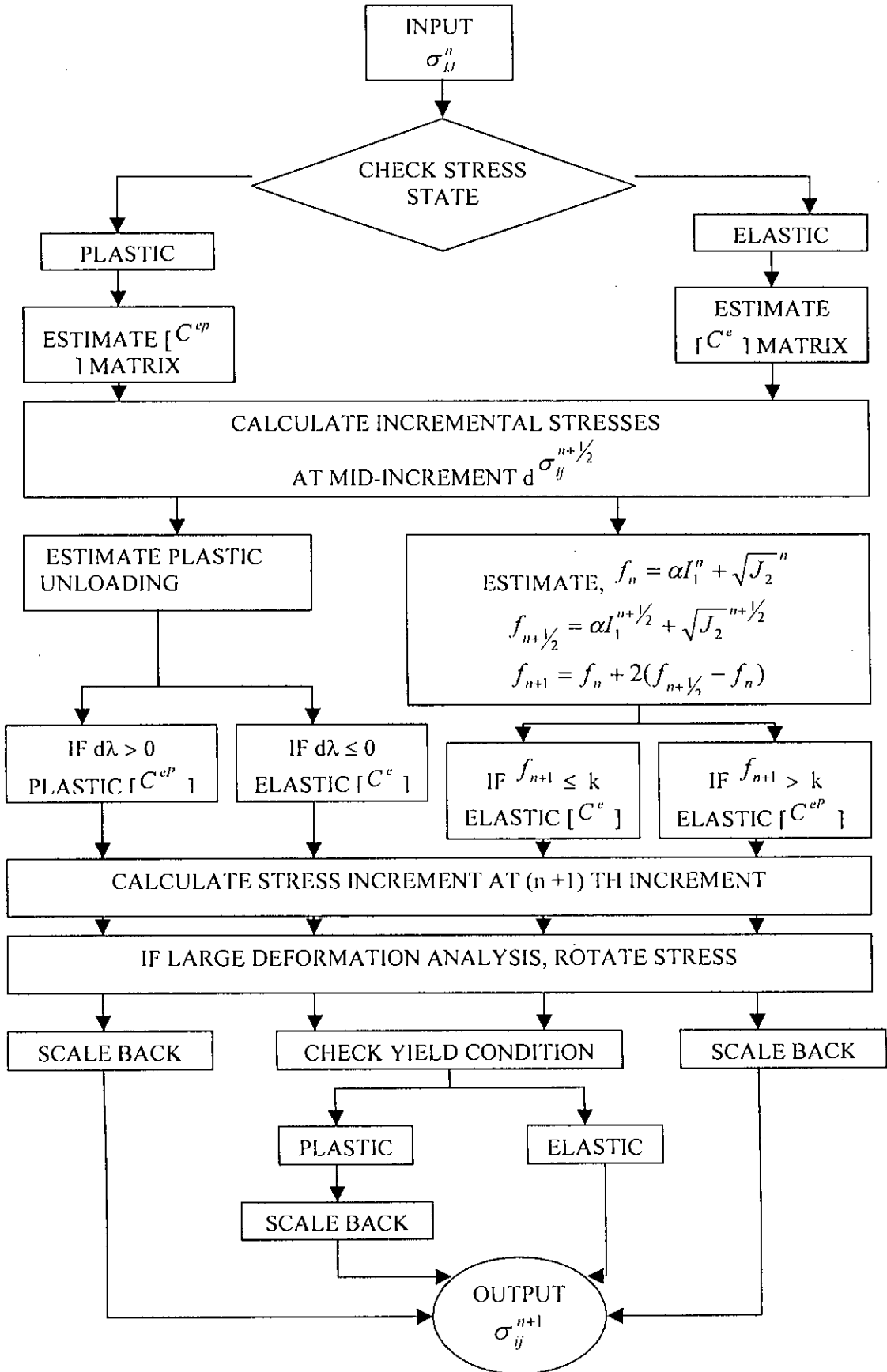


Fig. 2.61 Flow Chart for the Implementation of Coulomb and Prager Models in Cap Model (after Chen and Mizuno, 1990)

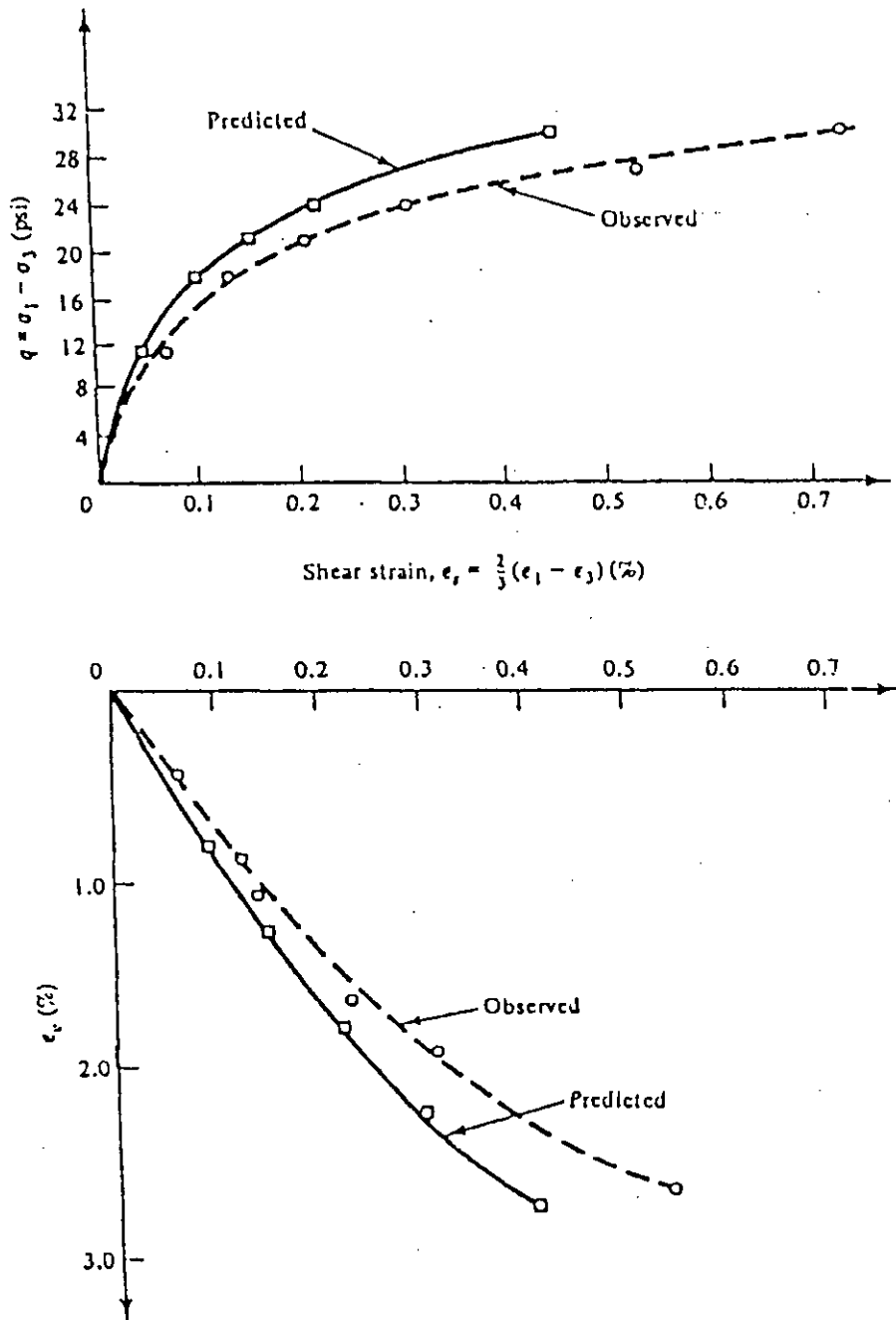


Fig. 2.62 Comparison of Cap Model Prediction and Test Results from Drained Test for Unstabilized Soil (after Desai and Siriwardane, 1984)

## CHAPTER 3

### LABORATORY INVESTIGATIONS, EQUIPMENT AND INSTRUMENTATION

#### 3.1 General

The individual scopes, limitations, apparatus and testing procedures for various tests performed are discussed in the relevant sections of this chapter. Sets of variables considered in the testing programme included a wide range of type of clay, type of admixture, clay-water/cement ratio, curing time, mixing water content of the clay slurry and effective confining pressure. The engineering behaviour of the treated clays was investigated by performing unconfined compression, direct shear, one-dimensional consolidation, triaxial drained and undrained tests.

The details of the experimental investigations followed in the research are discussed in the current chapter. Sampling procedure, methodology of soil sample preparations, test procedures, test programme and test apparatus used in the study are presented.

#### 3.2 Geology and Sub-Soil Conditions of the Project Sites

Bangladesh is a part of Bengal basin at the lower reaches of the three mighty rivers the Ganges, the Brahmaputra and the Meghna and their associated tributaries. Bangladesh, therefore, may be called the delta of this river system. The delta consists of a number of overlapping sub-deltas that were formed by intermingling of light coloured quaternary sediments that have been deposited by the three mighty rivers. The Himalayas were the major sources of these sediments. These sediments start from 0 m to about 8 m above mean sea level; other soil layers are marine deposition which is the result of changes in sea levels during the quaternary period. The sub-surface strata are constantly subsiding by the weight buildup of these sediments, compacted and maintaining the surface level in a condition of geological isostasy.

A lot of marshy and boggy areas are covered in Bangladesh and soft clays in this country are mainly available in the alluvial flood plain deposits, depression deposits and estuarine and tidal plain deposits. Geotechnical aspects for soil of Bangladesh were reported by Safiullah (1991) and Serajuddin (1992), while Mollah (1993) reported the geotechnical conditions of the deltaic alluvial plains of Bangladesh. Geological Map of Bangladesh is shown in Fig. 3.1 while Fig. 3.2 shows the various symbols used in the map. Based on geological considerations, Bangladesh can be conveniently divided into five major regions. These five regions are as follows:

- (i) North-western region or Gangetic plain: Rajshahi, Pabna division plus Dinajpur, Rangpur and Bogra districts.
- (ii) North-eastern region or Suma valley: Entire Sylhet division and North-eastern part of Mymensingh division.
- (iii) Central and eastern region: Dhaka division, South-eastern part of Mymensingh, Tangail, Gazipur and Western part of Comilla districts.
- (iv) South-western region: Khulna division plus Kushtia, Gopalganj, Faridpur, Jessore, Barisal, Patuakhali districts.
- (v) South-eastern region: Chittagong division plus Noakhali, Cox's Bazar, Rangamati, Banderban districts.

The layer features, thickness and different components of soil (mainly clay, silt and sand) at each layer of any district are similar and dissimilar with other districts in Bangladesh. The layer features and related components of soil (mainly clay, silt and sand) for different districts (Town) of Bangladesh are found on the basis of field tests i.e., Standard Penetration Test (SPT) and Geological Map of Bangladesh (Alam et al., 1990). The top layer of soil strata about 25 to 35 ft (7.6 to 10.7 m) contains clay and silt, and below these layers of soil strata contain sand and silt.

The samples used in the present investigation were collected from the Gazipur, Gopalganj and Khulna districts. The sample locations are shown in Fig. 3.1. The sub-soil conditions of Gazipur, Gopalganj and Khulna districts are summarized in the following paragraphs.

Sub-soil conditions in Gazipur district consists of inter-stream and older alluvial deposits contain yellowish-gray or gray to reddish-gray, light yellowish-gray/ brown, orange, light to brick-red and grayish-white soft to medium stiff / stiff clay, silty clay, silt from existing ground level to about 13 m depth and about from 13 to 15 m depth contain yellowish brown loose sandy silt and then about from 15 to 30 m depth contain brown medium dense to dense fine to medium sand.

Sub-soil conditions in Gopalganj district consists of stream and inter stream deposits contain light to yellowish-gray, gray, bluish-gray soft to medium stiff clay, silty clay, silt from existing ground level to about 9 m depth and about from 9 to 11 m depth contain gray loose sandy silt and about from 11 to 30 m depth contain gray medium dense to dense fine to medium sand.

Sub-soil conditions in Khulna district consists of tidal and deltaic deposits contain light to greenish gray, yellowish-gray, gray, bluish-gray, yellowish-gray soft to medium stiff clay, silty clay, silt with occasionally organic soil layers from existing ground level to about 15 m

depth and about from 15 to 30 m depth contain gray medium dense to dense fine to medium sand.

### 3.3 Properties of Soft Base Clays Used

The clays were collected from the south-western region, central and eastern region of Bangladesh. Samples of soft clay were collected from the location at Gazipur, Gopalganj and Khulna districts of Bangladesh as mentioned earlier. The natural water content of clays was in a range of 53% to 70%. The water table was varied from 1.0 to 2.0 m depth below from the existing ground level at time of collection. The high plastic clay was collected from a low land beside boundary wall of Titas Gas office in Gazipur. The low to medium plastic clays were collected from low land beside Embankment (Chainage: 12 km) of Gopalganj-Bhatiapara road in Gopalganj as from Foundation trench of Academic Building, Khulna University of Engineering and Technology (KUET) in Khulna. The basic index properties of the clays are shown as below:

Location (Districts)	Natural water content	LL (%)	PL (%)	PI (%)	Unified Soil Classification System
Gazipur	70	78	32	47	CH
Gopalganj	62	47	25	22	CL
Khulna	53	33	20	13	CL

### 3.4 Sampling Procedure

Soil sampling was carried out by open excavation at a depth of about 2.0 to 3.0 m as disturbed samples used for cement and lime treatment. Disturbed samples were collected in plastic polythene bags, secured and tied up tightly to make these airtight to prevent loss of natural water content and not to be changed in dry state. Undisturbed samples were retrieved using 100 mm diameter and 450 mm long open-drive tube sampler from depths of 2.0 to 3.0 m. This depth was chosen so that the sample obtained would be uniform in composition for finding the actual in-situ base clay conditions. The site was also chosen for its natural clayey soil conditions. All sampling tubes were immediately sealed at both ends with paraffin wax to prevent the loss of natural moisture. All samples were then transported from above districts to Geotechnical Engineering Laboratory of BUET and stored in a about constant-temperature humid room for later extrusion.



### **3.5 Admixtures Used**

Cement and lime are used as admixtures in this research. Both materials are the suitable binding material for soft soil improvement.

#### **3.5.1 Type of Cement Used**

"Holcim" as Hyundai cement, Type 1 Portland Cement, refined by the Holcim Cement Company, Bangladesh, was used in this research works. The major compositions of the cement are listed in Table 3.1. A total of 20 bags of cement were purchased from the market, one in each month. Immediately after receiving per bag cement at Geotechnical Engineering Laboratory, cement powder of weight 2 kg was packed in double-layered plastic polythene bags. In order to prevent hydration of the cement powder and to maintain the freshness of the powder, the plastic polythene bags were secured and tied up tightly to make these airtight.

#### **3.5.2 Type of Lime Used**

Quicklime powder or Calcium oxide (CaO), commercially produced locally by burning lime stone in Sylhet, Bangladesh, consisting of not less than 95% CaO was used this research works. The quicklime powder was purchased from market in a packet condition as a 2 kg lime sealed per bag. To ensure that the quicklime was not exposed to air and moisture, to prevent slaking and carbonation prior to the lime treatment of the clay samples, to take care was taken it all times.

#### **3.5.3 Admixture Content**

The clay-water/cement ratio (designated as  $w/c$  ratio) has been used as a prime parameter in this research, which governs the engineering behaviour of soil samples. The clay-water/cement ratio ( $w/c$  ratio) is defined as the initial water content in clay divided by the cement content. The cement content is found in percentage by dividing the percentage initial mixing water content by  $w/c$  ratio. The cement content ( $c$ ) of the test samples, is defined as the ratio of the weight of cement powder to the dry weight of the soil and is expressed as a percentage. Similarly, lime content ( $l$ ) is defined as the ratio of the weight of lime used to the dry weight of soil that was treated, expressed as a percentage. Knowing the total weight of soil and the water content of the base clay to be treated, the amount of cement or lime to be used was calculated.

### **3.6 Methodology Used for Sample Preparation**

The intentional increase in water content is to simulate the high water content increase taking place in the wet method of dispensing cement admixture in deep mixing at low land and the significant increase taking place in jet grouting. The clay with its water content corresponding to the above simulating levels quantity of cement resulting in clay-water / cement ratio (designated as  $w/c$ ) of 7.5, 10 and 15 was thoroughly mixed so as to ensure uniform

dispersion of the cementing agent (ordinary Portland cement). The initial water content (designated as  $w_i$ ) would be 120%, 150%, 200% and 250%. Cement contents (designated as  $c$ ) as low as 8% and as high as 33% were adopted for the clay-cement mixtures of initial clay water content of 120% at  $w_i/c$  of 15 and initial clay water content of 250% at  $w_i/c$  7.5, respectively. The estimated required amount of the base clay was thoroughly mixed with cement slurry with gloved hands. The artificially prepared clay paste was passed through a 2-mm sieve for removal of shell pieces and other bigger size particles. The cement slurry was prepared with the required amount of cement with water. The mixing of the hardening agent and the clay was done until the mixture was uniformly mixed, the mixing being done within 10 minutes. Such a uniform paste was transferred to cylindrical split moulds of 50 mm diameter  $\times$  100 mm height and 75 mm diameter  $\times$  100 mm height with connecting 50 mm height top collars and bottom ended cap, taking care to prevent any air entrapment by shaking but without compaction blows. Cylindrical moulds of 50 mm diameter  $\times$  100 mm height were used for unconfined compression and triaxial compression test samples preparation. Cylindrical moulds of 75 mm diameter  $\times$  100 mm height were used for one-dimensional consolidation and direct shear test samples preparation. After 24 hours the cylindrical samples were dismantled. All the cylindrical samples were wrapped in thick polythene bags and these were stored in a room of approximate constant temperature ( $25 \pm 2^\circ\text{C}$ ) until the lapse of different planned curing times.

### **3.7 Preparation of Specimens for Testing**

When the samples had been allowed to cure for the required time, the prepared cement treated clay was opened from the polythene bag. Then the sample was trimmed to the size required for the specific test to be conducted, i.e., to 38 mm diameter  $\times$  76 mm height for the unconfined compression and triaxial compression tests and to 63.5 mm diameter  $\times$  25.4 mm height for the consolidation and direct shear tests. The water content of the clay was determined with trimmed out soil and the unit weight of the sample was determined by measuring the weight and dimension (diameter and height) prior to the testing. One-dimensional consolidation, direct shear and triaxial compression tests were carried out on treated samples after 4 and 12 weeks of curing time. Unconfined compression tests were run on treated samples after 1, 2, 4, 12, 24, 52 and 104 weeks of curing time.

### **3.8 Scope of Experimental Investigations**

#### **3.8.1 Test Variables**

In order to carry out the comprehensive study of the strength and deformation characteristics of the cemented clays, the effects of several test variables were considered. The test variables include as follows:

- (i) type of clay
- (ii) type of admixture
- (iii) initial mixing water content
- (iv) clay-water/admixture ratio
- (v) curing time
- (vi) effective confining pressures
- (vii) drainage condition during testing

Depending on the plasticity of clays, the soils are selected in this research at different zone of Bangladesh. So, the types of clay were considered as a variable in this research. There are so many marshy, boggy and low land in Bangladesh and clays of these area contain high water content overall all seasons, so the different amount of high mixing water content were considered as another variable in this study. Sometimes, water drainage managements and applied pressure systems were controlled on these low land area for various purposes. To increase the variety boundaries of the research, type and different amount of binding materials were counted as the test variable. Maturity of stabilization samples depend on effective times, so curing time were a very essential parameter. Practically, one month and three months are very reasonable time for application of loads, importance of these two curing times were stressed in this study. Ultimate goal of this research, to improve these low land soils for construction of lightly loaded and temporary structure by deep mixing method to intrusion of cement/lime treated clay's columns. This laboratory investigation on strength and deformation for treated clays is an attempt to model deep mixing method for a vast area to improve its strength and compressibility. The details of the test variables are summarized as shown in Table 3.2.

### **3.8.2 Characteristics of the Base Clay**

The initial properties of the base clay, prior to the cement stabilization was important in order to determine the relative influences of cement treatment. It was also required to establish the degree of improvement caused by cement stabilization on the properties of the untreated clay. So, the basic physical, chemical, mineralogical and micro-structural properties of the base clay were established first, prior to the testing work of treated samples. The strength-deformation properties were determined by the unconfined compression, direct shear, consolidation and triaxial tests for in-situ base clay from undisturbed samples. Table 3.3 shows the scope of experimental work for the untreated base clay.

### **3.8.3 Characteristics of Treated Clays**

The final properties of base clay were completely changed after cement and lime treatment on the basis of different curing times. Experiments were conducted to determine the changeable

engineering parameters for cement and lime treated clay. The following properties of the treated clays were determined.

- (i) The basic physical, chemical, mineralogical and micro-structural properties of cement treated clays.
- (ii) Strength and deformation characteristics of both cement treated and lime treated clays were determined from unconfined compression test and one-dimensional consolidation tests.
- (iii) Strength and deformation characteristics of cement treated clays were determined from consolidated direct shear test, UU, CIU and CID triaxial compression tests.

Table 3.3 shows the scope of experimental investigation for cement treated clay.

#### **3.8.4 Number of Treated Samples depending on Test Variables**

According to test variables using type of clay, mixing water content and clay-water/admixture ratio, the total number of treated samples are shown in Table 3.4. Three soft clays were used in this study having plasticity index (PI) values of 47%, 22% and 13%. The clays with PI values of 47%, 22% and 13% are designated as C1, C2 and C3 respectively. There are four types of initial mixing water content ( $w_i$ ) used in this study such as 120%, 150%, 200% and 250%. There are three types of clay-water/cement ratio ( $w_c/c$ ) used in this study such as 7.5, 10 and 15. In this respect, the total numbers of cement treated samples are counted to thirty six. There are two types of binding material also used in this research such as cement and lime. Binding material cement is successfully applied with the proper ratio on each mixing high water content but lime is successfully applied with proper ratio on 120% and 150% mixing water content only and lime is failed to bind with the ratio on 200% and 250% mixing water content because the binding capacity of lime was out of boundary line with that ratio on much high water content i.e., 200% and 250%. In this respect, the total numbers of lime treated samples are counted to be eighteen.

### **3.9 Chemical, Mineralogical, Micro-structural and Physical Properties**

A summary of the chemical, mineralogical, micro-structural and physical tests for the untreated and treated clays conducted in this study has already been presented in Table 3.3.

#### **3.9.1 Chemical Property Tests and Test Programme**

The chemical properties of the base clays include the soil pH, organic content, salt concentration, cation exchange capacity, exchangeable cations, and electrical conductivity. The chemical properties were determined according to the procedures guided by BS 1377 (1990) and Jackson (1985). The chemical tests were performed in the Environment Engineering Laboratory of the Bangladesh University of Engineering and Technology

(BUET), Environment Engineering Laboratory of the Dhaka University of Engineering and Technology (DUET) and Soil Research Laboratory of the Soil Resource Development Institute (SRDI).

### 3.9.1.1 pH Test

The pH of dilute soil solution has been determined by the colourimetric method. Certain dyes, known as pH indicators, change colour in a definite manner, according to the acidity or alkalinity of the solution in which they are mixed. The best-known indicator is litmus, which is red in an acidic soil solution and blue in an alkaline soil solution. The colour is converted to numerical pH chart. The neutral soil solution is expressed by numerical pH value 7. If pH value exists above 7, soil solution is alkaline and pH value exists below 7, soil solution is acidic in nature. The low pH reveals that the clay contains a significant amount of  $H^+$  ions.

The pH of dilute soil solution has also been determined by the digital indicator for untreated and treated samples. In this method, Metrohm 691 glass electrode pH meter is directly pushed in soil suspensions, where soil and water ratio used as 1 : 2.5. pH tests were conducted on forty two treated clays and three on base clays. The details summary of pH test programme are shown in Table 3.5.

### 3.9.1.2 Loss on Ignition Test

Loss on ignition of soil solid is the reduction of temporary chemical substances which are identified as peat, mucks, and soil containing relatively undecayed or undecomposed vegetable matter or fresh plant materials such as wood, grass or alkaline and carbonaceous materials such as lignite, coal, carbonate etc and also efflorescence effect of treated cement. Loss on ignition is defined by the percentage of weight difference in between the conditions,  $110 \pm 5^\circ C$  temperatures during 24 hours and  $445 \pm 10^\circ C$  temperatures during 6 hours. At high temperature,  $445^\circ C$ , all burning matters are burned within 6 hours and rested only soil solid portions. Three tests on base clay and twenty four tests on treated samples were conducted by loss on ignition. The details summary of loss on ignition test programme is shown in Table 3.6.

### 3.9.1.3 Organic Content Test

Organic matter in soil is derived from a wide variety of animal and plant remains so there can be a great variety of organic compounds It has undesirable effects on the engineering behaviour of soils. A measure of the organic content of soils is necessary in order to make allowance for these effects. The undesirable effects on the engineering behaviour of soils are minimized and improved by chemical stabilization. The organic content of soil has been determined by the Dichromate wet oxidation. The organic content of dilute soil solution by dichromate oxidation method is the percentage of  $(0.67 \times V/m)$ , where V is the volume of potassium dichromate used to oxidize the organic matter in the soil, initial mass m, which is

the mass of passing 10 mm sieve.  $V$  is measured by titration with ferrous sulphate and is given by  $V = 10.5 \times (1 - y/x)$ . Where  $y$  = total volume of ferrous sulphate used in the test and  $x$  = volume used in standardization test. According to Organic content test was three base clays and eighteen treated samples. The details summary of organic content test programme are shown in Table 3.7.

#### 3.9.1.4 Electrical Conductivity Test

The salinity of clay is measured by the electrical conductivity (EC) test. The amount of salts are dissolved in the pore water which are responsible for amount of soluble cations. When clay particles settle in water during stabilization, deposits formed have a flocculated structure. The degree of flocculation of a clay deposit depends upon the location, type and concentration of clay particles, amount of cement and the presence of salts in water. Clays settling out in a salt water solution have a more flocculent structure than clays settling out in a fresh water solution. The amount of salts in clay act as an electrolyte and reduces the repulsive forces between particles. Stabilized soils with a flocculent structure are light in weight and have a high void ratio and water content. However, these soils are quite strong and can resist external forces because of strong bond due to attraction between particles. The stabilized soils are insensitive to vibration. In general, the stabilized soils with flocculated structure, have a low compressibility, a high permeability and a high shear strength.

The electrical conductivity (EC) was determined by Metrohm 644 conductivity meter from soil solution, where soil and water ratio used as 1 : 5. The electrical conductivity of the hydrogen ions ( $H^+$ ) in a very dilute soil solution is almost double that of the hydroxyl ions ( $OH^-$ ). Electrical conductivity of a solution can therefore be related to its pH, and although the converse is far more complex, this property is made by electrometric method of determining pH. According to electrical conductivity tests were programme, the eighteen tests were performed on treated clays and carried out of three tests were performed on base clays. The details summary of electrical conductivity test programme are shown in Table 3.7.

#### 3.9.1.5 Cation Exchange Capacity Test

The cation exchange capacity (CEC) for Potassium, Sodium, Calcium and Magnesium were determined through Atomic Absorption spectrometer and Na, K were determined by Flame photometer from soil extraction where 1N  $NH_4OAc$  were used for extracting solution. Total nitrogen was determined by Kjeldahl method accordingly 3 steps namely digestion, distillation and titration. The apparatus were used centrifuge machine, centrifuge tube (50 ml), volumetric flask (100, 250, 1000 ml), funnel (7.5 cm dia), filter paper and beaker. The reagents were ammonium acetate ( $CH_3COONH_4$ ), glacial acetic acid  $C_2H_4(OH)(COONa)_3H_2O$ , ammonia ( $NH_3$ ), ammonium chloride ( $NH_4Cl$ ), ammonium oxalate  $(NH_4)_2C_2O_4 \cdot H_2O$ , silver nitrate ( $AgNO_3$ ), sodium chloride ( $NaCl$ ), isopropyl alcohol (99%).

Cation exchange carpeting test programme, eighteen tests were performed on treated clays and conducted three tests were performed on base clays. The details summary of cation exchange test programme are shown in Table 3.7.

#### **3.9.1.6 Exchangeable Cations Test**

The exchangeable cations were measured from soil extract (extracting soil using 1M KCl) titrate with 0.02M NaOH also using a few drops of phenolphthalein indicator. In this test, the amount of  $\text{Na}^+$ ,  $\text{K}^+$ ,  $\text{Ca}^{++}$  and  $\text{Mg}^{++}$  are determined by chemical reactions. Exchangeable cations test were run on the number of eighteen tests were performed on treated clays and the number of three tests were performed on base clays. The summary of exchangeable cations test programme are shown in Table 3.7.

#### **3.9.2 Mineralogy Test and Test Programme**

The determination of the clay mineralogy of the untreated and treated clays were done by X-ray Diffraction (XRD) analysis in Materials and Metallurgical Engineering Laboratory of BUET, soil laboratory of Soil Research Development Institute (SRDI) and Atomic Energy Research Centre (AERC). The results for XRD of BUET have been calculated by manually graphical and tabular analysis but the result for XRD of SRDI and AERC by directly computerized analysis and thus the outputs are given on fair printed copies.

X-ray diffraction (XRD) analysis of untreated and cement treated Bangladesh clays was carried out using a Philips X'Pert-PRO X-ray diffractometer. XRD patterns were obtained using a  $\text{Cu K}\alpha$  ( $\lambda = 1.54178 \text{ \AA}$ ) x-ray tube with input voltage of 40 kV and current of 30 mA. A continuous scan mode and scan rate of 2-degree per minute was selected. Air-dried powdered samples (particle size less than  $75 \mu\text{m}$ ) of treated and untreated soil samples were used. Mineralogical analysis of X-ray diffraction pattern of untreated clay was carried out based on the characteristic Bragg angle given by Brown (1961), Grim (1981) and Mitchell (1993). For treated clay, the Bragg data were taken from the standard Powder Diffraction File (JCPDS, 1995). According to mineralogy tests programme, the number of nine tests were performed on treated clays and the number of three tests were performed on base clays. The details summary of mineralogy test programme are shown in Table 3.8.

#### **3.9.3 Microstructure Test and Test Programme**

The analysis of microstructure of the untreated and treated clays were performed by Scanning electron microscope (SEM) analysis in Materials and Metallurgical Engineering laboratory of BUET. The SEM setup is donated from The Netherlands to BUET. According to microstructure tests programme, the number of twelve tests were performed on treated clays and the number of three tests were performed on base clays. The details summary of microstructure test programme are shown in Table 3.9. Scanning electron microscope (SEM) analyses of treated and untreated clay were carried out by a Philips 4100 field emission

scanning electron microscope with a Model XL-30. The soil sample was dried completely by Drying method. Air drying may be suitable for very stiff soil (i.e., cement-treated soil) since it does not undergo significant shrinkage (Mitchell, 1993). However, for soft clay with water content, air drying takes longer and causes more particle rearrangement. For soft clay, the stress induced during oven drying may result in some breaking of fabric, for this freeze drying method is adopted (Safiullah, 1984). In the present study, to compare the micro fabric of untreated stiff clay and treated hard clay, a Drying method is adopted. The method causes less sample disturbance and shrinkage than air or oven drying.

In Order to minimize disturbance to the microstructure of the soil, the Drying method (Mitchell, 1993) was used to dry the soil specimen prior to SEM analysis. The soil samples were finally dried by raising the temperature and of the chamber to 32°C and 80 bars respectively. After drying soil samples were broken up by finger pressure to a size of about 10 mm diameter × 10 mm high without any disturbance to the broken face of the samples. The broken soil samples placed on an aluminum stub by a double-sided conducting tape, with the broken face facing upwards. Prismatic specimens were carefully sculptured out of the bulk specimen dried by of the techniques using a sharp modeling-knife and in the case of the very hard samples a fine hacksaw proved useful for coarse trimming. Regarding the specimens taken, two was deemed to be optimum number. After fracturing the specimens were carefully trimmed to approximately 1 cm cube for specimens. The back of the specimens so obtained flat and then fixed to a clean microscope stub using a glue. After mounting the fracture surfaces were peeled using 100 applications of Sello-tape in order a cleaned and representative surface. The prepared surface of each specimen was vacuum coated with a layer of gold palladium (200-300A) thick to prevent charge build up on the specimen. Surfaces not requiring examination were painted with colloidal silver to improve the electrical contact between the specimen and stub.

The specimen could be observed in a video screen to the desired magnification and photographed. It was possible to control and measure the movement of the specimen in three orthogonal directions as well as in rotation and tilt. Therefore it was suitable for taking stereo pictures. Microphotography techniques each specimen placing inside the microscope chamber was first observed at low level of magnification (3 to 4 times) over the whole specimen surface. After a thorough observation in low magnification, areas of interest were selected. These areas were subsequently observed at different higher magnifications. Stereo micrographs were taken using an angle of tilt of around 5 to 10. In order to maintain constant magnification focusing was carried out using the specimen height control. An attempt was also made to maintain constant contrast and brightness conditions.



### **3.9.4 Physical Property Tests and Test Programme**

The test results pertaining to the basic engineering properties of the untreated and treated clays are presented in Chapter 4. The fundamental engineering properties of the untreated and treated clays are: (i) water content (ii) Atterberg limits (iii) specific gravity (iv) degree of saturation (v) total and dry unit weights (vi) void ratio and (vii) grain size distribution. These basic engineering properties of the untreated and treated clays were determined according to procedures presented in ASTM (1989) except liquid limit and plastic limit. For the determination of liquid limit and plastic limit of the untreated base clays, natural samples as obtained from the field were directly used. However, for the determination of liquid limit and plastic limit of cement treated clays, the samples were first cured for required duration and then the samples were broken into small pieces. The broken pieces were mixed with water for determining liquid limit and plastic limit.

The basic engineering tests on cement treated clay samples are comprised basically the same tests carried out on untreated samples, except the determination of grain size distribution. The changes in grain size distribution due to cement treatment were rather difficult to determine accurately. The usual hydrometer method could not be expected to render a true picture for the cementation of soil. The grain size distribution for samples were taken place after cement treatment would be broken down grain size and failed the system if the usual laboratory procedures in preparing soil samples for the determination of the grain size distribution are adopted (Kamaluddin, 1995). For this reason, grain size distribution concept is converted to specific surface area distribution concept. The smallest grain size, the highest specific surface area. The details summary of physical properties of untreated and treated clay test programme are shown in Table 3.10. A total number of four hundred twenty three tests for each type of physical properties were performed on treated and untreated clays.

### **3.10 Determination of Engineering Properties and Test Programme**

In this research, the engineering properties were determined by four major types of tests such as unconfined compression test, direct test, consolidation test and triaxial compression (unconsolidated undrained, isotropically consolidated undrained and isotropically consolidated drained) test.

#### **3.10.1 Unconfined Compression Test**

##### **3.10.1.1 Testing Programme**

The unconfined compression testing programme was designed to provide an economical and fast method means of comparing the effects of variable cement content and to find optimum cement content, if any, and to monitor the characteristics of strength gain of the treated clay with time. The unconfined compression tests indicated the initial profile of stress-strain-strength characteristics of the treated samples. The main experimental programme was

designed on the basis of unconfined compression tests. These tests were performed according to the manuals recommended by ASTM (1989). There are two limitations for unconfined compression tests such as (i) no effect of lateral restraint and (ii) no information about the internal soil conditions (c.g., the degree of saturation, the pore water pressure and volume change). The details summary of unconfined compression test programme is shown in Table 3.11. A total number of four hundred seventy seven unconfined compression tests were performed on treated and untreated clays.

### **3.10.1.2 Test Apparatus**

A standard soil test apparatus manufactured by SOIL TEST was used for unconfined compression test. It consists of a compression type-loading ram. A screw-jack-activated load yoke applied the load. The deformation of the specimen was measured by a dial gauge (having resolution of 0.0254 mm.) and the axial load capacity of machine was measured by a means of calibrated proving ring load of 2.8 kN. Loading rate is usually controlled manually by turning lever. The axial strain of 1.50 mm per minute can be applied.

### **3.10.1.3 Specimen Preparation and Set-up**

The size of test specimens in this research for unconfined compression test is 38 mm diameter  $\times$  76 mm height, prepared from cement treated samples of size 50 mm diameter  $\times$  100 mm height. The trimming of the specimens was done with wire saw and or a cutting plate and trimming frame, the set-up which is called Soil Lathe. After the sample dimensions were measured, it was placed into a split former, which facilitated the trimming of the specimen to a correct height by cutting at both ends of the specimen. For the computation of the unit weight, the trimmed specimen was weighed without the split former. Wax paper was used to cover the top and the bottom ends of the trimmed specimen to minimize the ends effect, which was then placed on the loading frame of the compression machine. The specimen axis was carefully aligned as exactly perpendicular on the centre of loading frame in the machine.

### **3.10.1.4 Testing Procedure**

The loading platform was adjusted until the upper platen just in contact with the specimen at the time of specimen had been mounted on the compression machine. The contact point can be confirmed from response of the load dial for the proving ring. The proving ring and the deformation dials were set to zero after the specimen had been correctly mounted and aligned. The specimen was sheared at a controlled rate of strain of 1.00 mm/min (about 1% strain per minute). The applied load and deformation of the specimen tested can be read respectively from the dial of the proving ring and the attached strain gauge. When the shearing started, appropriate proving ring readings were taken at every equal interval until the load on the sample decreased significantly. When the failure mode has been reached, the geometry of the tested specimen at the failure phase was sketched and the angle of the failure plane was

measured with respect to horizontal for mode of failure study. The failure specimens were placed in the oven for 24 hours in the process of determining the water content in the test sample.

### **3.10.2 One Dimensional Consolidation Test**

#### **3.10.2.1 Testing Programme**

One dimensional consolidation testing programme was chosen for this study in order to investigate the effects of cement treatment on the consolidation characteristics of soft high, medium and low plastic Bangladesh clays. The effects of type of clay, mixing water contents, cement contents and curing time on the improvement in consolidation properties have been studied. The main object was to assess the effects of stabilization on the preconsolidation pressure, compression index, and coefficient of consolidation, coefficient of volume compressibility and coefficient of permeability. One- dimensional consolidation tests were outlined to the procedures based on ASTM (1989). The maximum stress level of 1600 kPa was used for all treated and untreated clay. A total number of one hundred fifty nine consolidation tests were performed on cement treated and untreated base clays, which are summarized in Table 3.12.

#### **3.10.2.2 Test Apparatus and Accessories**

A standard soil test apparatus manufactured by SOIL TEST was used for one dimensional consolidation test. The consolidation machine consists of a confining ring, top and bottom porous stones, top cap, water reservoir and strain gauge with clamp assemblies. It has a lever-arm type of loading device with an arm ratio of 1 : 10, together with standard 63.5 mm diameter × 25 mm height floating ring consolidometers were used. The sample ring was clamped to the base. A thin layer of grease is applied inside the ring in order to minimize friction. For the load sequence applied, the corresponding hanger loads were computed in accordance with the known lever arm ratio, and taking into account the weights of the loading cap and top porous stone on the samples. The calculated load sequence were 0.40, 0.80, 1.60, 3.25, 6.50, 13, 26, 52 kg and the load corresponding stresses sequence were 12.5, 25, 50, 100, 200, 400, 800, 1600 kPa respectively for the consolidation tests. The height, diameter and weight of the specimen rings were also measured. The top and bottom porous stones were deaired by boiling, cooled, and kept in deaired water until use.

#### **3.10.2.3 Specimen Preparation and Set-up**

Prior prepared treated samples of size 75 mm diameter × 100 mm height were used for consolidation specimen preparation. A thin walled retaining ring 63.5 mm inner diameter × 25.4 mm height as trimming tool is designed to minimize sample disturbance during mounting. The trimming tool holds the specimen and the ring through an outer support ring

which is turn fixed to the rotating ring guide. The soil sample was first placed at the rotating base of the trimming tool. The specimen was trimmed to the required size by alternately pressing the cutting edge into the soil sample and trimming the excess soil ahead of the ring with a spatula. The cutter shaves off a very thin slice and hence does not disturb the soil ahead of it. The trimming procedure was continued until the cutting shoe touched the rotating base. The outer ring along and the sample ring were then removed from the trimming frame. The outer ring was then separated from the sample ring. Excess soil in the sample ring was then trimmed using a straight edge wire saw and the surface made flush. A recess tool was then used to trim 1 mm deep soil from the top so as to place the top porous stone and the top cap in position. After sampling, the ring with the soil sample was weighed. Water content determinations were made from the soil trimmings. Soaked filter papers were used at both ends of the sample. The bottom porous stone was placed on the oedometer cell base and the sample was positioned on the porous stone very carefully. The consolidometer unit was assembled. The pre-leveled loading beam was lowered until the loading arm just touched the loading cap without exertion any pressure on the sample.

#### **3.10.2.4 Testing Procedure**

The ready ring with the soil sample was first assembled in the consolidometer and then aligned in the loading frame. A small seating load of 7 kPa was used to place the equipment in compression before the displacement recording device, strain gage is set. Displacements were recorded by strain gage. The stresses were applied in the sequence of 12.5, 25, 50, 100, 200, 400, 800, 1600, 800, 400, 100 and 50 kPa from the next morning. Thus one load-unload cycle was also studied. The loads were changed according to the required loading sequence. Adjustment of the lever arm was done before each loading. At the starting of each loading, the deformations were recorded at times of 0, 0.10, 0.25, 0.50, 1, 2, 4, 8, 15, 30 minutes, 1, 2, 4, 8, 24 hours. The container of the oedometer was filled de-aired and distilled water at certain stages of the loading sequence. If the water was added before this stress, there was a possibility of swelling of the sample. For cement treated clay, a stress of  $\sigma_{v_0}$  was normally adopted, at which water was added to the sample. For all samples, it was checked whether swelling occurred or not, after addition of water to the sample by seeing the dial gauge reading (whether the displacement reading is going forward or backward). In general, the loads were kept for 24 hours per increment in order to reach the end of the primary stage and to obtain the characteristics settlement time curve which also includes at least one log cycle of secondary compression. At the end of the last increment, the soil sample was taken out of the consolidometer, weighed, oven dried for 24 hours and re-weighed.

### 3.10.3 Direct Shear Test

#### 3.10.3.1 Testing Programme

A direct shear testing programme was chosen for this study in order to investigate the effects of cement treatment on the cohesion and friction characteristics of soft high, medium and low plastic Bangladesh clays. It was studied the effect of variables, such as clay type, clay water contents, cement contents and curing time on the improvement in cohesion and friction properties. Consolidated drained direct shear test has been carried out. The main goal was to measure the effects of stabilization on the strength parameters (effective cohesion,  $c'$  and effective angle of internal friction,  $\phi'$ ). Direct shear tests were outlined to the procedures based on ASTM D3080 (1989). The maximum stress level of 400 kPa was used for direct shear on treated and untreated clay. A total number of 123 direct shear tests was performed on treated and untreated clay, which is summarized in Table 3.13.

#### 3.10.3.2 Test Apparatus and Accessories

A standard testing apparatus shear box (63.5 mm in diameter x 25.4 mm high) manufactured by SOIL TEST was used for this test. The shear box was split in two halves, hence it is known as a shear box. Fig. 3.6 shows line details for the direct shear apparatus. The box is circular in section and it was split horizontally at the center of the soil specimen. The lower half of the box was rigidly held in position in a container. The container itself along with the lower part of box slides and could be pushed forward at a constant rate by a geared jack, driven by an electric motor. The upper half of the box shears against a calibrated steel-proving ring. The movement of the lower part of the box was transmitted through the specimen to the upper part and hence, on to the proving ring. The resulting deformation indicates shear force. The specimen was held between metal grids and porous stones. Normal load was applied on the specimen from a loading yoke bearing upon a metal pressure pad through a steel ball. The pressure pad fits into the box over the upper porous plate. The volume change during consolidation and during the shearing process was measured by mounting a dial gauge (having the resolution of 0.0254 mm) at the top of the box. The rate of shear displacement or strain within the specimen could be controlled precisely. The shear box had also the arrangement for permitting drainage of water through the porous stones, and for submerging the specimen in water. The corresponding hanger loads, 32.5 kg, 65 kg and 130 kg were computed in accordance with the applied stress 100 kPa, 200 kPa and 400 kPa respectively on the samples. The height, diameter and weight of the specimen rings are also measured after testing.

#### 3.10.3.3 Specimen Preparation and Set-up

Prior prepared treated samples of size 75 mm diameter x 100 mm height were used for direct shear specimen preparation. A thin walled retaining ring 63.5 mm inner diameter x 25.4 mm

height as trimming tool was designed to minimize sample disturbance during mounting. The trimming tool holds the specimen and the ring through an outer support ring which was turn fixed to the rotating ring guide. The soil sample was first placed at the rotating base of the trimming tool. The specimen was trimmed for the required size by alternately pressing the cutting edge into the soil sample and trimming the excess soil ahead of the ring with a spatula. The cutter shaves off a very thin slice and hence did not disturb the soil ahead of it. The trimming procedure was continued until the cutting shoe touched the rotating base. The outer ring along and the sample ring were then removed from the trimming frame. The outer ring was then separated from the sample ring. Excess soil in the sample ring was then trimmed using a straight edge wire saw and the surface made flush. After sampling, the ring with the soil sample was weighed. Water content was determined from the soil trimmings. Soaked filter papers were placed at bottom ends of the shear box. The loaded ring unit was placed and assembled on the shear box. Pressure was applied on soil sample and sample was transferred into shear box from sampling ring. The leveled loading beam was placed until the loading arm just touched the loading point without exertion any pressure on the sample.

#### **3.10.3.4 Testing Procedure**

The ring with the soil sample was first assembled in the shear box and then aligned in the loading frame. The required load for 100 kPa, 200 kPa and 400 kPa was used to place on hanger, the equipment in compression after the displacement recording device, strain gages were set and waited for primary consolidation. In each test, sample was consolidated for completing time about 2 hours. The container of the shear box was filled de-aired and distilled water just after of the loading. Vertical displacements were recorded by strain gage up to the time when readings were stable in position. Adjustment of the loading arm was done by starting motor at very low speed. The rate of shear was very slow. At the starting of loading, the proving ring, vertical and horizontal deformations readings were recorded at times of 0, 0.10, 0.25, 0.50, 1, 2, 4 minutes. When the shear fully started, appropriate proving ring and vertical dial gage readings were taken at every 10 horizontal dial gage divisions until the load on the sample decreased significantly. In these tests, the time for failure of a samples was approximately 4 to 5 hours. At the end of the test, the soil sample was taken out of the shear box, weighed, oven dried and re-weighed. The failed specimens were placed in the oven for 24 hours in the process of determining the water content in the test sample.

#### **3.10.4 Triaxial Test**

##### **3.10.4.1 Testing Programme**

In the UU, CIU and CID triaxial tests, the variables considered were type of clay, clay water content, cement content, curing time, the pre-sheared confining pressure and conditions of drainage. In order to have an idea pertaining to the stress-strain-strength behaviour of the treated samples at 4 and 12 weeks curing time were chosen for triaxial tests. The pre-sheared

confining pressures were 50, 100, 200 and 400 kPa for both undrained (CIU) and drained (CID) triaxial tests on isotropically consolidated samples. A summary of the triaxial testing programme is presented in Table 3.14. A total number of two hundred twenty two tests for each undrained and drained triaxial tests was performed on treated and untreated clays. The equipment used for the triaxial tests consisted of the cells, the loading devices, and the measuring units and instruments.

#### **3.10.4.2 Triaxial Cell**

A standard soil test apparatus manufactured by SOIL TEST was used for triaxial compression test. The triaxial machine consists of three main components, namely the cell base, the removable perspex cylinder, and the top head assemble. In the entire testing programme, free top cap system was used. The cell base, machined from anticorrosive light alloy, forms the pedestal on which the sample is placed and includes three different connections, namely: (i) the line to the cell chamber, used to fill the triaxial cell with de-aired, distilled water and through which pressure is applied (hydrostatic pressure increments) on the triaxial specimen; (ii) two drainage lines connected to the bottom of the test specimen. One drainage line is used in combination with a pore pressure transducer to measure pore pressure during undrained loading; while the other is used to apply the back pressure and/or as a bottom drainage line connected to volume change burettes; and (iii) a drainage line connected to the top of the sample. The back pressurizing for the saturation of the specimen was applied through the two drainage lines. The base connection lines are fitted with Klinger valves to close or open the connections. The removable cylinder, made of transparent Perspex material, encloses the pressurized water, and can withstand a working stress of 1700 kPa. The chamber assembly is clamped by stainless steel tie rods, and attached to the base by wing nuts on stainless steel studs with pilots for easy location. The top head assembly consists of a stainless steel piston or loading ram which was ground and honed to a close-sliding fit with the cell bush. The cell top assembly also includes ports for oil injection and air release.

#### **3.10.4.3 Loading Device**

The required stress conditions were created on the specimen by a combination of two dead weight suspended by hangers with dash-pot system. The piston uplift force of dash-pot is completely compensated by the hanger with dead weight. One was used to apply constant cell and back pressures to the triaxial cell. A capable of applying strain-controlled loading was used for the application of the deviator stress through a load cell. The deviator stress was measured through a load cell. With the aid of load hangers and dead weights, the specimens could be sheared along a wide range of pre-determined stress space.

#### **3.10.4.4 Measurement of Strains and Pore Pressure**

Axial deformations of specimen were measured with the displaced strain gage with an accuracy of 0.01 mm per revolution. In undrained tests, a pressure transducer of capacity 1700 kPa measured the excess pore pressure during shearing process with an accuracy of 0.1 kPa, connected to the bottom of the specimen. In the consolidation process and the drained tests, the change in volume of the specimen was monitored with the use of the volume change indicator (burette) with capacity of 10 cc (with an accuracy of 0.02 cc), which were connected to the back pressure line. This system is similar to that given by Head (1990). The interface of the de-aired water and coloured kerosene in the burette can be clearly seen due to the difference in their densities, and the volume changes were observed by monitoring the movement of the interface.

#### **3.10.4.5 Calibration of Pressure Transducer**

The calibration factor of each pressure transducer was estimated by regression analysis from the relationship between the applied pressure and the corresponding pressure transducer reading as shown in Fig. 3.3. The pressure transducers of capacity 1700 kPa were used for the measurement of pore pressure.

#### **3.10.4.6 Calibration of Displacement Strain Gauge**

The calibration factor of each displacement strain gage was found by regression analysis from the relationship between the applied displacement and the corresponding displacement gauge reading. The deformation readings were made on strain gauges with smallest reading of 0.0254 mm/division and maximum travel range is 25 mm.

#### **3.10.4.7 Calibration of Proving Ring for Measuring Load**

The calibration factor for proving ring was obtained based on the mean curve drawn from the relationship between proving ring reading and the known loads applied from the universal testing machine. Proving ring (Calibrated load constant, 0.4077 lb/division) of sufficiently range was used to measure load readings. The maximum capacity was 2.8 kN of the proving ring.

#### **3.10.4.8 Triaxial Testing Sample Preparation**

The required size of the test specimens for unconfined compression test is 38 mm diameter × 76 mm height, trimmed from prior prepared cement treated samples of size 50 mm diameter × 100 mm height. The initial moisture content was determined from the trimmings residue. The weight of the specimen was taken for unit weight determination.



#### 3.10.4.9 Setting-up of Specimen

The base of the triaxial cell was connected to the pressure line, drainage line and a pore pressure transducer. The entire pressure and drainage lines, including pore pressure transducers, were always flushed with de-aired water to get rid of any entrapped air. The porous stones were also de-aired and saturated. Filter papers, saturated porous stones, O-rings and membranes were prepared for the prompt sealing of the specimen after trimming. Filter paper strips were soaked in de-aired water at all times before they were used. De-aired distilled water was always used throughout the investigations. The trimmed specimen was mounted on the pedestal of the cell base. Then, the saturated porous stones and the filter papers were placed at both ends of the specimen along with side drains.

In order to accelerate consolidation, eight filter paper strips as side drains were placed vertically around the sample at equal spacing. These filter papers should not cover more than 50% of the specimen area. Both ends of the filter paper strip were extended to the porous stones for easy drainage. The sides of the top loading cap and the base pedestal were then lightly coated with silicone grease. The sample was enclosed within a membrane using a membrane stretcher sleeve, with both ends of the membrane rolled over the bottom pedestal and the top cap. The ends of the membranes were sealed with two O-rings at top end and three O-rings at bottom end.

Care was taken to keep the specimen concentric with both the pedestal and the shaft piston. The precautions were also taken to minimize the suction of water by the specimen during the setting-up procedure. The perspex cylinder with top head assembly was mounted and fixed to the cell base. The chamber surrounding the specimen was filled with de-aired water up to the top of the cell. The water is flashed by top open with a few time to conform for de-aired.

#### 3.10.4.10 Saturation of Specimen

For fully saturated specimens, selected back pressure of 100 kPa was applied in this stage. The cell pressure and back pressure were gradually increased with pressure increment of 25 kPa. During the application of pressure, the cell pressure was always maintained higher than the back pressure at value equal to initial effective stress of the sample. When the back pressure reached 100 kPa and cell pressure was 110 to 125 kPa depending on initial effective stress, then the specimen was left for 24 hours at least. At the end of the 24 hours saturation period, the state of saturation was checked by the pore pressure response under undrained conditions, i.e., closing both top and bottom drainage lines and increasing the cell pressure to estimate the pore pressure increasing. The Skempton B value of 0.90 to 0.98 was the index criterion of sufficient saturation. When the specimen showed such a B value, saturation of the specimen was deemed to be sufficient and the consolidation process of the specimen was commenced.

#### **3.10.4.11 Consolidation of Specimen**

The consolidation phase was started after full saturation of the specimen. The initial reading of the burette and the displacement had been taken, then the drainage valves were closed and the piston was clamped. The cell pressure (i.e., the consolidation pressure plus the back pressure) was raised to the desired value gradually (with the back pressure line closed) and the counterbalance force is provided by the hanger weight. The consolidation was initiated by reopening the drainage valves and unlocking the piston simultaneously. The volume and the axial displacement changes with time were recorded. Complete consolidation was determined mainly by measuring excess pore pressure. The presence of any excess pore pressure in the specimen was checked with the back pressure valve closed for one hour. The consolidation condition is considered as isotropic and the first loading increment starts at 25 kPa. For each step, displacement readings with time were recorded by strain gage and volume change readings from burette versus time up to the end of consolidation were recorded both manually.

#### **3.10.4.12 Shearing of Specimen**

All the specimens were allowed one day of consolidation or swelling process to ensure the full dissipation of excess pore pressure within the specimen. All undrained and drained tests were strained controlled.

#### **3.10.4.13 Unconsolidated Undrained Triaxial Compression Test**

The shearing stage was started without isotropic consolidation of the specimen. The drainage valves were closed and the strain gauge was set at zero position. The applied cell pressure was 200 kPa. The sample was loaded by driving the base platen upwards. All unconsolidated undrained triaxial tests were strain-controlled compression tests. Strain rate of 0.76 mm per minute was used for treated clays. The proving ring dial gauge reading and the corresponding pore pressure transducer reading were recorded. The sample was then sheared and the proving dial gauge reading and the corresponding pore pressure transducer reading were recorded at specified deformation of the sample. Shearing was continued until the proving ring dial reading remained constant or decreased for a few reading of strain dial gauge. At the end of the test, cell base was lowered and cell pressure was released. The cell was disassembled and sample was carefully removed from the cell. The weigh of the sample was taken and its water content was determined.

#### **3.10.4.14 Consolidated Undrained Triaxial Compression Test**

The shearing stage was started after the completion of isotropic consolidation of the specimen. All the drainage valves were closed and the cell pressure valves were open. After consolidation and up to prior to start of shearing, the piston ram was fixed to keep the prevailing stress condition within the cell. Shearing was then commenced by increasing the axial stress with constant cell pressure. The effective cell pressure were considered 50, 100,

200 and 400 kPa. The sample was loaded by driving the base platen upwards. All undrained triaxial tests were strain-controlled compression tests. Strain rate of 0.060 mm per minute was used for treated and untreated clays. Readings of pore pressure were monitored through pressure transducers but readings of axial displacement of sample and the axial load were recorded manually. Readings were taken at close intervals of time at the early stage of shearing, thereafter at larger intervals. After the failure of the specimen, shearing was continued as much as possible, until a larger axial strain was attained. To study the post-failure behaviour of the specimens is found by this test.

#### **3.10.4.15 Consolidated Drained Triaxial Compression Test**

The back pressure line was kept open and the cell pressure was maintained constant through the test. The back pressure was considered 100 kPa. The effective cell pressure were considered 50, 100, 200 and 400 kPa. The sample was allowed to drain via the burette during shearing. In this test series, samples were sheared at a strain rate of 0.020 mm per minute for treated and untreated samples. Axial load and axial displacement of the sample were recorded manually. The volume change was recorded from the burette. After the failure of the specimen, shearing was continued, whenever possible, up to the stage of larger strain in order to study the residual behaviour of the specimens.

#### **3.10.4.16 Isotropic Compression Test**

In triaxial machine, the isotropic compression tests can be easily performed. For specific cell pressure, the volume change of samples were recorded during consolidation. These tests represent equilibrium states of volume and effective stress and so creep has been neglected. The results of the test were used for analyses using critical state. Several tests were performed for various treated and untreated clays.

#### **3.10.4.17 End of Testing of Triaxial Test**

The drainage lines were closed and the cell pressure was reduced to atmospheric pressure in one step at the end of the test. The triaxial cell was released immediately as possible as early and cleaned. The mode of failure and the inclination of failure planes were drawn. The specimen was then weighed and dried in the oven for 24 hours.

### **3.11 Extra Precaution Measures During Triaxial Test**

In triaxial tests, some precaution measures applied to be considered. According to the suggestions of Head (1990), precautions were in order to minimize the effects of end restraints, a thin coat of vacuum silicone grease was applied on top of the pedestal and on the underside of the top cap. The lubricated end platens were most successful in reducing end restraints. The ratio of the length to the diameter of the sample was also at least two in all the tests conducted. Leakage through O-rings and membranes was always checked. Two membranes may be used with smooth talc lubricating the interface. The sides of the base

pedestal and the top cap may be lightly coated with vacuum silicon grease and 2 O-rings at top and 3 O-rings at bottom may be placed to seal the membranes with sample at both ends. De-aired distilled water may be used in the tests. The de-airing of the distilled water may be done for at least 10 hours in de-airing apparatus to remove dissolved air from the water. All lines in the triaxial set-up were carefully flushed with deaired water prior to every test. System flexibility was checked during every stages of testing.

### 3.12 Processing and Analysis of Triaxial Test Data

The test results were processed based on the following usual assumptions:

(i) A right cylindrical shape specimen was remained and (ii) Stresses and strains were uniform throughout the soil samples during testing.

#### 3.12.1 Calculation of Stress

In this research, the compressive stress was taken as positive. The principal stresses in such a way that lateral stresses are always equal, which acted on a soil specimen under cylindrical triaxial test. The total stresses as axial stress acting on the specimen is denoted by  $\sigma_1$  and lateral stress by  $\sigma_3$ . When the soil specimen is saturated and pore water pressure in the soil is  $u$ , then the corresponding effective stresses in the specimen are  $\sigma_1'$  and  $\sigma_3'$ . The equations are defined as follows:

$$\sigma_1' = \sigma_1 - u \quad (3.1)$$

$$\sigma_3' = \sigma_3 - u \quad (3.2)$$

In the tests, the stress condition is  $\sigma_1' > \sigma_2' = \sigma_3'$ , where  $\sigma_1'$  is effective stress on the end caps of the sample and  $\sigma_1' = \sigma_3'$  is the cell pressure. The stress parameter  $q$  (deviator stress) and  $p$  (mean normal stress) which are also a function of the invariant of stress tensor are limited as follows:

$$p' = \frac{1}{3}(\sigma_1' + 2\sigma_3') \quad (3.3)$$

$$\text{and, } q = \sigma_1 - \sigma_3 = \sigma_1' - \sigma_3' \quad (3.4)$$

#### 3.12.2 Calculation of Strains

The axial strain  $\epsilon_1$  has been defined as

$$\epsilon_1 = \int_{L_0}^L \frac{dL}{L} = \ln\left(\frac{L}{L_0}\right) \quad (\text{Compression being positive}) \quad (3.5)$$

The volumetric strain  $\epsilon_v$  is given by

$$\epsilon_v = \int_{V_0}^{V'} \frac{dV}{V} = \ln\left(\frac{V}{V_0}\right) \quad (\text{Compression being positive}) \quad (3.6)$$

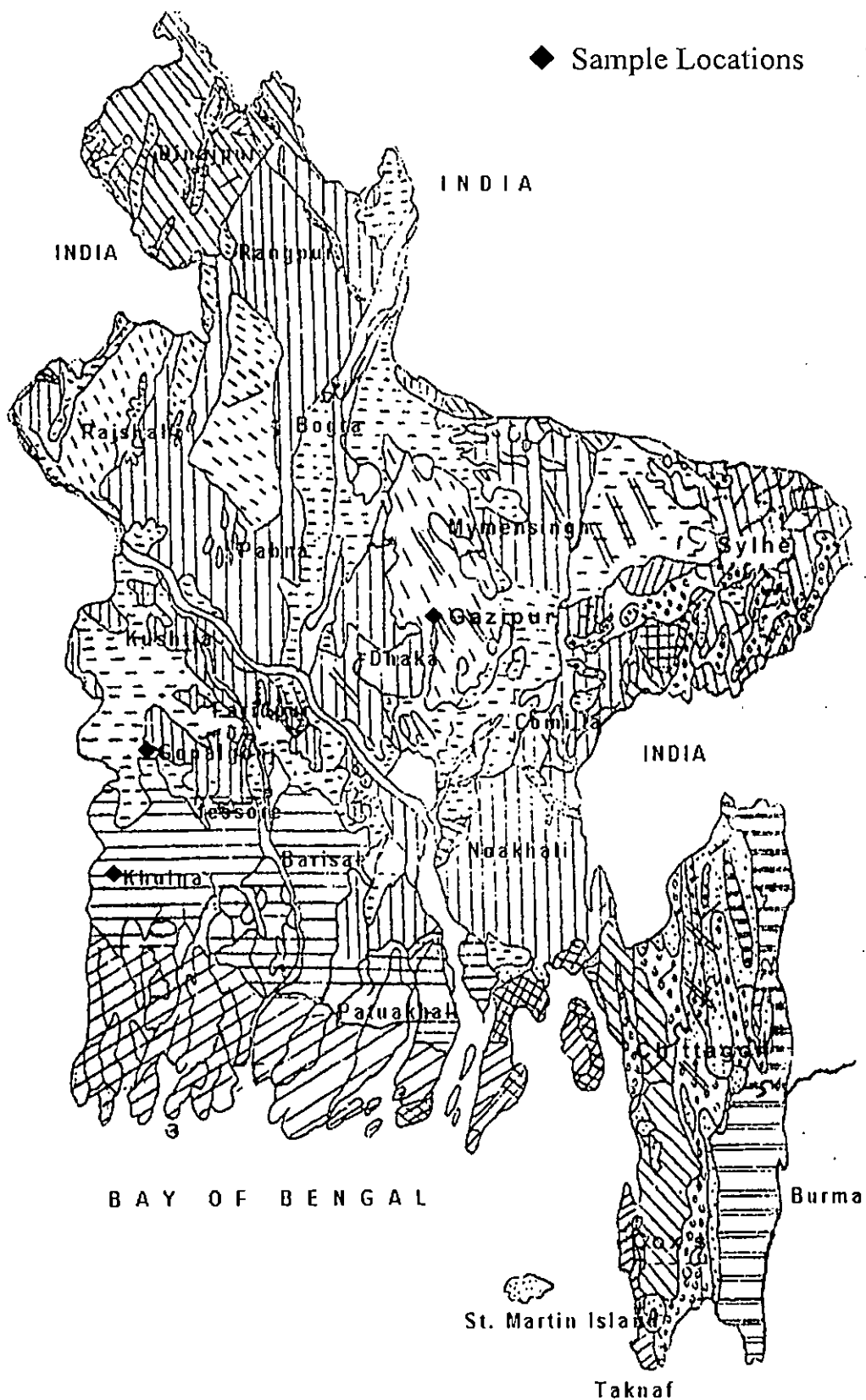


Fig. 3.1 Geological Map of Bangladesh

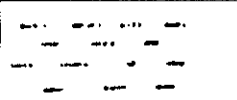



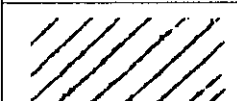
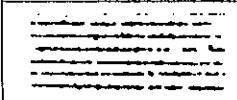
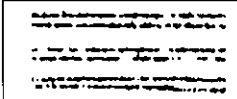
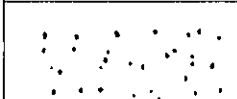
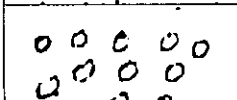

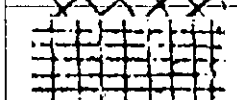
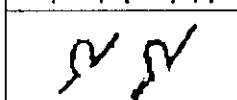
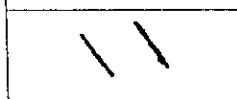
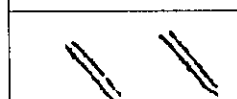
	<b>Stream Deposits:</b> Stream bed, meander bolt, flood plain and low level terrace deposits, undivided including some swamp deposits.
	<b>Older Alluvial Deposits:</b> Medhupur clay mostly red end orange clay deposits slightly higher than inter-stream deposits (old).
	<b>Inter-stream Deposits:</b> Silt, sand and gravel deposit of a slightly higher attitude than adjacent flood-plain and low level terrace deposits.
	<b>Piedmont Deposits (Barind):</b> Detrital materials derived from highlands of India deposited on gentle slopes to the south and the west.
	<b>Tidal Deposits:</b> Tidal delta deposits and deltaic flood plain deposits.
	<b>Deltaic Deposits:</b> Deltaic flood plain deposits. Tidal and deltaic deposits are separated primarily on the basis of difference in land use, vegetation and drainage pattern.
	<b>Sedimentary Rocks:</b> Grayish-yellow, medium grained and cross bedded sandstones, gray sandy shale, gray shale and limestone, thickness up to 10,000 ft.
	<b>Sedimentary Rocks:</b> Yellowish-brown, medium to coarse grained sandstone and mottled clay and sandy clay thickness up to 5,000 ft.
	<b>Sedimentary Rocks:</b> Sylhet lime stones, gray, medium grained, hard, massive lime stones: thickness up to 2,000 ft, chittagong lime stones: gray brown, coarse grained, medium hard lime stones:
	<b>Coastal Deposits:</b> Beach sand and sandbars deposits tidal deposits.
	<b>Swamp Deposits:</b> Vegetables, Organic, and Peat deposits.
	<b>Folds:</b> Stratum tilted, bent or buckled rock deposits
	<b>Faults:</b> Fractured, broken down rock deposits.
	<b>Fault trace:</b> Light Fractured rock deposits.

Fig. 3.2 Symbols Used in Geological Map of Bangladesh

**Table 3.1 Properties of Type 1 Portland Cement Used in the Study**

Physical Properties	Test Result	Chemical Properties	Test Result (By Weight, %)
Specific Gravity, $G_s$	3.17	Calcium Oxide (CaO)	64.67
Bulk Density ( $\text{g/cm}^3$ )	1.02	Magnesium Oxide (MgO)	2.15
Fineness, Specific Surface Area, ( $\text{m}^2/\text{kg}$ )	280 – 303	Potassium Oxide ( $\text{K}_2\text{O}$ )	0.57
Normal Consistency (%)	24 – 25	Sodium Oxide ( $\text{Na}_2\text{O}$ )	0.23
Initial Setting Time (min), > 45 minute	100 – 153	Silicon dioxide ( $\text{SiO}_2$ )	21.87
Final Setting Time (min), < 375 minute	241 – 320	Aluminium Oxide ( $\text{Al}_2\text{O}_3$ )	7.26
Compressive Strength (Mpa), 3 days	18.10 – 22.50	Ferric Oxide ( $\text{Fe}_2\text{O}_3$ )	2.91
Compressive Strength (Mpa), 7 days	24.60 – 25.30	Sulfurtrioxide ( $\text{SO}_3$ )	1.45
Loss of Ignition (%)	0.80	Insoluble Residue	0.29

**Table 3.2 Summary of the Test Variables Used**

Test Variables	Description
Type of Soil	High Plastic Clay, designated as C1 (PI = 47%)
	Medium Plastic Clay, designated as C2 (PI = 22%)
	Low Plastic Clay, designated as C3 (PI = 13%)
Type of Admixture	Cement
	Lime
Initial Mixing Water Content	120%, 150%, 200% and 250%
Clay-water /Admixture Ratio	2, 2.5, 4, 7.5, 10, 15 and 30
Curing Time	1, 2, 4, 12, 24, 52 and 104 weeks
Confining Pressure	50, 100, 200 and 400 kPa
Stress Conditions for Tests	Unconfined Compression Tests
	Consolidation Tests
	Triaxial Compression Tests
	Direct Shear Tests
Drainage Condition	Undrained Triaxial Tests
	Drained Triaxial Tests
	Drained Direct Shear Tests

Table 3.3 Summary of Experimental Investigations

Samples	Tests	Description
Untreated Clays (High, Medium and Low Plastic Base Clays) and Treated Clays (with Various ratio of Cement or Lime Content and Curing Time)	Chemical Analysis	pH, Organic Content, Loss on Ignition, Cation Exchange Capacity, Exchangeable Cations, Electrical Conductivity
	Basic Engineering Properties	w, S <sub>r</sub> , G <sub>s</sub> , PI, PL, LL, Unit Weight and Void Ratio, Specific Surface area Analysis
	Mineralogy Analysis	X-ray Diffraction Analysis
	Microstructure Analysis	Scanning Microscopic Analysis
	Unconfined Compression Tests	Without confining pressure
	Direct Shear Tests	Normal Pressure = 100, 200 and 400 kPa
	Consolidation Test	Loading Sequence: 12.5, 25, 50, 100, 200, 400, 800, 1600, 800, 400, 200, 100, 12.5 kPa
	CIU and CID Triaxial Compression Tests	Pre-shear Effective Consolidation Pressure = 50, 100, 200 and 400 kPa, Back Pressure = 100 kPa
UU Triaxial Compression Tests	Confining Cell Pressure = 200 kPa,	

Table 3.4 Total Number of Treated Samples Used

Initial water content (w <sub>i</sub> )	Clay-water/Cement (wc/c) Ratio = 7.5			Clay-water/Cement (wc/c) Ratio = 10			Clay-water/Cement (wc/c) Ratio = 15		
	C1	C2	C3	C1	C2	C3	C1	C2	C3
120%	C1	C2	C3	C1	C2	C3	C1	C2	C3
150%	C1	C2	C3	C1	C2	C3	C1	C2	C3
200%	C1	C2	C3	C1	C2	C3	C1	C2	C3
250%	C1	C2	C3	C1	C2	C3	C1	C2	C3
Initial water content (w <sub>i</sub> )	Clay-water/Lime (wc/l) Ratio = 7.5			Clay-water/Lime (wc/l) Ratio = 10			Clay-water/Lime (wc/l) Ratio = 15		
	C1	C2	C3	C1	C2	C3	C1	C2	C3
	120%	C1	C2	C3	C1	C2	C3	C1	C2
150%	C1	C2	C3	C1	C2	C3	C1	C2	C3



**Table 3.5 Summary of pH Test**

Type of soil	Initial Water Content (%)	Clay-Water/ Cement Ratio	Curing Time (week)	Number of Tests
3-Base Clays	In-situ	-	-	3
C1, C2, C3 Clays	120	2, 4, 7.5, 15	4, 12	24
C1, C2, C3 Clays	150, 200, 250	15	4, 12	18

**Table 3.6 Summary of Loss of Ignition Tests**

Type of soil	Initial Water Content (%)	Clay-Water/ Cement Ratio	Curing Time (week)	Number of Tests
3-Base Clays	In-situ	-	-	3
C1, C2, C3 Clays	120	2, 4, 7.5, 15	4, 12	24

**Table 3.7 Summary of Organic Matter, Electrical Conductivity, Cation Exchange Capacity and Exchangeable Cation Tests**

Type of soil	Initial Water Content (%)	Clay-Water/ Cement Ratio	Curing Time (week)	Number of Tests
3-Base Clays	In-situ	-	-	3
C1, C2, C3 Clays	120	4, 7.5, 15	4, 12	18

### 3.8 Summary of X-ray Diffraction Test

Type of soil	Initial Water Content (%)	Clay-Water/ Cement Ratio	Curing Time (week)	Number of Tests
3-Base Clays	In-situ	-	-	3
C1, C3 Clays	120	2, 4, 7.5	4	6
C2 Clays	120	4, 7.5	4	2
C1 Clays	120	4	12	1

### 3.9 Summary of Microstructure Test

Type of soil	Initial Water Content (%)	Clay-Water/ Cement Ratio	Curing Time (week)	Number of Tests
3-Base Clays	In-situ	-	-	3
C1, C2, C3 Clays	120	4, 7.5	4, 12	12

**Table 3.10 Summary of Physical Properties Test**

Type of soil	Initial Water Content (%)	Clay-Water/ Cement Ratio	Curing Time (week)	Number of Each Tests
3-Base Clays	In-situ	-	-	3
C1, C2, C3 Clays	120, 150, 200, 250	2, 2.5, 4, 7.5, 10, 15, 30	1, 2, 4, 12, 24	420

**Table 3.11 Summary of Unconfined Compression Test**

Type of soil	Initial Water Content (%)	Clay-Water/ Cement Ratio	Clay-Water/ Lime Ratio	Curing Time (week)	Number of Tests
3-Base Clays	In-situ	-	-	-	3
C1, C2, C3 Clays	120	2, 2.5, 4, 7.5, 10, 15, 30	-	1, 2, 4, 12, 24, 52, 104	147
C1, C2, C3 Clays	150, 200, 250	7.5, 10, 15	-	1, 2, 4, 12, 24,	135
C1, C2, C3 Clays	120	-	2, 2.5, 4, 7.5, 10, 15, 30	1, 2, 4, 12, 24, 52, 104	147
C1, C2, C3 Clays	150	-	7.5, 10, 15	1, 2, 4, 12, 24,	45

**Table 3.12 Summary of Consolidation Test**

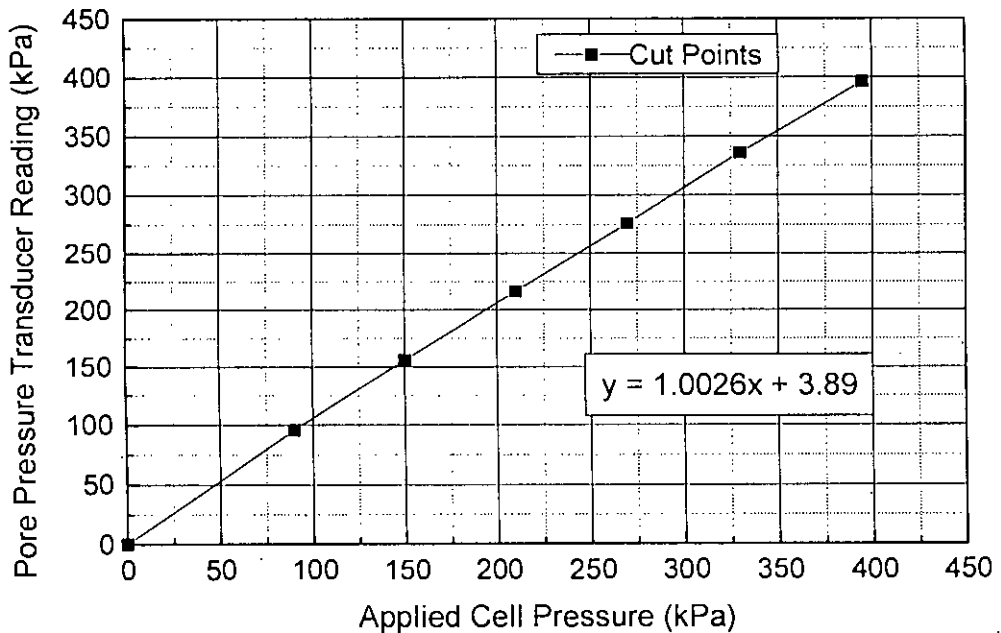
Type of soil	Initial Water Content (%)	Clay-Water/ Cement Ratio	Clay-Water/ Lime Ratio	Curing Time (week)	Number of Tests
3-Base Clays	In-situ	-	-	-	3
C1, C2, C3 Clays	120, 150, 200, 250	7.5, 10, 15	-	4, 12	72
C1, C2, C3 Clays	120, 150	7.5	-	1, 24	12
C1, C2, C3 Clays	120, 150	-	7.5, 10, 15	1, 4, 12, 24	72

**Table 3.13 Summary of Direct Shear Test**

Type of soil	Initial Water Content (%)	Clay-Water/ Cement Ratio	Curing Time (week)	Number of Tests
3-Base Clays	In-situ	-	-	3
C1, C2, C3 Clays	120, 150, 200, 250	2.5, 4, 7.5, 10, 15	4, 12	120

**Table 3.14 Summary of Triaxial Compression Test**

Type of soil	Initial Water Content (%)	Clay-Water/ Cement Ratio	Curing Time (week)	Number of Tests
3-Base Clays	In-situ	-	-	3 Nos. CIU test 3 Nos. CID test
C1, C2, C3 Clays	120, 150, 200, 250	7.5, 10, 15, 30	4, 12	96 Nos. CIU test 96 Nos. CID test
C1, C2, C3 Clays	120	7.5, 10, 15, 30	4, 12	24 Nos. UU test

**Fig.3.3 Calibration Chart for Pore Pressure Transducer Used**

## CHAPTER 4

### CHEMICAL, MINERALOGICAL AND PHYSICAL PROPERTIES OF CEMENT TREATED CLAYS

#### 4.1 General

This chapter explains the physicochemical as well as microstructural behaviour and integrate them with the physical properties of treated clays at high water content. The basic index and physical properties of the base clays used in the research are presented to establish the relevant reference properties, prior to treatment. The observed properties include the physical, chemical, mineralogical and microscopic properties. These are presented in order to establish relevant reference behaviour for the counterpart, cemented clays. For this, a large number of tests on various treated clays were conducted with different values of initial mixing water content, clay-water/cement ratio and curing period. The experimental programme of untreated clays was set in accordance with that for treated clays so that a datum profile can be established for the base clays and parametric relevance can be drawn between treated and untreated clays. The basic chemical, mineralogical, microscopic and physical properties for both treated and untreated clays are presented and discussed in the following sections.

#### 4.2 Chemical Properties of Untreated Base and Cement Treated Clays

Most of the important chemical properties have been studied for both treated and untreated clays. The soil pH value, cation exchange capacity, exchangeable cations, organic content, loss on ignition, nitrogen and phosphorous, electrical conductivity parameters were considered as the chemical properties in this study. The chemical properties were studied for three base clays with different plasticity from the location in Gazipur, Gopalganj and Khulna districts of Bangladesh. The chemical response for three base clays were quite different. The clays C1 (PI = 47%), C2 (PI = 22%) and C3 (PI = 13%) were treated by using mixing clay-water contents ( $w_i$ ) 120%, 150%, 200% and 250% and clay-water/cement ratios ( $w_c/c$ ) 2, 4, 7.5, 10 and 15, where chemical tests were applied on the final products at different curing times. The result of each chemical properties for the treated and untreated clays are presented in graphical and tabular form.

##### 4.2.1 Soil pH Value

The pH values of the base clays was found to be 8.3, 6.6 and 7.8 for C1 clay, C2 clay and C3 clay, respectively. The neutral soil solution is expressed by numerical pH value 7. If pH value exists above 7, soil solution is alkaline and pH value exists below 7, soil solution is acidic in nature. According to the criteria, C1 clay and C3 clay are alkaline in nature and C2 clay is acidic in nature. The low pH reveals that the clay contains a significant amount of  $H^+$  ions.

The comparisons of the variation for pH value with clay-water/cement ratio are shown in Fig. 4.1 for treated clays. From Fig. 4.1, it has been found that the pH values decrease with increasing clay-water/cement ratio. The pH value for C1 clay is higher than that of C3 clay but the pH value for C2 clay is lower than that of C3 clay. The effect of cement content and curing time on pH value of treated clays are shown in Fig. 4.2. The pH values increase with increasing cement content but the pH values decrease with increasing curing time. At lower cement content, the pH value suddenly changes. It can be seen from Fig. 4.2 that the pH value (8.3 to 11.9) rises rapidly with increasing cement content (0 to 16%) but the rate of the rise pH value (11.9 to 12.6) moderated with increasing cement content (16 to 60%) for typical C1 clay. This is because as possibly, due to hydrolysis of cement constituent with high metallic oxide occur promptly at lower cement level, then pH rises rapidly and afterward reach in equilibrium position at higher cement level and including other reasons.

At very high cement content, the pH value approaches 12.6, which corresponds to that of  $\text{Ca}(\text{OH})_2$ . The increase of pH with an increase of cement content is due to crowding of the  $\text{Ca}^{+2}$  ion concentration on the clay surface, leading to changes in fabric of the cement-treated clay (i.e., the formation of a flocculated clay-cement matrix). The similar effect of pH on fabric changes of a clay-water-electrolyte system has been reported by Santamarina et. al. (2001) and Chew et. al. (2004). Furthermore, the cement content at which the pH values moderate also agree closely with that at which the water content reduction moderates. Thus, the trends of water content reduction and pH increase support the presence of un-reacted lime at high cement content postulated.

Figure 4.3 shows the effect for mixing clay-water content and type of clay on final pH value of treated clays. It is found that the rate of pH value increases with increasing the initial mixing water content of soil during stabilization at same clay-water/cement ratio and curing time. It can be seen from Fig. 4.3 that for C1 clay at wc/c ratio 15 (i.e. cement content 8%) and curing time 4 weeks, with respect to base clay values, the pH values increases 26.5%, 34.9%, 39.7% and 43.4% for initial mixing water contents 120%, 150%, 200% and 250% respectively.

From the Fig. 4.2, comparing the pH values for treated and untreated samples of each clays, the pH values for treated samples are higher than that of untreated samples. The treated clays at initial mixing water content 120%, wc/c ratio 7.5 (i.e. cement content 16%) and curing time 4 weeks, with respect to base clay values, the pH values increases 51%, 59% and 80% for C1 (PI = 47%) clay, C2 (PI = 22%) clay and C3 (PI = 13%) clay respectively.

#### 4.2.2 Loss on Ignition

Effect of cement content, curing time and clay type on loss on ignition values of the treated clays are presented in Fig. 4.4. The loss on ignition of the base clays was found to be 11.38%, 4.56% and 3.94% for C1 (PI = 47%) clay, C2 (PI = 22%) clay and C3 (PI = 13%) clay

respectively. The loss on ignition for C1 clay is higher than that of C2 clay and C3 clay. During chemical stabilization, loss on ignition of soil is minimized by chemical reactions. The loss on ignition values decrease with increasing curing time because soil become strengthen due to hydration reactions. The effect for cement content and type of clay on loss of ignition value of treated soils at initial water content, 120% and curing time, 4 weeks and 12 weeks are shown in Fig. 4.4. From the figure, it can be seen that for each treated clays have the minimum loss on ignition at a particular cement content. The minimum loss on ignitions are observed at against 28%, 18% and 22% cement content for C1 clay, C2 clay and C3 clay respectively. Afterward, loss on ignition increases with increasing cement content for treated clays. For typical high plastic (C1, PI = 47%) clay, the loss on ignition (from 11.4 to 8%) decreases rapidly with increasing cement content (from 0 to 28%) but loss on ignition (from 8 to 9.6%) increases moderately with increasing cement content (from 28 to 60%).

### 4.2.3 Organic Content

The organic content of the treated and untreated clays were determined by wet oxidation methods. The organic content contains organic matter and organic carbon. The organic content of the treated and untreated clays are shown in Fig. 4.5. Organic content are 6.99%, 3.52% and 4.64% for untreated C1 (PI = 47%) clay, C2 (PI = 22%) clay and C3 (PI = 13%) clay respectively. Relatively small amount of organic material for treated clays have a effect on the strength increase. Some other accelerating agent (e.g., gypsum) has often been used together to stabilize organic soil when cement alone is not effective (Broms, 1986). Arman and Muhfakh (1972) also reported that the strength decreases with increasing organic matter. Generally, the effect of cement / lime decreases with increasing organic content.

The organic content increases with increasing plasticity of soil. The organic content for C1 clay is greater than that of C2 clay and C3 clay. Comparing the organic content in between untreated and treated soils, the values for treated soils are lower than that of untreated soils. During chemical stabilization, organic content of soil is minimized by chemical reactions. The organic content decreases with increasing curing time because soil become strengthen due to hydration and pozzalonic reactions. The effect for cement content and type of clay on organic content of treated soils at initial water content, 120% and curing time, 4 and 12 weeks are shown in Fig. 4.5. From Fig. 4.5, it can be seen that for each treated clays have the minimum organic content at a particular cement content. The minimum organic content have been observed at against 12%, 10% and 11% cement content for C1 clay, C2 clay and C3 clay respectively. Afterward, organic content increases with increasing cement content for treated clays. For typical high plastic C1 (PI = 47%) clay, the organic content (from 4.5 to 1.5%) decreases rapidly with increasing cement content (from 0 to 8%) and organic matter (from 1.50 to 3.25%) increases moderately with increasing cement content (from 8 to 30%). This is because as possibly, the organic matter having organic acid and carbon-oxalic acid react with

metallic oxide effectively, results reduces organic matter and afterward reach in equilibrium position.

#### 4.2.4 Electrical Conductivity

The electrical conductivity (EC) of the base clays were determined to be 0.23 ds/m, 0.92 ds/m and 0.78 ds/m for C1 (PI = 47%) clay, C2 (PI = 22%) clay and C3 (PI = 13%) clay respectively with signifying that the clays are non-saline in nature because the EC values up to 2 ds/m (desicemal/meter), the soils are called non-salinity. The range of values indicates that the pore water contains a low amount of soluble cations. The salinity of clay is measured by the electrical conductivity test. Kamaluddin (1995) reported that the electrical conductivity value was 2.29 ds/m for untreated Bangkok clay (PI = 60%). It is indicated that the Bangkok clay has salinity problems.

The effect for cement content, curing time and type of clay on electrical conductivity of treated soils at initial water content, 120% and curing time, 4 and 12 weeks are shown in Fig. 4.6. It is found that the electrical conductivity (EC) of soil is increased by reactions with increasing cement content (decreasing clay-water/cement ratio). For typical high plastic C1 (PI = 47%) clay, the EC (from 0.23 to 7.56 ds/m) increases rapidly with increasing cement content (from 0 to 16%) and EC (from 7.56 to 9.38 ds/m) increases moderately with increasing cement content (from 16 to 30%). It can be inferred that the flocculation of cement treated particles changes the EC values, because EC values indicate the salinity of clay-cement slurries. Salt concentration is one of reason of flocculated type structures and including other reasons. The EC values increases with increasing curing time because chemical reactions proceed on and flocculated structures are increased. The degree of flocculation of a clay deposit depends upon the type and concentration of clay particles, amount of cement and the presence of salts in water. The amount of salts in clay act as an electrolyte and reduces the repulsive forces between the particles (Arora, 2000). It is also evident that EC values increases with increasing plasticity of soil.

#### 4.2.5 Cation Exchange Capacity

The cation exchange capacity (CEC) of base clays were found to be 26 meq/100g, 23 meq/100g and 18 meq/100g for C1 (PI = 47%) clay, C2 (PI = 22%) clay and C3 (PI = 13%) clay, respectively. This means that C1 clay tends to absorb cations and it's 16.7 numbers of chemical equivalents per hundred grams of oven dry soil. CEC is the sum of the exchangeable cations that a mineral can absorb at a specific pH, i.e., a measurement of the negative charges carried by the mineral. Kamaluddin, (1995) reported that the cation exchange capacity (CEC) of the Bangkok clay (PI = 60%) was found to be 28.2 meq/100g while Chew et. al. (2004) reported that the cation exchange capacity (CEC) of the Singapore clay (PI = 52%) was found to be 33.3 meq/100g.



Effect of CEC on cement content, curing time and type of clay is shown in Fig. 4.7 at initial water content 120%, wc/c ratio of 7.5 (i.e. cement content 16%) and curing time of 4 weeks and 12 weeks. From Fig. 4.7 it is clear that the rate of cation exchange capacities increases with increasing cement content. For typical high plastic C1 (PI = 47%) clay at 4 weeks, the CEC (from 26 to 41 meq/100gm) increases rapidly with increasing cement content (from 0 to 16%) and CEC (from 41 to 48 meq/100gm) increases moderately with increasing cement content (from 16 to 30%). It can be inferred that the hydrolysis, hydration, pozzolanic reactions are responsible for changing the CEC values of clay-cement slurries. Thus Clay-water-electrolyte system changes CEC values of clay fabric and including others changes.

The cation exchange capacity (CEC) also increases with increasing curing time. Fig. 4.7 also shows that the cation exchange capacity at 12 weeks for C1 clay (highest measured 57 meq/100gm) is higher than that of C3 clay (highest measured 50 meq/100gm) while the cation exchange capacity for C2 clay (highest measured 45 meq/100gm) is lower than that of C3 clay and subsequently, C1 clay gains more strength than that of C3 clay while C3 clay gains more strength than that of C2 clay (which has been found from unconfined compression test as presented in the next chapter). So it is evident that cation exchange capacity increases with increasing plasticity of soil.

#### 4.2.6 Exchangeable Cations

Cation exchange capacity is the sum of the exchangeable cations which means the clay tends to absorb cations. The clays will absorb cations and/or anions that neutralize the layer charge, but which are exchangeable. This means that it can be readily replaced by another anion or cation when brought into contact with these ions in aqueous solution. The cation exchange capacity and exchangeable cations are varied on the type clays. During the chemical stabilization, the cation exchange capacity and exchangeable cations of base are continuously changed. The exchangeable cations of the untreated base clays and cement treated clays are summarized in Table 4.1.

The effect for cement content, curing time and type of clay on exchangeable cation ( $\text{Ca}^{2+}$ ) of treated soils at mixing water content ( $w_i$ ) of 120% is shown in Fig. 4.8. It has been found that  $\text{Ca}^{2+}$  ion increases with increasing curing time. There is a consistent of results, reported by Rao and Rajashekar (1996). It seems to suggest for exchangeable cation,  $\text{Ca}^{2+}$  from the figure that a certain percentage of cement (say more than 4%) is required to complete the hydration as well as pozzolanic reaction between cement and clay particles. Fig. 4.8 shows that the  $\text{Ca}^{2+}$  ion for C1 clay is higher than that of C3 clay while the  $\text{Ca}^{2+}$  ion for C2 clay is lower than that of C3 clay. For typical high plastic (C1, PI = 47%) clay at 4 weeks, the  $\text{Ca}^{2+}$  ion (from 17 to 32 meq/100gm) increases rapidly with increasing cement content (from 0 to 16%) and  $\text{Ca}^{2+}$  ion (from 32 to 34 meq/100gm) increases moderately with increasing cement content (from 16 to 30%). Table 4.1 shows the following variations:

- exchangeable cations  $Mg^{2+}$  increases with increasing plasticity index.
- exchangeable cations  $Na^+$  and  $K^+$  decreases with increasing plasticity index.
- exchangeable cations  $Ca^{2+}$ ,  $Na^+$  and  $K^+$  increases with increasing cement content.
- exchangeable cation  $Mg^{2+}$  decreases with increasing cement content.

From the Table 4.1, comparing the exchangeable cations for treated and untreated samples of each clays, it can be observed that the cation exchange capacities for treated samples are higher than that of untreated samples. For treated clays, exchangeable cations increase with increasing curing time. It can be inferred that the rapidly rising the pH values indicate the crowding of  $Ca^{2+}$  ion concentration and the formation of flocculated clay-cement matrix on the clay surface. The exchangeable cations that a mineral can absorb at a specific pH value, i.e., a measurement of the negative charges carried by the mineral. As increasing cement content, the pH value approaches 12.6, which corresponds to that of  $Ca(OH)_2$ . The increase of pH with an increase of cement content is due to crowding of the  $Ca^{2+}$  ion concentration on the clay surface, leading to changes in fabric of the cement-treated clay (i.e., the formation of a flocculated clay-cement matrix). The flocculated nature of the fabric has been attributed to the cation exchange process, which results in  $Ca^{2+}$  ions replacing  $Mg^{2+}$ ,  $K^+$  and  $Na^+$  cations (Locatc et al., 1990; Shen, 1998). The adsorption of  $Ca^{2+}$  ions onto the mineral particle surface leads to a decrease in repulsion between successive diffused double layers and results in more edge-to-face contacts between successive mineral sheets. Thus, clay particles flocculate into larger size clusters, which has been confirmed in SEM images in the next section. As the silicates and aluminates from the mineral component go into solution, they react with the adsorbed  $Ca^{2+}$  ions on the mineral particle surface and form CSH (Calcium silicate hydrate) and CASH (Calcium aluminium silicate hydrate), which induces cementation of the flocculated clay particles and forms clay-cement clusters, which has been confirmed in X-ray diffraction in the next section. Similar to that reported by Rao and Rajasekaran (1996), Kamruzzaman (2002) and Chew et al. (2004).

#### 4.2.7 Nitrogen and Phosphorus

Due to chemical stabilization, the nitrogen and phosphorus in soil are also changed. The nitrogen and phosphorus of the treated and untreated clays are summarized in Table 4.2. The nitrogen of the base clays were found to be 0.037%, 0.027% and 0.024% for C1 (PI = 47%) clay, C2 (PI = 22%) clay and C3 (PI = 13%) clay respectively. The phosphorus of the base clays were found to be 4.62 micro gm/gm, 6.23 micro gm/gm and 7.74 micro gm/gm for C1 clay, C2 clay and C3 clay respectively. The nitrogen for C1 clay is higher than that of C2 and C3 clay but the phosphorus for C1 clay is lower than that of C2 and C3 clay. The nitrogen and phosphorus are both increased with increasing cement content. The nitrogen increased with increasing curing time, while the phosphorus decreased with increasing curing time. As the pH values of treated samples are increased, the phosphorus are also increased. The amount of nitrogen and phosphorus in soil have no role on strength and deformation function but have

remarkable role on soil fertilization function. So, the effects of cement stabilization on environmental position of treated soils are explained here by the amount of nitrogen and phosphorus.

#### **4.2.8 Chemical Effect for Potential Acidity or Buffering Capacity**

Kamaluddin (1995) reported that the clays, which have high in organic content ( $\geq 6\%$ ) having a large reserve of potential acidity or buffering capacity. Buffering capacity was defined as the capacity of the soil to release exchangeable  $H^+$  into the soil solution to restore the equilibrium pH and due to which there is no soil reaction until the reserve  $H^+$  is exhausted. The chemical tests' results show that prior to cement treatment, the base clay already contains a moderate amount of calcium cations, both in the adsorbed state and dissolved state in the pore water. Secondly, another important property which has a significant bad influence on the effectiveness of cement treatment should be marked as the high organic content of the soil. Low pH value of the soil results in high degree of acidity. Thus, it shows that the clay has got high buffering capacity, i.e., it bears a large reserve of potential acidity. So, a relatively large amount of cement is needed to first exhaust the reserve acidity, and thereafter, to raise the pH value to the desired value at which the cement-clay reactions are enhanced.

The modification of the clay particles is brought about by the dissolution of the silicates and aluminates originating from the clay particles themselves and the amorphous components in the high pH environment, caused by the highly reactive  $Ca(OH)_2$ . The material thus dissolved is associated with calcium ions, producing additional cementing matter which, in turn, connect with adjacent clay particles. The ideal conditions for cement-clay reactions arise at high pH ( $pH > 12$ ), at which the solubility of soil pozzolans (Silicates and aluminates) is high. Thus it can be inferred that for the soft Bangladesh clay which was used as base clay, a large portion of the cement used was needed mainly for the above mentioned purpose, i.e., to first exhaust the large reserve of potential acidity of the soil since the soil, in its equilibrium or intact state, already possessed a moderate amount of calcium. After neutralization of the reserve acidity, the balance cement is used up to raise the pH value in order to bring about the clay-cement interactions. The base clay C2 has got high buffering capacity, i.e., it bears a large reserve of potential acidity, which has been confirmed in pH value determination in the previous section.

#### **4.2.9 Summary for Effect of Cement Treatment on Chemical Properties**

Concluding remarks of each chemical properties are summarized in Table 4.3. The effect for each variable on chemical properties are listed in a tabular form. From Table 4.3, one can easily observe the final effects of chemical properties for each variable during cement stabilization of clays at high water content.

### 4.3 Mineralogical Properties of Untreated Base and Cement Treated Clays

The clay minerals contained in the cohesive soil demonstrate physicochemical interactions with hardening agents to affect properties of the treated soil and it is important to study the relations with mineral compositions of cohesive soils. The basic mineralogical properties of the treated and untreated clays are summarized in Tables 4.4 and 4.5 for understanding the effect of cement, clay type and curing time. Diffraction patterns were obtained with X-ray diffractometer using Cu K $\alpha$  radiation, Fe-filter, and fixed scanning speed per minute. The clay mineral constituents of the base clay were identified as Illite, Montmorillonite and Kaolinite and expressed as percentages of the total amount of clay minerals in the soil. A silt fraction was identified to contain in the base clay. The silt fraction was found to contain mainly quartz and a smaller fraction of feldspar. Calcium silicate hydrate (CSH) and calcium aluminum silicate hydrate (CASH) were identified to contain in the treated clays.

Mineralogical analysis of X-ray diffraction pattern of untreated clay was carried out based on the characteristic Bragg angle given by Brown (1961) and Mitchell (1992). For treated clay, the Bragg data were taken from the standard Powder Diffraction File (JCPDS 1995). Figures 4.9(a) and 4.9(b) show the XRD pattern of untreated soils for C3 clay and C1 clay respectively. As shown in Fig. 4.9, illite, Montmorillonite, quartz, and kaolinite are clearly indicated for the untreated Bangladesh clays. In untreated clays reveal several peaks, which indicates the presence of illite (at 4.46, 3.19, 2.88, 2.16 and 2.04 Å), montmorillonite (at 3.53, 2.55 and 2.25 Å), quartz (at 4.28, 3.34 and 1.82 Å), and kaolinite (at 7.07, 2.45 and 2.28 Å). Of these, illite is the predominant mineral as shown in Table 4.4. This is consistent with the measured activity,  $A$  of 0.64, 0.35 and 0.23 and cation exchange capacity (CEC) of 32.2 meq/100 gm, 28.1 meq/100 gm and 16.7 meq/100 gm for C1 (PI = 47%) clay, C2 (PI = 22%) clay and C3 (PI = 13%) clay respectively. Mitchell's (1993) reported that both parameters fall within range of activity of 0.20 - 1.0 and cation exchange capacity of 10 - 40 meq/100 gm for illite.

The effects of cement content are explained in Figs. 4.10, 4.11 and 4.12 up to 4 weeks curing time and addition with the effect of curing is explained in Fig. 4.13 up to 12 weeks curing time. As shown in Figs. 4.10(a) and 4.10(b), corresponding measurements with 16% cement-treated clays for C3 clay and C1 clay respectively and Figs. 4.11(a) and 4.11(b), corresponding measurements with 30% cement-treated C3 clay and C1 clay respectively. And the Figs. 4.12(a) and 4.12(b), corresponding measurements with 60% cement-treated C3 clay and C1 clay respectively. The Fig. 4.13, corresponding measurements with 30% cement-treated C1 clay only up to 12 weeks curing time. In these Figures, the cement content is defined as the ratio of the mass of cement to the mass of soil solid. In cement-treated clays reveal several new peaks, which indicates the presence of calcium silicate hydrate (CSH) (at 3.85, 3.61, 3.19, 3.04, 2.12, 1.87 and 1.59 Å) and calcium aluminum silicate hydrate (CASH) (at 5.01, 3.28, 2.73, 2.45, 1.99 and 1.67 Å). Figure 4.14 shows the amounts of constituents in

the soil samples which were determined using the semi quantitative procedure suggested by Pierce and Siegel (1969). The mass of CSH and CASH was normalized by the mass of the treated soil solid; this quantity is hereafter termed the cementations product content. As Fig. 4.14 shows, although the cementations product content increases approximately linearly at higher cement content but nonlinear line at lower cement content and pass through the origin. This suggests that, at cement content up to 20%, the rate of increase in CSH and CASH content is higher. It should be mentioned that there is some uncertainty in the accuracy of the semi quantitative procedure. Nonetheless, the consistency in the trend of the nine samples is significant and suggests that the cause may be deterministic. The change in composition of the clay can be seen from Table 4.4 and Table 4.5, which show the mass of the various constituents of improved soil after 4 weeks and 12 weeks of curing time respectively. The initial mass of soil solid in each sample is 100 g. As Table 4.4 shows, kaolinite appears to have vanished in all eight of the cement-treated soil specimens. This suggests that kaolinite is rapidly exhausted by the pozzolanic reaction and is consistent with the highly pozzolanic behaviour of kaolinite (see, e.g., Eades and Grim 1960). It is also consistent with the rapid increase in cementitious product (CSH + CASH) at low cement content. For typical high plastic (C1, PI = 47%) clay, the cementitious product (from 0 to 52% by wt.) increases rapidly with increasing cement content (from 0 to 30%) and cementitious product (from 52% to 82% by wt.) increases moderately with increasing cement content (from 30 to 60%) as shown Fig. 4.14. From Table 4.4, the cementitious product for C1 clay is higher than that of C3 clay while the cementitious product for C2 clay is lower than that of C3 clay.

At low cement content, cementitious products are formed by the hydration and pozzolanic reaction with the latter using up the kaolinite. At higher cement content, exhaustion of the kaolinite leads to completion of the pozzolanic reaction and additional cementitious products are formed only by the hydration reaction (Kamruzzaman, 2002). There is always a substantial amount of isomorphous substitution of silicon of by aluminium in silica sheet. Consequently, the mineral has a larger negative charge than in montmorillonite. The link between different structural units is through non exchangeable potassium ( $K^+$ ) and not through water. This bonds for the units are more firmly than in montmorillonite. The lattice of illite is stronger than that of montmorillonite, and is, therefore, less susceptible to cleavage. Illite swells less than montmorillonite. However, swelling for both more than in kaolinite. The space between different structural units is much smaller than that in montmorillonite, as the potassium ions just fit in between the silica sheet surfaces. The properties of the mineral illite are somewhat intermediate between that of kaolinite and montmorillonite. The bond between the non-exchangeable  $K^+$  ions, though stronger than that in montmorillonite is considerably weaker than bond of kaolinite. The swelling of illite is more than that of kaolinite, but less than that of montmorillonite (Arora, 2000).

From Table 4.4, it can be seen that the amount of illite and quartz showed consistent trend with change in cement content and plasticity of soil. Illite decreases and quartz increases with an increase in cement content but illite and quartz decrease with a increase in plasticity of soil. The amount of CSH and CASH content increases with decrease in plasticity of soil. The amount of montmorillonite, on the other hand, also show the consistent trend of reduction with an increase in cement content. From Table 4.5, it can be seen that Illite and montmorillonite decreases and quartz increases with an increase in curing time. The amount of CSH and CASH products increase with increasing in curing time. This suggests that the illite and montmorillonite are less involved in the pozzolanic reaction than kaolinite, which is consistent with the findings reported by Porbaha et al. (2000). On the other hand, Eades and Grim (1960) reported that both pure kaolinite and pure illite undergo pozzolanic reaction with lime although illite appears to require a higher lime content to initiate the pozzolanic reaction but Chew et al. (2004) reported for marine clay that different minerals kaolinite and illite undergo pozzolanic reaction with cement. At the present research, it is found for Bangladesh clays that different minerals kaolinite, montmorillonite, and illite undergo pozzolanic reaction with cement.

There are, however, two important differences between Eades and Grim's (1960) research and the present research. Firstly, Eades and Grim (1960) used lime as the reactant where as the present research uses cement. In soil-cement mixes, lime is not present initially, but is instead, produced by hydration reaction of the cement. Secondly, Eades and Grim's (1960) study was on pure clay mineral, whereas the Bangladesh clays used in the present research comprises several different minerals. There are, more or less, similarity between Chew et al. (2004) research and the present research, but only one difference that montmorillonite mineral has been found in this study.

#### **4.4 Micro-structural Properties of Untreated Base and Cement Treated Clays**

Scanning Electro Micrograph (SEM) analysis was carried out in order to understand the bridging (cementation) effect and to indicate the probable weak / failure zone in the cement treated clay matrix. The drying method was used to sample preparation, prior to SEM analysis in order to minimize the disturbance of the microstructure for soil. Details of the sample preparation techniques have been reported in the last Chapter 3.

Figures 4.15(a) and 4.15(b) show SEM images of untreated for C1 (PI = 47%) clay and C3 (PI = 13%) clay respectively. As shown in these figures, untreated clays exhibits a fairly open type of microstructure, with the platy clay particles assembled in a dispersed arrangement. However, the micrograph of 16% cement treated clays at curing 4 weeks, shown in Figs. 4.16(a) and 4.16(b) for C1 clay and C3 clay, respectively, results in an open structure, with some sign of reticulation. As the cement content increases to 30% at curing age of 4 weeks, the flocculated nature of the structure becomes more evident, with clay particle clusters

interspersed by large openings as can be seen from Fig. 4.17. At the same time, the platiness of the structure becomes less evident and degree of reticulation appears to increase. As the cement content highest increases up to 30% at curing 4 weeks (Fig. 4.17), the flocculated nature of the structure becomes most evident, with clay particle clusters interspersed by large openings. The increase in the degree of reticulation and formation of clay cement clusters is due to the formation of cementitious products, calcium silicate hydrate (CSH)/calcium aluminum silicate hydrate (CASH). The increase in the degree of reticulation can be attributed to an increase in the amount of CSH, which is reticular in nature (e.g., Locate et al. 1990). As a similar significant improvement result was observed and reported by Kamruzzaman et al. (2004). The formation of cementitious products (CSH + CASH) is also confirmed from the X-ray Diffraction (XRD) analysis in the present research. Similar results were also reported by Chew et al. (2004).

The effect of curing time on the formation of cementitious products can also be explained by the SEM images. The clay cement clusters are formed for 16% cement treated clays with in the period of 12 week curing as can be seen from Fig. 4.18. As the curing time increases through 4 to 12 weeks, the flocculated nature of the structure becomes more evident, with the formation of clay cement clusters. At the same time, the platiness of the structure becomes less evident and degree of reticulation appears to increase. The micrograph of 30% cement treated clays cured at 12 weeks as shown in Fig. 4.19 appears to be different from the 16% cement treated clays samples cured up to 4 weeks (Fig. 4.16). As can be seen from Figs. 4.19, the clay-cement clusters are appeared to be platy in nature and at same time the clusters are interspersed by large openings. This is attributed to the fact that at prolonged curing periods ( $\geq 1$  year). Significant portion of  $\text{Ca}^{2+}$  ions diffuses within the cement treated clays matrix to permit the pozzolanic reaction, similar to that reported by Kamruzzaman et al. (2004) and Chew et al. (2004). For lime treated clay, Locate et al. (1990) suggested that CASH appears to be platy and CSH is reticular in nature. Thus, it seems that at prolonged curing time ( $\geq 1$  year) the behaviour of cement treated clay is mainly governed by the platy nature of cementitious product, which is believed to be the calcium aluminum silicate hydrate (CASH). The presence of platy and reticular cementitious products in the clay cement matrix is the main cause for the development of long-term strength. This is consistent with the results of the XRD analysis discussed above, as well as with SEM results for lime-treated clay (Locate et al., 1990; Berube et al., 1990; Rao and Rajasekaran 1996). The flocculated nature of the fabric has been attributed to the cation exchange process, which results in  $\text{Ca}^{2+}$  ions replacing  $\text{K}^+$  cations (Locate et al. 1990; Shen 1998). The adsorption of  $\text{Ca}^{2+}$  ions onto the illite and montmorillonite particle surface leads to a decrease in repulsion between successive diffused double layers and results in more edge-to-face contacts between successive illite and montmorillonite sheets. Thus, clay particles flocculate into larger size clusters. As the silicates and aluminates from the kaolinite go into solution, they react with the adsorbed  $\text{Ca}^{2+}$  ions on the illite and montmorillonite particle surface and form CSH and CASH, which induces

ccementation of the flocculated clay particles and forms clay-cement clusters, similar to that reported by Kamruzzaman et al. (2004) and Chew et al. (2004). Thus, the overall effect in one of removal of kaolinite material from the clay matrix and addition of cementitious material between flocculated particles. The dissolution of kaolinite and the flocculation process both result in a more open clay structure, with cement-clay clusters interspersed by large voids.

#### **4.5 Physical Properties of Untreated Base and Cement Treated Clays**

##### **4.5.1 Colour**

The base clays used in this study were retrieved from depths of 2.0 m to 3.0 m. The narrow range of sampling depth was adopted to obtain each samples with similar initial properties and history and is expected to have the same initial structure, water content and index properties. The clays used in this study were undisturbed and fairly homogeneous, and various in colour. The colour is varied from location to location, depth to depth, soil to soil and indicator to indicator. The observed colour of base clays were grayish brown for C1 (PI = 47%) clay, brown for C2 (PI = 22%) clay and yellowish brown for C3 (PI = 13%) clay. At time of treatment, the colour of base clays were changed by chemical reaction with deep gray coloured cement. The observed colour of treated clays were grayish light brown for C1 clay, light brown for C2 clay and light yellowish brown for C3 clay. The gray colour cement converted to the colour of each untreated clays to light in position.

##### **4.5.2 Grain Size Distribution and Surface Area Distribution**

The basic physical properties of the clays can be explained by grain size and surface area distribution. The percentage sand, silt and clay of base clays were determined by hydrometer analysis. The percent of clay, silt and sand are shown in Table 4.6. In this table, the percent of clays were 73%, 41% and 32%, the percent of silts were 23%, 51% and 58%, and the percent of sands were 4%, 8% and 10%, for C1 (PI = 47%) clay, C2 (PI = 22%) clay and C3 (PI = 13%) clay respectively. Fig. 4.20 presents expresses a comparison of the grain size distribution curves for three base clays.

The basic engineering tests on cement treated clay samples comprised basically the same tests carried out on untreated samples, except the determination of grain size distribution. The changes in grain size distribution due to cement treatment were rather difficult to determine accurately. The usual hydrometer method could not be expected to render a true picture for the cement treated clays as reported by Kamaluddin (1995). The grain size distribution concept is converted to specific surface area distribution concept. The lowest the grain size, the highest the specific surface area and vice versa are presented as shown in Fig. 4.21. From Fig. 4.21, it has been found that specific surface area increases with increasing plasticity index (i.e. increasing clay content) of soils.



### 4.5.3 Water Content

The clays used in this study were undisturbed and disturbed samples. The in-situ water contents were determined from undisturbed samples as possible as early after sampling. The water content is varied from season to season, location to location, depth to depth and soil to soil. In this study, the water content is defined as the ratio of weight of water to the weight of total dry solids, which consists of soil and cement solids, and is determined by heating the soil in an oven at temperature of 105°C for 24 hours. The in-situ water content of base clays are shown in Table 4.6. The water content of treated and untreated clays were measured during unconfined compression and triaxial tests. The natural water content of base clays were 70%, 62% and 53% for C1 clay, C2 clay and C3 clay respectively. At time of treatment, the initial mixing water content of base clays were changed by chemical reaction with cement. The final water contents ( $w_f$ ) of treated clays have been found to depend on applied initial water ( $w_i$ ), clay-water/cement ratio ( $w/c$  ratio) i.e. cement content ( $c$ ) and curing time. The water content of treated clays are shown in Tables 4.7, 4.8 and 4.9 for C1 (PI = 47%) clay, C2 (PI = 22%) clay and C3 (PI = 13%) clay, respectively.

The effect of clay-water/cement ratio and curing time on water content is shown in Figs. 4.22(a) and 4.22(b) for C1 clay and C2 clay, respectively. From Fig. 4.22, it can be seen that water content increases with increasing clay-water/cement ratio (i.e., decreasing cement content) and increasing curing time at particular curing time for all clays.

The effect of cement content, type of clay and curing time on final water content of treated clays are shown in Fig. 4.23. In this figure, the immediate reduction of the water content from that of the slurry clay is due to the addition of dry cement, so it should therefore be regarded as the initial water content. As the cement content increases, the water content of the improved soil decreases but the relative differences in the changes in the water content are not proportional to the differences in the amount of cement additive used. Fig. 4.23 shows the relations between water content and cement content of the sample before treatment, water content of sample after treatment. Cement content up to 16% refers to Part A (Fig. 4.23a) which corresponds to sharp reduction of water content (17%, 26% and 37% for C1 clay, C2 clay and C3 clay respectively), whereas Part B (from 16% up to 60% cement) experiences reduction of only 16%, 13% and 24% for C1 clay, C2 clay and C3 clay respectively. Moreover, it can be seen that this reduction process of water content continues until it reaches a higher mixing ratio of cement, where it reaches an asymptotic value of water content. It is also evident that the reduction process ceases beyond 30% to 35% of cement content leaving the water content of the treated clay almost constant thereafter. The immediate decrease in the water content after mixing was recorded from 8% to 60% cement for various clays (Fig. 4.23). Chew et al. (2004) reported that the similar behaviour for reduction of water at 28 days, 7 days and immediate after mixing of initial water, 120% with different cement content. Bergado et al. (2003), Miura et al. (2001) and Kamaluddin (1995) found that the same

consistent of results for the effect of cement and curing time on water content of treated clays. According to the relationship suggested by Broms et al. (1980), for lime treated clay, the reduction in water content ( $\Delta w_c$ ) is as follows:

$$\Delta w_c = \frac{(w_n + 32).X}{(100 + X)}$$

Where X is the lime added as a percentage of the weight of the base clay, and  $w_n$  is the original natural water content, in percentage.

The above expression leads to an underestimation for the cement treated clay at low water content. The alternate relationship at low water content (1% decrease in water content per 1% of hardening agent) proposed by Broms et al., (1980) gave reasonable value for cement content up to 7.5%, and beyond 7.5%, it overestimates the percentage of the water content that is reduced. All the 4-week water contents show a very rapid decrease at cement content of less than 16%, which then moderated substantially at higher cement contents (Fig. 4.23). Furthermore, the vertical offset between the three curves increases at low cement content, but stabilizes to a roughly constant vertical offset at higher cement content. Both these observations are consistent with the earlier-proposed notion that, the extent of hydration and pozzolanic reaction still increases with the cement content, and water is utilized in both reactions. At higher cement content, the exhaustion of the kaolinite further inhibits pozzolanic reaction, leaving only the hydration reaction. Thus, the increase in water usage moderated at higher cement contents. Moreover, since the their individual reaction activities.

The variation of final water with mixing water content relationships in Fig. 4.24 are approximately linear at clay-water/cement ratio, 7.5 for all treated clays.

The comparison of the variation for water content with clay-water/cement ratio and curing time are shown in Figs. 4.25 and 4.26 respectively for all clays. From these figures, the effect for plasticity of clay, curing time and clay-water/cement ratio on final water content of treated clays are clearly observed. The slope of curve for increase of water content with increasing clay-water/cement ratio and curing time for C3 clay is greater than that of C2 and C1 clays. During soil stabilization at clay-water/cement ratio and curing time, the loss of water for C2 clay is more than that of C1 clay but the loss of water for C3 clay is more than that of C2 clay i.e. the more water holding capacity, the more plasticity of soil. The curing time effect on the treated samples is illustrated in Fig. 4.26. It can be seen that the water content of cement treated clay decreases with curing time up to 12 weeks curing time for Part A (e.g., 24%, 29% and 44% for C1 clay, C2 clay and C3 clay respectively). Lower reduction of water content (e.g., 4%, 3% and 6% for C1 clay, C2 clay and C3 clay respectively) occurs in Part B (from 12 weeks up to 24 weeks), thereafter the reduction process slows down. Fig. 4.26 shows that much of the decrease in water content takes place within the first one week of curing. This is not surprising since water is absorbed and transformed into hydrated CSH, CAH and CASH

during the hydration and pozzolanic reactions, and will not be expelled by reheating the cementitious products to 105°C. This notion has been readily verified by conducting simple experiment with an amount of cement. Since both the hydration and pozzolanic reactions involve cement, the total amount of immediate water loss is proportional to the relative amount of cement as shown in Fig. 4.23. Water content continues to decrease for longer curing time, which can be attributed to the fact that the formation of the primary and secondary cementitious materials proceeds slowly and continuously, which are confirmed by X-ray diffraction analysis and SEM development images in this study. Similar results were reported by Kamruzzaman et al. (2004) and Chew et al. (2004). The formation of hydrated gel and pozzolanic reaction continue last for months, even years and the water loss also continue.

#### 4.5.4 Unit Weight

The basic physical properties of the clays can be also explained by the wet unit weight and dry unit weight. The unit weights of treated and untreated clays are measured during unconfined compression and triaxial compression tests. The values of wet unit weight and dry unit weight of base clays have already been presented in Table 4.6. The dry unit weight of base clays are 8.85 kN/m<sup>3</sup>, 9.05 kN/m<sup>3</sup> and 9.44 kN/m<sup>3</sup> for C1 (PI = 47%) clay, C2 (PI = 22%) clay and C3 (PI = 13%) clay, respectively. From this analysis, it can be remarked that the dry unit weight increases with decreasing plasticity of soil.

The dry unit weight of treated clays are shown in Tables 4.7, 4.8 and 4.9 for C1 clay, C2 clay and C3 clay, respectively. It can be seen that dry unit weight for treated samples are lower than that of untreated samples. It is also evident from the data presented in Tables 4.7, 4.8 and 4.9 that dry unit weight decreases with increasing mixing water content of soil during chemical stabilization at same clay-water/cement ratio and curing time. The rate of decrease for dry unit weight for C3 clay is lower than that of C2 clay. The rate of decrease for dry unit weight for C2 clay is lower than that of C1 clay.

Effect of dry unit weight on clay-water/cement ratio at different curing time are shown in Fig. 4.27(a) and 4.27(b) for C1 clay and C3 clay, respectively. From the figures, it has been found that dry unit weight increases with decreasing clay-water/ cement ratios (i.e. increasing cement content) at a particular curing time. The influence of curing time is also illustrated in the Fig. 4.27 which shows that at a particular wc/c ration, the longer curing time produces treated clay of higher unit weight. Bergado et al. (2003), Miura et al. (2001) and Kamaluddin (1995) also found similar results for the effect of cement and curing time on unit weight of cement treated clays.

The variation of dry unit weight with initial mixing water content at different clay-water/cement ratio are shown in Figs. 4.28(a) and 4.28(b) for C2 clay and C3 clay respectively. From the figures, it can be seen that dry unit weight decreases with increasing

mixing water content at particular clay-water/cement ratio for all clay because more mixing water content occupied more pore volume.

#### 4.5.5 Specific Gravity

The basic physical properties of the clays can also be explained by specific gravity. The specific gravity values of base clays are shown in Table 4.6 which shows that the values of specific gravity are 2.680, 2.673 and 2.668 for C1 (PI = 47%) clay, C2 (PI = 22%) clay and C3 (PI = 13%) clay, respectively. It can be seen that the specific gravity decreases with decreasing plasticity of soil for untreated clays.

Tables 4.7, 4.8 and 4.9 summarize the changes incurred in the values of specific gravity due to cement stabilization for C1 clay, C2 clay and C3 clay respectively. Cement causes significant reduction in specific gravity and this change is dependent on cement content and curing time. From Tables, comparing the specific gravity for treated and untreated samples of each clays, the specific gravity for treated samples are lower than that of untreated samples.

The rate of decrease for specific gravity of treated clays at high water content, for C3 clay is higher than that of C2 clay. The rate of decrease for specific gravity for C2 clay is higher than that of C1 clay. It is clear that the rate of decrease for specific gravity decreases with increasing initial mixing water content of soil during soil stabilization at same clay-water/cement ratio and curing time because at high water content, treated clays hold a large fabric that is an arrangement of particles, particle group and pore spaces in the soil as well as cementation. A cluster is a grouping of particles or aggregates into large fabric units and a fabric composed of grouping of clusters (Mitchell, 1993).

Effect of clay-water/cement ratio and curing time on specific gravity is shown in Figs. 4.29(a) and 4.29(b) for C1 clay and C3 clay, respectively. From the figures, it is observed that specific gravity increases with increasing clay-water/cement ratios (i.e. decreasing cement content) at particular curing time. Fig. 4.29 also shows that specific gravity decreases with increasing curing times at particular clay-water/cement ratio.

The variation of specific gravity with initial mixing water content at different clay-water/cement ratio are shown in Figs. 4.30(a) and 4.30(b) for C2 clay and C3 clay, respectively. It can be observed from Fig. 4.30 that specific gravity increases with increasing initial mixing water content at particular clay-water/cement ratio. Cementation causes significant reduction in specific gravity and this change is dependent on type of clay, cement content and curing time. It has been found from present study that the influence of the curing time on the specific gravity is not significant. At the early period of curing, significant influence of cement content on specific gravity has been observed. Longer curing period has got in significant effect on specific gravity. Bergado et al. (2003), Miura et al. (2001) and

Kamaluddin (1995) found that the same consistent of results for the effect of cement and curing time on specific gravity of treated clays.

#### 4.5.6 Atterberg Limits

The basic physical properties of the clays can easily be explained by Atterberg limits. The Atterberg limits of base clays are shown in Table 4.6. In this table, plasticity indices are 47%, 22% and 13% for C1 clay, C2 clay and C3 clay respectively. Activity of clays depend on plasticity index and clay content, which is defined as the ratio of plasticity index and clay content. The activity of clays are 0.64, 0.35 and 0.23 for C1 clay, C2 clay and C3 clay respectively. It can be seen that the activity of clays decreases with decreasing plasticity of soil.

The effect of cement content and curing time on Atterberg limits are shown in Figs. 4.31(a) and 4.31(b) for C2 clay and C3 clay, respectively. From the Figs. 4.31, comparing the Atterberg limits for treated and untreated samples of each clays, the Atterberg limits for treated samples at high water content are higher than that of untreated samples. But at higher cement content for treated samples, the plastic limit are higher than that of untreated samples but the plasticity index are lower than that of untreated samples. The plastic limit increases with increasing cement content and the plasticity index decreases with increasing cement content.

From Fig. 4.31, it has been observed that liquid limit and plasticity index decrease with increasing curing time and increasing cement content (i.e. decreasing clay-water/cement ratio) but plastic limits increase with increasing curing time and increasing cement content (i.e. decreasing clay-water/cement ratio). The samples with curing time, 4 weeks and 12 weeks, showed a minor decreased of liquid limit, while the sample after 4 weeks rendered the value of liquid limit almost unchanged or higher than that of the base clay. The plastic limit was significantly increased with cement content and curing time and thus, reduction in the plasticity index was due to increase in the plastic limit. The increase in the plastic limits was such that the plasticity index of the treated soil reduced significantly. Higher cement content and longer curing time dominate the reduction process of the plasticity index of the treated clays.

The liquid limit increase significantly at low cement content ( $\leq 12\%$ ) before dropping slightly at higher cement contents. As the Fig. 4.31 shows the rates of increase in the liquid and plastic limits with respect to the cement content are almost equal at low cement content. This is consistent with the notion of water trapped with intra-aggregate pores. However, the rates of change of these two Atterberg limits at higher cement content are not the same. This suggests that the entrapped water hypothesis explains much, but not all, of the observed changes in the plastic and liquid limits. One possible reason for this is the deposition of cementitious products on the surfaces of the flocculated clay clusters, which would lower the

surface activity of these clusters. This has been explained the decrease in liquid limit between 4-week curing and 12-week curing periods. The rapid hydration reaction is accompanied by the much slower pozzolanic reaction over time. The findings of mineralogy study indicate that kaolinite is preferentially attacked in comparison to illite and montmorillonite. The secondary cementitious products appear to be deposited on or near the surfaces of the clay clusters. This gives rise to a reduction in entrance pore diameter but an increase in particle size. The continued increase in particle size leads to an increase in the plastic limit over time with increase in cement content. The deposition of secondary cementitious products on the clay cluster, on the other hand, leads to a decrease in surface activity of the illite clusters. As a result the liquid limit decreases over time and at higher cement content. Similar effects were reported by Kamruzzaman et al. (2004) and Chew et al. (2004).

A particle with a large specific surface is attributed as having a higher liquid limit because of a larger double layer. Hence, this contributes to an additional explanation for the increase of the liquid limit at low cement content. Chew et al. (2004) reported that the similar trend of Atterberg limits for cement treated Singapore marine clay at 7 days and 28 days of curing time. Bergado et al. (2003) and Kamaluddin (1995) found that the same consistent of results for the effect of cement and curing time on Atterberg limits of treated clays. A number of research works on regional treated samples of Bangladesh reported similar effect for such physical properties (Ahmed, 1984; Serajuddin and Azmal, 1991; Serajuddin, 1992; Rajbongshi 1997; Molla, 1997; Shahjahan, 2001; Hasan, 2002; Siddique and Rajbongshi, 2001, 2002; Siddique and Hossain, 2003; Ansary et al., 2003; Toyeb, 2006).

Effect of mixing water content and clay type on Atterbeg's limits is shown Fig. 4.32. It has been observed that LL, PL and PI increase with increasing mixing water content. In should be noted that the trend of change in the liquid limit with cement content and curing time seems to depend heavily on the soil type. Sivapullaiah et al. (2000) reported a similar increasing trend on lime-treated black cotton soil after 7 days of curing. Kinuthia et al. (1999) also reported a similar trend for lime-treated kaolinitic, measured a few hours after mixing. On the other hand, Locat et al.'s (1996) data on lime-treated Louiseville clay after 100 days of curing suggest a general increase in liquid limit with the lime content, Brandl (1981) reported divergent trends for two soils with the more plastic soil (containing montmorillonite) showing a significant decrease in liquid limit after 7-day and 270-day curing and a less plastic soil showing a corresponding increase. The general trend appears to be one of decreased liquid limit if the untreated soil is highly plastic and increased liquid limit in soil of low plasticity. Taken in light of the mechanisms postulated above, this suggests that, in soils of high plasticity, the encapsulation of the clay clusters by deposited cementitious products has a dominant effect, leading to lowering rate of the liquid limit. On the other hand, in soils of low plasticity, the presence of entrapped water has a dominant effect, leading to a higher rate in the liquid limit.

Figure 4.33 shows the normalized plasticity index of cement treated clays (C1, C2 and C3) at initial mixing water content, 120%. The plasticity index (PI) of treated clays is normalized with their respective final water content. As can be seen, the normalized plasticity index reduces with the increase of cement content. The normalized behaviour pattern is approximately independent of curing time and unique relationships for the particular cemented clay. Based on the experimental result of this study, the following empirical equations are thus proposed as:

$$PI/w_f = -0.166\ln(c) + 0.99 \quad \text{for C1 clay} \quad (4.1)$$

$$PI/w_f = -0.160\ln(c) + 0.85 \quad \text{for C2 clay} \quad (4.2)$$

$$PI/w_f = -0.156\ln(c) + 0.79 \quad \text{for C3 clay} \quad (4.3)$$

Where,  $w_f$  = Final water content of the hardened cemented clay

$c$  = Amount of cement in percentage of dry weight of soil solid

Using above equations, plasticity index of cement treated clays can be estimated if the final water content and amount of cement are known. Similar analysis was also performed by Kamruzzaman (2002), where  $PI/w_f = -0.12\ln(c) + 0.73$  has been found for Singapore marine clay.

#### 4.5.7 Void Ratio

The basic physical properties of the clays can be defined by void ratio. The void ratio of treated and untreated clays were estimated from consolidation tests. The void ratio of base clays are shown in Table 4.6. In this table, the void ratios are 1.81, 1.96 and 2.10 for C1 (PI = 47%) clay, C2 (PI = 22%) clay and C3 (PI = 13%) clay respectively at effective vertical pressure, 12.5 kPa. From this analysis, it can be remarked that the void ratio decreases with increasing plasticity of soil. The void ratio of cement treated clays are shown in Table 4.7, 4.8 and 4.9 for C1 clay, C2 clay and C3 clay respectively at effective vertical pressure, 12.5 kPa. Tables show that the void ratio for treated samples are higher than that of untreated samples. It has also been found that the void ratio for all clays decreased with increasing cement content (decreasing  $w/c$  ratio) and curing time. Bergado et al. (2003), Miura et al. (2001) and Kamaluddin (1995) also found similar results for the effect of cement and curing time on void ratio of treated clays.

It has been also observed that the rate of void ratio of cement treated clays increases with increasing the initial mixing water content of soil during soil stabilization at same clay-water/cement ratio and curing time and that void ratio decreases with increasing plasticity index of the clays. A comparative study with the base clay revealed that at high water content, the cement treated samples have higher void ratio. Cement treatment caused a notable change in the values of void ratio.

#### 4.5.8 Degree of Saturation

The degree of saturation of treated and untreated clays have been estimated using water content, specific gravity and consolidation test data. The degree of saturation of soil is varied from location to location, depth to depth and soil to soil. The degree of saturation of base clays are shown in Table 4.6. The degrees of saturation are 89%, 84% and 78% for C1 (PI = 47%) clay, C2 (PI = 22%) clay and C3 (PI = 13%) clay respectively. It can be seen that the degree of saturation decreases with decreasing plasticity of soil. The degree of saturation of treated clays are shown in Tables 4.7, 4.8 and 4.9 for C1 clay, C2 clay and C3 clay respectively. It has been found that the values of degree of saturation for treated samples are higher than that of untreated samples and that the degree of saturation decreases with increasing curing time.

It has also been found that degree of saturation increases with increasing initial water content of soil during soil stabilization at same clay-water/cement ratio and curing time. It has been also been observed that degree of saturation increases with increasing plasticity index of clay. When compared with the base clay, the cement treated samples were found to have comparatively lower degrees of saturation for curing periods up to twelve weeks; while lower curing periods resulted in higher degree of saturation. Similarly, low cement content produced a higher value of degree of saturation. In general, higher saturation is obtained with more mixing clay-water/cement ratio. Ultimately, it has been found that the degree of saturation for all clays decreased with increasing cement content and curing time. Bergado et al. (2003), Miura et al. (2001) and Kamaluddin (1995) found that the same consistent of results for the effect of curing time but different effect of cement on degree of saturation of treated clays.

#### 4.5.9 Summary for the Effect of Cement Treatment on Basic Properties

Concluding remarks on the effect of cement treatment on basic engineering properties are summarized in Table 4.10. The effect for variables on basic properties are provided in a tabular form. From this table, the effects of physical properties for each variable during cement stabilization of soft clays at high water content can be observed.



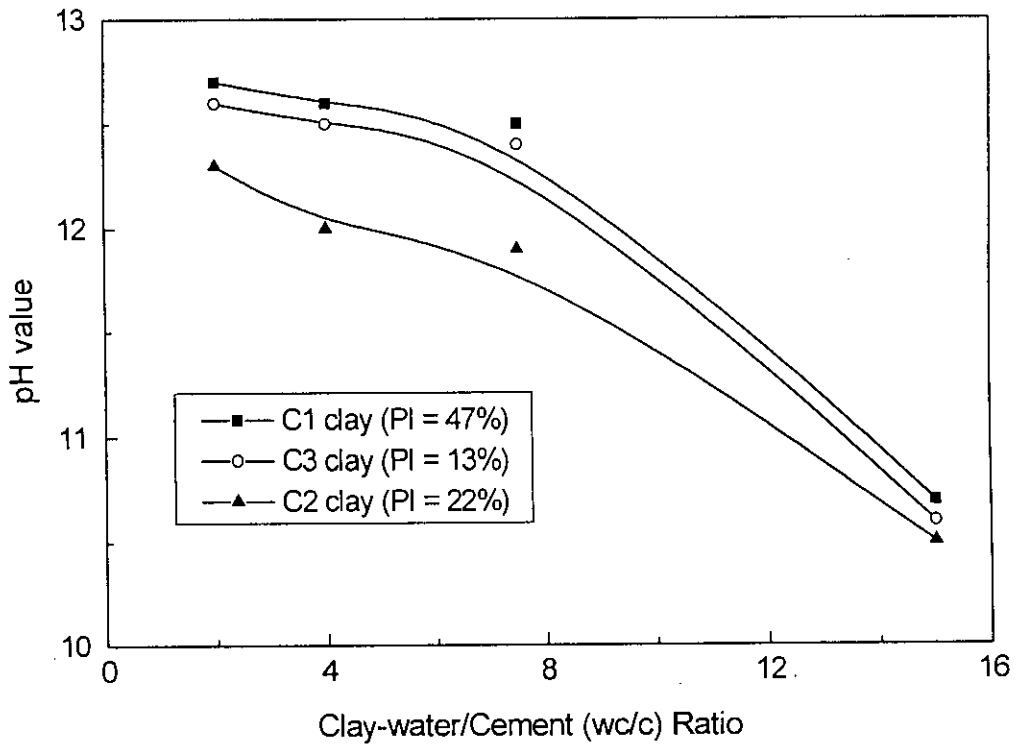


Fig. 4.1 Effect of Clay-water/Cement Ratio and Clay Type on pH value for Cement Treated Clays (mixing water = 120%)

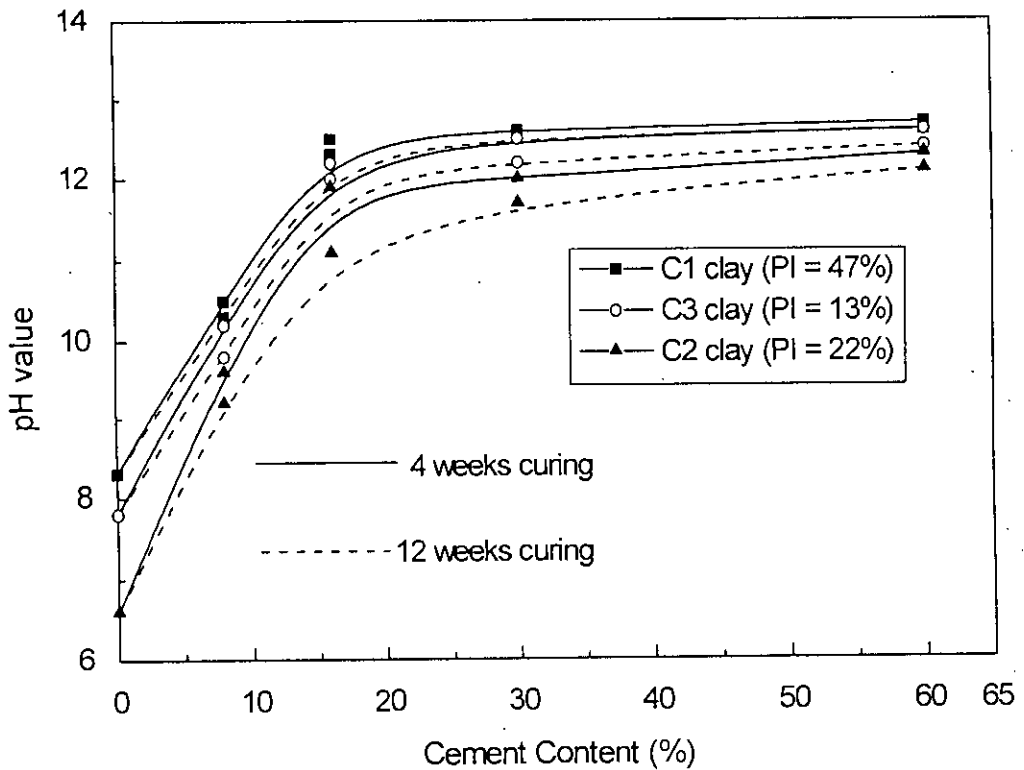


Fig. 4.2 Effect of Cement Content, Curing Time and Clay Type on pH value for Cement Treated Clays (mixing water = 120%)

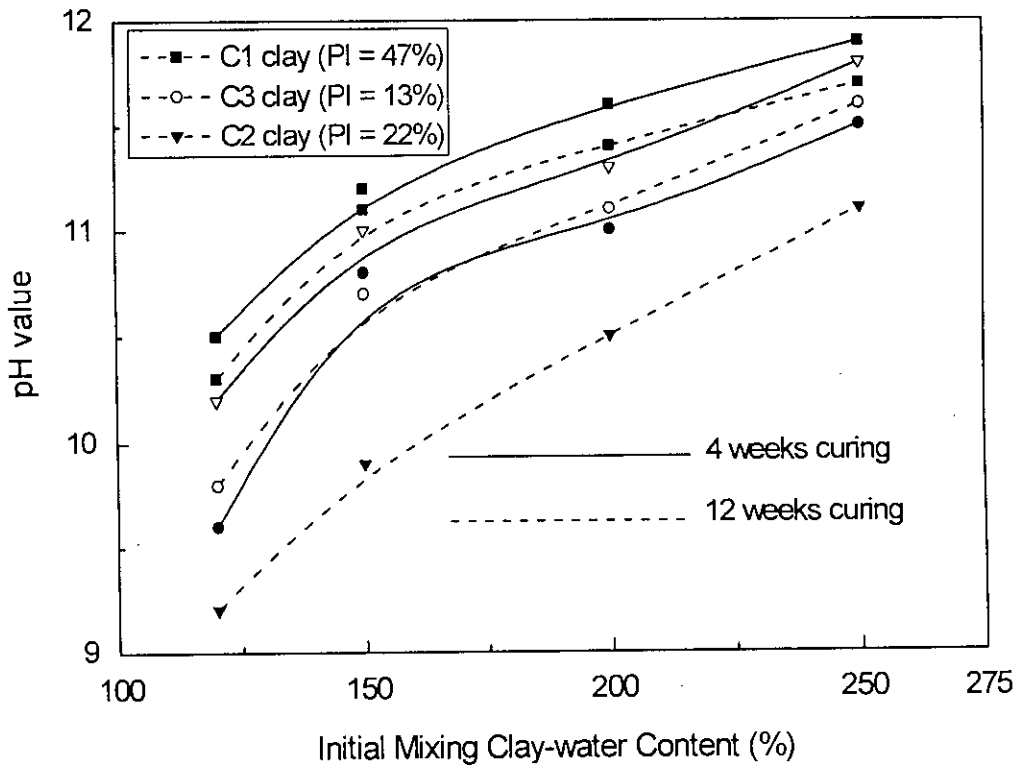


Fig. 4.3 Effect of mixing Water Content, Curing Time and Clay Type on pH value for Cement Treated Clays (wc/c ratio = 15)

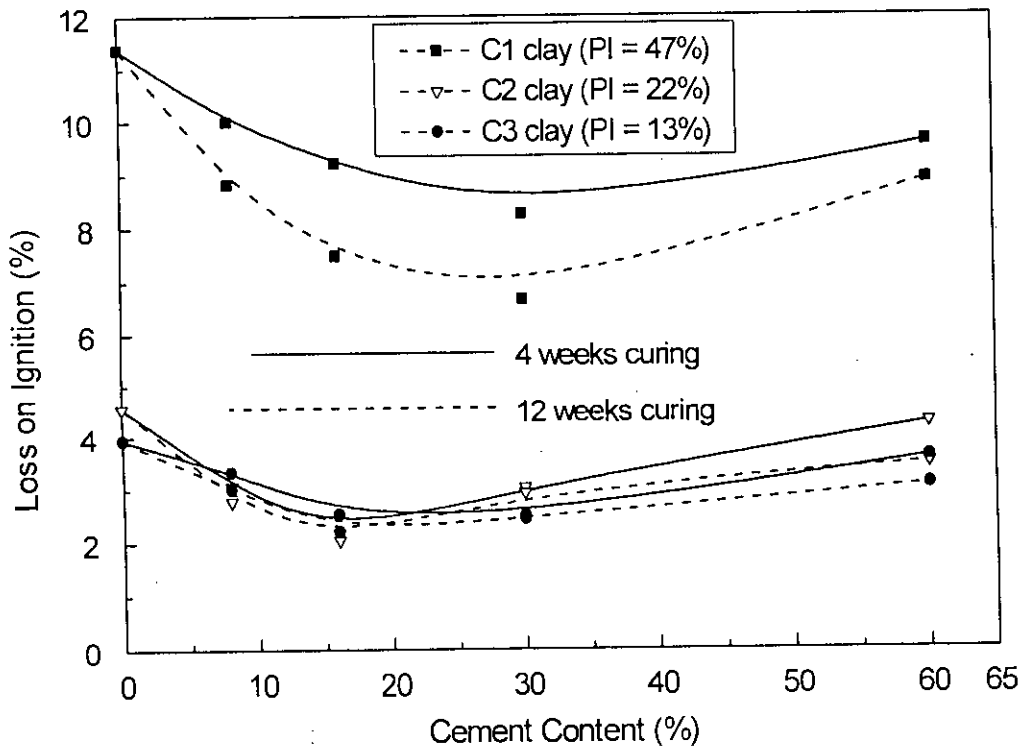


Fig. 4.4 Effect for Cement Content, Curing Time and Clay Type on Loss of Ignition value for Cement Treated Clays (mixing water = 120%)

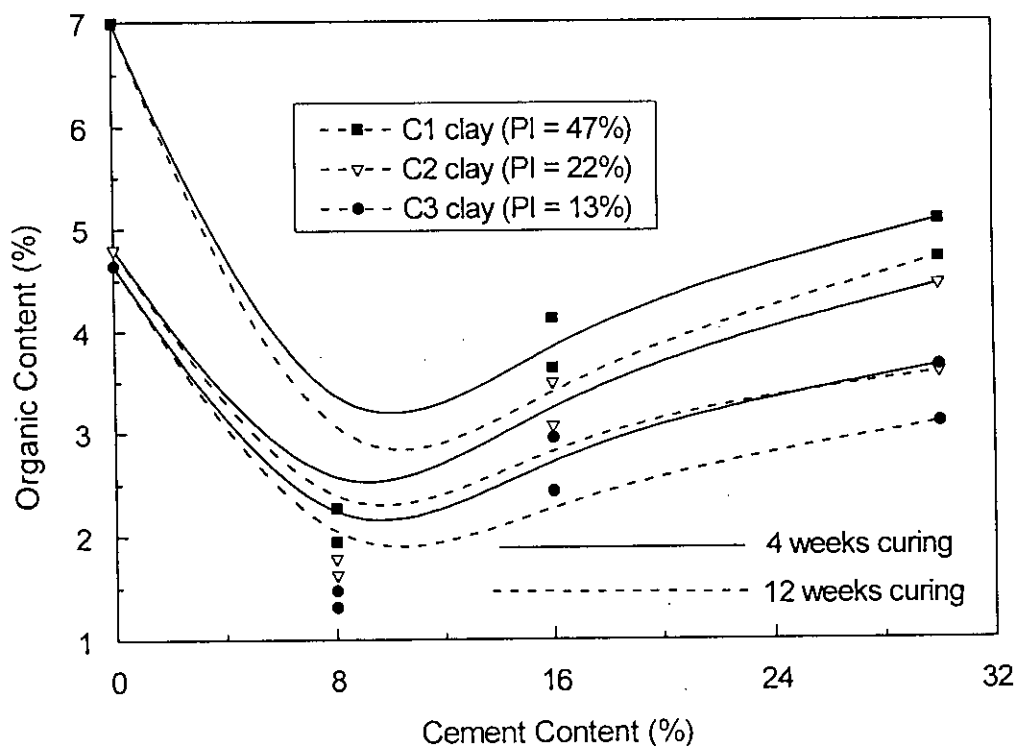


Fig. 4.5 Effect for Cement Content, Curing Time and Clay Type on Organic Content of Treated Soils (mixing water = 120%)

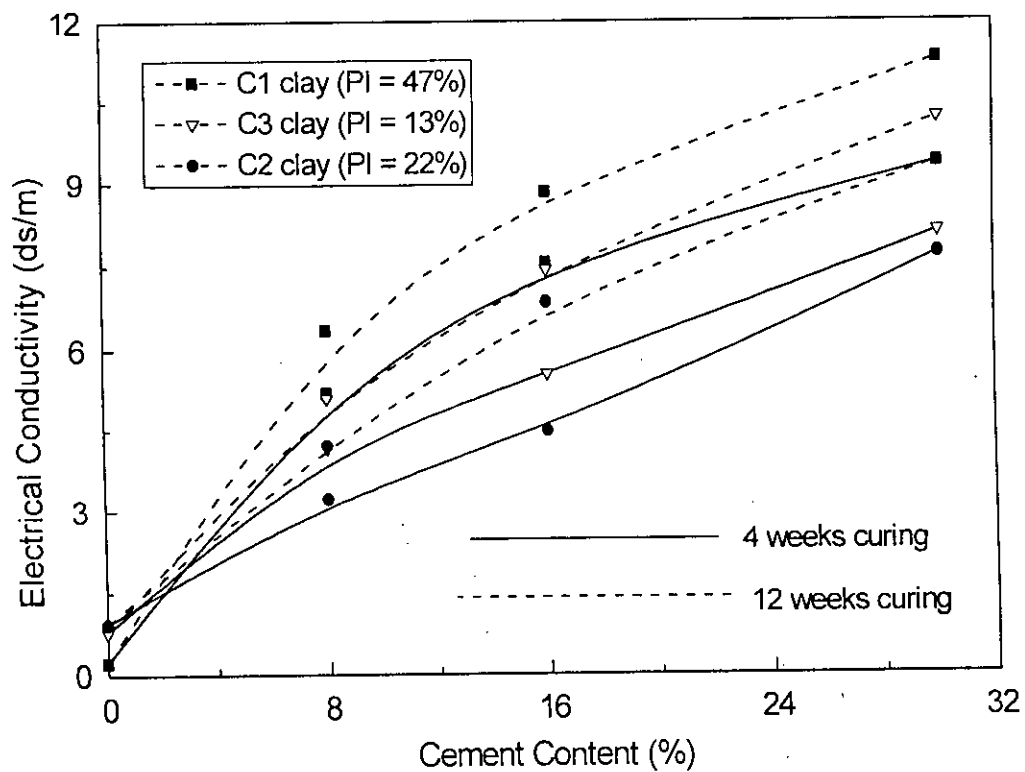


Fig. 4.6 Effect for Cement Content, Curing Time and Clay Type on Electrical Conductivity of Treated Soils (mixing water = 120%)

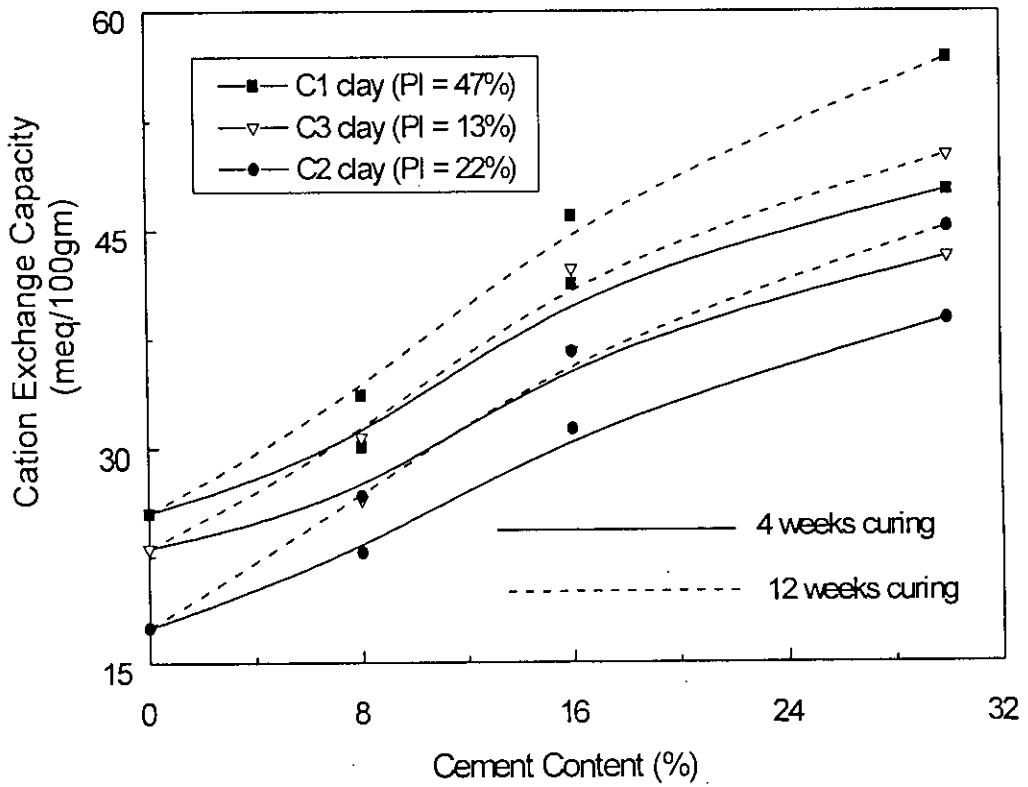


Fig. 4.7 Effect for Cement Content, Curing Time and Clay Type on Cation Exchange Capacity (CEC) of Treated Soils (water = 120%)

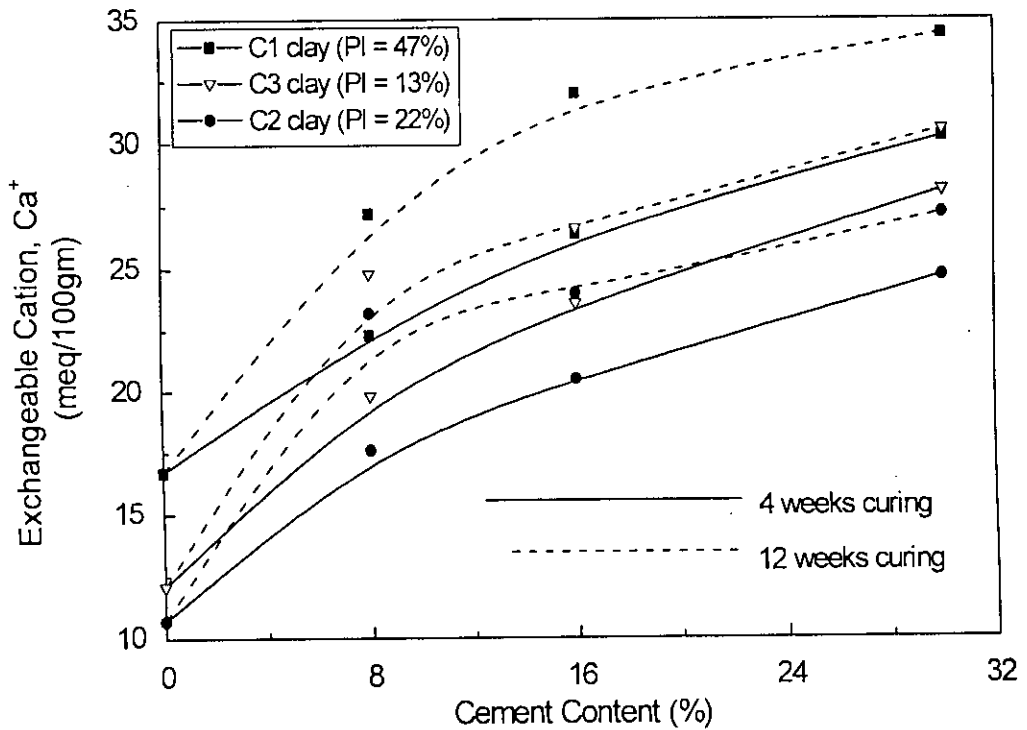


Fig. 4.8 Effect for Cement Content, Curing Time and Clay Type on Exchangeable Cation (Ca<sup>2+</sup>) of Treated Soils (water = 120%)

**Table 4.1 Effect for Cement Content, Curing Time and Clay Type on Exchangeable Cations for Treated Clays**

Curing Time (w)	Cement Content (%)	Exchangeable Cations (meq/100 gm) (Initial Mixing Water = 120%)											
		C1 clay				C2 clay				C3 clay			
		Ca <sup>2+</sup>	Mg <sup>2+</sup>	Na <sup>+</sup>	K <sup>+</sup>	Ca <sup>2+</sup>	Mg <sup>2+</sup>	Na <sup>+</sup>	K <sup>+</sup>	Ca <sup>2+</sup>	Mg <sup>2+</sup>	Na <sup>+</sup>	K <sup>+</sup>
Base	0	16.7	5.8	0.21	0.27	10.7	4.5	0.26	0.33	12.1	3.3	0.35	0.45
4 w	8	22.3	4.0	0.34	0.51	17.6	3.1	0.42	0.53	19.8	2.7	0.48	0.59
	16	26.4	3.2	0.53	0.74	20.5	2.3	0.60	0.68	23.6	2.3	0.57	0.76
	30	30.2	1.9	0.64	0.84	24.7	2.1	0.72	0.78	28.1	1.8	0.72	0.86
12 w	8	27.2	4.8	0.41	0.57	23.2	3.8	0.46	0.61	24.8	3.0	0.57	0.69
	16	32.0	3.6	0.62	0.85	24.6	2.9	0.66	0.76	26.6	2.7	0.67	0.88
	30	34.4	2.3	0.70	0.96	27.2	2.4	0.79	0.87	30.5	2.0	0.81	0.99

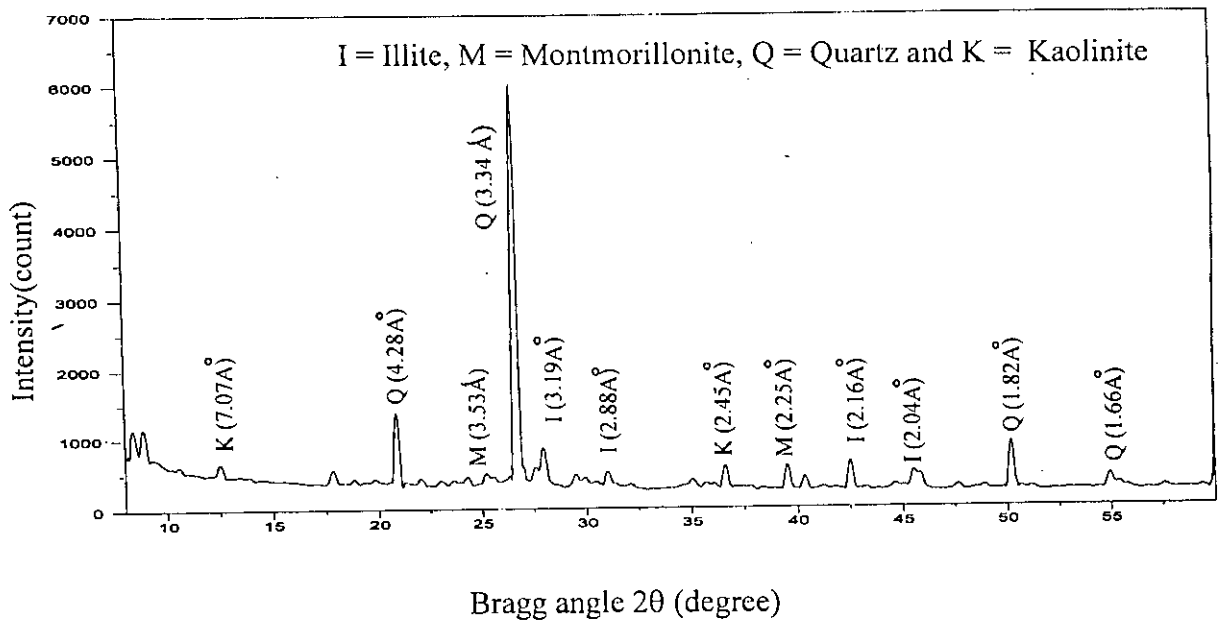
**Table 4.2 Effect for Cement Content, Curing Time and Clay Type on Nitrogen and Phosphorus for Treated clays**

Curing Time (week)	Cement Content (%)	wc/c Ratio	Nitrogen (%) (w <sub>i</sub> = 120%)			Phosphorus (micro gm/gm) (w <sub>i</sub> = 120%)		
			C1 clay	C2 clay	C3 clay	C1 clay	C2 clay	C3 clay
4 w	0	base clay	0.037	0.027	0.024	4.62	6.23	7.74
	8	15	0.072	0.068	0.041	9.68	11.56	13.23
	16	7.5	0.102	0.097	0.093	12.28	14.13	18.82
	30	4	0.141	0.130	0.110	20.43	24.61	29.20
12 w	8	15	0.076	0.071	0.053	8.66	10.06	12.15
	16	7.5	0.123	0.106	0.098	10.38	12.16	16.72
	30	4	0.163	0.142	0.128	18.24	20.55	26.23

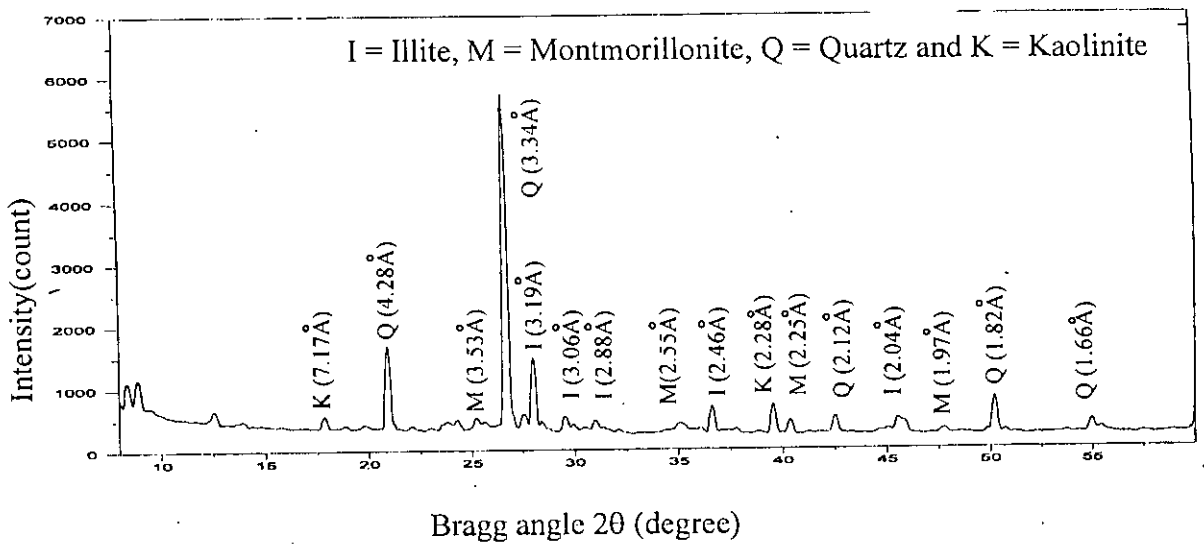
**Table 4.3 Effect of Cement Treatment on Chemical Engineering Properties**

Chemical properties	General effect in comparison to untreated clay	Effect of increasing cement content	Effect of increasing curing time	Effect of increasing initial water content	Effect of increasing plasticity of clay
pH value	Increases significantly (52 to 82%)	Increases significantly	Decreases with time increasing	Increases at higher water content	Increases with increasing plasticity
Loss on Ignition	Immediate decrease (27 to 52%)	Reduces significantly	Reduces substantially	Decreases at higher water content	Decreases with decreasing plasticity
Organic Matter and Carbon	Decreases (41 to 68%)	Decreases at higher cement	Decreases at longer time	Decreases at higher water content	Increases with increasing plasticity
Electrical Conductivity	Increases (80 to 139%)	Increases at higher cement	Increases with time increasing	Decreases at higher water content	Decreases with decreasing plasticity
Cation Exchange Capacity	Increases (106 to 154%)	Increases significantly	Reduces with time increasing	Decreases at higher water content	Increases with increasing plasticity
Ca <sup>2+</sup> Cations	Increases significantly (122 to 159%)	Increases at higher cement	Decreases at longer time	Reduces at higher water content	Decreases with decreasing plasticity
Nitrogen	Increases (3.8 to 4.6 times)	Increases at higher cement	Increases with time increasing	Decreases at higher water content	Increases with increasing plasticity
Phosphorus	Increases (3.7 to 4.4 times)	Increases at higher cement	Decreases with time increasing	Reduces at higher water content	Decreases with increasing plasticity

(\* Indicated results up to 4 weeks curing, 30% cement and 120% mixing water for range of clays)

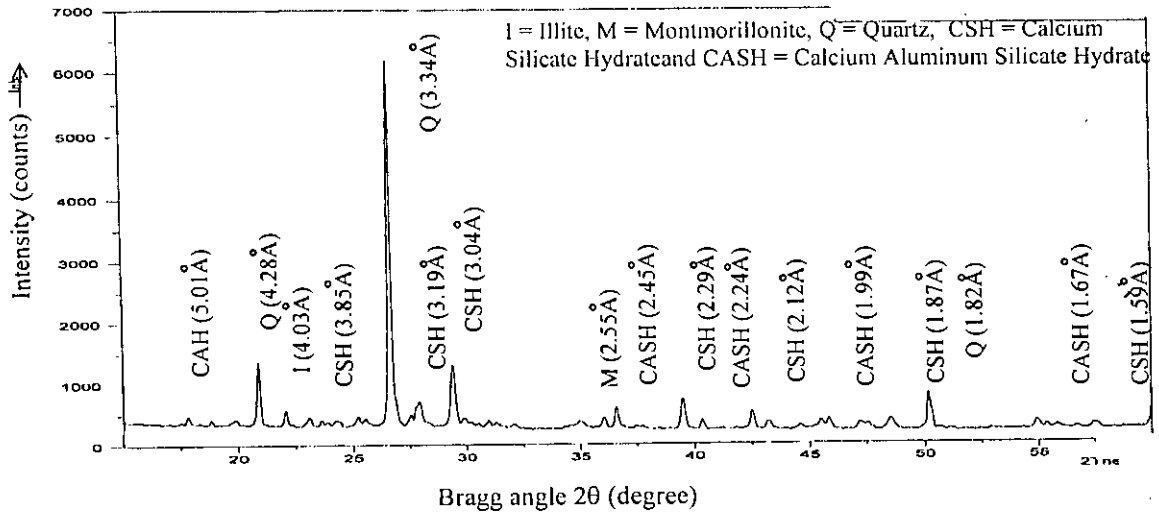


(a)

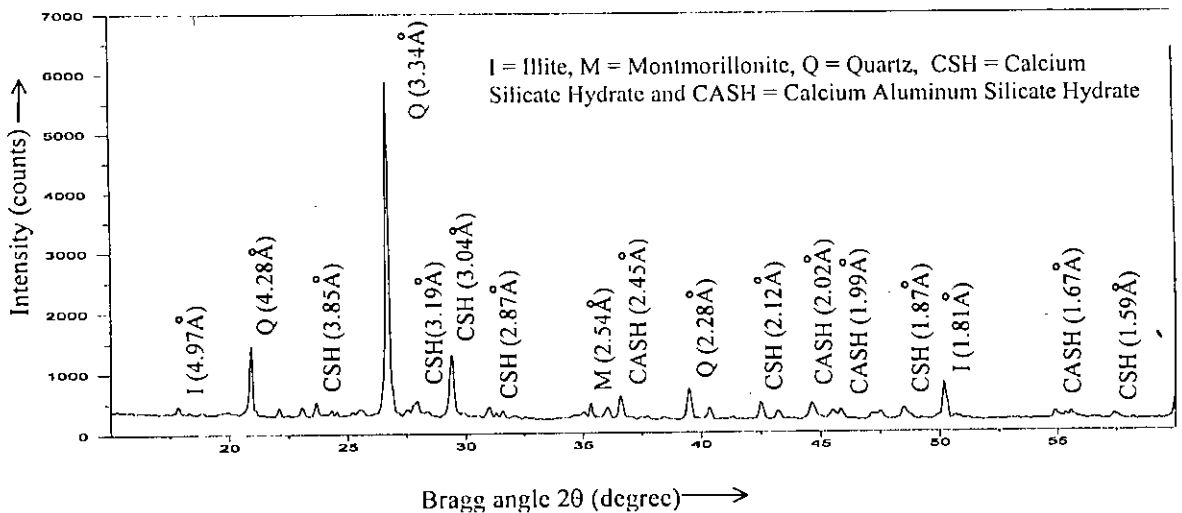


(b)

Fig. 4.9 X-Ray Diffraction Patterns of Untreated Base Clays (a) C3 clay (PI = 13%) and (b) CI clay (PI = 47%)



(a)



(b)

Fig. 4.10 X-Ray Diffraction Patterns at 4 weeks Curing time and 120% Mixing water of 16% Cement Treated Clays (a) C3 clay and (b) C1 clay

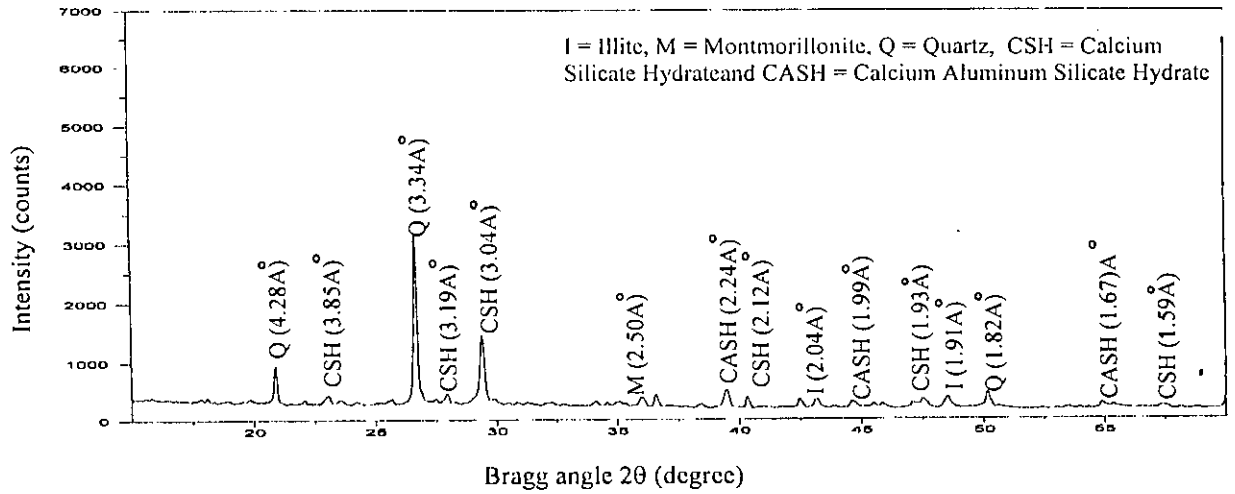


**Table 4.4 Effect of Cement and Clay Type on Semi-Quantitative Proportions Clay Minerals Cementitious Compounds ( $w_i = 120\%$ , Particle Size  $< 63 \mu\text{m}$ )**

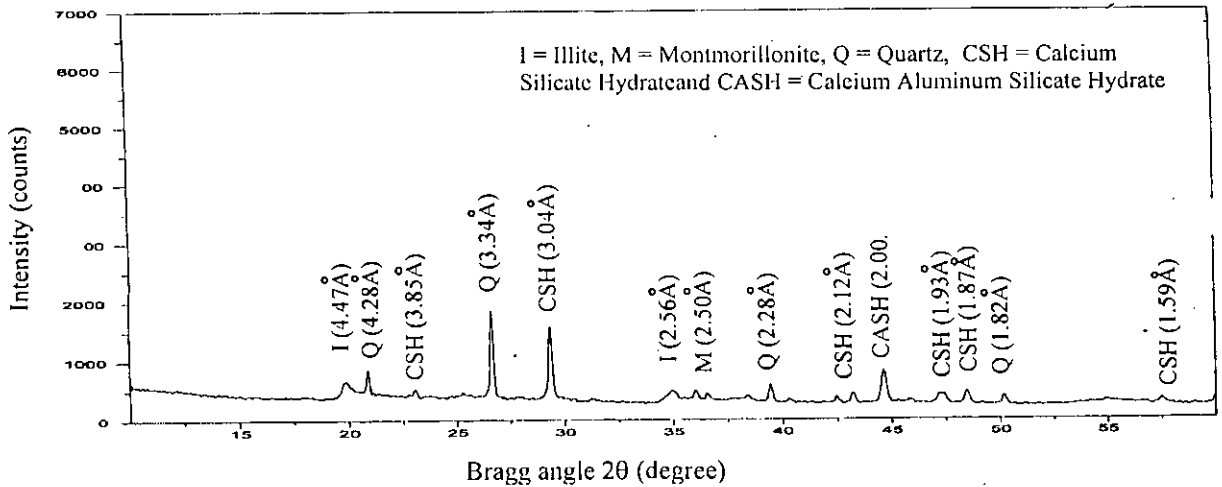
Curing time	Cement content (%)	Clay-type	Normalized mass of mineral (% by Weight)					
			Total mass	Illite	Montmorillonite	Quartz	Kaolinite	CSH+CASH
Untreated	-	C3	100	21	9	64	6	0
		C2	100	18	15	63	4	0
		C1	100	19	12	61	8	0
4 weeks	16	C3	116	15	7	59	0	35
		C2	116	16	10	60	0	30
		C1	116	14	8	53	0	41
	30	C3	130	11	6	63	0	50
		C2	130	9	7	71	0	43
		C1	130	10	8	60	0	52
	60	C3	160	10	5	70	0	75
		C1	160	8	6	64	0	82

**Table 4.5 Effect of Curing on Semi-Quantitative Proportions of Clay Minerals Cementitious Compounds ( $w_i = 120\%$ , Particle Size  $< 63 \mu\text{m}$ )**

Normalized mass of mineral (% by wt.)	Untreated C1 clay	30% cement Treated C1 clay	
	-	4 weeks Curing	12 weeks Curing
Total mass (% by wt.)	100	130	130
Illite (% by wt.)	19	11	7
Montmorillonite (%)	12	9	4
Quartz (% by wt.)	61	58	59
Kaolinite (gm)	8	0	0
CSH+CASH (% by wt.)	0	52	60

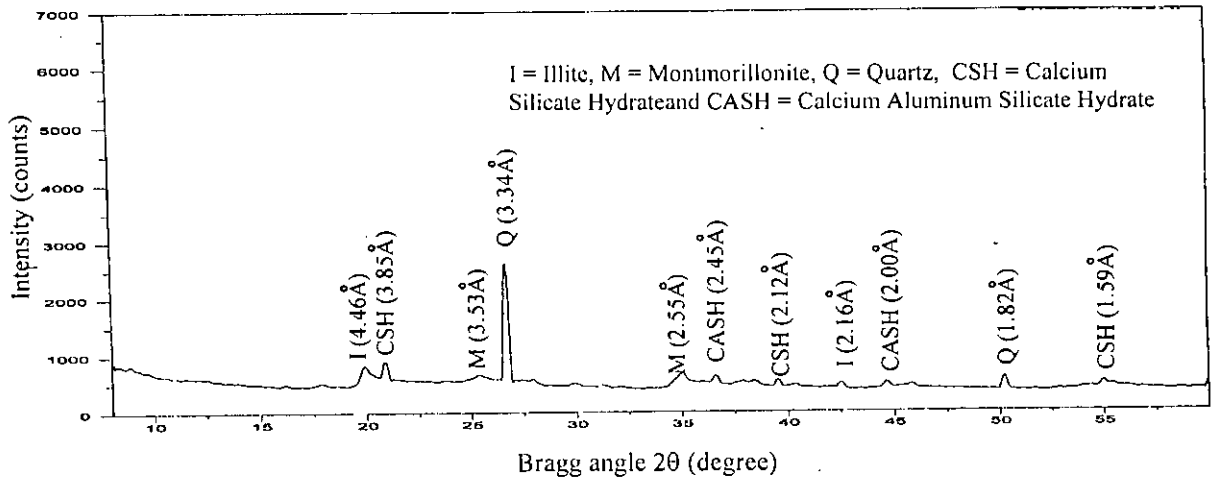


(a)

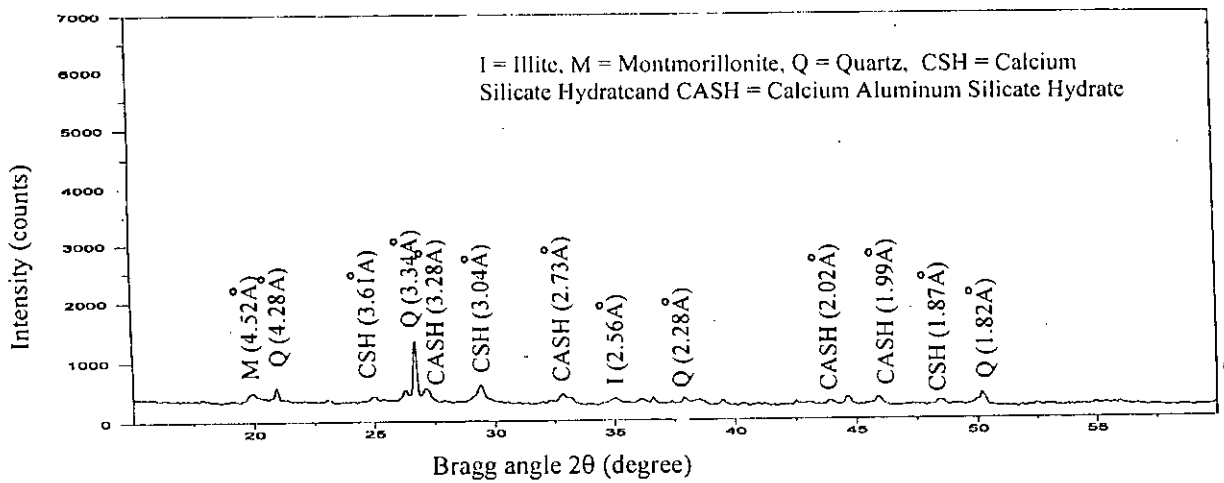


(b)

Fig. 4.11 X-Ray Diffraction Patterns at 4 weeks Curing time and 120% Mixing water of 30% Cement Treated Clays (a) C3 clay and (b) C1 clay



(a)



(b)

Fig. 4.12 X-Ray Diffraction Patterns at 4 weeks Curing time and 120% Mixing water of 60% Cement Treated Clays (a) C3 clay and (b) C1 clay

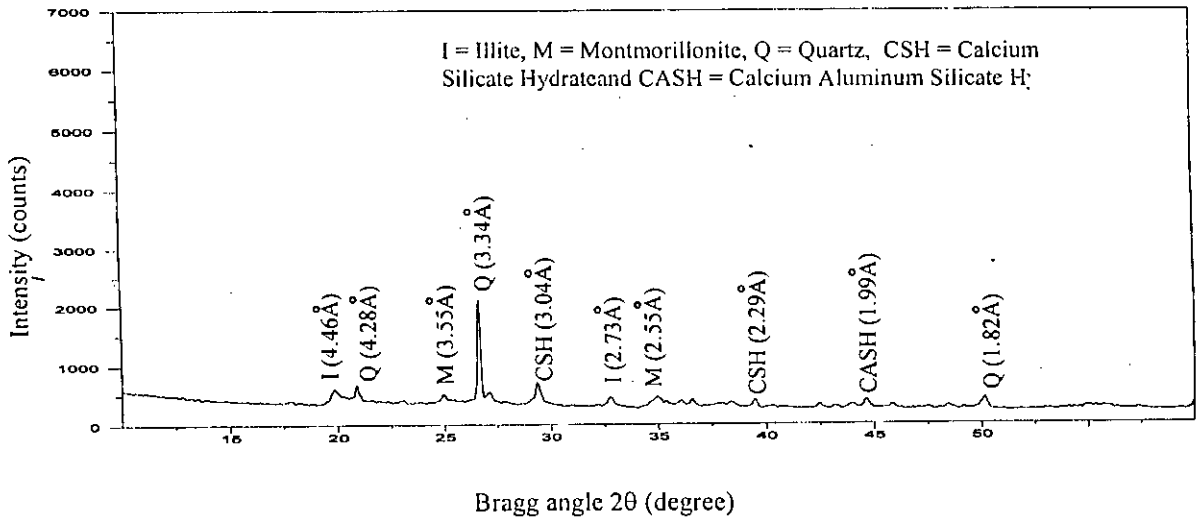


Fig. 4.13 X-Ray Diffraction Patterns at 12 weeks Curing time and 120% Mixing water of 30% Cement Treated C1 clay

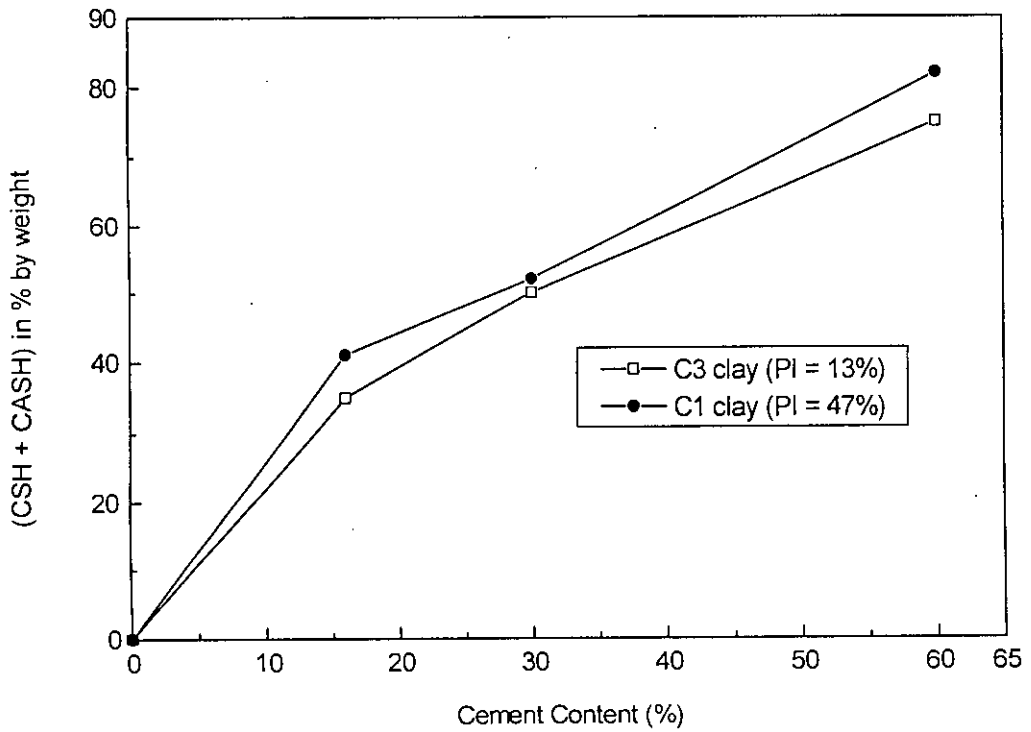
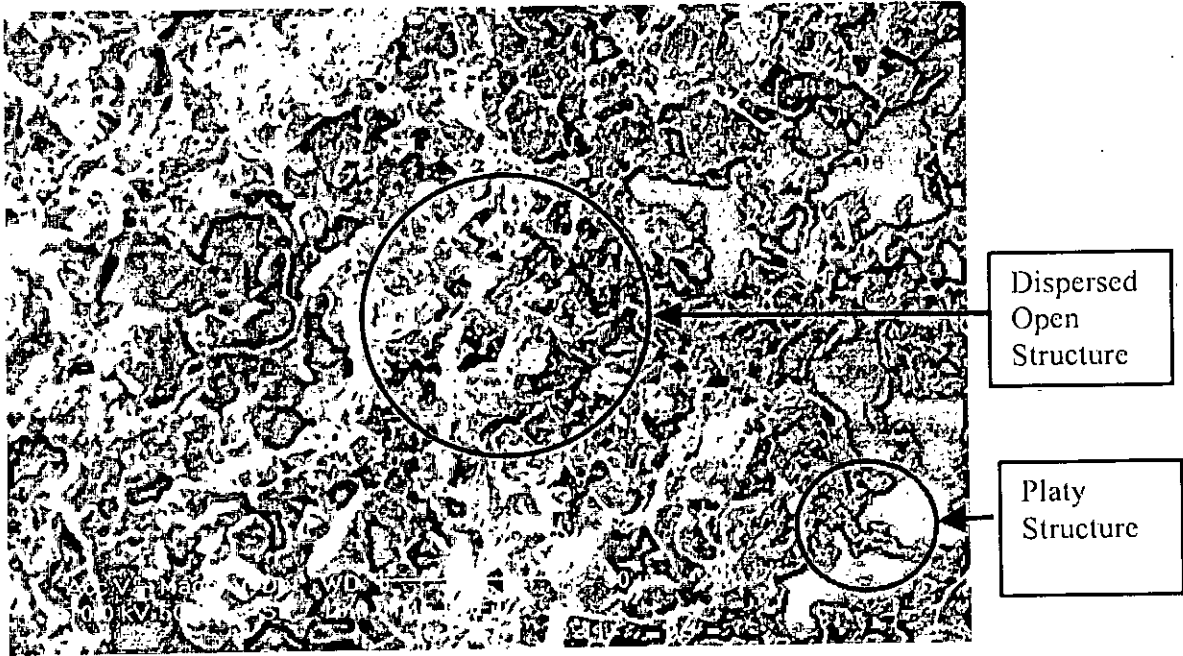
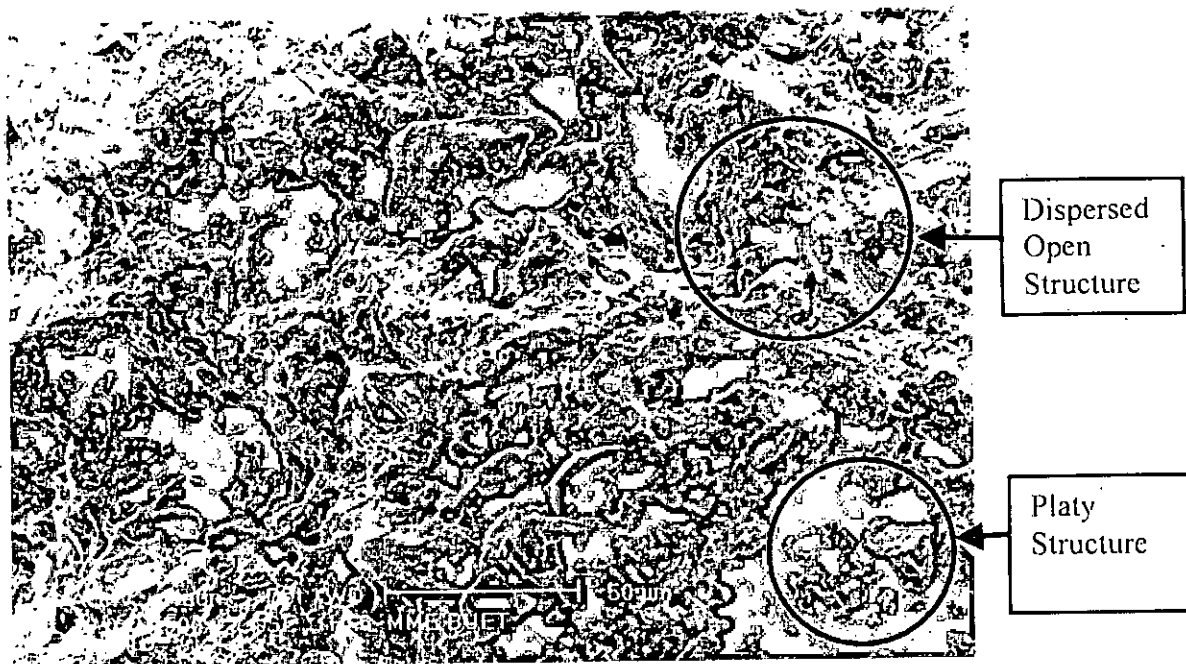


Fig. 4.14 Relationship between Cement Content and Cementitious Products (CSH + CASH) of treated clays (4 weeks curing and 120% water)

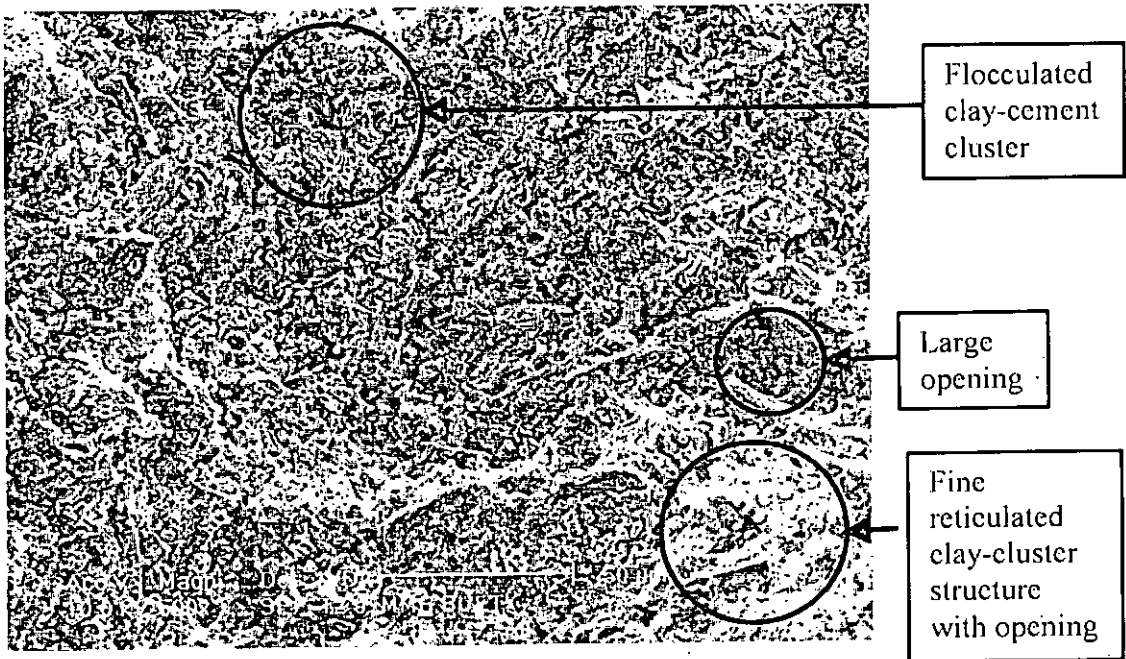


(a)

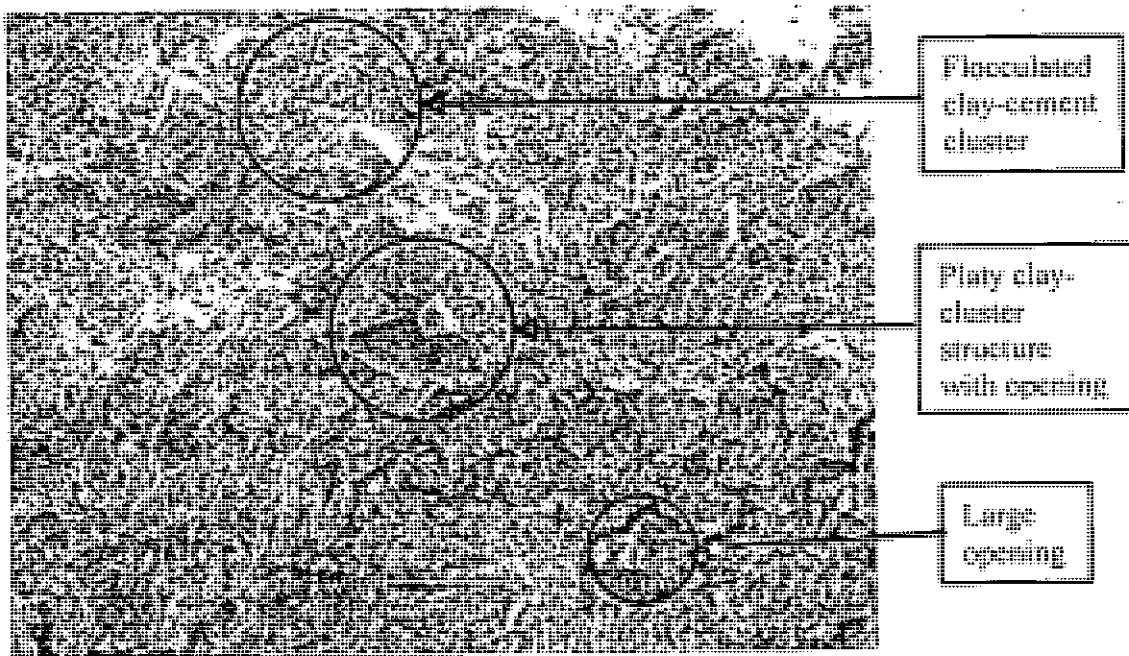


(b)

Fig. 4.15 SEM Image of Untreated (Remoulded) Clays (a) C1 clay and (b) C3 clay



(a)



(b)

Fig. 4.16 SEM Image of 16% Cement Treated Clays (a) C1 clay and (b) C3 clay (4 weeks curing time and 120% mixing water)

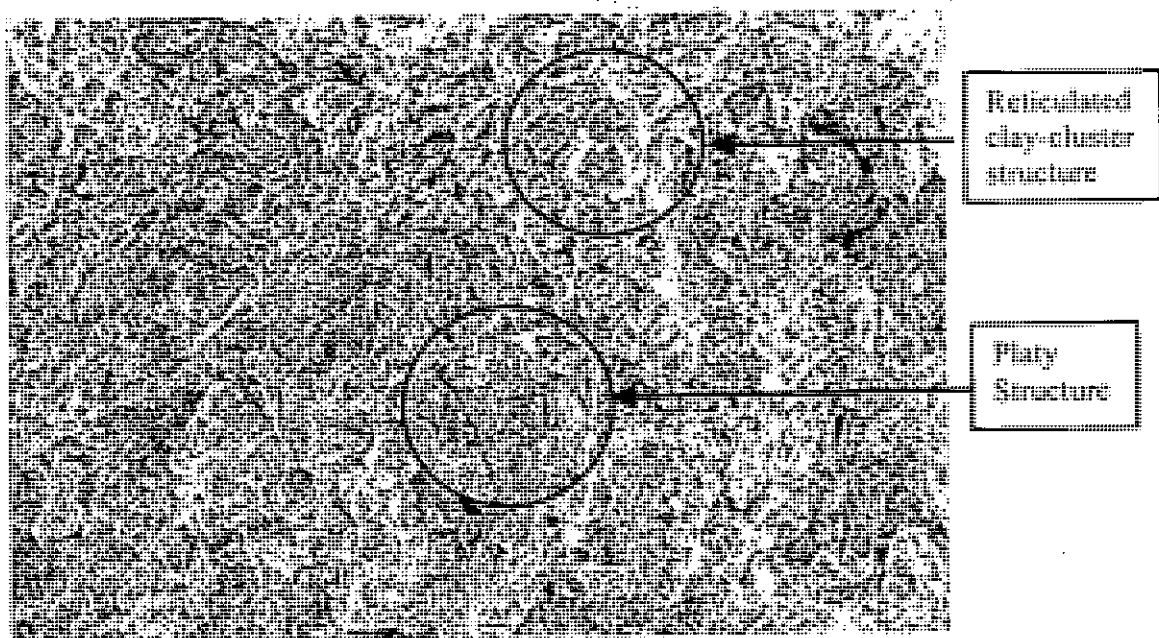


(a)

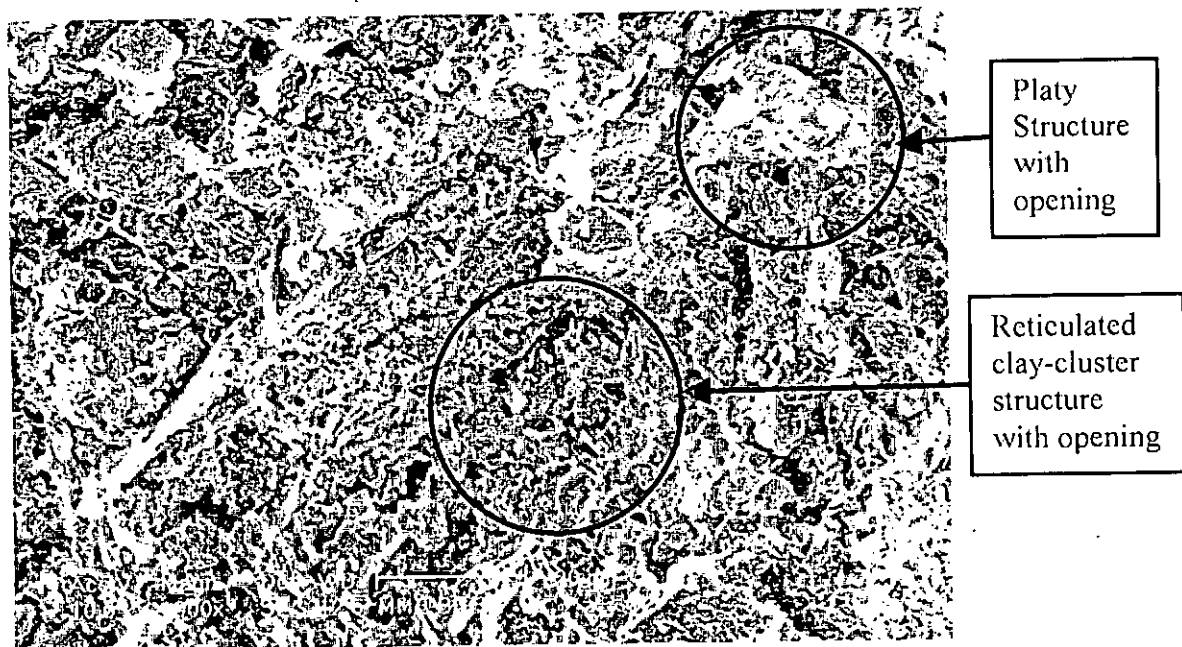


(b)

Fig. 4.17 SEM Image of 30% Cement Treated Clays (a) C1 clay and (b) C3 clay (4 weeks curing time and 120% mixing water)



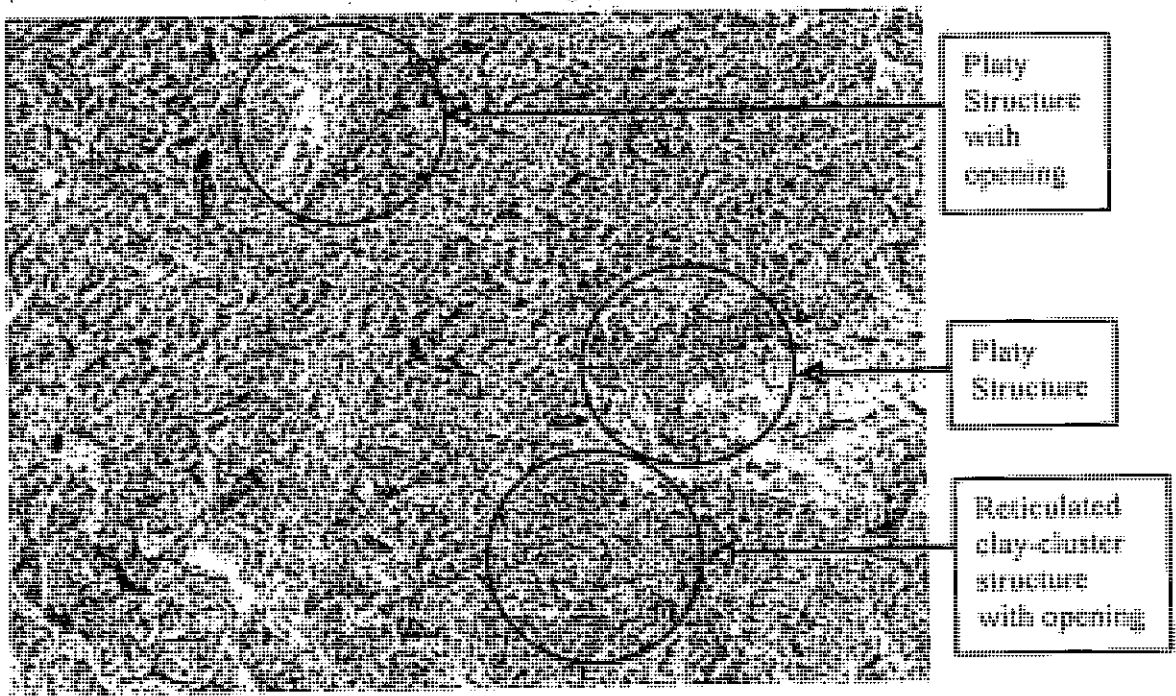
(a)



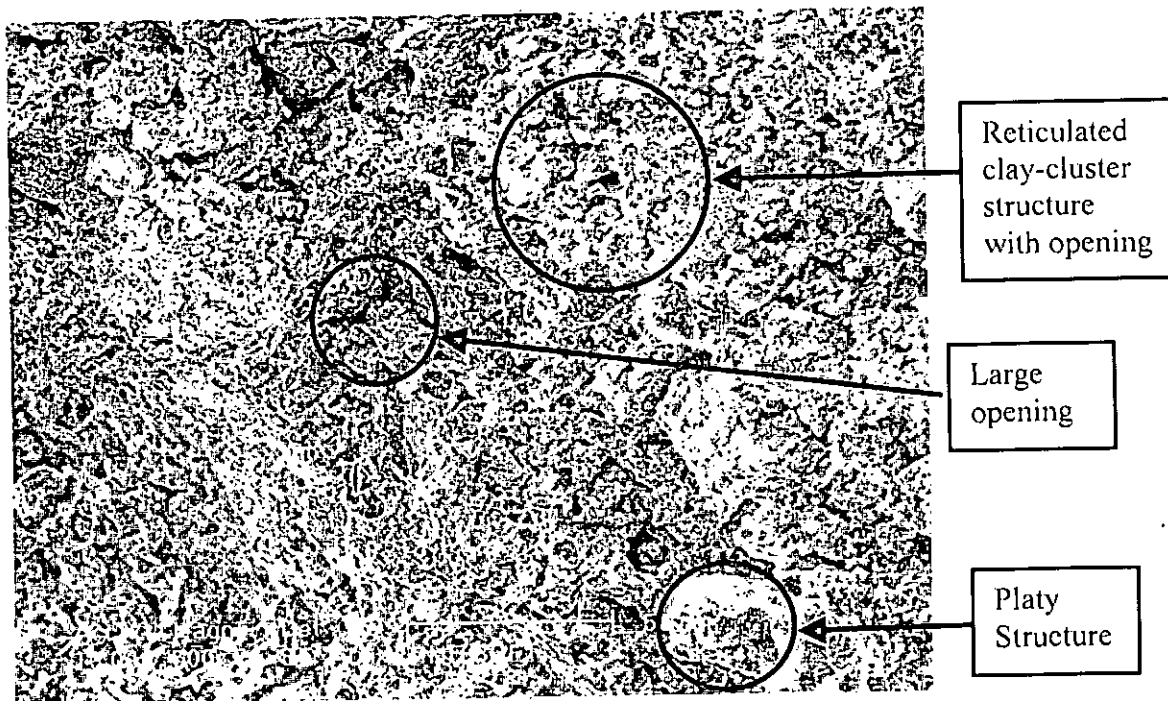
(b)

Fig. 4.18 SEM Image of 16% Cement Treated Clays (a) C1 clay and (b) C3 clay (12 weeks curing time and 120% mixing water)





(a)



(b)

Fig. 4.19 SEM Image of 30% Cement Treated Clays (a) C1 clay and (b) C3 clay (12 weeks curing time and 120% mixing water)

Table 4.6 Characteristics Values (Physical Properties) of Untreated Base Clays

Properties	Characteristics Values		
	C1 clay	C2 clay	C3 clay
Type of Soil			
Liquid Limit, LL, (%)	78	47	33
Plastic Limit, PL, (%)	31	25	20
Plasticity Index, PI, (%)	47	22	13
Natural Water Content, $w_n$ (%)	43	36	27
Liquidity Index, LI	0.83	1.68	2.54
*Clay (%)	73	41	32
*Silt (%)	23	51	58
*Sand (%)	4	8	10
Bulk Unit Weight, $\gamma_t$ (kN/m <sup>3</sup> )	15.05	14.67	14.45
Dry Unit Weight, $\gamma_d$ (kN/m <sup>3</sup> )	8.85	9.05	9.44
Specific Gravity, $G_s$	2.680	2.673	2.668
Initial Void Ratio, $e_0$	1.81	1.96	2.10
Activity of clays, $A_c$	0.64	0.35	0.23
Unified Soil Classification System	CH	CL	CL

Table 4.7 Physical Properties of Cement Treated C1 (PI = 47%) Clay

Curing (weeks)	w <sub>i</sub> (%)	wc/c ratio	c (%)	w <sub>r</sub> (%)	$\gamma_d$ (kN/m <sup>3</sup> )	G <sub>s</sub>	e at 12.5 kPa	S <sub>r</sub>
4	120	7.5	16	96.7	6.37	2.661	2.32	97.8
		10	12	103.4	5.94	2.667	2.41	98.1
		15	8	108.9	5.47	2.670	2.53	98.6
	150	7.5	20	111.5	6.05	2.663	2.77	98.3
		10	15	117.3	5.84	2.668	2.85	98.4
		15	10	124.9	5.41	2.672	2.97	99.8
	200	7.5	26.67	129.6	5.98	2.665	3.10	98.1
		10	20	142.8	5.73	2.670	3.30	98.7
		15	13.33	155.7	5.27	2.673	3.63	99.0
	250	7.5	33.33	160.2	5.68	2.668	3.75	98.7
		10	25	169.4	5.42	2.673	3.98	98.9
		15	16.67	189.8	5.19	2.676	4.31	99.2
12	120	7.5	16	87.3	6.45	2.658	1.79	96.7
		10	12	96.1	6.07	2.664	1.99	96.9
		15	8	103.6	5.62	2.668	2.27	97.3
	150	7.5	20	106.4	6.15	2.660	2.39	97.2
		10	15	112.6	5.96	2.663	2.63	97.4
		15	10	119.8	5.53	2.667	2.33	98.0
	200	7.5	26.67	125.1	6.05	2.662	2.87	97.6
		10	20	133.6	5.84	2.665	3.12	97.8
		15	13.33	145.8	5.46	2.669	3.42	98.2
	250	7.5	33.33	151.7	5.88	2.664	3.35	98.0
		10	25	161.7	5.55	2.671	3.67	98.2
		15	16.67	177.4	5.34	2.674	4.10	98.4

Table 4.8 Physical Properties of Cement Treated C2 (PI = 22%) Clay

Curing (weeks)	w <sub>i</sub> (%)	wc/c ratio	c (%)	w <sub>f</sub> (%)	$\gamma_d$ (kN/m <sup>3</sup> )	G <sub>s</sub>	e at 12.5 kPa	S <sub>r</sub>
4	120	7.5	16	87.4	6.98	2.634	2.47	96.7
		10	12	95.4	6.72	2.653	2.61	96.9
		15	8	103.6	6.43	2.660	2.83	97.3
	150	7.5	20	108.4	6.81	2.641	2.94	97.4
		10	15	113.8	6.62	2.654	3.09	97.7
		15	10	119.9	6.31	2.662	3.26	97.9
	200	7.5	26.67	123.1	6.70	2.647	3.34	97.6
		10	20	131.9	6.52	2.657	3.58	97.8
		15	13.33	145.4	6.17	2.665	3.95	98.0
	250	7.5	33.33	150.4	6.38	2.649	4.07	97.9
		10	25	163.6	6.02	2.660	4.43	98.2
		15	16.67	175.4	5.87	2.668	4.75	98.5
12	120	7.5	16	80.8	7.04	2.614	2.21	95.2
		10	12	86.6	6.87	2.637	2.39	95.5
		15	8	98.3	6.56	2.651	2.73	96.8
	150	7.5	20	105.2	6.93	2.612	2.85	96.2
		10	15	108.6	6.74	2.639	2.97	96.5
		15	10	113.8	6.49	2.660	3.13	96.7
	200	7.5	26.67	118.8	6.82	2.611	3.21	96.6
		10	20	135.8	6.66	2.641	3.67	97.0
		15	13.33	139.4	6.34	2.661	3.82	97.2
	250	7.5	33.33	145.0	6.46	2.662	3.91	97.2
		10	25	154.9	6.18	2.644	4.19	97.7
		15	16.67	165.1	5.98	2.663	4.49	97.9

Table 4.9 Physical Properties of Cement Treated C3 (PI = 13%) Clay

Curing (weeks)	w <sub>i</sub> (%)	wc/c ratio	c (%)	w <sub>f</sub> (%)	γ <sub>d</sub> (kN/m <sup>3</sup> )	G <sub>s</sub>	e at 12.5 kPa	S <sub>r</sub>
4	120	7.5	16	74.8	7.52	2.617	2.63	95.3
		10	12	79.3	7.31	2.631	2.81	95.5
		15	8	92.7	6.83	2.644	2.95	96.1
	150	7.5	20	95.5	7.44	2.626	3.01	95.9
		10	15	103.1	7.22	2.640	3.18	96.3
		15	10	109.4	6.76	2.654	3.38	96.6
	200	7.5	26.67	115.1	7.28	2.631	3.52	96.3
		10	20	122.1	7.12	2.650	3.86	96.5
		15	13.33	133.6	6.67	2.661	4.21	96.7
	250	7.5	33.33	139.5	7.18	2.640	4.33	96.6
		10	25	147.5	6.88	2.657	4.58	96.8
		15	16.67	158.8	6.59	2.665	5.12	96.9
12	120	7.5	16	64.5	7.64	2.611	2.40	92.1
		10	12	72.1	7.43	2.619	2.64	93.5
		15	8	82.2	6.94	2.631	2.84	94.1
	150	7.5	20	88.4	7.55	2.621	2.91	94.6
		10	15	96.3	7.34	2.633	3.08	94.9
		15	10	103.6	6.84	2.641	3.26	95.2
	200	7.5	26.67	106.6	7.42	2.625	3.41	95.1
		10	20	115.2	7.22	2.642	3.64	95.6
		15	13.33	126.0	6.71	2.648	3.96	95.8
	250	7.5	33.33	125.1	7.32	2.630	4.12	95.8
		10	25	135.3	6.96	2.647	4.40	96.0
		15	16.67	151.4	6.73	2.660	4.82	96.3

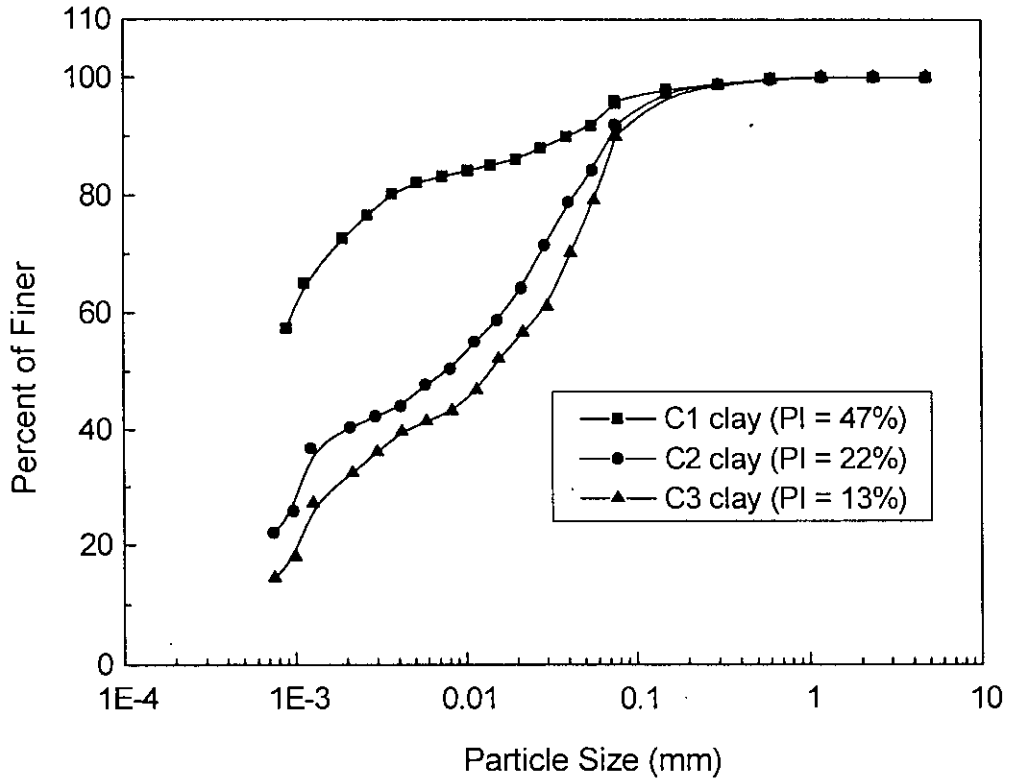


Fig. 4.20 Comparison of Grain Size Distribution Curve of Untreated Base Clays

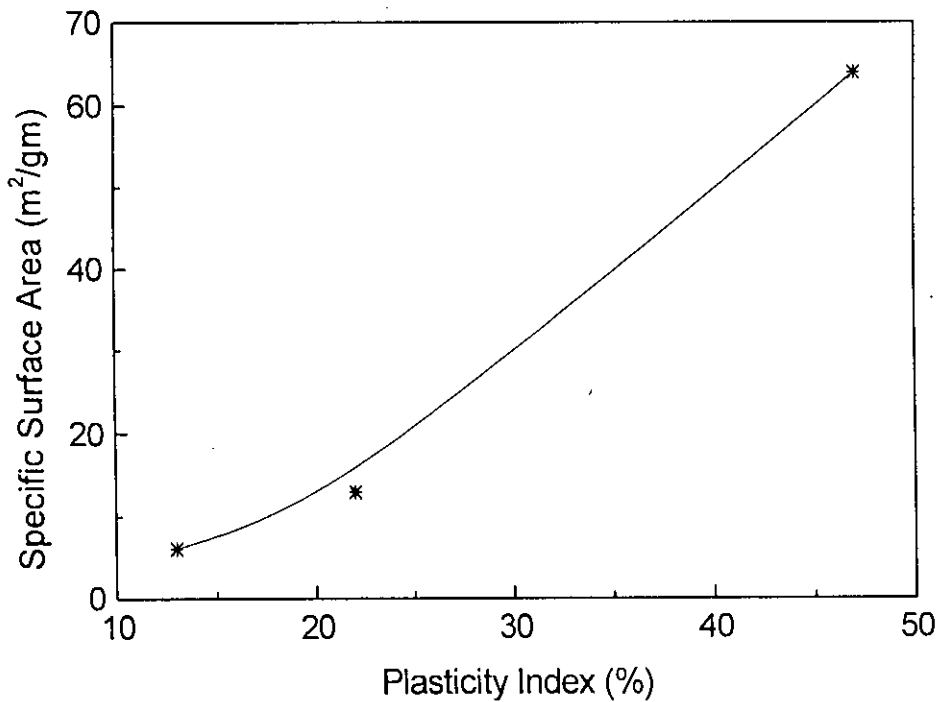
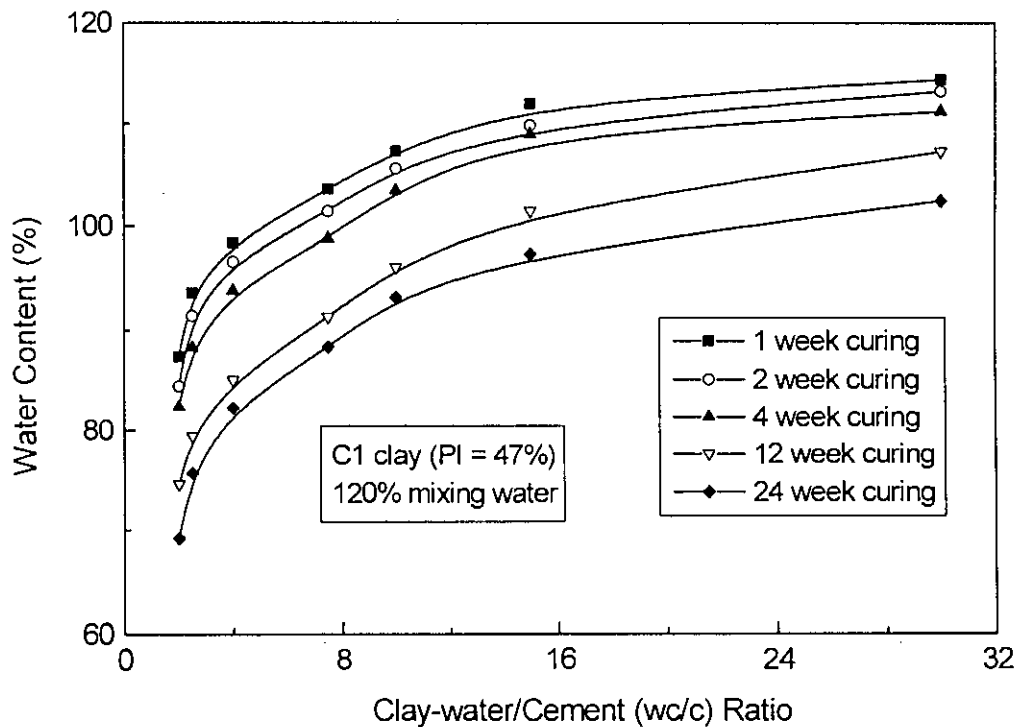
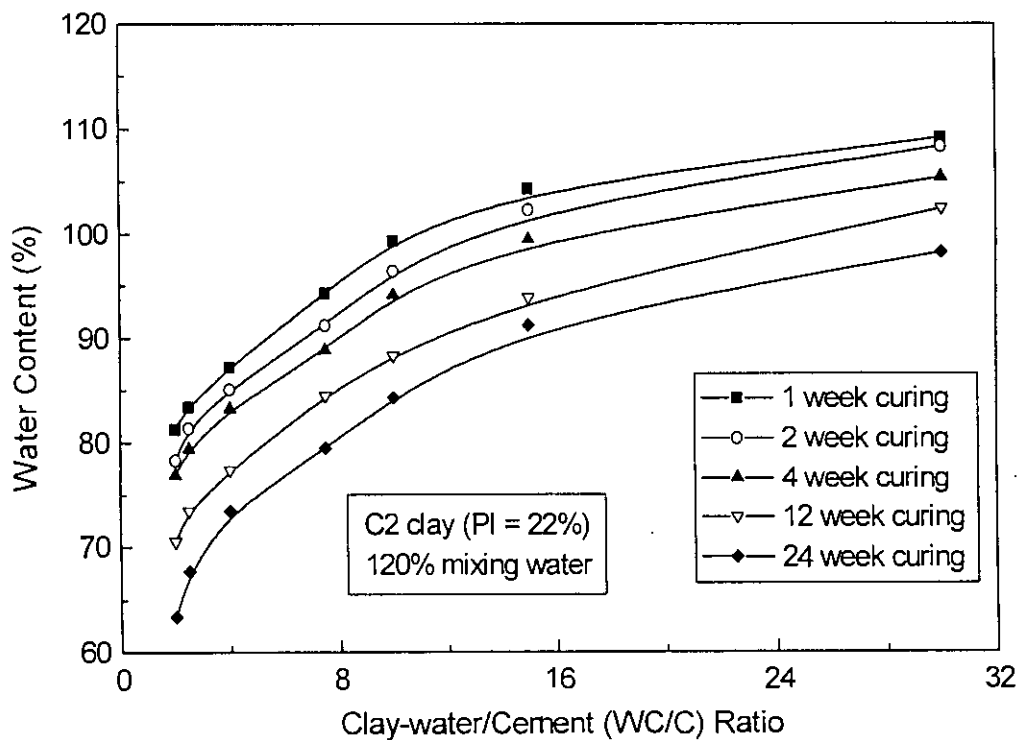


Fig. 4.21 Variation of Specific Surface Area with Plasticity Index of Untreated Base Clays



(a)



(b)

Fig. 4.22 Effect of Clay-water/Cement ratio and Curing Time on Water Content of Cement Treated Clays (a) C1 clay and (b) C2 clay

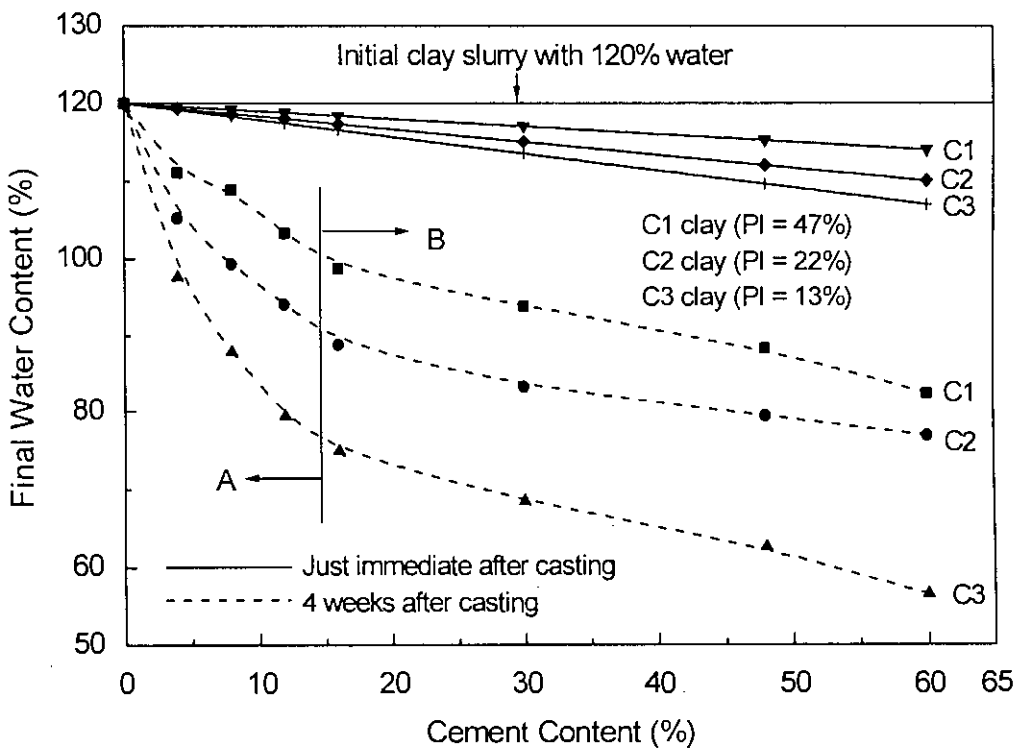


Fig. 4.23 Effect of Cement Content, Clay Type and Curing Time on Final Water Content of Cement Treated Clays

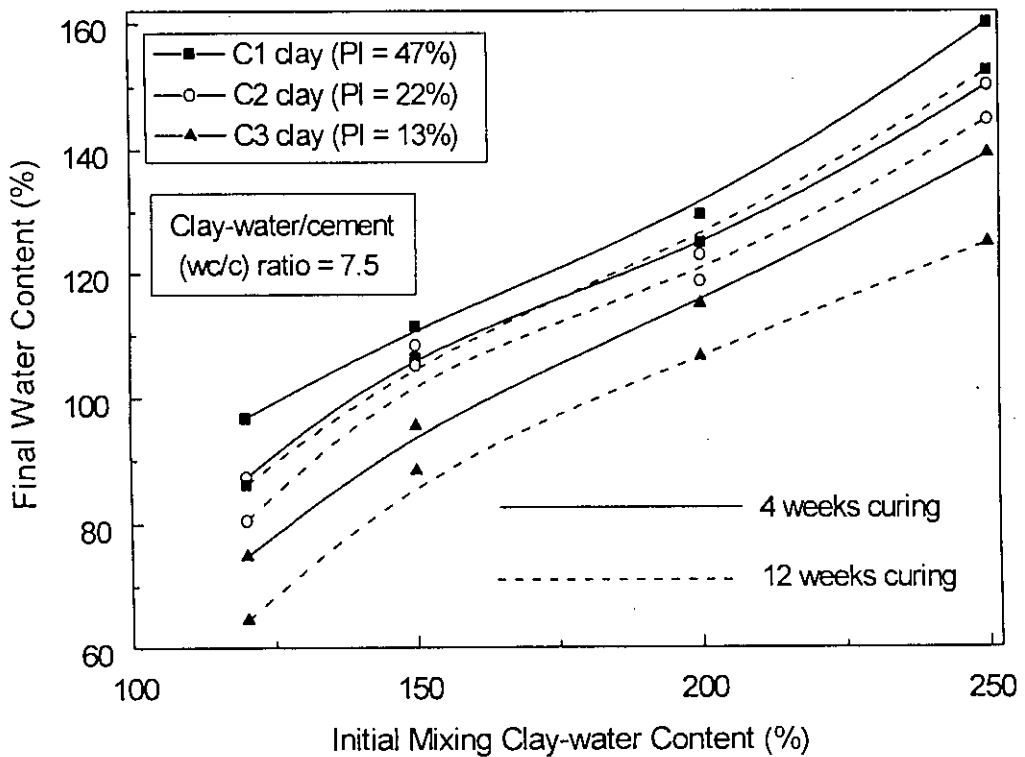


Fig. 4.24 Effect of Initial Mixing Clay-water Content, Clay Type and Curing Time on Final Water Content of Cement Treated Clays



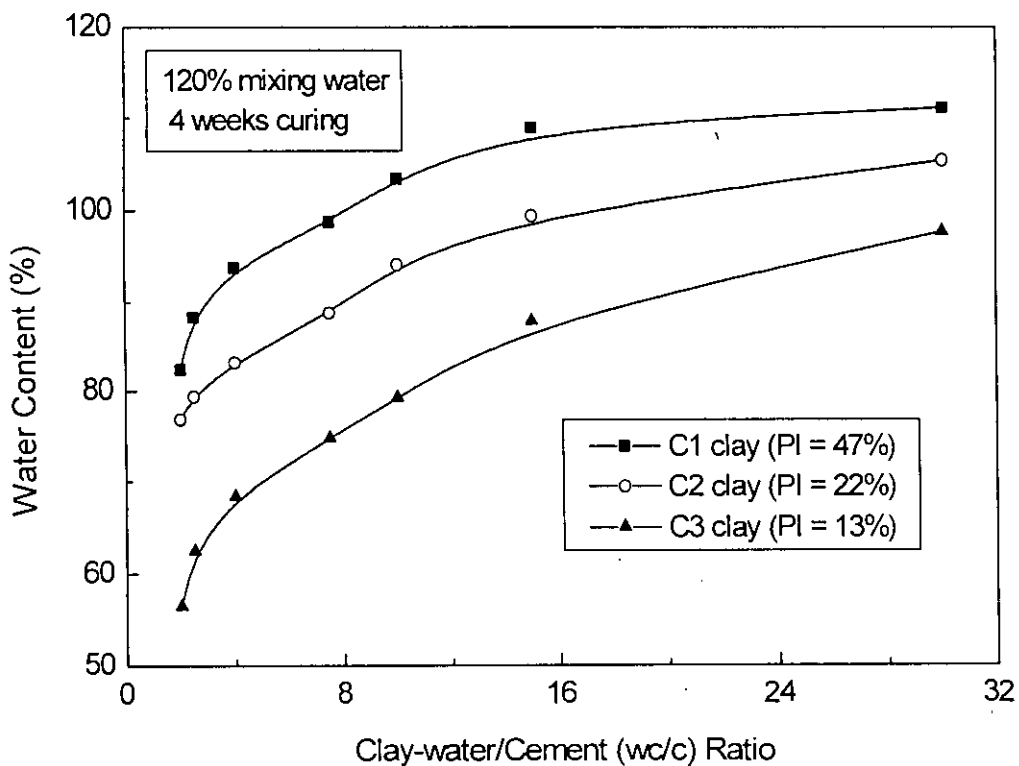


Fig. 4.25 Effect of Clay-water/Cement Ratio and Clay Type on Water Content of Cement Treated Clays

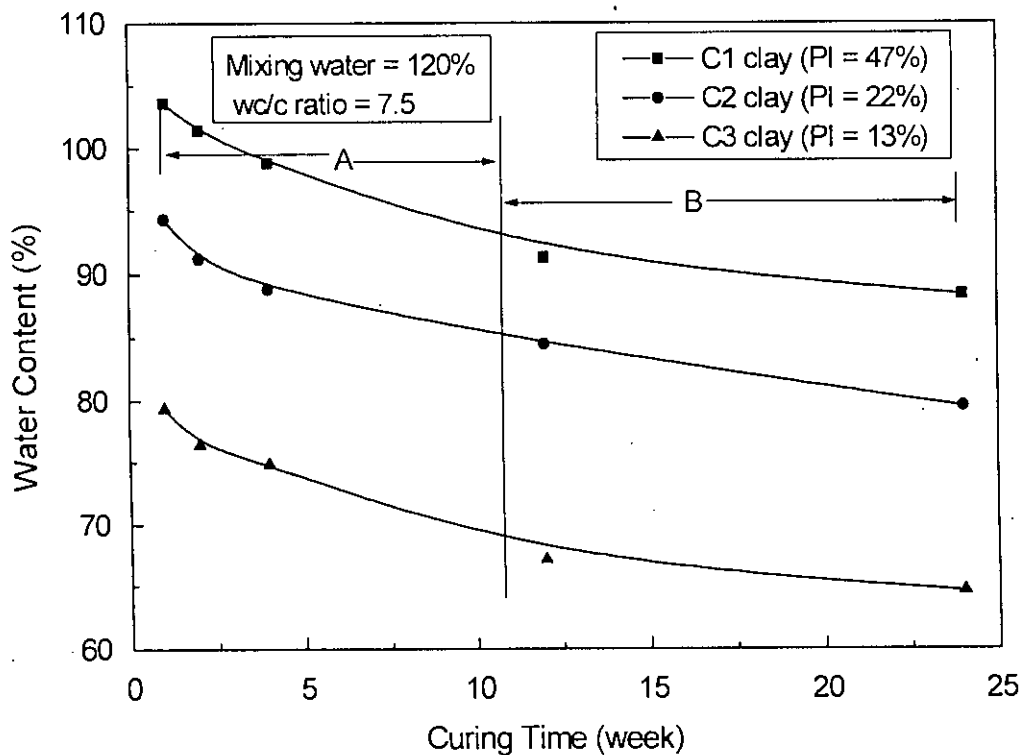
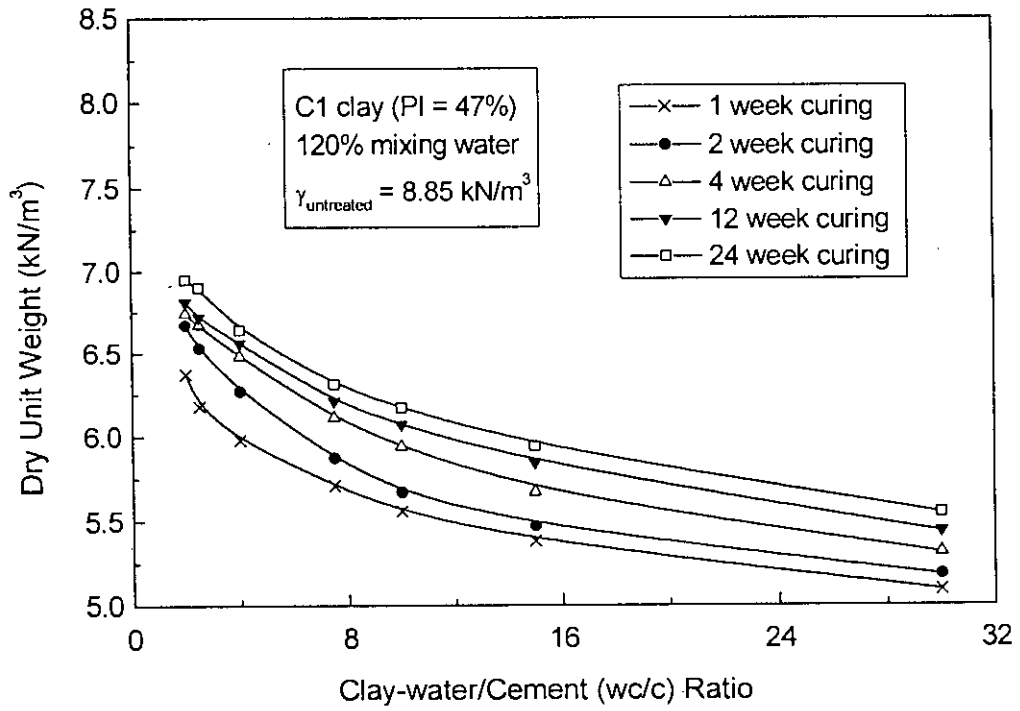
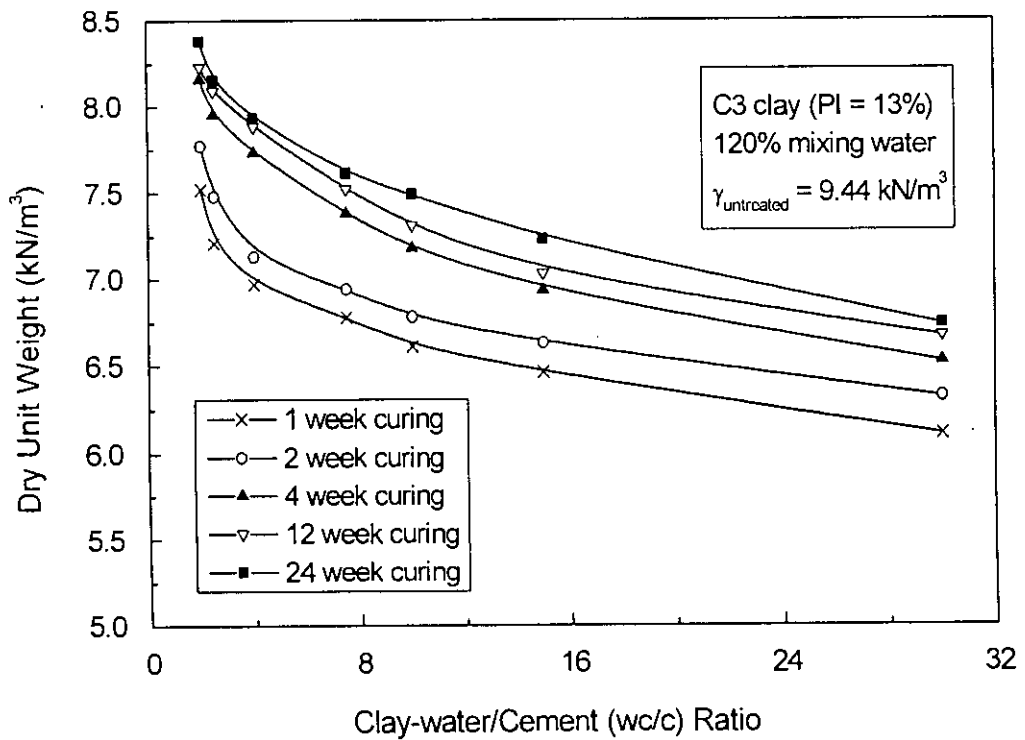


Fig. 4.26 Effect of Curing Time and Clay Type on Water Content of Cement Treated Clays

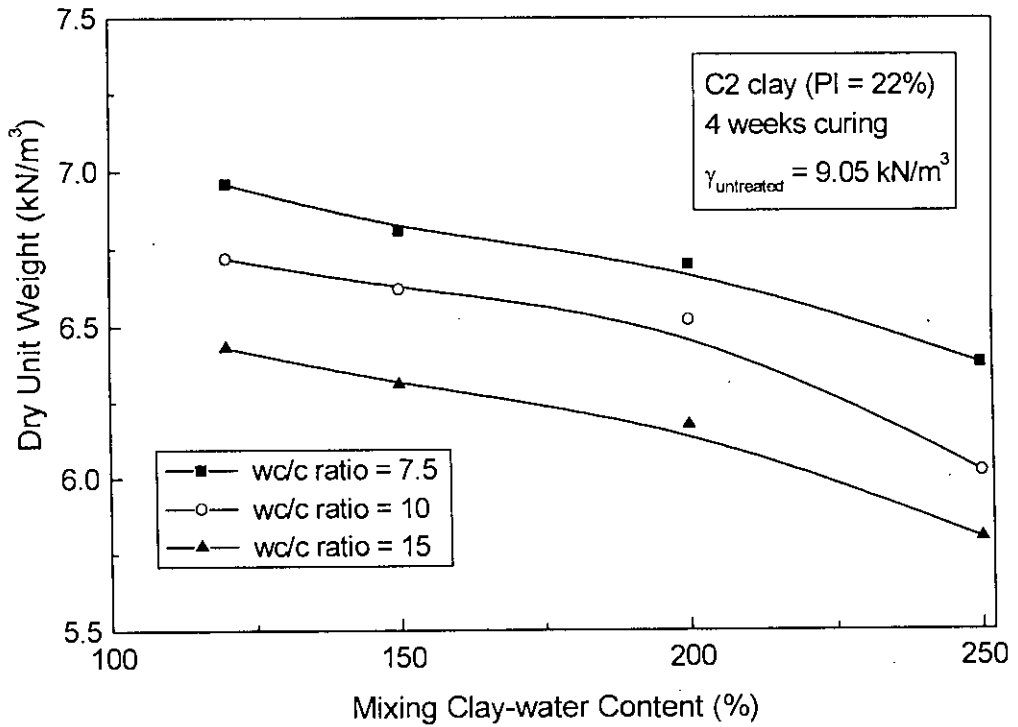


(a)

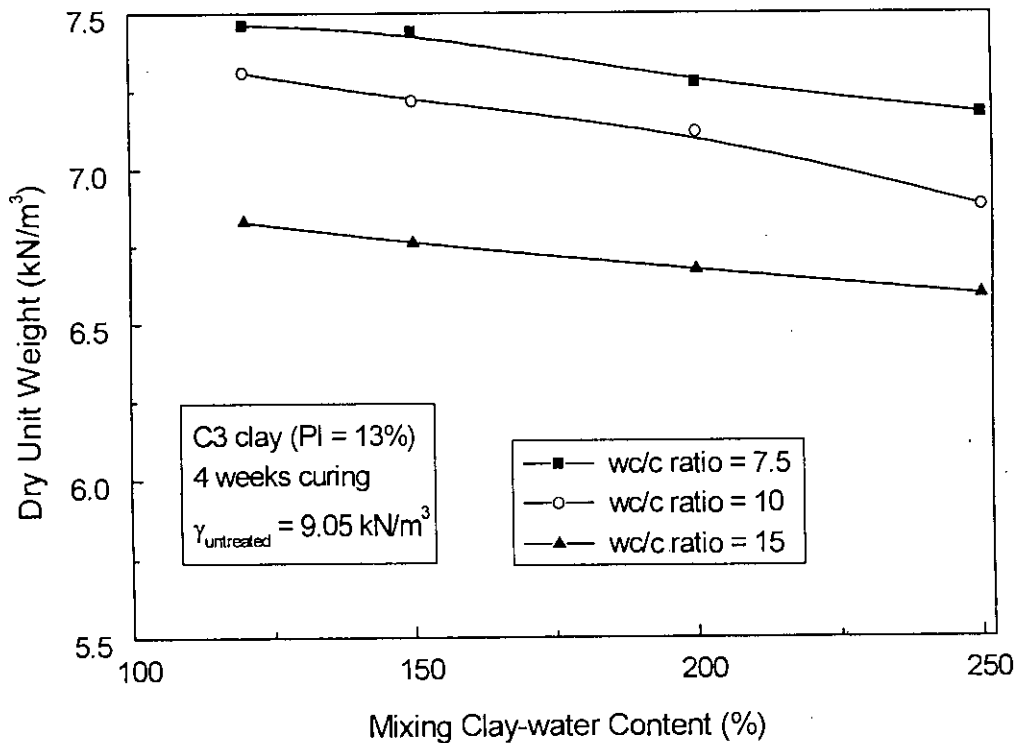


(b)

Fig. 4.27 Effect of Clay-water/Cement ratio and Curing Time on Dry Unit Weight of Cement Treated Clays (a) C1 clay and (b) C3 clay

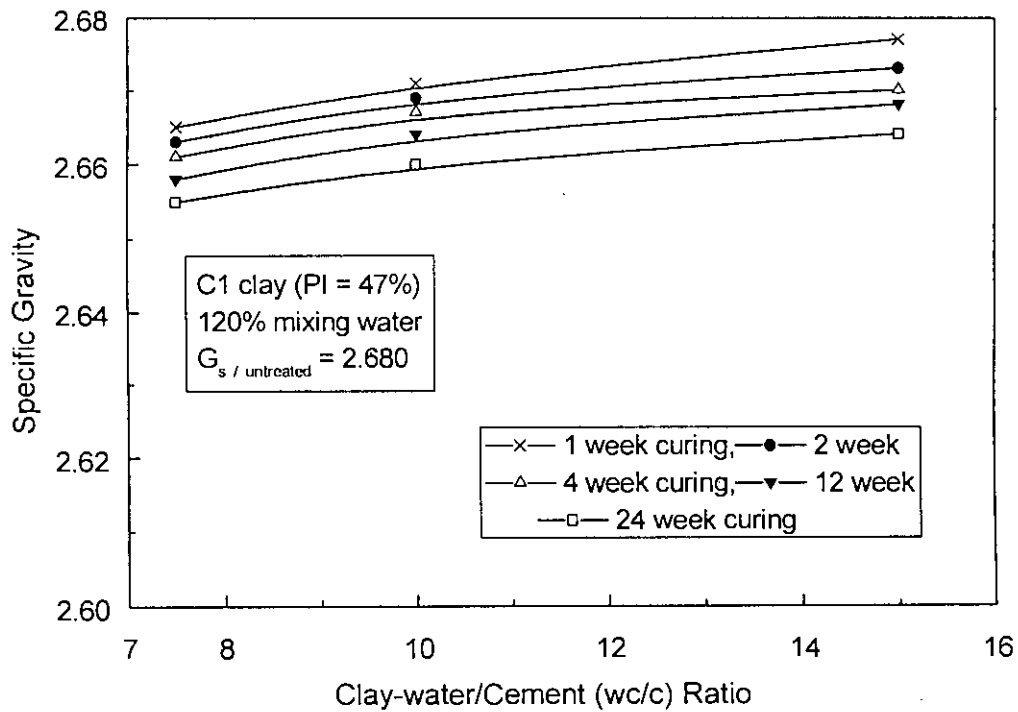


(a)

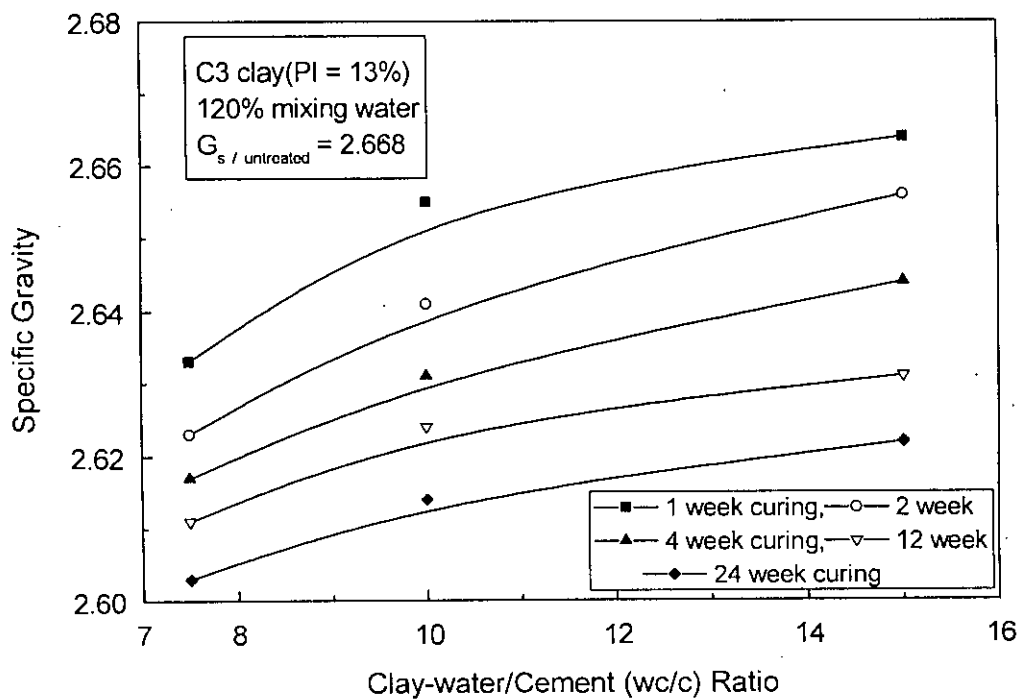


(b)

Fig. 4.28 Effect of Mixing Clay-water Content and w/c Ratio on Dry Unit Weight of Cement Treated Clays (a) C2 clay and (b) C3 clay

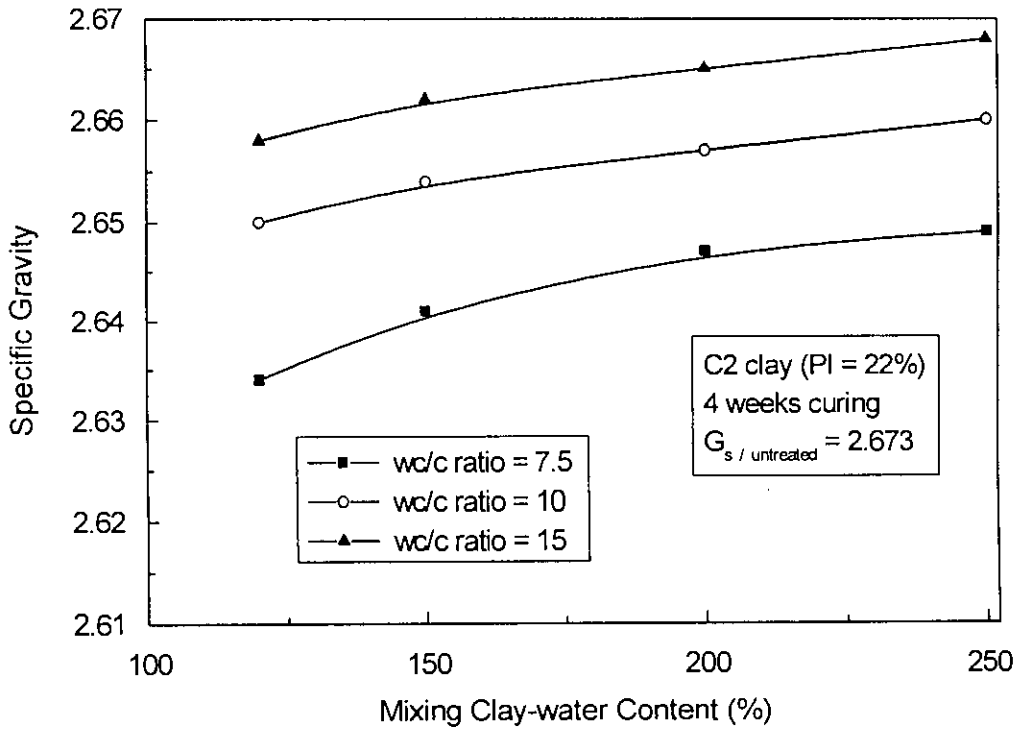


(a)

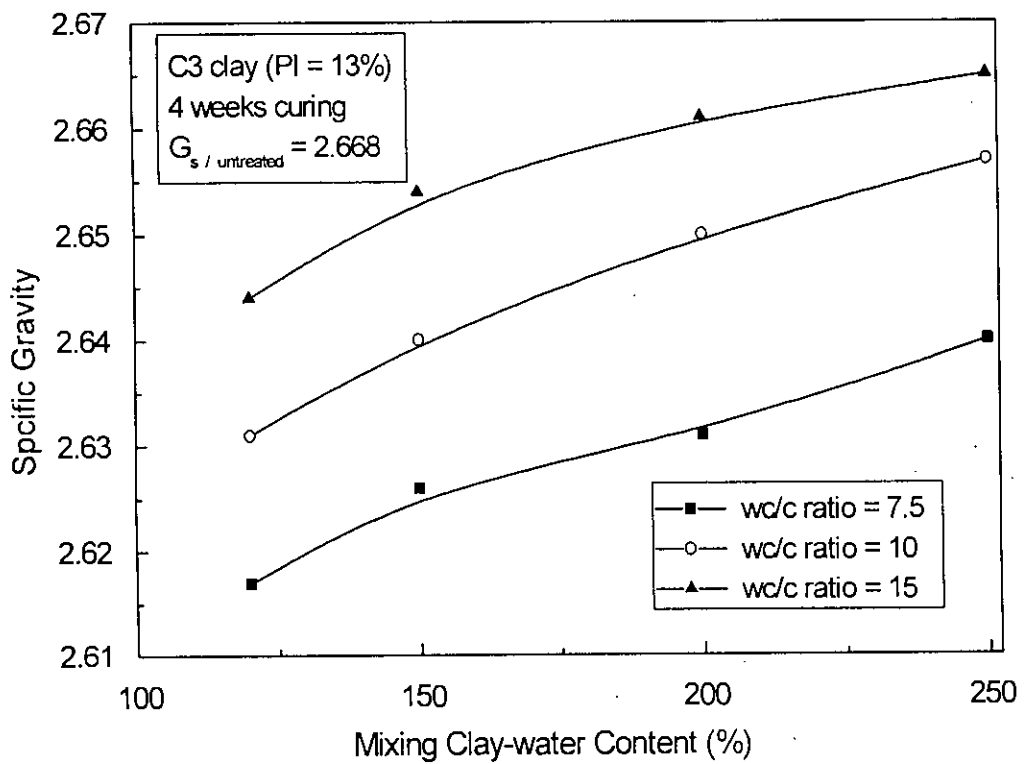


(b)

Fig. 4.29 Effect of Clay-water/Cement Ratio and Curing Time on Specific Gravity of Cement Treated Clays (a) C1 clay and (b) C3 clay

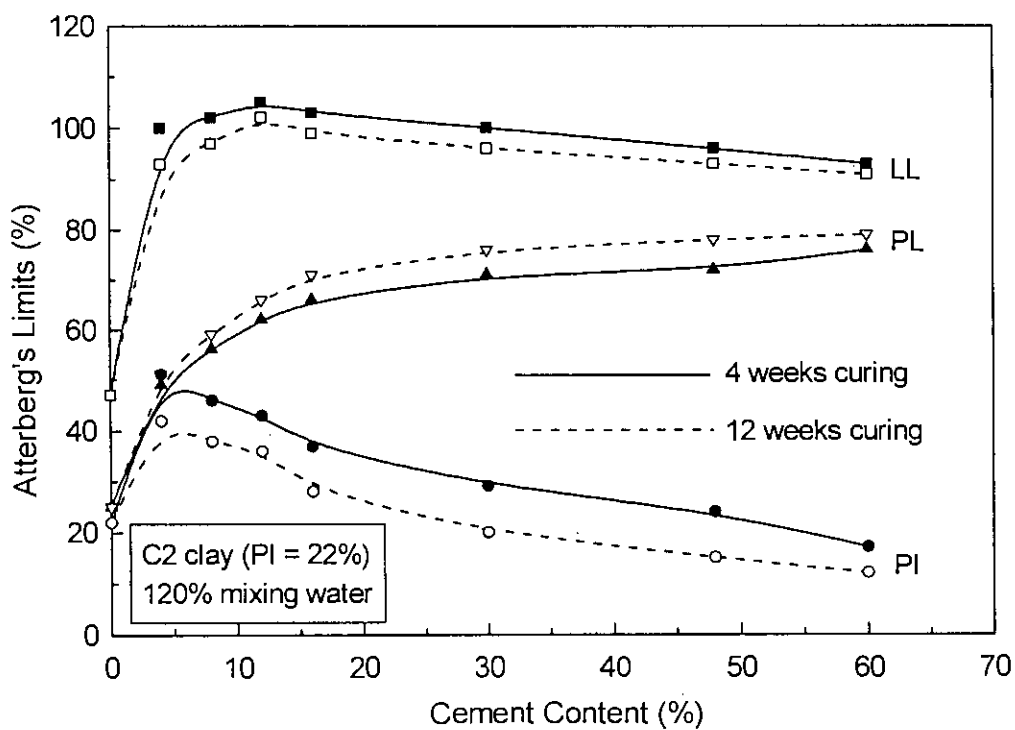


(a)

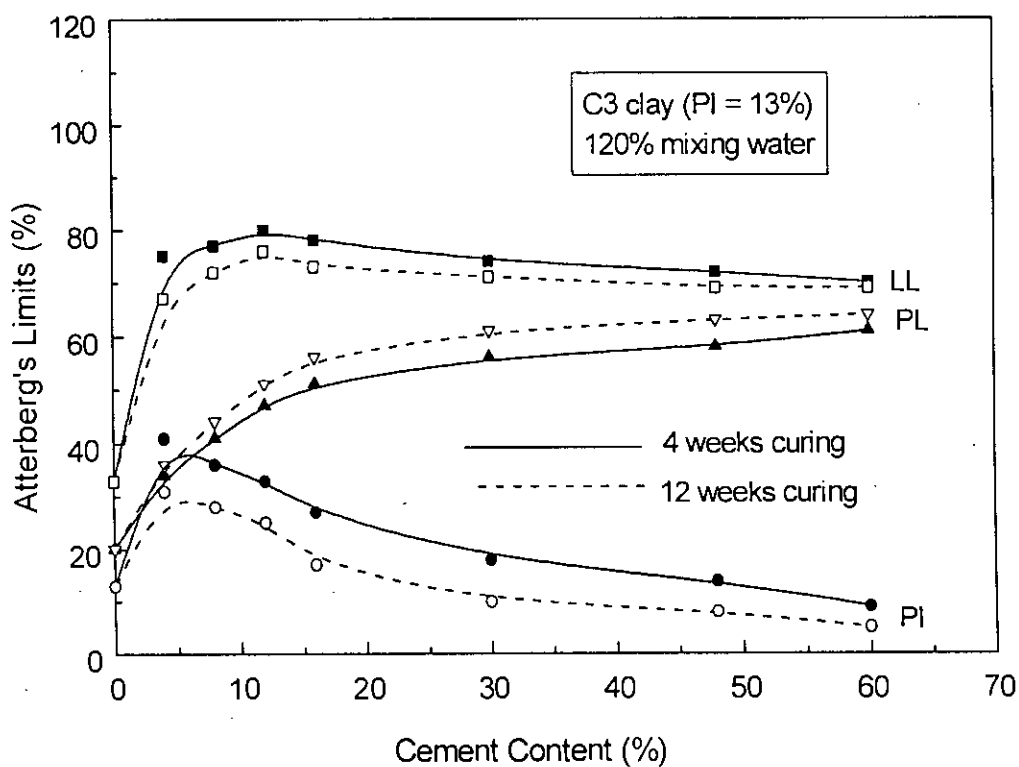


(b)

Fig. 4.30 Effect of Mixing Clay-water Content and wc/c Ratio on Specific Gravity of Cement Treated Clays (a) C2 clay and (b) C3 clay



(a)



(b)

Fig. 4.31 Effect of Cement Content and Curing Time on Atterberg's Limits of Cement Treated Clays (a) C2 clay and (b) C3 clay

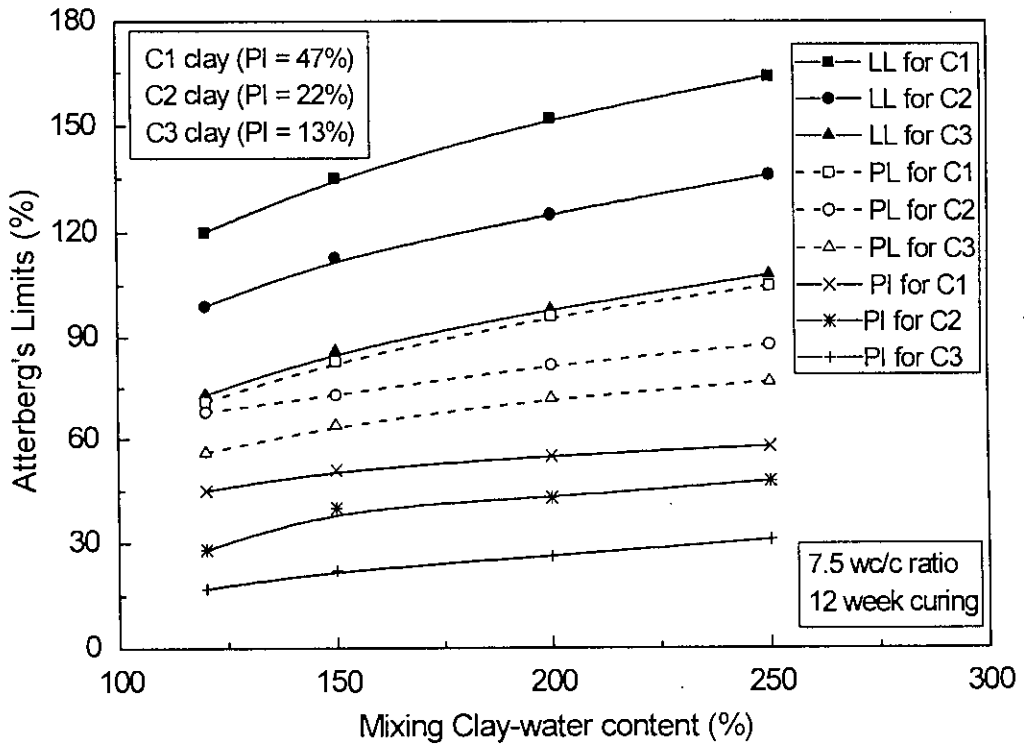


Fig. 4.32 Effect Mixing Water Content and Clay Type on Atterberg's Limits of Cement Treated clays

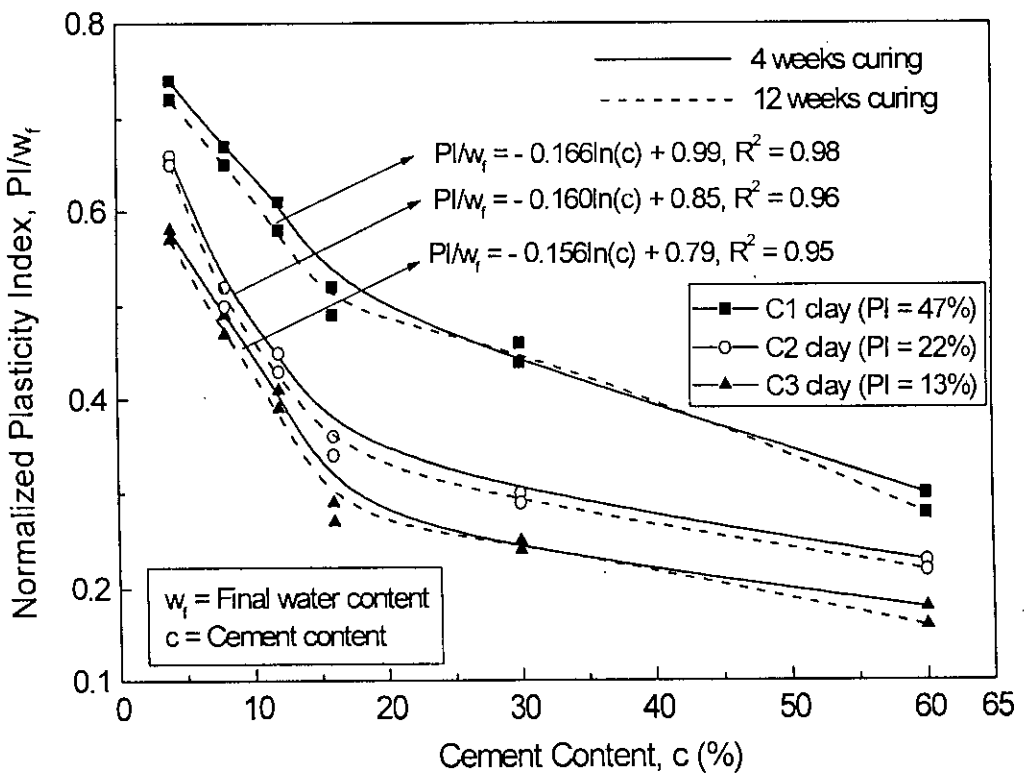


Fig. 4.33 Normalized Plasticity Index of Cement Treated clays (mixing water = 120%)

**Table 4.10 Effect of Cement Treatment on Physical Properties**

Physical properties	General effect in comparison to untreated clay	Effect of increasing cement content	Effect of increasing curing time	Effect of increasing initial water content	Effect of increasing plasticity of clay
Specific gravity	Decreases about 1% to 4%	Reduces significantly	Decreases with time increasing	Increases at higher water content	Increases with increasing plasticity
Water content	Immediate decrease about 5% to 11%	Reduces significantly	Reduces substantially	Increases at higher water content	Increases with increasing plasticity
Unit weight	Decreases about 20% to 35%	Increases at higher cement	Increases at longer time	Decreases at higher water content	Reduces with increasing plasticity
Plastic limit	Increases significantly (50% to 170%)	Increases at higher cement	Increases with time increasing	Increases at higher water content	Increases with increasing plasticity
Liquid limit	Immediate increases about 52% to 142%	Insignificant change	Reduces with time increasing	Increases at higher water content	Decreases with decreasing plasticity
Plasticity index	Reduces about 47% to 65%	Reduces at higher cement	Decreases at longer time	Increases at higher water content	Increases with increasing plasticity
Void ratio	Increases about 25% to 108%	Reduces at higher cement	Reduces with time increasing	Increases at higher water content	Increases with increasing plasticity
Degree of saturation	Decreases significantly (10% to 24%)	Decreases at higher cement	Decreases at longer time	Increases at higher water content	Decreases with decreasing plasticity

(\* Indicated results up to 4 weeks curing, 16% cement and 120% mixing water for range of clays)



## CHAPTER 5

### STRENGTH, STIFFNESS AND DEFORMATION CHARACTERISTICS OF TREATED CLAYS

#### 5.1 General

This chapter deals with the experimental results and discussions for basic stress-strain-strength characteristics based on consolidation, unconfined compression, triaxial (drained and undrained) compression and direct shear tests for treated and untreated C1 (PI = 47%) clay, C2 (PI = 22%) clay and C3 (PI = 13%) clay. These are also presented in order to establish relevant reference behaviour for the counterpart of cement treated Bangladesh clays. In parallel these, presents the results and discussion on the basic engineering properties of the treated and untreated clays from the series of relevant tests conducted. For this, a large number of tests on various treated clays were conducted with different values of initial mixing water content, clay-water/cement ratio, curing period, confining stress and drainage condition.

The experimental programme of untreated clays was set in accordance with that for treated clays so that a datum profile can be established for the base clays and parametric relevance relation can be drawn between treated and untreated clays. In the chapter, the results of tests conducted on treated samples for C1, C2 and C3 clays are presented with special emphasis on the behaviour of the treated samples with respect to the untreated samples. In order to assess the degree of improvement of the clay after treatment, investigation of the initial properties of the base clay is important. In this chapter, references and comparisons of the untreated characteristics have been made from previous studies to show the effects of cement and lime treatment on the strength and deformation behaviour of the soft clay.

The experimental observations on compressibility and permeability characteristics of treated and untreated C1, C2 and C3 clays from one-dimensional consolidation tests. Important aspects of deformation characteristics of the treated clay were analyzed with reference to untreated clay. The effects of cement and lime treatment on one-dimensional consolidation behaviour are presented.

Important aspects of the basic soil properties of the treated and untreated Bangladesh clays from unconfined compression tests are presented, in which the influences of type of clay, water content, cement content and curing time are explained. The results of the comprehensive series of unconfined compression tests are then discussed, specifically to illustrate the significant effects of cement treatment on the strength and deformation characteristics of the C1, C2 and C3 clays. The optimum range of cement content and the effective curing period are established based on the results of unconfined compression tests. The strength development and its normalized behaviour were studied. From the unconfined

compression tests, a comprehensive set of values pertaining to strength, strain at peak  $q_u$ , stiffness and physical properties were obtained.

The experimental investigations on shearing stress and resistance characteristics of treated clays from direct shear tests are also presented and discussed in this chapter. Important aspects of effective cohesion and friction characteristics of the treated clays were analyzed. The effects of cement treatment on cohesion and friction behaviours are observed from consolidated drained direct shear tests. From the direct shear tests, a comprehensive set of values pertaining to strength, normal strain and friction angles were obtained for a wide range of cement content and curing time. The variables, which were considered, include the type of clay, water content, cement content, the curing time and the applied normal stress range.

The results of the drained and undrained stress-strain behaviour from triaxial tests are critically discussed, specifically to illustrate the important effects of cement treatment on the strength and deformation characteristics of the clays. Sets of parametric variation employed in the tests were the type of clay, water content, cement content, curing period, pre-sheared consolidation pressure and loading conditions. Important aspects of strength and deformation characteristics of treated C1, C2 and C3 clays are pointed out using the Critical State Concept (CSC) to include the characteristics seen in stress-strain relationship, stress paths, pore pressure development and observations made concerning strength envelopes, failure state and residual conditions, among others. Comparisons are made between the initial behaviour of the untreated clays with treated clays, whenever necessary.

## 5.2 Compressibility Characteristics of Cement Treated and Lime Treated Clays

One-dimensional consolidation tests were carried out to study the compressibility characteristics of cement and lime treated clay samples and their relative improvement over that of the untreated clay. The influences of mixing ratio ( $w_c/c$ , clay-water/cement ratio and  $w_c/l$ , clay-water/lime ratio) [i.e., 7.5, 10 and 15], curing time (i.e., 1, 2, 4, 12 weeks), types of clay (depending on plasticity index) and mixing water content (i.e., 120%, 150%, 200% and 250%) have been investigated on different compressibility parameters including change in void ratio ( $e$ ), volumetric strain ( $\epsilon_v$ ), yield stress ( $\sigma'_y$ ) or Pre-consolidation pressure ( $\sigma'_p$ ), compression index ( $C_c$ ) and swell index ( $C_s$ ), coefficient of consolidation ( $c_v$ ) and coefficient of volume compressibility ( $m_v$ ). These results of the tests have been used to discuss the effects of stucturation i.e. the formation of cementation bond strength and destucturation i.e. the breakdown of cementation bond strength.

Summary of the compressibility properties for untreated base clays, cement treated clays and lime treated clays are shown in Tables 5.1, 5.2 and 5.3 respectively. The ( $e$ - $\log \sigma'_v$ ) typical relationship for untreated clays show that up to the maximum past pressure ( $\sigma'_p = 70$  kPa, 65 kPa and 61 kPa for C1, C2 and C3 clays respectively), the compressibility characteristics virtually do not change much. Beyond  $\sigma'_p$  value, it is shown a very significant drop in the void

ratio indicating that the clays are highly compressible. The compression index ( $C_c$ ) of untreated clays was found to be 0.737, 0.781 and 0.863 for C1, C2 and C3 clays respectively at the maximum stress level 1600 kPa. The swelling curve is similar and parallel to the initial part of the curve. The swell index ( $C_s$ ) of untreated clays was found to be 0.124, 0.127 and 0.131 for C1, C2 and C3 clays respectively at the minimum stress level 25 kPa. The clays have an overconsolidation ratio of 1.33, 1.26 and 1.18 for C1, C2 and C3 clays respectively; which was previously attributed to secondary consolidation processes (Sridaran et al, 1991, Nagaraj et al, 1991). The values of the coefficient of consolidation ( $c_v$ ) have been calculated by logarithm of time methods and taken as (3.37 to 0.90)  $\text{m}^2/\text{year}$ , (4.00 to 1.05)  $\text{m}^2/\text{year}$  and (5.20 to 1.40)  $\text{m}^2/\text{year}$  for C1 (PI = 47%) clay, C2 (PI = 22%) clay and C3 (PI = 13%) clay respectively at  $\sigma_v' = 12.5$  kPa to  $\sigma_{vm}' = 1600$  kPa, while the coefficient of volume of compressibility ( $m_v$ ) have been found,  $(6.24$  to  $1.50) \times 10^{-4}$   $\text{m}^2/\text{kN}$ ,  $(6.74$  to  $1.62) \times 10^{-4}$   $\text{m}^2/\text{kN}$  and  $(7.12$  to  $1.71) \times 10^{-4}$   $\text{m}^2/\text{kN}$ .

### 5.2.1 Effect of Clay-Water/ Admixture Ratio on Compressibility Characteristics

A summary of the compressibility parameters of cement treated and lime treated clay is shown in Table 5.2 and 5.3, respectively. The effects of clay-water/ admixture ratio ( $w/c$  and  $w/l$ ) and also curing time, types of clay and mixing water content on different compressibility characteristics such as ( $e$ - $\log\sigma_v'$ ) relationships, ( $\epsilon_v$ - $\log\sigma_v'$ ) relationships, compression index ( $C_c$ ) and swell index ( $C_s$ ), ( $c_v$ - $\log\sigma_v'$ ) relationships and ( $m_v$ - $\log\sigma_v'$ ) relationships are discussed individually for cement and lime treated clays in the following sections.

#### 5.2.1.1 Void Ratio Versus Effective Vertical Pressure Curve

The  $e$ - $\log\sigma_v'$  relations of clay mixtures with 150% water at mixing ratios of 7.5, 10 and 15 after 4 weeks of curing have been presented in Figs. 5.1(a) and 5.1(b) for cement-treated and lime-treated clays, respectively. The  $e$ - $\log\sigma_v'$  relationships are plotted so as to take care of the effect of the difference in void ratio for the vertical stresses less than the yield stress. In this range the cementation component is the dominant factor to resist compression. It has been found that the yield stress and the deformation behaviour at pre-yield stress of all samples having identical mixing ratio are practically the same. But samples provide higher compression indices beyond yield stress ( $\sigma_y'$ ). This is due to the break up of cementation bond, which is similar to the behaviour of naturally cemented clay. The compression indices at post yield state of clay-cement mixtures having an identical initial water content are in almost the same order, even if they are made up from different cement content. It has been found that the lower the value of clay-water/ admixture ratio ( $w/c$ ,  $w/l$ ), the greater the enhancement of the yield stress. The lime-treated clays are gained comparatively more higher void ratio and lower yield stress than those of cement-treated clays. The mixing ratio affects not only the deformation characteristic, but also the rate of hardening related to mineralogy,

hydration and pozzolanic reactions. Miura et al. (2001) and Bergado et al. (2003) found that the same consistent of results for compressibility characteristics of treated clays.

### 5.2.1.2 Volumetric Strain Versus Effective Vertical Pressure Curve

Typical  $\epsilon_v$ - $\log\sigma'_v$  relations of clay mixtures with 150% water at clay-water/ admixture ratios of 7.5, 10 and 15 after 4 weeks of curing have been presented in Figs. 5.2(a) and 5.2(b) for cement-treated and lime-treated clays respectively. The  $\epsilon_v$ - $\log\sigma'_v$  relationships have been plotted so as to take care of the effect of the difference in void ratio for the vertical stresses less than the yield stress. In this range the cementation component is the dominant factor to resist compression. The lime-treated clays are gained comparatively higher volumetric strains than those of cement-treated clays. Although the curves exhibit some similarity to that of conventional normally consolidated untreated clay, it still possesses many fundamental differences due to the effect of the treatment. This type of parallel behaviour among the natural samples is implied in a unique state Boundary Surface. The parallel characteristics of treated each clays at higher values of consolidation pressure beyond  $\sigma'_v$  value signify that at the time of consolidation, which is a shearing process, the bonded particles or clusters generally become dissociated, releasing the locked-in energy. This effect of dissociation of bonded particles accompanied by the release of locked-in energy transforms the soil mass more close to the untreated one and hence it's compressibility behaviour acts accordingly. Miura et al. (2001) and Kamaluddin (1995) also reported that the same types behaviour of the cementation effect for treated clays.

### 5.2.1.3 Compression Index and Swell Index

Figs. 5.3 and 5.4 illustrate the effect of clay-water/admixture ratio on  $C_c$  and  $C_s$  values respectively. Figs. 5.3 and 5.4 show that  $C_c$  and  $C_s$  values results due to the hardening effect imposed on the treated soil mass, increase with the increase of clay-water/admixture ratio (decrease of cement / lime content). However, at lower ratio, almost reduction of  $C_c$  is noticed and the reduction of  $C_s$  values is very marginal and approaching almost zero. Test results show that the swelling index reduces significantly due to the effect of cementation in soft clay. This observation implies that the treated clay sample is consistent with the heavily over-consolidated soil behaviour. For treatment, considering admixture content,  $C_c$  and  $C_s$  for lime treated clays are greater than those of cement treated clays. Balasubramaniam et al. (1999) also reported that the similar type comparison between lime and cement treated clays. It can be inferred that physicochemical changes in the clay-cement structure which leads the reduction in  $C_c$  values (including other changes in the compressibility characteristics). This observation is consistent with the findings of Liu and Carter (1999) and Chew et al. (2001), who showed that during virgin yielding, the structured soil is more compressible than the reconstituted soil. This suggests that at higher stresses (beyond the apparent pre-consolidation pressure), the treated samples exhibit normally consolidated behaviour with larger  $C_c$ .

#### 5.2.1.4 Coefficient of Consolidation

One important effects of cementation on the consolidation characteristics of soft clay are to increase the values of the coefficient of consolidation ( $c_v$ ). Figs. 5.5(a) and 5.5(b) illustrate the characteristics of the variation in  $c_v$  values with increasing effective pressures for cement-treated and lime-treated clays respectively at 4 weeks curing and clay-water/ admixture ratio = 7.5, 10 and 15. It is found that the variations of  $c_v$  for mixing ratio are nearly parallel. Fig. 5.5 shows that the lower clay-water/admixture ratio (higher the cement / lime content), the lower is the value of  $c_v$ . For cement content, the reduction of  $c_v$  are more pronounced than those lime content at the same condition. For treated clays,  $c_v$  generally decrease with increasing consolidation pressure similar to those of natural soft untreated clays. It is also noted that the coefficient of consolidation of untreated clays, which are much smaller than treated clay samples. It also appears that at a particular clay-water admixture ratio and effective vertical pressure,  $c_v$  values for lime treated clay are higher than those of cement treated clay. It is inferred that physicochemical changes in the clay-cement structure which leads the increase in  $c_v$  values. Similar types of behaviour for the treated Bangkok clay samples were noticed by Kamaluddin et al. (1997).

#### 5.2.1.5 Coefficient of Volume Compressibility

Figs. 5.6(a) and 5.6(b) illustrate the variation of coefficient of volume compressibility ( $m_v$ ) with effective pressures for cement treated and lime treated clays respectively at 4 weeks curing and clay-water/ admixture ratio = 7.5, 10 and 15. It has been found that the non-linear variation of  $m_v$  is nearly parallel. The coefficient of volume compressibility decreases with an increase in the effective stress. One important effect of cementation on the compressibility characteristics of soft clay is to increase the values of the coefficient of volume compressibility. For treated clays,  $m_v$  generally decreases with increasing consolidation pressure similar to those of natural soft untreated clays. Fig. 5.6 also shows that the lower clay-water/admixture ratio (higher the cement / lime content), the lower is the value of  $m_v$ . For cement content, the reduction of  $m_v$  are more pronounced than those lime content at the same condition. Miura et al. (2001); and Horpibulsuk and Miura (2001) revealed that the compressibility behaviour of treated clay are influenced by the cementation and fabric. Fabric is the arrangement of the particles, particle group (cluster) and pre-space (spacing between clusters) in soil (Mitchell 1993).

### 5.2.2 Effect of Curing Time on Compressibility Characteristics

#### 5.2.2.1 Void Ratio Versus Effective Vertical Pressure Curve

The effect of curing time on  $e$ - $\log \sigma_v'$  relationships is presented in Figs. 5.7(a) and 5.7(b) for cement treated and lime treated clays, respectively. The gradual reduction process of compressibility of treated clay with time is quite obvious in these figures, indicating the

incremental influence of the curing time parameter. The increase of apparent pre-consolidation pressure ( $\sigma'_p$  or  $\sigma'_y$ ) is due to the effect of structuration (existing of cementation bond) for increasing curing time of treated clay particles. The curves of treated clays in Fig. 5.7 shows approximate parallel behaviour as implied by the natural untreated clay in a unique State Boundary Surface. Apparently, the  $e$ - $\log\sigma'_v$  relationships for 4 weeks curing time with cement / lime content, are very similar to each other and they possess some analogical characteristics of treated clays for 12 weeks curing time. For cement content, the reduction of void ratio are more pronounced than those lime content at the same curing condition. The treated clays exhibit similar type compressibility properties and do not show large changes due to curing time. The phenomenon suggests that with time in the clay matrix, calcium hydroxide reacts with the silicates and aluminates (pozzolans) in the clay to form cementing materials or binders, consisting of calcium silicates and/or aluminums hydrates (principally dihydrates). The higher curing time, the larger is the degree of improvement of the consolidation properties. Miura et al. (2001) and Chew et al. (2001) reported the same consistent of results for compressibility characteristics of cement treated clays.

### 5.2.2.2 Volumetric Strain Versus Effective Vertical Pressure Curves

The effect of curing time on  $\epsilon_v$ - $\log\sigma'_v$  relationships is shown in Figs. 5.8(a) and 5.8(b) for cement treated and lime treated clays respectively. The gradual reduction process of compressibility of treated clay with time is quite obvious in Fig. 5.8, indicating the incremental reduction of volumetric strain influence of the curing time parameter. This pronouncement of the hardening effect due to curing time is further accelerated and governed as the value of cement / lime content in the clay matrix is enhanced. It can be noticed that as curing time increases the volumetric strain gradually decreases. Gradual hardening of clays accompanied by reduction of compressibility is quite remarkable and the hardening process is active. Miura et al. (2001) and Kamaluddin (1995) also reported that the same types behaviour of the cementation effect for treated clays.

### 5.2.2.3 Compression Index and Swell Index

Figs. 5.9 and 5.10 illustrate typical variation of  $C_c$  and  $C_s$  values with increasing curing time for C3 clay, respectively. For the same clay-water/ admixture ratio and mixing clay-water content, the compressibility and swelling exhibited by the treated clays slowly decrease with increasing higher curing time. Figs. 5.9 and 5.10 shows that the samples initially caused substantial reduction of  $C_c$  and  $C_s$  value during the period of first month. After 4 weeks and up to 12 weeks curing period, smaller changes in the  $C_c$  values can be noticed. That means the curing time has rendered maximum effectiveness during the first month (4 weeks) and thereafter, it has got little influence on the compression indices. Miura et al. (2001) and Chew et al. (2001) found that the same consistent of results for compression and swell indices of treated clays. It can be seen from Fig. 5.9 and 5.10 that at the same curing time,  $C_c$  and  $C_s$

values for lime treated clays are higher than those of cement treated clays. Balasubramaniam et al. (1999) also reported that the similar type comparison between lime and cement treated clays.

#### 5.2.2.4 Coefficient of Consolidation

The effect of curing time on coefficient of consolidation ( $c_v$ ) values is shown in Figs. 5.11(a) and 5.11(b) for cement treated and lime treated clays respectively. It can be seen that the higher the curing time, the lower the value of  $c_v$ . It also appears from Fig. 5.11 that at a particular curing time and effective vertical pressure,  $c_v$  values for lime treated clays are higher than those of cement treated clays. It is inferred that physicochemical changes in the clay-cement structure with time which leads the increase in  $c_v$  values. Bergado et al. (2003) also found that the higher the curing time, the lower the value of  $c_v$ .

#### 5.2.2.5 Coefficient of Volume Compressibility

The effect of curing time on coefficient of volume compressibility ( $m_v$ ) values is shown from Figs. 5.12(a) and 5.12(b) for cement treated and lime treated clays respectively. It can be seen that at a particular effective vertical pressure, higher the curing time, the lower is the value of  $m_v$ . The non-linear variation of  $m_v$  is nearly parallel. It is splendid for curing time that samples of same cement/ lime content also exhibit similar behaviour. Figs. 5.12 also show that at the same curing time and effective vertical pressure,  $m_v$  values for lime treated clays are higher than those of cement treated clays.

### 5.2.3 Effect of Clay Type on Compressibility Characteristics

#### 5.2.3.1 Void Ratio Versus Effective Vertical Pressure Curves

Effect of clay type on  $e$ - $\log\sigma'_v$  relationships for cement treated and lime treated clays at a particular  $w_c/c$  ratio, mixing water content and curing time is shown in Figs. 5.13(a) and 5.13(b) for cement treated and lime treated clays, respectively. It can be seen from Figs. 5.13 that at a particular  $\sigma'_v$ , there is a trend of increasing void ratio with the decrease in plasticity index of the clays for both cement and lime treated clays. Figs. 5.13 also show that yield stress (pre-consolidation pressure) increases with increasing plasticity of the clays for both cement and lime treated clays. It is also evident that for the same clay, pre-consolidation pressure for cement treated clay is higher than that of lime treated clay.

#### 5.2.3.2 Volumetric Strain Versus Effective Vertical Pressure Curve

Figs. 5.14(a) and 5.14(b) present  $\epsilon_v$ - $\log\sigma'_v$  relationships for cement-treated and lime-treated clays respectively at a particular  $w_c/c$  ratio and mixing water content. It has been found that the deformation behaviour at pre-yield stress of all clay samples are identical but different  $\epsilon_v$  values after yielding. The  $\epsilon_v$  values for C1 clay are lower than those of C2 clay and  $\epsilon_v$  values of C2 clay are lower than those of C3 clay. This is due to the break up of cementation bonds

have more resistant for more plastic clay. Therefore at a particular effective vertical pressure,  $\epsilon_v$  increases with the decrease in plasticity index. For the same clay at a particular  $w/c$  ratio,  $\epsilon_v$  values for lime treated clays are higher than those of cement treated clays.

### 5.2.3.3 Compression Index and Swell Index

Figs. 5.15 and 5.16 illustrate the variation of  $C_c$  and  $C_s$  values respectively with clay-water/admixture ratio for cement treated and lime treated clays. Figs. 5.15 and 5.16 show that  $C_c$  and  $C_s$  values results due to the hardening effect imposed on the treated soil mass depend on plasticity of soil (i.e., type of clay). For the same  $w/c$  ratio and curing time, the compressibility and swelling exhibited by the treated mass for C3 clay are higher than that of C1 and C2 clays. Therefore, it appears that  $C_c$  and  $C_s$  increases with the decrease in plasticity index of clays. For the same clay,  $C_c$  and  $C_s$  values for lime treated clays are higher than those of cement treated clays. It can be inferred that physicochemical changes depend on montmorillonite mineral in the clay, which affects the  $C_c$  and  $C_s$  values (including other changes in the compressibility and swelling characteristics). Kamaluddin (1995) also reported that the similar behaviour for treated clays.

### 5.2.3.4 Coefficient of Consolidation

The effect of clay-type on coefficient of consolidation ( $c_v$ ) values is shown in Figs. 5.17(a) and 5.17(b) for cement treated and lime treated clays, respectively. It can be seen that  $c_v$  value results due to the consolidation effect imposed on the treated soil mass depend on plasticity of soil (type of clay). For the same clay type,  $c_v$  values for lime treated clays are higher than those of cement treated clays. It can also be seen from Fig. 5.17 that the higher the plasticity index, the lower is the value of  $c_v$ . It can be inferred that physicochemical changes depend on illite and kaolinite mineral in the clay which controls the  $c_v$  values. The changing of these clay minerals due to cementation have been confirmed from X-ray diffraction analysis in this study.

### 5.2.3.5 Coefficient of Volume Compressibility

The effect of clay-type on coefficient of volume compressibility ( $m_v$ ) values is shown in Figs. 5.18(a) and 5.18(b) for cement treated and lime treated clays, respectively. The figure reveals that  $m_v$  results due to the consolidation effect imposed on the treated soil mass depend on plasticity of soil (type of clay). For the same clay,  $m_v$  values for lime treated clays are higher than those of cement treated clays. It appears from Fig. 5.18 that at a particular effective vertical stress,  $m_v$  decreases with increasing plasticity index of clay. It can be inferred that physicochemical changes depend on illite and kaolinite mineral in the clay which leads the  $m_v$  values.



## 5.2.4 Effect of Mixing Clay-Water Content on Compressibility Characteristics

### 5.2.4.1 Void Ratio Versus Effective Vertical Pressure Curve

Figs. 5.19(a) and 5.19(b) present the effect of mixing water content on  $e$ - $\log\sigma'_v$  relations for cement treated and lime treated clays respectively. The clay-cement mixture were made up from four conditions of clay water content (120%, 150%, 200% and 250% for cement-treated clays) but the clay-lime mixture were made up from two conditions of clay water content (120% and 150% for lime-treated clays). This is why for practical problems, lime is failed as a non-effective binding material at very high mixing water content i.e., 200% and 250%. Fig. 5.19 shows that at the same mixing water content, void ratio for lime treated clays are higher than those of cement treated clays. It is found that the deformation behaviour at pre-yield stress of all samples having identical  $w/c$  are practically the same but different after the yield stress. The samples with a higher clay-water contents are stable at higher void ratios. It appears from Fig. 5.19 that a particular effective vertical pressure the void ratio decreases with decreasing mixing water content. Fig. 5.19 also shows that yield stress (pre-consolidation pressure) increases with the decrease of initial mixing water content. Similar effects are reported by Locat et al. (1996), Chew et al. (2004) and Miura et al. (2001).

### 5.2.4.2 Volumetric Strain Versus Effective Vertical Pressure Curve

Effect of mixing water content effect on  $\epsilon_v$ - $\log\sigma'_v$  relations is shown in Figs. 5.20(a) and 5.20(b) for cement treated and lime treated clays respectively. The  $\epsilon_v$ - $\log\sigma'_v$  relationships are plotted so as to take care of the effect of the difference in void ratio for the vertical stresses less than the yield stress. In this range the cementation component is the dominant factor to resist compression. The samples with a higher clay-water contents are stable at higher volumetric strain beyond yield stress, especially for samples made up at a high water content of 250%. It is found that as water content decreases, the volumetric strain gradually decreases. It also appears that at the same mixing water content,  $\epsilon_v$  values for lime treated clays are higher than those of cement treated clays. This is due to the break up of cementation bond, which is similar to the behaviour of naturally cemented clay. The rate of volumetric strain increases for hardening related depends on physicochemical changes for hydration and pozzolanic reactions. These physicochemical changes due to cementation have been confirmed in the previous chapter of this study.

### 5.2.4.3 Compression Index and Swell Index

Figs. 5.21 to 5.22 illustrate the characteristics of the variation of  $C_c$  and  $C_s$  values respectively with clay-water/cement ratio at curing time 4 weeks and different water content for cement-treated and lime-treated clays. Figs. 5.21 and 5.22 show that a particular  $w/c$  ratio,  $C_c$  and  $C_s$  values resulting due to the hardening effect imposed on the treated soil mass, increase significantly with the increase of mixing clay-water content. At the same mixing water

content,  $C_c$  and  $C_s$  values for lime treated clays are higher than those of cement treated clays. It can be inferred that physicochemical changes in the clay-cement structure that leads the reduction in  $C_c$  values due to lowering of mixing water content (including other changes in the compressibility characteristics). This observation is consistent with the findings of Liu and Carter (1999) and Chew et al. (2001), who showed that during virgin yielding, the structured soil is more compressible than the reconstituted soil. This suggests that at higher stresses (beyond the apparent pre-consolidation pressure), the treated samples exhibit normally consolidated behaviour with larger  $C_c$ .

#### 5.2.4.4 Coefficient of Consolidation

Figs. 5.23(a) and 5.23(b) present the variation in  $c_v$  values with increasing mixing high water content at 4 weeks curing and mixing ratio of 10 for cement treated and lime treated clays respectively. It can be seen from Fig. 5.23 that at the same mixing water content,  $c_v$  values for lime treated clays are higher than those of cement treated clays. A substantial increase in  $c_v$  values was found to have occurred within higher mixing water content. It is postulated that the highest enhancement of  $c_v$  value with same mix ratio is deemed to occur in the vicinity of higher water content i.e., 250%.

#### 5.2.4.5 Coefficient of Volume Compressibility

The effect of mixing water content on coefficient of volume compressibility ( $m_v$ ) is shown in Figs. 5.24(a) and 5.24(b) for cement treated and lime treated clays, respectively. Fig. 5.24 shows that at the same mixing water content,  $m_v$  values for lime treated clays are higher than those of cement treated clays. It has been found that for mixing water contents of 120%, 150%, 200% and 250%, the non-linear variation of  $m_v$  is nearly parallel. A substantial decrease in  $m_v$  values was found to have occurred within lowering the mixing water content. Miura et al. (2001) revealed that the compression behaviour of cement admixed clays were influenced by amount of mixing water content, degree of cementation and type of fabric.

#### 5.2.5 Compressibility Effects on SEM Images

To verify the effect of apparent destructuration, two treated soil samples with 16% cement content were stressed up to a consolidation pressure of 400 and 1600 kPa, and SEM analysis was carried out. Fig. 5.25 shows SEM images at zero pressures for untreated and 16% cement treated C1 clay, while Fig. 5.26 shows SEM images for 16% cement treated C1 clay at 400 kPa and 1600 kPa pressure. In these two tests, SEM samples were obtained in the vertical plane after consolidation to the desired stresses. As can be seen from Fig 5.25(b) that the treated clay matrix appears in the form of large clay-cement cluster associated with large inter-cluster void space when it is not compressed. When the sample is stressed up to the consolidation pressure of 400 kPa, the large clay-cement clusters collapse and inter-cluster void spaces reduce, but small intra-cluster pores still remain as it was, as shown in Fig

5.26(a). At very high consolidation pressure (i.e., 1600 kPa), as can be seen from Fig. 5.26(b), both inter and intra-aggregate pore spaces reduce significantly, and thereby reduce the resulting void ratio. Results for void ratio as shown in Tables 4.7, 4.8 and 4.9, suggest that the treated clay particles have more inter and intra-aggregate pore spaces with larger pore volume. Thus, the SEM images in Figs 5.25 and Fig. 5.26, suggest that only the clay-cement cluster collapses at high stresses and the collapsing is progressive. The small intra-cluster pores are not compressed until the pressure far beyond the pre-consolidation pressure. And at that time all inter-cluster voids would have been collapsed. Kamruzzaman (2002) found the same loading effects for compressibility characteristics in SEM images of treated Singapore clay. This is because the treated clay has a larger pore volume than the untreated clay as can be seen from the SEM images of Figs. 5.25(a) and 5.25(b).

### 5.2.6 Intrinsic Compression Line and Generalized Compression Line

The cement treated (cement = 8%, 12% and 16%) and lime treated (lime = 8%, 12% and 16%) clays have been plotted along with untreated clays in the  $I_v$ - $\log\sigma_v'$  plane as shown in Figs. 5.27(a) and 5.27(b), respectively. The Intrinsic Compression Lines (ICL) have been found by plotting void index,  $I_v = (e - e_{100})/C_c$  against  $\log\sigma_v'$ . Here void index are considered as a parameter for measuring the intrinsic hardening potential of the treated clays. The figures render confirmation of the over-consolidation effect of the treated clays brought about by cement and lime treatment. The untreated clays lies along with ICL. The figures show that cement and lime treatment displaces the relationship with an increasing value of  $\sigma_v'$  comparing untreated state of clays. The cement and lime treated clay plots shift rightward to the untreated clay plot of ICL. As the cement content or lime content increases, the curves are shifted with an increasing value of  $\sigma_v'$  as shown by the bands of cement or lime content. Kamaluddin et al. (1995) found that the same results for the cement treated Bangkok clay samples. The ICL of the clays studied can be expressed by the following equations.

$$I_v = 1.26 - 0.015 \log\sigma_v' + 1 \times 10^{-5} (\log\sigma_v')^2 - 4.76 \times 10^{-9} (\log\sigma_v')^3 \quad \text{for untreated clays} \quad (5.1a)$$

$$I_v = 0.89 - 0.007 \log\sigma_v' - 1.12 (\log\sigma_v')^2 + 7.05 \times 10^{-3} (\log\sigma_v')^3 \quad \text{for cement treated} \quad (5.1b)$$

$$I_v = 1.09 - 0.009 \log\sigma_v' - 1.16 (\log\sigma_v')^2 + 6.35 \times 10^{-4} (\log\sigma_v')^3 \quad \text{for lime treated} \quad (5.1c)$$

From the test results, it is of interest to note that for a particular clay admixed with cement or lime, the compression behaviour at post-yield state is only dependent upon cement content or lime content, irrespectively of clay water content. The Intrinsic Compression Line (ICL) is taken the effect of cement content and lime content into account. Comparing cement and lime treatment from Fig. 5.27, it has been found that ICL for cement clays are sifted more rightward than those of lime treated clays.

There are two unknown parameters required to obtain ICL, which are compression index and  $e_{100}$ . Since the  $e_{100}$  can be written in terms of  $C_c$ , the modification of the Intrinsic Compression

Line has been obtained by plotting normalized void ratio,  $e/e_{100}$  versus vertical pressure,  $\sigma_v'$  as shown in Fig. 5.28. This line is designated as Generalized Compression Line (GCL). The GCL for cement treated and lime treated clays have been plotted along with untreated clays in the  $e/e_{100}$ - $\log\sigma_v'$  plane as shown in Figs. 5.28(a) and 5.28(b), respectively. The GCL of the clays studied can be expressed by the following equations.

$$e/e_{100} = 1.17 - 0.006 \log\sigma_v' \quad \text{for untreated clays} \quad (5.2a)$$

$$e/e_{100} = 1.09 - 0.0024 \log\sigma_v' \quad \text{for cement treated clays} \quad (5.2b)$$

$$e/e_{100} = 1.12 - 0.0032 \log\sigma_v' \quad \text{for lime treated clays} \quad (5.2c)$$

The Generalized Compression Line (GCL) considers the effect of cement content and lime content into account. Comparing cement and lime treatment from Fig. 5.28, it has been found that GCL for cement clays are also shifted more rightward than those of lime treated clays. From ICL and GCL for treated clays, it can be concluded that cement is more effective and active binding material than those of lime, because in both cases, it has been confirmed that cement treated clays experienced more yield strength and over-consolidated behaviour than those of lime treated clays.

Horpibulsuk (2002) also reported that the same type relation between  $I_v$  and  $e/e_{100}$  with  $\log\sigma_v'$  for cement treated Bangkok clays, such as  $I_v = 2.45 - 1.285 \log\sigma_v' + 0.015 (\log\sigma_v')^3$  and  $e/e_{100} = 2.025 - 0.504 \log\sigma_v'$  respectively. The advantage of these lines are that it can take the effect of cement / lime content into account with only one unknown parameter,  $e_{100}$ . In the absence of laboratory compression test data on cement admixed clay, the  $e_{100}$  can still be predicted if a vertical pressure and its corresponding void ratio are known. Since the magnitudes of the yield stress,  $\sigma_y'$  and unconfined compressive strength,  $q_u$  depend on the degree of cementation (bond strength), it appears logical to relate these two parameters as reported by Horpibulsuk (2002). As a result, the Generalized Compression Line (GCL) can be simply obtained by conducting the unconfined compression test to indirectly obtain the yield stress. Miura et al. (2001) have recommended that the yield stress is preferable to be determined by the method proposed by Sridharan et al. (1991). The yield stress is obtained as the point of two straight lines extended from the linear portions on either end of the compression curve plotted as void ratio against logarithm of effective vertical pressure.

It has been known from chemical properties test for cement treated clays in this research that the compression behaviours are also affected by the clay composition such as clay minerals, salt concentration, organic matter, sulfate content, etc. since it influences the bond strength development (Chew et al., 2001). Even if the Generalized Compression Line (GCL) is generated from only a certain types of clay used in this research mixed with cement due to the limited test results, there is a possibility of applicability of the Generalized Compression line to different clays at any curing time.

### 5.3 Permeability Characteristics of Cement Treated and Lime Treated Clays

Co-efficient of permeability of untreated and cement and lime treated samples were determined from one-dimensional consolidation test data. The coefficient of permeability is the direct function of coefficient of consolidation, coefficient of volume compressibility and wet unit weight, and numerical value of  $k$  is the product of these three parameters. A comparison of coefficient permeability of untreated and treated clays at effective vertical pressure of 18.75 kPa is shown in Table 5.4. The permeability characteristics values for untreated base clays, cement treated clays and lime treated clays are shown in Table 5.4. The values of the coefficient of permeability ( $k$ ) have been found,  $(4.28 \text{ to } 0.27) \times 10^{-9}$  m/sec,  $(4.94 \text{ to } 0.32) \times 10^{-9}$  m/sec and  $(6.16 \text{ to } 0.53) \times 10^{-9}$  m/sec at average  $\sigma'_v = 18.75$  kPa to 1200 kPa for untreated C1 (PI = 47%), C2 (PI = 22%) and C3 (PI = 13%) clays, respectively.

#### 5.3.1 Effect of Clay-Water/ Admixture Ratio on Permeability Characteristics

The coefficient of permeability and effective vertical stress,  $k$ - $\log \sigma'_v$  relationships of cement treated and lime treated clays are shown in Figs. 5.29(a) and 5.29(b) respectively at 150% mixing water content, 4 weeks curing and clay-water/ admixture (wc/c, wc/l) ratio = 7.5, 10 and 15. Test results reveal that at the same effective vertical stress, the treated clay has higher permeability than that of the untreated clay. This implies that at the same depth below the ground surface, the treated clay contain a higher void ratio than the untreated clay. This has been verified from the  $e$ - $\log \sigma'_v$  relation of treated and untreated clays in previous section. It can be seen from Fig. 5.29 that  $k$  value increases with increasing clay-water/admixture ratio (decreasing admixture content). It has been found that the variation of  $k$  with  $\log \sigma'_v$  is nearly parallel and non-linear. It is evident that higher the mixing ratio (lower the cement / lime content), the higher is the value of  $k$ . The figures reveal that  $k$  results due to the drainage effect imposed on the treated soil mass, decrease significantly with the increase of admixture content. For cement content, the reduction of  $k$  are more pronounced than lime content at the same condition. However, for both admixtures reduction of  $k$  has been noticed due to increase vertical effective pressure. It is inferred that physicochemical changes in the clay-cement structure orientation which leads the increase in  $k$  values. Kamruzzaman (2002) reported the same type results.

#### 5.3.2 Effect of Curing Time on Permeability Characteristics

Figures 5.30(a) and 5.30(b) illustrate the typical variation of  $k$  values with curing time for cement treated and lime treated clays respectively. It can be seen from Fig. 5.30 that at particular vertical effective stress coefficient of permeability decreases with increasing curing time. Fig. 5.30 also shows that at the same vertical effective stress and curing time coefficient of permeability for lime treated clay is higher than that of cement treated clay. Kauschinger et al. (1992) and Chew et al. (2004) reported that the same consistent of results for the effect of cement and curing time on permeability of treated clays. This is most probably due to

impervious hardened cement hydrates with time, which prevent the movement of the pore water in the enclosed matrix.

### 5.3.3 Effect of Clay Type on Permeability Characteristics

The coefficient of permeability of treated clay is also affected by the soil-type. Effect of clay-type effect on coefficient of permeability ( $k$ ) values is shown in Figs. 5.31(a) and 5.31(b) for cement treated and lime treated clays respectively. Fig. 5.31 shows that  $k$  values result due to the consolidation effect imposed on the treated soil mass depend on plasticity of soil (type of clay). It can also be seen from Fig. 5.31, higher the plasticity index, the lower is the value of  $k$ . The non-linear variation of  $k$  is nearly parallel for each type of clay. The permeability is the function of void ratio and greatly influenced nearly against consolidation pressure, 100 kPa. It can also be seen that for all the clay at a particular vertical effective pressure  $k$  is higher for the lime treated clay than for cement treated clay. Due to treatment considering clay-type,  $k$  increased for lime content are more than that of cement content. It is also noted that the coefficient of permeability for untreated clays, which is much smaller than that of treated clay samples. It can be inferred that physicochemical changes depend on illite and kaolinite mineral in the clays which leads the  $k$  values (including other changes in the coefficient of permeability characteristics). The physicochemical changes have been confirmed in the previous chapter of this study.

### 5.3.4 Effect of Mixing Clay-Water Content on Permeability Characteristics

The effect of mixing water content on  $k$ - $\log \sigma_v'$  relationship is shown in Figs. 5.32(a) and 5.32(b) for cement treated and lime treated clays respectively. At the same mixing water content,  $k$  for lime treated clay is higher than for cement treated clay. It is evident from Fig. 5.32 that the higher mixing clay-water content, the higher the values of void ratio (pore size) and permeability. The short-term rise in permeability can be explained by double layer analysis. Because of the addition of  $\text{Ca}^{2+}$  ions from the cement, there is an increase in the concentration of cations and an increase in the valence within the soil matrix, which are confirmed from chemical properties test for cement treated clays in this research. An increase in the concentration and valence decreases the double layer, resulting in a decrease in repulsion and causing flocculation of the clay particles. The flocculated particles with large pore size resulted in an increase of permeability. The longer-term drop in permeability is consistent with the decrease in pore size as CASH and CSH are deposited onto clustered clay particles. This phenomenon would be consistent with treated clay that has rather large inter-cluster voids ( $\leq 3 \mu\text{m}$ ), which are enclosed by layers of cementations products (CASH and CSH) with much smaller entrance pore diameters by intra-cluster voids ( $\leq 2 \mu\text{m}$ ). In such instances, the permeability would be controlled by the pore diameter rather than the intra-cluster void diameter. This is consistent with the notion of void infilling postulated above, but it would also require the infilling be limited to surfaces of the clusters, with the interior of the

clusters remaining largely unfilled. As a pozzolanic reaction occurs with time, cementitious products gradually fill the intra-cluster void and strengthen the contacts between soil particles, thereby rendering the soil less permeable. The production of cementitious products for treated clays is confirmed from mineralogy and SEM images test in this research. Kamruzzaman (2002) and Chew et al. (2004) reported that the same consistent of results.

### 5.3.5 Permeability and Void Ratio Relations of Cement Treated and Lime Treated Clays

Figs. 5.33(a) and 5.33(b) show that reasonable relationships between void ratio and permeability for cement treated and lime treated clays respectively at different clay-water/admixture ratio and mixing water content.

As shown in Fig. 5.28(a), the effect of clay-water/cement ( $wc/c$ ) ratio of 7.5 at different water content, coefficient of permeability ( $k$ ) can be correlated with void ratio ( $e$ ) for the cement treated clays ( $PI = 13$  to  $47\%$ ) studied in this research by the following relations:

$$e = a \ln(k) + b \quad (5.3)$$

where,  $a = 0.4$  to  $0.5$  and  $b = 2$  to  $3$  for mixing water contents varying from  $120\%$  to  $250\%$  at  $wc/c$  ratio of  $7.5$  for cement treated clays.

Similarly, for lime treated clay the effect of clay-water/lime ( $wc/l$ ) ratio of  $7.5$  and  $15$  at different water content ( $120\%$  and  $150\%$ ), coefficient of permeability ( $k$ ) can be correlated with void ratio ( $e$ ) for the lime treated clays ( $PI = 13$  to  $47\%$ ) studied in this research by the equation 5.3, where  $a = 0.5$  to  $0.6$  and  $b = 2$  to  $2.25$  for mixing water contents varying from  $120\%$  to  $150\%$  and at  $wc/l$  ratio varying from  $7.5$  to  $15$ . The regression equations for treated clay appear to be independent of the curing time and cement content, being almost entirely dependent on the void ratio and permeability. Chew et al. (2004) reported that the relationship ( $\log e - \log k$ ) as  $e = 0.26 \ln(k) + 6.86$  for cement treated Singapore clay with mixing water content  $120\%$  at  $wc/c$  ratio varying from  $4$  to  $6$ .

## 5.4 Stress-Strain, Strength and Stiffness Characteristics from UC Test

The stress-strain, strength and stiffness characteristics have been studied from unconfined compression (UC) test of cement and lime treated clay samples containing different plasticity.

### 5.4.1 Stress-Strain Behaviour for Cement Treated and Lime Treated Clays

Typical stress-strain behaviour of cement and lime treated samples at curing time  $4$  and  $12$  weeks have been obtained from unconfined compression tests as shown in Figs. 5.34 and 5.35 respectively for C1 clay.

Shear types of failures were observed. The stress-strain curves shown that the samples exhibit a strength that reaches a peak and then reduces gradually as straining continues. In general,

stress-strain curves of the treated samples were found to increase abruptly to peak values, then suddenly decreased to low residual values at low clay-water/cement ratio and long curing time. From the aspect of stress-strain relationships, the overall behaviour was categorized into brittle, quasi-brittle and ductile. Comparatively, brittle, quasi-brittle and ductile types for the cement treated clays, while quasi-brittle and ductile types for the lime treated clays have been found. The similar stress-strain behaviour of all stabilized clays having the same clay-water/admixture ratio have been observed. The unconfined compressive strength of cement and lime treated clays are listed in Table 5.5. Higher strain, low strength and mild peak were found to be associated with ductile behaviour for samples of higher clay-water/admixture ratio, whereas, lower strain, higher strength and sharp peak exhibited brittle behaviour for samples of lower clay-water/admixture ratio. Chew et al. (2004), Miura et al. (2001) and Balasubramaniam et al (1999) also reported similar stress-strain behaviour for treated clays.

#### 5.4.2 Strength Characteristics for Cement Treated and Lime Treated Clays

The strength is defined as the peak stress gained at which the sample failed, known as unconfined compressive strength and simply abbreviated as  $q_u$ . The strength has been studied in light of some previous techniques.

##### 5.4.2.1 Strength Activeness

Fig. 5.36 illustrates the effect of admixture content and curing age on unconfined compressive strength of cement and lime treated C3 clay. As can be seen, unconfined compressive strength increases with the increase in admixture content (i.e. decrease in water/admixture ratio) and increasing curing time. Based on the observation in Fig. 5.36, the unconfined compressive strength and admixture content relationship can be divided into 3 zones: Inactive Zone, Active Zone and Inert Zone. The cement content up to 4% shows only very low marginal improvement of unconfined compressive strength even at 2 years of curing, and is termed as inactive zone. It seems to suggest that a certain percentage of cement (say more than 4%) is required to complete the hydration as well as pozzolanic reaction between cement particles and clay particles. The end result of the complete cementation is to increase the shear strength and this zone is termed as active zone. The upper limit of this zone varies from about 34% to 38% of admixture content. In this zone, significant improvement of strength is observed with increasing admixture content and longer curing time. The rapid gain in strength is attributable to the fact that the pozzolanic reactions permit the efficient diffusion of available  $Ca^{2+}$  ions within the treated clay matrix. At this zone, the rate of hydration reaction is very high and thus, the bridging (cementation) effect is very significant and efficient. Hence, the increased amount of cementitious reaction products CSH (calcium silicate hydrate) and CASH (calcium aluminum silicate hydrate) caused a sharp increase in shear strength. It has been confirmed in X-ray diffraction test in this study.



Beyond the admixture content of 38%, i.e. beyond the active zone, the rate of increase of strength reduces and seems to be asymptotic. Such region is referred here as inert zone. The possible reason for such zone lies on that, the reactions are still going on but greater difficulty for calcium ions to diffuse within the treated clay matrix such that no further improvement of strength is observed. The greater difficulty arises due to the exhaustion of admixture content, which leads to the imbalance proportion of calcium ions and soil silica/alumina. This is because of the completion of cementitious reaction (pozzolanic reaction) due to the exhaustion of cement. It is possible that the reactions are going on but the calcium ion solutes diffuse very slowly within the treated clay matrix such that no further improvement of strength is observed. The conclusion has also been supported by Locat et al. (1990) and Kamruzzaman et al. (2004) for lime treated and cement treated clays, respectively.

Similarly, the effects of curing time on unconfined compression strength have been in Fig. 5.37 of cement and lime treated C1 clay. The unconfined compression strengths of cement and lime treated clays are listed in Table 5.5. Comparatively, cement treated clays are gained higher strength than that of lime treated clays, For a certain clay-water/ admixture (wc/c and wc/l) ratio, the development of strength with curing time can be sub-divided into active, quasi-active and inert zones (Fig. 5.37). Fig. 5.37 shows that earlier periods of curing are more active than that of the later. During the first to fourth weeks of curing, the development of strength is very rapid and dominant. Thus, for the parameter of curing time, one to twenty four weeks can be considered as the most effective and active zone in terms of hardening effect. Beyond the twenty four weeks, though the hardening potential does not enhance much, moderate improvement can still be noticed generally. The improvement becomes almost stagnant and latent after about fifty two weeks, termed as quasi-active zone. Beyond this range, the hardening influence decreases and does not produce great potentiality for improvement and can be termed as inert zone. The zone of 24 to 52 weeks curing period can be set as a boundary zone that makes a demarcation between the active zone and the inert zone for types of clays. Kamaluddin (1995) reported such a demarcation boundary zone for Bangkok clay.

#### 5.4.2.2 Strength Development Index (SDI)

The strength development indices for cement and lime treated C2 clay are presented in Figs. 5.38 and 5.39 with respect to admixture content and curing time respectively. These indices render a clear understanding about the degree of relative strength improvement that resulted due to cement /lime treatment with variables such as cement content/lime content and curing time. The strength increase of specimens with 4% admixture content is insignificant. The degree of relative strength gained for C1 clay has been found to be higher than those of C2 and C3 clay. The degree of relative strength gained for cement treated clays are higher than those of lime treated clays. Kamaluddin (1995), Rajbongshi (1997) and Hasan (2002) also

reported significant increase in strength development index with admixture content and curing time.

#### 5.4.2.3 Normalized Strength

Normalization techniques have been attempted for cement and lime treated C3 clays. A typical normalized behaviours are shown in Figs. 5.40 and 5.41 with respect to admixture content and curing time respectively. The reason for choosing the strengths for highest admixture content (60%) and highest curing time (104 weeks) lies on the fact that all samples were found to attain an ultimate and steady state at this stage, which produced a unique and stable  $q_u$  value for each clay samples. These parameters are independent of clay-water/admixture ( $w_c/c$  and  $w_c/l$ ) ratios and curing times in the sense that it produces similar effect for all values. The normalized behaviour of the samples exhibits to overall narrow band with more closed values ranging from low and high levels bounded by two polynomial curves of third order. Such normalization can be useful for finding the strength for a range of the treated clay once the ultimate strength acquired at longer curing periods. The narrowness for band curves of lime treated clays are higher than those of cement treated clays. The nature of normalized curves for Fig. 5.40 is totally different than those of Fig. 5.41. Kamaluddin (1995) also found similar normalized behaviour for Bangkok clay.

#### 5.4.2.4 Effect of Plasticity of Clay on Unconfined Compressive Strength

A summary of the unconfined compressive strength of the three clays has already been presented in Table 5.5. The effects of plasticity index on unconfined compression strength are presented in Fig. 5.42 at different clay-water/admixture ratio for cement and lime treated clays. At a particular clay-water/admixture ratio, unconfined compressive strength, in general, is increased with increasing plasticity. The effect of plasticity index on unconfined compression strength for different curing time is presented in Fig. 5.43. It can be seen from Fig. 5.43 that at a particular curing time unconfined compressive strength, in general, is increased with increasing plasticity. At a particular curing time, strength is increased with increasing plasticity. The effect of plasticity index on unconfined compression strength for different mixing water content is presented in Fig. 5.44 and found that at a particular mixing water content, unconfined compressive strength is also increased with increasing plasticity. It has been found that cement treated clays gained higher strength than those of lime treated clays. In all cases, C1 clay of highest plasticity achieved highest strength. High plastic clay has high sensitivity, high water holding capacity and more clay cluster hardness capacity than those of other clays. For this, the high plastic clay has been achieved more strength than other clays for cement and lime treatment at high water content. Ahnberg, et al. (1995) and Taki and Yang (1991) also found that the similar difference in strength for different types of soil with different plasticity index due to cement and lime stabilization. For the improvement of soft clay at a high water content by cement and lime admixtures, it is concluded that high

plastic (C1) clay undergoes better improvement than low plastic (C3) clay but low plastic clay undergoes better improvement than medium plastic (C2) clay. This is because as possibly, the chemical properties response such as pH value, electrical conductivity, exchangeable cations and finally cementitious products for C2 clay (PI = 22%) have lowest values than those of C1 clay (PI = 47%) and C3 clay (PI = 13%), which have been found in this study. Another possible cause, according to the criteria of pH value determination for the base soil, C1 clay and C3 clay are alkaline in nature and C2 clay is acidic in nature, which have exchangeable  $H^+$  ion. Thus, it may be called that C2 clays have a large reserve of potential acidity or buffering capacity. As buffering capacity was defined as the capacity of the soil to release exchangeable  $H^+$  ion into the soil solution to restore the equilibrium pH and due to which there is no soil reaction with cement until the reserve  $H^+$  ion is exhausted. And it is also added other causes.

It has been found that the amount of mixing water and type of clay have great role on the development of strength. The strength is increased with increasing curing time and admixture content (lowering  $w/c$  and  $w/l$  ratio). The test results show that the engineering behaviour of stabilized clays are dependent upon the clay-water/admixture ratio ( $w/c$  and  $w/l$ ) and fabric (the structure of clays). The role of  $w/c$  and  $w/l$  are that the lower the  $w/c$  and  $w/l$ , the greater the yield stress, resulting in enhancement of the yield surface, which means that the failure strain gets decreased; hence, the strength increases (Figs. 5.34 and 5.35). However, the fabric and clay-water content govern the stress-strain behaviour. The higher water content, the greater spacing between clusters; this leads to a decrease in ultimate strength (see Fig. 5.44). The comparative study between cement and lime stabilization, it has been found that cement stabilization are more effective than that of lime stabilization. The lime stabilization is not effective at very high water contents (i.e., binding properties of lime are failed at mixing water 200% and 250%). Ahmed (1984), Serajuddin and Azmal (1991), Serajuddin (1992), Siddique and Rajbongshi (2002), Hasan (2002), Siddique and Hossain (2003), Ansary et al. (2003) and Toyeb (2006) reported that the similar effects of cement and lime content and its curing time on strength characteristics for different regional and coastal soils of Bangladesh.

#### 5.4.2.5 Strength Relationship Based on Yield and Ultimate Conditions

The magnitudes of the yield strength,  $\sigma_y'$  (found from consolidation test at confined condition) and unconfined compressive strength,  $q_u$  (found from compression test at unconfined condition) depend on the degree of cementation (bond strength), it appears logical to relate these two parameters, it was reported by Horpibulsuk (2002). Depending on this logic, Figure 5.45 represents the relationship between  $\sigma_y'$  and  $q_u$ , which is generated based on test results of cement admixed clays studied (C1, C2 and C3 clays). In this figure, the test results are generalized on four way depending on initial mixing water ( $w_i$ ) contents (120%, 150%, 200% and 250%) with mixed tests data for three types of clay at  $w/c$  ratio of 7.5, 10 and 15 and curing time of 4 weeks. The equations for the relationship between  $\sigma_y'$  and  $q_u$ , are as follows:

$$\sigma_y' = 2.56 q_u \quad \text{for } wc/c = 7.5 \quad (5.4a)$$

$$\sigma_y' = 2.07 q_u \quad \text{for } wc/c = 10 \text{ and} \quad (5.4b)$$

$$\sigma_y' = 1.34 q_u \quad \text{for } wc/c = 15 \quad (5.4c)$$

with coefficient of correlations of 0.97, 0.99 and 0.94 respectively.

Horpibulsuk (2002) found that the relationship between  $\sigma_y'$  and  $q_u$ , which was  $\sigma_y' = 2.20 q_u$ , for cement admixed clays, while Takahashi and Kitazume (2004) also found that the same relation, which was  $\sigma_y' = (1.27 \text{ to } 2.55) q_u$ . Miura et al. (2001) have recommended that this relationship is preferable to be determined generalized compression line (GCL) by the method proposed by Sridraran et al. (1991).

#### 5.4.2.6 Strength Prediction Based on Clay-water/Cement Ratio's Concept for Cement Treated Clays

Strength prediction of cement stabilized clays have been discussed based on the test results of C1, C2 and C3 clays studied. The predication referred to the clay-water content/cement ratio's concept was proposed by Horpibulsuk et al., (2000) as follows: "..... for given clay-cement mixtures, the strength at any curing time depends on only one factor clay-water content/cement ratio,  $wc/c$ ". The observed relationship between unconfined compressive strength after a certain period of curing has been expressed by a formula having the following equation:

$$q_u = \frac{A}{B^{(wc/c)}} \quad (5.5)$$

where,  $q_u$  is the unconfined compressive strength of cement stabilized clay at a stated age,  $wc/c$  is the clay-water content/cement ratio, A and B are constant depending on the characteristic of clay, type of cement and curing time.

Fig. 5.46 shows a typical strength prediction of cement stabilized C1 clay, which agrees well with this proposed method. The coefficients of correlation were found to be higher than 0.97 for all clays. The B-value is 1.24 for all clays at all curing time. But the A-values are different for curing time, which are found as follows:

Curing Time (week)	A- value		
	C1 clay	C2 clay	C3 clay
1	1241	943	1054
4	1562	1211	1354
12	1771	1395	1557
52	2952	2211	2492

While, Horpibulsuk et al., (2000) reviewed the results for cement treated Bangkok clay that the A-values were 969, 1130 and 1739 kPa for 7, 14 and 28 day-curing time, respectively and the B-value was 1.24 ( $R^2 = 0.99$ ). From above prediction, the B-value can be taken as 1.24 for the all cases of (C1, C2 and C3) clays studied but the A-values are different. For every curing time, the A-values of stabilized clays for C1 clay are highest. Among the clays presented here, such the C1 clay provide the highest strength at the same conditions of curing time, clay-water content and cement content. Since B-value is identical for all clays, the same strength ratio equation of cement stabilized clays at a particular curing time have been obtained in terms of clay water content/cement ratio as follows:

$$\left( \frac{q_{(wc/c)_1}}{q_{(wc/c)_2}} \right) = 1.24 \{ (wc/c)_2 - (wc/c)_1 \} \quad (5.6)$$

where  $q_{(wc/c)_1}$  is the strength to be estimated at clay water content/cement ratio of  $(wc/c)_1$  and  $q_{(wc/c)_2}$  is the strength value at clay water content/cement ratio of  $(wc/c)_2$ . From this prediction, it reveals that the  $wc/c$  does not play any role on the strength development with time. As a result, the strength normalization of stabilized clays as shown in Fig. 5.47 by the 28 day-strength, (i.e., 4 week-strength) can be performed by the liner regression analysis in terms of curing time only as follows:

$$\frac{q_D}{q_{28}} = a + b \ln D \quad (5.7)$$

where,  $q_D$  is the strength after D days of curing,  $q_{28}$  is the 28 day-strength, D is the curing time, a and b are constant depending upon the type of clay. It is found here that  $a = -0.51$  and  $b = 1.07$  for the clays studied. While, the a and b for inland clays have investigated by Nagaraj et al. (1996) as -0.18 and 0.46, respectively.

The interrelationship among strength, curing time and clay water content/cement ratio,  $wc/c$  for predicting strength development of generalized cement stabilized clays studied can be expressed by combination of equation nos. (5.6) and (5.7) as follows:

$$\left( \frac{q_{(wc/c)_1, D}}{q_{(wc/c)_2, 28}} \right) = 1.24 \{ (wc/c)_{28} - (wc/c)_1 \} (-0.513 + 1.07 \ln D) \quad (5.8)$$

where  $q_{(wc/c)_1, D}$  is the strength of cement admixed clay to be estimated at clay-water /cement ratio of  $(wc/c)_1$  after D days of curing and  $q_{(wc/c)_2, 28}$  is the strength of cement admixed clay at clay-water/cement ratio of  $(wc/c)$  after 28 days of curing. While, Horpibulsuk et al. (2000) found that following relationship for Ariake clay:

$$\left( \frac{q_{(wc/c).D}}{q_{(wc/c).28}} \right) = 1.24 \left\{ \left( \frac{wc}{c} \right) 28^{-\left( \frac{wc}{c} \right) \cdot D} \right\} (0.116 + 0.2471 \ln D)$$

### 5.4.3 Failure Strain Behaviour for Cement Treated and Lime Treated Clays

The failure strain in unconfined compression test has been defined as the strain at peak axial stress and abbreviated as  $\epsilon_f$ . The treated samples with ductile behaviour have higher failure strain and with brittle behaviour have lower failure strain.

#### 5.4.3.1 Effect of Mixing Ratio, Curing and Clay Type on Axial Strain at Failure

Axial strain at failure reduces significantly as the admixture (cement and lime) content increases. Within 4 weeks of the curing period, the failure strains reduce and lie between 2.68% to 1.52%, 3.42% to 2.30% and 3.26% to 2.12% for samples of C1, C2 and C3 clays respectively having cement contents for 4% to 60% (average  $\epsilon_f$  for base clays = 3.67%, 3.65% and 3.83% for C1 clay, C2 clay and C3 clay respectively). For longer periods beyond 4 weeks, the failure strains of treated samples reduce further, lie between 2.91% to 1.10% for all values of cement content. Figs. 5.48(a) and 5.48(b) show the typical relationship between failure strain and clay-water/ admixture ratio for cement and lime treated C1 clays respectively with mixing water content of 120%. Failure strain increases with increasing admixture ratio (or decrease in admixture content). Fig. 5.48 also shows that failure strain for lime treated clays are higher than those of cement treated clays at same mixing ratio.

The effect of curing time on failure strain for cement and lime treated clays have been presented in Fig. 5.49 for both cement and lime treated clays. It can be seen from Fig. 5.49 that failure strain reduces considerably with curing time. It has been also been found that at a particular curing time failure strain increases with decreasing plasticity index of clays. Effect of clay type on axial strain at failure is shown in Fig. 5.50. It can be seen from Fig. 5.50 that at a particular clay water admixture ratio failure strain increases with the decreasing plasticity index of clays.

#### 5.4.3.2 Failure Strain Prediction for Cement Treated Clays

Figs. 5.51 and 5.52 present the relation of  $\epsilon_f$  and  $q_u$  in an arithmetic plot in terms of  $wc/c$  ratio and curing time for cement treated C2 (PI = 22%) and C3 (PI = 13%) clay, respectively at mixing water content of 120%. Such plots are meaningful to delineate the ductile and brittle behaviour of the samples. The relationship has produced a definite trend of reduction of failure strain with incremental values of cement content and curing time. At higher values of curing time, the failure strains are smaller and are with more scatters, whereas samples with low strength produce higher values of  $\epsilon_f$  with constraint in a narrow band. Ductile behaviour is associated with low strength and higher failure strain. On the contrary, higher strength and low failure strain correspond to brittle behaviour. Generally, higher cement content (lower

wc/c ratio) and curing time are the main parameters to cause the treated mass brittle. In Figs. 5.51 and 5.52, the brittle characteristics have been seen at relatively higher values of  $q_u$ , where samples cluster along the best-fit line. On the other hand, ductile behaviour can be observed at the region of relatively lower values of  $q_u$  where samples show comparatively less wider scatter. The best-fit line shows a coefficient of correlation greater than 0.90. The relations  $\epsilon_f$  (in mm/mm) and  $q_u$  (in kPa) of the plot in terms of curing time of cement treated clays studied are linear equations which can be expressed as follow:

$$\epsilon_f = 2.34 - 7.01 \times q_u / 10^4 \quad \text{for C1 clay} \quad (5.9a)$$

$$\epsilon_f = 2.83 - 7.60 \times q_u / 10^4 \quad \text{for C2 clay} \quad (5.9b)$$

$$\epsilon_f = 3.00 - 8.04 \times q_u / 10^4 \quad \text{for C3 clay} \quad (5.9c)$$

The mathematical relations show that C1 clay has achieved lower failure strain than that of C2 clay and C3 clay. While, Kamaluddin (1995) reported the relationship ( $\epsilon_f$ ,  $q_u$ ) for cemented Bangkok clay at low mixing water content as  $\epsilon_f = 3.3 - 19 \times q_u / 10^4$ .

#### 5.4.4 Stiffness Characteristics for Cement Treated and Lime Treated Clays

The stress-strain behaviour of unconfined compression test for soils is generally non-linear. For this, modulus of elasticity (stiffness) is classified two types, namely initial (stiffness) tangent modulus and secant (stiffness) modulus. Initial stiffness is defined as the slope of tangent at initial starting point of non-linear stress-strain curve and simply abbreviated as  $E_i$ . Secant stiffness is defined as the slope of straight line passing through the cut point of half of the peak stress strength and the origin of non-linear stress-strain curve and simply abbreviated as  $E_{50}$ .

##### 5.4.4.1 Effect of Mixing Ratio, Curing Time and Clay Type on Initial Stiffness

The modulus of elasticity (stiffness) was found to be a function of cement content (c) and curing time. Generally, lower cement content (higher wc/c ratio) and lower curing time generate correspond to the smaller values of the modulus (stiffness). Figs. 5.53(a) and 5.53(b) show the relationship between initial stiffness and clay-water/ admixture ratio for cement and lime treated C1 clays respectively at mixing water content of 120% used for clay slurries. It can be seen from Fig. 5.53 that initial stiffness increases with decreasing admixture ratio or increasing admixture content. Fig. 5.53 also shows that initial stiffness for cement treated clays are higher than those of lime treated clays at same mixing water ratio.

The effect of curing time on initial stiffness for cement and lime treated clays is presented in Fig. 5.54. A sharp increase of the initial modulus has been observed with increasing curing time for cement and lime treated clays. Fig. 5.54 also shows the effect of clay type on initial stiffness. It can be seen that, at a particular curing time,  $E_i$ , in general, increases with increasing plasticity. Fig. 5.55 shows the effect of initial stiffness on wc/admixture ratio. It

can be seen from Fig. 5.55 that initial stiffness decreases with the increasing wc/admixture ratio (i.e. decreasing admixture content). Fig. 5.55 also shows the effect of clay type on initial stiffness. It can be seen that, at a particular wc/admixture ratio,  $E_i$  in general, increases with increasing plasticity. The relative initial stiffness gained for C1 clay is higher than those of C2 and C3 clay. These samples with lower mixing ratio exhibit brittle behaviour during shearing. On the other hand, samples with higher mixing ratio (i.e., lower cement / lime content) are associated with lower initial stiffness and lower  $q_u$  value, exhibits ductile behaviour during shearing. Bergado et al. (2003) and Porbaha et al. (2000) found that the similar behaviour for stiffness of treated clays.

#### 5.4.4.2 Initial Stiffness Prediction for Cement Treated Clays

Figs. 5.56 and 5.57 present the relationship between initial stiffness ( $E_i$ ) and  $q_u$  in an arithmetic plot in terms of wc/c ratio and curing time respectively for cement treated C2 (PI = 22%) and C3 (PI = 13%) clay at mixing water content of 120%. Data points of these relations lie closely on a straight narrow band in such a way that the relationship between  $E_i$  and  $q_u$  can be approximated to linearity. The best-fit line shows a coefficient of correlation greater than 0.98. The predicted relations in between  $E_i$  (in MPa) and  $q_u$  (in kPa) in the arithmetic plot in terms of curing time of cement treated clays studied can be expressed by the following equations:

$$E_i = 3.02 \times (q_u^{1.5})/10^3 \quad \text{for C1 clay} \quad (5.10a)$$

$$E_i = 3.35 \times (q_u^{1.5})/10^3 \quad \text{for C2 clay} \quad (5.10b)$$

$$E_i = 3.13 \times (q_u^{1.5})/10^3 \quad \text{for C3 clay} \quad (5.10c)$$

Kamaluddin (1995) reported that the relation for cement treated Bangkok clay at low mixing water content as  $E_i = 6.2 \times (q_u^{1.5})/10^3$ .

#### 5.4.4.3 Effect of Mixing Ratio, Curing Time and Clay Type on Secant Stiffness

For the soil possessing elasto-plastic behaviour with a dominating plastic component, the incremental modulus changes continuously with strain. In that case, the initial (stiffness) tangent modulus does not represent the elastic modulus of the curve and instead of that, the secant (stiffness) modulus becomes more representative and useful than the initial tangent modulus. Thus, it is convenient to use the secant stiffness ( $E_{50}$ ) in such cases. The effect of clay-water/admixture ratio on secant modulus is illustrated in Figs. 5.58(a) and 5.58(b) for cement and lime treated C1 clays respectively. Fig. 5.58 shows that secant stiffness increases with decreasing admixture ratio. It is also evident from Fig. 5.58 that secant stiffness for cement treated clays are higher than those of lime treated clays at same mixing ratio.

The effect of curing time on secant stiffness for cement and lime treated clays is presented in Fig. 5.59. A sharp increase in secant stiffness has been observed with increasing curing time.



Fig. 5.59 also shows the effect of clay type on secant stiffness. It can be seen at a particular curing time there is a trend of increase in secant stiffness with increasing plasticity index. Fig. 5.60 shows the effect of  $w_c$ /admixture ratio on secant stiffness. It can be seen from Fig. 5.60 that secant stiffness decreases with the increasing  $w_c$ /admixture ratio (i.e. decreasing admixture content). Fig. 5.60 also shows the effect of clay type on secant stiffness. It can be seen that, at a particular  $w_c$ /admixture ratio, secant stiffness, in general, increases with increasing plasticity.

High plastic clay has high sensitivity, high water holding capacity and more clay cluster hardness capacity than those of other clays. For this, the high plastic clay has been achieved more stiffness than other clays for cement and lime treatment at high water content. Ahnberg, et al. (1995) and Taki and Yang (1991) also found that the similar different stiffness for different types of soil with different plasticity index from cement and lime stabilization.

#### 5.4.4.4 Secant Stiffness Prediction of Cement Treated Clays

Figs. 5.61 and 5.62 present typical relationships between secant elastic modulus,  $E_{50}$  and  $q_u$  in an arithmetic plot in terms of  $w_c/c$  ratio and curing time respectively of cement treated C2 (PI = 22%) and C3 (PI = 13%) clay at mixing water content of 120%. Such a linear relationship can be useful for prediction of secant modulus. It is quite apparent that the data points lie closely on a straight narrow band that can be approximated to linearity. The best fit line shows a coefficient of correlation greater than 0.98. The predicted relations  $E_{50}$  (in MPa) and  $q_u$  (in kPa) in the arithmetic plot of cement treated clays studied are expressed by the following equations:

$$E_{50} = 2.72 \times (q_u^{1.5})/10^3 \quad \text{for C1 clay} \quad (5.11a)$$

$$E_{50} = 2.91 \times (q_u^{1.5})/10^3 \quad \text{for C2 clay} \quad (5.11b)$$

$$E_{50} = 2.78 \times (q_u^{1.5})/10^3 \quad \text{for C3 clay} \quad (5.11c)$$

Kamaluddin (1995) reported the relation ( $q_u$ ,  $E_{50}$ ) for cement treated Bangkok clay at low mixing water content as  $E_{50} = 5.8 \times (q_u^{1.5})/10^3$ .

#### 5.4.5 Failure Mode and Brittleness Characteristics for Cement Treated Clays

A shear type of failure was noticed generally in the case of treated samples. Angles of failure plane were found generally between 35° and 50° with the horizontal by investigations during tests. Cement treatment caused a transformation of the plastic clay into mainly brittle and quasi-brittle characteristics. The development of the brittle behaviour of the cement treated clay originates from the mixing period. It has been found that physicochemical, mineralogical and micro-structural tests that the hydration of cement creates a rather strong bond between various mineral substances and forms a matrix that efficiently encloses clay-clusters then on-bonded particles. The matrix develops a cellular structure by the enclosed clay-clusters and

the strength of the clay matrix depends entirely on the cellular structure. Since the matrix pins the particles, cement reduces plasticity on the one hand, and increases shear strength on the other. The brittleness on the treated clay develops due to formation of the cellular structure. Bergado et al. (2003), Porbaha et al. (2000) and Kamaluddin (1995) also observed that the similar behaviour for treated clays.

The results show that brittleness is more pronounced with low failure strains. The strains at peak failure strengths are observed to be 1.1% to 3.42% for all samples covering all  $w_c/c$  ratio and curing times as shown in Fig. 5.48. The degree of brittleness was found to be a function of clay-water/cement ( $w_c/c$ ) ratio, clay type, mixing water content and curing time. The higher the value of cement content (lower  $w_c/c$  ratio), the greater the degree of stiffness and brittleness of the treated clay. Low cemented samples such as up to 4% showed a ductile type of behaviour and their failure strains are comparatively higher than other treated samples.

Though the effect of curing time is similar to that of cement content, the results reveal that hardening effects rendered by curing have lesser influence than that of cement. Some samples of longer curing periods (i.e., 24, 52 and 104 weeks) exhibited extreme brittle behaviour bringing about sudden failure as shown in Fig. 5.36. The failure occurred of these samples by breaking into small pieces. A large number of samples had to be discarded due to sudden premature failure.

## **5.5 Stress-Strain Behaviour and Strength Parameters from Direct Shear Test**

### **5.5.1 Shear Stress and Shear Displacement Relations for Cement Treated Clays**

Figs. 5.63(a) and 5.63(b) show typical relationship between shearing stress and horizontal displacement from consolidated drained direct shear test at  $w_c/c$  ratio of 7.5, mixing water content 120% and curing time of 4 weeks. It has been found that cement treated clays have gained more shear strength and shear straining than that of base clays. Relatively, cement treated C1 clay has gained more shear strength and less shear straining than that of cement treated C2 and C3 clays. It can be seen from Fig. 5.63 that there are distinct peak points in stress-displacement curves and the curves for low normal stress condition located well below than those of high normal stress condition specimens. The shear stress-displacement curves show that the samples exhibit a shear strength that reaches a peak and then reduces gradually as shear displacement continues. Taha et al. (1998) also reported that the similar results from direct shear test.

### **5.5.2 Vertical and Horizontal Displacement Relations for Cement Treated Clays**

Figs. 5.64(a) and 5.64(b) show typical relationship between vertical and horizontal displacement for cement treated C1 and C3 clays respectively. For cement treated clays, vertical expansion (dilation) was observed at low normal stress and experienced vertical contractions or settlement throughout the shearing stage at higher normal stress. Vertical

settlements dominated for specimens at highest normal stress levels (200 kPa and 400 kPa). Settlement initially took place upon shearing, and then vertical expansion (dilation) dominated for treated specimens prevails at lowest normal stress level (100 kPa). It has been found that cement treated clays have gained lower vertical settlements than that of base clays. Relatively, cement treated C1 clay has gained lower vertical settlements than that of cement treated C2 and C3 clays at higher normal stress levels but cement treated C1 clay has gained higher vertical expansion (dilation) than that of cement treated C2 and C3 clays at same lower normal stress levels. These results are very important in geotechnical problems involving vertical shear such as in the case of pile foundations. Similar vertical and horizontal displacement relationship were also reported by Taha et al. (1998).

### 5.5.3 Effect of Clay Type, Cement and Curing on Shear Strength Parameters

Typical failure envelopes from direct shear tests are presented in Figs. 5.65(a) and 5.65(b) for the cement treated C1 and C3 clays respectively. A summary of effective shear strength parameters,  $c'$  and  $\phi'$  for cement treated clays is listed in Table 5.6. It has been found that the effective cohesion and friction angle of samples having higher cement (lower  $w_c/c$  ratio) are greater than that of samples contained lower cement (higher  $w_c/c$  ratio). This is possibly due to the effect of stiffness and more lubricating effect in cement treated condition that prevents soil slippage and frictional movement. The apparent cohesion of cement treated C1 clay was higher than those of cement treated C2 clay and C3 clay but the friction angle of cement treated C1 clay were lower than those of cement treated C2 clay and C3 clay.

The effect of clay-type, cement content and curing time on cohesion for treated clays is shown in Fig. 5.66. The cohesion of treated clays has been found to increase with increasing curing time because the stiffness and lubrication are increased due to hydration of cementation with time. Fig. 5.66 also shows that cohesion of treated clays increased with increasing cement content (or decreasing  $w_c/c$  ratio) due to more cementation. Fig. 5.66 also shows that at particular cement content and curing time effective cohesion, in general, increases with increasing plasticity index.

The effect of clay-type, cement content and curing time on friction angle for treated clays is shown in Fig. 5.67. The figure shows that at a particular curing time friction angle of treated clays increased with increasing cement content (or decreasing  $w_c/c$  ratio) due to more cementation. Fig. 5.67 also shows that friction angle of treated clays decreased with increasing curing time because the soil slippage and frictional movement are less prevented due to hydration of cementation with time. Fig. 5.67 also shows that at a particular cement content and curing time effective friction angle, in general, decreases with increasing plasticity index. Kamruzzaman et al. (2004) also reported similar effects of cement content and curing time on effective shear strength parameters ( $c'$  and  $\phi'$ ) for cement treated clays.

Similar behaviour for cohesion and friction of improved soil were investigated by Shibuya and Ozawa, (1992).

#### 5.5.4 Effect of Clay-water Content on Strength Parameters

The effect of clay-water content and curing time on cohesion for treated clays are shown in Fig. 5.68. It can be seen from Fig. 5.68 that at a particular curing time, the cohesion of treated clays is decreased with increasing clay-water content because the stiffness and non-lubrication are decreased due to hydration of cementation at high water content. The effect of clay-water content and curing time on friction angle for treated clays is shown in Fig. 5.69, which shows that at a particular curing time, the friction angle of treated clays is decreased with increasing clay-water content because the soil slippage and frictional movement are less prevented due to hydration of cementation at high water content. Similar result were reported by Radwan (1988).

#### 5.5.5 Relationship between Strength from Direct Shear and Unconfined Compression Tests for Cement Treated Clays

The relationship between the direct shear (DS) and unconfined compression (UC) test results for C1, C2 and C3 clays treated with 8% to 48% cement content and cured for 4 weeks is shown in Fig. 5.70. Although, there are some data points scattered, the plot demonstrates a general validity. From the regression analysis, the following relationships have been obtained:

$$c' = 99.86 - 0.103q_u + 0.003q_u^2, \text{ (} c' \text{ and } q_u \text{ in kPa)} \quad (5.12a)$$

$$\text{or } c' = 0.103 - 0.113q_u + 2.976q_u^2, \text{ (} c' \text{ and } q_u \text{ in kg/cm}^2\text{)} \quad (5.12b)$$

where  $c'$  is the effective cohesion, i.e., shear strength from a direct shear test for zero normal stress ( $\tau_{10}$ ) and  $q_u$  is the unconfined compressive strength for all specimens cured up to 4 weeks. It should be pointed out that the loading condition applied in these direct shear tests represents shallow soil-cement stabilization. In addition, the mode of simple shear is perhaps difficult to achieve in shear box tests on stiff soils. Similar relationship was proposed by Porbaha et al. (2000) as  $c'(\tau_{10}) = 0.53 + 0.37q_u - 0.0014q_u^2$ , where,  $c'$  and  $q_u$  in  $\text{kg/cm}^2$  for all specimens cured up to 4 weeks.

#### 5.6 Stress-Strain Characteristics for Cement Treated Clays from Unconsolidated Undrained Triaxial Compression Test

The stress-strain behaviour of cement treated samples cured for 4 weeks from unconsolidated undrained (UU) triaxial compression tests with confining pressure,  $\sigma_3 = 200$  kPa is shown in Figs. 5.71(a) and 5.71(b) for C1 and C3 clays respectively. While Figs. 5.72(a) and 5.72(b) show the stress-strain behaviour of cement treated samples cured for 12 weeks for C1 and C3 clays respectively.

From Figs. 5.71 and 5.72, it can be seen that, in general, the stress-strain curves of the treated samples were found to increase abruptly up to the peak deviator stress, then suddenly decreased to low residual values upon further straining. The overall behaviour of the treated samples can be categorized into brittle, quasi-brittle and ductile types. Brittle characteristics were observed for higher cement content (such as  $w/c$  ratio 7.5 and 10), rendering a comparatively lower value of  $\epsilon$  at  $q_{max}$  whereas ductile characteristics were observed for lower cement content ( $w/c$  ratio of 15 and 30). Ductile samples were observed to be associated with a mild peak whereas brittle samples were observed to be associated with a sharp peak. The samples with higher cement content and curing time were observed to possess brittle behaviour accompanied with low values of strains at  $q_{max}$ . The brittle samples always exhibited sharp peaks associated with abrupt falling characteristics. The residual strain of the brittle sample is much lower than that of the ductile sample. It reveals that the lower the  $w/c$ , the greater the enhancement of the cementation bond strength inducing higher undrained shear strength.

A comparison of undrained shear strength and strain at failure obtained from UU triaxial compression and unconfined compression tests is shown in Table 5.7. It has been found that undrained shear strengths obtained from UU triaxial compression test are average about 1.2 times higher than those obtained in UC test but failure strains for UU triaxial compression test are average increased to about 2 times than those obtained from unconfined compression tests.

### **5.7 Stress Path, Stress-Strain, Pore Pressure and Failure Envelopes Characteristics for Cement Treated Clays from CIU Triaxial Compression Tests**

The stress path, stress-strain and pore pressure characteristics have been studied from isotropically consolidated undrained (CIU) triaxial compression tests of cement treated clay samples. Failure envelopes of the cement treated clays have also been examined.

#### **5.7.1 Effective Stress Paths for Untreated Base and Cement Treated Clays**

##### **5.7.1.1 Effective Stress Paths for Untreated Samples**

The conventional undrained and drained tests with constant cell pressure were carried out on isotropically consolidated samples. Typical stress paths are shown in Fig. 5.73(a) and 5.73(b) for untreated C1 and C3 clays, respectively. The stress paths are straight line for drained tests and curve line for undrained tests and rise at a slope of 1:3 from the initial value of  $p'_0$  for each sample in the deviator stress ( $q$ ) versus mean effective pressure ( $p'$ ) plot. The failure envelop in the  $q$ - $p'$  plots, derived from maximum deviator stresses, is a straight line passing through the origin, with a slope  $M = 0.98, 0.91$  and  $0.94$  for C1, C2 and C3 clays, respectively. The undrained stress paths for the untreated clay samples (Fig. 5.73) are typical of normally consolidated clays and demonstrate a high degree of consistency indicating the

normalizable behaviour. The relevant stress points fall approximately on the same straight line passing through the origin. The maximum deviator stress condition is being referred to here as critical state line at which unlimited shear distortions occur without an increase in the shear stress or without change in the volumetric strains. Kamaluddin (1995) also found that the same natured stress paths for untreated Bangkok clay.

#### 5.7.1.2 Effects of Clay-water/Cement Ratio on Effective Stress Paths

Figures 5.74(a) and 5.74(b) present typical undrained effective stress paths for cement treated C1 and C3 clays, respectively at a different  $w_c/c$  ratio and cured for 4 weeks. Fig. 5.74 consists of stress paths of treated clays for  $p_o' = 200$  kPa. The clay-water/cement ratio used was 7.5, 10, 15 and 30 with mixing water content 120% for each clay. Fig. 5.74 shows that the stress paths evidently, belong to different category of states such as normally consolidated, lightly, moderately and heavily over-consolidated state. Effective stress paths for treated clays is similar to that of normally consolidated state for high  $w_c/c$  ratio of 30 (i.e., low cement content of 4%), lightly over-consolidated state for  $w_c/c$  ratio of 15 (i.e., cement content of 8%), moderately over-consolidated state for  $w_c/c$  ratio of 10 (i.e., cement content of 12%) and heavily over-consolidated state for  $w_c/c$  ratio of 7.5 (i.e., high cement content of 16%). The stress paths for heavily over-consolidated clays in which very small pore pressures were developed, propagate approximately at constant  $p'$ , i.e., parallel to  $q$ -axis. Such a behaviour is generally found from natural over-consolidated clays and this aspect strongly supports the elastic wall concept of the Cambridge stress-strain theories; the specimens remaining on elastic wall exhibits constant plastic volumetric strain. Kamaluddin (1995) also found similar stress paths for cement treated Bangkok clay.

The samples for  $w_c/c = 10$  and 7.5 (cement = 12% and 16%) behave to be on the dry side of the critical state and the stress paths are the constant- $p_o'$  at the onset of the test, then start to curve in a manner that indicates phase transformation into dilative nature. After approaching the Hvorslev strength envelope, they tend to seek the failure state, either moving on the Hvorslev envelope or failing with strain softening.

The stress path for untreated clay is also shown in Fig. 5.74. Now comparing the treated clays with untreated clay, evidently, cement treatment has caused severe alterations in the characteristics of the base clay. The degree of alteration is different for different samples depending on the amount of cement ( $w_c/c$  ratio). The varieties of the stress paths of samples with cement = 4% to 16% (i.e.,  $w_c/c = 30$  to 7.5) signify not only that the treatment renders enormous potential for the alteration of parameters, rather cement content is dominating function for the changes. The Gradual improvement process is revealed from the characteristic shapes of the stress paths. The stress path alter it's direction from decreasing  $p_o'$ -value with smaller undrained strength magnitude to increasing  $p_o'$ -value with higher undrained strength, i.e., the sample transform from normally consolidated to lightly over-

consolidated treated clays indicate less pore pressure generation which results in less rounded stress path with low plastic volumetric deformation of compressive or dilative nature depending on the value of the  $w/c$  ratio.

Three different failure criteria can be deemed for untreated clays. The relevant stress points fall on the same straight line passing through the origin. In this study, the maximum deviator stress line is considered as the failure line and will be referred to as the Critical State Line. The failure condition of the treated clay with low cement content and CSL of untreated clay have been found to be closely related. In general, the treated clays have been observed to fall from peak deviator stress in a constant- $p_o'$  route and finally lie close to the CSL of untreated clay.

### 5.7.1.3 Effects of Curing Time and Clay Type on Effective Stress Paths

Fig. 5.75 shows the typical stress paths of the treated specimens cured for 4 weeks and 12 weeks for C1 and C2 clays at  $w/c$  ratio of 10 and mixing water content of 120%. It can be seen from Fig. 5.75 that the samples behave like heavily over-consolidated clays; very small pore pressures are developed and the stress paths for the samples proceed along paths of increasing  $p'$ . The shapes of the stress paths for same values cement are similar; revealing the behaviour of over-consolidated characteristics; though they exhibit different undrained shear strength depending on the plasticity of soil. A comparison of the stress paths reveals the transformed behaviour quite clearly. Samples with 12% cement content ( $w/c$  ratio of 10 and mixing water content of 120%) have been metamorphosed from an over-consolidated state into a comparatively slight lower degree of over-consolidation.

Now the curing time effect for treated clays can be seen if we consider stress paths for 4 weeks curing compared with 12 weeks curing. This is due to the fact, as stated earlier, that higher curing time does improve the clay significantly; because sufficient hydration products of cement (which are main cementitious compounds formed) are needed to form the hardened skeleton matrix. During cement-clay interaction, the main cementitious hydration products are formed and the hydrated lime is deposited as a separate crystalline solid phase. These cement particles bind the adjacent soil grains together during hardening and form a hardened skeleton matrix, which encloses unaltered clay particles. The effects of cementitious compounds during curing time on treated clays have been confirmed in the X-ray diffraction analysis in this research.

The curing time 4 weeks, sample can be found to be well rounded which reflects the behaviour of low OCR sample (lightly over-consolidated clay), while the sample with 12 weeks shows the characteristics of slight higher over-consolidation. In the figures, for C1 clay, the effect of curing time is little more than that of C2 clay for same cement content, the increase in curing time has imparted an apparent increase of over-consolidation in the samples resulting in a less rounded stress path with low plastic volumetric change and less pore

pressure development. The increase of curing time is also produced in the sample a characteristic of higher ratio of over-consolidation, in which the stress paths rise almost vertically and parallel to the  $q$ -axis for the full range of deviator stress up to the peak, resulting in the generation of less pore pressure. It is noticeable, as reiterated earlier, that curing time is a secondary dominating factor to create a hardening effect on the clay than that of cement. Always a moderate or mild type of physicochemical changes has been noticed due to the elapse of time, which has also been confirmed from the results of chemical and physical properties obtained in this research.

#### 5.7.1.4 Effects of Mixing Water Content on Effective Stress Paths

The effect of mixing water content on effective stress paths can be seen for C1 clay from Fig. 5.76, where the stress paths for  $w_c/c$  ratio = 10, mixing water contents of 120%, 150%, 200% and 250% and curing time of 4 weeks have been shown. The stress paths can be seen to be well rounded which reflects the behaviour of medium OCR sample (moderately over-consolidated clay). For samples of C1 clay, the increase of water content up to 200% and 250% is also produced in the sample a characteristic of higher ratio of over-consolidation, in which the stress paths rise almost vertically and parallel to the  $q$ -axis for the full range of deviator stress up to the peak, resulting in the generation of less pore pressure. It is noticeable, that mixing water content is a secondary dominating factor to create a hardening effect on the clay than that of cement. Always a moderate type of physicochemical changes has been noticed due to the change in mixing water content.

#### 5.7.1.5 Effects of Pre-Shear Consolidation Pressure on Effective Stress Paths

Fig. 5.77 shows the effective stress paths plotted in terms of mean effective stress,  $p'$  in order to depict the effect of pre-shear effective consolidation pressure,  $p_o'$  on the effective stress paths on untreated and treated samples of C1 clay. The salient effect of cement is to change the stress-strain-strength characteristics of the soft clay from normally consolidated to over-consolidated behaviour. The degree of over-consolidation has been influenced by pre-shear consolidation pressure among other factors (such as cement content, curing time, clay type and mixing water content). For a comparative study of stress paths of the treated clays, reference can be drawn to the stress paths of the untreated clay, which belongs to the normally consolidated state. In Fig. 5.77, the samples (12% cement and 4 weeks curing having  $p_o' = 50, 100, 200$  and  $400$  kPa) imply low OCR behaviour (normally consolidated to over-consolidated), resulting in convex curves curving toward origin with decreasing  $p_o'$ -value and behaves similar to the samples belonging to the wet side under State Boundary Surface. The effect of  $p_o'$  can be discerned from the characteristics' curves of each sample and their gradual transformation behaviour from one extreme to other extreme of  $p_o'$ -value. The sample at  $p_o' = 200$  kPa shows well-rounded stress path with positive pore pressure generation that conforms more to a moderate over-consolidated state, whereas 50 kPa sample shows behaviour



indicating similarity to lightly over-consolidated state with stress path nearly parallel to  $q$ -axis. Stress path of the sample, having cement of 12%, mixing water content of 120% and cured for 4 weeks, showed higher over-consolidation behaviour at  $p_o' = 400$  kPa and higher; whereas the samples having  $p_o' = 100$  kPa show semi-rigid types of lightly over-consolidation. The paths end up with residual states lying close to the failure envelope of the untreated clays. Ghee et al. (2004) and Bergado et al. (2003) also reported similar types of stress paths evidently, belong to different category ranging from a low OCR value to a high OCR value depending on amount of cement content, curing period and pre-shear consolidation pressures.

In Figure 5.77, the samples with  $p_o' = 200$  and 400 kPa exhibit signs of transformation at the point where the path deviates from the constant- $p'$  line. At this point, the path encounters a large curvature and has been defined as the Point of Phase Transformation, where upon transformation begins to take place from one stage to another with further increase in shear stress. Until this point is reached, the effective pressure being developed during the shear. However, upon passage through the Point of Phase Transformation, the pore pressure begins to build up. The axial strain is small and recoverable until this point is reached, and much larger axial strain is produced for further increase in shear stress in excess of that at the said transformation Points and by linking these points, a locus as illustrated in Fig. 5.77 can be established. The transformation line thus developed is the demarcation that separates the initial elastic phase from the remaining phase where plastic component dominates. It is notable that for the sample with cement = 12% and curing = 4 weeks, the lower the over-consolidation ratio, the larger the stress ratio value at which the samples begin to exhibit phase transformation. A consistent picture of phase transformation emerges for these samples; the corresponding transformation points (P1 and P2) have been marked on the stress paths. A second order polynomial function was found to represent this locus. The phase transformation of treated clay occurred at lower levels than the critical state line for untreated clay.

Resulting from cement treatment, there are samples that correspond to the heavily over-consolidated state. The stress paths of the samples with low  $p_o'$  indicate that samples remaining on the dry side, first move on a constant- $p'$  line (corresponding to AB of inset diagram), then approach Hvorslev surface and tend to seek failure state either moving on the Hvorslev surface or moving parallel along tension failure line at 3 : 1 slope (BC) until they reach the failure envelope of the corresponding treated clay. After reaching the  $q_{max}$  level (at C), the stress path incurs strain softening process by falling in a line (CD) sub-parallel to  $q$ -axis. At this stage, the sample comes down with destructured state then end up at residual state after reaching close to the critical state line of the untreated clay.

### 5.7.1.6 Pertinent Features of Undrained Stress Path for Treated Clays

An elastic structural response gives rise to constant- $p'$  effective stress paths for a saturated specimen. The degree of curvature of the stress paths is dictated by the generation of pore pressure. Therefore, the degree of curvature of the effective stress path is a measure of the phase transformation of a specimen. In general, the treated samples sheared from the very low stress levels fails without significant transformation, and the tendency to dilate at stresses close to failure is manifested in the decrease in pore pressure. These samples behaviour in such a way that as if they belong to dry side. They initially mobilize stresses in a constant- $p'$  route and then keep on increasing  $p'$ -value and finally tend to transform with dilation at values of  $q$  close to the Hvorslev strength envelope. The increase of  $p'$  from this low stage develops and expands the initial elastic phase.

Fig. 5.78 shows that it is possible to convert the untreated clay like to normally consolidated behaviour (U) and treated clay like to over-consolidated behaviour (ABCDE). For treated clays, part of stress path (AB), initial small strain phase which is parallel to the  $q$ -axis with constant- $p'$  line then starts to curve in such a way that indicates abrupt change in pore pressure dissipation and parts of stress path (BC and CD) are large strain phase, which are changed curve pattern at point of contraflexure / transformation point due to pore pressure dissipation. It is important to emphasize that the concept of transformation behaviour has been used in a wider sense; the initial transformation point (B) refers to the stress point where the generation of pore pressure starts to be significant. An investigation in this study showed that the angle of contraflexure for transformation line of the treated clays varies slope between 1.80 to 1.07 : 1 and generally gets reduced when  $p_o'$  goes higher. The part (DE) represented strain softening, which is the extension after failure strength.

## 5.7.2 Stress-Strain Behaviour for Untreated and Cement Treated Clays

### 5.7.2.1 Deviator Stress-Axial Strain Relationships for Untreated Samples

A series of undrained triaxial compression tests was run on isotropically consolidated specimens of untreated clay. Each specimen of this series (three samples) was consolidated isotropically to different initial effective pre-shear consolidation pressures ( $p_o'$ ) of 50, 100, 200 and 400 kPa. Typical deviator stress versus axial strain curves for samples of C1 and C3 clays are shown in Figs. 5.79(a) and 5.79(b), respectively. The deviator stress increases sharply with increasing strain with a mild peak or without well-defined peaks as observed at failure. Generally, a slight strain softening beyond the peak was noticed. After a axial strain of about 8%, the  $q$ - $\epsilon_a$  relationships appear to be such that the deviator stress at any particular strain level is approximately proportional to pre-shear consolidation pressure. The overall nature of the curves seems to indicate that the samples are behaving as if they are normally consolidated to lightly overconsolidated. Such an over-consolidation can only arise from the secondary consolidation effect prior to undrained shear. It seems that in a laboratory study of

the undrained behaviour of soft clays, the pre-shear consolidation stress has a pronounced effect. The specimens which were consolidated to higher values of  $p_o'$  sustain higher values of peak deviator stress but the shapes of the  $q$ - $\epsilon_a$  curves are similar.

### 5.7.2.2 Effects of $wc/c$ Ratio on Deviator Stress-Axial strain Relationships

The effect of clay water/cement ( $wc/c$ ) ratio on  $q$ - $\epsilon_a$  relationship for treated samples of C1 clay is shown in Fig. 5.80 at  $wc/c$  ratio of 7.5, 10, 15 and 30. In these plots, the improvement of the sample of high  $wc/c$  ratio of 30 (i.e., low cement content of 4%) has been found to be much smaller peak deviator stress than for the samples of low  $wc/c$  ratio (i.e., high cement content) of 30 higher cement content and lie close to the untreated clay (Fig. 5.79). It can be seen from Fig. 5.80 that  $q$ - $\epsilon_a$  relationships are largely dependent on  $wc/c$  ratio. After reaching the peak deviator stress, all the  $q$ - $\epsilon_a$  relationships have been found to fall under varying rates depending on the parameter,  $wc/c$ , revealing that cement is the paramount factor that controls the post-treatment relationships of  $q$ - $\epsilon_a$  relationships. A general trend exists in Fig. 5.80 that the maximum deviator stress increases with decreasing clay-water/cement ratio (i.e., increasing value of cement content). It has also been found that generally the axial strain at the maximum deviator stress is reduced when  $wc/c$  ratio has been decreased (i.e., cement content has been increased). This is because these samples of low cement content acquire low hardening potential and their behaviour is more similar to untreated clay than to treated clay possessing higher content of hardening agent. On the other hand, the  $q$ - $\epsilon_a$  relationships for higher cement content, such as 12% and 16% ( $wc/c$  ratio = 10 and 7.5), are different than those of samples having low cement content and render greater strength and stiffness to the clays. From such response, a conclusion can thus be drawn pertaining to the definition of low and high cement content in terms of stiffness development benefits. All these behaviour of CIU tests support the UC and UU tests results, where a boundary was sought to define active and inert zone. From the above test results, it is revealed that the  $wc/c$  is the prime parameter influencing the engineering behaviour for cement-stabilized clay. Nagaraj et al. (1996), Horpibulsuk et al. (2000) and Miura et al. (2001) also reported similar behaviour for stress-strain of cement treated clays.

### 5.7.2.3 Effects of Curing Time and Clay-type on Stress-Strain Relationships

The effects of curing time and clay type on  $q$ - $\epsilon_a$  relationships can be seen from Fig. 5.81. It can be seen from Fig. 5.81 that the deviator stresses of 12 weeks samples increase sharply towards well-defined higher peak values followed by a large amount of strain softening, especially for the typical cases of  $wc/c$  ratio of 10 (cement content of 20% and mixing water of 200%). Similar behaviour was observed for  $wc/c$  ratio, 7.5 and 15 samples at 4 weeks and 12 weeks curing time. Another aspect pertains to the strain softening that incurs during shearing. The peak deviator stresses for samples of C1 are higher than those of C2 and C3

clays for both 4 and 12 weeks curing time. So, at a particular curing time, peak deviator stress increases with increasing plasticity index of the clays.

#### 5.7.2.4 Effects of Mixing Water Content on Stress-Strain Relationships

Typical effect of mixing water content on  $q$ - $\epsilon_a$  relationships for treated samples of C2 clay is shown in Fig. 5.82 at clay-water/cement ( $wc/c$ ) ratio of 10 and curing time of 4 weeks. Fig. 5.82 shows that at particular  $wc/c$  ratio here is a trend of increasing peak deviator stresses with the increase in mixing water content. This is because at a fixed  $wc/c$  ratio, increase in mixing water content leads to increase in the cement content. As a consequence, all samples having the same  $wc/c$  both made up at low and high clay-water contents exhibit identical deviator stress versus axial strain response. Miura et al. (2001) also found similar behaviour for stress-strain of treated clays.

#### 5.7.2.5 Effects of Pre-Shear Pressure on Stress-Strain Relationships

Typical effect of pre-shear effective consolidation pressure ( $p_o'$ ) on  $q$ - $\epsilon_a$  relationships for sample of C1 clay cured for 4 and 12 weeks with clay-water/cement ratio of 10 and mixing water content of 250%, is shown in Fig. 5.83. It can be seen from Fig. 5.83 that the deviator stresses of samples increase sharply towards well-defined peak values followed by a large amount of strain softening, especially for the cases of high pre-shear effective consolidation pressures of 400 kPa. The effects of pre-shear consolidation pressure on  $q$ - $\epsilon_a$  relationships for samples of C2 and C3 clay at 4 weeks curing time with clay-water/cement ratio, 10 and 15 with mixing water contents, 120%, 150%, 200% and 250% were also investigated. In general, it has been found that the samples consolidated to higher pre-shear consolidation pressure attain higher values of maximum deviator stress.

Typical effects of  $p_o'$  on  $q$ - $\epsilon_a$  relationships at large  $wc/c$  ratio have been presented in Figs. 5.84(a) and 5.84(b) for samples of C2 clay cured for 4 and 12 weeks, respectively. It can also be seen that similar to samples of low  $wc/c$  ratio (Fig. 5.83) the deviator stresses of samples increase sharply towards well-defined peak values followed by a large amount of strain softening, especially for the cases of high  $p_o'$  of 400 kPa. The characteristic shape of the  $q$ - $\epsilon_a$  curves is for the deviator stress to increase to a peak value, then strain-softens to a lower value of  $q$ . Thus pre-shear consolidated volumes are affected largely by the  $p_o'$ , with in turn affects the relationship of  $q$ - $\epsilon_a$ . On the other hand, the samples with lower  $p_o'$  of 50 to 100 kPa have very similar  $q$ - $\epsilon_a$  relationships. This is because the volume changes during consolidation to this range of stresses were very small, and therefore, the pre-shear void ratios are very close for these samples. It can also be seen from Fig. 5.84 that at a particular  $p_o'$ , peak deviator stress increases with the increase in curing time.

Here it may be mentioned that one-dimensional consolidation test results gave the apparent pre-consolidation pressure ( $\sigma_p'$ ) for samples cured for 4 weeks of about 350 to 500 kPa. Thus

for the case of  $p_o' < \sigma_p'$ , large change in void ratios occur, resulting into large deformation in the consolidated sample. Since the consolidated volumes are different, the  $q$ - $\epsilon_a$  relationships for the case of  $p_o' < \sigma_p'$  will be very different from the  $q$ - $\epsilon_a$  relationships for the case  $p_o' > \sigma_p'$  and hence will be largely effected by the pre-shear consolidation pressure.

#### 5.7.2.6 Normalized Deviator Stress-Axial Strain Relationships

The specimens which were consolidated to higher values of  $p_o'$  sustain higher values of  $q_f$  but the shapes of the  $q$ - $\epsilon_a$  curves are similar. It is therefore possible to normalize the curves by plotting  $q/p_o'$  against  $\epsilon_a$ , where  $p_c' = p_o'$  for undrained case. Fig. 5.85 illustrates the normalized behaviour in the  $q/p_o'$ - $\epsilon_a$  plots for typical untreated base C1 clay. A unique normalized behaviour is evident from the plot in Fig. 5.85.

Fig. 5.86 shows the normalized stress and strain relationships for C1 clay samples treated with 12% cement at mixing water content of 120% and cured for 4 weeks with various pre-shear consolidation pressures. The overall trend of increasing normalized value of the deviator stress with increasing cement content can be seen from the Fig. 5.86. It is also evident that generally the lower the value of  $p_o'$ , the greater is the normalized value of the deviator stress. It deserves mentioning that the untreated clay produces unique normalized behaviour in the  $q/p_o'$ - $\epsilon_a$  relationships (Fig. 5.85).

The normalized  $q/p_o'$ - $\epsilon_a$  relationships for C1 clay with clay-water/cement ratio of 30 and mixing water content of 120% and cured for 4 and 12 weeks are presented in Figs. 5.87(a) and 5.87(b) respectively for different pre-shear consolidation pressures  $p_o'$  of 50, 100, 200 and 400 kPa. The effects of normalization are clearly observed from the plots in Fig. 5.87. For samples having low cement content (i.e. 4%), it can be seen from Fig. 5.87 that the normalized ratios of samples increase sharply towards well-defined peak values followed by a large amount of strain softening, especially for the case of effective pre-shear consolidation pressure of 50 kPa.

It is interesting to note that the residual part of the curves of the samples having low cement content such as 4% and consolidated at  $p_o' = 50$  to 400 kPa, shows merging behaviour (Fig. 5.87). This can be explained from the fundamental understanding. Physicochemical reactions involving clay-water content and cement content result in grouping or cementation of particles into larger clusters. At the time of shearing process, these bonded particles or clusters gradually become dissociated releasing the locked-in energy. This way, destructuration (breaking of cementing bond) occurs in the cemented soil in a manner such that it transforms into destructured soil having a common destructured nature. When a sample of low cement content is consolidated isotropically to a comparatively higher stress, such dissociation of the particles is deemed to be happened during the process of shearing, resulting in a structure at the residual state with characteristic very similar to each other irrespective of cement content. Such behaviour of samples with low cement content subjected

to higher  $p_o'$  is supposed to produce normalized behaviour at the residual states. Kamaluddin (1995) also reported similar CIU strength normalization results.

### 5.7.3 Pore Pressure Characteristics for Untreated and Cement Treated Clays

#### 5.7.3.1 Pore Pressure-Axial strain Relationships for Untreated Samples

Figs. 5.85(a) and 5.85(b) present typical pore pressure-axial strain responses at different  $p_o'$  for untreated samples of C1 and C3 clays, respectively. It is generally known that the pore pressure generated during undrained shear is not a unique property of the soil but it depends on the applied  $p_o'$  as can be seen from Fig. 5.85. It can be seen that maximum pore pressure developed increased with the increase in  $p_o'$ . Pore pressure-axial strain responses for the untreated typical samples that can be observed for normally consolidated clays.

#### 5.7.3.2 Effects of wc/c Ratio on Pore Pressure Change-Axial Strain Relationships

Fig. 5.86 presents typical influence of wc/c ratio on  $\Delta u$ - $\epsilon_a$  relationships for specimen of 4 weeks curing time and sheared from  $p_o'$  of 200 kPa for samples of C1 clay. It can be seen from Fig. 5.86 that at a particular  $p_o'$ , peak  $\Delta u$  increases with decreasing wc/c ratio (increasing cement content). From Fig. 5.86, the effect of cement content can be generalized by grouping the cement contents into three groups: low cement content (high wc/c ratio 15 and 30), medium cement content (medium wc/c ratio 10) and high cement content (low wc/c ratio 7.5) with having mixing water content of 120%. At medium consolidation stress,  $p_o'$  of 200 kPa, the  $\Delta u$ - $\epsilon_a$  relationships rise to peak  $\Delta u$  values are obtained 234 kPa at  $\epsilon_a = 4.13\%$ , 179 kPa at  $\epsilon_a = 4.31\%$ , 132 kPa at  $\epsilon_a = 4.50\%$ , and 89 kPa at  $\epsilon_a = 5.28\%$ , for wc/c ratio 7.5, 10, 15 and 30, respectively thereafter, the pore pressures decrease to lower values. It is seen that the after reaching the peak  $\Delta u$ , pore pressures fall under varying rates with an increase in axial strain. The falling characteristics after peak depend very much on the wc/c ratio. The rate of increase is greater for lower wc/c ratio.

#### 5.7.3.3 Effects of Curing Time and Clay Type on Pore Pressure Change-Axial Strain Relationships

Fig. 5.87 shows the influence of curing time and clay type on  $\Delta u$ - $\epsilon_a$  relationships for sample of C1, C2 and C3 clays. It can be seen from Fig. 5.87 that samples cured for 12 weeks attain low peak pore pressures at lower strains than those of samples cured for 4 weeks. A comparative study also shows that 12 weeks samples attain peak pore pressures at lower strains than those of 4 weeks samples. Similar results were obtained for wc/c ratios of 7.5 and 15. The peak pore pressure change for both 4 and 12 weeks curing for C1 are higher than those of C2 and C3 clays. So, at particular curing time, there is a trend of increase in peak  $\Delta u$  with the increase in plasticity index of soils. The 4 weeks' samples show that the curves rise to a distinct and well-defined peak accompanied by a significant amount of pore pressure dissipation after the peak, which refers to the increased value of OCR. But the effect of curing

time for lower cement content and resemble to the behaviour of normally consolidated or lightly over-consolidated state. Normally, the pore pressure is decreased with increasing curing time. Chew et al. (2001) also reported similar results.

#### 5.7.3.4 Effects of Mixing Water on Pore Pressure Change-Axial Strain Relationships

Fig. 5.88 shows typical influence of mixing water content on  $\Delta u$ - $\epsilon_a$  relationships for samples of C2 clay cured for 4 weeks curing time and at a  $w/c$  ratio of 10. It can be seen from Fig. 5.88 that there is a trend of increase in peak  $\Delta u$  with increasing mixing water content. Samples with high clay water content of 250% exhibit lower axial strain at higher peak pore pressures and shear modulus. However, the peak pore pressures of the samples made up both at low and high clay water contents are almost of the same order.

#### 5.7.3.5 Effects of Pre-shear Effective Consolidation Stress on Pore Pressure Change-Axial Strain Relationships

The development of pore pressure with axial strain for samples of C1 clay cured for 4 weeks at 250% mixing water content and  $w/c$  of 10 is shown in Fig. 5.89 for various values of pre-shear effective consolidation pressure ( $p_o'$ ). It can be seen from Fig. 5.89 that the higher the value of  $p_o'$ , the greater is the pore pressure generation. At low values of  $p_o'$  (e.g., 50 kPa and 100 kPa), large amount negative pore pressure has been generated. An overall characteristic of the treated clay is noticeable that the peak pore pressure has been mobilized always at much lower value of axial strains than those of untreated clay. For natural base clay,  $\Delta u$  keeps on increasing with  $\epsilon_a$  without showing any maximum value, i.e.,  $u_{max}$  is located at the end-of-test condition, which reflects one of the characteristics of the normally consolidated clay (Fig. 5.85).

Typical effects of  $p_o'$  on  $\Delta u$ - $\epsilon_a$  relationships at large  $w/c$  ratio 30 (i.e., low cement content of only 4%) are presented in Figs. 5.90(a) and 5.90(b) for samples of C2 clay cured for 4 and 12 weeks, respectively. The relationships are significantly influenced by pre-shear effective consolidation pressure at low cement content; the samples for high pressure possess extra added characteristics in the  $\Delta u$ - $\epsilon_a$  relationships. A comparative study shows that samples consolidated at pressures (200 kPa and 400 kPa) attain high peak pore pressures at higher strains than those of low pressure consolidated samples (50 kPa and 100 kPa). The relationships are significantly influenced by curing time at low cement content. It can be seen from Fig. 5.90 that peak  $\Delta u$  for generated for samples cured for 12 weeks is lower than that of samples cured for 4 weeks. Low pre-shear effective consolidation pressure, generated large amount negative pore pressure and effects of curing time on negative pore pressure have also been observed. On the other hand, shorter curing time propagates smaller values of negative pore pressure. The increase of effective consolidation pressure tends to diminish the negative effect of cement treatment.

The untreated clays develop maximum pore pressure at the residual state. This can be found for  $p_o'$  of 200 kPa and 400 kPa, where it can be seen that low cement contents tend to resemble to the untreated clay. Samples treated with higher cement contents have also been found to be in the process of transformation towards lower OCR state, revealing the fact the much higher pressure is required to convert these samples into untreated behaviour. Thus, it is evident that increase of consolidation stress increases the positive effects of cement treatment. The result shows that at low  $p_o'$ , unique relationship (different from untreated curves) exists from initial starting point up to the peak positive value of pore pressure for all the cement content. This aspect of unique relationship covering all cement content diminishes with increase of  $p_o'$  and tends to merge with untreated clay. This therefore supports the postulation that the increase of consolidation stress tends to diminish the negative effect of cement treatment. Similar behaviours of pore pressure for cement treated clays were also observed by Kamaluddin (1995), Chew et al. (2001) and Kamruzzaman (2002).

#### 5.7.3.6 Normalized Pore Pressure Change-Axial Strain Relationships

Fig. 5.94 shows the normalized pore pressure change-axial strain curves for typical untreated base C1 clay while Fig. 5.95 shows the different behaviour of normalized pore pressure and axial strain relationships  $\Delta u/p_o' - \epsilon_a$  for cement treated C1 clay samples at mixing water content of 120% and cured for 4 weeks with various pre-shear consolidation pressures. The overall trend of increasing normalized value of the pore pressure with cementing can be found in Fig. 5.95. It is also evident from Fig. 5.95 that generally the lower the values of  $p_o'$  (50 and 100 kPa), the greater is the normalized value of the pore pressure but generated small amount negative normalized pore pressure at higher axial strain.

The influence of curing time on normalized behaviour of  $\Delta u/p_o' - \epsilon_a$  relationships for cement treated clays can also be observed in Figs. 5.96(a) and 5.96(b) for samples cured for 4 weeks and 12 weeks respectively with the same  $w_i = 120\%$ ,  $wc/c$  ratio = 30 and cement = 4%. The relationships are significantly influenced by curing time at low cement content; the cured samples for a longer time possess extra added characteristics in the  $\Delta u/p_o' - \epsilon_a$  relationships. A comparative study shows that 12 weeks samples attain high normalized values at lower strains than those of 4 weeks samples. At low pre-shear consolidation pressure, samples generated large amount of negative normalized values and effects of curing time on negative normalized values are also observed (Fig. 5.96). The overall trend of decreasing normalized values of the pore pressure with increasing curing time has been found. Similar normalized behaviours of pore pressure for cement treated Bangkok clay were also reported by Kamaluddin (1995).

#### 5.7.4 Peak and Deconstructed Envelopes of Cement Treated Clays

The failure envelopes are derived from the points of peak deviator stress ( $q_{max}$ ) and deconstructed envelopes are derived from the points of end-of-test deviator stress ( $q_{end}$ ), both obtained from CIU tests are studied in this research.



#### 5.7.4.1 Peak Deviator Stress Conditions and Undrained Failure Envelopes

The failure envelopes derived from the points of peak deviator stress ( $q_{max}$ ) obtained from CIU tests for cement treated clays are shown in Figs. 5.91(a) and 5.91(b) for samples of C1 and C3 clays, respectively. For cement treated clays, the maximum deviator stress criterion of failure envelopes can be used. The treated clays possess various degrees of over-consolidation depending mainly on cement, curing time and pre-shear consolidation pressure ( $p_o'$ ). The occurrence of  $q_{max}$  depends upon the degree of over-consolidation. For treated soil with high over-consolidation, the peak deviator stress ( $q_{max}$ ) occurs at much lower strain than corresponding failure strain and thus the criterion of peak deviator stress ( $q_{max}$ ) becomes inconsistent and valid to refine the residual states of the treated soil mass. Thus in this study, the maximum deviator stress criterion has been considered to define the failure condition. Bergado et al. (2003), Porbaha et al. (2000) and Kamaluddin (1995) also reported similar behaviour for failure envelopes with mean effective pressure of treated clays.

In Fig. 5.91, the envelopes drawn through the points of peak deviator stress are much higher than that of untreated clays. Fig. 5.91 shows that the strength tends to increase linearly with the magnitude of the effective consolidation stresses. In general, the failure envelopes are found to be curve. The lowest envelope of the treated clays is for  $wc/c$  ratio of 30 cured for 4 weeks and the envelope adjacent to it belongs to the samples cured for 12 weeks having the same clay-water/cement ( $wc/c$ ) ratio. These two curves can fall on a unique failure envelope. Thus the finding shows that  $wc/c$  ratio of 30 does not render sufficient effect even at higher curing time. The envelopes for  $wc/c$  ratio of 30 show a smaller improvement over  $wc/c$  ratio of 15 samples. On the other hand, for the higher  $wc/c$  ratio (10 and 7.5), the envelopes have been found to shift upwards significantly, suggesting that these higher percentages of cement content (lower  $wc/c$  ratio) are most effective for cement stabilization. For these two cement contents, the curing time effect is also pronounced when compared with respect to low range cement content. One noticeable aspect is that the parameter of  $wc/c$  ratio renders greater impact on hardening potential than the curing time. The curing time factor is observed as quite effective. And the rate of strength increment is found to decrease at higher consolidation stresses. Now, the failure envelopes appear to be more curved for all type treated clays. Failure envelopes of samples of C1 clay have greater strength than that of samples of C2 and C3 clays. Thus it is evident that the degree of overall curvature of the failure envelope for each type of clay depends on the range of consolidation stresses and hence increases with increasing cement content and curing time.

#### 5.7.4.2 Residual State and End-of-Test Destructured Envelope Behaviour

The conditions at residual states or end-of-test conditions of cement treated clays are plotted in Figs. 5.92(a) and 5.92(b) for samples of C1 and C3 clays, respectively. Observation can be made that the residual strengths of the treated samples approach are end-of-test destructured

envelope (referred to as the critical state line) of the untreated clay. From the figure, in spite of some scattering of the data, it is quite clear and can be suggested that these residual points will ultimately plot near to the end-of-test destructured envelope of the untreated clay. The physical and chemical reactions resulting after addition of cement bring about changes in the soil structure, which have been already investigated. A transformation in the soil structure occurs, resulting into flocculation and coagulation of the soil particles into large size aggregate or clusters. When the soil shears under load, the cemented particles dissociate. Dismembering of the cluster particles brings about drastic changes of the structure of the treated clay and transforms it to a new structure close to that of untreated clay. Thus at the last stage of shearing, which refers to a very large level of strain, all the treated clays are deemed to behave similarly to the failure condition of the untreated base clay. The behaviour after the maximum deviator stress condition can be regarded as unstable; this unstable phase is manifested by the strain-softening characteristics of cement treated clays (the reduction in deviator stress in constant- $p'$  path after  $q_{max}$  is reached).

The undrained stress paths fall along approximately vertical or constant-  $p'$  paths until the residual or end-of-test states. This residual state is referred to as the states defining the end-of-test destructured condition for cement treated clay. It has further been suggested that if complete destructuration of the treated clays would be achieved and neglecting any permanent changes in soil structure due to cement treatment, an end-of-test destructured envelope would be obtained. A details examination of these residual points shows that these do not exactly fall on the critical state line of the untreated clay, but rather plot above the line in such a way that they constitute an envelope, which has referred in this study as destructured envelope. SEM results of CIU triaxial sheared sample suggest in the next section that complete destructuration only take place on the shear plane at which the clay-cement cluster crushes.

End-of-test destructured envelopes of samples of C1 clay have greater strength than that of samples of C2 and C3 clays. The destructured envelope is still somewhat different from that of the untreated clay in as much as some permanent changes in the soil may have taken place during the chemical reactions between the cement and the clay, which could not completely be reversed or destroyed during the tests for all type treated clays. It seems that cementation bond controls the initial stage of the shearing; thereafter fabric of the clay dominates the behaviour. The behaviour of these samples can be considered as lightly over-consolidated behaviour, resulting in a manner similar to the sample belonging to the wet side of the State Boundary Surface. On the other hand, the treated sample with low confining pressure (i.e. 50 kPa), which is far lower than the yield stress, shows semi-rigid type of behaviour. Hence, the development of positive pore pressure is very small. For this type of sample, the stress path is almost parallel to  $q$  axis. The cementation bond dominates the behaviour of this type of treated clay and the role of fabric is minimum during shearing.

### 5.7.5 SEM Images at Shear Stage for Cement Treated Clays from CIU Test

The effect of cementation as well as fabric after the shearing can be seen from the SEM images of treated clay at which the confining pressure was 400 kPa as shown in Fig. 5.93. This sample was chosen as it has gone through more destructuration at the consolidation stage. As can be seen from Fig. 5.93(b) that both inter and intra-cluster voids are found to be negligible in the shear plane as compared to the intact sample as shown in Fig. 5.93(a). However, the SEM image of sheared sample out side the shear plane as shown in Fig. 5.93(c) has been found to be different from the shear plane image. Results from particle size analysis reveal that some breakage of the treated clay particles also occurs in addition to the crushing of clay-cement cluster. Both inter and intra cluster voids are found to be very negligible in the shear plane as compared to the intact sample. However, the image of the sample outside of the shear plane is found to be quite different from that within the shear plane. For sample outside the shear plane, the breaking of large clay-cement clusters is apparent but still contain small clusters in the form of reticulation. At this stage, no breakage of treated clay particles is observed. More inter-cluster voids are visible as compared to the image of sample within the shear plane. It is concluded that during the isotropic consolidation, the cementation bond in the form of clay-cement cluster did not completely break down, and may affect the subsequent shearing stage.

## 5.8 Stress-Strain and Volumetric Strain Characteristics from CID Triaxial Compression Tests

The stress-strain and volumetric strain characteristics have been studied from isotropically consolidated drained (CID) triaxial compression tests for cement treated samples C1, C2 and C3 clays. Failure envelopes of the treated samples have also been investigated.

### 5.8.1 Stress-Strain Behaviour of Untreated and Cement Treated Clays

#### 5.8.1.1 Deviator Stress- Axial Strain Relationships of Untreated Clays

The deviator stress-axial strain,  $q-\epsilon_a$  relationships for untreated samples of clays C1 and C3 clays are shown in Figs. 5.94(a) and 5.94(b), respectively. These curves are of the same shape for all clays. Fig. 5.94 show that samples which have been consolidated to higher  $p_o'$  exhibit higher values of deviator stress. Compared with the results of CIU tests, the stress-strain curves from CID tests increase less sharply with increasing strain, suggesting that the drained stiffness is less than the undrained stiffness. Furthermore, the stress-strain curves show that the axial strains of CID tests are greater than those of CIU tests. A unique type of relationship is evident among the untreated samples. These curves possess certain definite patterns. The usual trend exists, the higher the  $p_o'$ , greater is the value of deviator stress. The overall nature of the curves seems to indicate that the samples are behaving as if they are normally consolidated to lightly overconsolidated.

### 5.8.1.2 Effect of $w/c$ Ratio on Deviator Stress-Axial strain Relationships

Typical effect of  $w/c$  ratio on  $q-\epsilon_a$  relationships for treated samples of C1 clay is shown in Fig. 5.95. It can be seen from Fig. 5.95 that at a particular mixing water content and curing time, peak deviator stress increases with decreasing  $w/c$  ratio (i.e., increasing cement content). It has been observed that after attaining the peak deviator stress, all the  $q-\epsilon_a$  relationships have been found to fall under varying rates depending on the value of  $w/c$  ratio, revealing that cement is the paramount factor that controls the post-treatment relationships of  $q-\epsilon_a$ . It has also been found that generally the axial strain at the maximum deviator stress is reduced when  $w/c$  ratio has been decreased (i.e., cement content is increased). This is because these samples of high  $w/c$  ratio acquire low hardening potential and their behaviour is more similar to untreated clay than to a treated clay possessing higher content of hardening agent. On the other hand, the  $q-\epsilon_a$  relationships for higher cement content, such as 12% and 16% ( $w/c$  ratio = 10 and 7.5), are different than those of samples having low cement content and render greater strength and stiffness to the clays.

A comparison of shear strength and strain at failure obtained from CIU and CID triaxial compression tests is shown in Table 5.8 for different  $w/c$  ratio. It has been found that shear strengths obtained from CID triaxial compression test are average about 1.15 times higher than those obtained in CIU test but failure strains for CID triaxial compression test are increased to average about 1.10 times than those obtained from CIU tests.

The experimental observations in this investigation indicate that it would be advantageous to include the cement content in the same parameter since it would take care of the bonding component of the state represented by water content. Hence, clay-water / cement ratio,  $w/c$ , is a convenient parameter to adjust cement content in water to get the same level of strength with the same curing time. From the above test results, it is revealed that the  $w/c$  is the prime parameter influencing the engineering behaviour of cement-stabilized clay. Horpibulsuk et al. (2000, 2001) also supported that the same clay-water content/cement ( $w/c$ ) ratio's concept. Miura et al. (2001) also reported similar stress-strain behaviour for Ariake clay.

### 5.8.1.3 Effects of Curing Time and Clay Type on Deviator Stress-Axial Strain

The effects of curing time and clay type on  $q-\epsilon_a$  relationships can be seen from Fig. 5.96 for samples for C1, C2 and C3 clays cured for 4 weeks and 12 weeks. Comparing samples cured for 4 weeks with those samples cured for 12 weeks, it can be seen that the deviator stresses of samples cured for 12 weeks increase sharply towards well-defined higher peak values followed by a large amount of strain softening, especially for the typical cases of cement content of 20% ( $w/c$  ratio = 10 and mixing water = 200%). Similar behaviour was observed for other  $w/c$  ratios of 7.5 and 15. Fig. 5.96 also shows that at a particular curing time, the peak deviator stresses samples of C1 are higher than those of samples of C2 and C3 clays. So, there has been a trend of increase in peak deviator stresses with the increase in plasticity index

of soils. A comparison of shear strength and strain at failure obtained from CIU and CID triaxial compression tests is shown in Table 5.8 for different curing time and clay type.

#### 5.8.1.4 Effect of Mixing Water on Deviator Stress - Axial strain Relationships

The effect of mixing water content on  $q$ - $\epsilon_a$  relationship for samples of treated C2 clay has been presented in Fig. 5.97 at  $w_c/c$  ratio of 10 for mixing water contents of 120%, 150%, 200% and 250% and curing time of 4 weeks. The  $q$ - $\epsilon_a$  relations of samples having the same  $w_c/c$  are identical at the initial state up to a certain level, and samples with high clay water contents of 200% to 250% exhibit higher deviator stresses. This can be explained by the fact that the cementation bond initially governs the engineering behaviour, and then the stress paths proceed up to a certain level where the cementation bond is broken down. At this level, the samples at high initial clay water contents of 200% to 250% exhibit higher shear modulus and higher axial strain because of the large spacing between clusters. As a consequence, all samples having the same  $w_c/c$  both made up at low and high clay-water contents exhibit identical deviator stress versus axial strain response. However, the peak deviator stresses of the samples made up both at low and high clay-water contents are almost of the same order. It, therefore, can be concluded that at a particular  $w_c/c$  ratio, mixing water content has got insignificant effect on peak deviator stress. Miura et al. (2001) found similar results for samples having the same  $w_c/c$  with different mixing water contents.

#### 5.8.1.5 Effect of Pre-Pressure Effective Consolidation Pressure on Deviator Stress-Axial strain Relationships

Typical effects of pre-shear effective consolidation pressure on  $q$ - $\epsilon_a$  relationships for samples of C1 clay cured for 4 weeks with clay-water/cement ratio of 10 and mixing water content of 250% is shown in Fig. 5.98. It can be seen that the deviator stresses of samples increase sharply towards well-defined peak values followed by a large amount of strain softening, especially for the cases of high effective consolidation pressure of 400 kPa. In general, Fig. 5.98 shows that samples consolidated to higher  $p_o'$  attains higher values of maximum deviator stress. Miura et al. (2001) also found similar results.

The effects of  $p_o'$  on  $q$ - $\epsilon_a$  relationships were also assessed for high  $w_c/c$  ratio of 30 (i.e., low cement content of only 4%) for curing time of 4 and 12 weeks. Typical effects of  $p_o'$  on  $q$ - $\epsilon_a$  relationships are shown in Figs. 5.99(a) and 5.99(b) for samples of C2 clay. It can be seen from Fig. 5.99 that similar to samples for low  $w_c/c$  ratio (Fig. 5.98), the deviator stresses of samples having high  $w_c/c$  ratio increase sharply towards well-defined peak values followed by a large amount of strain softening, especially for the cases of effective consolidation pressure of 400 kPa. Thus pre-shear consolidated volumes are affected largely by the  $p_o'$ , with in turn affects the relationship of  $q$ - $\epsilon_a$ . On the other hand, the samples with lower  $p_o' = 50$  to 100 kPa have very similar  $q$ - $\epsilon_a$  relationships. This is because the volume changes during consolidation to this range of stresses were very small, and therefore, the pre-shear void ratios

are very close for these samples. Higher volumetric deformation was noticed with higher level of axial strains in these samples. It can also be seen from Fig. 5.99 that at a particular  $p_o'$ , peak deviator stress of samples cured for 12 weeks are higher than that of samples cured for 4 weeks.

#### 5.8.1.6 Normalized Deviator Stress-Axial Strain Relationships

The normalized deviator stress-axial strain relationships ( $q/p_o' - \epsilon_a$ ) are shown in Fig. 5.106 for typical untreated base C1 clay. A unique normalized behaviour of lower normalized values have been found for each clay at higher values of  $p_o'$ .

Fig. 5.107 illustrates the normalized stress and axial strain relationships ( $q/p_o' - \epsilon_a$ ) for typical cement treated C1 clay samples at mixing water content of 120% and cured for 4 weeks with various pre-shear consolidation pressures. The overall trend of increasing normalized value of the deviator stress with increasing cement content has been found. It is also observed from Fig. 5.107 that the lower the value of  $p_o'$ , the greater is the normalized value of the deviator stress.

The effect of curing time on normalized deviator stress-axial strain relationships ( $q/p_o' - \epsilon_a$ ) for C1 clay with clay-water/cement ratio of 30 and mixing water content of 120% and cement content of 4% and cured for 4 and 12 weeks are shown in Figs. 5.108(a) and 5.108(b) respectively for different pre-shear effective consolidation pressures ( $p_o'$ ) of 50, 100, 200 and 400 kPa. The effects of normalization are clearly observed for the plots in Fig. 5.108. For samples containing low quantity of cement (i.e. 4%), it can be seen that the normalized values of samples increase sharply towards well-defined peak values followed by a large amount of strain softening due to curing time, especially for the cases of effective pressure of 50 kPa. This can be explained from the fundamental understanding. Physicochemical reactions involving clay-water content and cement content result in grouping or cementation of particles into larger clusters. At the time of shearing process, these bonded particles or clusters gradually become dissociated, releasing the locked-in energy, which is understood from micro-graph of microscopic analysis in this study. Kamaluddin (1995) also found similar normalization results for CID triaxial compression tests.

### 5.8.2 Volumetric Strain Characteristic of Untreated Base and Cement Treated Clays

#### 5.8.2.1 Volumetric Strain-Shear Strain relationships of Untreated Samples

Figs. 5.100(a) and 5.100(b) show the typical volumetric strain-axial strain response at different confining pressure for samples of untreated C1 and C3 clays, respectively. It is generally known that the volumetric strain generated during drained shear is not a unique property of the soil, but it depends on the applied stress increment. It can be seen from Fig. 5.100 that volumetric strain generated during drained shear depend considerably on  $p_o'$ .

Values of volumetric strain ( $\epsilon_v$ ) increase with increasing  $p_o'$ . It can be seen from Fig. 5.100 that  $\epsilon_v$ - $\epsilon_a$  relationships for the untreated samples typically resemble those of normally consolidated clays.

### 5.8.2.2 Effect of wc/c Ratio on Volumetric Strain-Axial Strain Relationships

Fig. 5.101 shows typical influence of wc/c ratio on  $\epsilon_v$ - $\epsilon_a$  relationships for samples of C1 clay cured for 4 weeks at mixing water content of 120%. From Fig. 5.101, the effect of cement content can be generalized by grouping the cement contents into three groups: low cement content (high wc/c ratio 15 and 30), medium cement content (medium wc/c ratio 10) and high cement content (low wc/c ratio 7.5). At each value of  $p_o'$  the  $\epsilon_v$ - $\epsilon_a$  relationships rise to peak  $\epsilon_v$  values and thereafter, the volumetric strains decrease to lower wc/c values. It has been seen that after attaining the peak value, the volumetric strains fall under varying rates with an increase in strain. The falling characteristics after peak depend very much on the wc/c ratio. The rate of increase is smaller for lower wc/c ratio. Fig. 5.101 also shows that at a particular mixing water content and curing time, peak volumetric strains increase with increasing wc/c ratio.

### 5.8.2.3 Effect of Curing and Clay Type on Volumetric Strain-Axial Strain

The curing time has got significant effect on  $\epsilon_v$ - $\epsilon_a$  relationships. The influence of curing time and clay type on volumetric strains is shown in Fig. 5.102 for samples of C1, C2 and C3 clays. A comparison of the plots shown in Fig. 5.102 shows that samples cured for 12 weeks samples attain low peak volumetric strains at lower strains than those of samples cured for 4 weeks. Fig. 5.102 also shows that at a particular curing time peak volumetric strains for samples of C1 clay are higher than those of C2 and C3 clays. So, at a particular curing time there is a trend of increasing peak volumetric strains with increasing plasticity index of soils.

### 5.8.2.4 Effect of Mixing Water on Volumetric Strain-Axial Strain Relationships

Fig. 5.103 shows typical influence of mixing water content on  $\epsilon_v$ - $\epsilon_a$  relationships for samples of C2 clay cured for 4 weeks and sheared from  $p_o'$  of 200 kPa. Fig. 5.103 shows that at a particular wc/c ratio, there is a trend of increase in peak  $\epsilon_v$  with increasing mixing water content. It can also be seen from Fig. 5.103 that after reaching the peak, volumetric strains fall under varying rates with an increase in axial strains. The falling characteristics after peak depend very much on the cement content and water content. The  $\epsilon_v$ - $\epsilon_a$  relations of samples having the same wc/c are identical at the initial state up to a certain strain level, and samples with high clay water content of 200% to 250% exhibit higher volumetric strains. This can be explained by the fact that the cementation bond initially governs the engineering behaviour, and then the stress paths proceed up to a certain level where the cementation bond is broken down. At this level, the samples at high initial clay water content of 200% to 250% exhibit lower shear modulus and higher volumetric strain because of the large spacing between

clusters. The higher the water content, the greater is the spacing between clusters; this leads to a decrease in shear modulus and an increase in volumetric strain. However, the peak volumetric strains of the samples made up both at low and high clay water contents are almost of the same order. The samples subjected to same effective cell pressures of 200 kPa exhibit similar characteristics up to a certain level. As a consequence, all samples having the same  $w_c/c$  both made up at low and high clay-water contents exhibit identical volumetric strain versus axial strain response. So, the  $w_c/c$  is a prime parameter governing the engineering behaviour of cement treated samples having different mixing water content. Miura et al. (2001) also reported similar results.

#### 5.8.2.5 Effect of Pre-shear Effective Consolidation Pressure on Volumetric Strain-Axial Strain Relationships

The influence of pre-shear effective consolidation pressure on  $\epsilon_v$ - $\epsilon_a$  relationships for samples of C1 clay cured for 4 weeks at 250% mixing water content and  $w_c/c$  ratio of 10 is shown in Fig. 5.104. The influence of  $p_o'$  is very clear. As can be seen from Fig. 5.104 that the higher the value of  $p_o'$ , the greater is the generated volumetric strains. Low  $p_o'$  generated large amount negative volumetric strains at higher axial strains. An overall characteristic of the treated clay that the peak volumetric strains is mobilized always at much lower value of axial strains than those of untreated clay. For natural base clay,  $\epsilon_v$  keeps on increasing with  $\epsilon_a$  without showing any maximum value, i.e., peak  $\epsilon_v$  is located at the end-of-test condition, which reflects one of the characteristics of the normally consolidated clay (Fig. 5.100).

The influence of pre-shear effective consolidation pressure on  $\epsilon_v$ - $\epsilon_a$  relationships was also investigated for high  $w_c/c$  ratio of 30 (i.e., low cement content of only 4%) for curing time of 4 and 12 weeks. Typical effects of  $p_o'$  on  $\epsilon_v$ - $\epsilon_a$  relationships are shown in Figs. 5.105(a) and 5.105(b) for samples of C2 clay. It can be seen from Fig. 5.105 that similar to samples for low  $w_c/c$  ratio (Fig. 5.104), peak  $\epsilon_v$  of samples having high  $w_c/c$  ratio increases with increasing  $p_o'$ . At low  $p_o'$ , samples having higher  $w_c/c$  ratio generated higher amount of negative volumetric strains at large axial strains than sample having low  $w_c/c$  ratio. The relationships are significantly influenced by curing time at low cement content. It can also be seen that at a particular  $p_o'$ , peak  $\epsilon_v$  for samples cured for 4 weeks are higher than those of samples cured for 12 weeks. Similar behaviour of volumetric strain for cement treated clays was also reported by Kamaluddin (1995) and Miura et al. (2001).

#### 5.8.2.6 Normalized Volumetric Strain-Axial Strain Relationships

Fig. 5.115 shows the normalized volumetric strain versus the axial strain relationship for typical untreated base C1 clay. A unique relationship between the normalized volumetric strain and the axial strain is evident. Higher normalized volumetric strain due to lower value of  $p_o'$  has been obtained. It is generally known that the volumetric change generated during drained shear is not a unique property of the soil, but it depends on the applied stress



increment. Fig. 5.116 presents the normalized volumetric strain-axial strain ( $\epsilon_v/p_o'-\epsilon_a$ ) relationships for typical cement treated C1 clay samples at mixing water content of 120% and cured for 4 weeks at various pre-shear consolidation pressures. The influence of curing time on normalized relationships for cement treated clays can be observed for the plots in Figs. 5.117(a) and 5.117(b) for samples cured for 4 weeks and 12 weeks respectively with the same  $w_i = 120\%$ ,  $wc/c$  ratio = 30 and cement = 4%. The relationships are significantly influenced by curing time at low cement content; the cured samples for a longer time possess extra added characteristics in the  $\epsilon_v/p_o'-\epsilon_a$  relationships. A comparative study shows that 12 weeks samples attain high normalized ratios at lower strains than those of 4 weeks samples. At low pre-shear consolidation pressure, generated large amount negative obliquity ratios and effects of curing time on negative normalized ratios have been clearly observed (Fig. 5.117). It is also evident from Fig. 5.117 that for treated clays the lower the  $p_o'$  (50 kPa), the greater is the normalized volumetric strain which is positive at lower axial strain and also generated small amount negative normalized volumetric strain at higher axial strain. It can be mentioned that untreated clay produces similar unique normalized behaviour in the  $\epsilon_v/p_o'-\epsilon_a$  relationships (Fig. 5.115). Similar normalized behaviours of volumetric strain for cement treated clays were also reported by Kamaluddin (1995).

### 5.8.3 Stress Ratio Versus Volumetric Strain, ( $\eta-\epsilon_v$ ) Relationships

For samples subjected to high effective cell pressures, their  $q-\epsilon_a$  and  $\epsilon_v-\epsilon_a$  relationships are the same at the initial state up to a certain stress ratio,  $\eta$  ( $q/p'$ ) and samples with higher clay-water content exhibit higher volumetric and shear strains at the same stress ratio,  $\eta$ . Such behaviour can be explained by the fact that, while the initial states of stress of all samples are inside the state boundary surfaces, they have the same mean effective yield stress in the  $K_o$ -line. This is attributed to the yield stress being the same (Mirua et al., 2001). Thus, the elastic behaviour is recognized for these samples. Samples with higher clay-water content undergo higher volumetric deformation when the states of stress are on the state boundary surfaces due to the break up of the cementation bond. The transformation of the small strain zone into the large strain zone occurs at a smaller stress ratio,  $\eta$  for samples with a higher clay water content, as illustrated in Figs. 5.106(a) and 5.106(b) for samples of C1 and C3 clays, respectively. Examination of the  $q-\epsilon_a$  relationship show that these figures (especially for the samples of higher  $p_o'$  or  $\sigma_3'$ ) contain an initial linear relationship where the stress states possess low strains followed by a break point and thereafter, the samples has been subjected to higher strain. This type of behaviour was found in undrained tests, which were referred to as small strain phase. Additional evidence of this type of phase will be sought in the stress ratio and volumetric strain  $\eta-\epsilon_v$  relationships. The large strain phase for samples of C1 clay is greater than that of samples of C2 and C3 clays. Similar stress ratio and volumetric strain relationships for cement treated clays were reported by Kamaluddin (1995) and Miura et al. (2001).

### 5.8.4 Peak and Destructured Envelopes Characteristics of Treated Clays

The failure envelopes derived from the points of peak deviator stress ( $q_{max}$ ) and destructured envelopes derived from the points of end-of-test deviator stress ( $q_{end}$ ) obtained from CID tests are studied in this research.

#### 5.8.4.1 Peak Deviator Stress Conditions and Drained Failure Envelopes

The peak deviator stress ( $q_{max}$ ) for the cement treated clays achieves greater values with increase of  $p_o'$  for both 4 and 12 weeks curing time as shown in Fig.5.107. For low cement content, the  $q_{max}$ - $p'$  relationships are almost linear but become curved at higher cement content. The untreated clay possesses linear relationships as well and plots at the lowest level. For low cement content ( $wc/c = 15$  and  $30$ ), the relationships are roughly similar irrespective of the curing time. On the other hand, higher values of cement content ( $wc/c = 7.5$  and  $10$ ) render greater potentiality in the increase of  $q_{max}$  with curing time and consolidation stress. Further, the rate of increase of  $q_{max}$  is greater at the region of higher  $p_o'$ . The variation of peak deviator stress with cement content is also shown in Fig. 5.107. It has been seen that the points of peak deviator stress for cement treated clays lie on envelopes higher than those for untreated clays, and these envelopes are curved and the influenced by cement content and curing time. In order to examine the effects of cement content, the failure envelopes were re-plotted in Figs. 5.107(a) and 5.107(b) for samples of C1 and C3 clays, respectively. Failure envelopes of samples of C1 clay have greater strength than that of samples of C2 clay and C3 clay. Thus it is evident that the degree of overall curvature of the failure envelope for each type of clay depends on the range of consolidation stresses and hence failure envelope increases with increasing  $p_o'$ . Bergado et al. (2003), Porbaha et al. (2000) and Kamaluddin (1995) also reported that the similar behaviour for failure envelopes with mean effective pressure of treated clays.

#### 5.8.4.2 Residual Stress States and End-of-Test Destructured Envelope

The end-of-test points are plotted in Figs. 5.108(a) and 5.108(b) for samples of C1 and C3 clay, respectively. As has been found earlier from the results of CIU tests, the end-of-test data points of drained tests are seen to lie close to the failure envelope for untreated soils. Beyond the peak deviator stress, the stress condition can be termed as unstable phase, which is manifested from the strain-softening behaviour and failing characteristics of the stress path in a constant- $p'$  route. These residual states can be regarded as a destructured condition.

It can be visualized clearly that if complete destructuration of the treated clay could be achieved and any permanent change in the soil structure could be neglected, then it is possible to obtain a unique destructured failure envelope irrespective of clay-type, cement content and curing time. The end-of-test destructured envelope is somewhat different from the failure envelope of untreated clay. This is because of the possible reason as the permanent change

occurred due to physicochemical reactions between the clay and cementations materials of the hardening agent, which could not be fully destroyed during the shearing process. For this reason a majority of the end-of-test stress states did not reach the failure envelope of the untreated clay even at much larger strains. However, the stresses which can be expected to actually be imposed on cement treated clays in the field are much lower than the maximum pre-shear consolidation pressure of 100 kPa used in the tests; the testing at much higher strains will have very little practical significance.

**Table 5.1 Characteristics Values of the Strength and Deformation Properties for Untreated Base Clays**

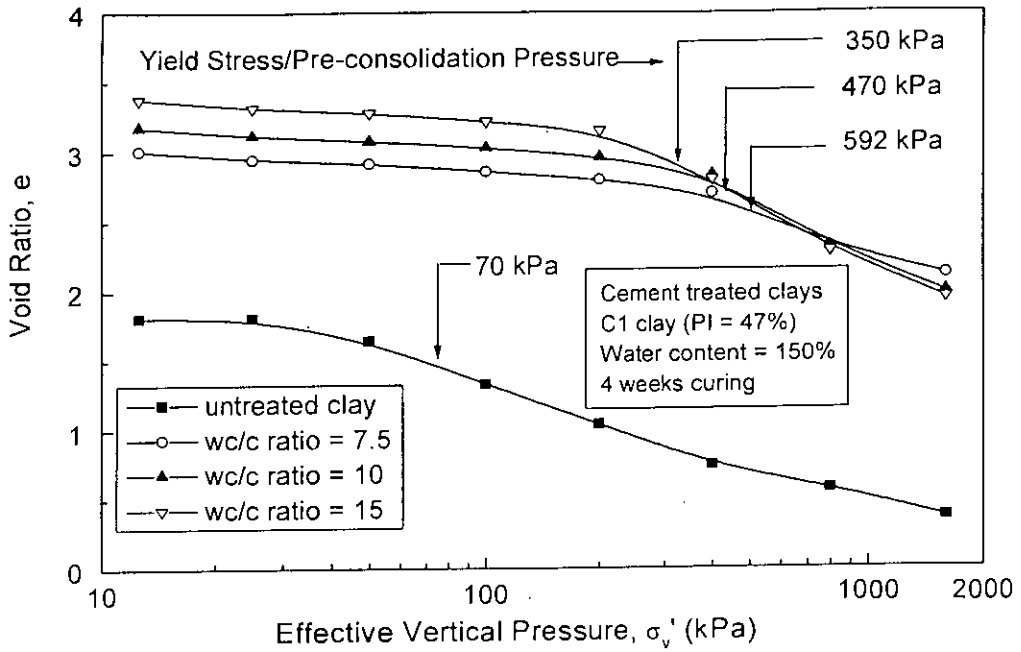
Properties	Characteristics Values		
	C1 Clay (PI = 47%)	C2 Clay (PI = 22%)	C3 Clay (PI = 13%)
In-situ Void Ratio, $e_o$	1.81	1.96	2.10
Coefficient of Consolidation, $c_v$ ( $m^2/year$ )	0.90 - 3.37	1.06 - 4.00	1.71 - 5.20
Coefficient of Volume Compressibility, $m_v$ ( $\times 10^{-4} m^2/kN$ )	1.50 - 6.24	1.62 - 6.74	1.71 - 7.12
Coefficient of Permeability, $k$ ( $\times 10^{-9} m/sec$ )	0.28 - 4.28	0.32 - 4.94	0.53 - 6.16
Compression Index, $C_c$	0.737	0.781	0.863
Swell Index, $C_s$	0.124	0.127	0.131
Preconsolidation Pressure, $p_c'$ (kPa)	70	65	61
Overconsolidation Ratio (OCR)	1.33	1.26	1.18
Unconfined Compressive Strength, $q_u$ (kPa)	50	41	58.5
Strain at Peak Stress, $\epsilon_f$ (%)	3.67	3.65	4.00
Undrained Shear Strength, $s_u$ (kPa)	49	46	44.5
Axial Strain at $s_u$ , $\epsilon_u$ (%)	11	10.7	10.2
Effective Cohesion, $c'$ (kPa)	15.2	13.5	10.8
Effective Angle of Internal Friction, $\phi'$ (degree)	9.8	10.4	11.6

Table 5.2 Compressibility Properties for Cement Treated Clays

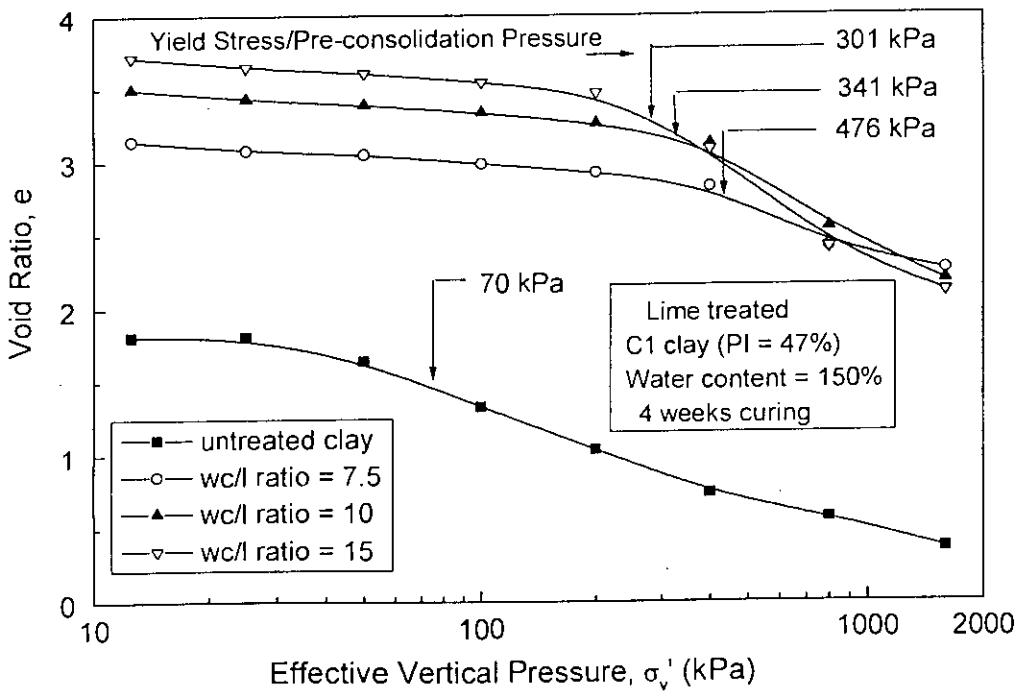
Curing (weeks)	$w_i$ (%)	wc/c Ratio	C1 clay (PI = 47%)			C2 clay (PI = 22%)			C3 clay (PI = 13%)		
			$p_c'$ (kPa)	$C_c$	$C_s$	$p_c'$ (kPa)	$C_c$	$C_s$	$p_c'$ (kPa)	$C_c$	$C_s$
4	120	7.5	540	0.822	0.004	505	0.855	0.007	525	0.882	0.009
		10	510	0.856	0.005	417	0.886	0.008	457	0.916	0.010
		15	445	0.933	0.006	395	0.963	0.009	418	0.982	0.012
	150	7.5	592	0.893	0.008	451	0.912	0.009	475	0.991	0.011
		10	470	0.906	0.009	429	0.943	0.011	447	1.082	0.013
		15	350	0.968	0.011	358	0.995	0.013	380	1.115	0.015
	200	7.5	440	0.992	0.010	410	1.065	0.014	422	1.154	0.016
		10	408	1.111	0.012	375	1.121	0.016	390	1.203	0.019
		15	387	1.126	0.014	318	1.148	0.018	331	1.228	0.021
	250	7.5	398	1.155	0.014	376	1.88	0.018	387	1.213	0.021
		10	378	1.188	0.015	354	1.201	0.020	365	1.261	0.024
		15	351	1.194	0.017	297	1.213	0.022	306	1.311	0.026
12	120	7.5	680	0.806	0.003	634	0.822	0.005	650	0.849	0.007
		10	638	0.823	0.004	601	0.856	0.006	631	0.877	0.008
		15	560	0.848	0.005	502	0.933	0.008	536	0.961	0.010
	150	7.5	638	0.857	0.007	605	0.893	0.008	620	0.945	0.009
		10	609	0.875	0.008	556	0.906	0.009	576	0.966	0.011
		15	534	0.946	0.009	491	0.968	0.011	501	1.003	0.013
	200	7.5	602	0.915	0.009	561	0.992	0.012	582	1.142	0.014
		10	558	0.928	0.011	502	1.111	0.014	526	1.182	0.016
		15	509	0.998	0.013	440	1.126	0.016	471	1.204	0.019
	250	7.5	580	1.101	0.012	538	1.155	0.016	567	1.181	0.019
		10	531	1.131	0.013	449	1.188	0.018	476	1.225	0.021
		15	473	1.154	0.015	412	1.194	0.019	438	1.287	0.024
Untreated base clays			70	0.737	0.024	65	0.781	0.027	61	0.863	0.031

Table 5.3 Compressibility Properties for Lime Treated Clays

Curing (weeks)	$w_i$ (%)	wc/c Ratio	C1 clay (PI = 47%)			C2 clay (PI = 22%)			C3 clay (PI = 13%)		
			$p_c'$ (kPa)	$C_c$	$C_s$	$p_c'$ (kPa)	$C_c$	$C_s$	$p_c'$ (kPa)	$C_c$	$C_s$
4	120	7.5	497	0.871	0.006	403	0.897	0.010	456	0.920	0.014
		10	461	0.902	0.007	359	0.930	0.011	400	0.970	0.017
		15	396	0.988	0.009	326	1.011	0.013	356	1.060	0.020
	150	7.5	476	0.930	0.010	406	1.030	0.013	436	1.063	0.016
		10	341	1.010	0.013	301	1.112	0.016	331	1.162	0.019
		15	301	1.220	0.017	256	1.42	0.020	274	1.62	0.023
12	120	7.5	577	0.780	0.005	523	0.820	0.010	547	0.870	0.012
		10	561	0.813	0.006	501	0.883	0.012	531	0.913	0.015
		15	466	0.873	0.008	402	0.933	0.015	436	0.973	0.018
	150	7.5	536	0.907	0.008	472	0.977	0.011	506	0.997	0.014
		10	449	1.000	0.011	371	1.050	0.014	402	1.100	0.016
		15	401	1.113	0.014	306	1.213	0.017	352	1.413	0.019
Untreated base clays			70	0.737	0.024	65	0.781	0.027	61	0.863	0.031

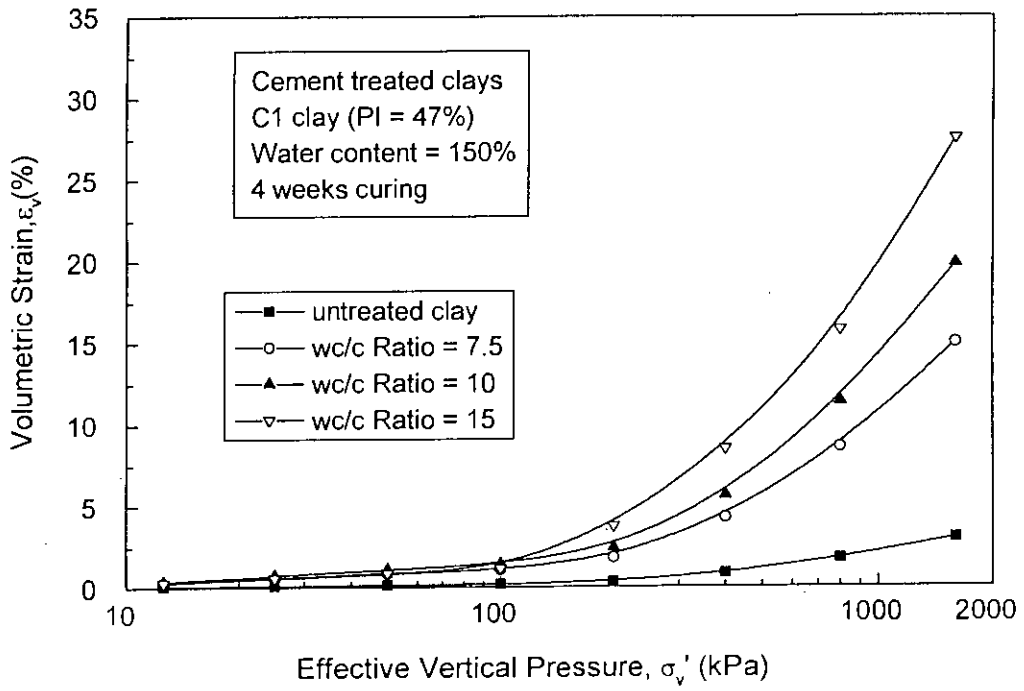


(a)

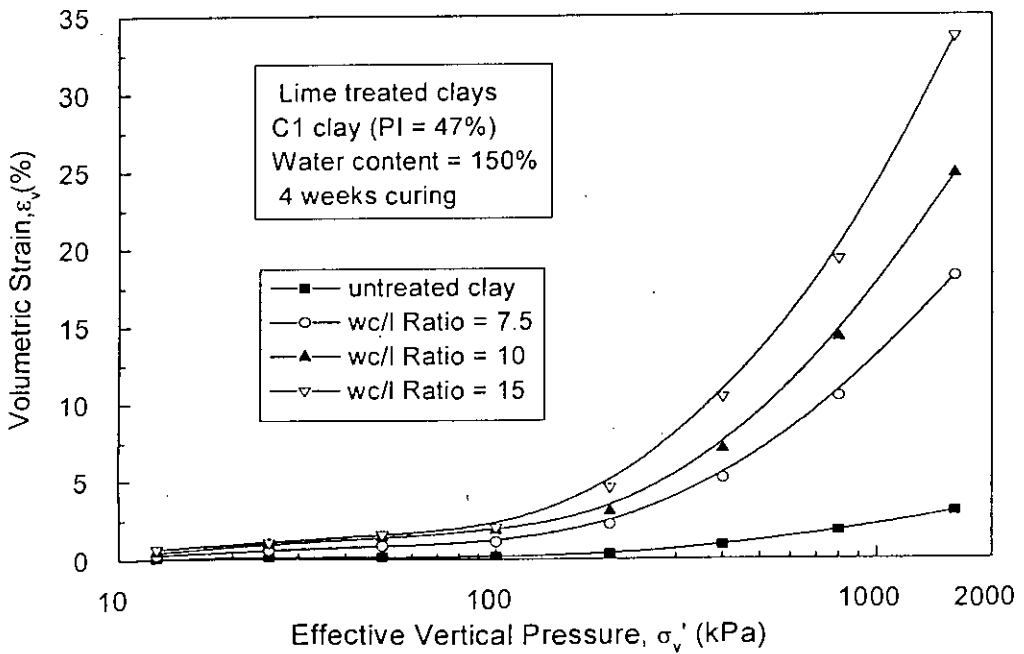


(b)

Fig. 5.1 Effect of Mixing Ratio on  $e - \log \sigma'_v$  Relationships of C1 Clay  
(a) Cement Treated and (b) Lime Treated



(a)



(b)

Fig. 5.2 Effect of Mixing Ratio on  $\epsilon_v$  -  $\log \sigma'_v$  Relationships of C1 Clay  
(a) Cement Treated and (b) Lime Treated



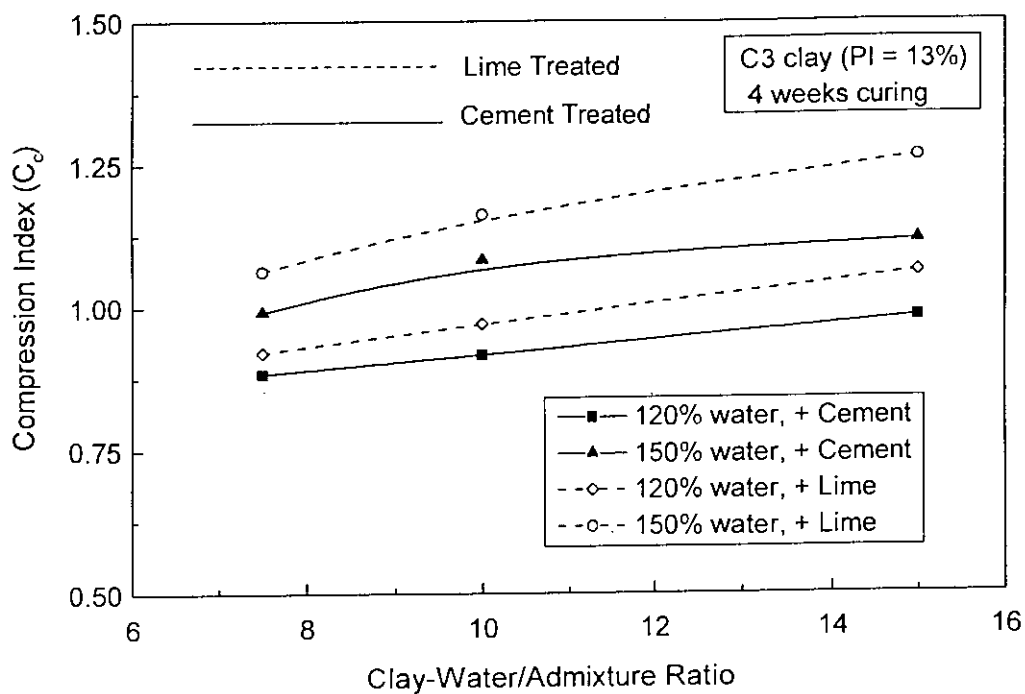


Fig. 5.3 Effect of Clay-Water/Admixture Ratio on Compression Index for Cement and Lime Treated C3 Clay

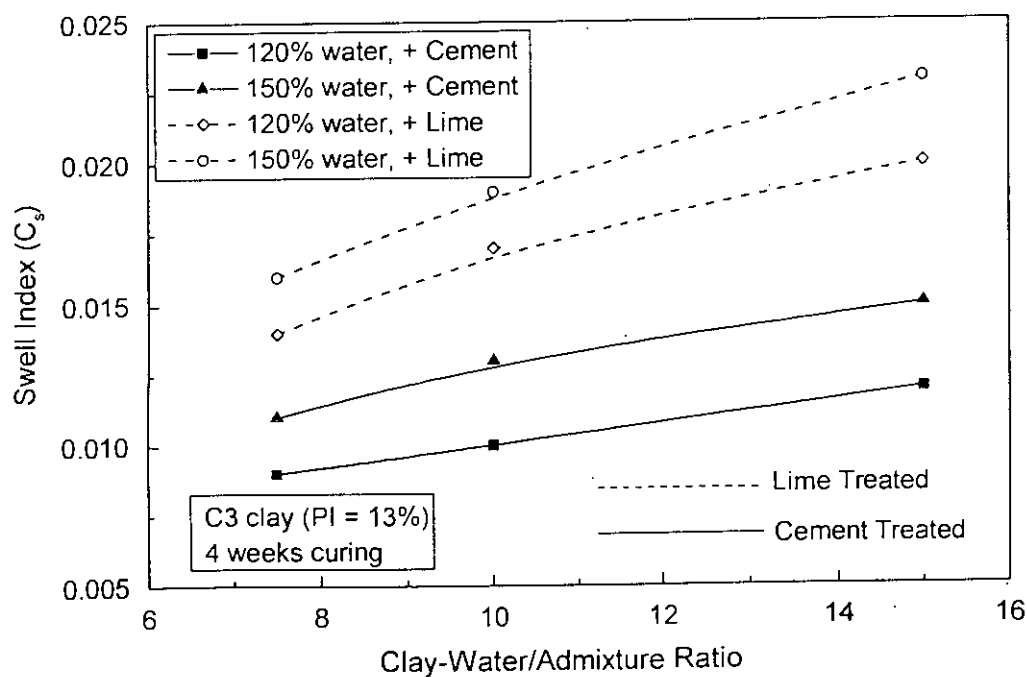
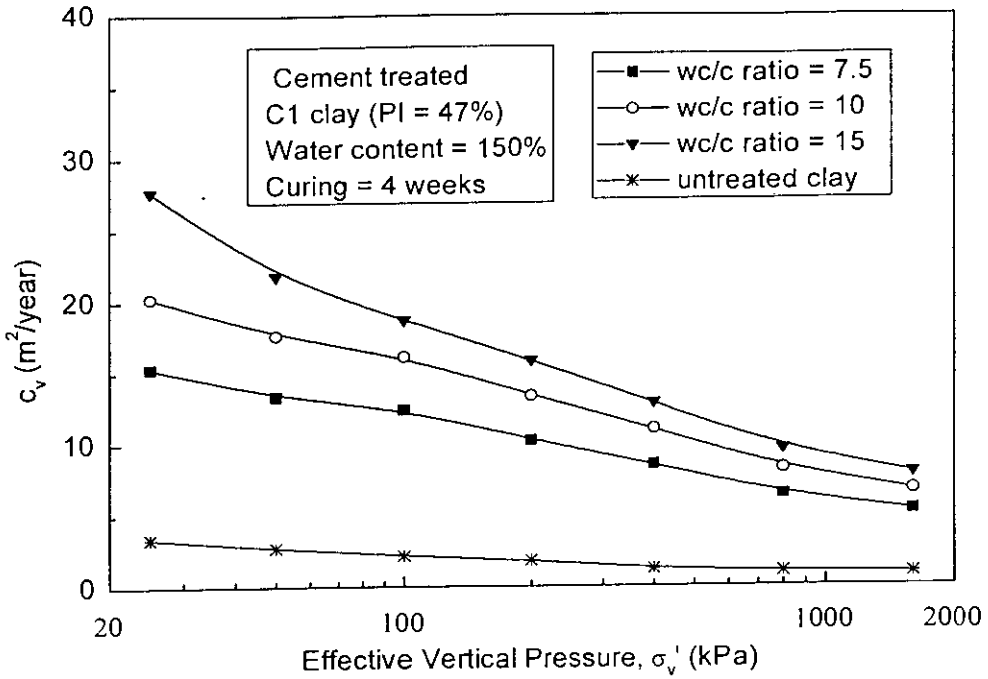
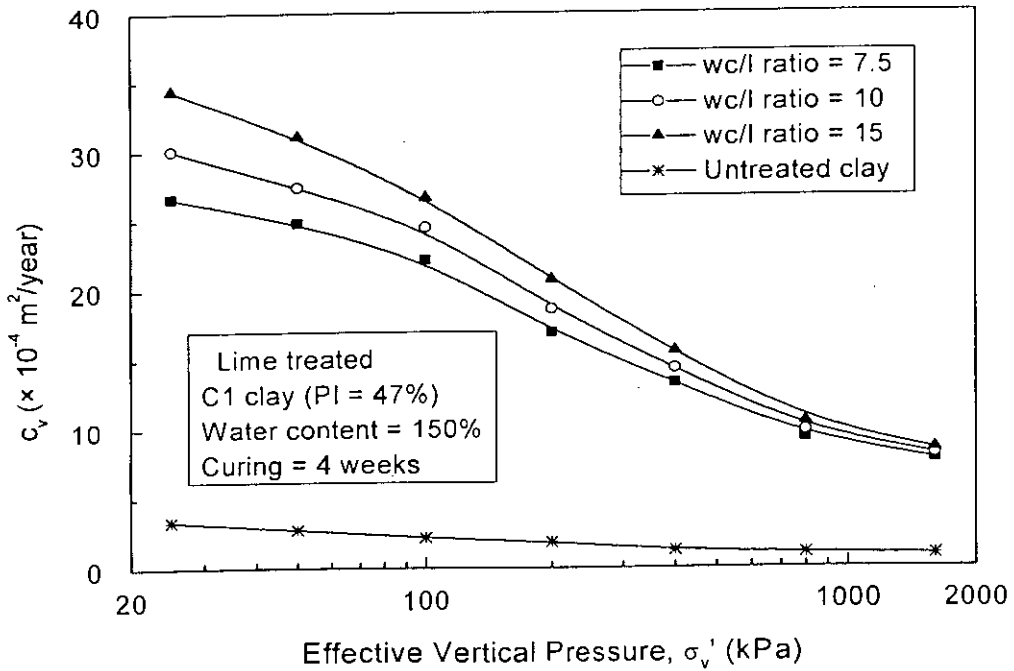


Fig. 5.4 Effect of Clay-Water/Admixture Ratio on Swell Index for Cement and Lime Treated C3 Clay

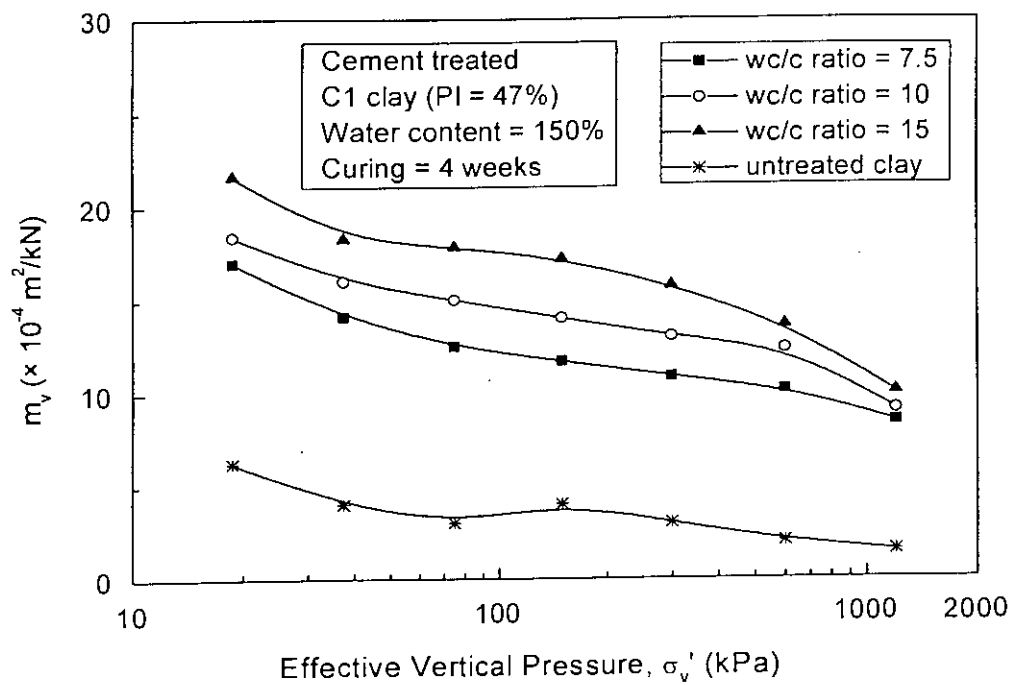


(a)

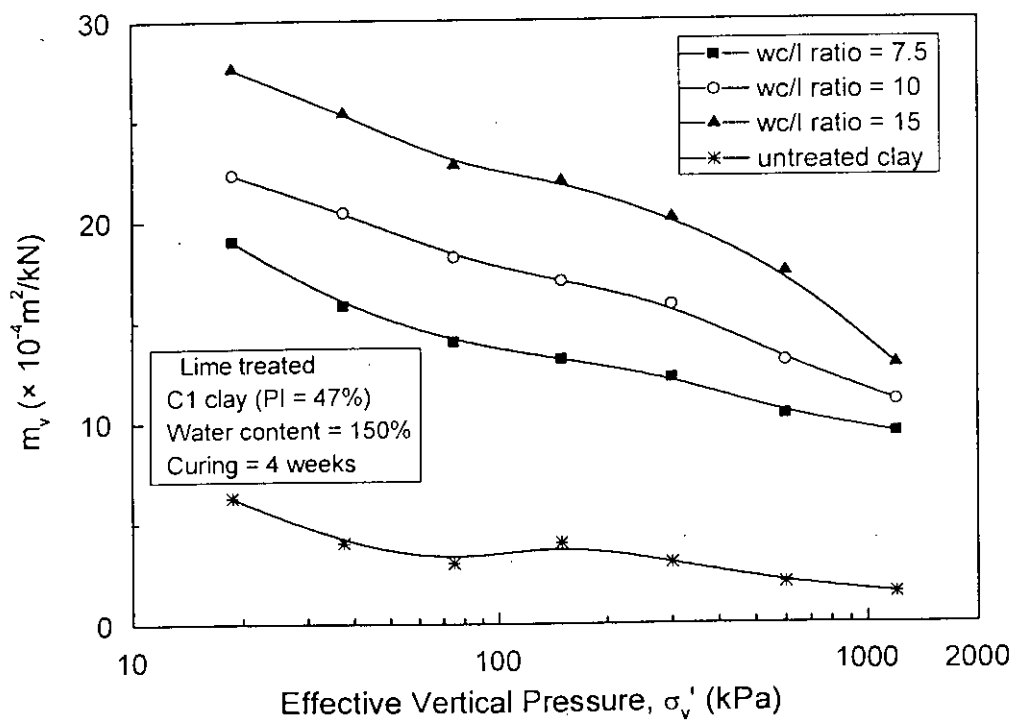


(b)

Fig. 5.5 Effect of Mixing Ratio on  $c_v - \log \sigma'_v$  Relationships of C1 Clay  
(a) Cement Treated and (b) Lime Treated

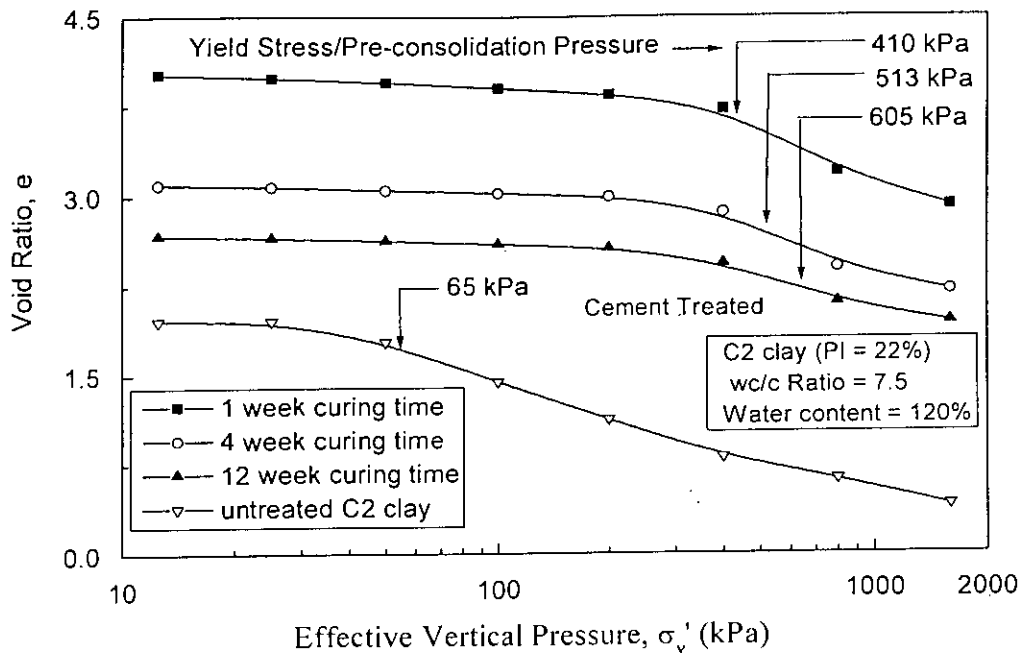


(a)

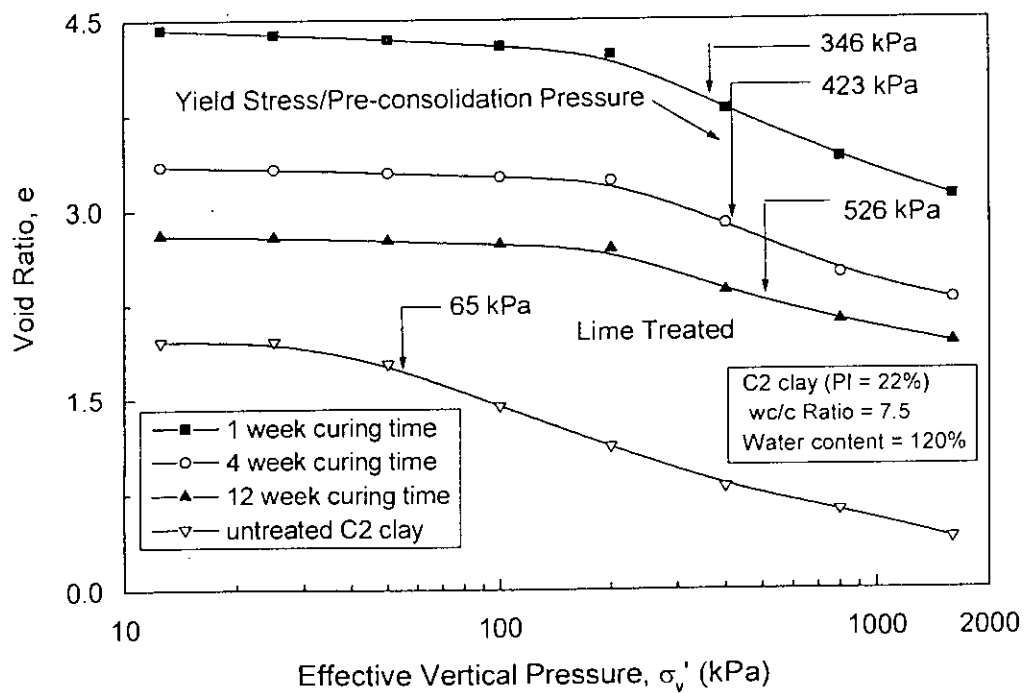


(b)

Fig. 5.6 Effect of Mixing Ratio on  $m_v - \log \sigma'_v$  Relationships of C1 Clay  
(a) Cement Treated and (b) Lime Treated

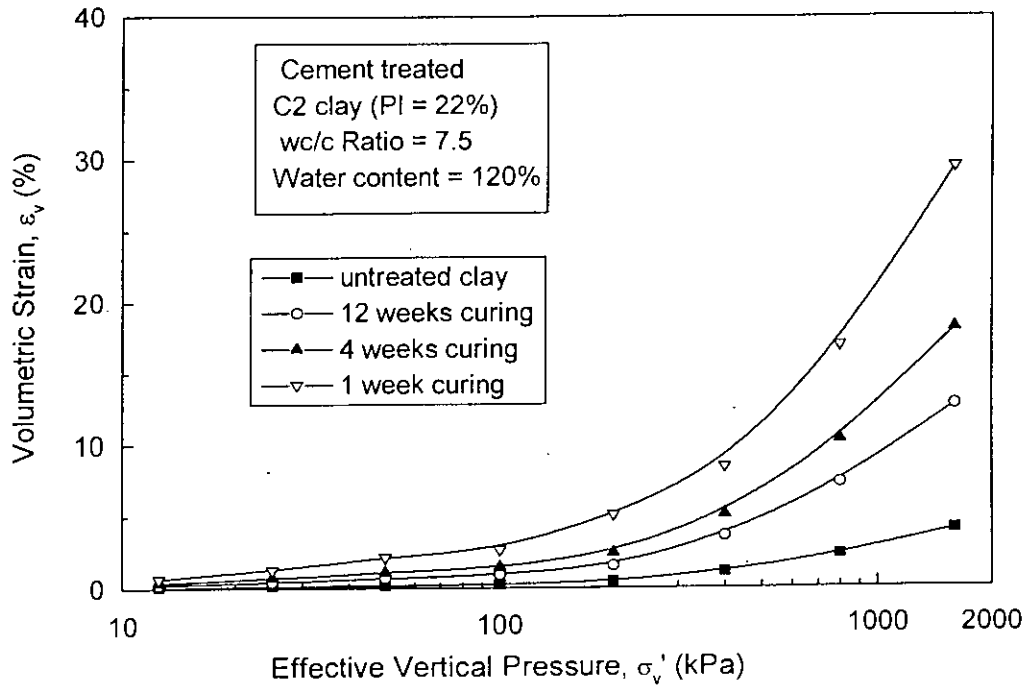


(a)

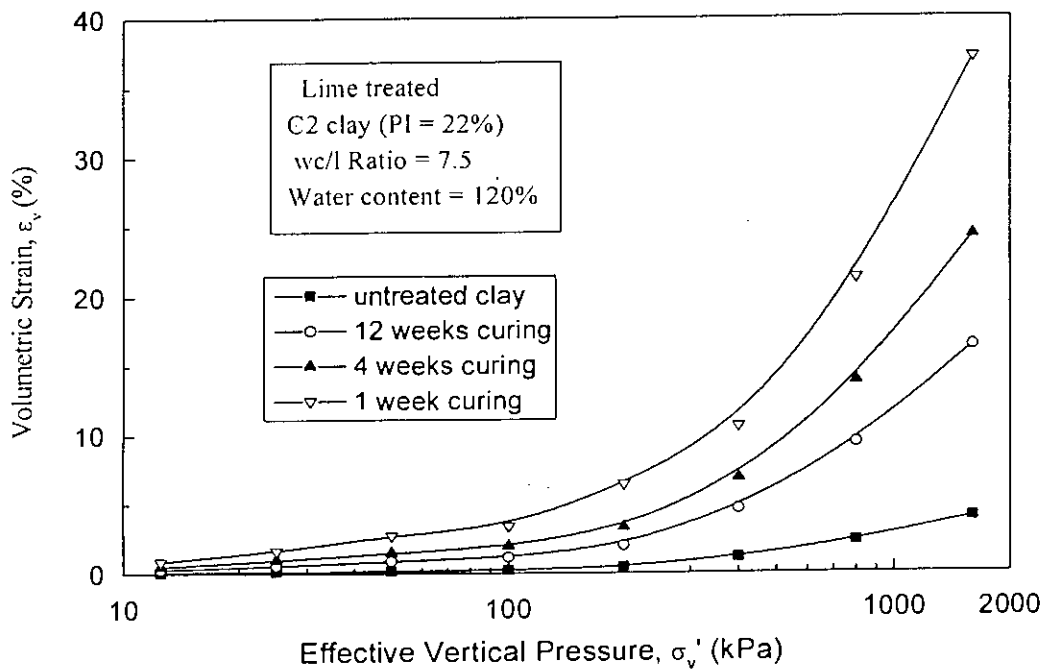


(b)

Fig.5.7 Effect of Curing Time on  $e - \log \sigma'_v$  Relationships of C2 Clay  
(a) Cement Treated and (b) Lime Treated



(a)



(b)

Fig. 5.8 Effect of Curing Time on  $\epsilon_v - \log \sigma'_v$  Relationships of C2 Clay  
(a) Cement Treated and (b) Lime Treated

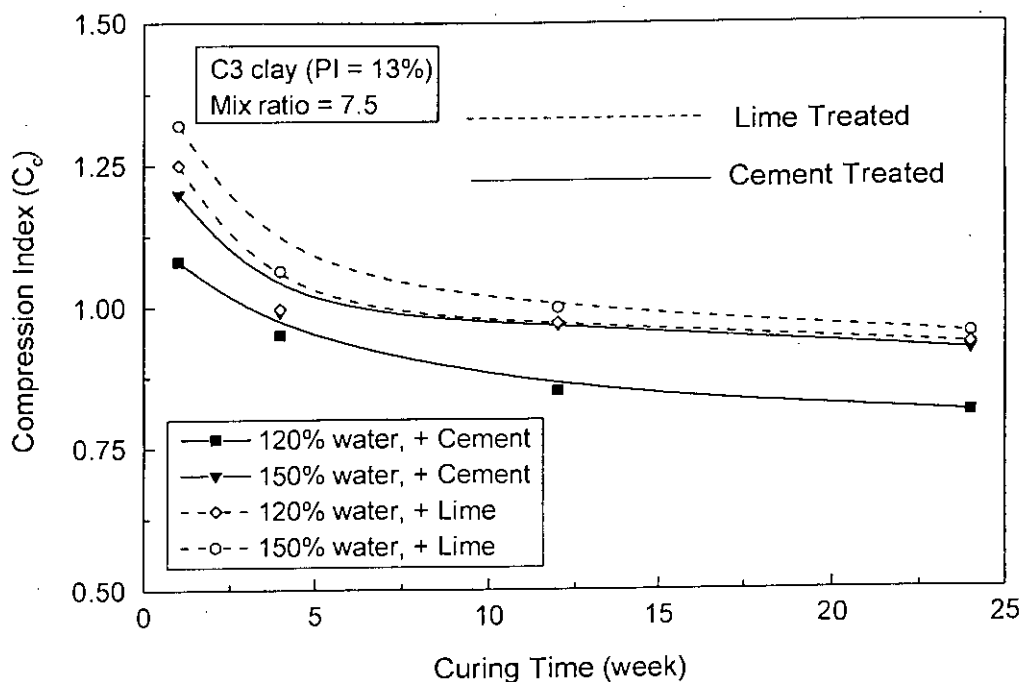


Fig. 5.9 Effect of Curing Time on Compression Index for Cement and Lime Treated C3 Clay

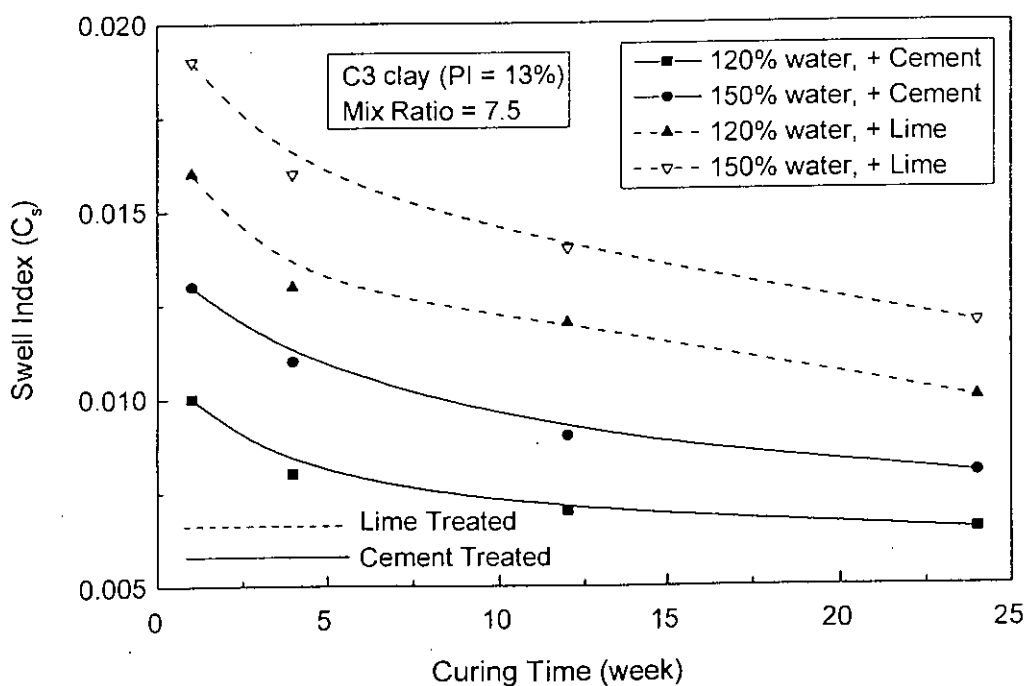


Fig. 5.10 Effect of Curing Time on Swell Index for Cement and Lime Treated C3 Clay

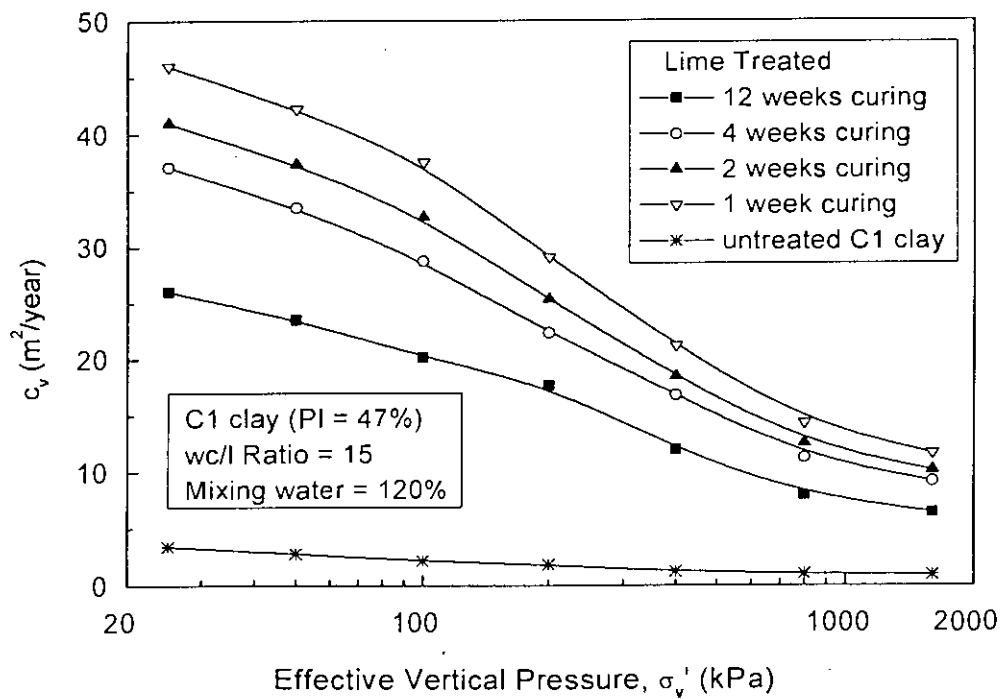
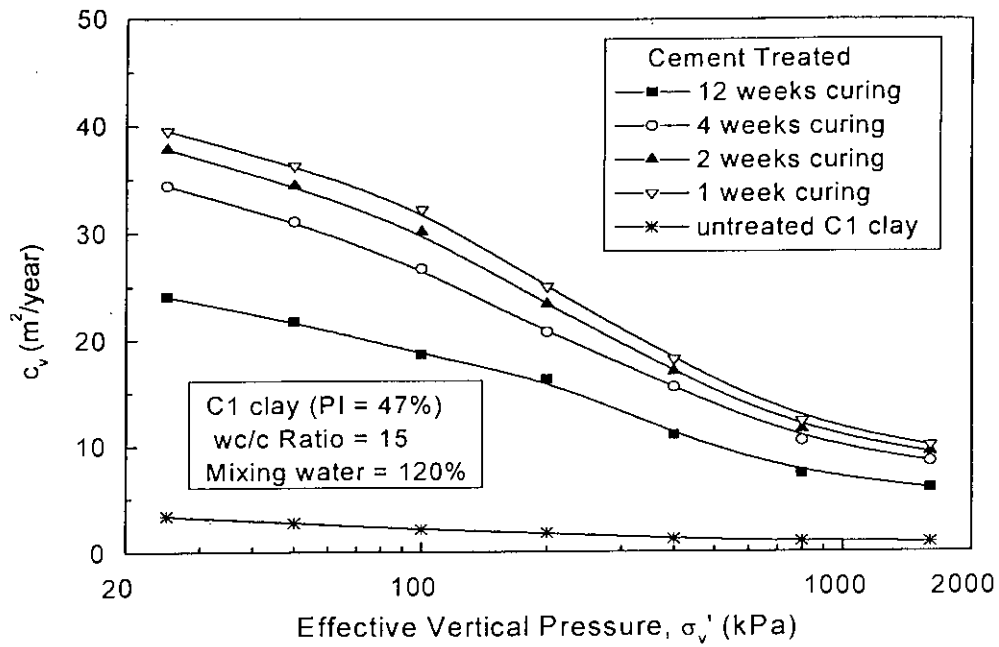
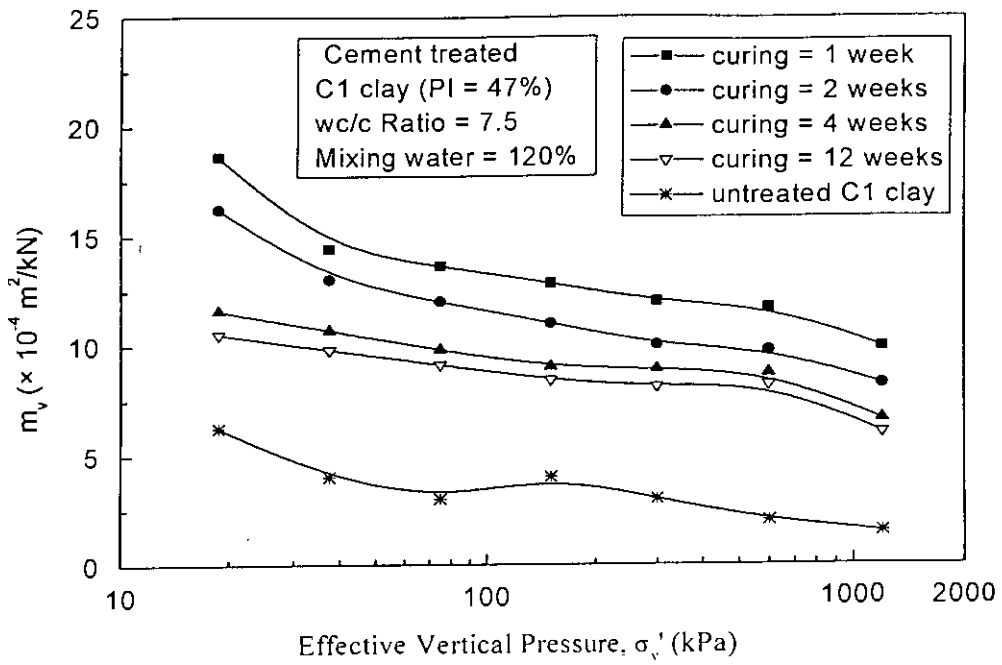
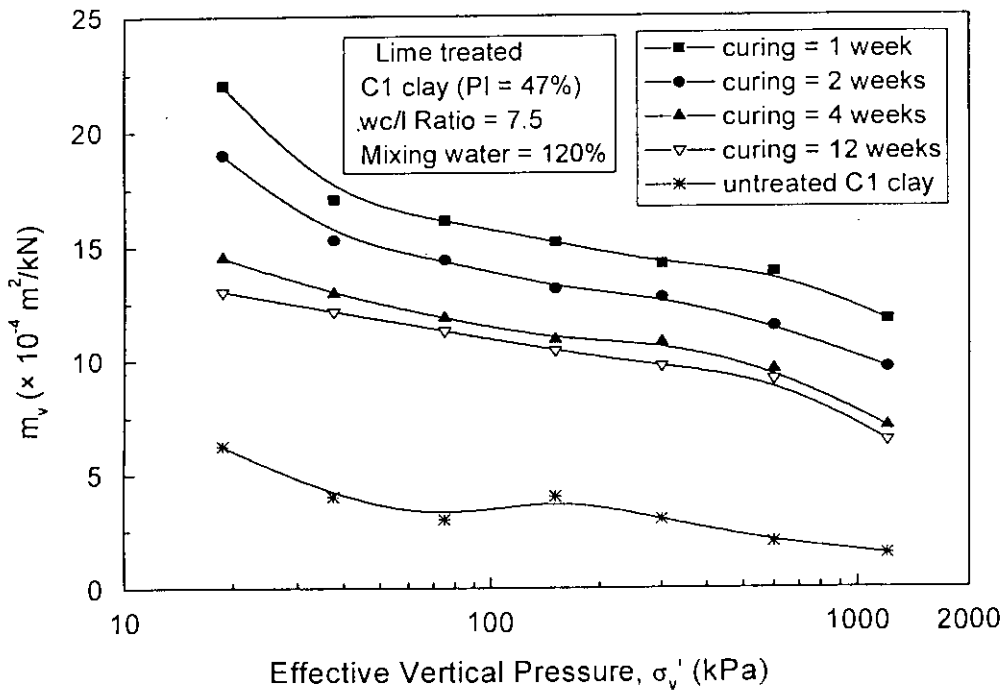


Fig. 5.11 Effect of Curing Time on  $c_v - \log \sigma'_v$  Relationships of C1 Clay  
(a) Cement Treated and (b) Lime Treated



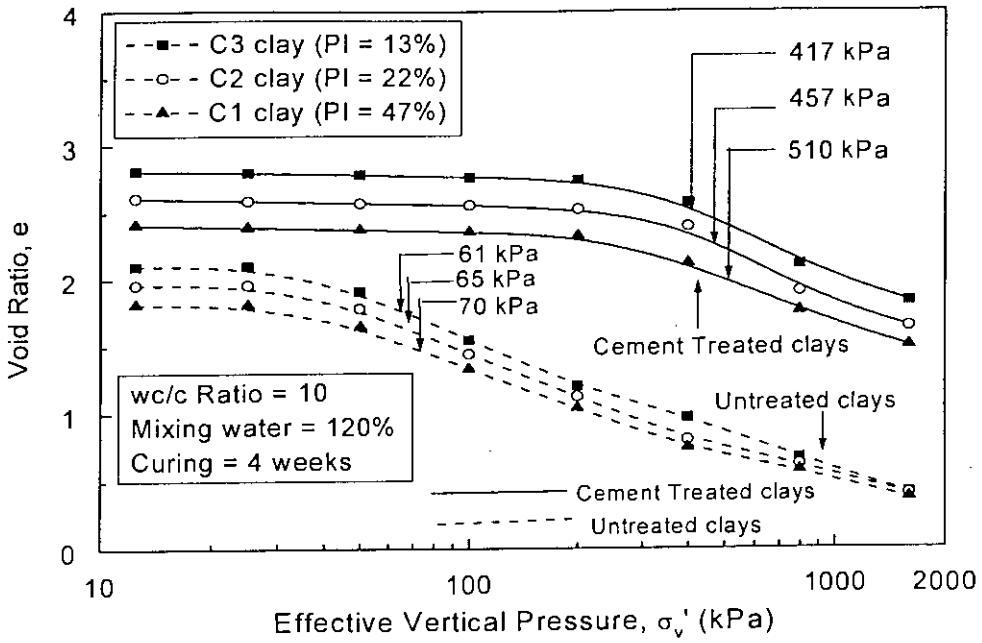
(a)



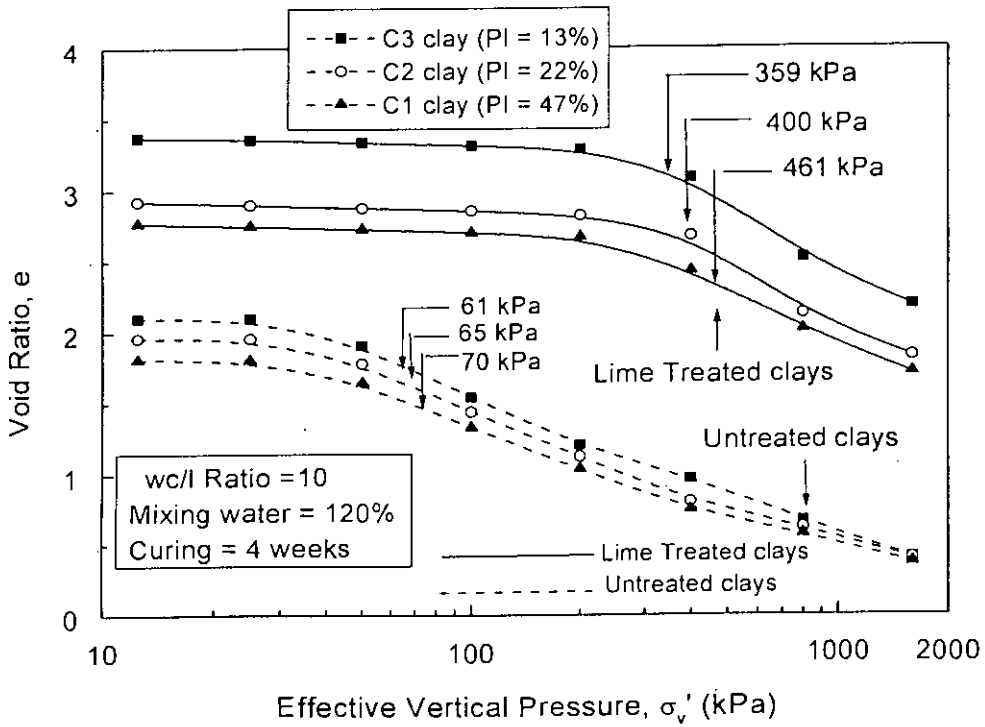
(b)

Fig. 5.12 Effect of Curing Time on  $m_v - \log \sigma'_v$  Relationships of C1 Clay  
(a) Cement Treated and (b) Lime Treated



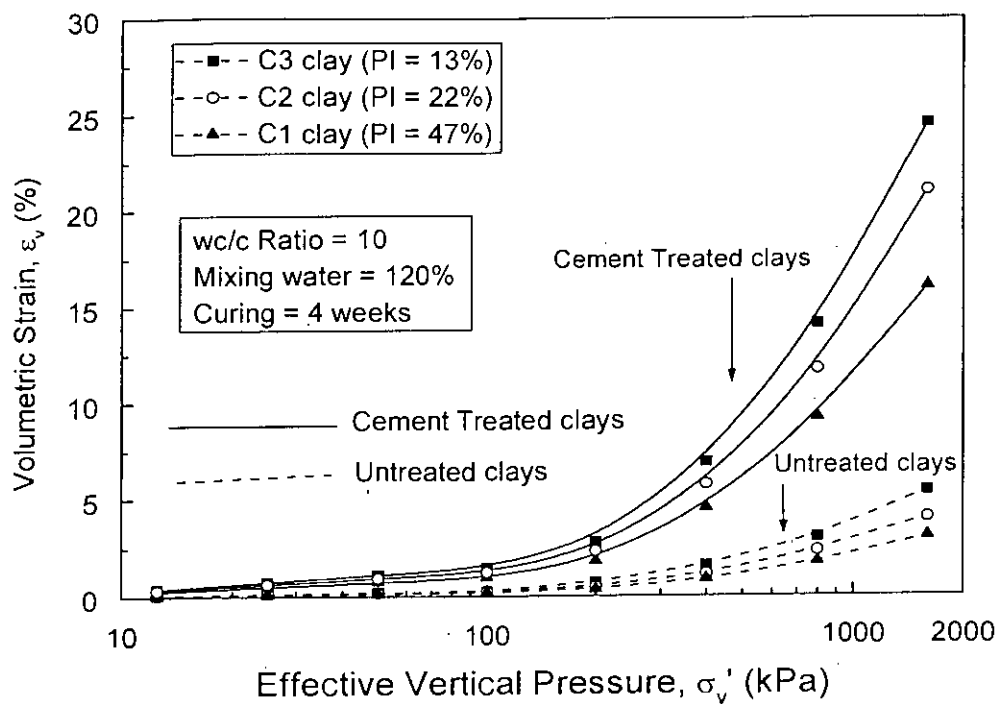


(a)

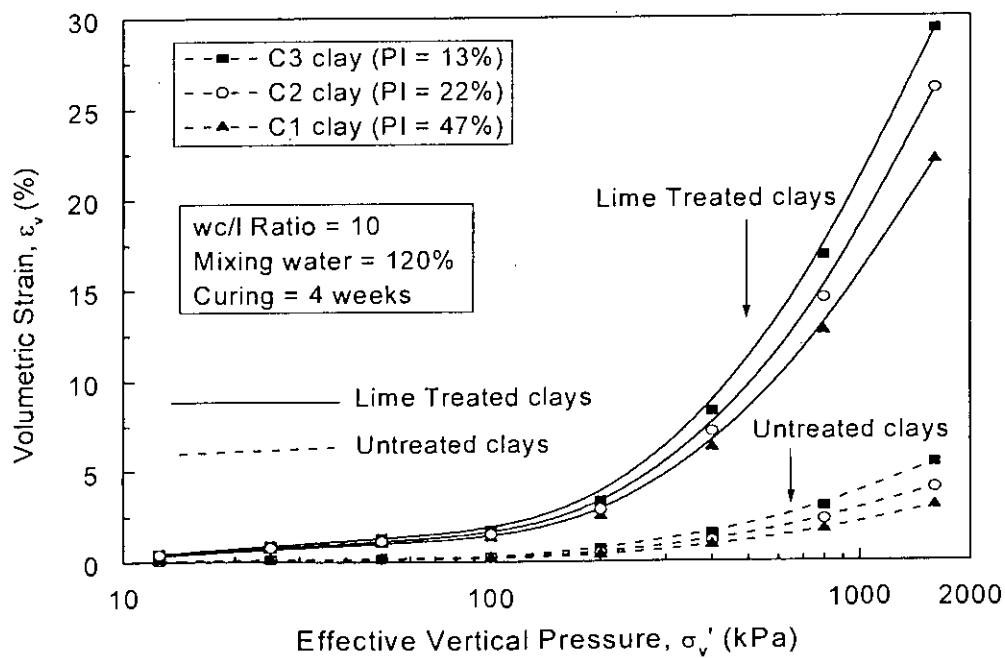


(b)

Fig. 5.13 Effect of Clay Type on  $e - \log \sigma'_v$  Relationships of Clays  
 (a) Cement Treated and (b) Lime Treated



(a)



(b)

Fig. 5.14 Effect of Clay Type on  $\epsilon_v - \log \sigma'_v$  Relationships of Clays  
 (a) Cement Treated and (b) Lime Treated

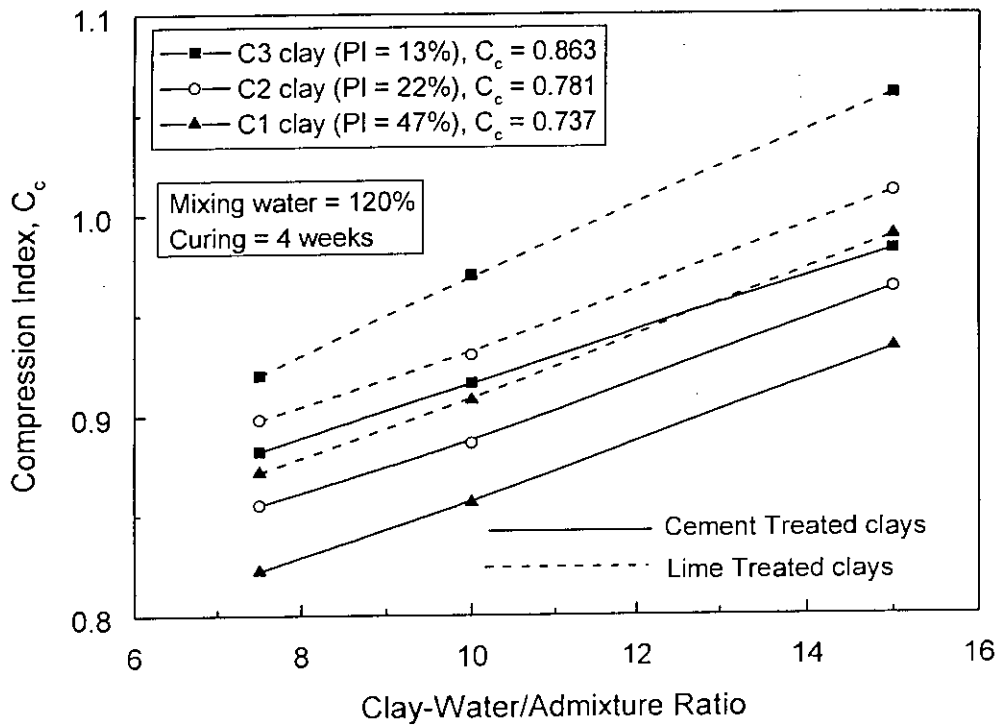


Fig. 5.15 Effect of Clay Type on Compression Index of Cement and Lime Treated Clays

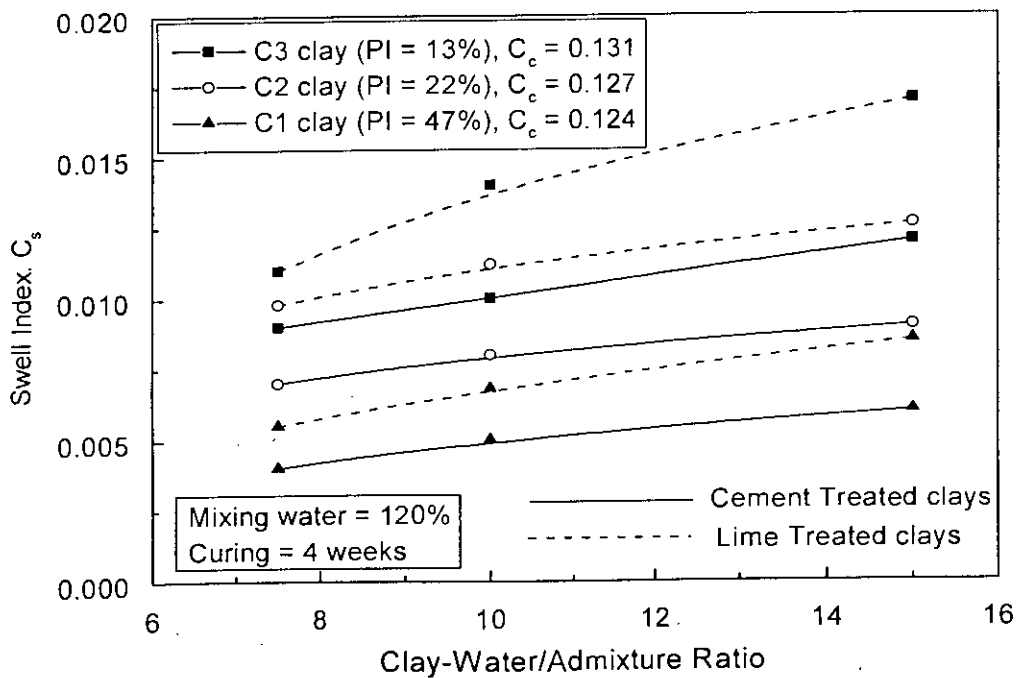
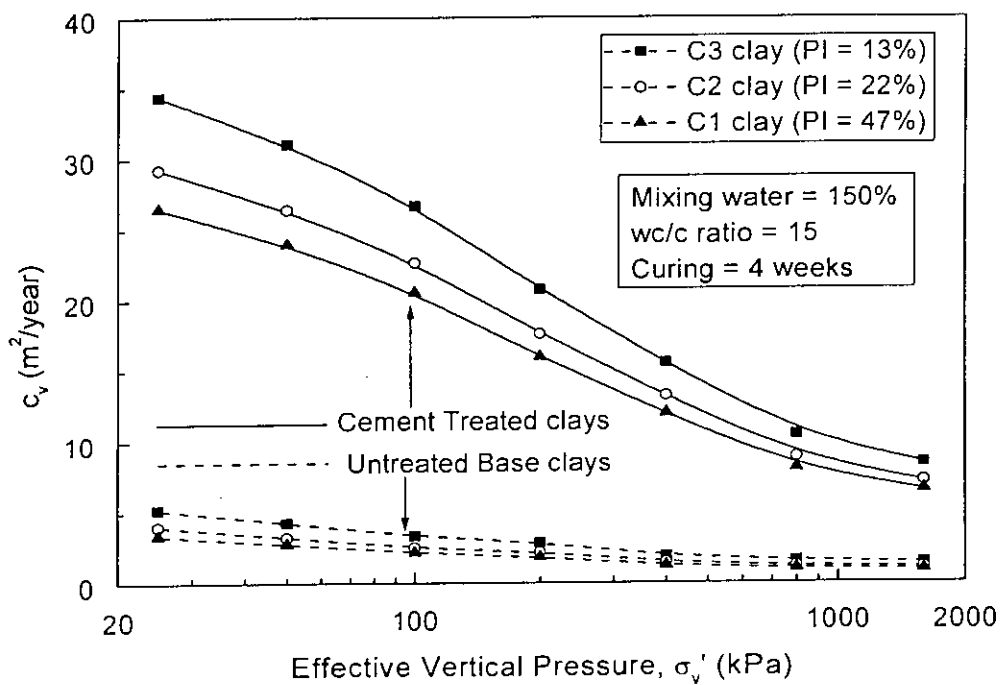
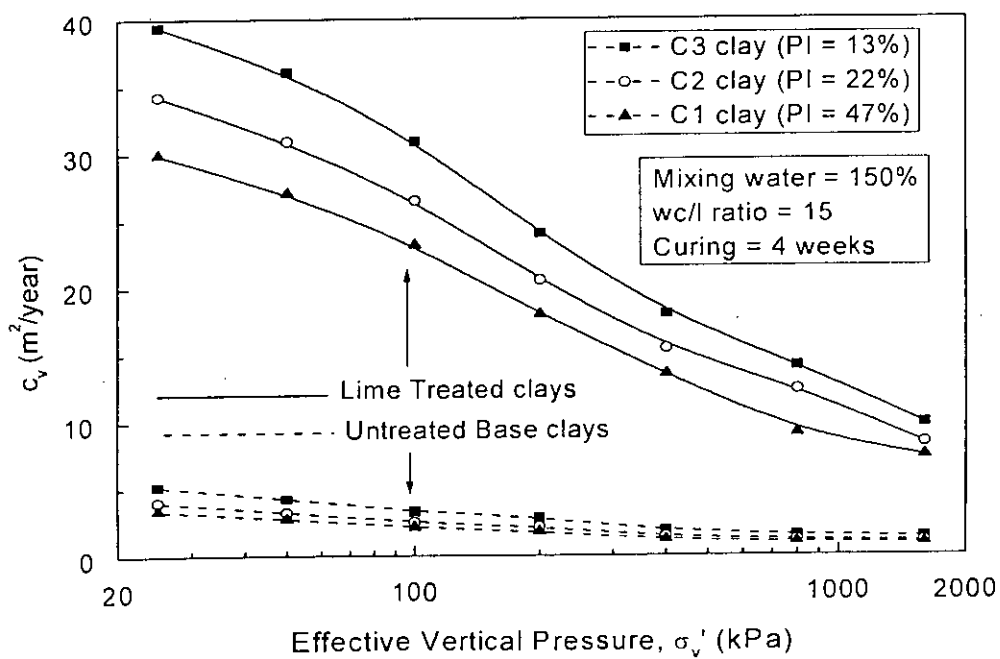


Fig. 5.16 Effect of Clay Type on Swell Index of Cement and Lime Treated Clays

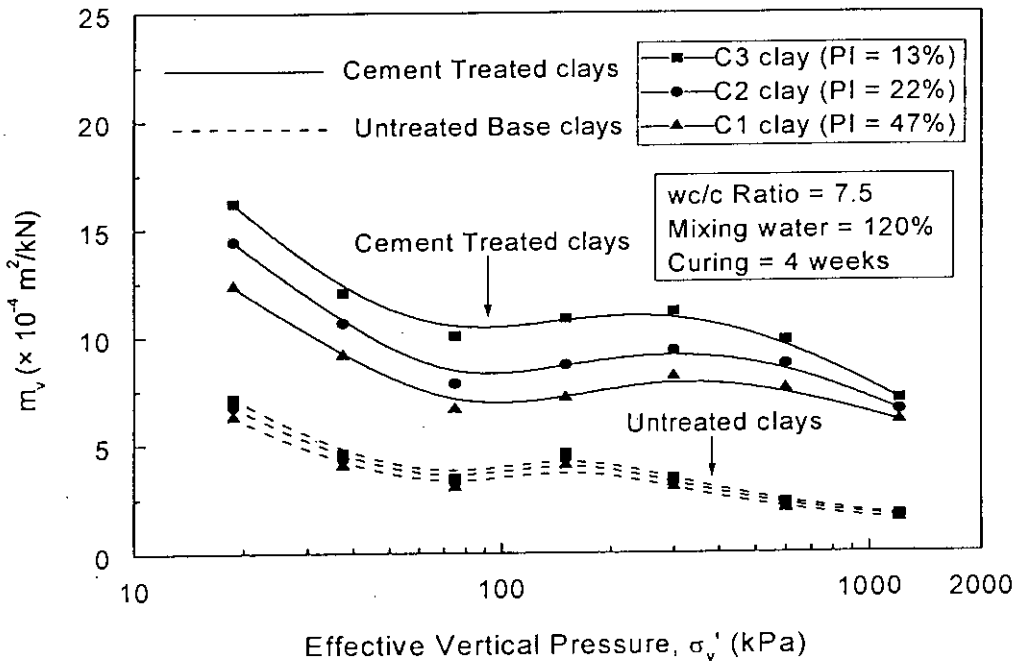


(a)

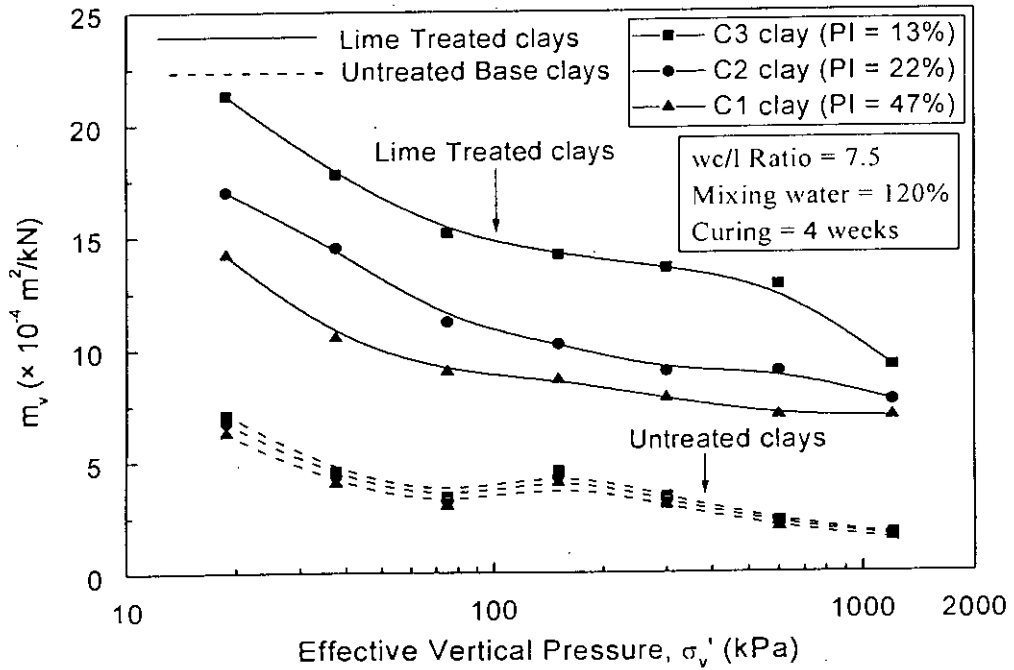


(b)

Fig. 5.17 Effect of Clay Type on  $c_v - \log \sigma'_v$  Relationships of Clays  
(a) Cement Treated and (b) Lime Treated

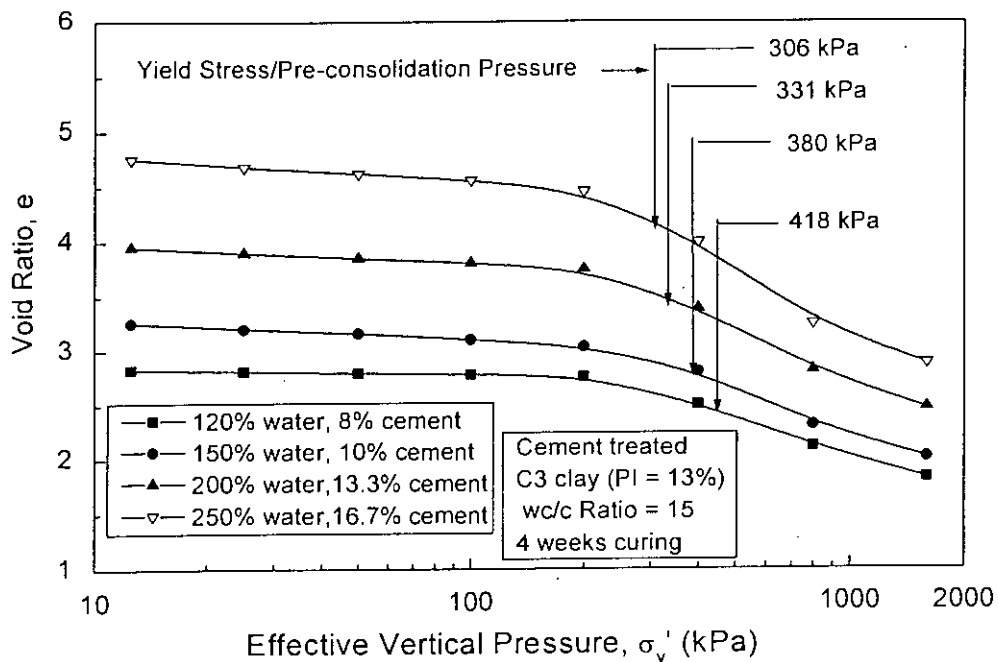


(a)

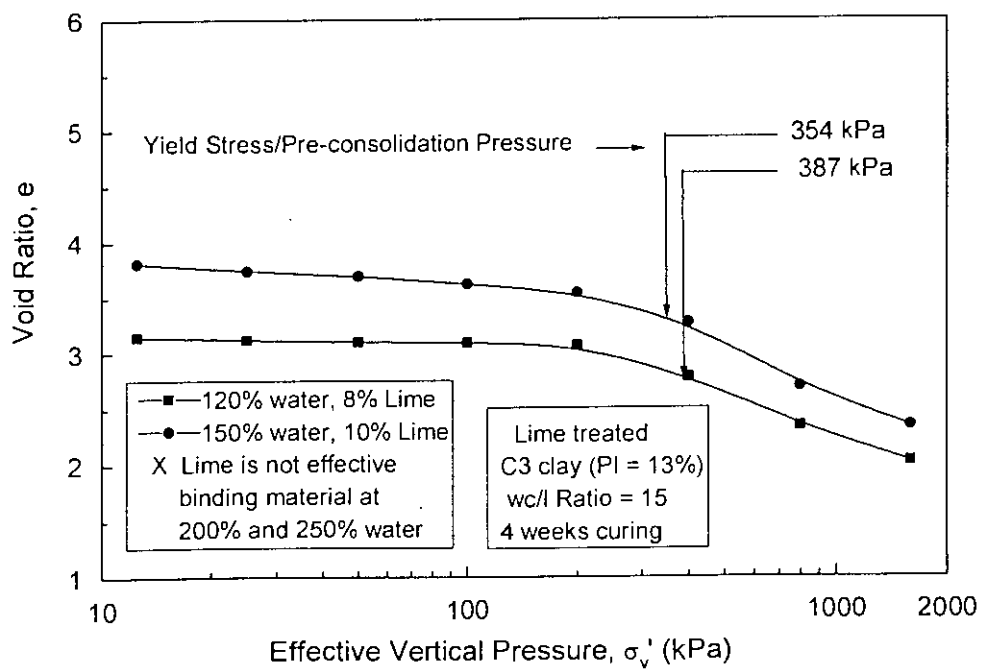


(b)

Fig. 5.18 Effect of Clay Type on  $m_v - \log \sigma'_v$  Relationships of Clays  
 (a) Cement Treated and (b) Lime Treated

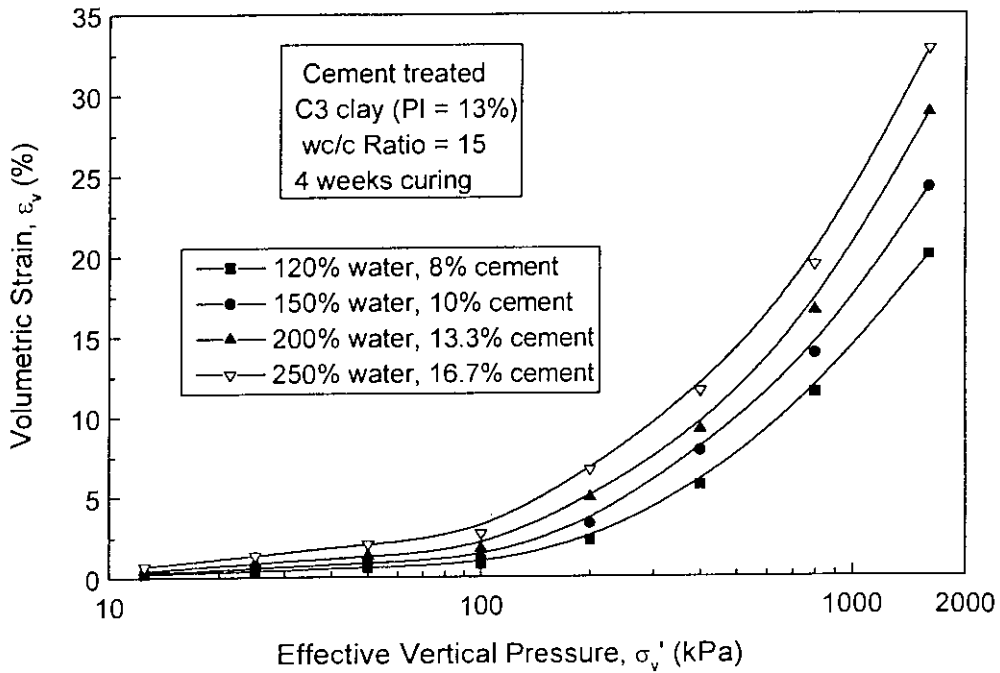


(a)

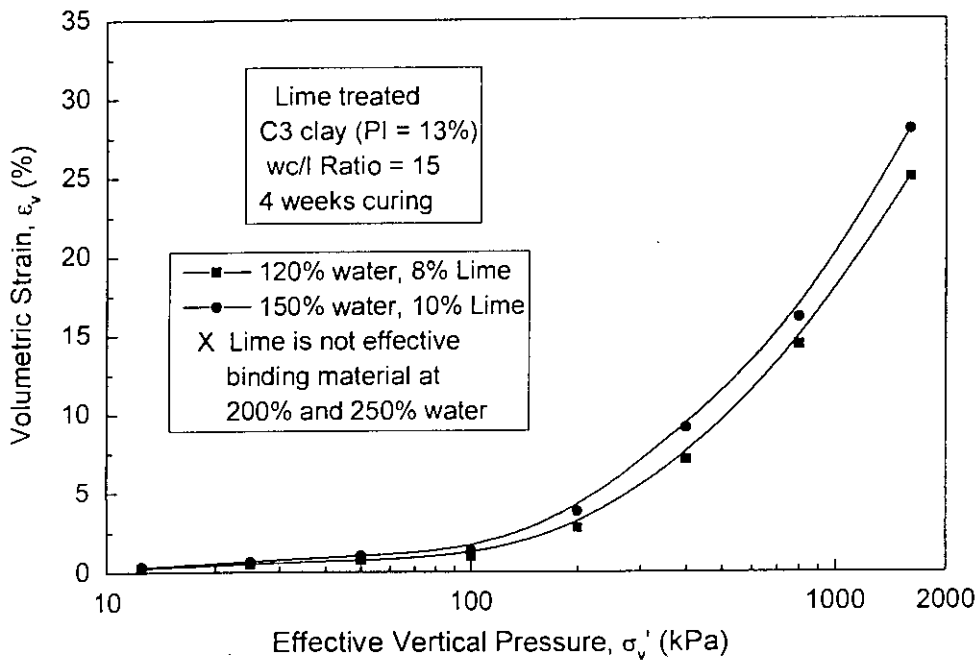


(b)

Fig. 5.19 Effect of Clay-Water Content on  $e - \log \sigma'_v$  Relationships of C3 Clay  
(a) Cement Treated and (b) Lime Treated



(a)



(b)

Fig. 5.20 Effect of Clay-Water Content on  $\epsilon_v - \log \sigma'_v$  Relationships of C3 Clay (a) Cement Treated and (b) Lime Treated

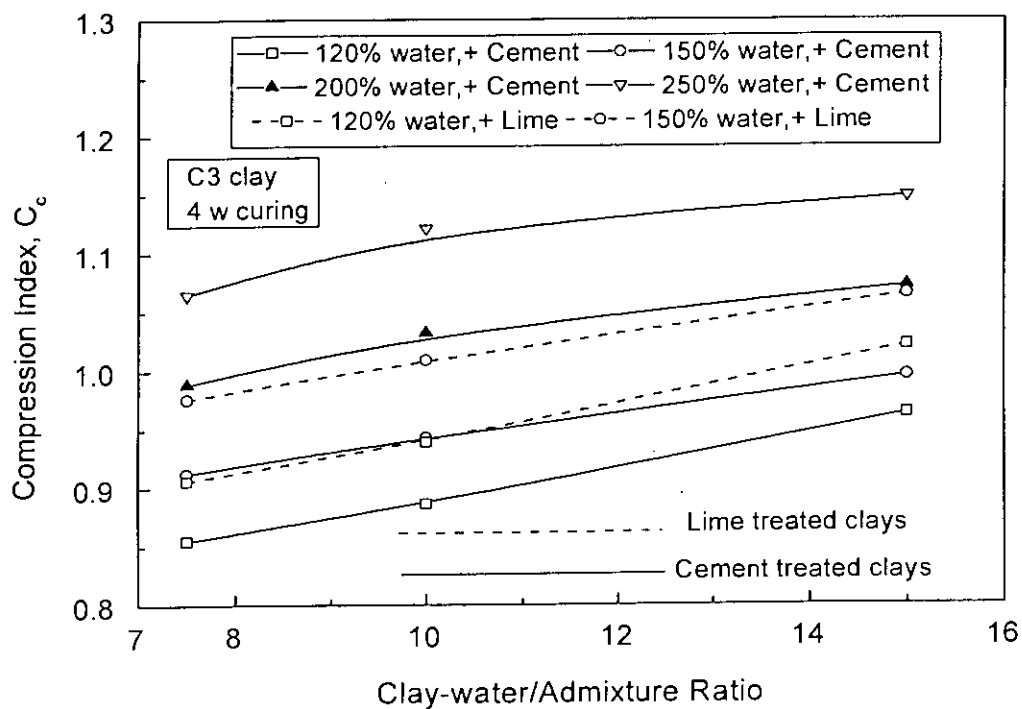


Fig. 5.21 Effect of Clay-Water Content on Compression Index for Cement and Lime Treated C3 Clay

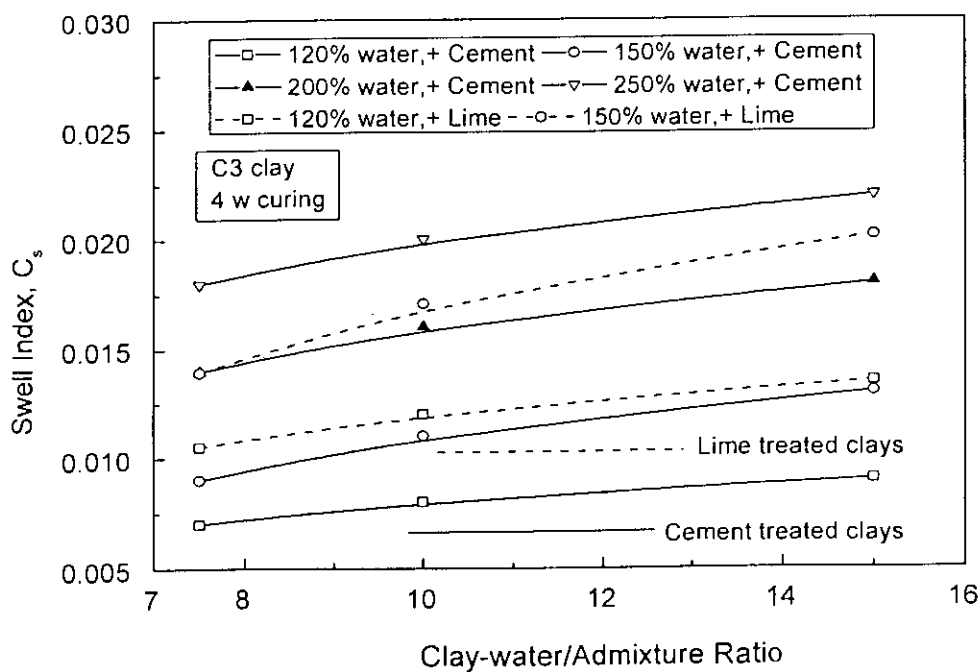
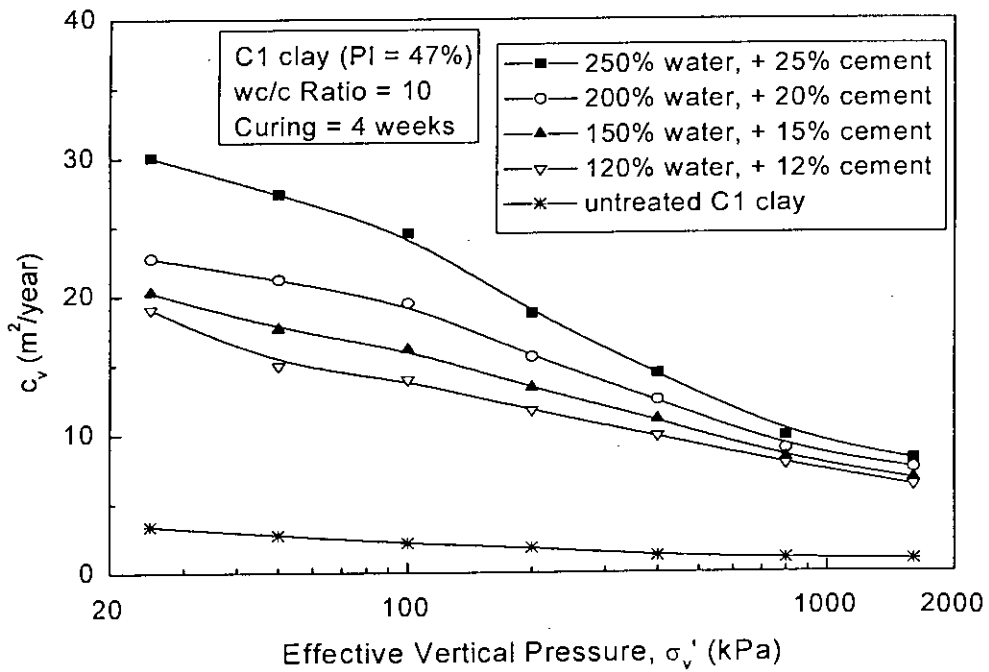
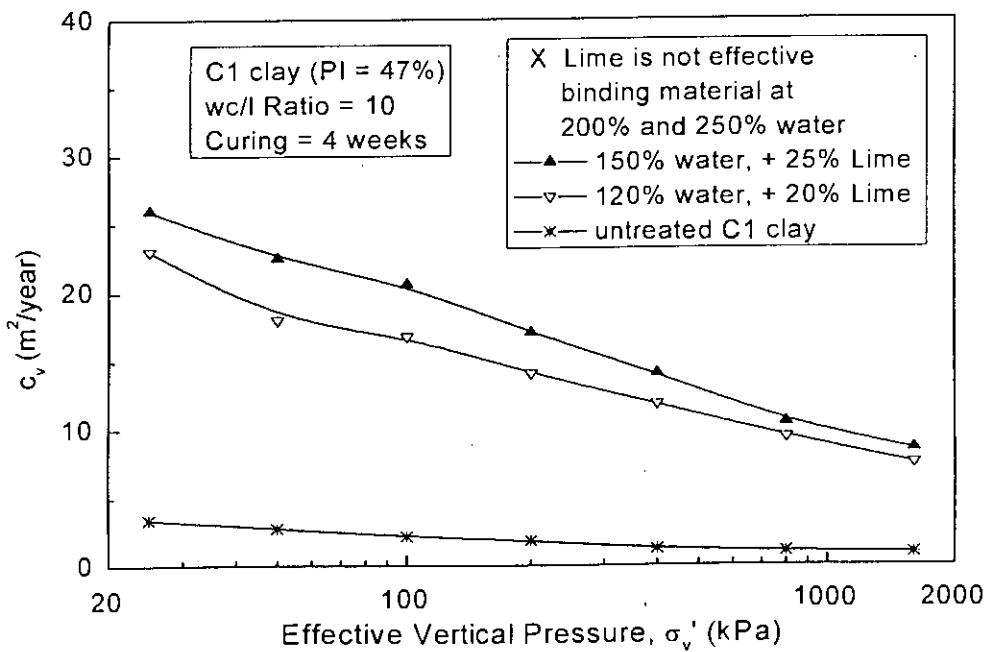


Fig. 5.22 Effect of Clay-Water Content on Swell Index for Cement and Lime Treated C3 Clay



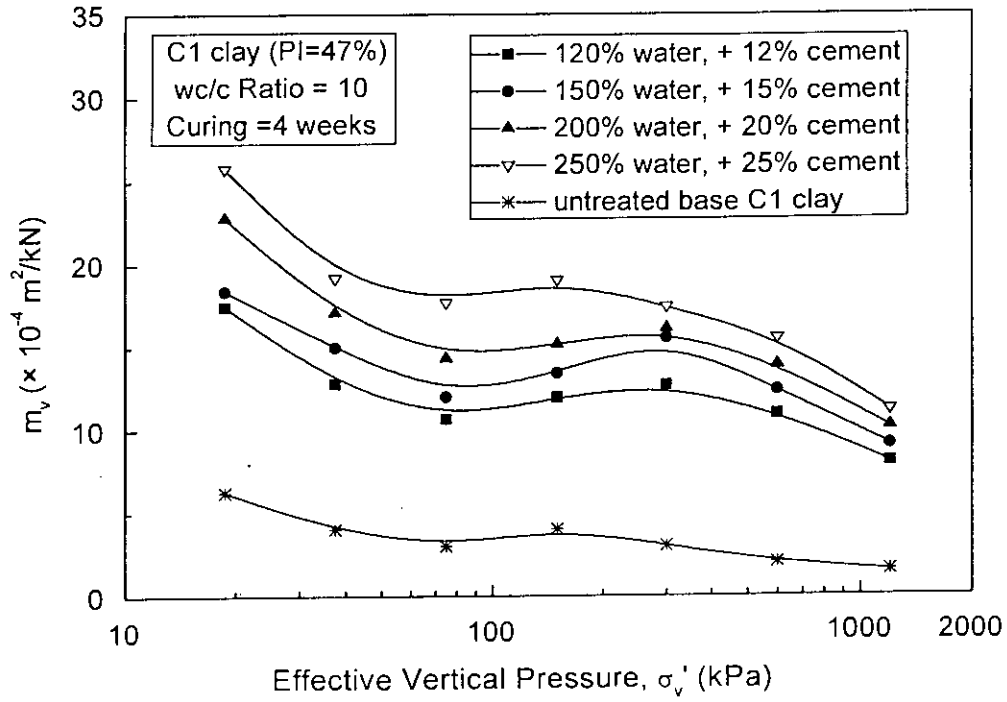


(a)

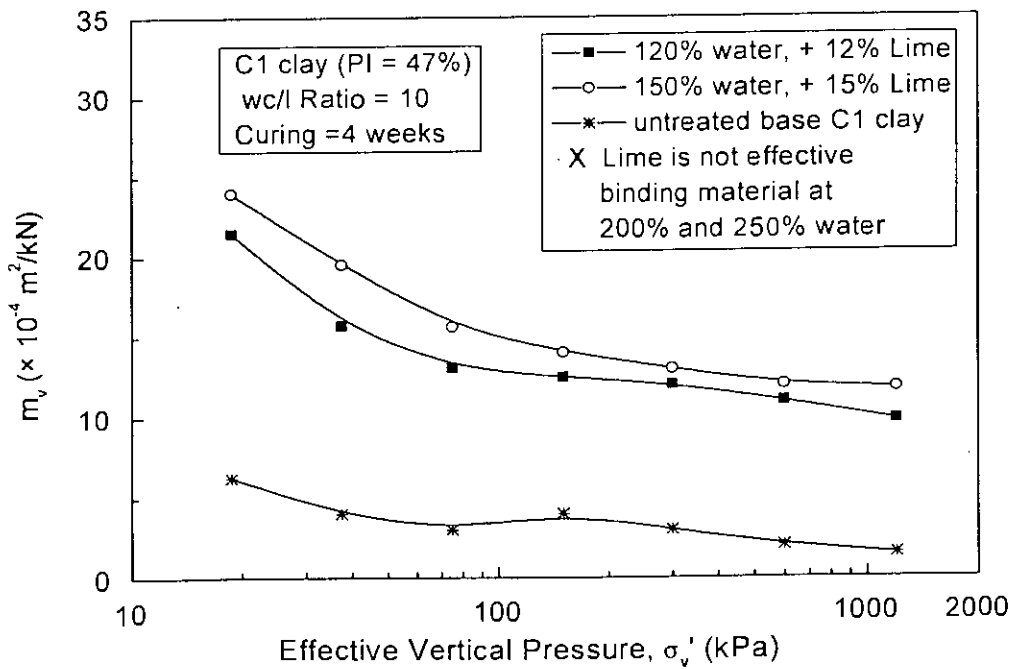


(b)

Fig. 5.23 Effect of Clay-Water Content on  $c_v - \log \sigma_v'$  Relationships of C1 Clay  
(a) Cement Treated and (b) Lime Treated

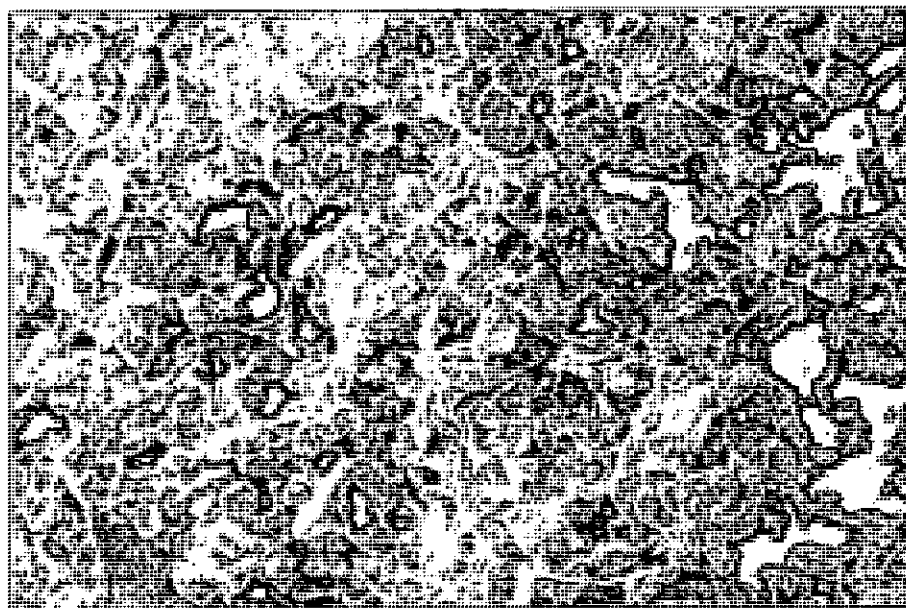


(a)

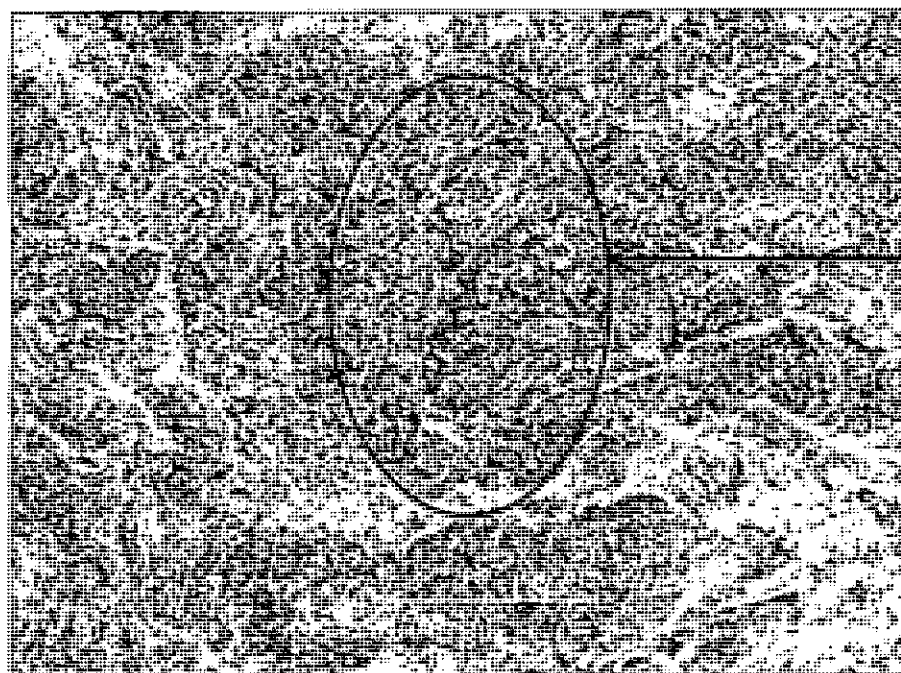


(b)

Fig. 5.24 Effect of Clay-Water Content on  $m_v - \log \sigma'_v$  Relationships of C1 Clay (a) Cement Treated and (b) Lime Treated

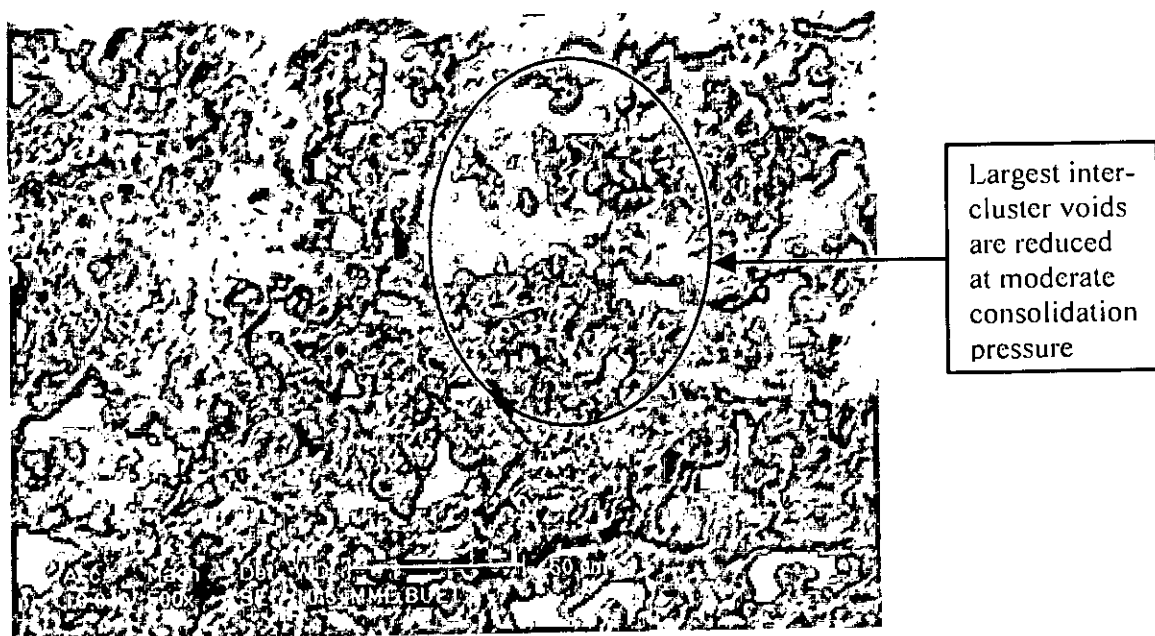


(a)



(b)

Fig. 5.25 SEM Images at Zero Pressure of CI Clays  
(a) Untreated (Remoulded) and (b) 16% Cement

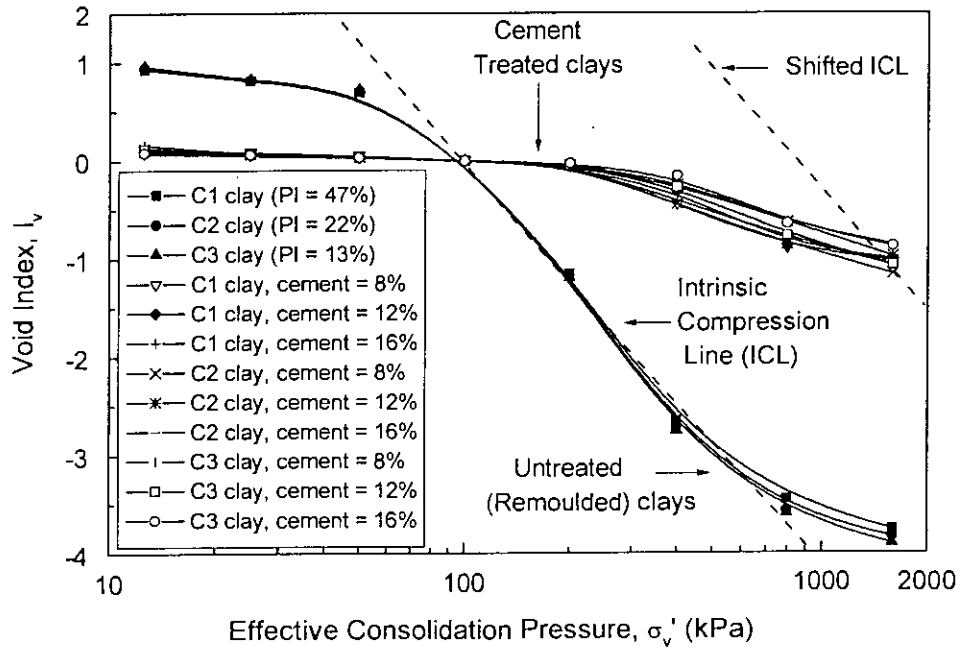


(a)

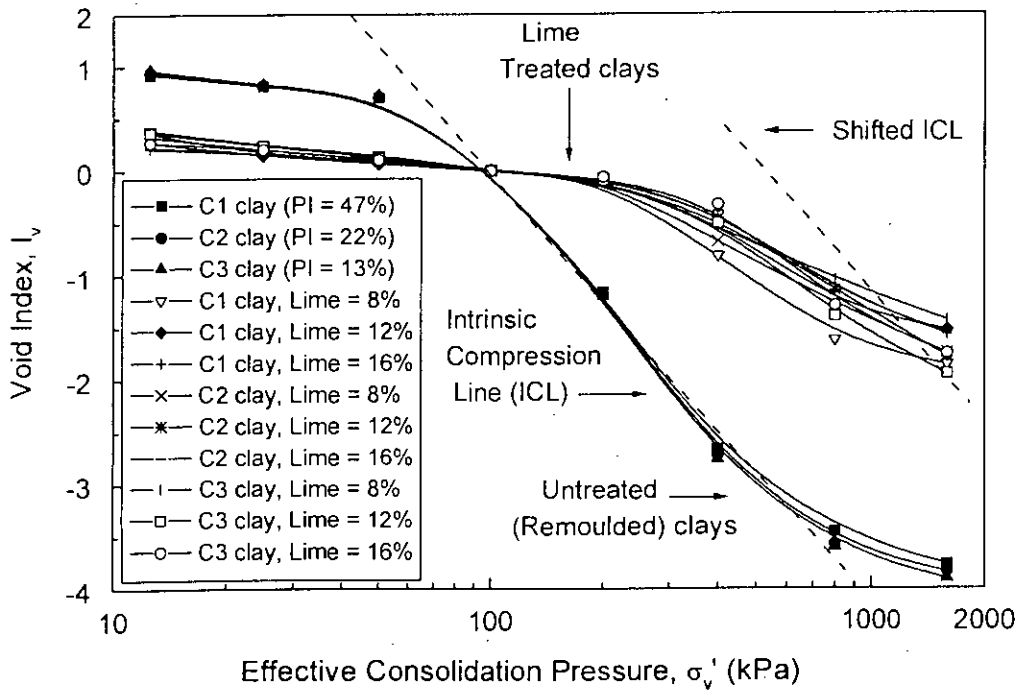


(b)

Fig. 5.26 SEM Images of 16% Cement Treated CI Clays at Different Consolidation Pressure at (a)  $\sigma'_v = 400$  kPa and (b)  $\sigma'_v = 1600$  kPa

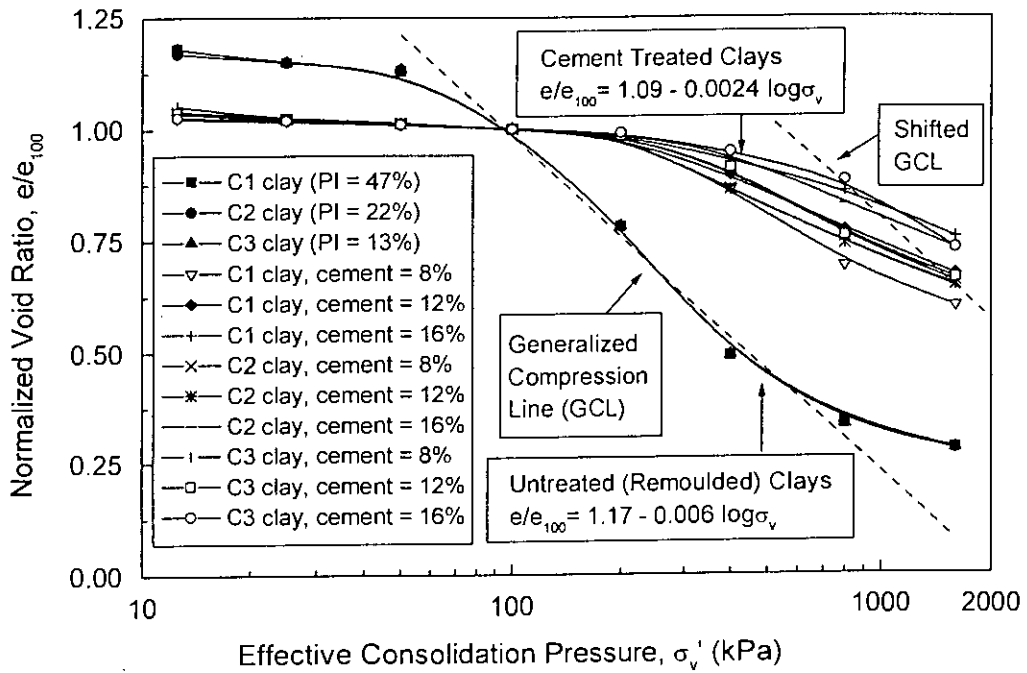


(a)

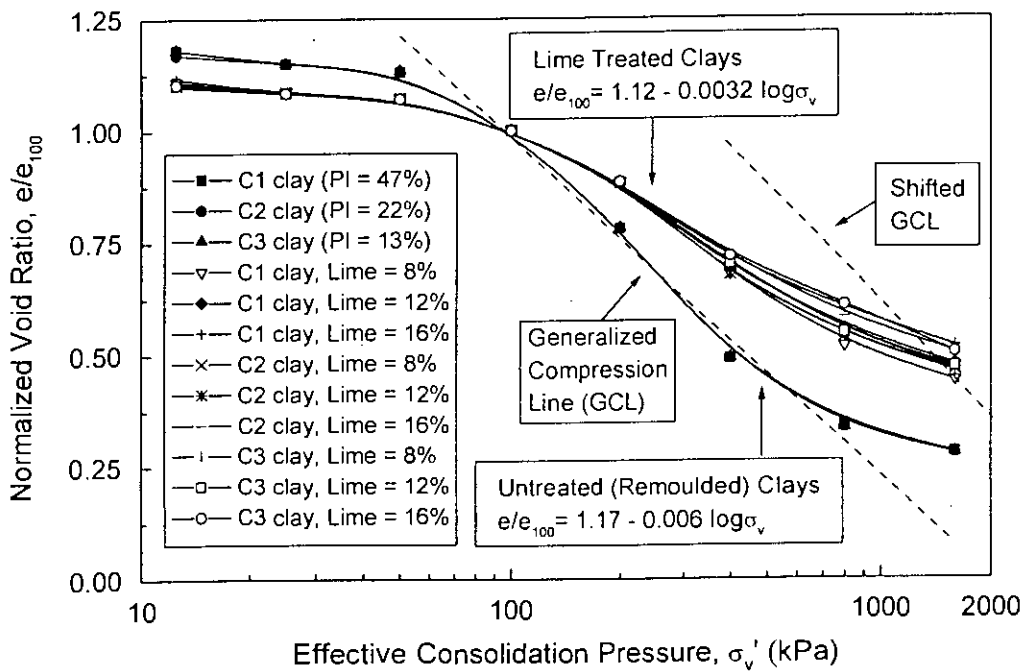


(b)

Fig. 5.27 Intrinsic Compression Line (ICL) for Clays (a) Cement Treated and (b) Lime Treated



(a)

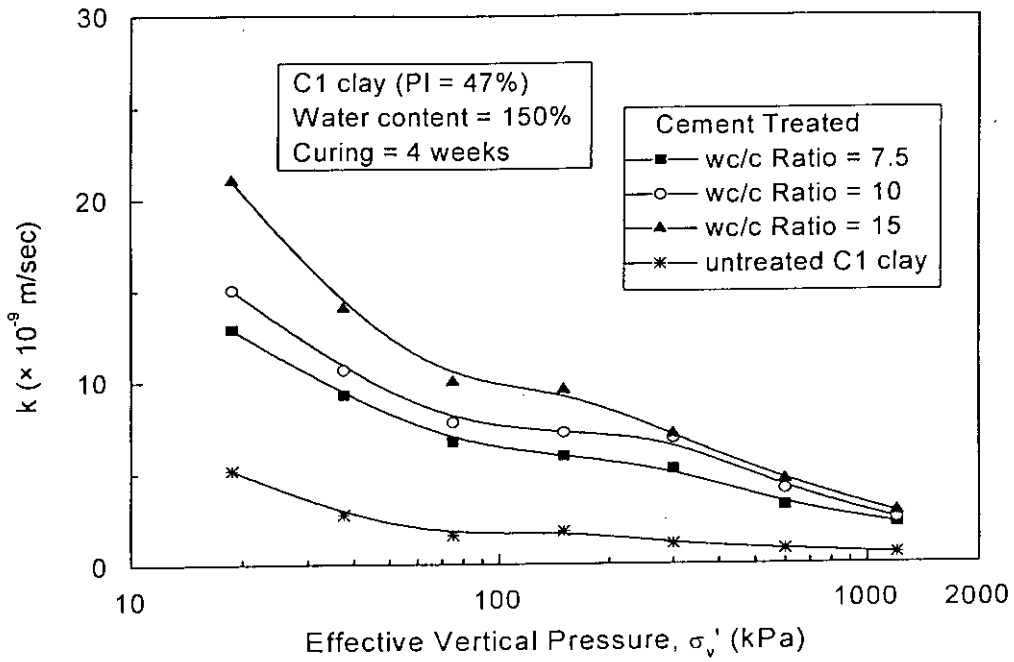


(b)

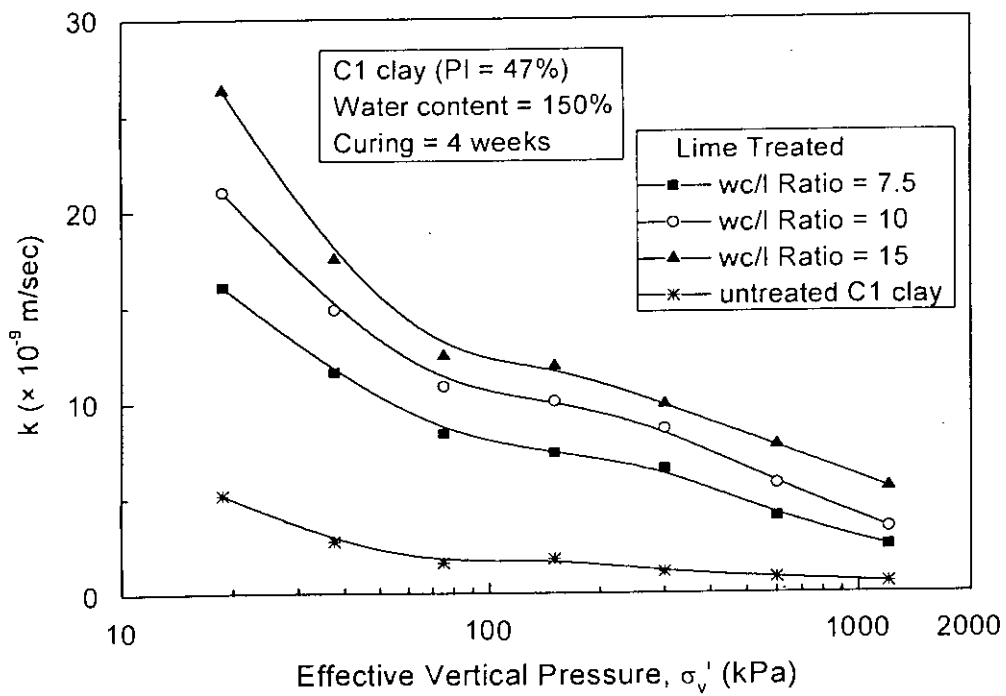
Fig. 5.28 Generalized Compression Line (GCL) for Clays (a) Cement Treated and (b) Lime Treated

**Table 5.4 Permeability Properties (4 weeks Curing) for Cement Treated and Lime Treated Clays**

Admix- ture	$w_i$ (%)	wc/c Ratio	C1 clay (PI = 47%)	C2 clay (PI = 22%)	C3 clay (PI = 13%)
			$k (\times 10^{-9} \text{ m/sec})$ at $\sigma_v' = 18.75 \text{ kPa}$	$k (\times 10^{-9} \text{ m/sec})$ at $\sigma_v' = 18.75 \text{ kPa}$	$k (\times 10^{-9} \text{ m/sec})$ at $\sigma_v' = 18.75 \text{ kPa}$
Cement	120%	7.5	10.9	13.6	17.5
		10	12.8	15.6	19.0
		15	16.2	20.1	23.1
	150%	7.5	12.9	14.1	16.7
		10	15.0	19.6	23.6
		15	21.0	24.1	26.6
Lime	120%	7.5	13.5	16.7	19.6
		10	16.1	20.1	25.6
		15	21.0	23.6	27.9
	150%	7.5	16.5	18.8	22.1
		10	22.8	25.3	28.1
		15	30.0	32.1	34.4
Untreated base clays			4.28	4.94	6.16



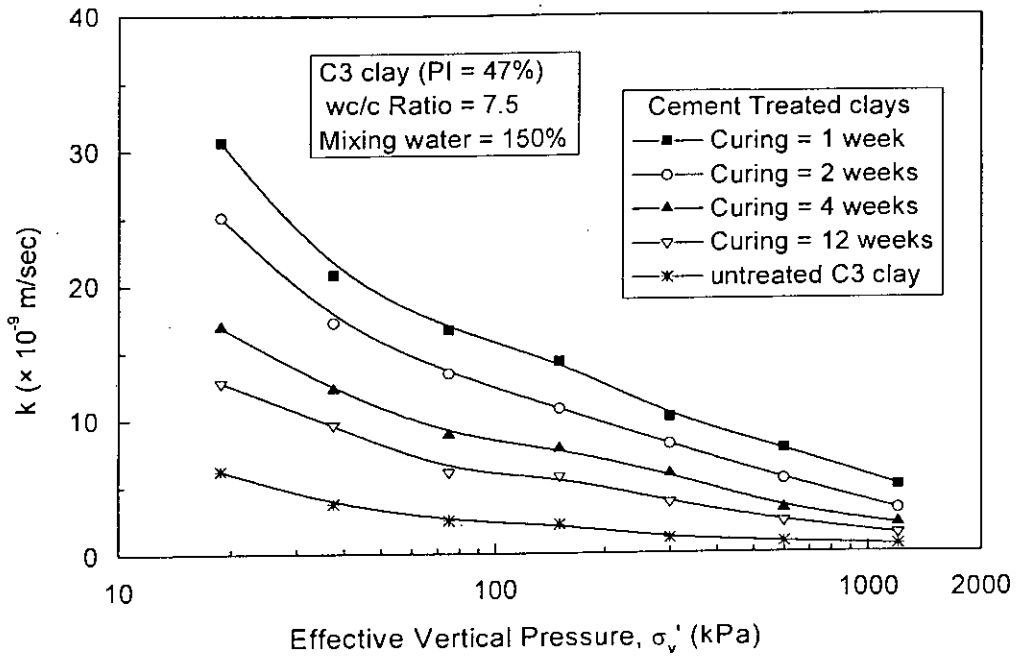
(a)



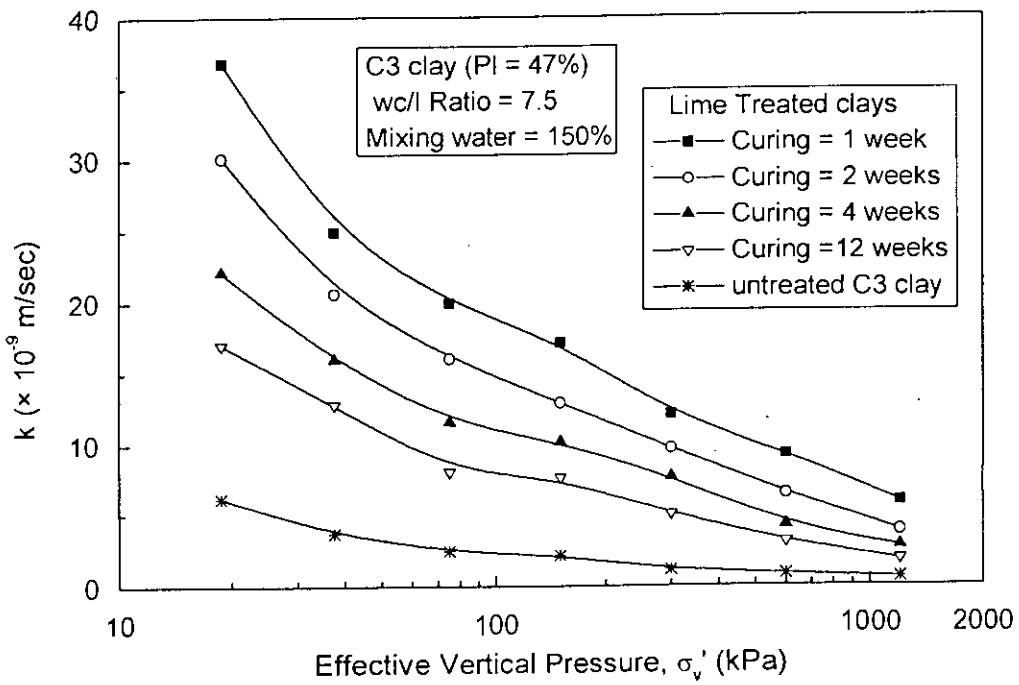
(b)

Fig. 5.29 Effect of Mixing Ratio on  $k - \log \sigma'_v$  Relationships of C1 Clay  
(a) Cement Treated and (b) Lime Treated



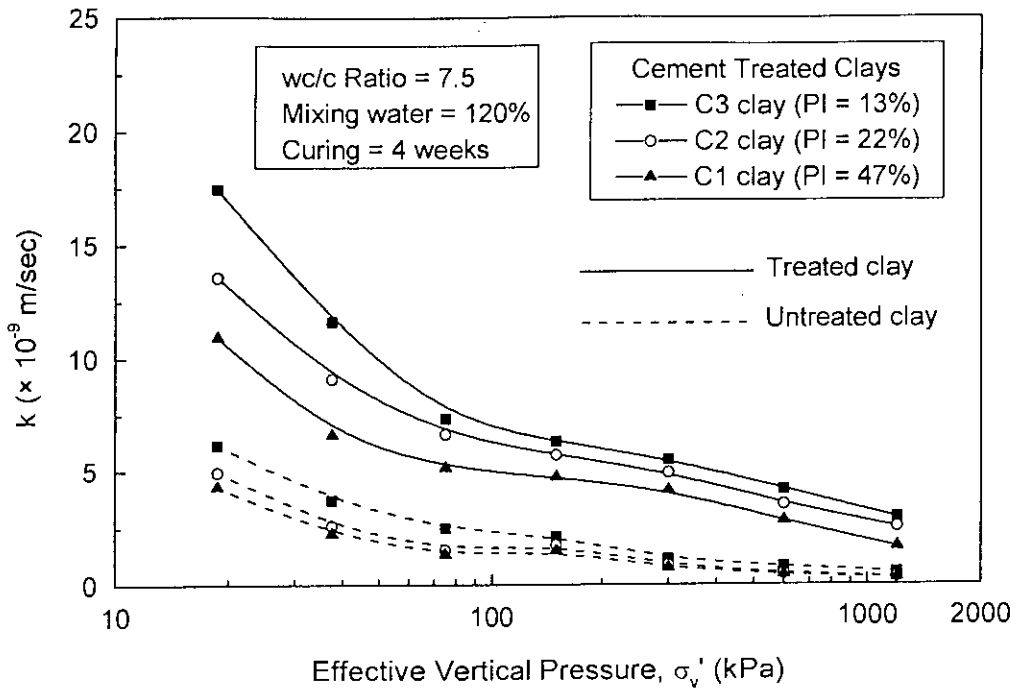


(a)

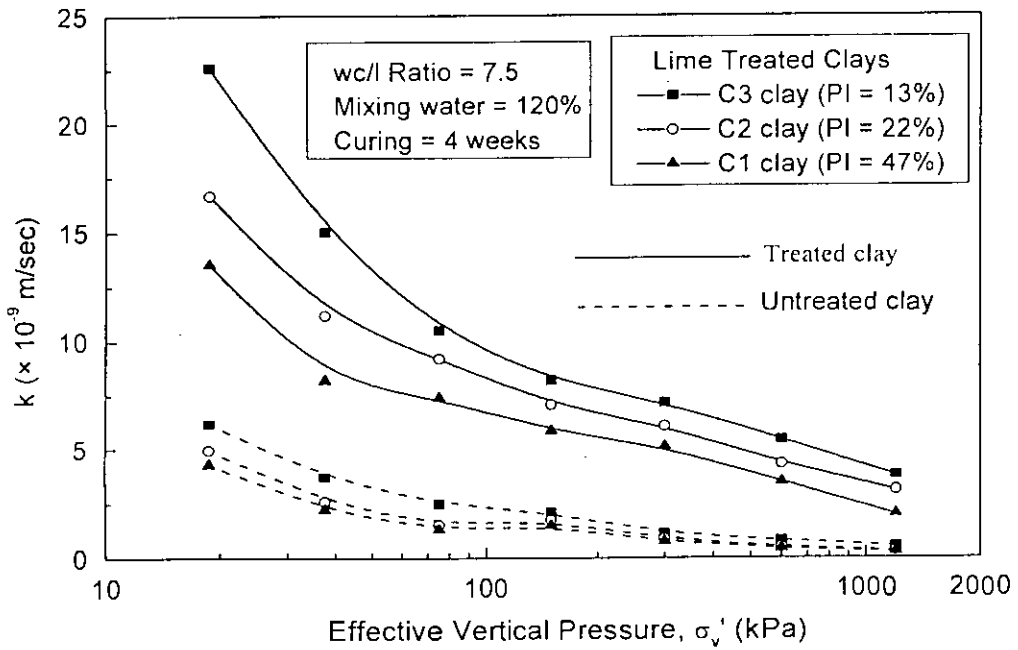


(b)

Fig. 5.30 Effect of Curing Time on  $k - \log \sigma'_v$  Relationships of C3 Clay  
(a) Cement Treated and (b) Lime Treated

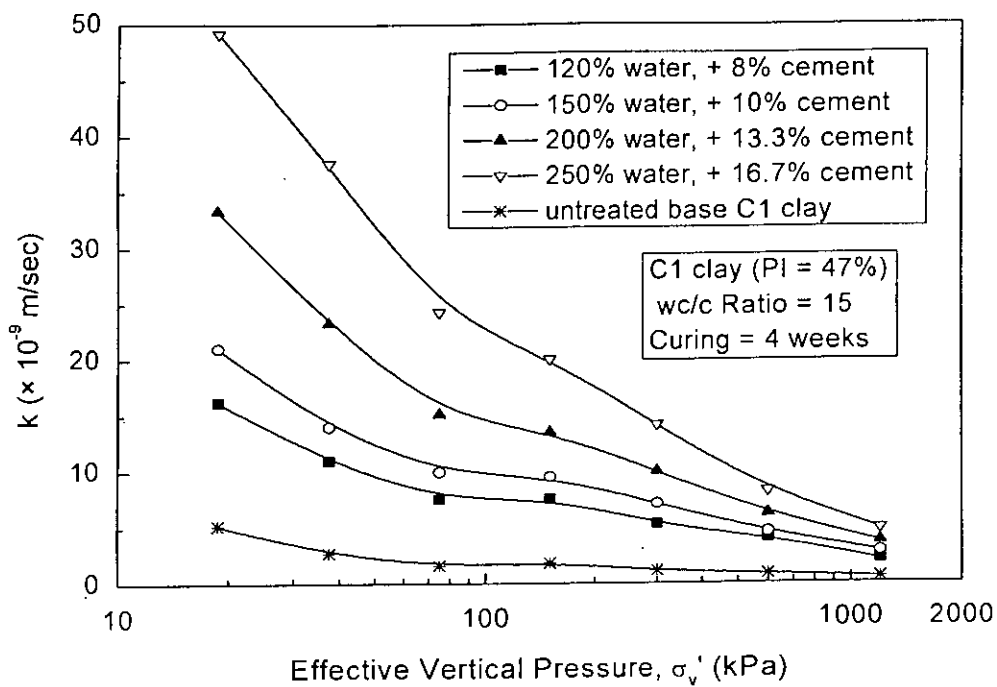


(a)

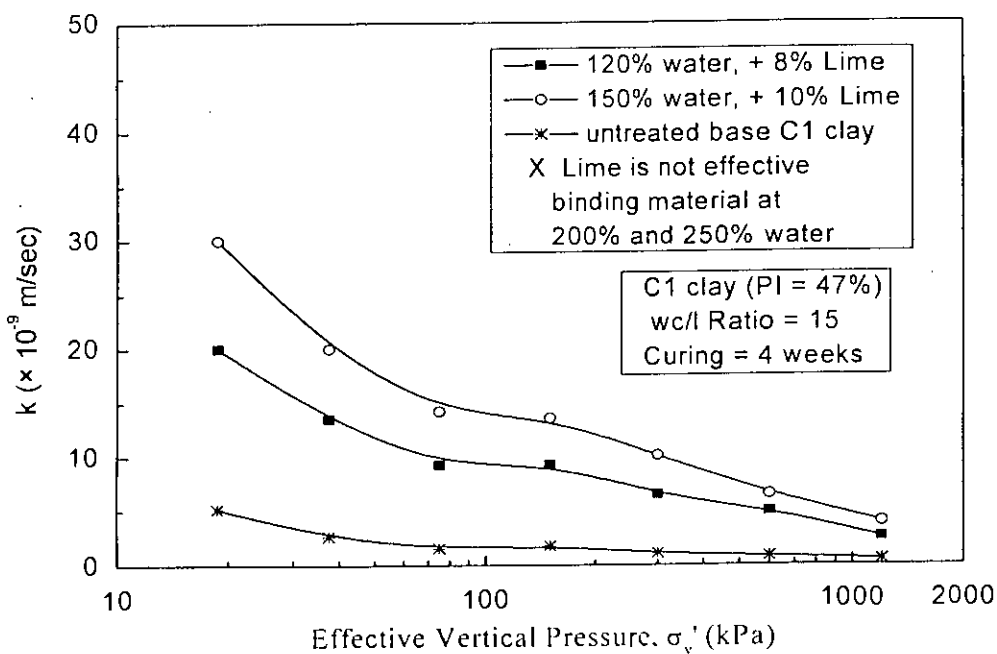


(b)

Fig. 5.31 Effect of Clay Type on  $k - \log \sigma'_v$  Relationships of Clays  
 (a) Cement Treated and (b) Lime Treated

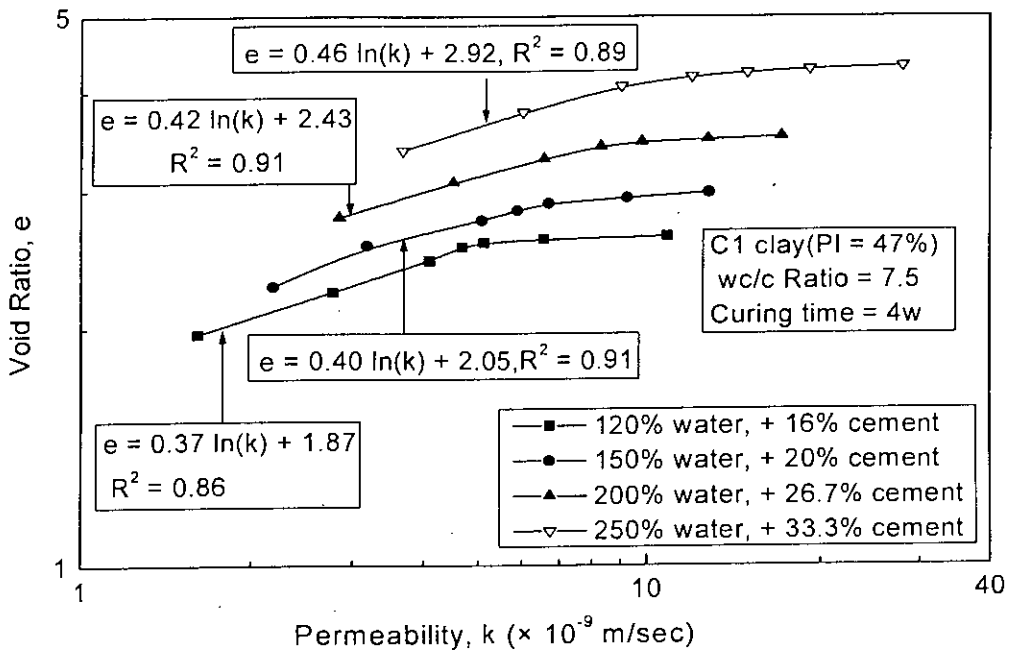


(a)

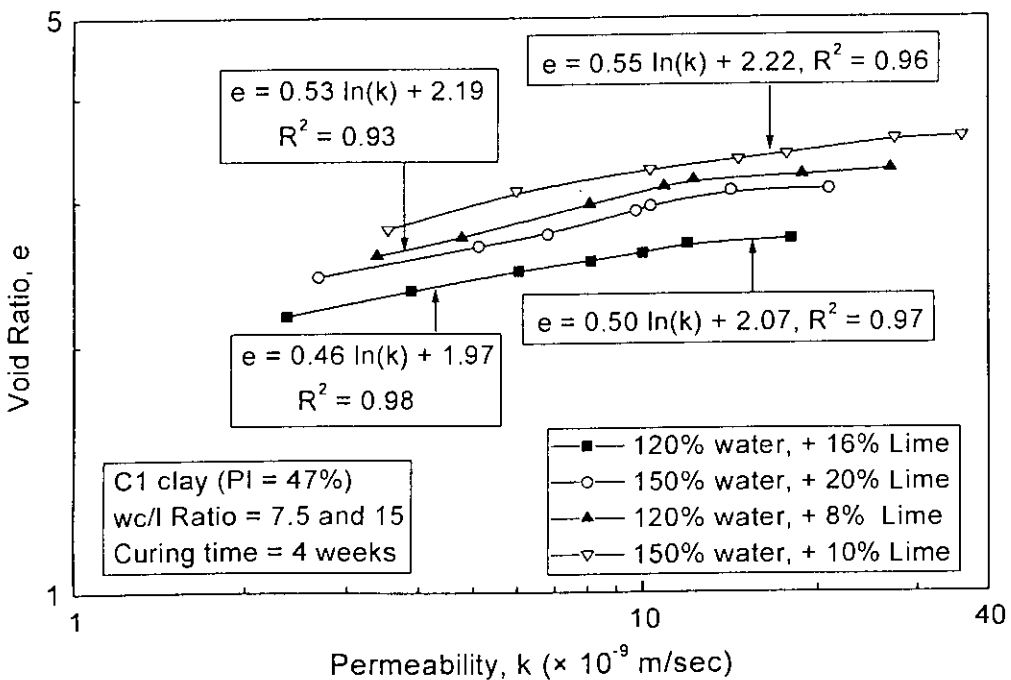


(b)

Fig. 5.32 Effect of Mixing Clay-Water Content Ratio on  $k - \log \sigma'_v$  Relationships of C1 Clay (a) Cement Treated and (b) Lime Treated

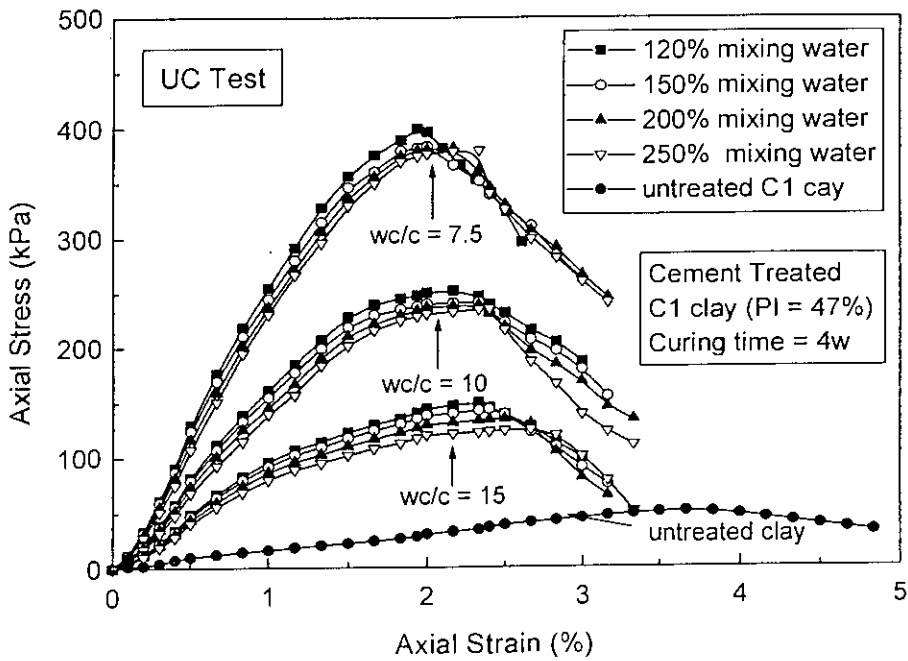


(a)

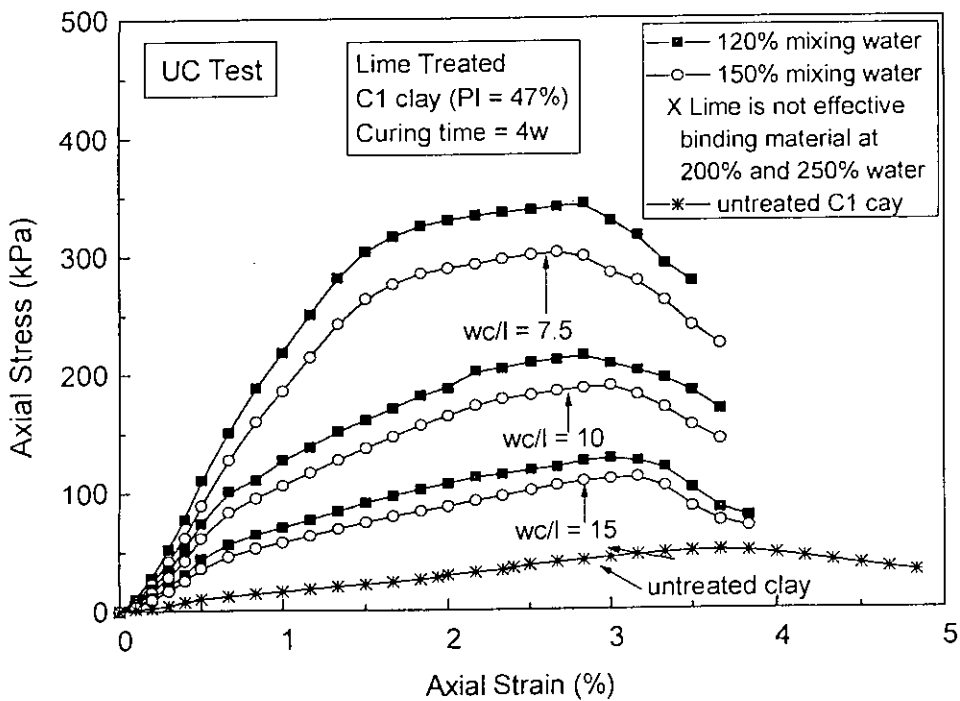


(b)

Fig. 5.33 Relationships between Void Ratio and Permeability for C1 clay  
(a) Cement Treated and (b) Lime Treated

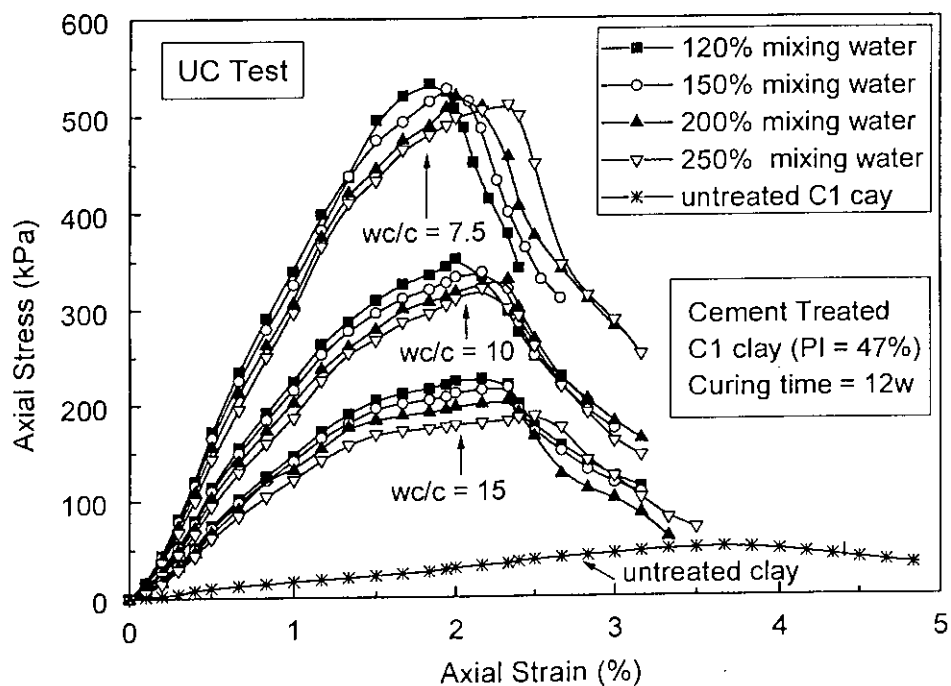


(a)

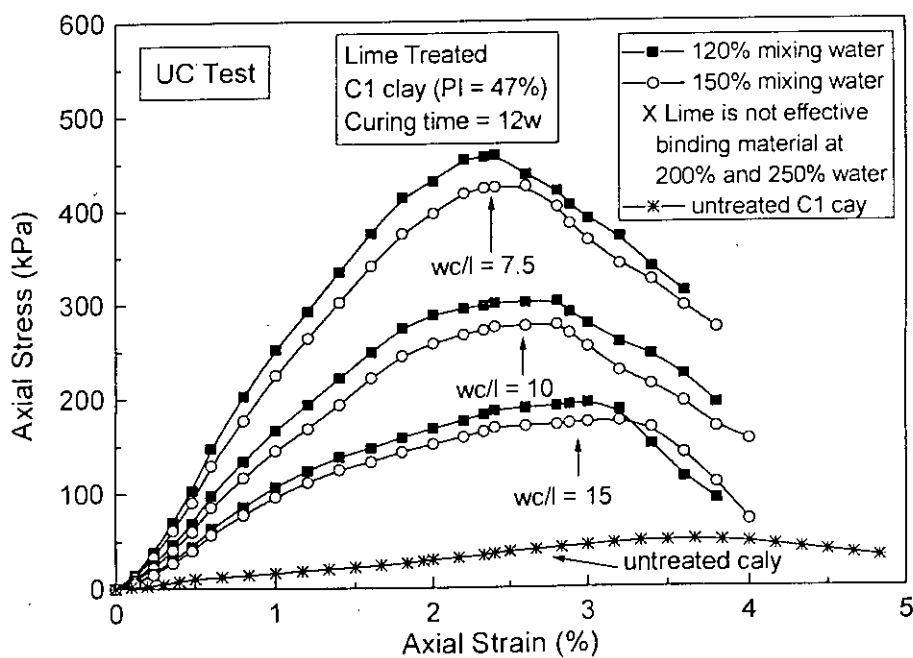


(b)

Fig. 5.34 Stress-Strain Behavior from UC Test at 4 weeks Curing of C1 clay (a) Cement Treated and (b) Lime Treated



(a)

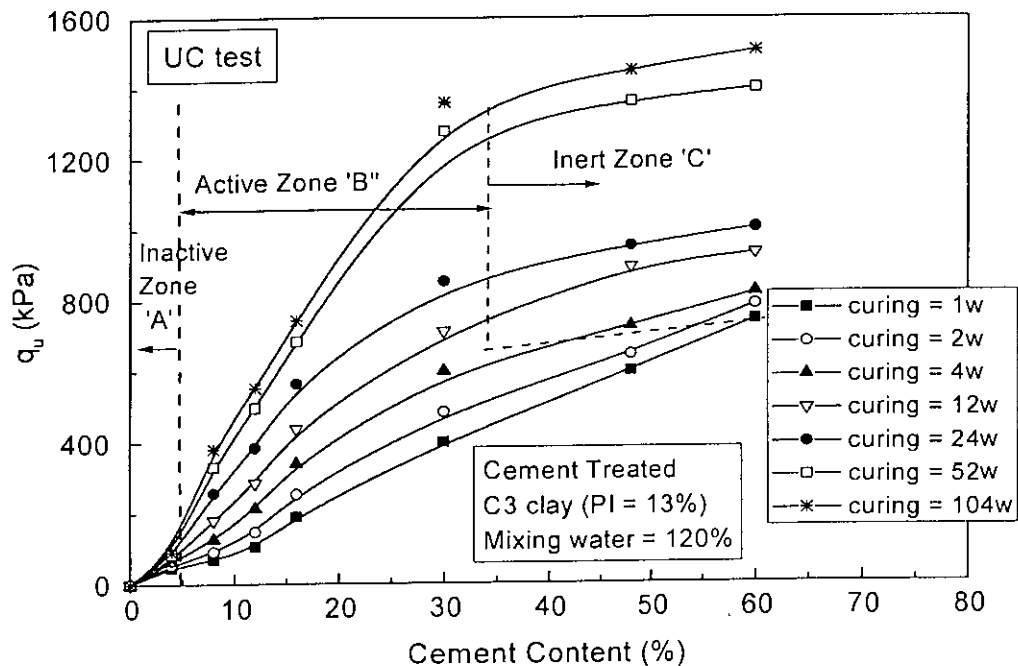


(b)

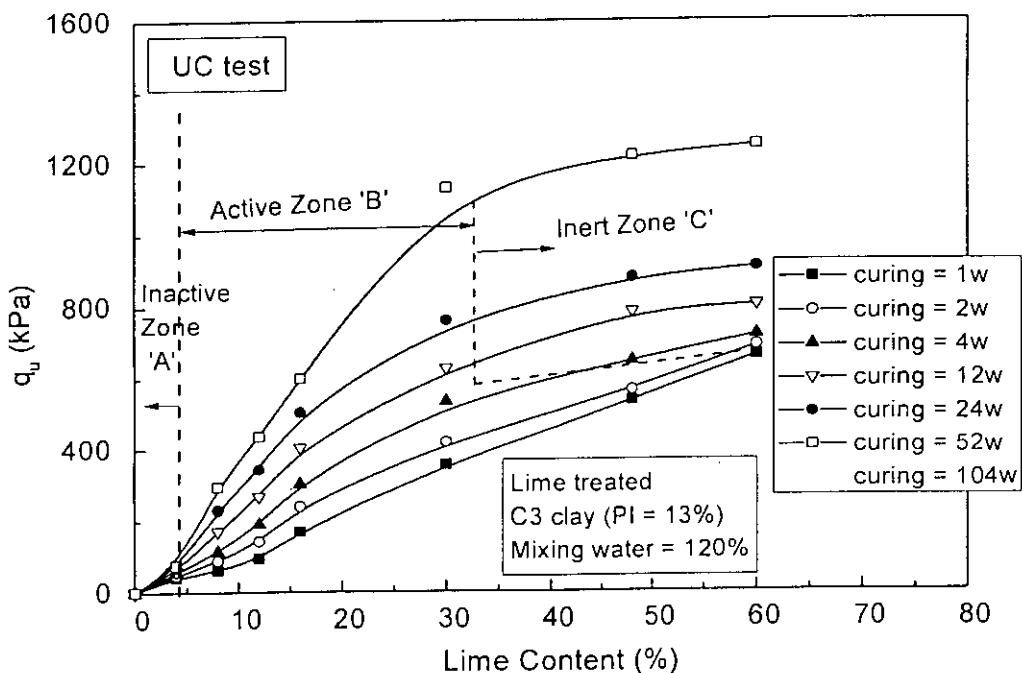
Fig. 5.35 Stress-Strain Behavior from UC Test at 12 weeks Curing of C1 clay  
(a) Cement Treated and (b) Lime Treated

**Table 5.5 Unconfined Compressive Strength ( $q_u$ ) in kPa for Cement Treated and Lime Treated Clays**

Admix- ture	$w_i$ (%)	wc/c Ratio	C1 Clay		C2 Clay		C3 Clay	
			Curing Time		Curing Time		Curing Time	
			4 w	12 w	4 w	12 w	4 w	12 w
Cement	120	7.5	399	533	291	405	339	438
		10	251	335	179	267	213	284
		15	149	226	106	172	126	180
	150	7.5	383	528	277	395	318	429
		10	241	338	175	260	200	266
		15	143	217	124	169	138	185
	200	7.5	381	520	272	390	314	421
		10	238	330	170	249	195	257
		15	134	207	95	155	112	165
	250	7.5	379	511	268	401	311	409
		10	235	321	172	258	189	265
		15	124	187	88	160	108	166
Lime	120	7.5	343	458	266	302	281	390
		10	215	302	158	201	192	257
		15	128	194	115	133	144	172
	150	7.5	302	425	235	278	272	312
		10	189	277	150	185	211	167
		15	112	169	103	123	124	154
Untreated base clays			50		41		58.5	



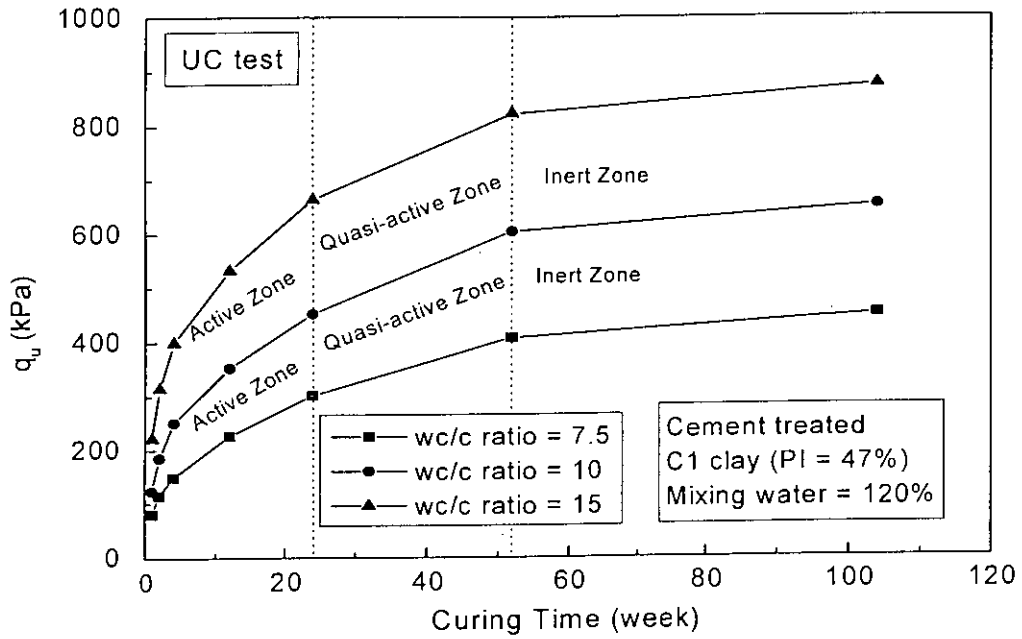
(a)



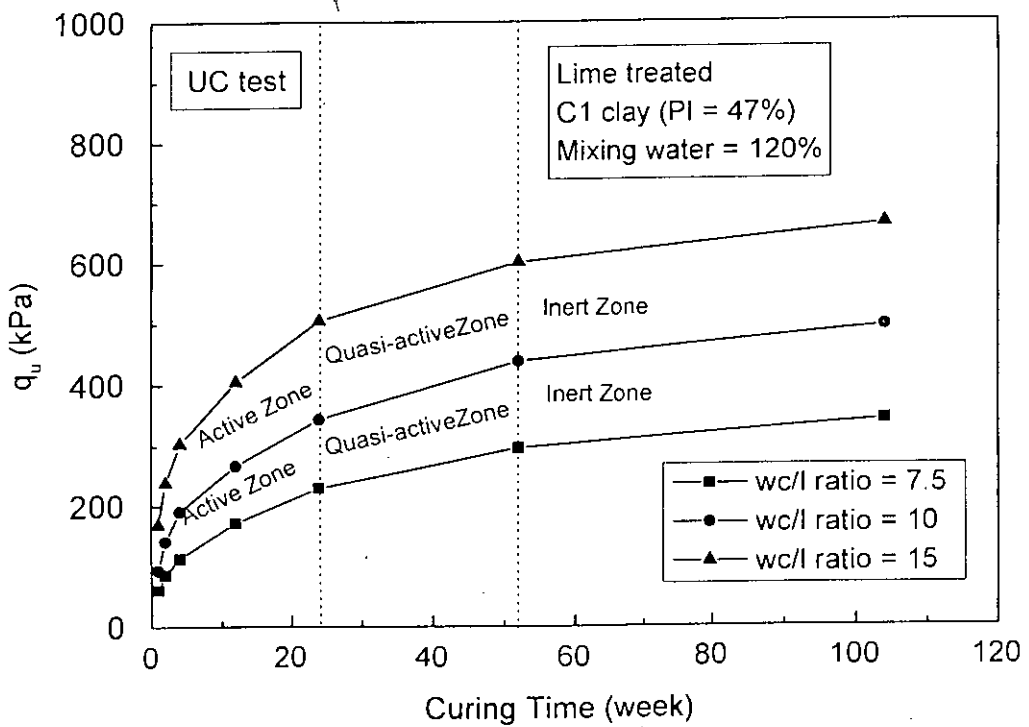
(b)

Fig. 5.36 Unconfined Compressive Strength and Cement Content Relationship at different Curing of C3 clay (a) Cement Treated and (b) Lime Treated



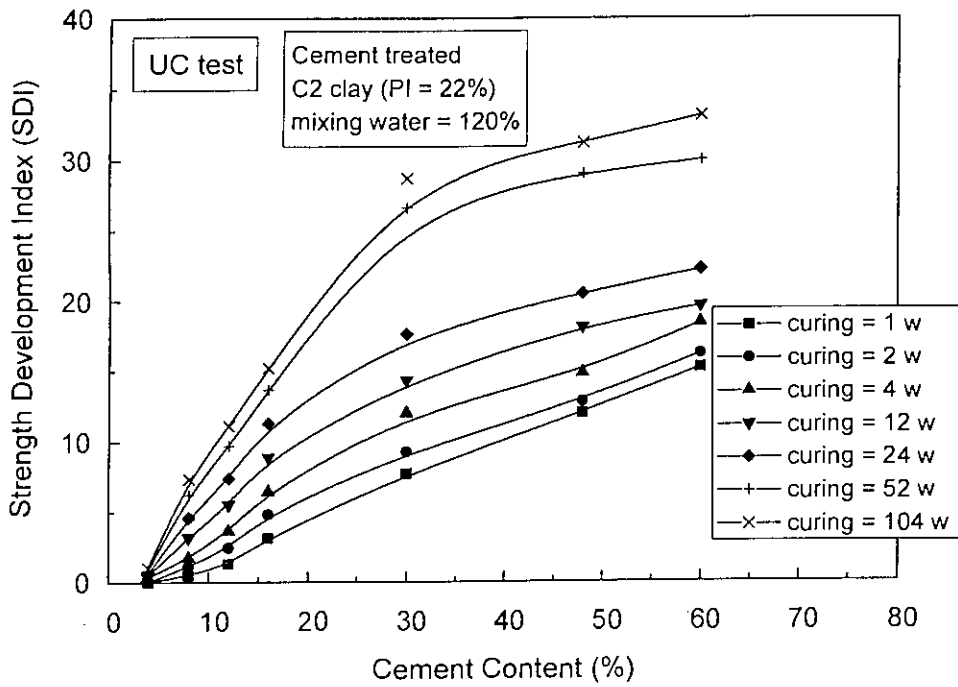


(a)

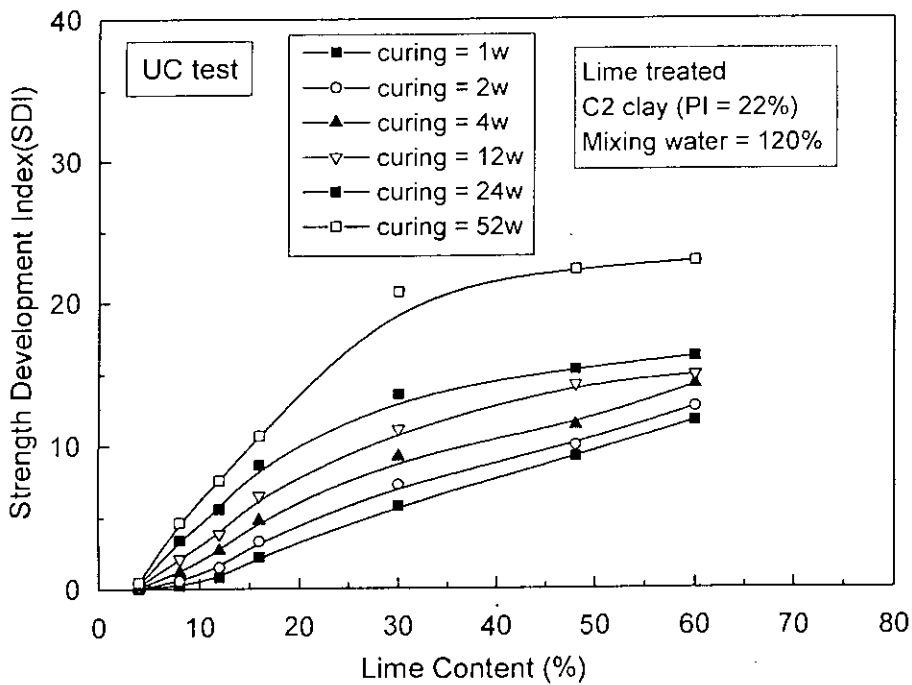


(b)

Fig. 5.37 Unconfined Compressive Strength and Curing Time Relationship at different wc/c Ratio of C1 clay (a) Cement Treated and (b) Lime Treated

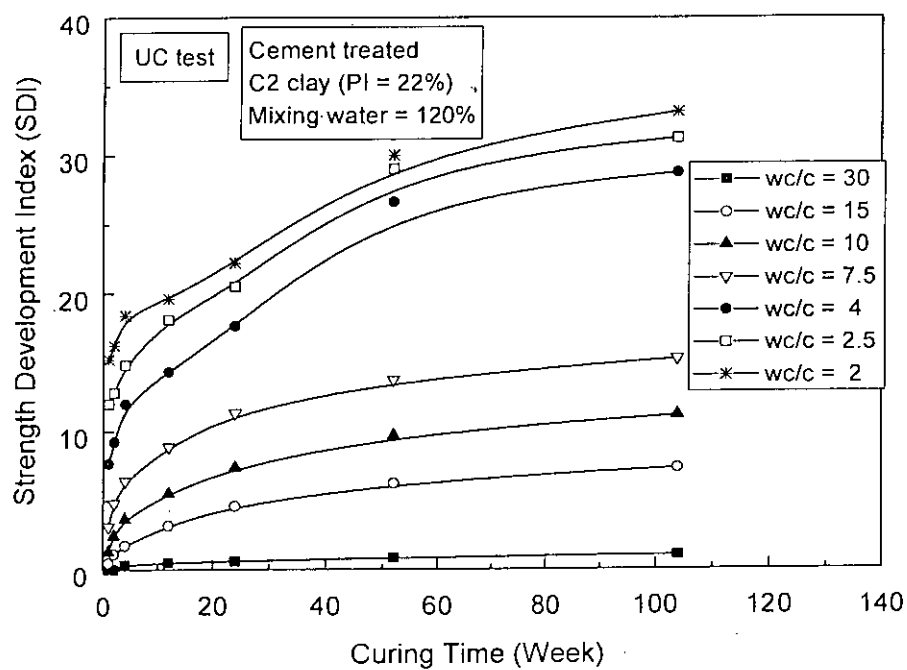


(a)

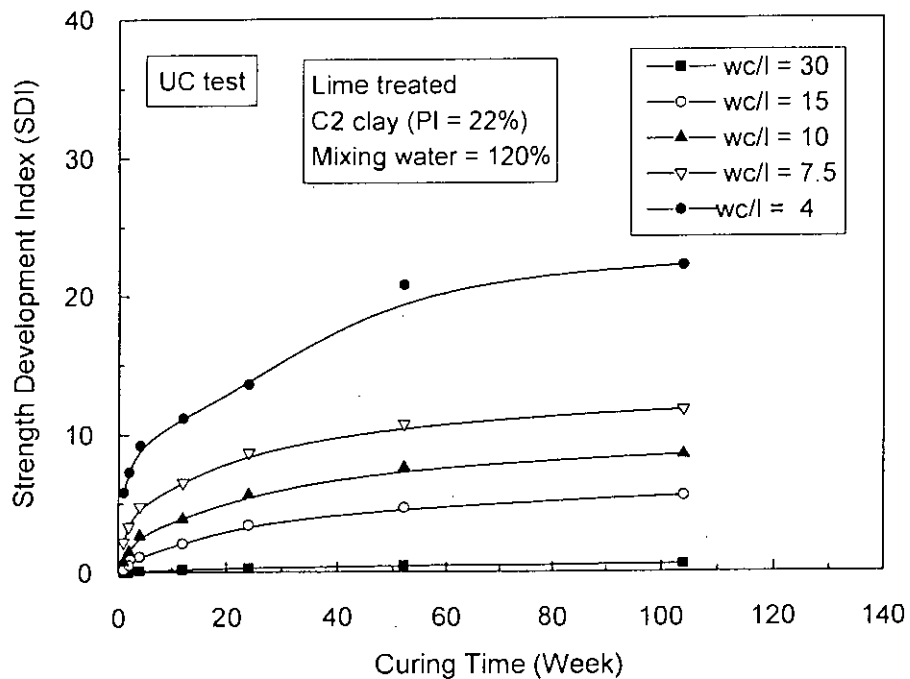


(b)

Fig. 5.38 Variation of Strength Development Index (SDI) with Cement Content of C2 clay (a) Cement and (b) Lime Treated

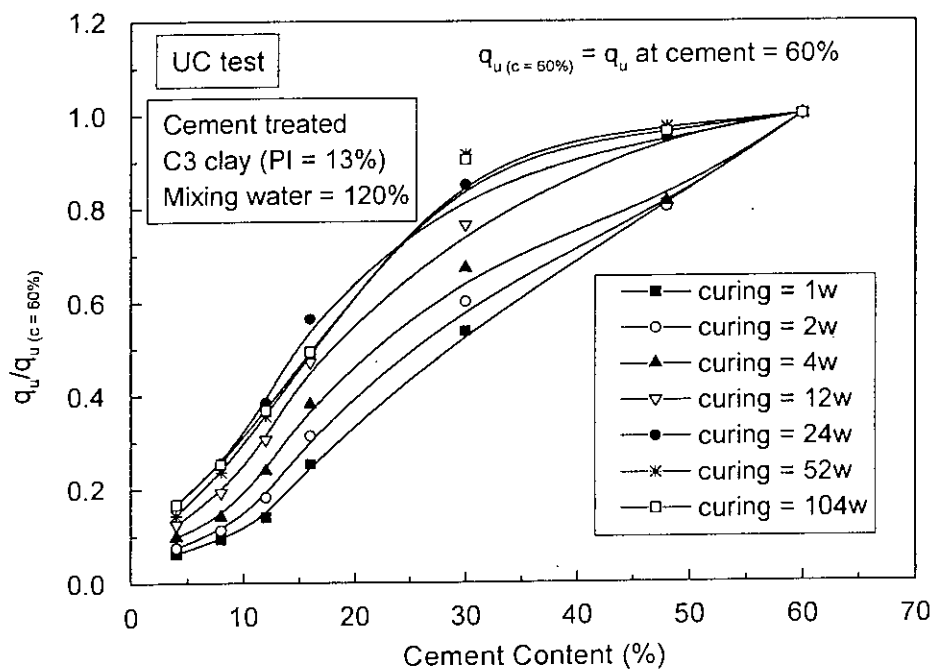


(a)

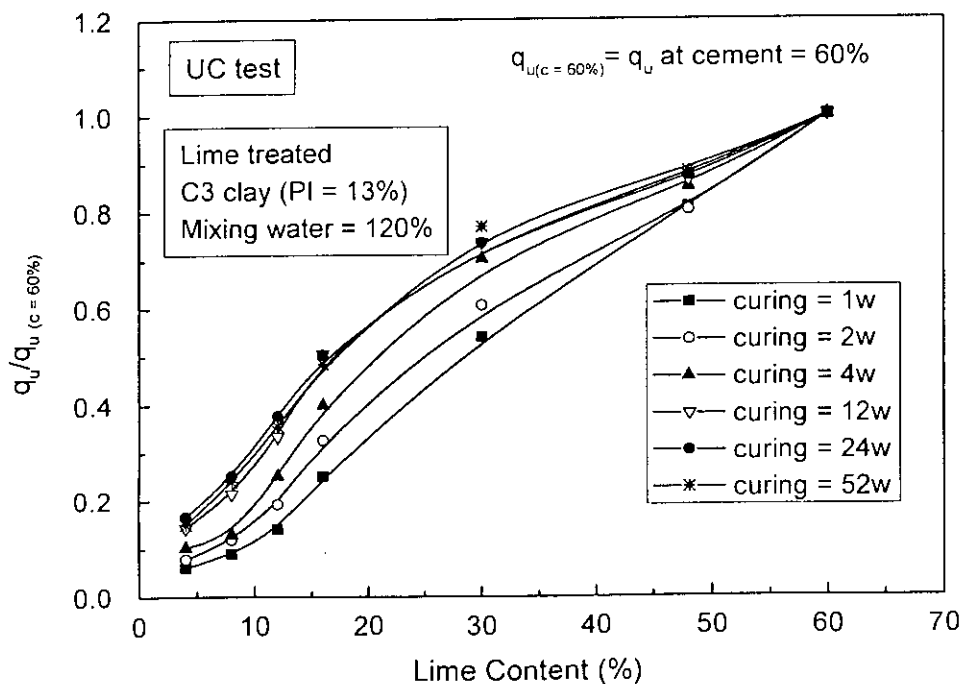


(b)

Fig. 5.39 Variation of Strength Development Index (SDI) with Curing Time of C2 clay (a) Cement Treated and (b) Lime Treated

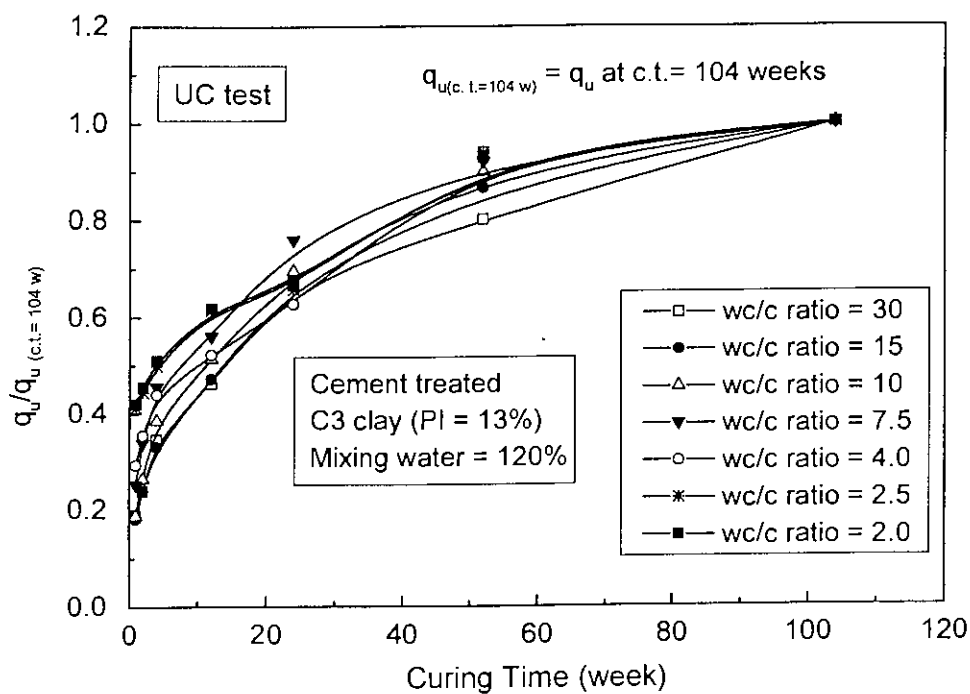


(a)

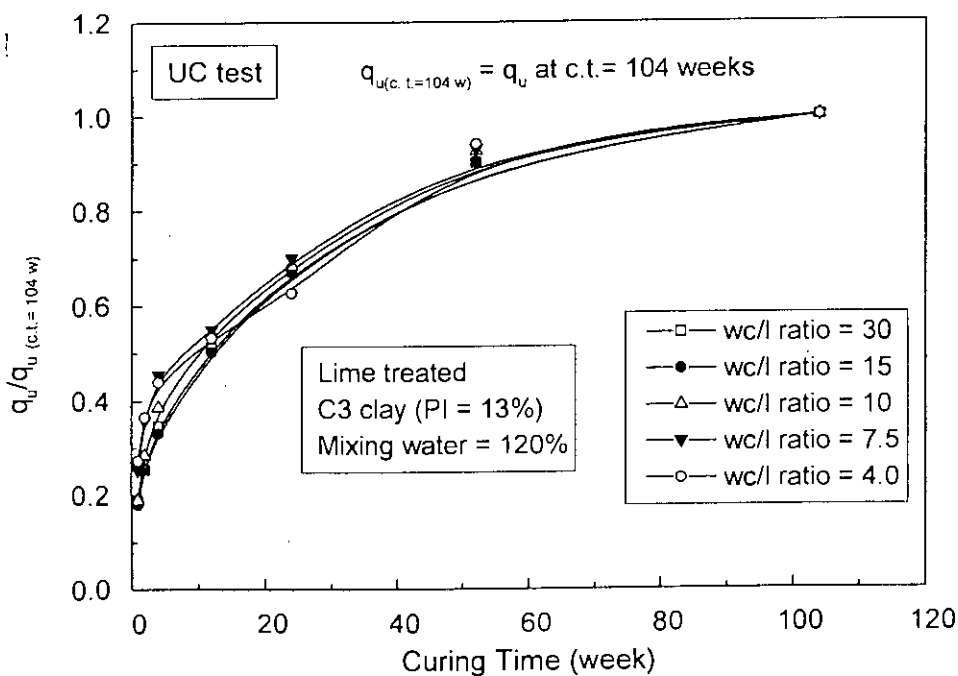


(b)

Fig. 5.40 Typical Normalized Behavior of Unconfined Strength with Cement at different Curing of C3 clay (a) Cement Treated and (b) Lime Treated



(a)



(b)

Fig. 5.41 Typical Normalized Behavior of Unconfined Strength with Curing Time at different of C3 clay (a) Cement Treated and (b) Lime Treated

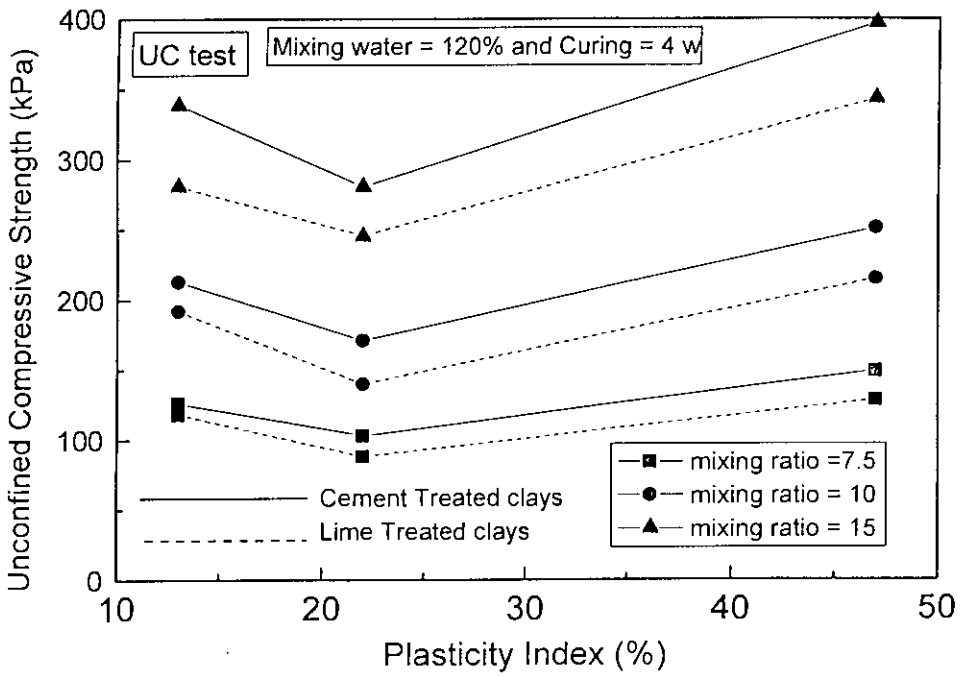


Fig. 5.42 Unconfined Compressive Strength and Plasticity Index Relationship at Various Clay-Water/Admixture Ratio for Cement and Lime Treated clays

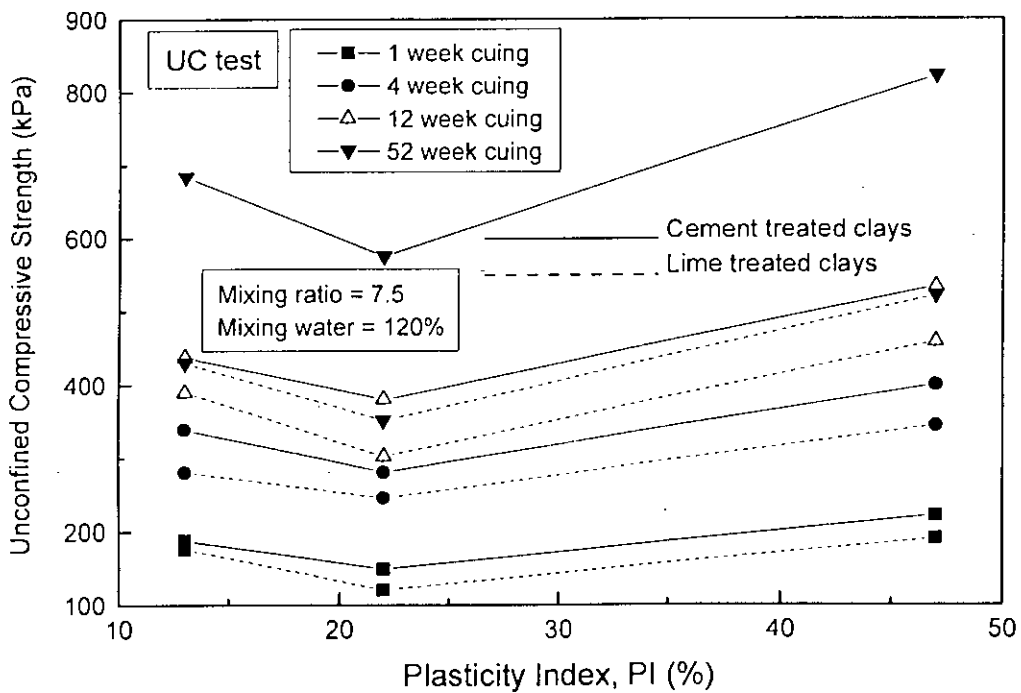


Fig. 5.43 Unconfined Compressive Strength and Plasticity Index Relationship at different Curing Time for Cement and Lime Treated clays

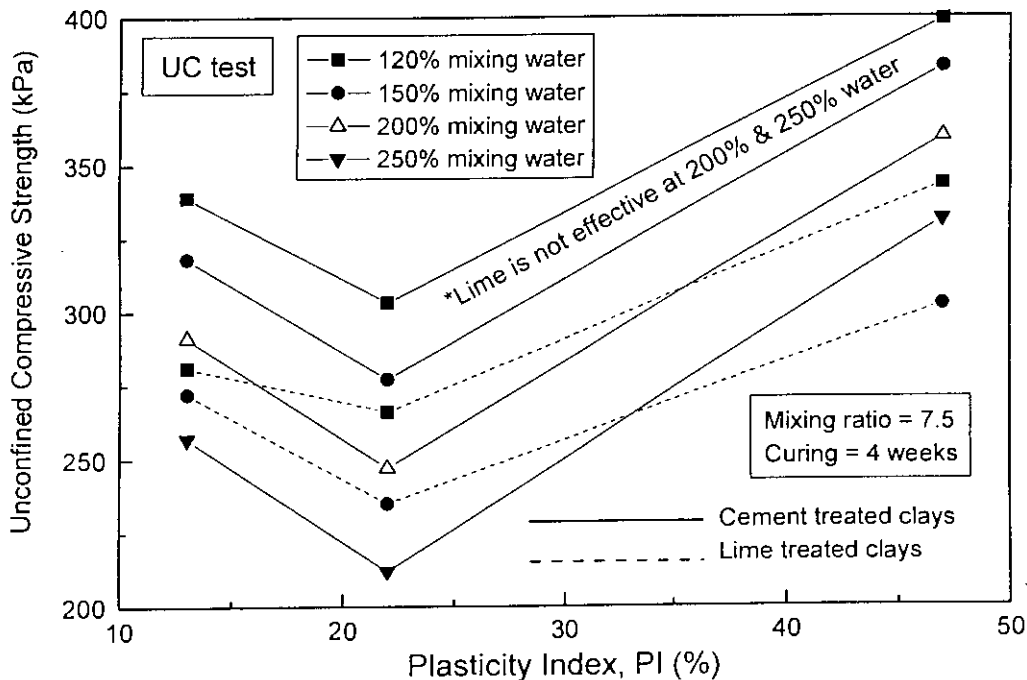


Fig. 5.44 Unconfined Compressive Strength and Plasticity Index Relationship at different Initial Mixing Water for Cement and Lime Treated clays

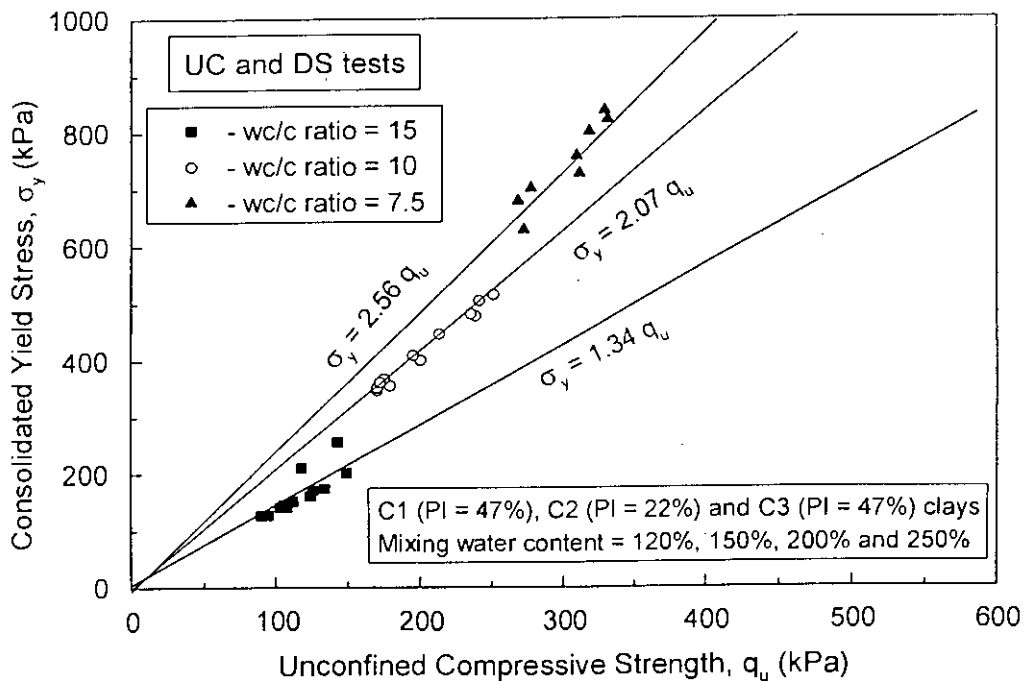


Fig. 5.45 Relationship between Unconfined Compressive Strength ( $q_u$ ) and Consolidated Yield Strength ( $\sigma_y$ ) of Cement Treated clays Studied

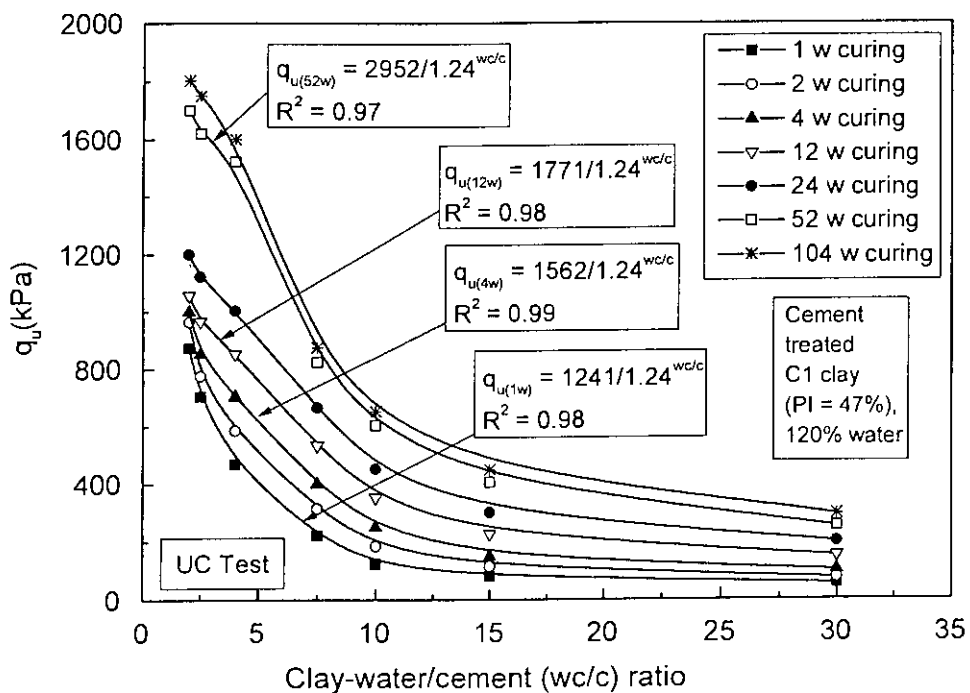


Fig. 5.46 Strength Prediction based on Clay-Water/Cement Ratio's Concept of Cement Treated C1 clay

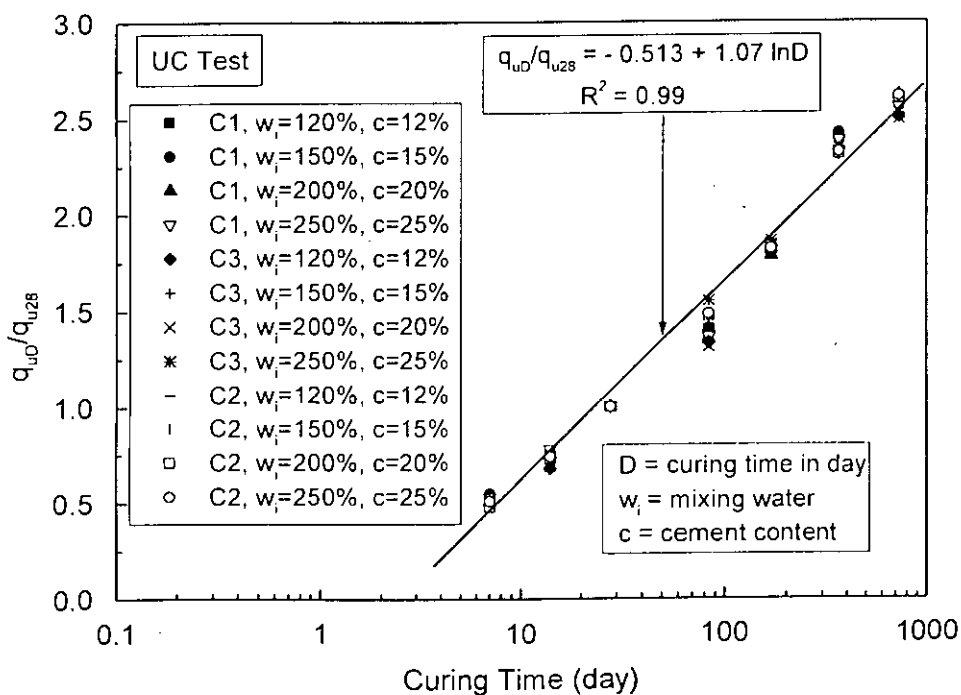
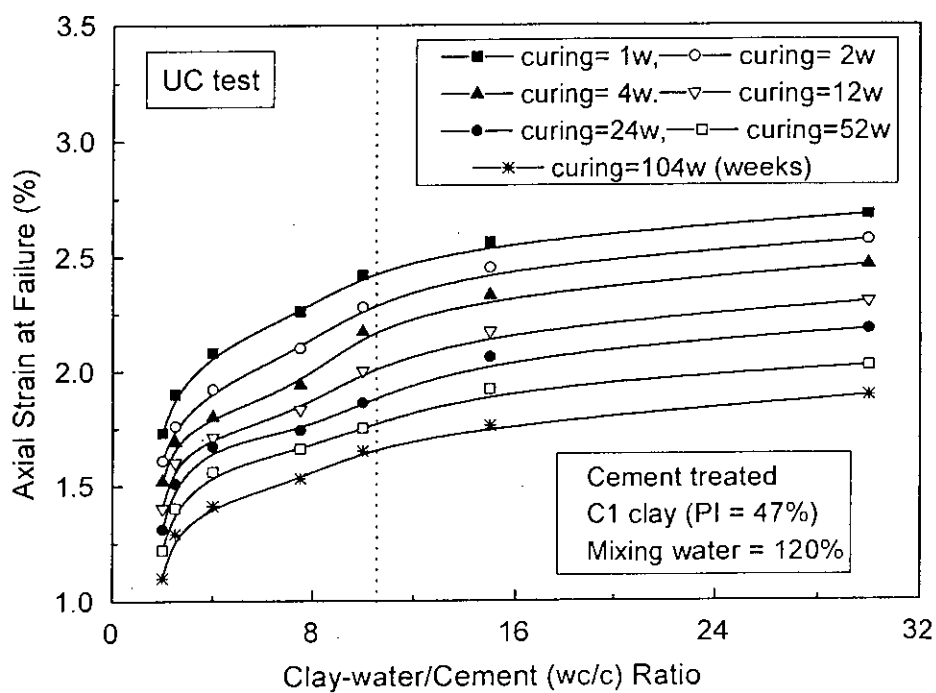
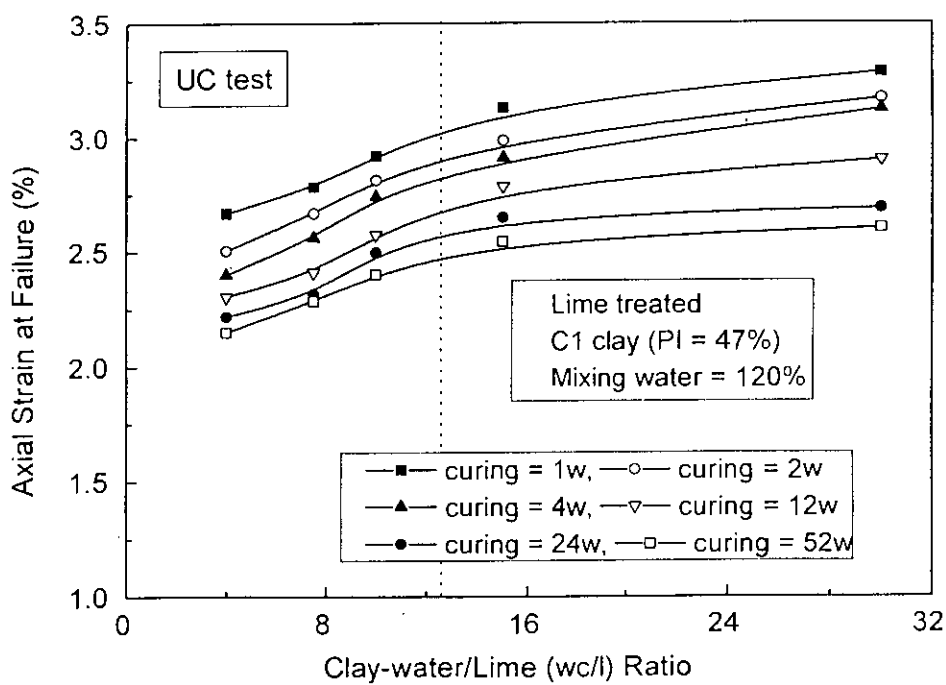


Fig. 5.47 Strength Development with Time and its Generalization of Clays Studied





(a)



(b)

Fig. 5.48 Relationship between Axial Strain at Failure and Clay-Water/Admixture Ratio of C1 clay (a) Cement Treated and (b) Lime Treated

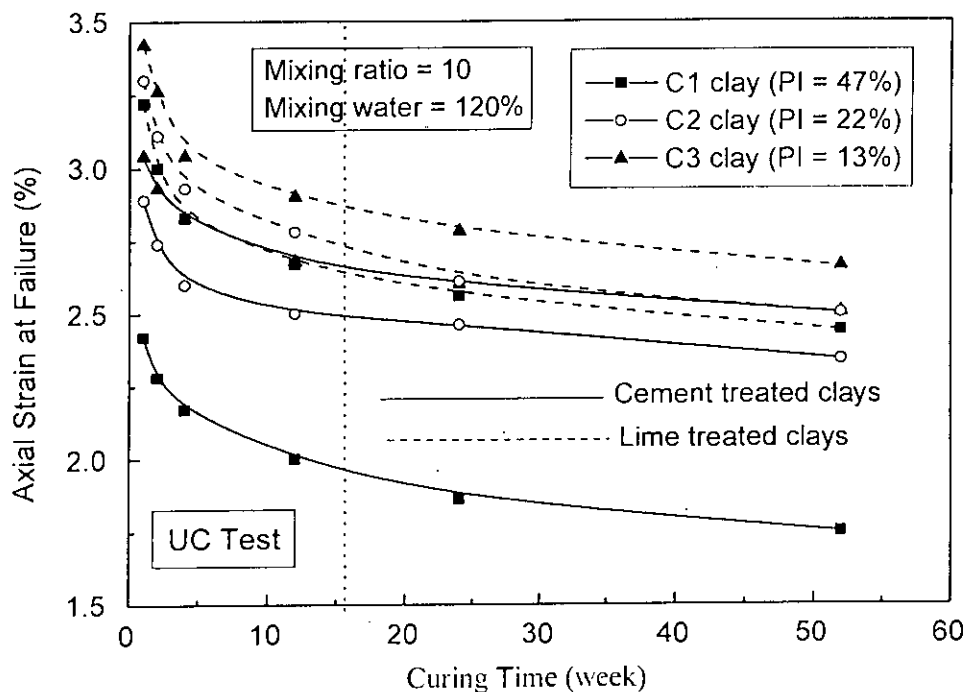


Fig. 5.49 Effect of Curing Time and Clay Type on Axial Strain at Failure of Cement and Lime Treated clays

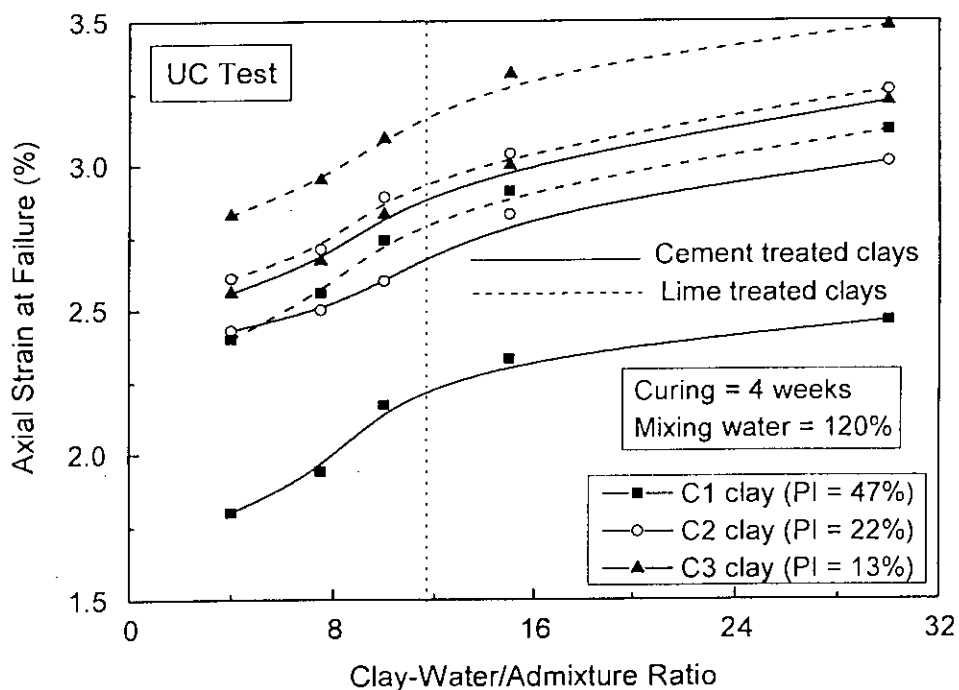


Fig. 5.50 Effect of Clay-Water/Admixture Ratio and Clay Type on Axial Strain at Failure of Cement and Lime Treated clays

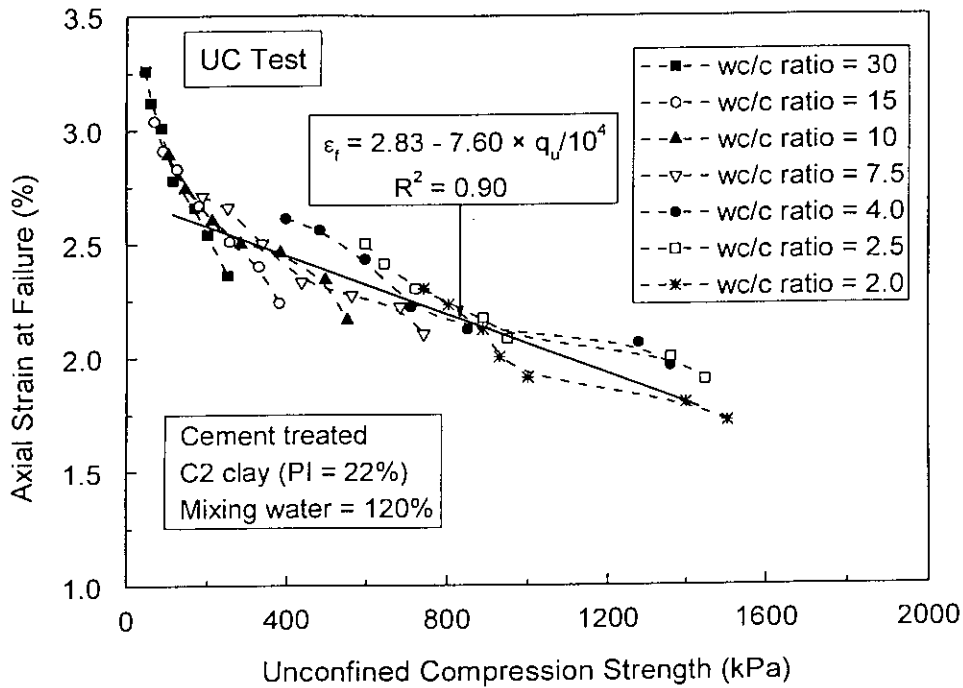


Fig. 5.51 Relationship between  $q_u$  and Axial Strain at Failure Shown in Terms of  $w/c$  Ratio for Cement Treated C2 clay

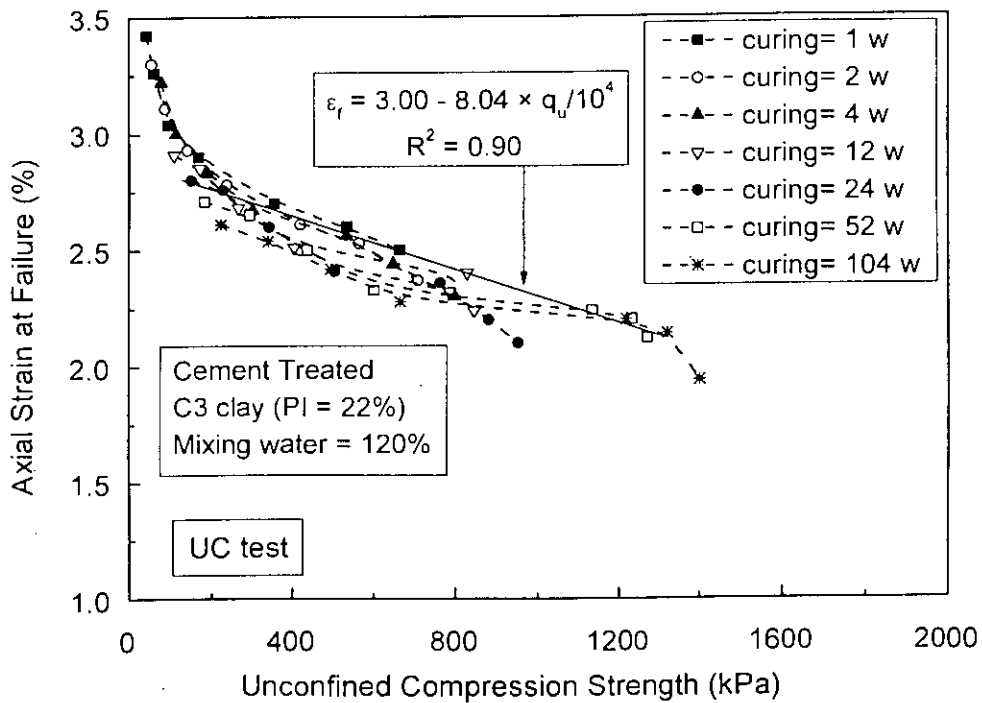
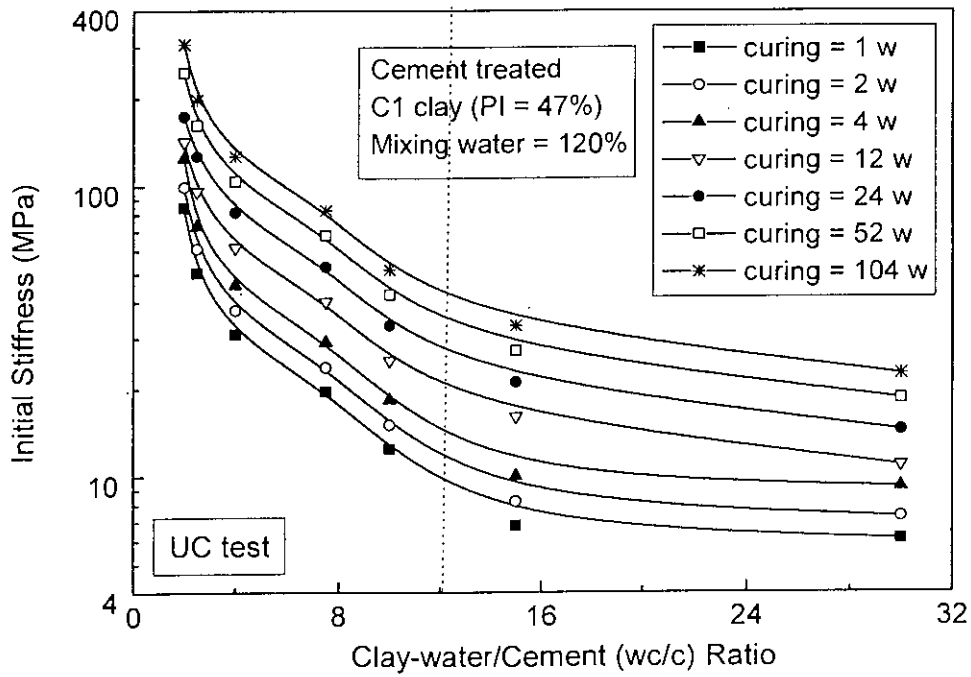
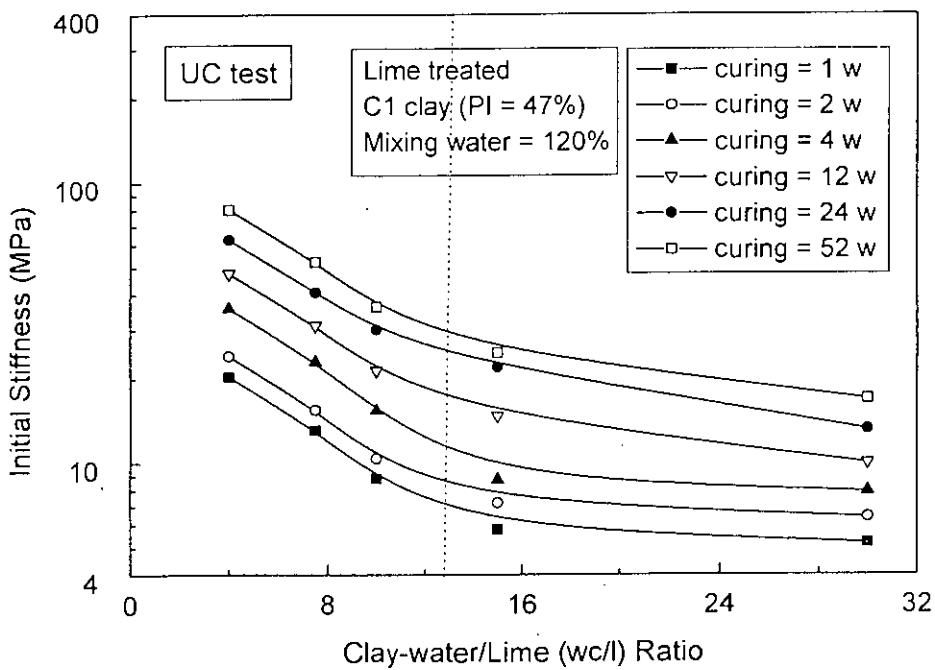


Fig. 5.52 Relationship between  $q_u$  and Axial Strain at Failure Shown in Terms of Curing Time of Cement Treated C3 clay



(a)



(b)

Fig. 5.53 Effect of Clay-Water/Admixture Ratio and Curing Time on Initial Stiffness of C1 clay (a) Cement Treated and (b) Lime Treated

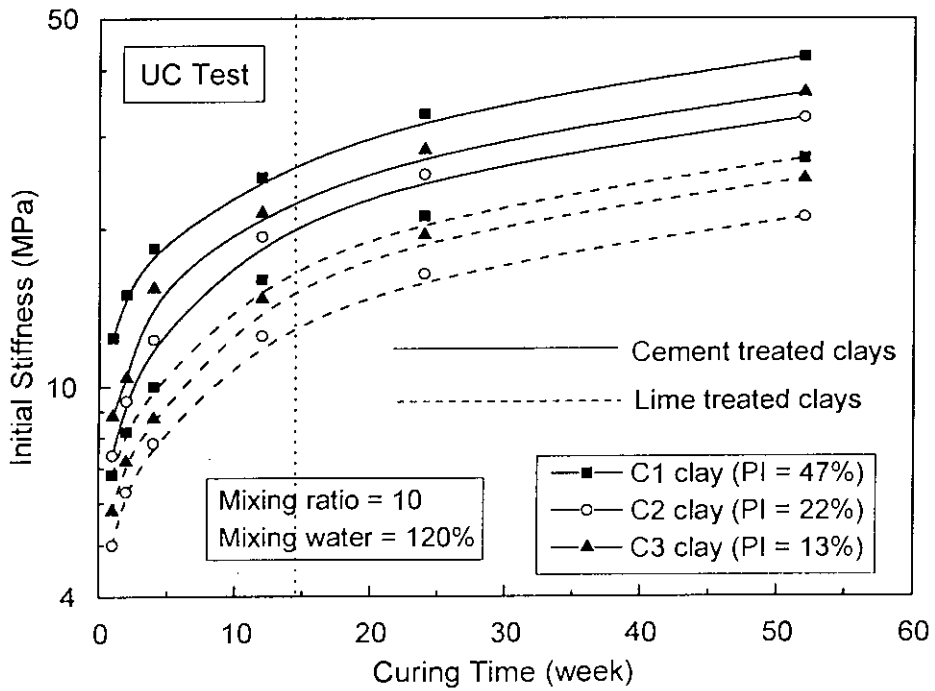


Fig. 5.54 Effect of Curing Time and Clay Type on Initial Stiffness of Cement and Lime Treated clays

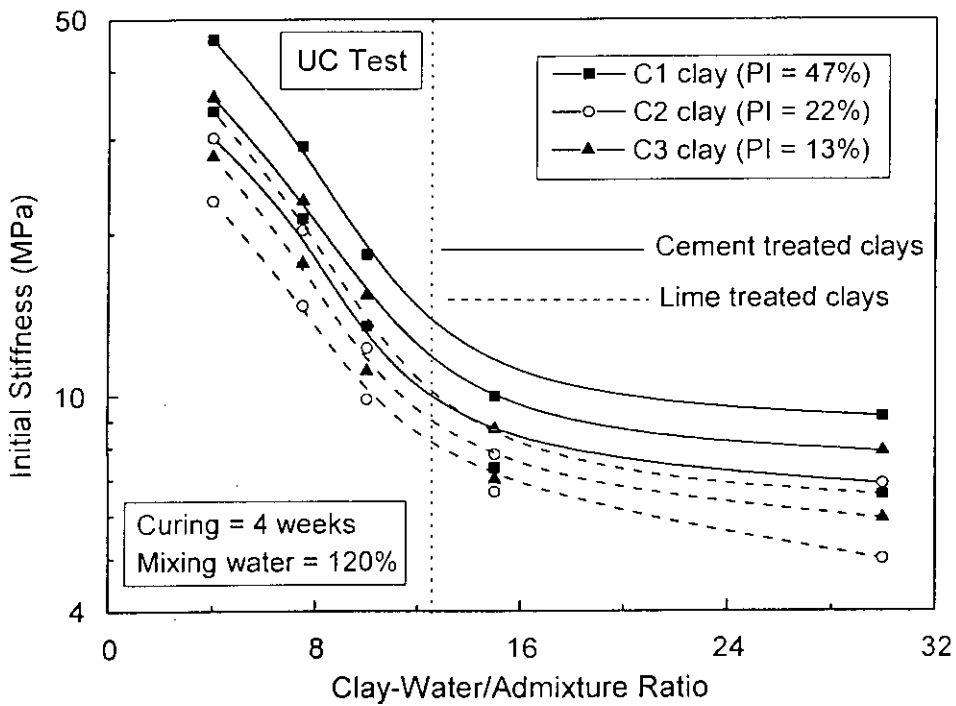


Fig. 5.55 Effect of Clay-Water/Admixture Ratio and Clay Type on Initial Stiffness of Cement and Lime Treated clays

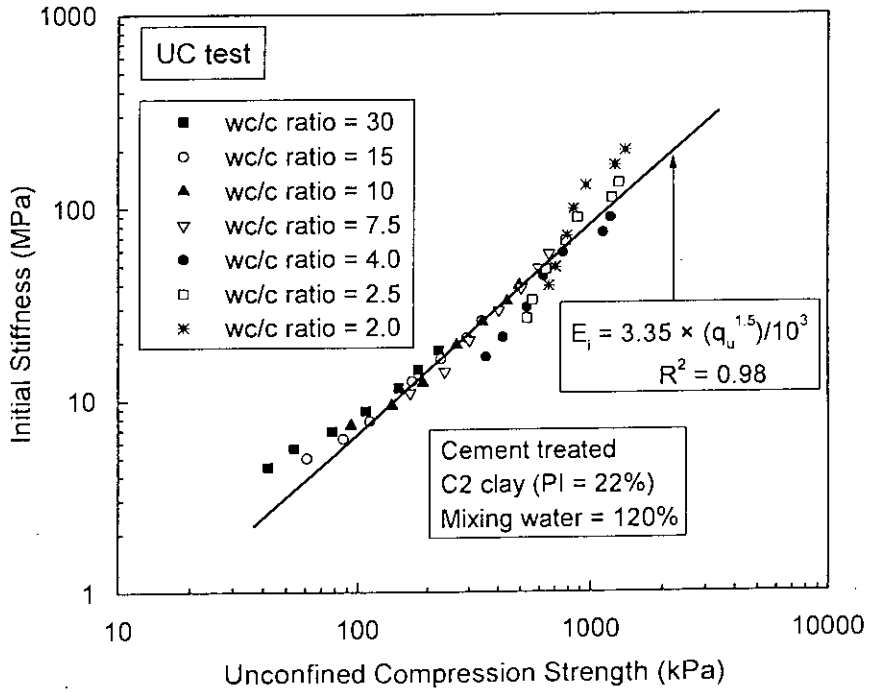


Fig. 5.56 Relationship between  $q_u$  and  $E_i$  Shown in Terms of  $w/c$  Ratio of Cement Treated C2 clay

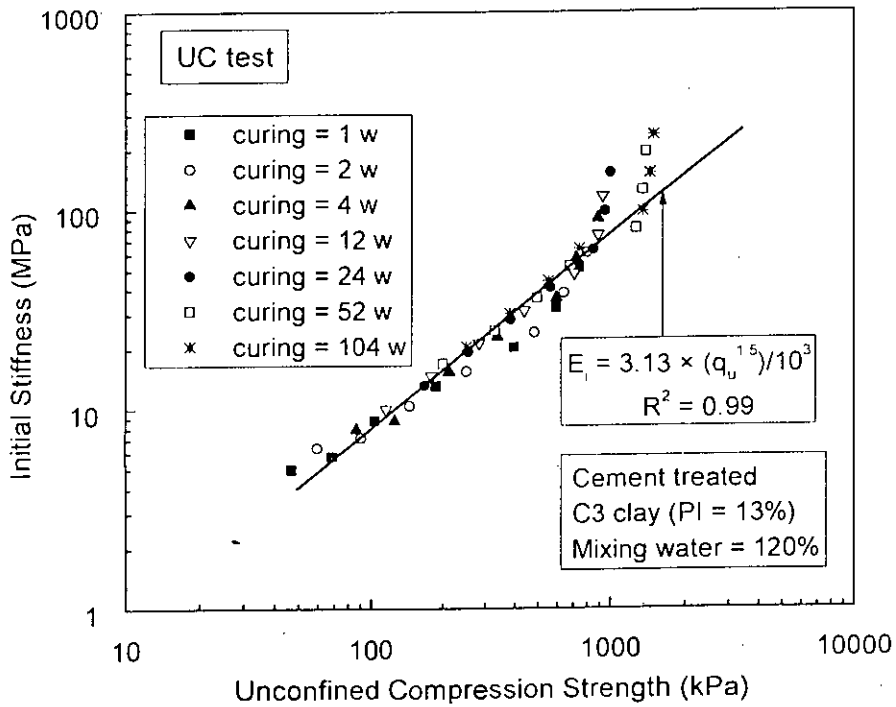
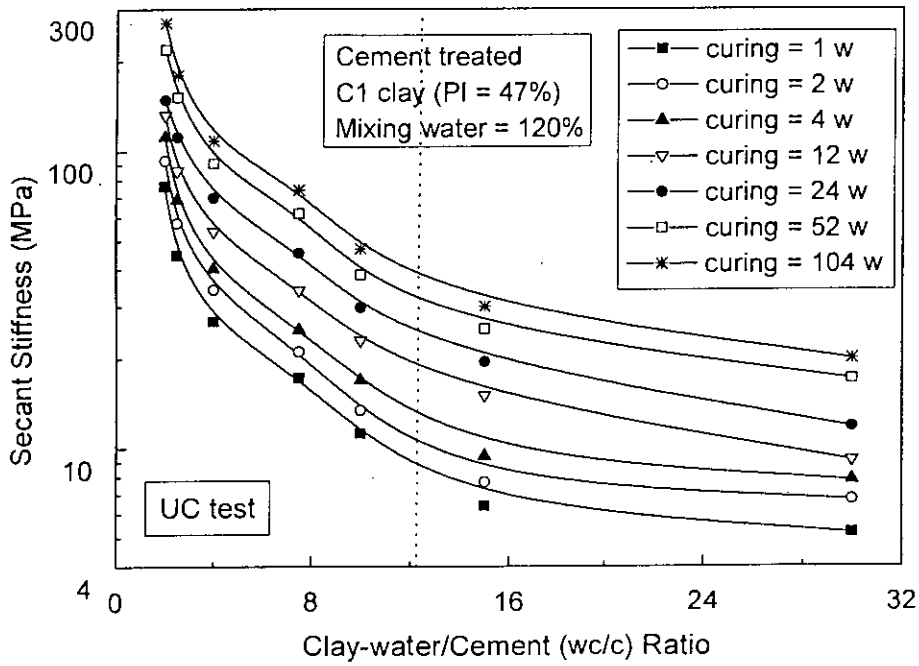
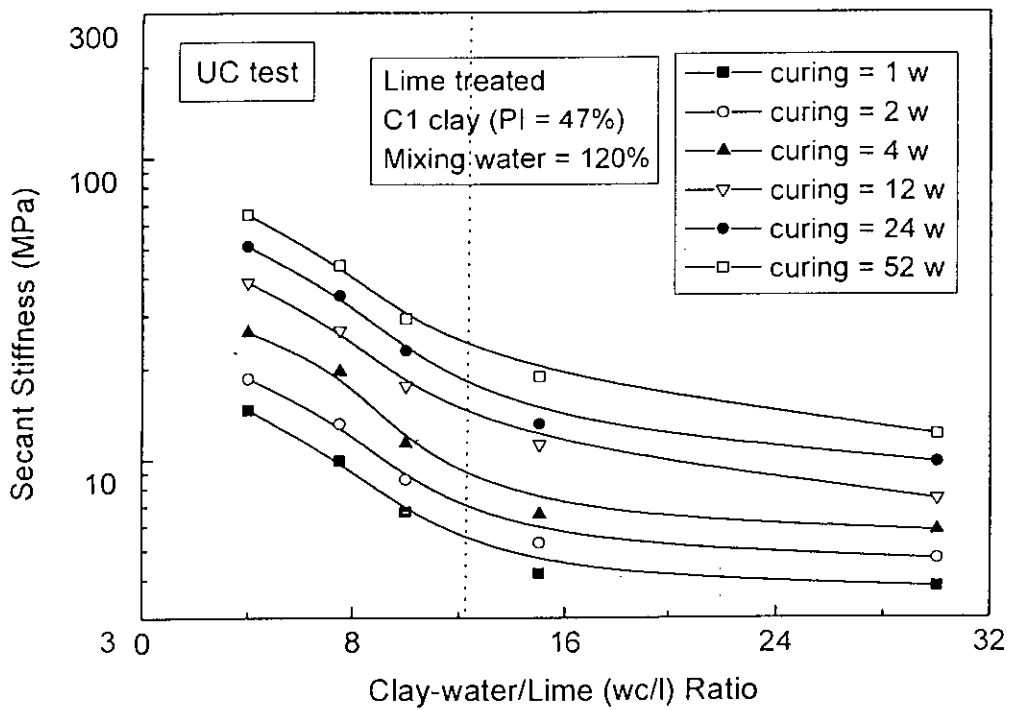


Fig. 5.57 Relationship between  $q_u$  and  $E_i$  Shown in Terms of Curing Time of Cement Treated C3 clay



(a)



(b)

Fig. 5.58 Effect of Clay-Water/Admixture Ratio and Curing Time on Secant Stiffness of C1 clay (a) Cement Treated and (b) Lime Treated

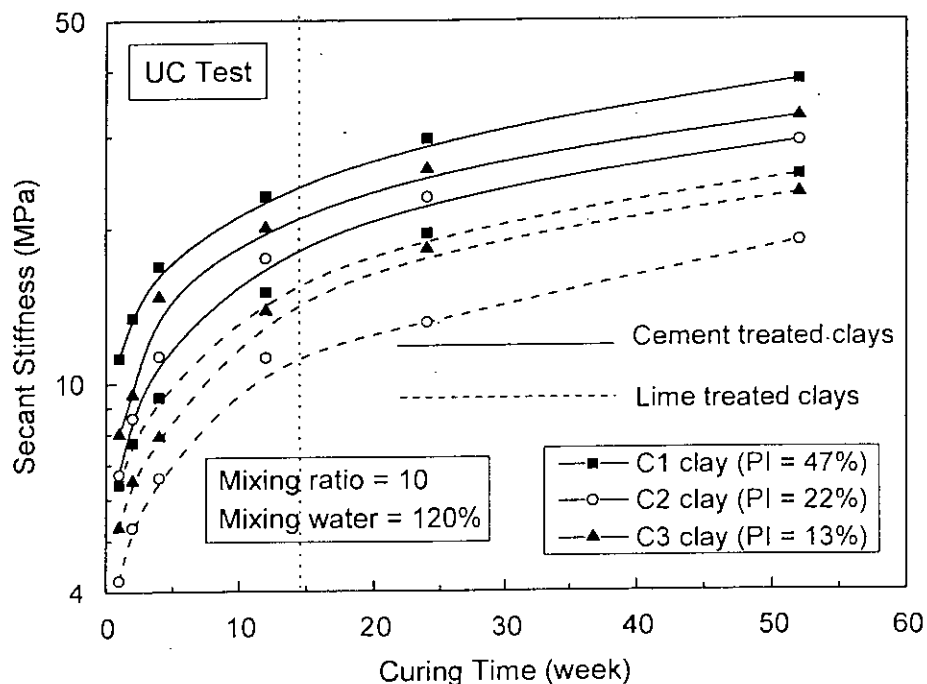


Fig. 5.59 Effect of Curing Time and Clay Type on Secant Stiffness of Cement and Lime Treated clays

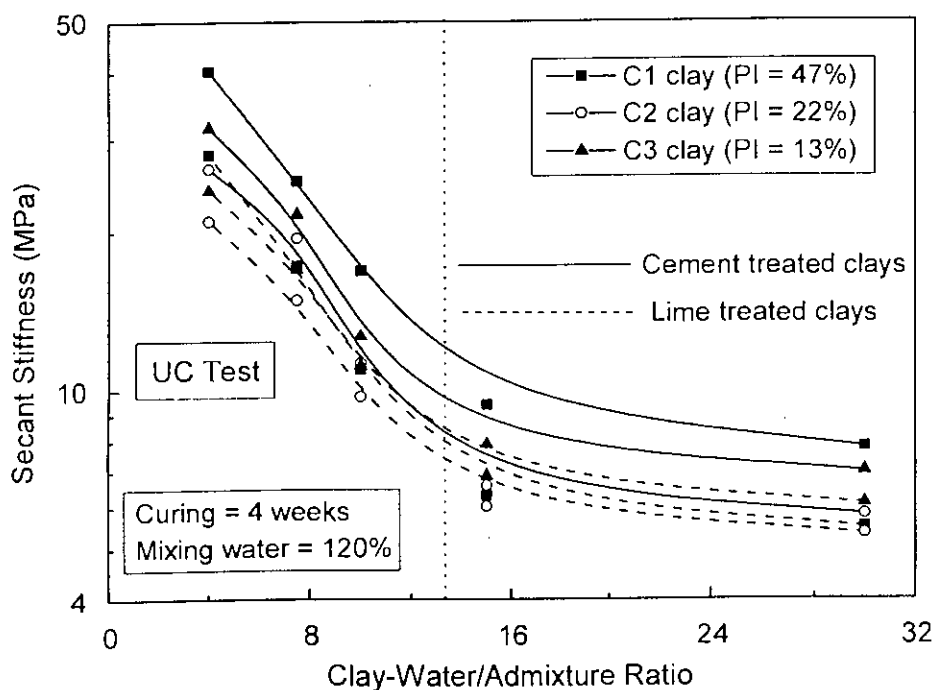


Fig. 5.60 Effect of Clay-Water/Admixture Ratio and Clay Type on Relations between Secant Stiffness of Cement and Lime Treated clays



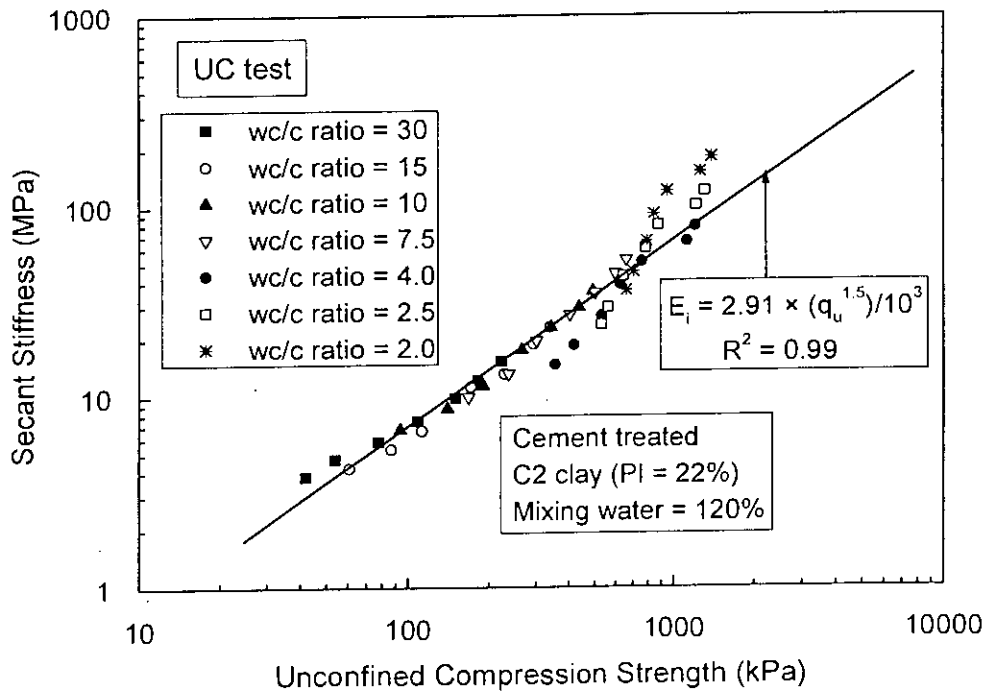


Fig. 5.61 Relationship between  $q_u$  and  $E_{50}$  Shown in Terms of  $w/c$  Ratio of Cement Treated C2 clay

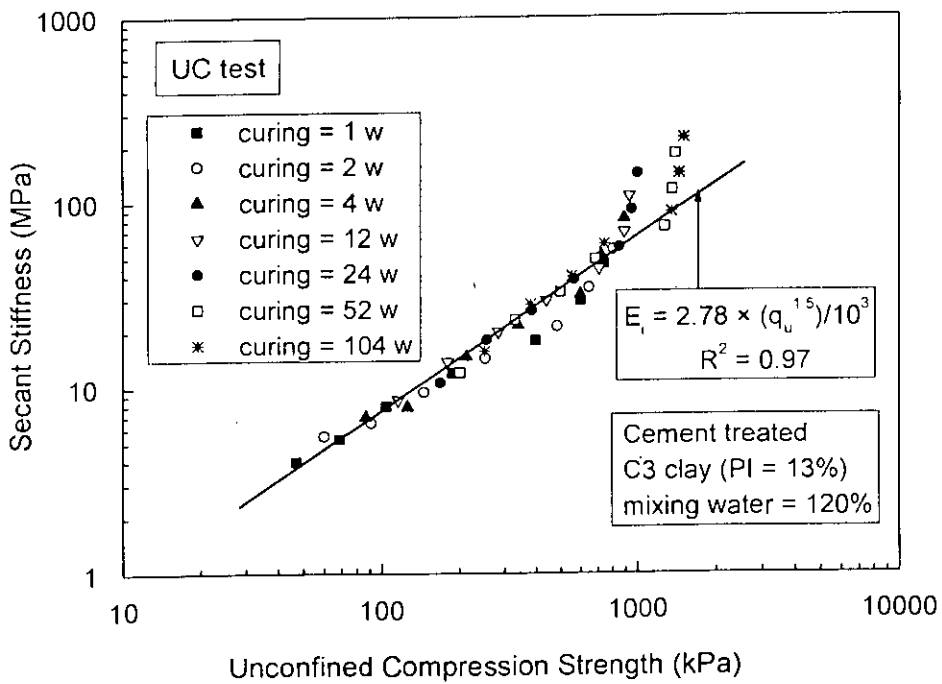
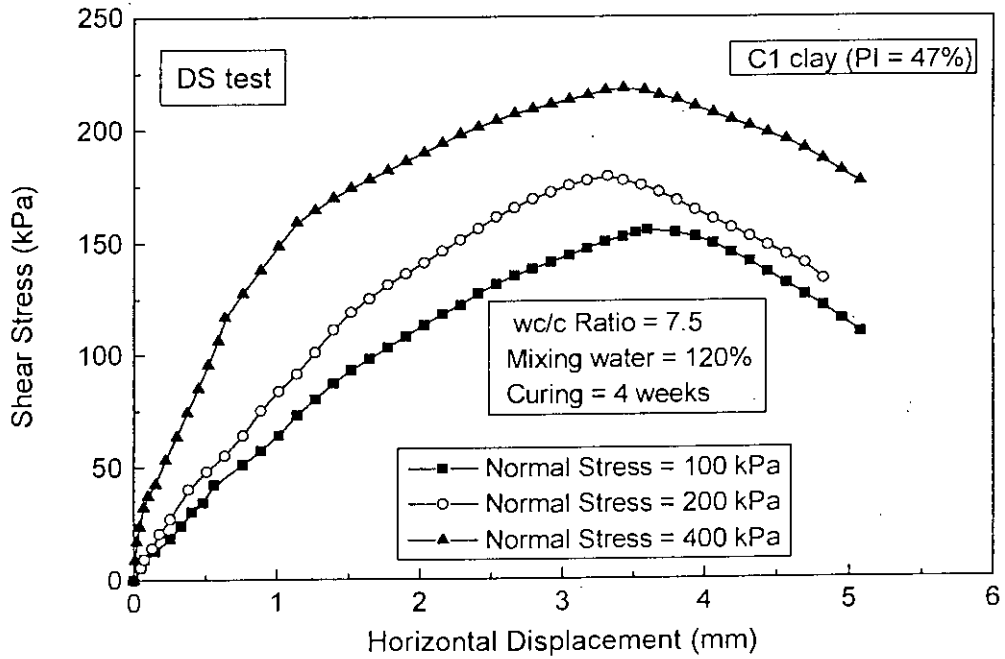
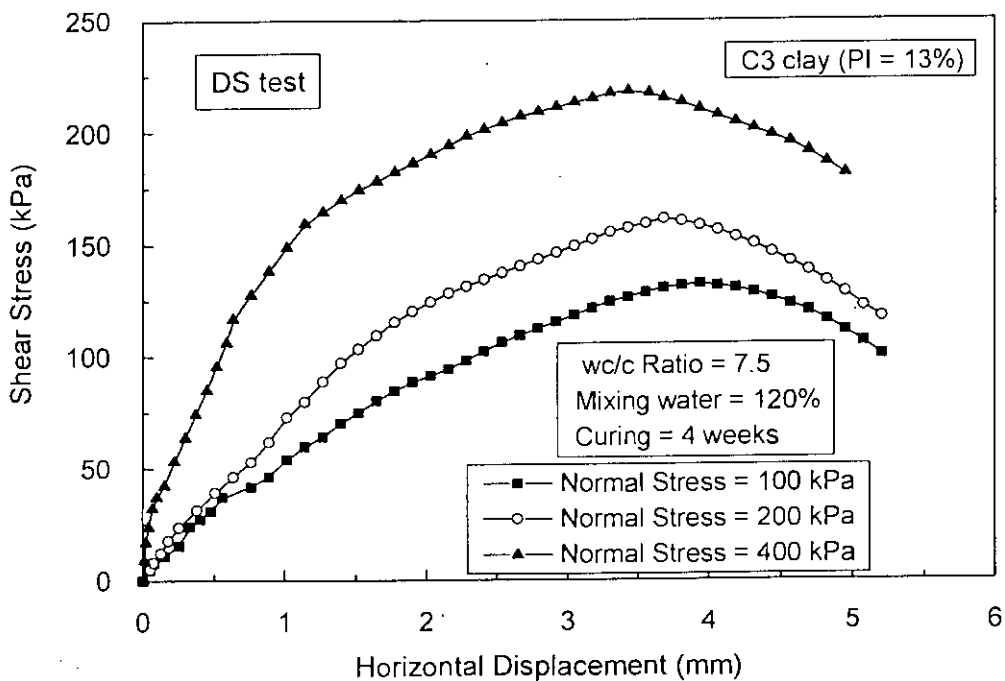


Fig. 5.62 Relationship between  $q_u$  and  $E_{50}$  Shown in Terms of Curing Time of Cement Treated C3 clay

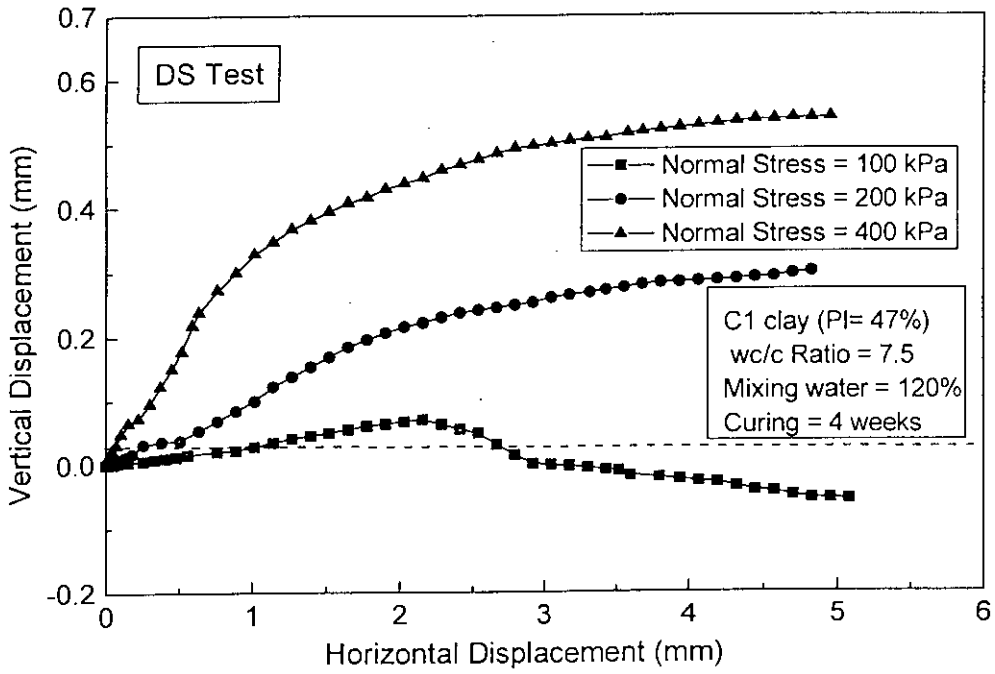


(a)

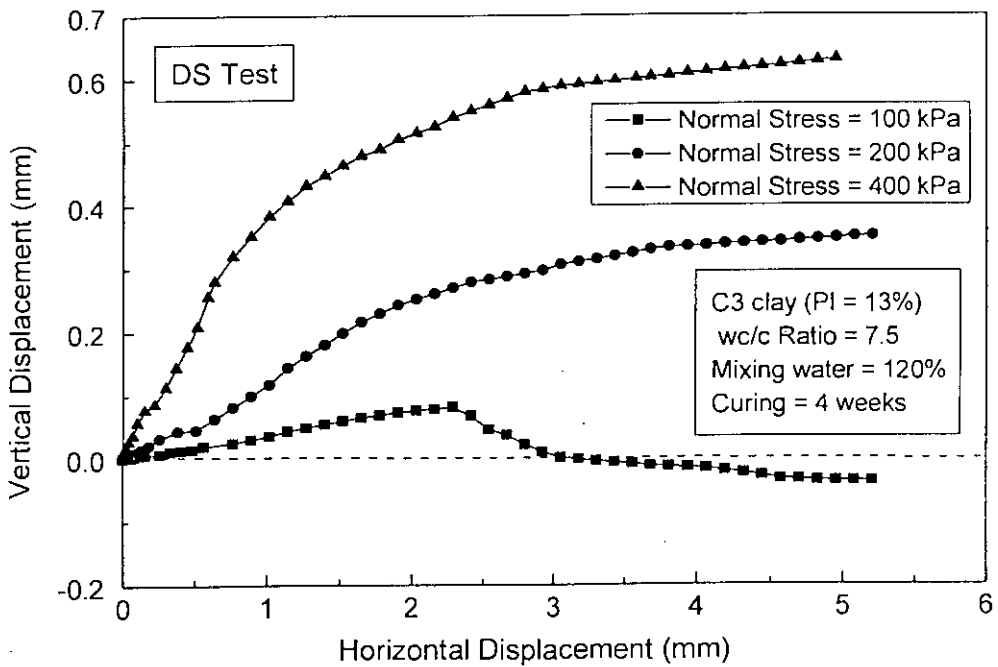


(b)

Fig. 5.63 Relationship between Shear Stress with Horizontal Displacement of Cement Treated Clays (a) C1 Clay and (b) C3 Clay

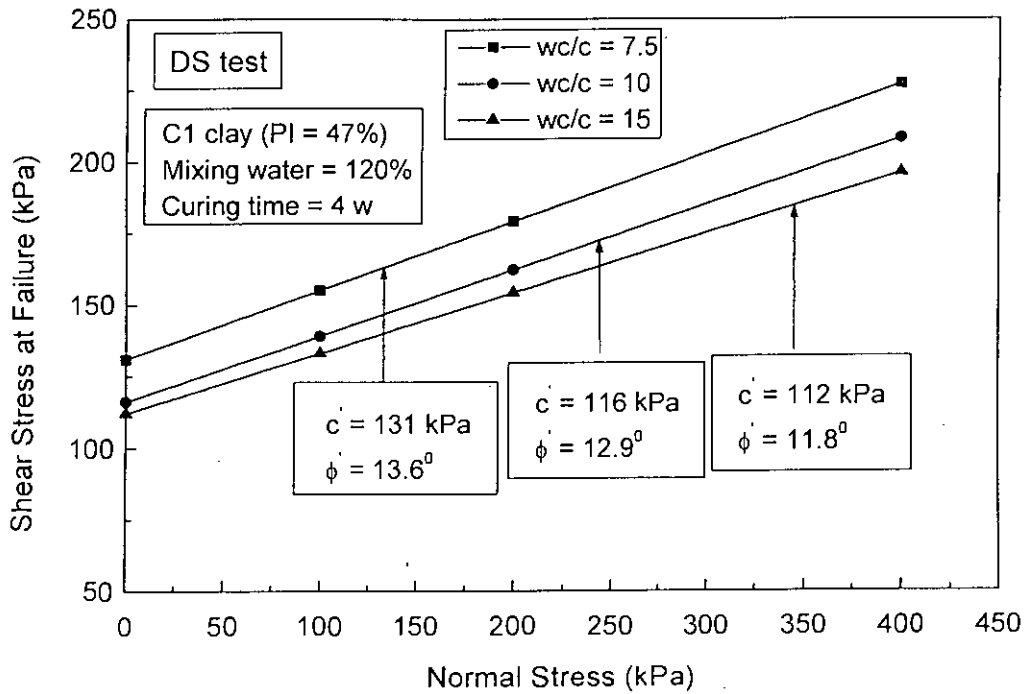


(a)

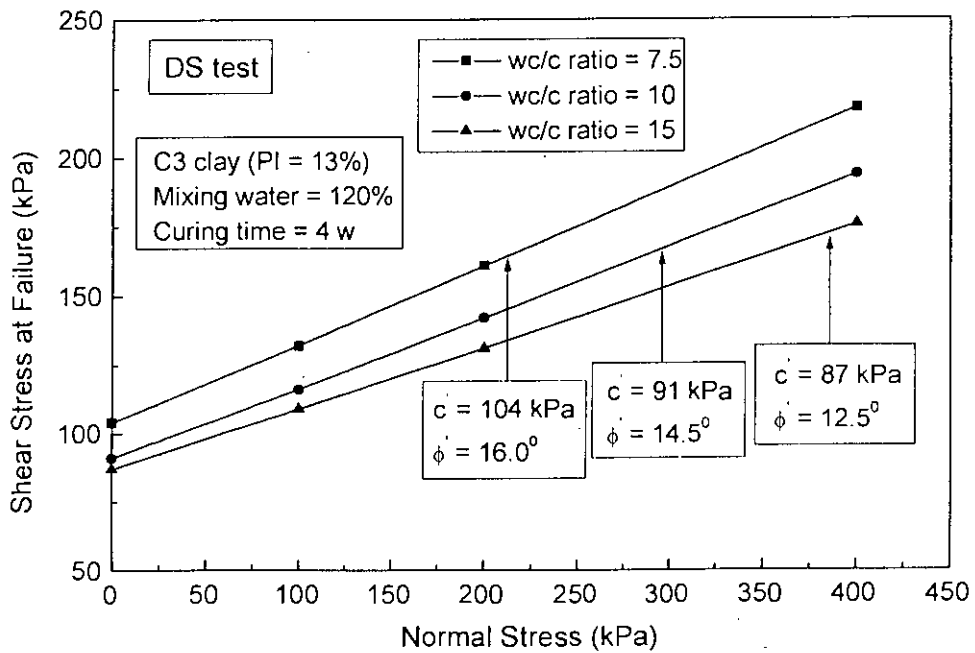


(b)

Fig. 5.64 Relationships between Vertical with Horizontal Displacement of Cement Treated Clays (a) C1 Clay and (b) C3 Clay



(a)



(b)

Fig. 5.65 Relationship between Shear and Normal Stress of Cement Treated Clays (a) C1 Clay and (b) C3 Clay

Table 5.6 Shear Strength Parameters  $e'$  and  $\phi'$  for Cement Treated Clays

Parameters	$w_i$ (%)	wc/c Ratio	C1 Clay		C2 Clay		C3 Clay	
			Curing Time		Curing Time		Curing Time	
			4 w	12 w	4 w	12 w	4 w	12 w
$c'$ in kPa	120	7.5	131	141	82	87	104	115
		10	116	134	77	82	91	101
		15	112	129	73	77	87	96
	150	7.5	114	128	74	80	86	99
		10	101	117	69	75	75	83
		15	97	112	64	69	70	78
	200	7.5	109	118	69	76	82	89
		10	96	112	65	70	71	79
		15	91	105	61	65	67	74
	250	7.5	101	110	64	71	75	80
		10	88	103	60	65	66	73
		15	83	97	55	59	63	69
$\phi'$ in degree	120	7.5	13.6	13.0	17.5	16.4	16.0	14.2
		10	12.9	12.2	15.4	14.6	14.1	13.0
		15	11.8	11	13.1	12.8	12.5	11.3
	150	7.5	12.2	12.0	13.5	13.1	15.4	15.2
		10	11.6	10.9	12.0	11.3	13.5	12.6
		15	10.5	9.8	10.1	9.8	12.0	10.8
	200	7.5	11.4	11.1	14.7	14.0	13.0	12.5
		10	10.8	10.1	12.9	12.3	11.4	10.6
		15	9.9	9.2	11.0	10.7	10.2	9.4
	250	7.5	10.6	10.4	13.3	12.9	11.8	11.0
		10	10.0	9.5	11.7	11.1	10.5	9.6
		15	9.2	8.6	9.9	9.5	9.1	7.9
$c'$	Untreated Clay		15.2		13.5		11.6	
$\phi'$	Untreated Clay		6.4		8.0		7.1	

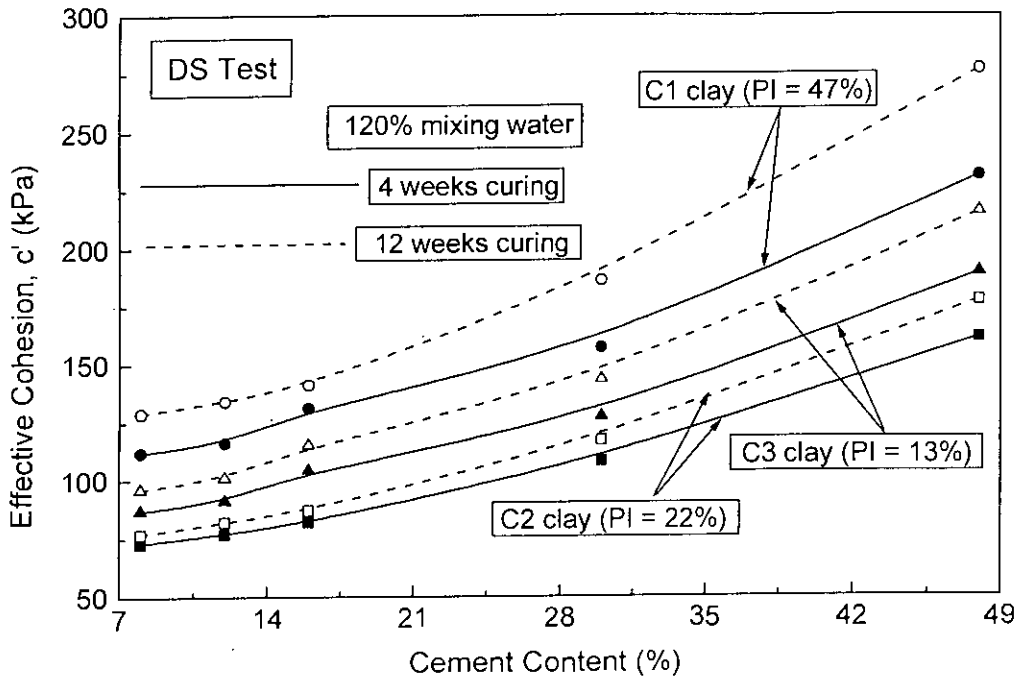


Fig. 5.66 Effect of Cement Content, Clay Type and Curing Time on Cohesion ( $c'$ ) of Treated Clays

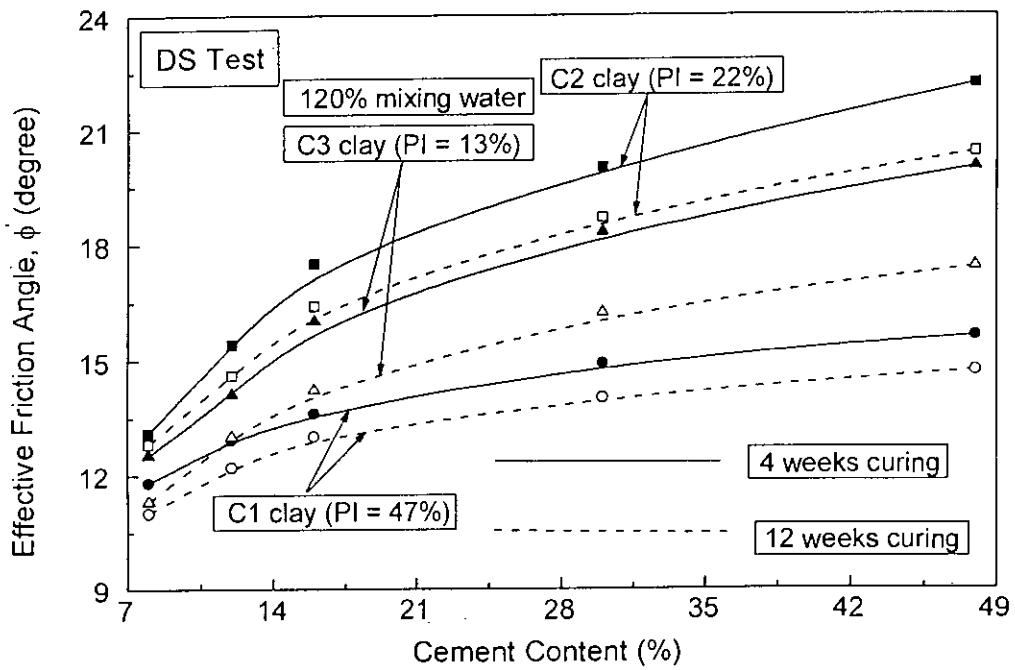


Fig. 5.67 Effect of Cement Content, Clay Type and Curing Time on Friction Angle ( $\phi'$ ) of Treated Clays

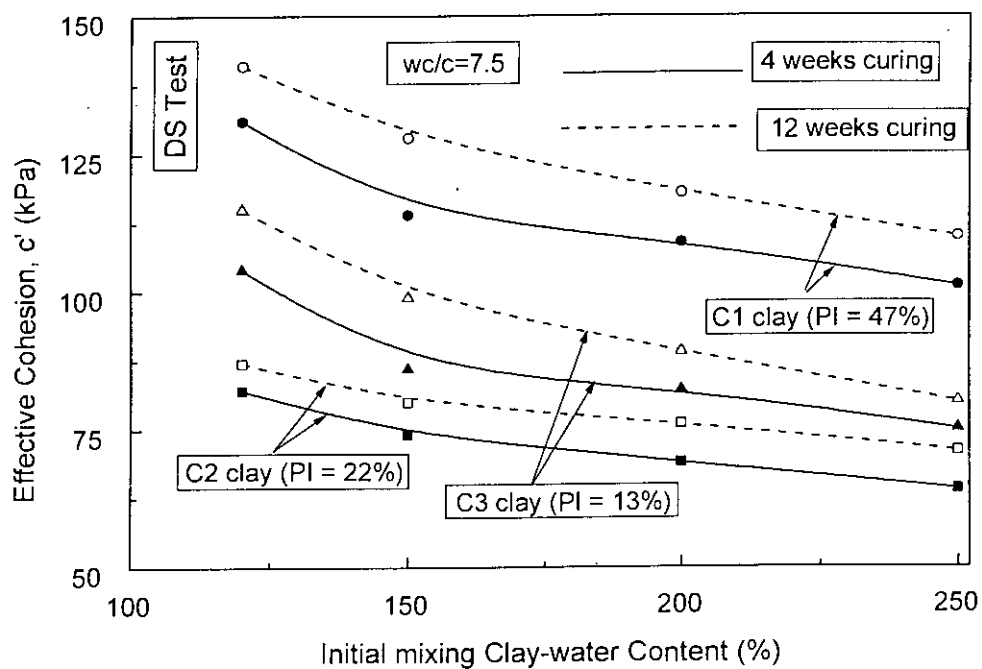


Fig. 5.68 Effect of Mixing Clay-water Content, Clay Type and Curing Time on Cohesion ( $c'$ ) of Treated Clays

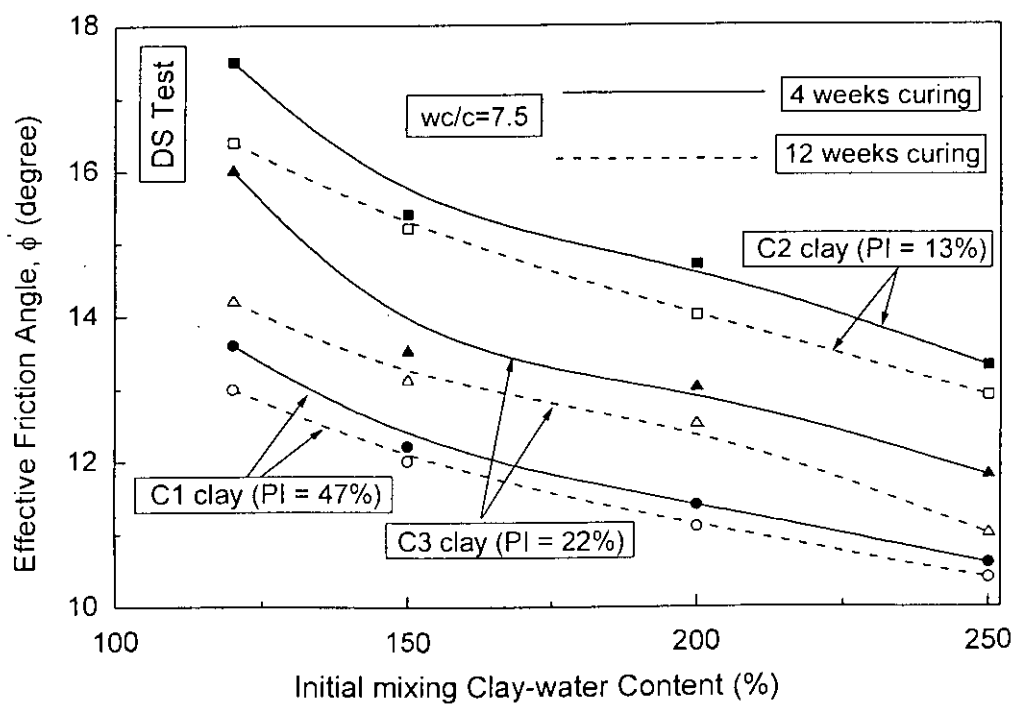


Fig. 5.69 Effect of Mixing Clay-water Content, Clay Type and Curing Time on Friction Angle ( $\phi'$ ) of Treated Clays

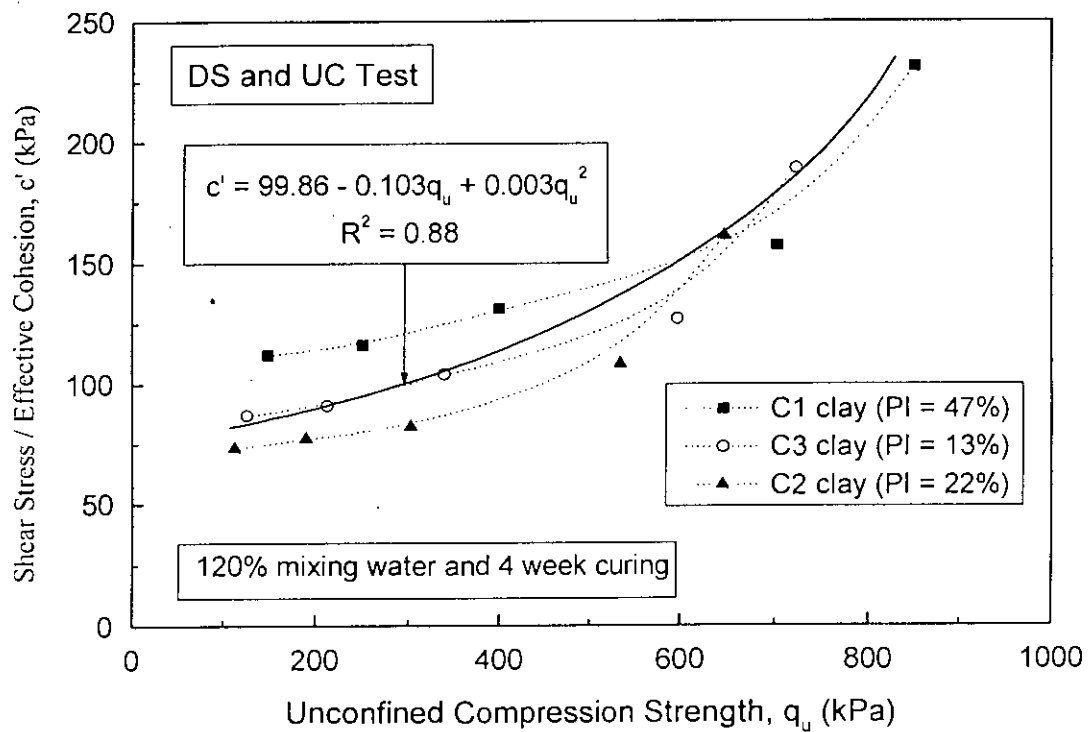
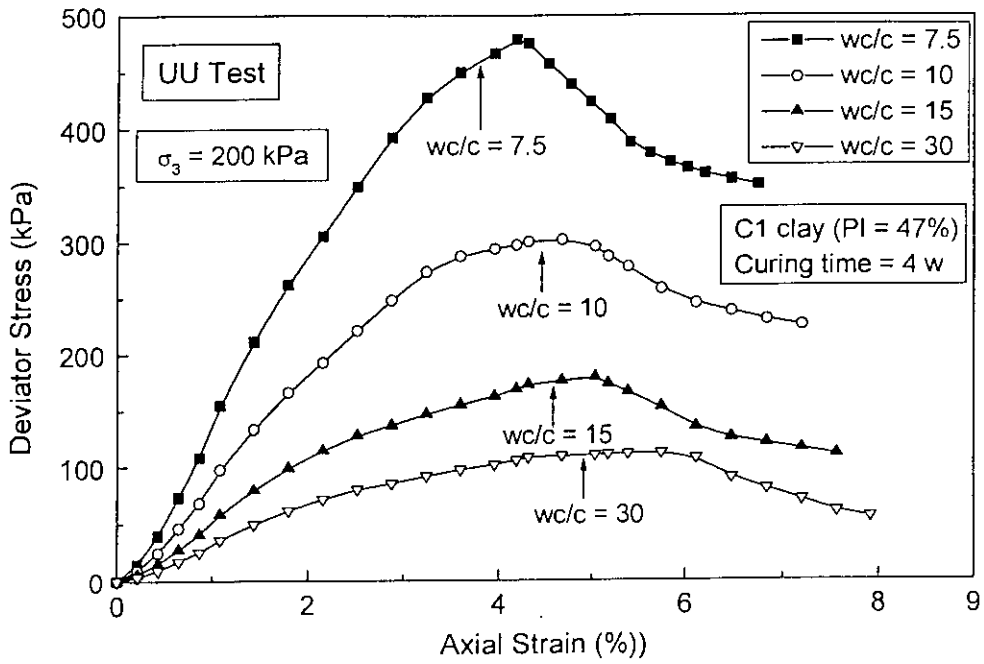
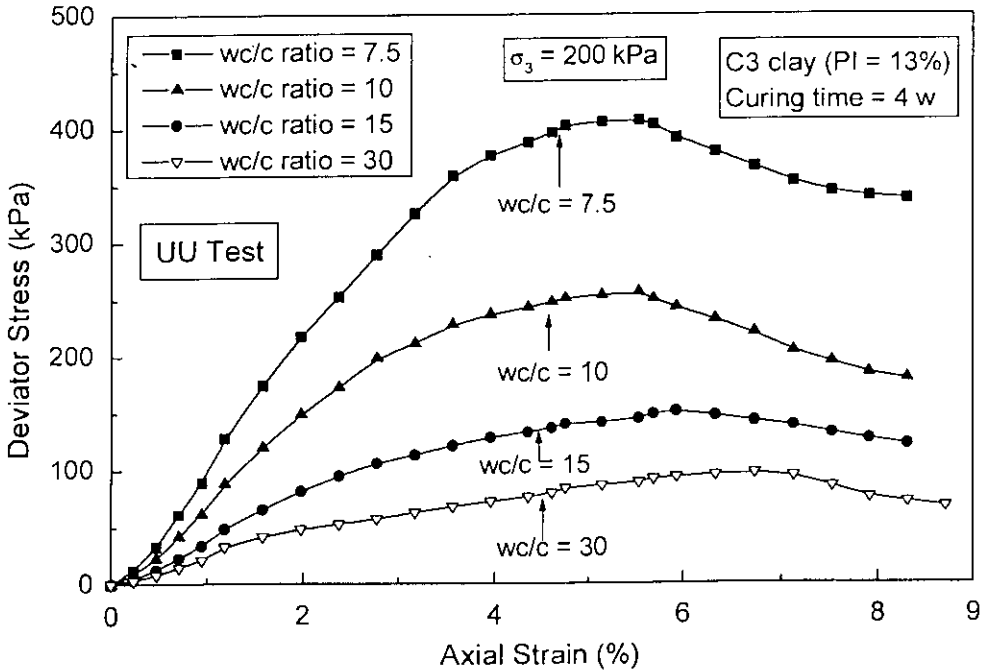


Fig. 5.70 Relationship between DS and UC Test Results of Cement Treated Clays



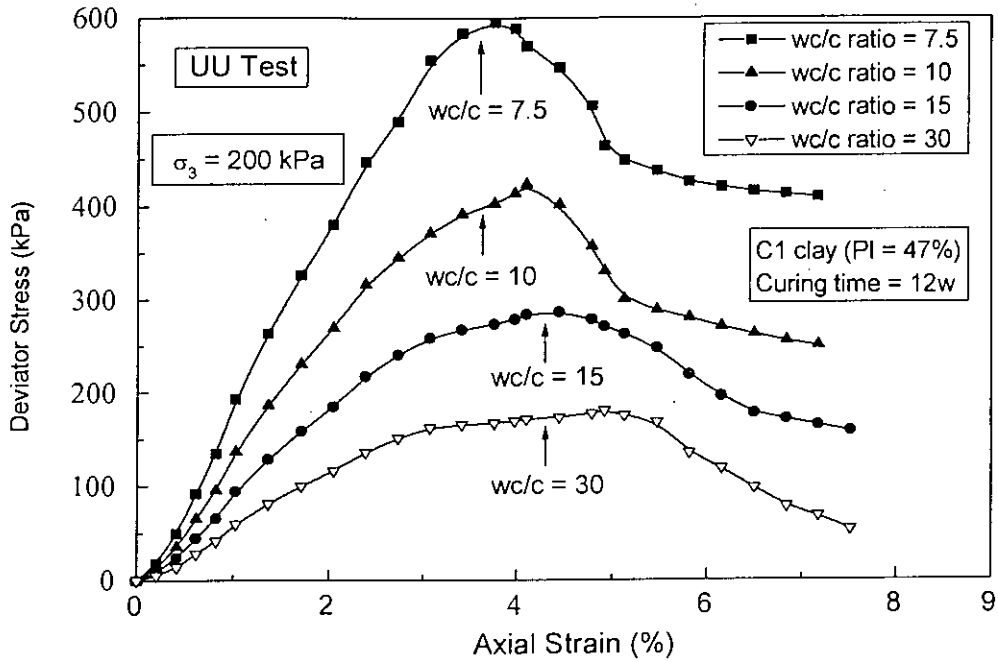


(a)

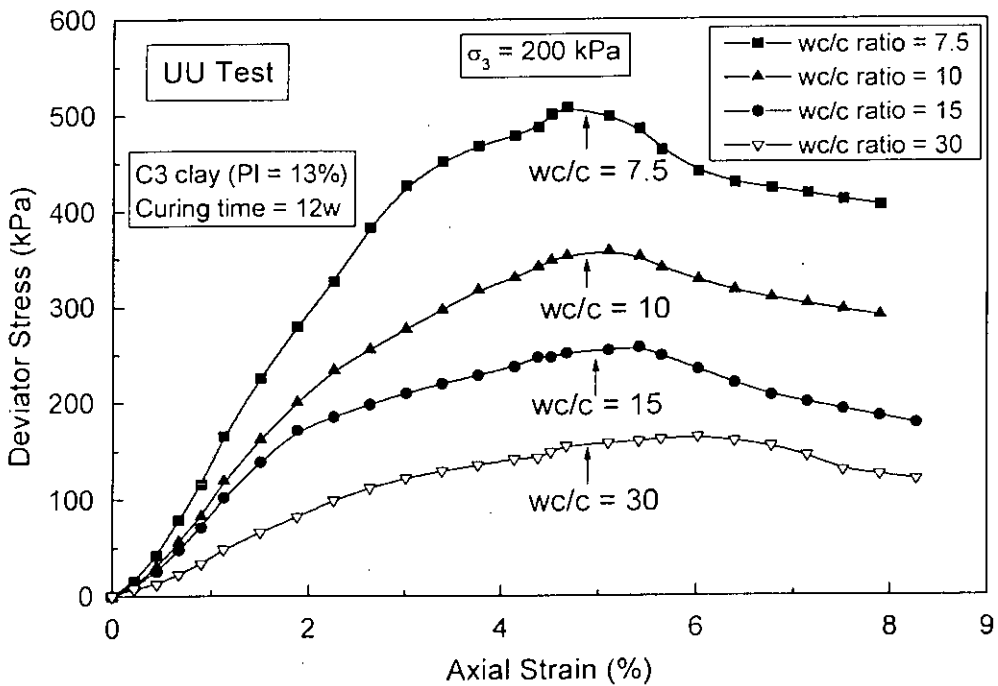


(b)

Fig. 5.71 Stress-Strain Characteristics from UU Test at 4 Weeks Curing of Cement Treated Clays (a) C1 Clay and (b) C3 Clay



(a)

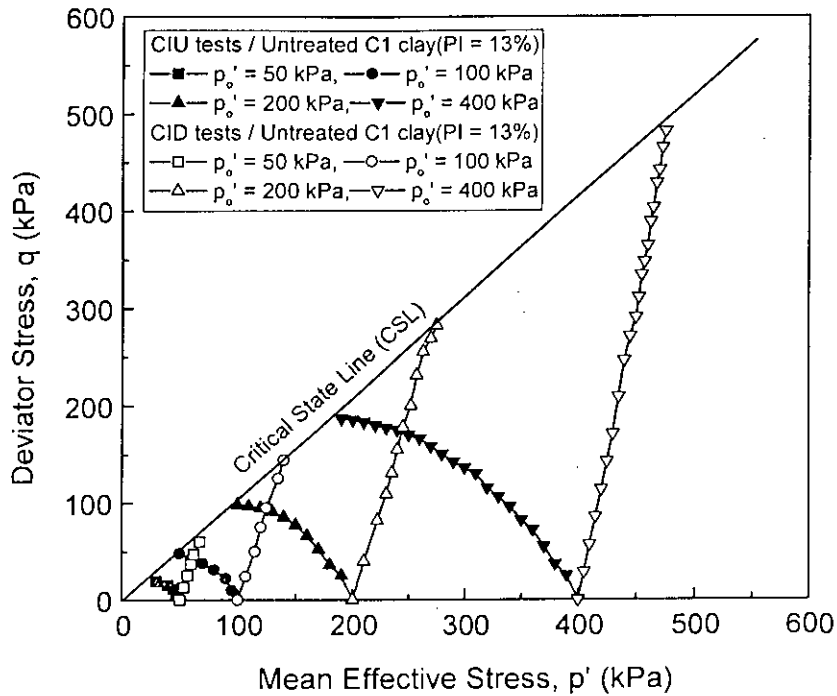


(b)

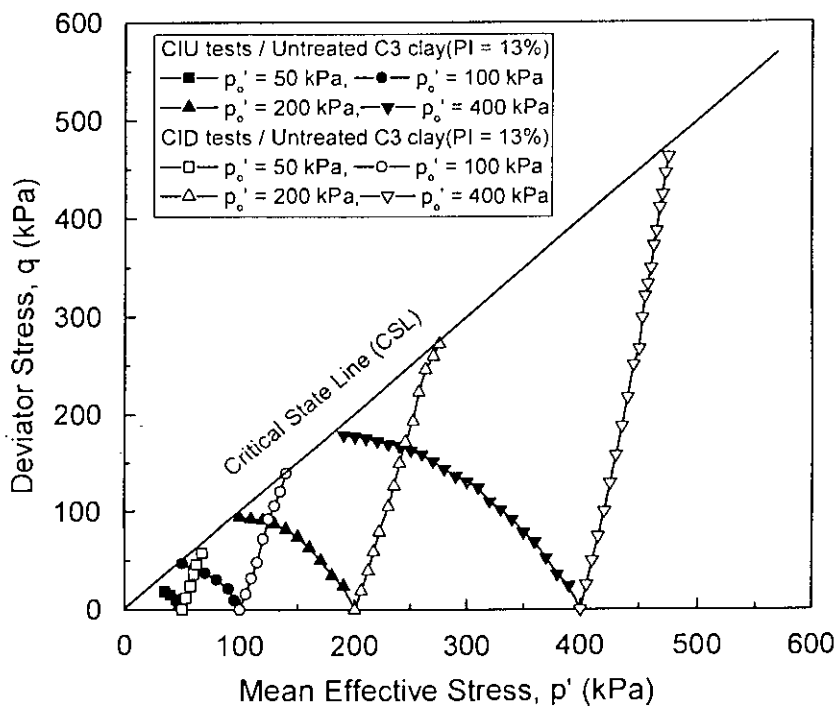
Fig. 5.72 Stress-Strain Characteristics from UU Test at 12 Weeks Curing of Cement Treated Clays (a) C1 Clay and (b) C3 Clay

**Table 5.7 Comparison of Undrained Shear Strength and Axial Strain at Failure of Cement Treated Clays from UC and UU Tests ( $\sigma_3 = 200$  kPa)**

Curing Time (week)	Clay Type	w/c Ratio	Undrained Shear Strength (kPa)		Axial Strain at Failure (%)	
			UC test	UU test	UC test	UU test
4 w	C1	7.5	200	240	1.94	1.83
		10	126	151	2.16	2.00
		15	75	93	2.33	2.17
		30	34	56	2.69	2.46
	C2	7.5	146	174	2.67	2.50
		10	92	108	2.85	2.67
		15	53	64	3.00	2.83
		30	27	45	3.23	3.01
	C3	7.5	170	219	2.40	2.33
		10	107	142	2.50	2.50
		15	63	91	2.83	2.67
		30	32	48	3.15	2.93
12 w	C1	7.5	267	299	4.19	3.76
		10	168	211	4.68	4.11
		15	113	143	5.04	4.45
		30	38	89	5.76	4.92
	C2	7.5	203	237	5.26	5.00
		10	134	160	5.64	5.14
		15	86	103	6.02	5.36
		30	30	69	5.64	6.43
	C3	7.5	219	254	5.54	4.67
		10	142	194	5.61	5.10
		15	90	129	5.94	5.41
		30	35	82	6.7	6.02

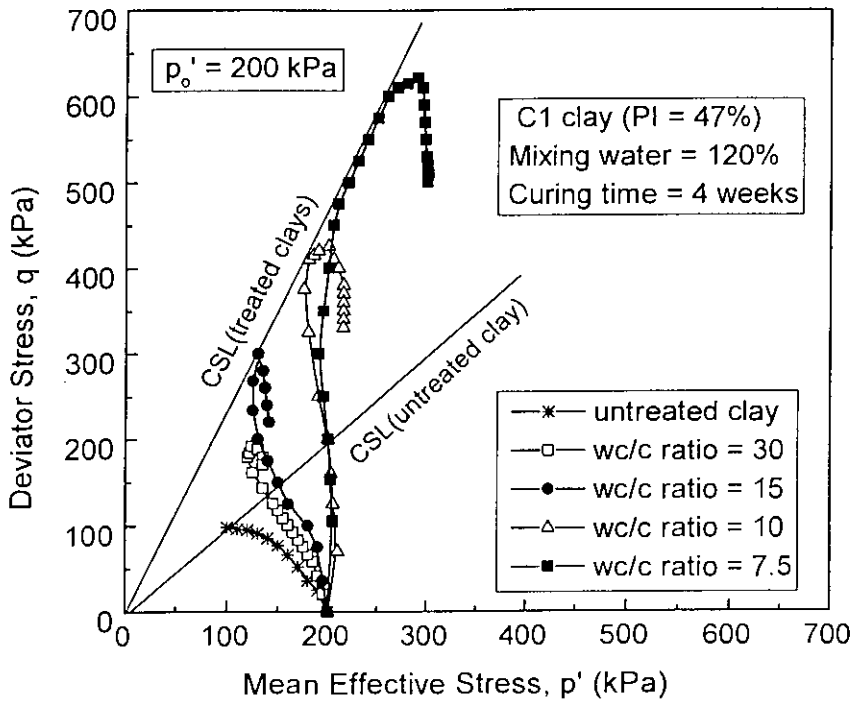


(a)

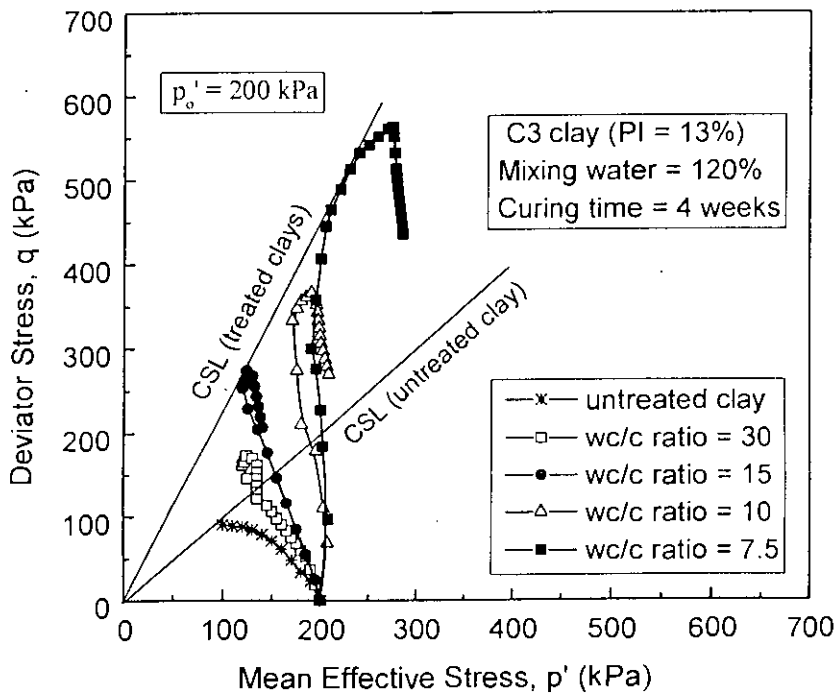


(b)

Fig. 5.73 Undrained and Drained Stress Paths of Untreated Base Clays  
(a) C1 Clay and (b) C3 Clay



(a)



(b)

Fig. 5.74 Undrained Stress Paths of Cement Treated Clays  
(a) C1 Clay and (b) C3 Clay

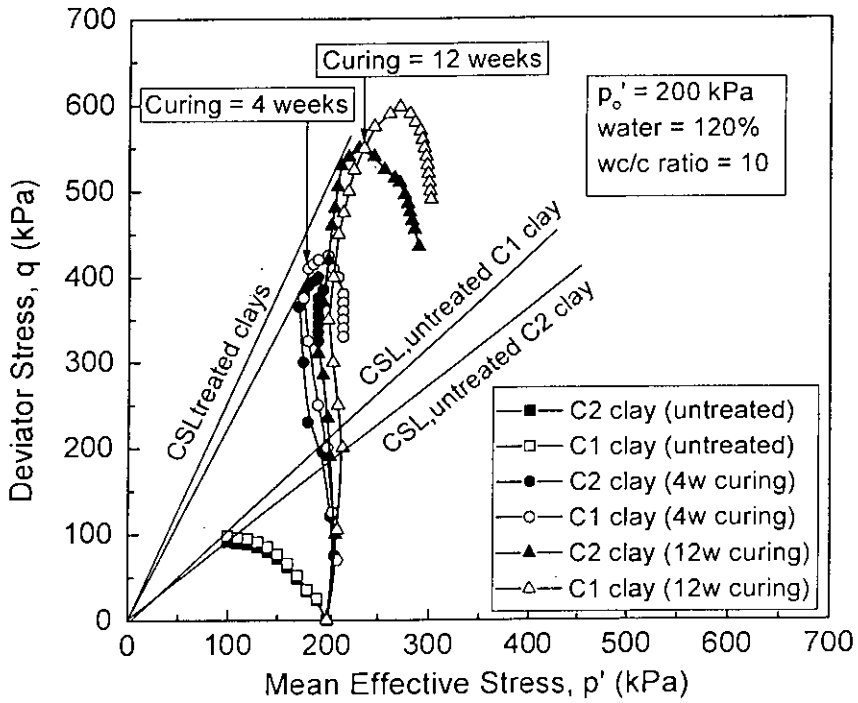


Fig. 5.75 Effect of Curing Time and Clay Type on Undrained Stress Paths of Cement Treated Clays

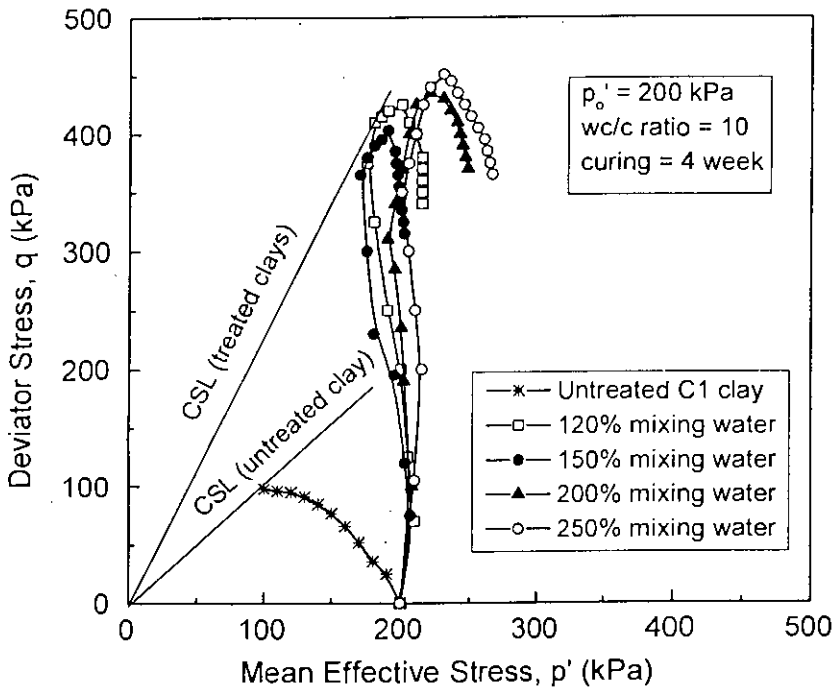


Fig. 5.76 Effect of Mixing Water Content on Undrained Stress Paths of Cement Treated Clays

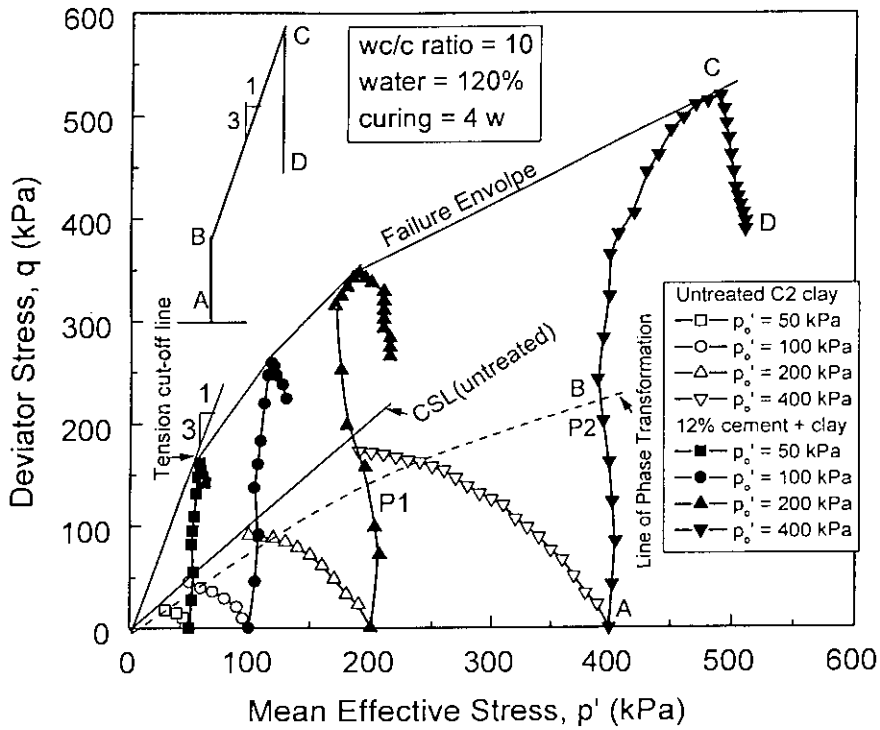


Fig. 5.77 Effect of Pre-Shear Effective Consolidation Pressure on Undrained Stress Paths of Cement Treated Clays

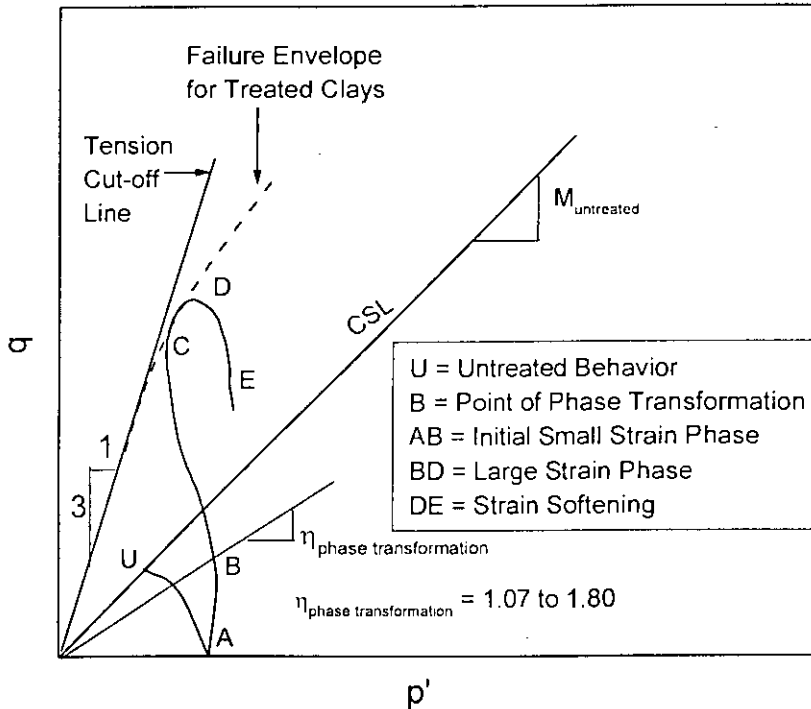
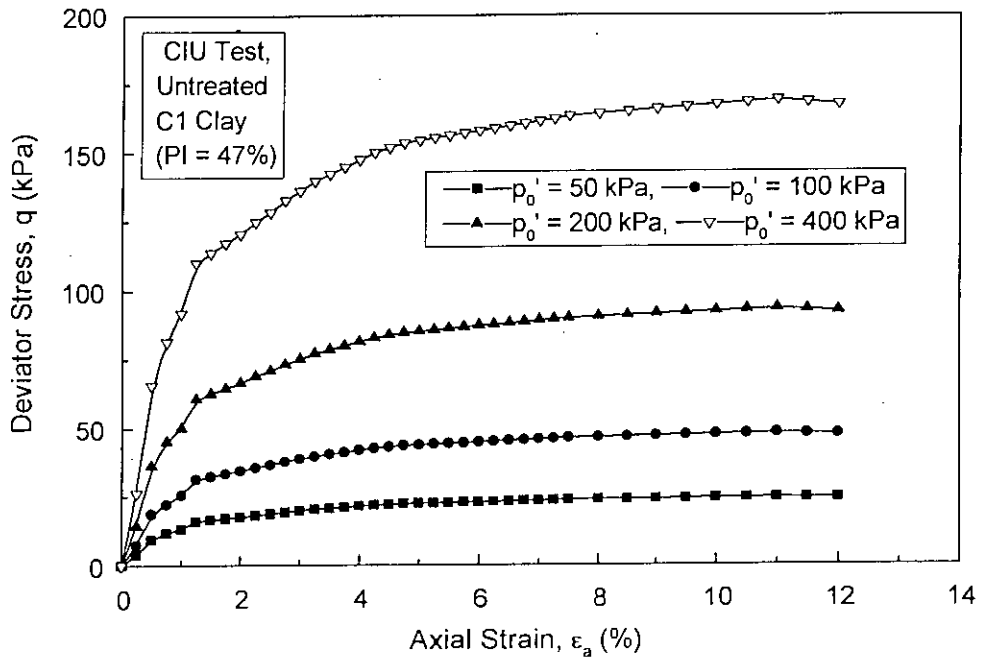
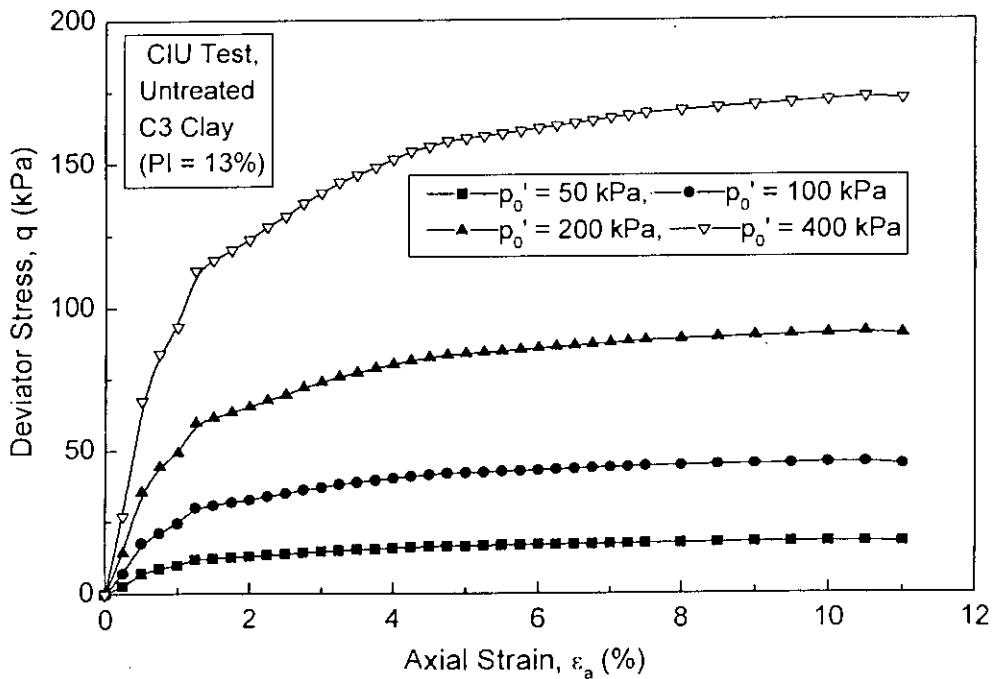


Fig. 5.78 Schematic Diagram of Undrained Stress Paths of Cement Treated Clays



(a)



(b)

Fig. 5.79 Deviator Stress Versus Axial Strain Response at Different Pre-Shear Effective Pressure of Untreated Base Clays (a) C1 Clay and (b) C3 Clay



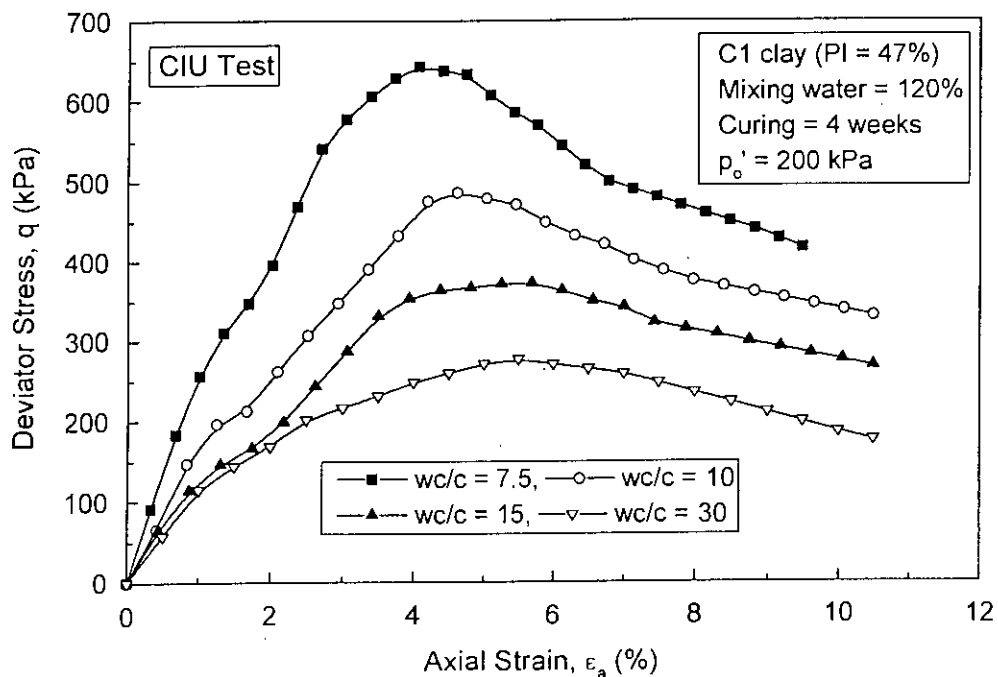


Fig. 5.80 Effect of Clay-Water/Cement ( $wc/c$ ) Ratio on Deviator Stress Versus Axial Strain Response of C1 Clay

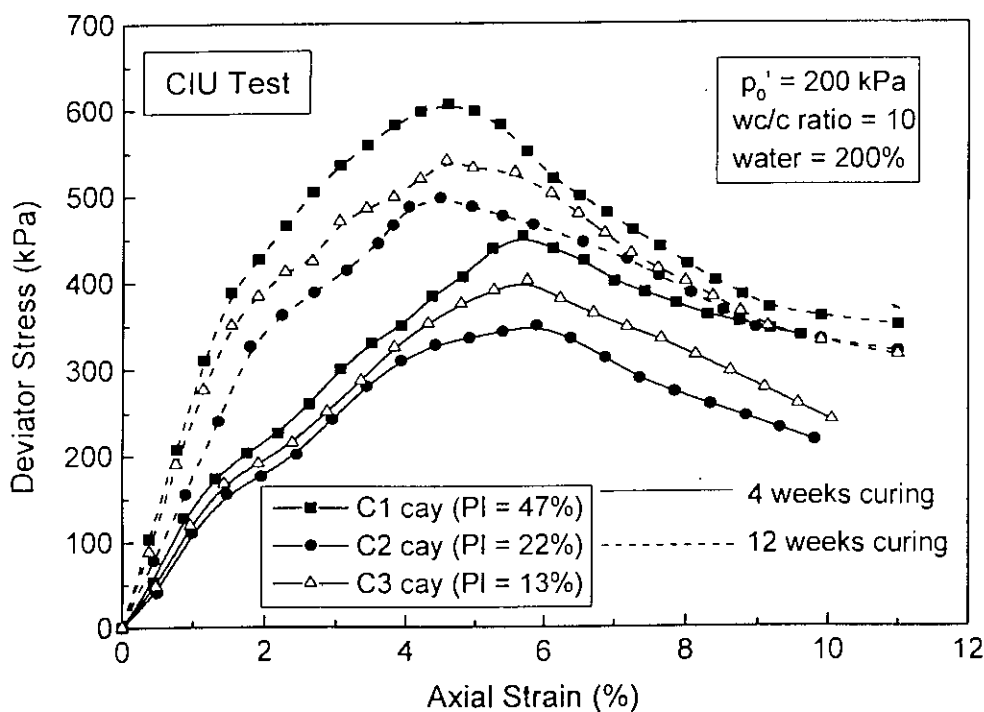


Fig. 5.81 Effect of Curing Time and Clay Type on Deviator Stress Versus Axial Strain Response

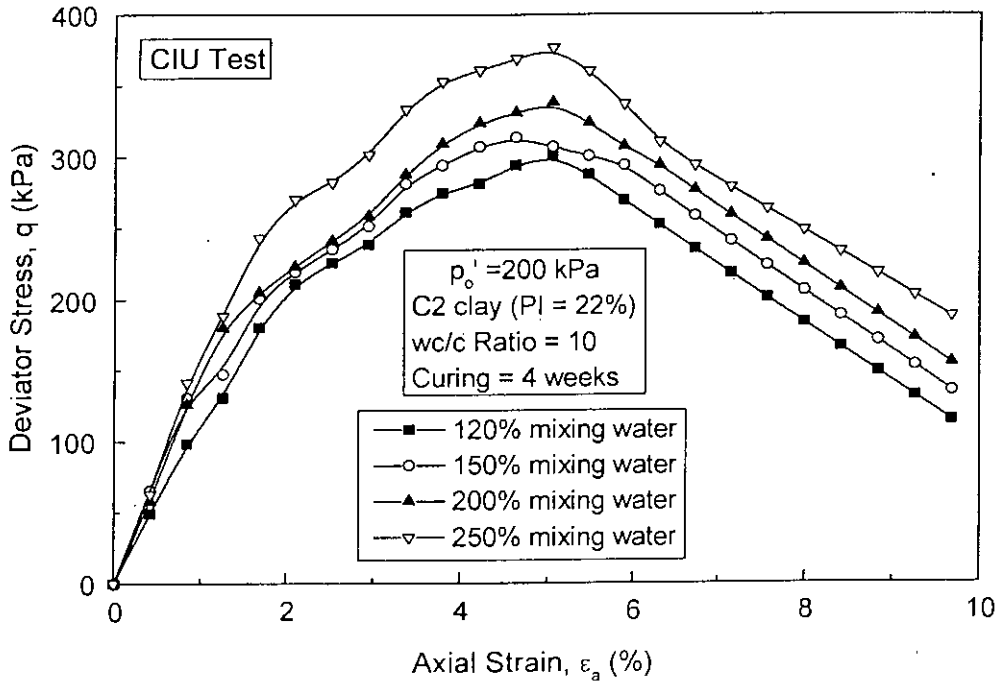


Fig. 5.82 Effect of Mixing Water Content on Deviator Stress Versus Axial Strain Response of C2 Clay

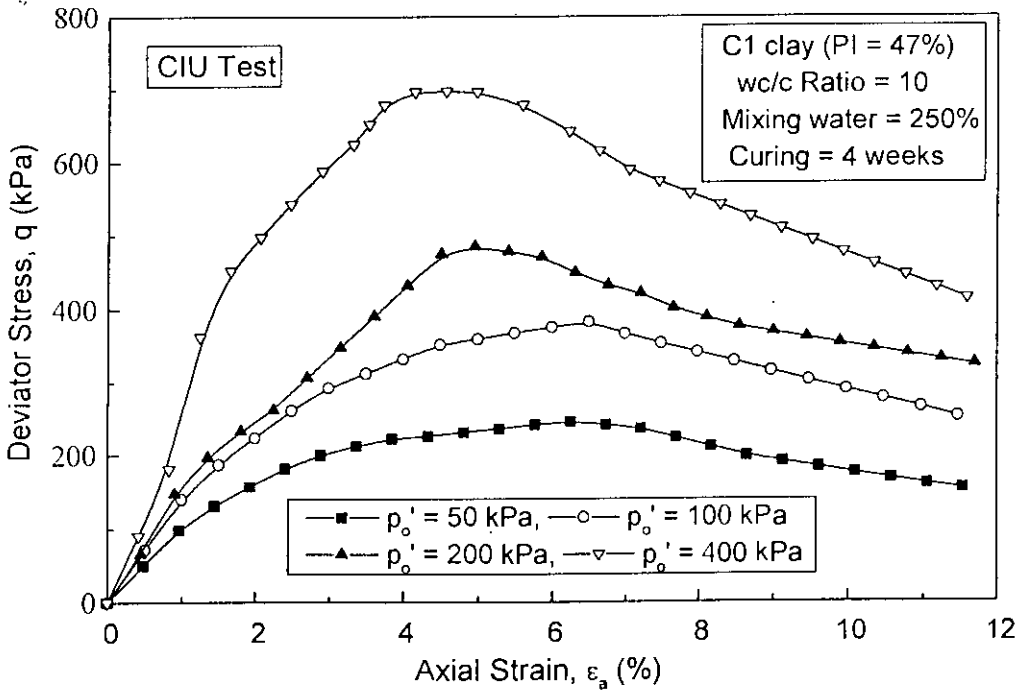
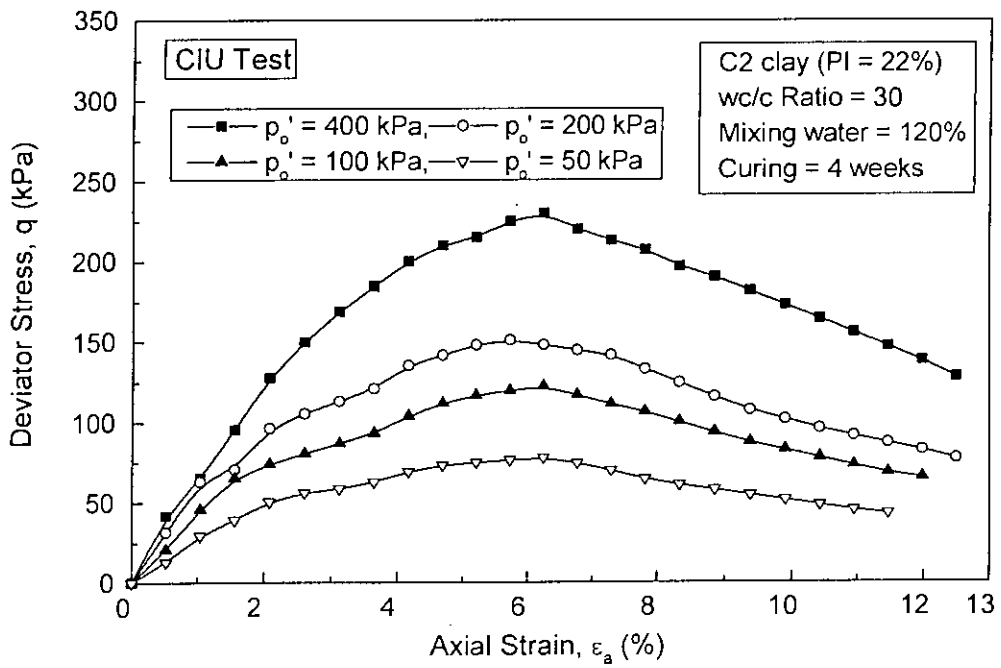
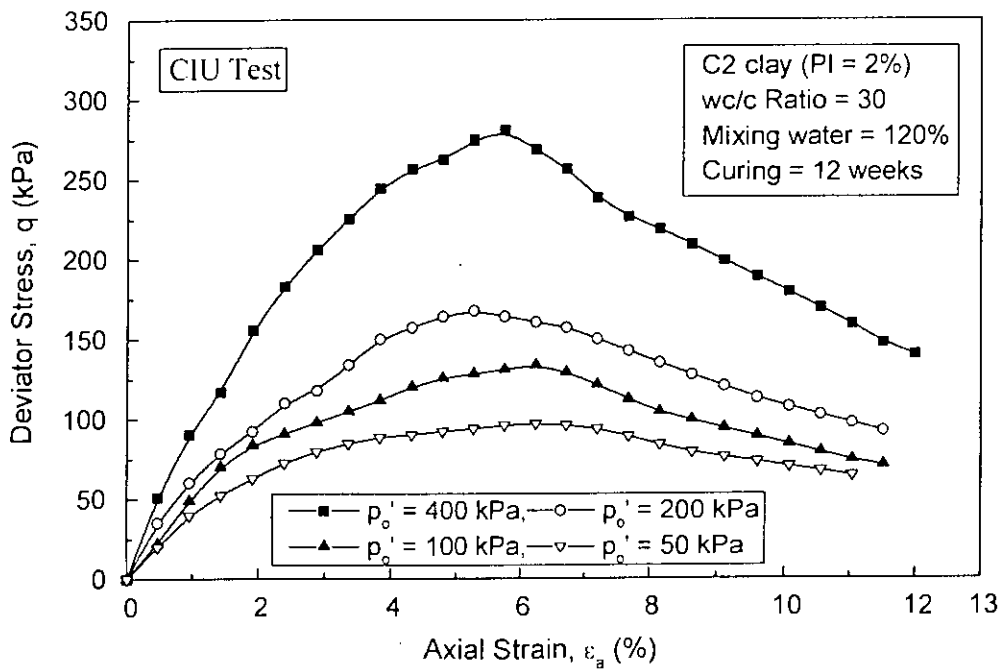


Fig. 5.83 Effect of Pre-Shear Effective Consolidation Pressure on Deviator Stress Versus Axial Strain Response of C1 Clay



(a)



(b)

Fig. 5.84 Effect of Pre-Shear Effective Pressure on Deviator Stress Versus Axial Strain Relations of C2 clay at Large  $wc/c$  (a) 4 w and (b) 12 w Curing

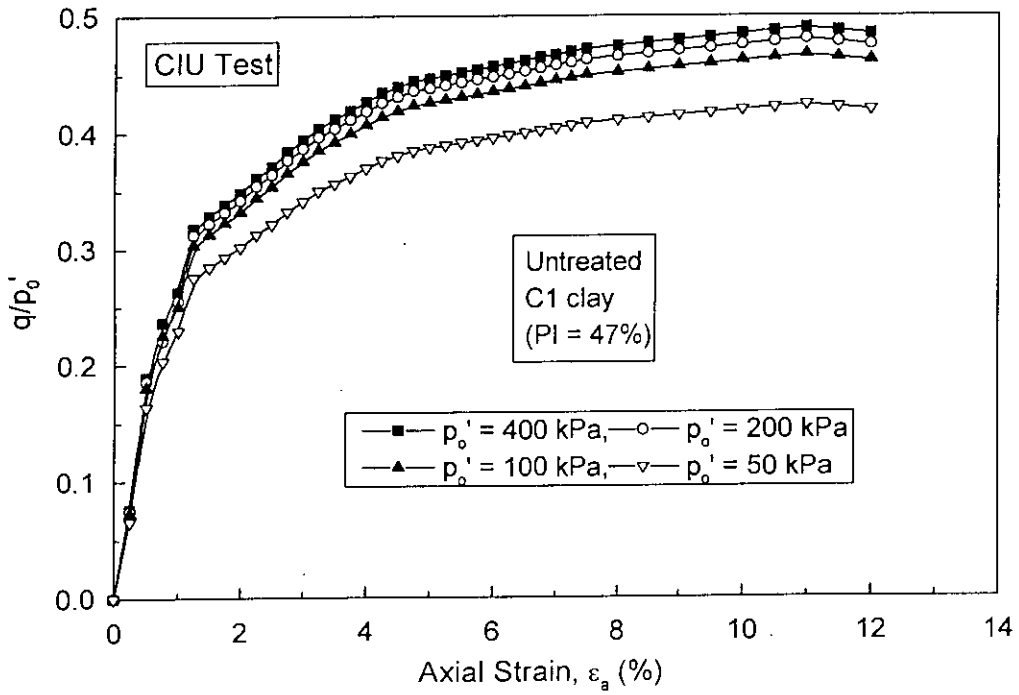


Fig. 5.85 Normalized Relationship Plots  $q/p'_0 - \epsilon_a$  for Untreated Base C1 Clay

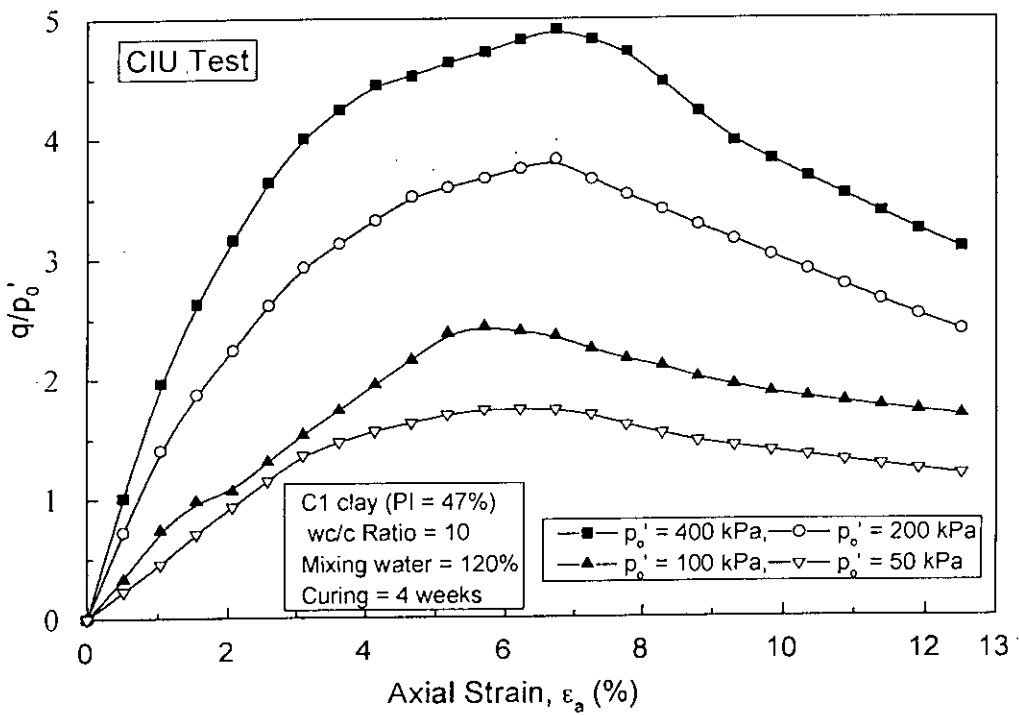
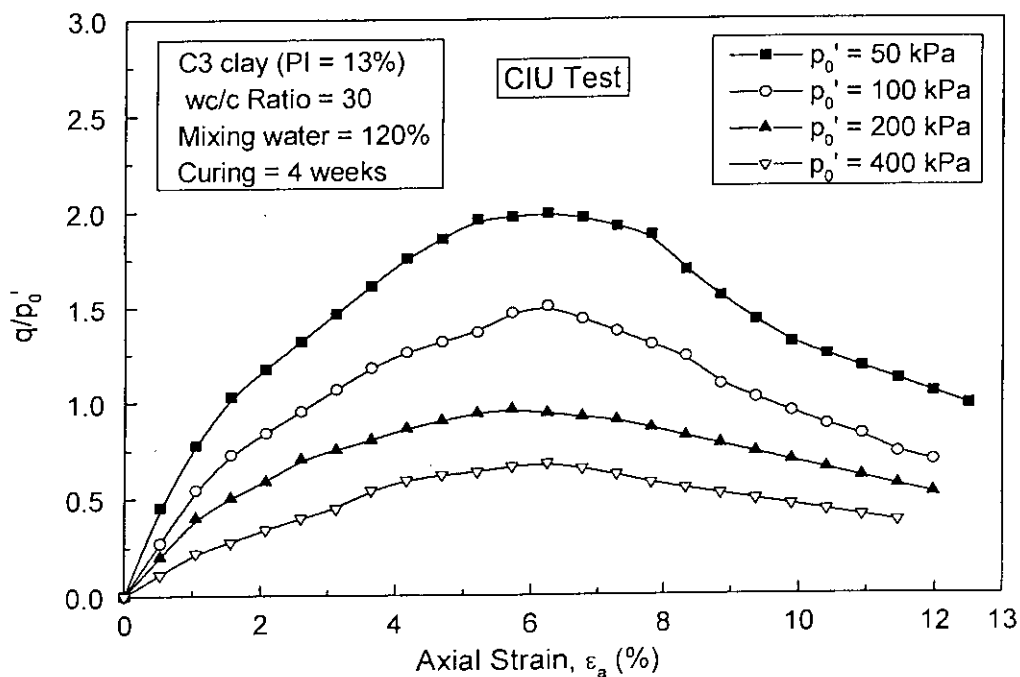
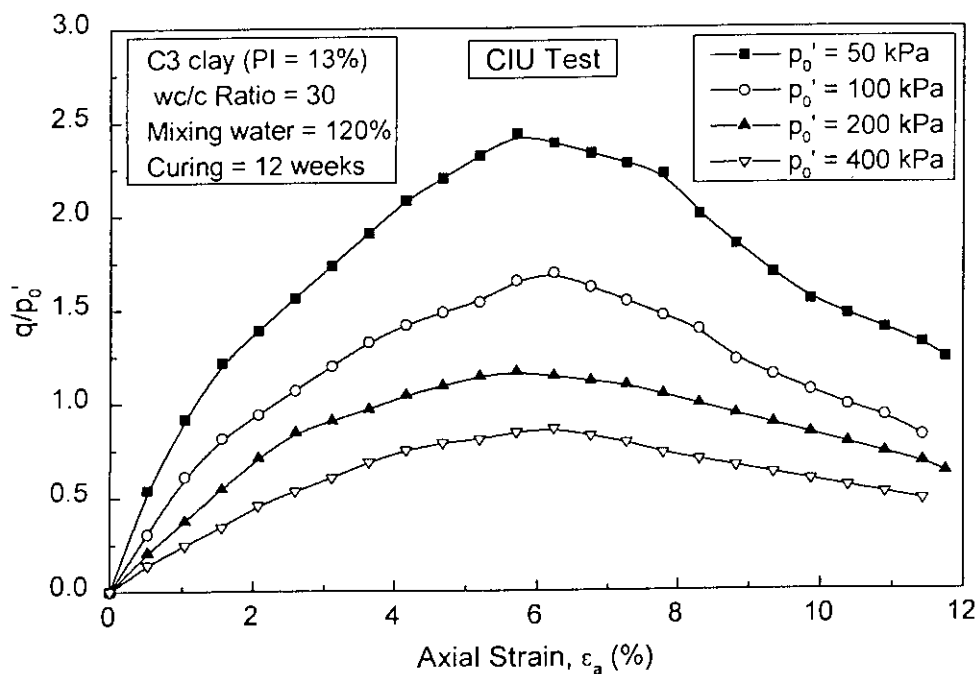


Fig. 5.86 Normalized Relationship Plots  $q/p'_0 - \epsilon_a$  for Cement Treated C1 clay

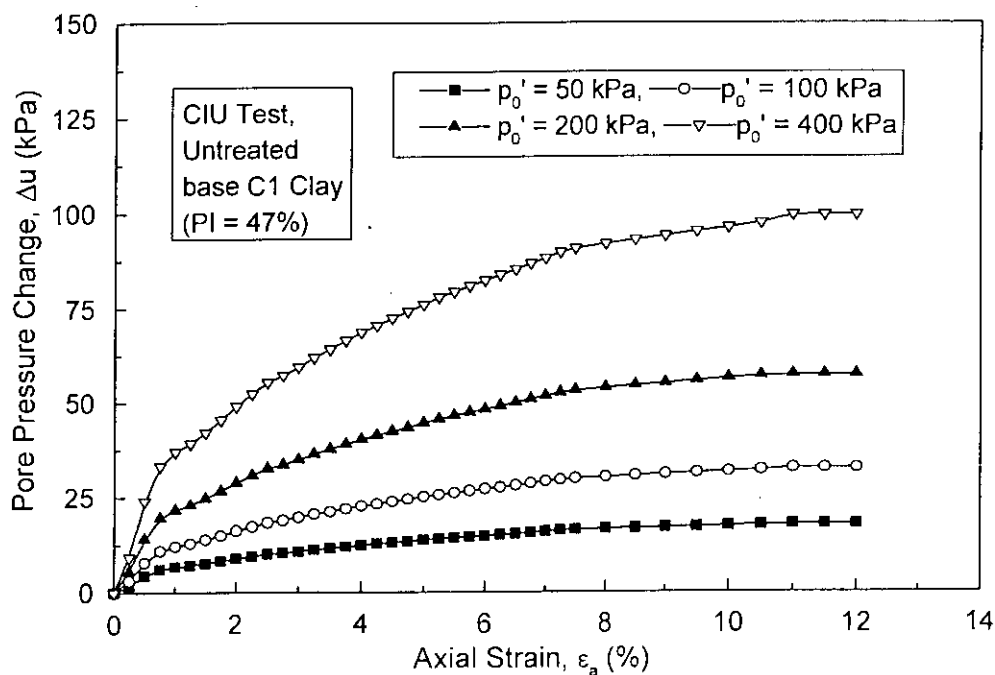


(a)

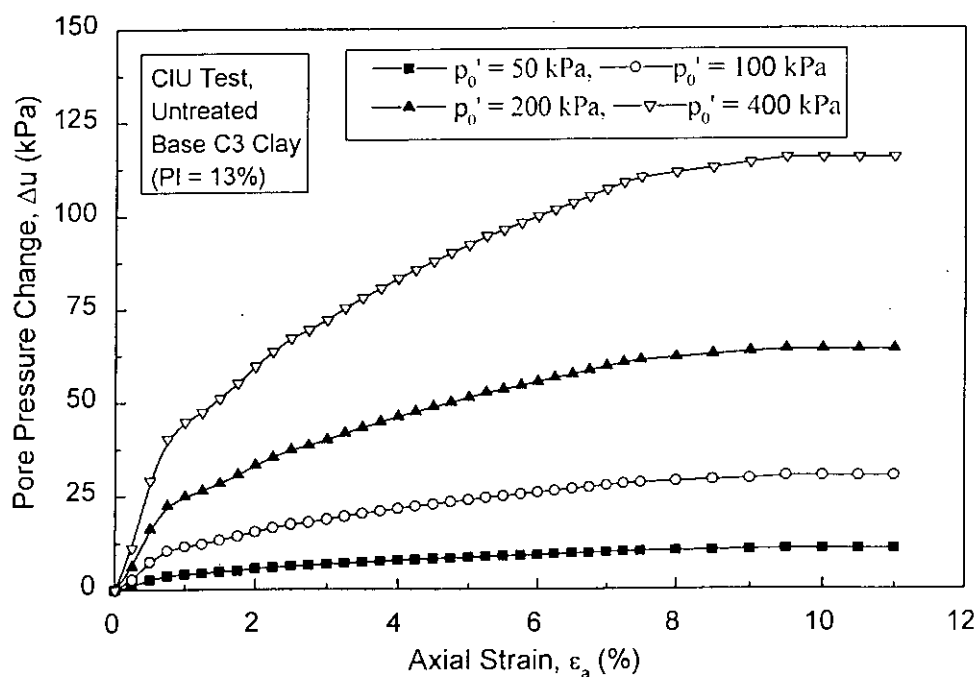


(b)

Fig. 5.87 Normalized Relationship Plots  $q/p'_0 - \epsilon_a$  for Treated C3 clay at Curing Time (a) 4 week and (b) 12 week



(a)



(b)

Fig. 5.88 Pore Pressure Versus Axial Strain Response at Different Pre-Shear Effective Pressure of Untreated Base Clays (a) C1 Clay and (b) C3 Clay

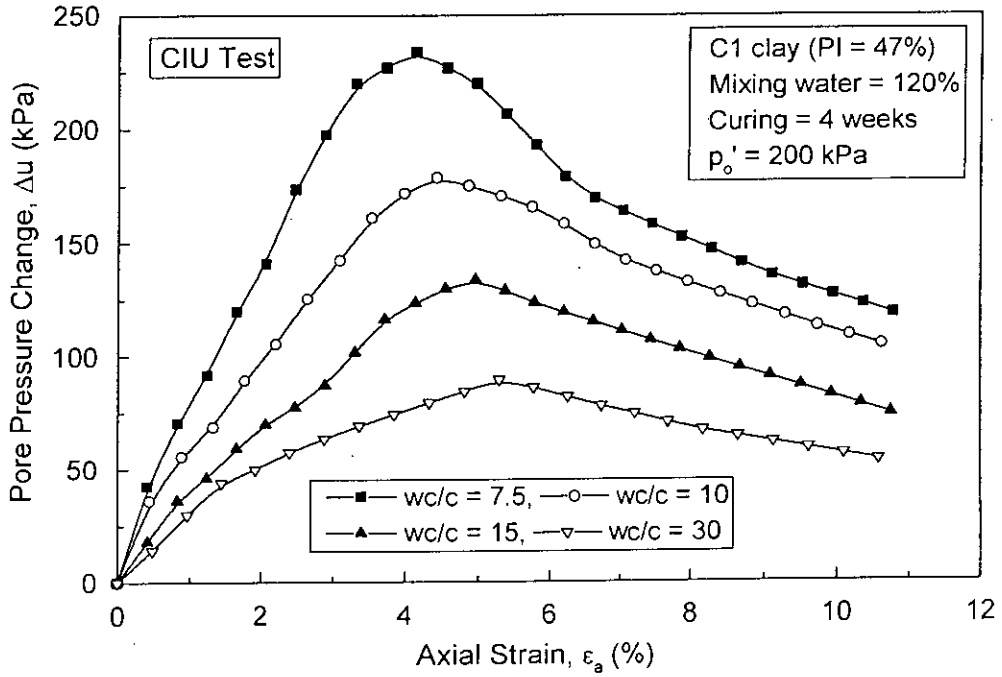


Fig. 5.89 Effect of Clay-Water/Cement (w/c) Ratio on Pore Pressure Versus Axial Strain Response of C1 Clay

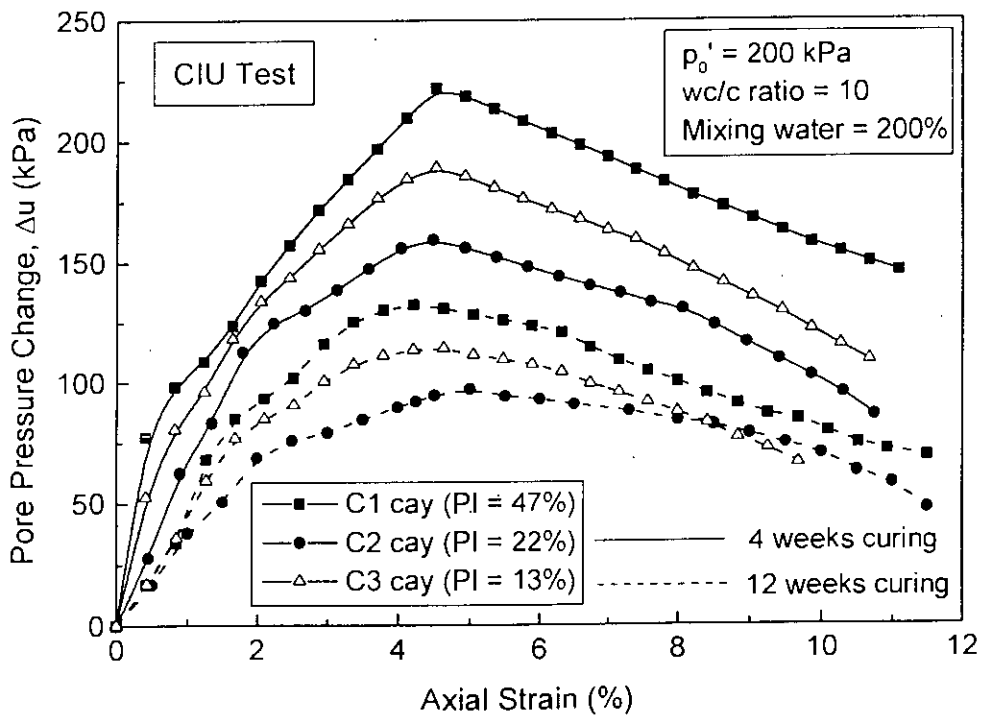


Fig. 5.90 Effect of Curing Time and Clay Type on Pore Pressure Versus Axial Strain Response

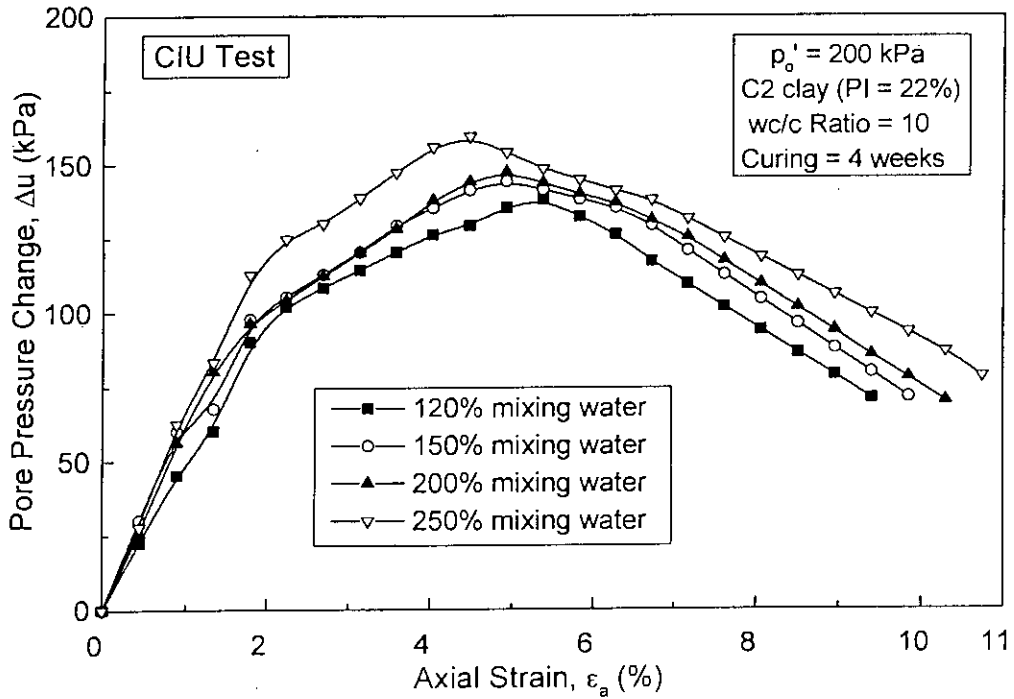


Fig. 5.91 Effect of Mixing Water Content on Pore Pressure Versus Axial Strain Response of C2 clay

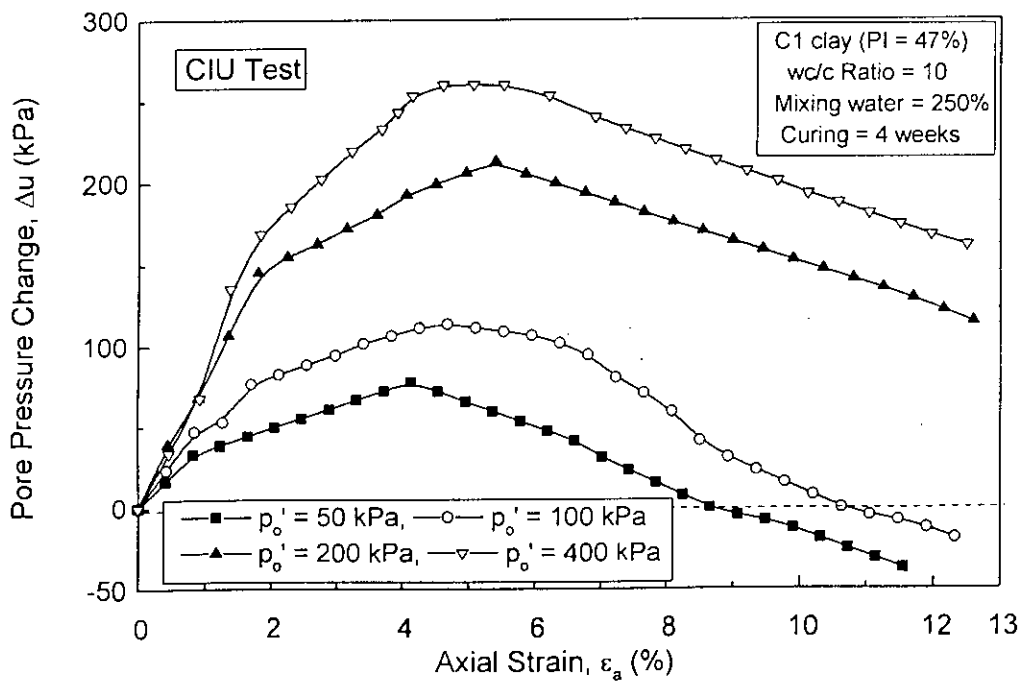
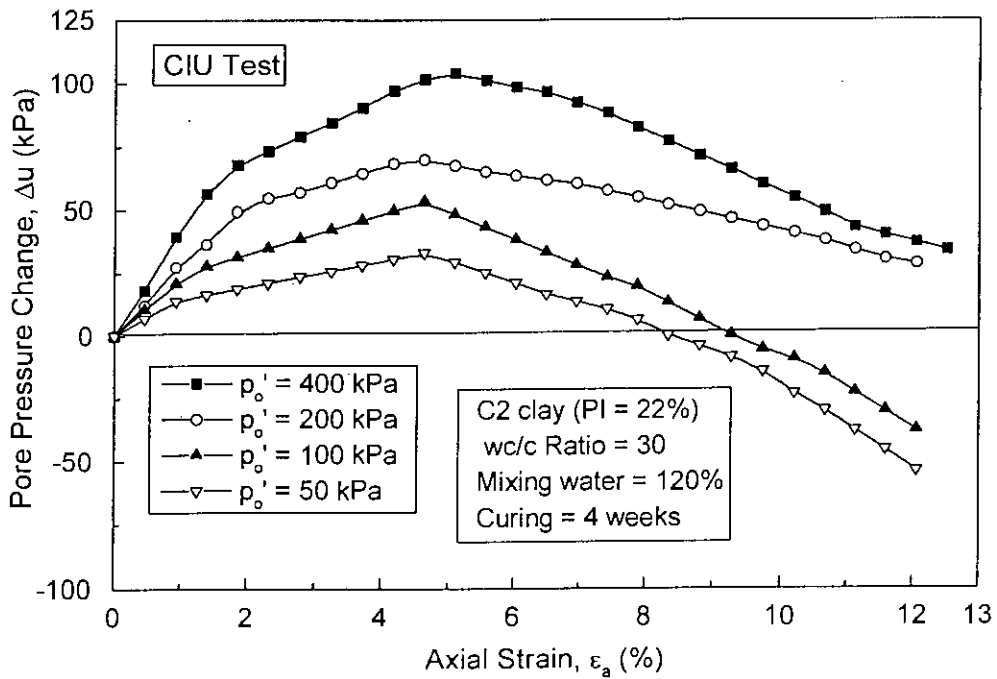
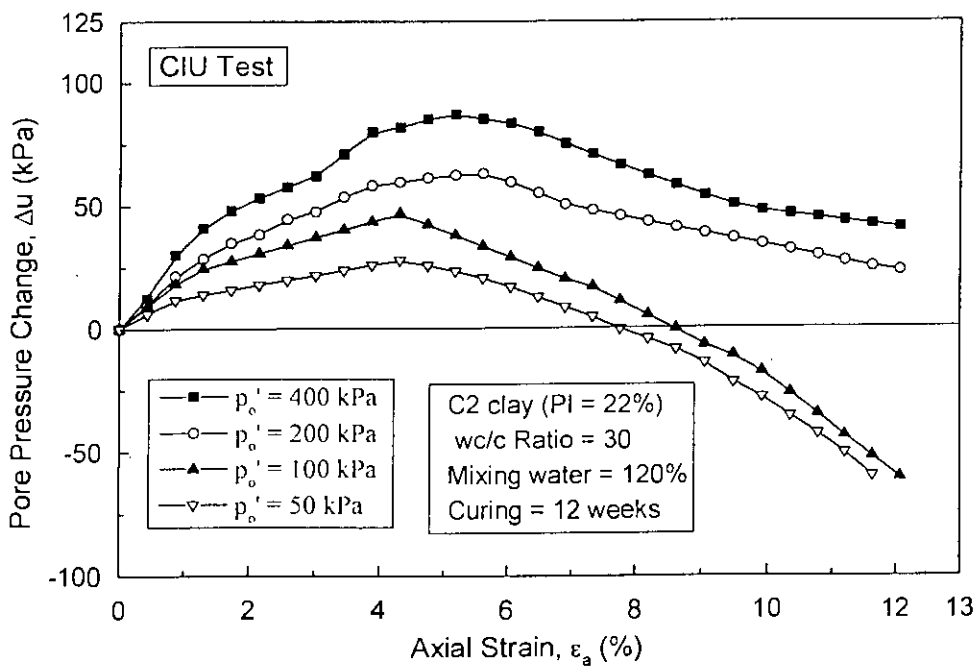


Fig. 5.92 Effect of Pre-Shear Effective Consolidation Pressure on Pore Pressure Versus Axial Strain Response of C1 Clay





(a)



(b)

Fig. 5.93 Effect of Pre-Shear Effective Pressure on Pore Pressure Versus Axial Strain Response of C2 clay at Large wc/c (a) 4 w and (b) 12 w Curing

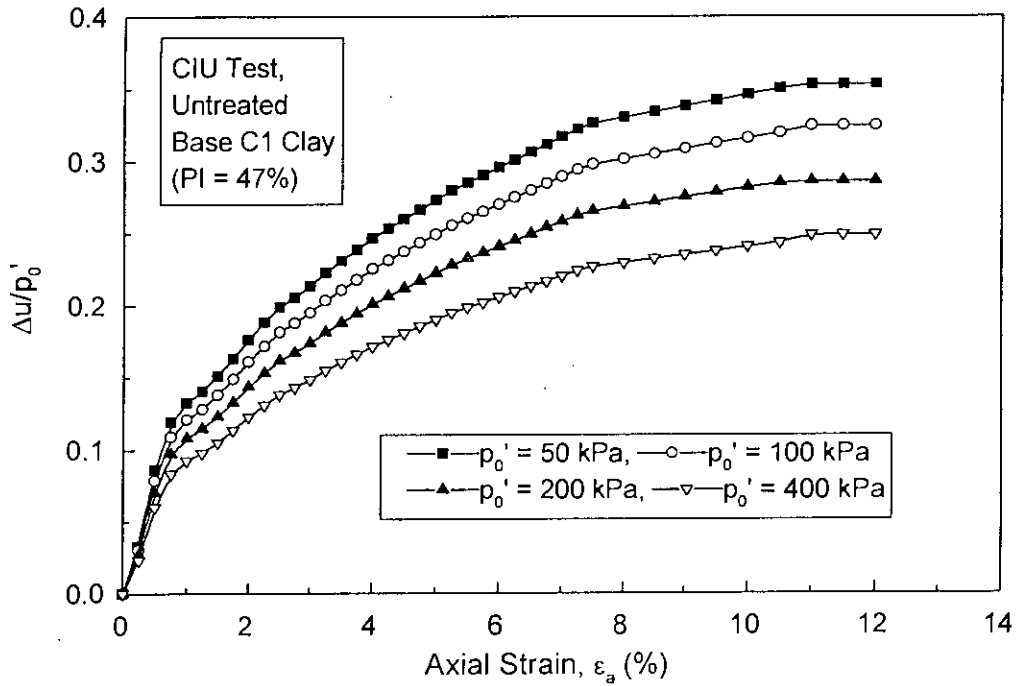


Fig. 5.94 Normalized Relationship Plots  $\Delta u/p'_0 - \epsilon_a$  for Untreated Base C1 Clay

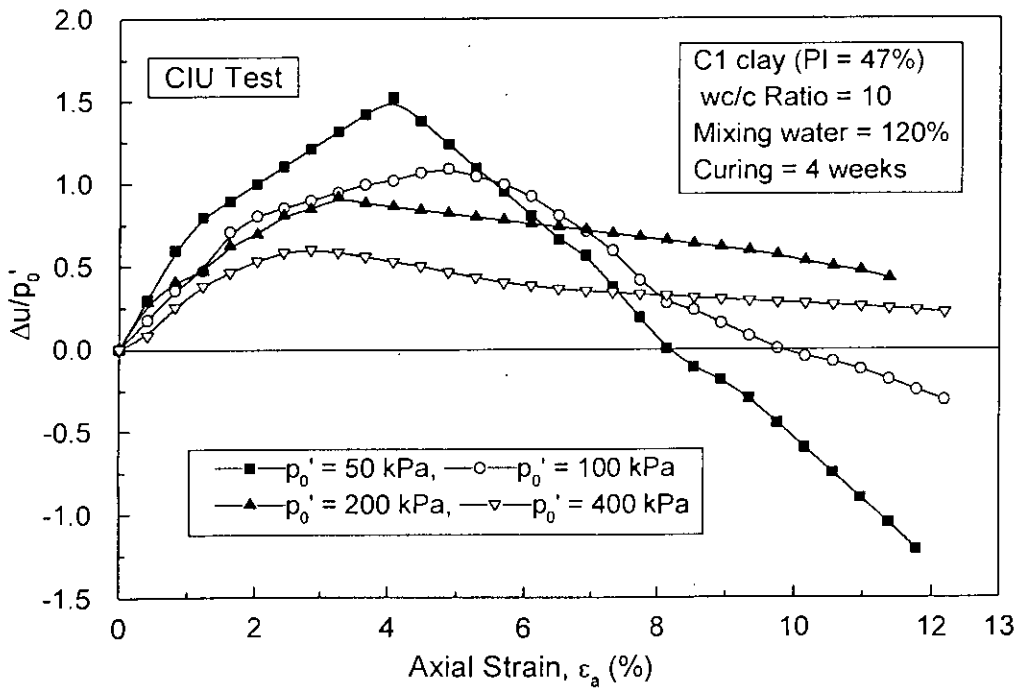
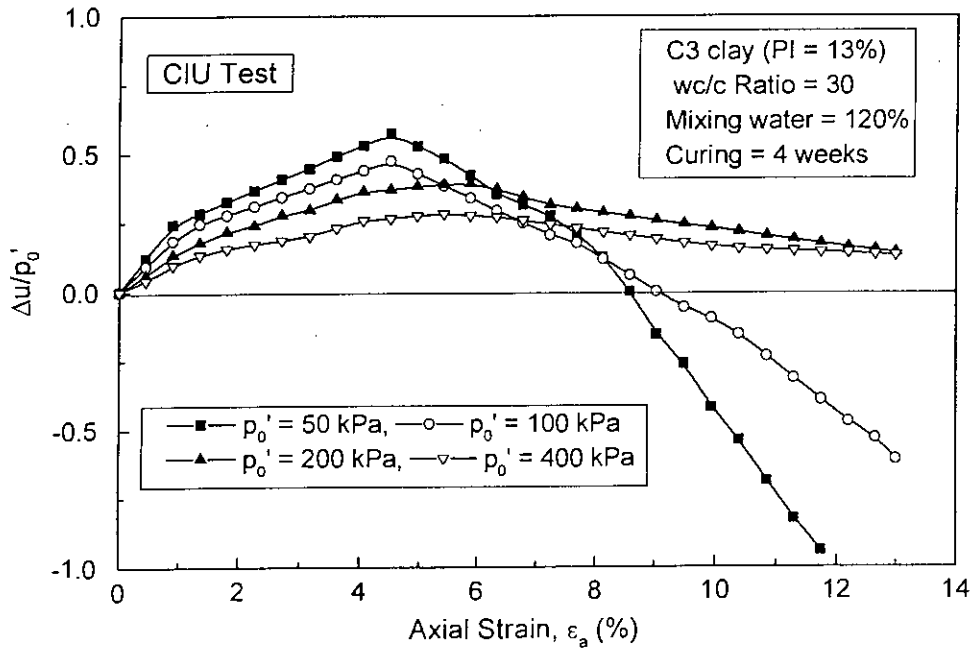
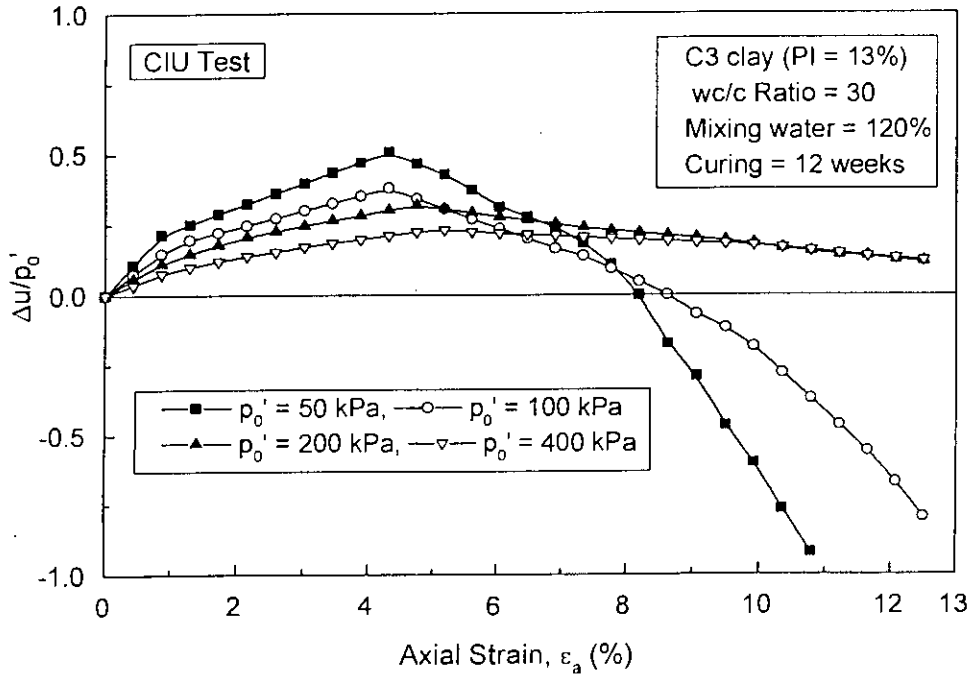


Fig. 5.95 Normalized Relationship Plots  $\Delta u/p'_0 - \epsilon_a$  for Cement Treated C1 clay

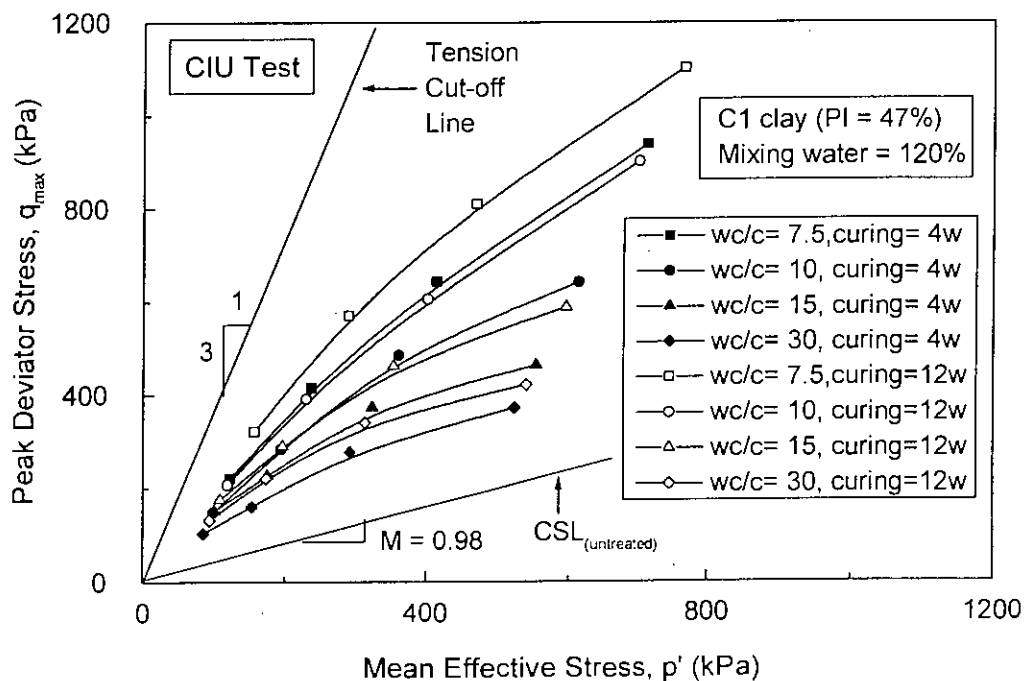


(a)

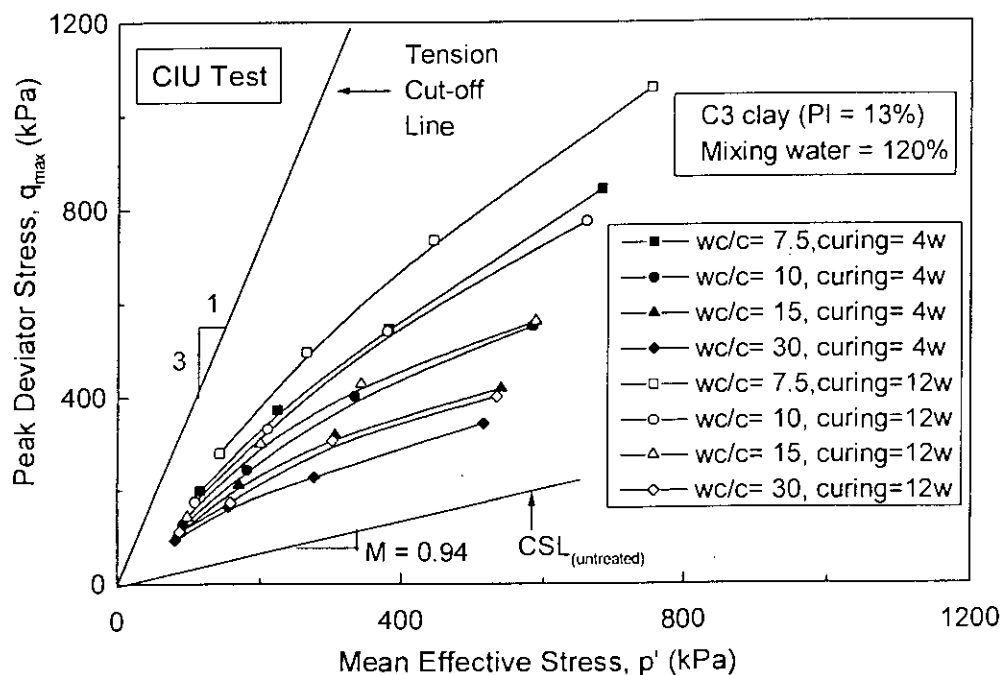


(b)

Fig. 5.96 Normalized Relationship Plots  $\Delta u/p'_0$ -  $\epsilon_a$  for Treated C3 clay at Curing Time (a) 4 week and (b) 12 week

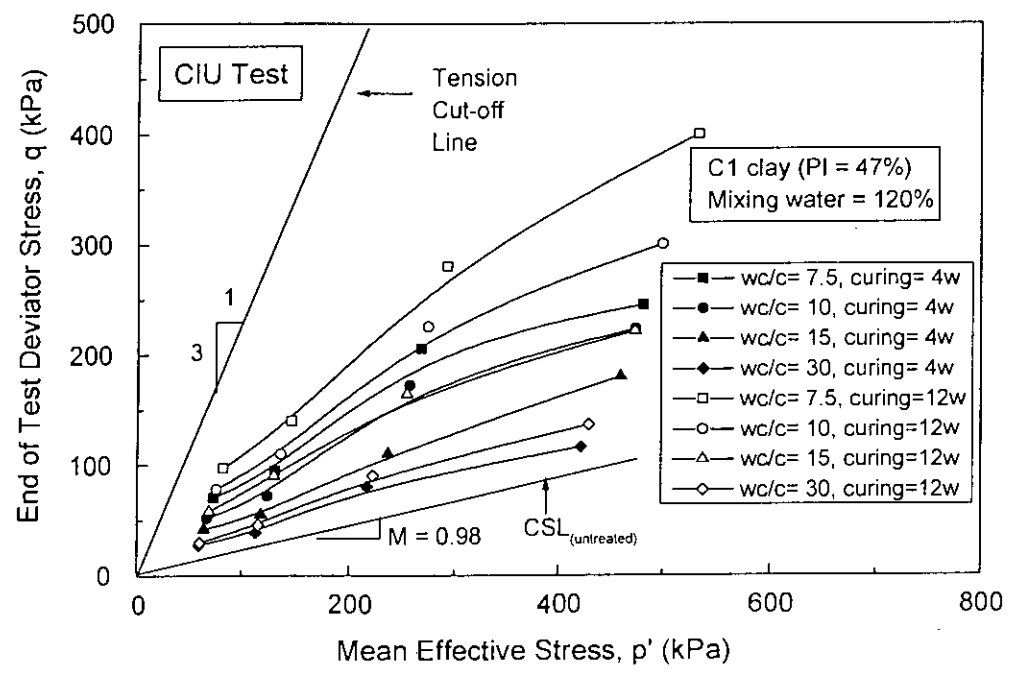


(a)

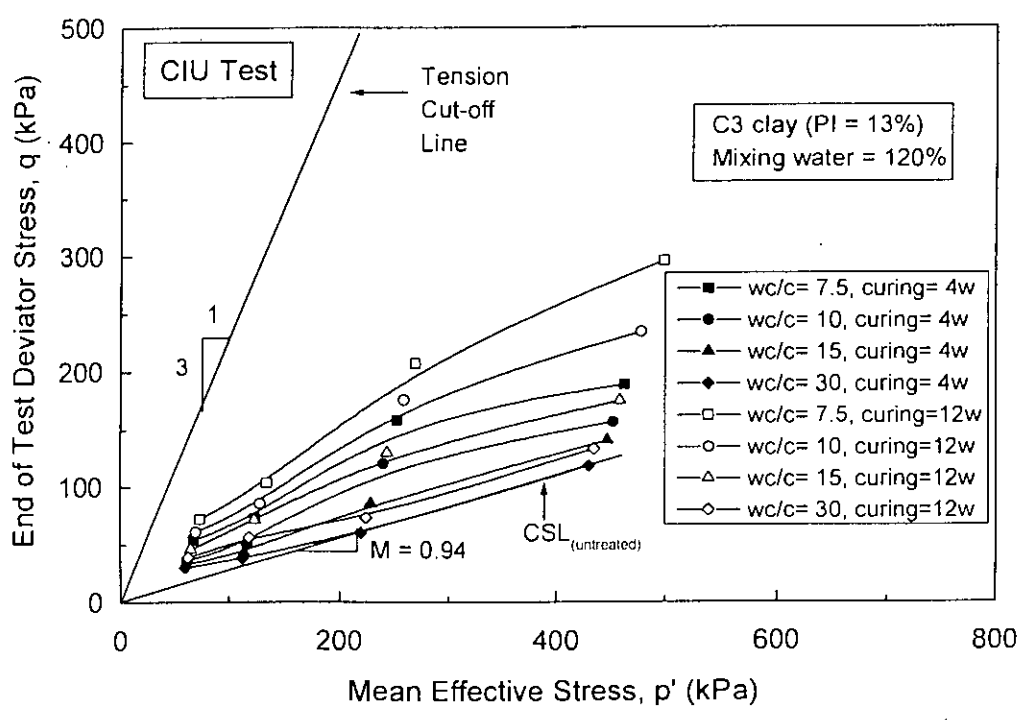


(b)

Fig. 5.97 Peak Deviator Stress Envelopes from CIU Tests of Cement Treated Clays (a) C1 Clay and (b) C3 Clay

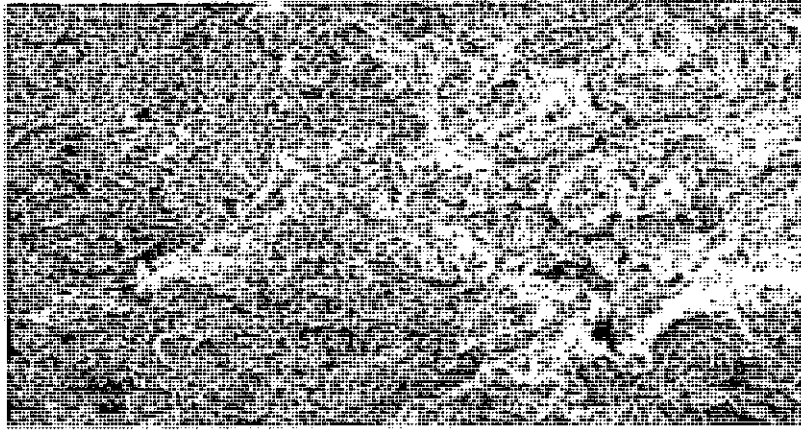


(a)

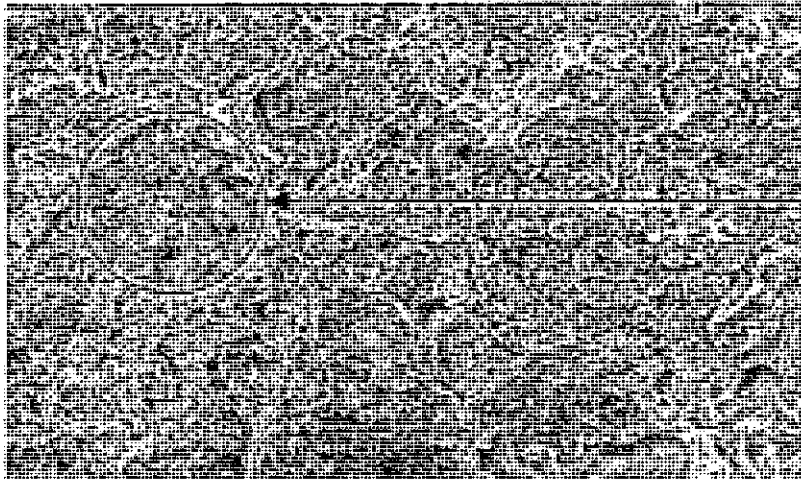


(b)

Fig. 5.98 End-of-Test Destructured Envelopes from CIU Tests of Cement Treated Clays (a) C1 clay and (b) C3 Clay

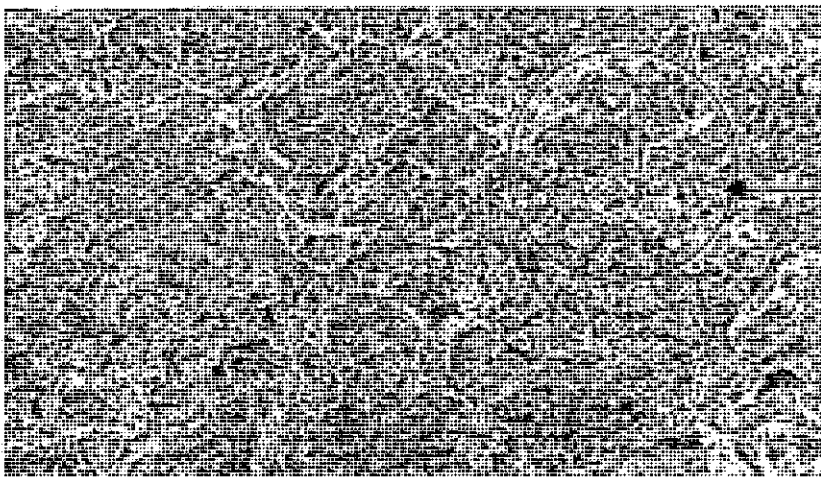


(a)



More  
destruction  
on the shear  
plane

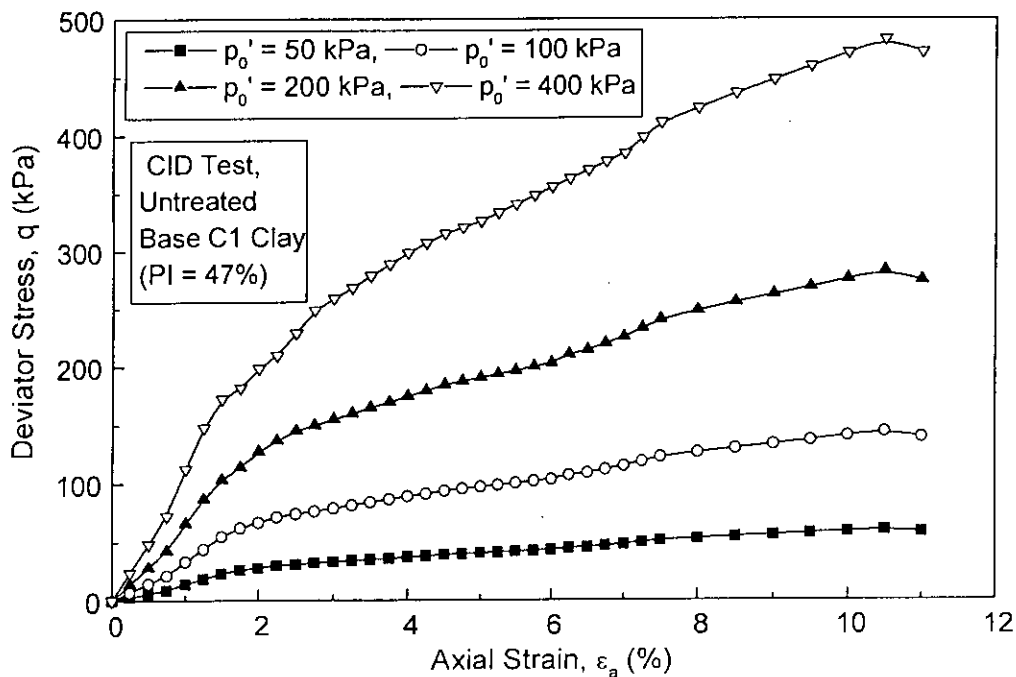
(b)



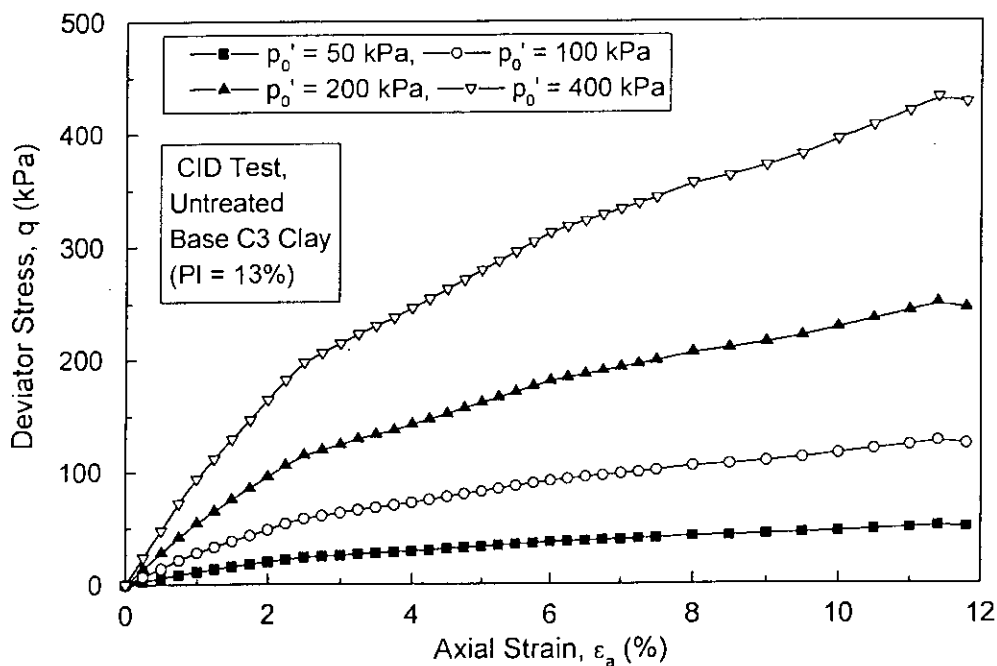
Breaking of  
large clay-  
cement clusters  
is apparent

(c)

Fig. 5.99 SEM Images of 12% Cement Treated CIU Triaxial Sheared Samples  
(a) 'Intact' Sample, (b) 'Shear Band' Sample and (c) 'Outside Shear Band' Sample

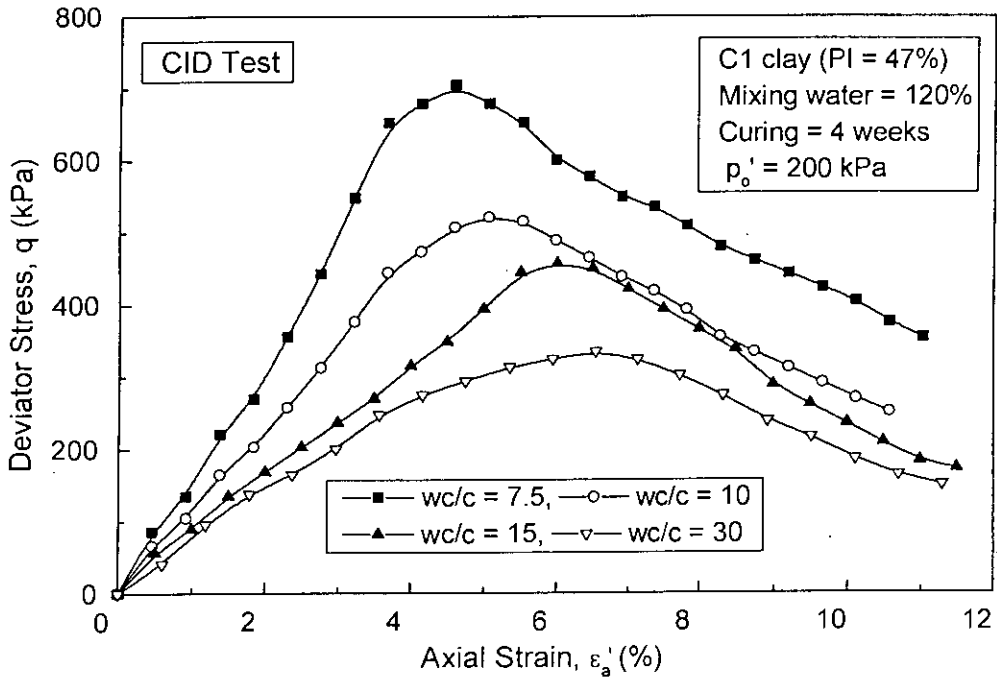


(a)



(b)

Fig. 5.100 Deviator Stress Versus Axial Strain Response at Different Pre-Shear Effective Pressure of Untreated Base Clays (a) C1 Clay and (b) C3 Clay



ig. 5.101 Effect of Clay-Water/Cement (wc/c) Ratio on Deviator Stress Versus Axial Strain response of C1 Clay

F

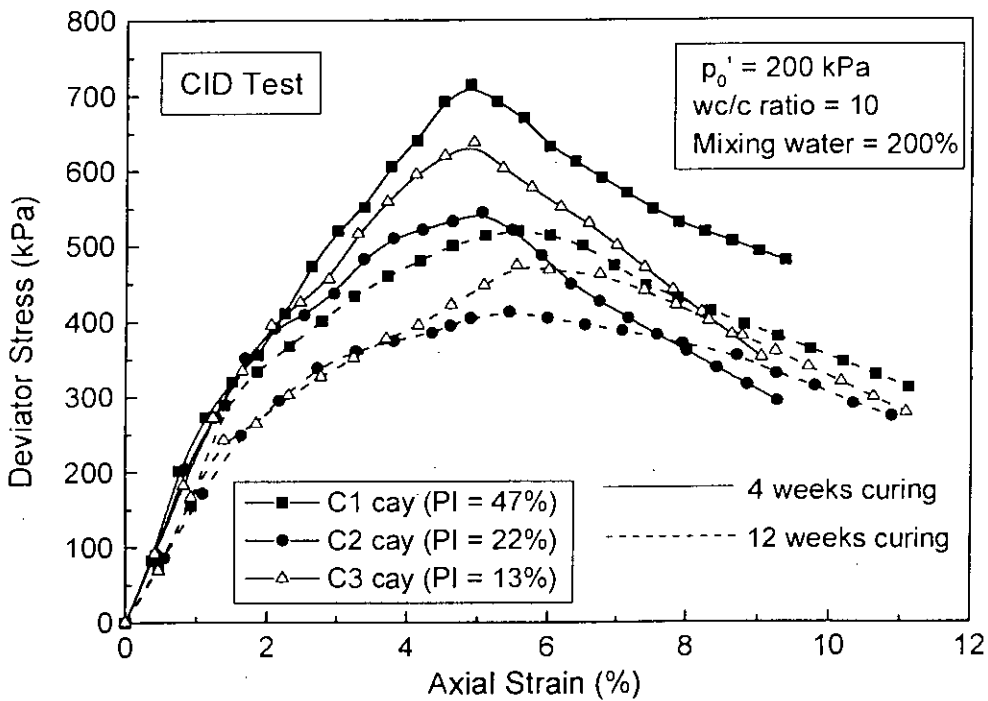


Fig. 5.102 Effect of Curing Time and Clay Type on Deviator Stress Versus Axial Strain Response



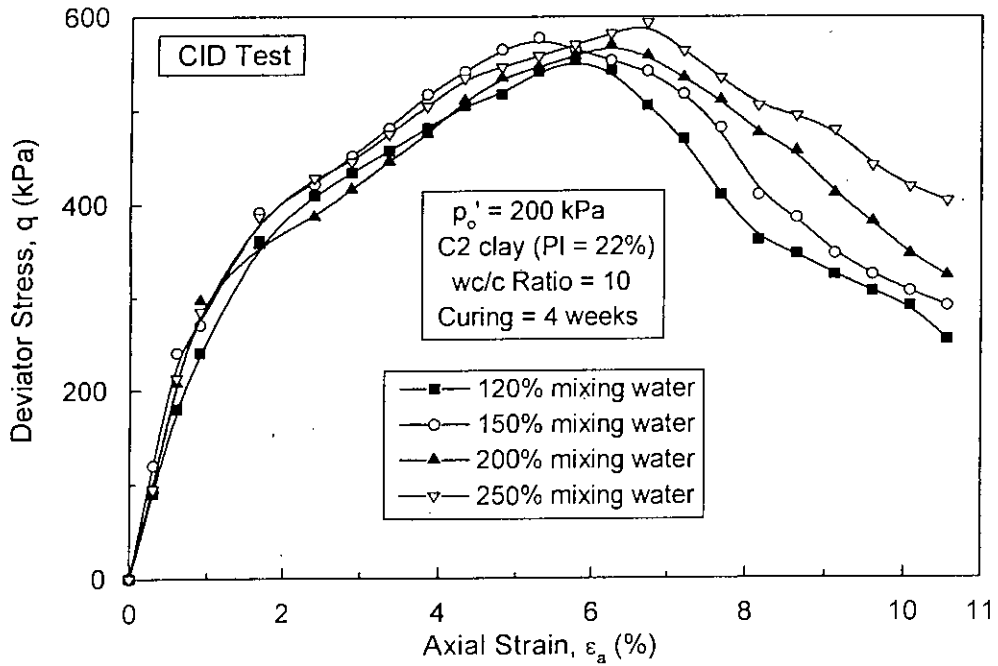


Fig. 5.103 Effect of Mixing Water Content on Deviator Stress Versus Axial Strain Response of C2 Clay

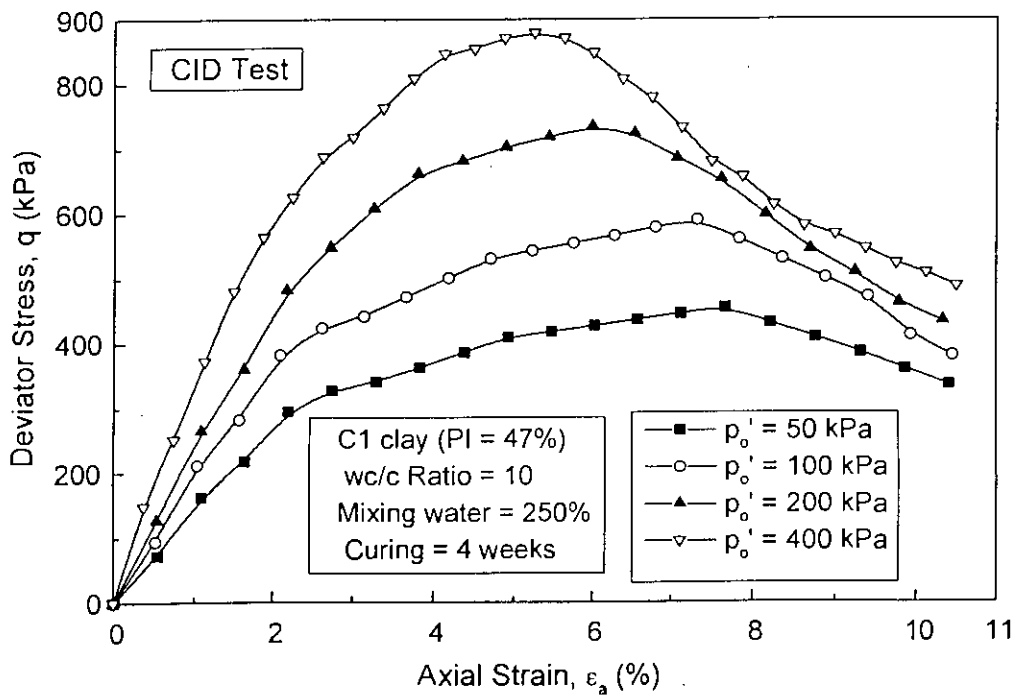
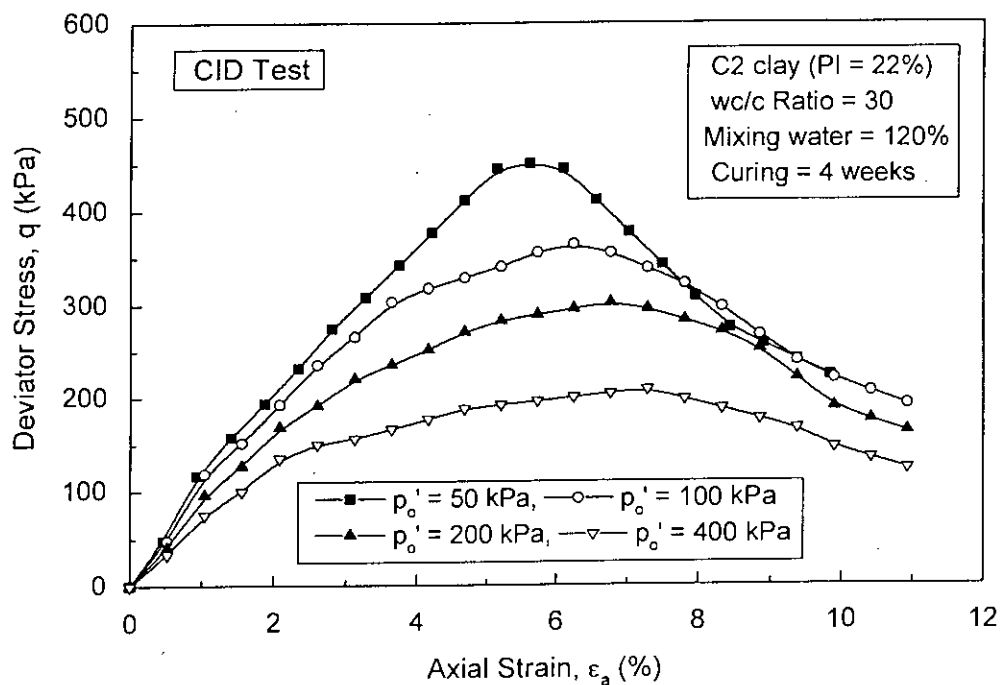
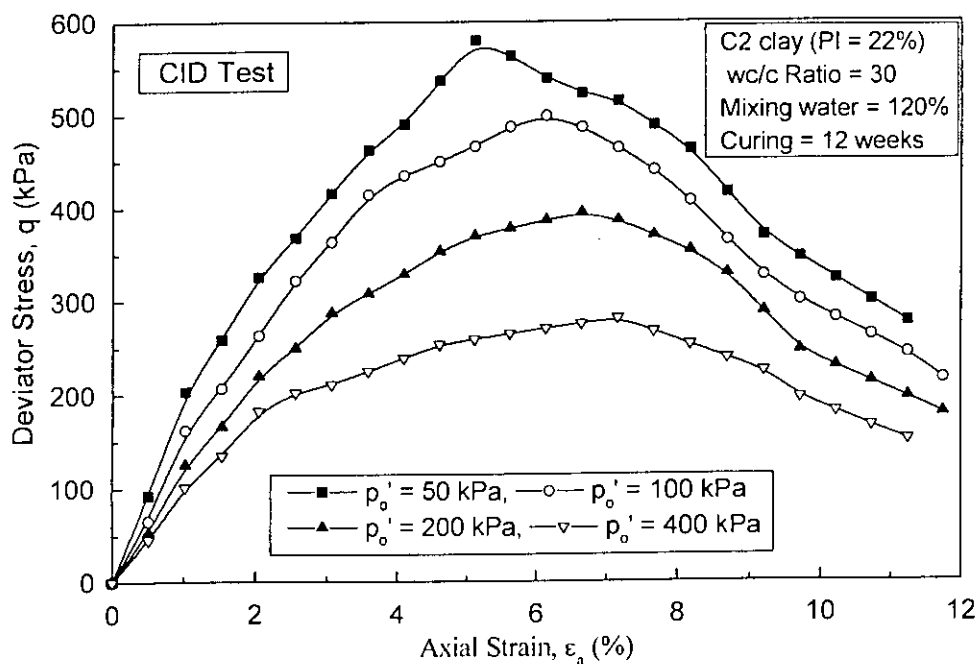


Fig. 5.104 Effect of Pre-Shear Effective Consolidation Pressure on Deviator Stress Versus Axial Strain Response of C1 Clay



(a)



(b)

Fig. 5.105 Effect of Pre-Shear Effective Pressure on Deviator Stress Versus Axial Strain Relations of C2 clay at Large  $w/c$  (a) 4 w and (b) 12 w Curing

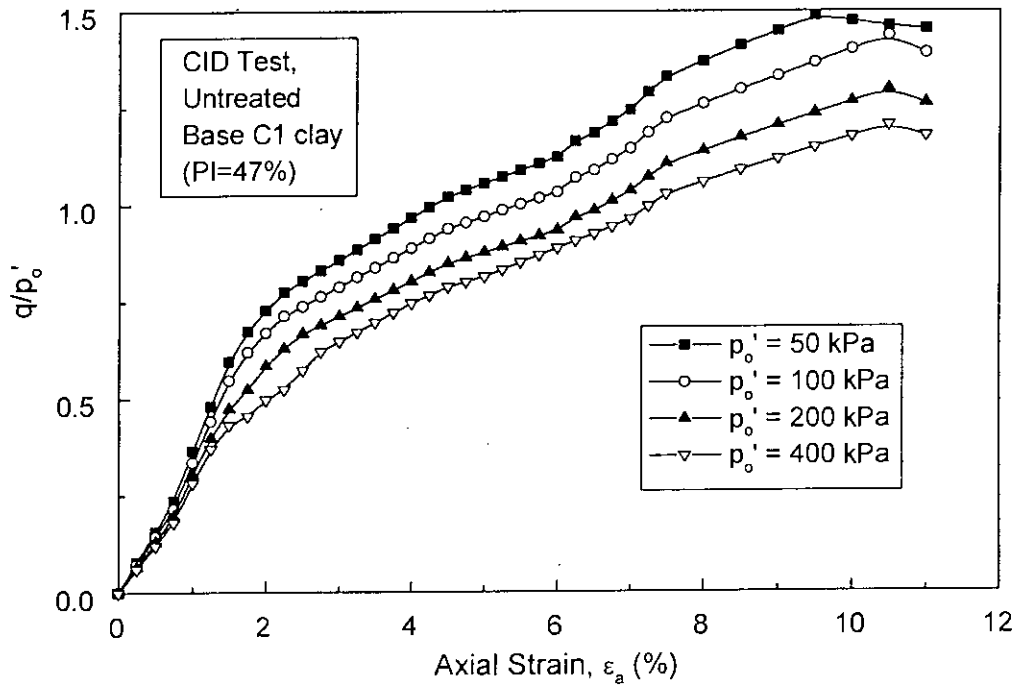


Fig. 5.106 Normalized Relationship Plots  $q/p'_o$  vs.  $\epsilon_a$  for Untreated Base C1 Clay

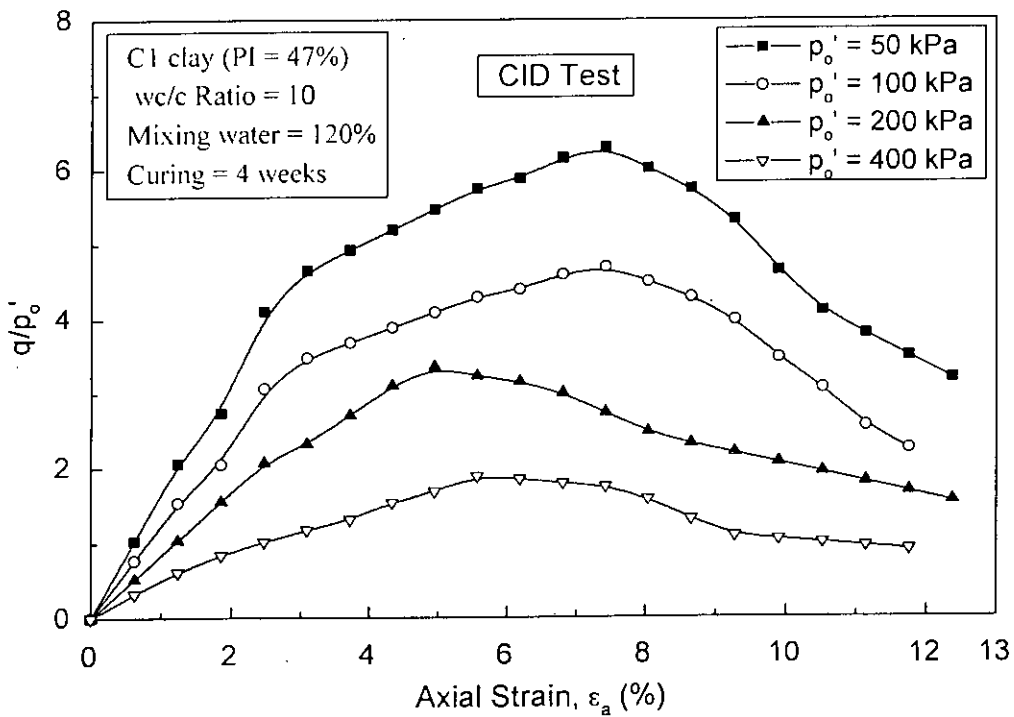
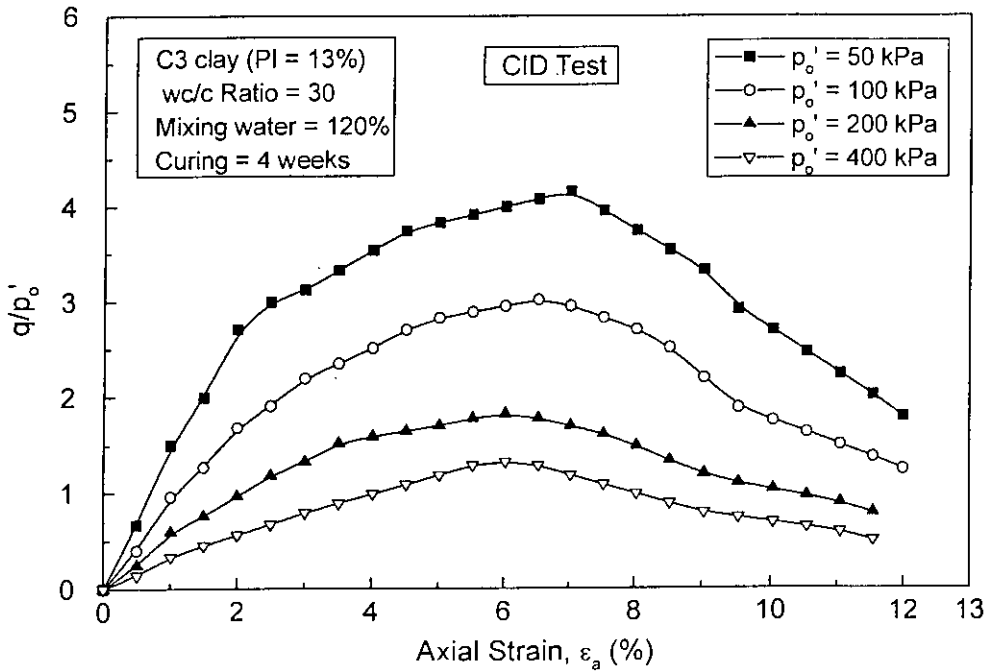
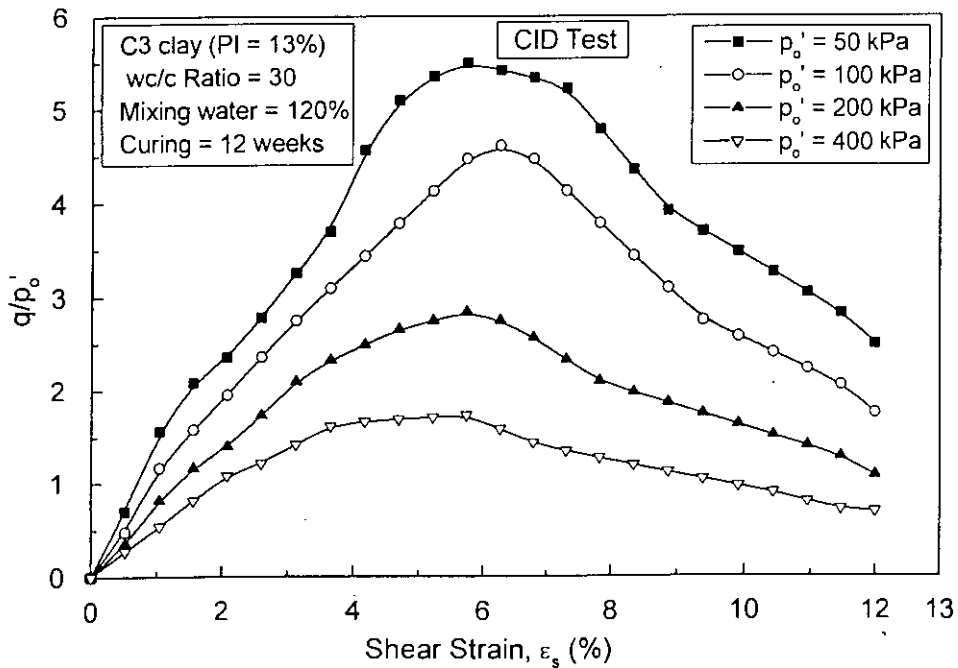


Fig. 5.107 Normalized Relationship Plots  $q/p'_o$  vs.  $\epsilon_a$  for Cement Treated C1 clay



(a)

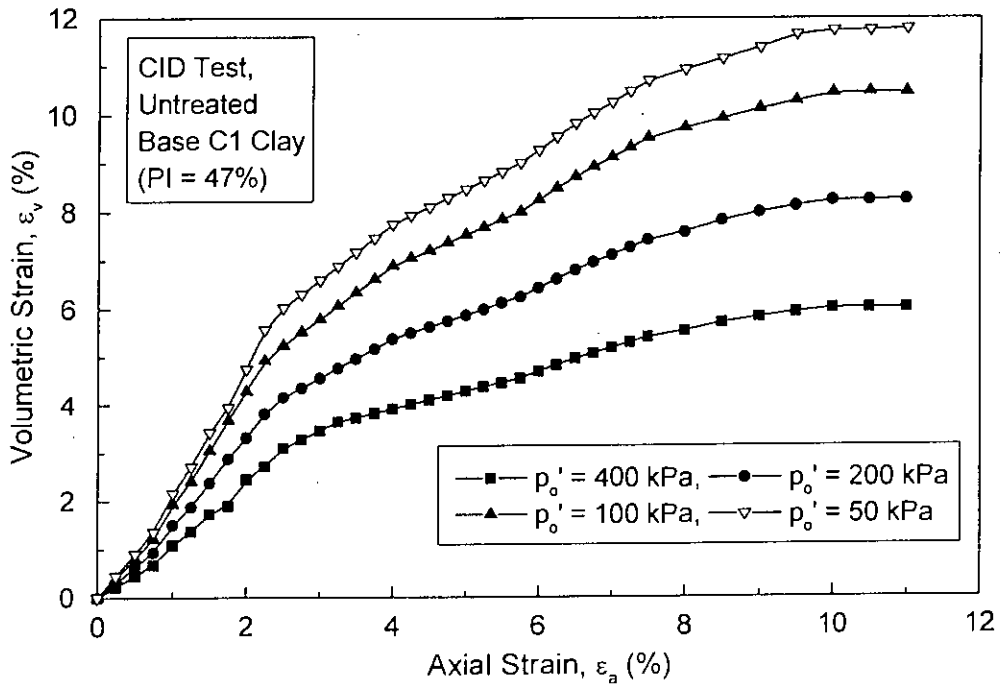


(b)

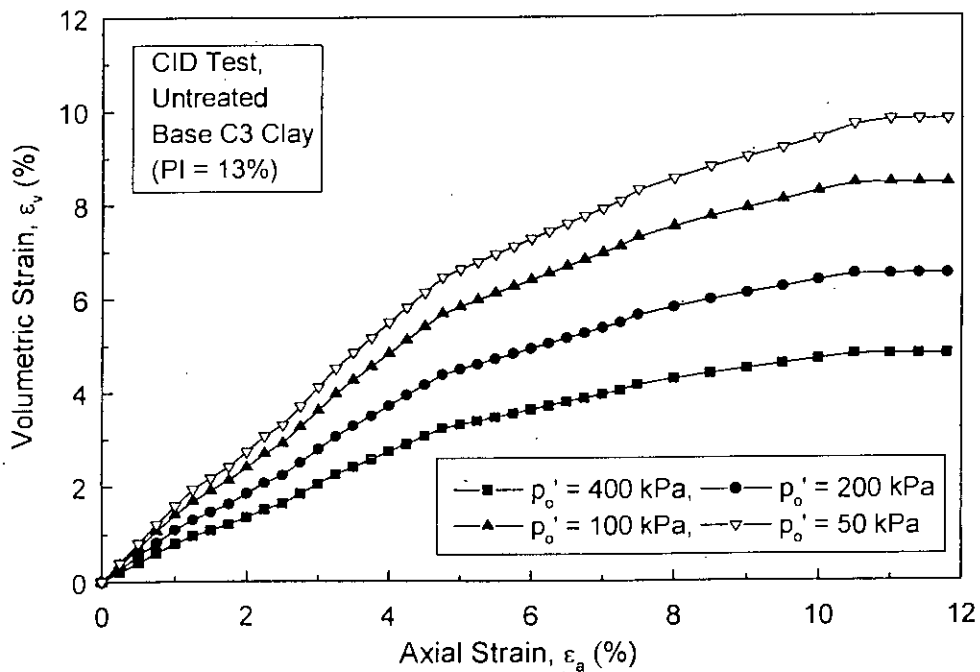
Fig. 5.108 Normalized Relationship Plots  $q/p'_0 \cdot \epsilon_a$  for Treated C3 clay at Curing Time (a) 4 week and (b) 12 week

**Table 5.8 Comparison of Shear Strength and Axial Strain at Failure of Cement Treated Clays ( $p_o' = 200$  kPa) from CIU and CID Tests**

Curing Time (week)	Clay Type	wc/c Ratio	Shear Strength (kPa)		Axial Strain at Failure (%)	
			CIU test	CID test	CIU test	CID test
4 w	C1	7.5	643	706	4.07	4.60
		10	485	521	5.12	5.56
		15	372	456	5.50	6.00
		30	276	335	5.68	6.54
	C2	7.5	474	561	4.71	4.95
		10	350	413	5.88	5.93
		15	271	365	6.31	6.73
		30	201	268	6.53	7.21
	C3	7.5	547	646	4.51	4.89
		10	402	474	5.74	5.83
		15	318	419	6.19	6.31
		30	228	317	6.41	6.92
12 w	C1	7.5	811	958	3.59	4.11
		10	606	715	4.38	4.87
		15	461	620	4.76	5.26
		30	340	445	4.93	5.64
	C2	7.5	564	645	3.88	4.34
		10	498	545	4.48	5.05
		15	389	426	4.88	5.73
		30	271	311	5.23	6.14
	C3	7.5	736	842	3.70	4.21
		10	541	638	4.56	4.92
		15	428	561	4.93	5.43
		30	306	404	5.09	5.86



(a)



(b)

Fig. 5.109 Volumetric Strain Versus Axial strain Response at Different Pre-Shear Effective Pressure of Untreated Base Clays (a) C1 and (b) C3 Clays

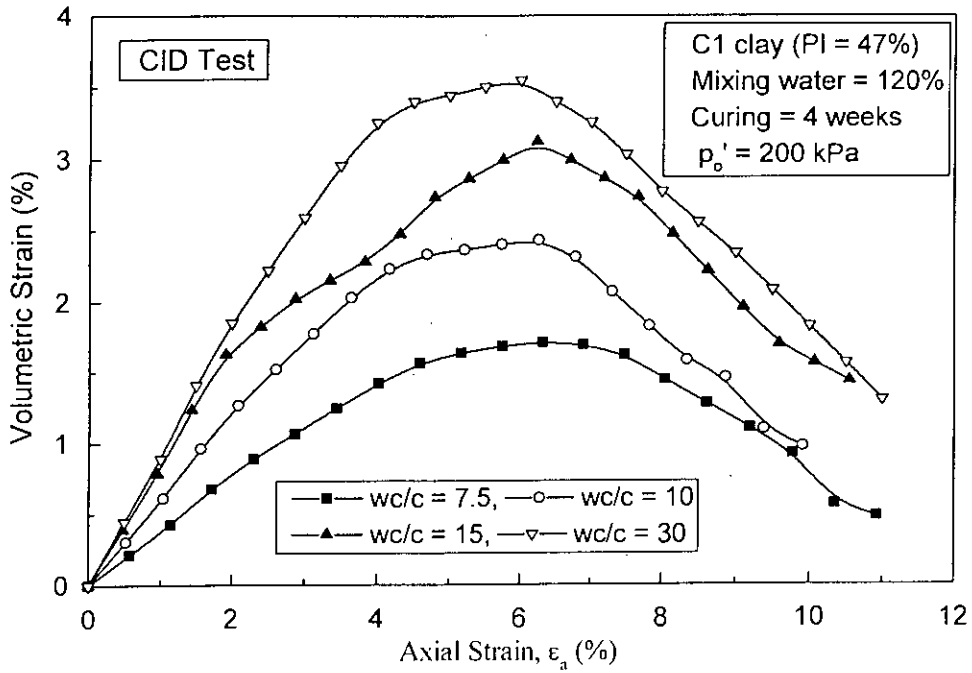


Fig. 5.110 Effect of Clay-Water/Cement (wc/c) Ratio on Volumetric Strain Versus Axial Strain Response of C1 Clay

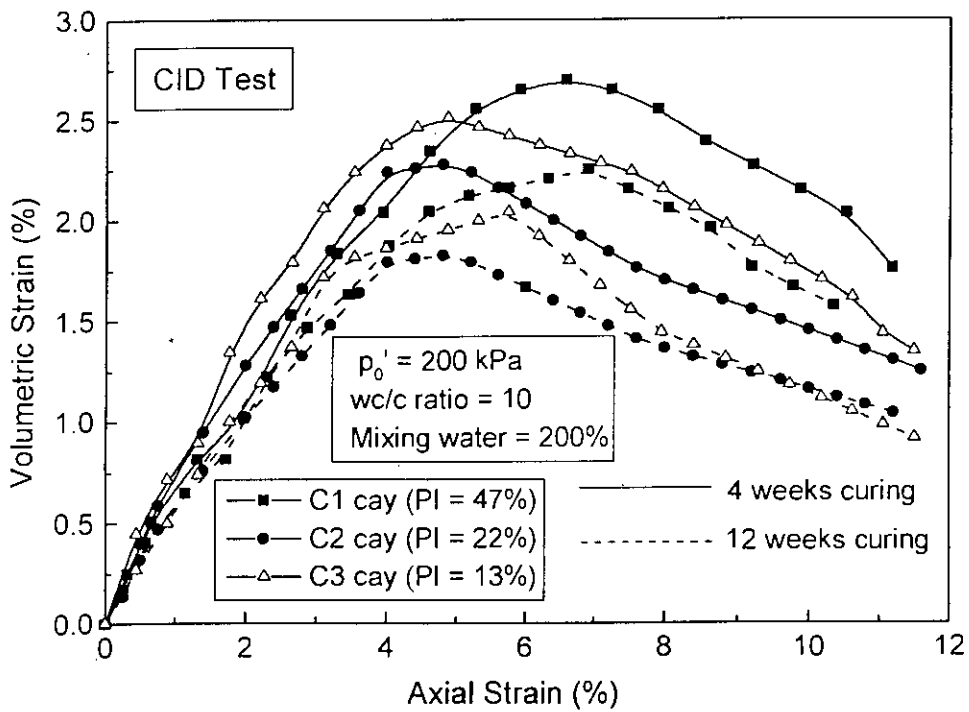


Fig. 5.111 Effect of Curing Time and Clay Type on Volumetric Strain Versus Axial Strain Response

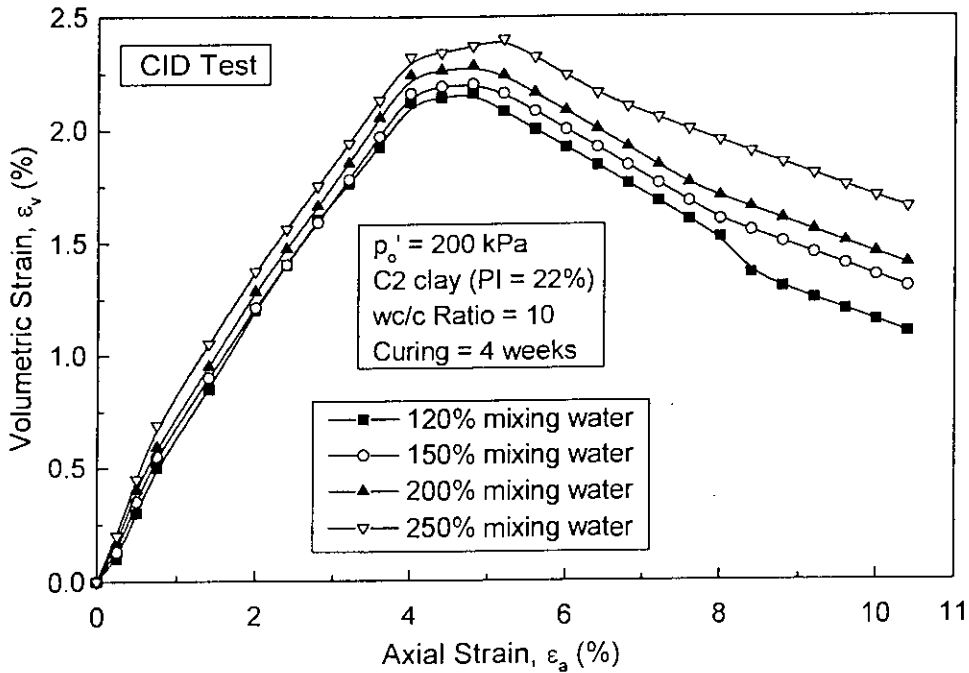


Fig. 5.112 Effect of Mixing Water Content on Volumetric Strain Versus Axial Strain Response of C2 Clay

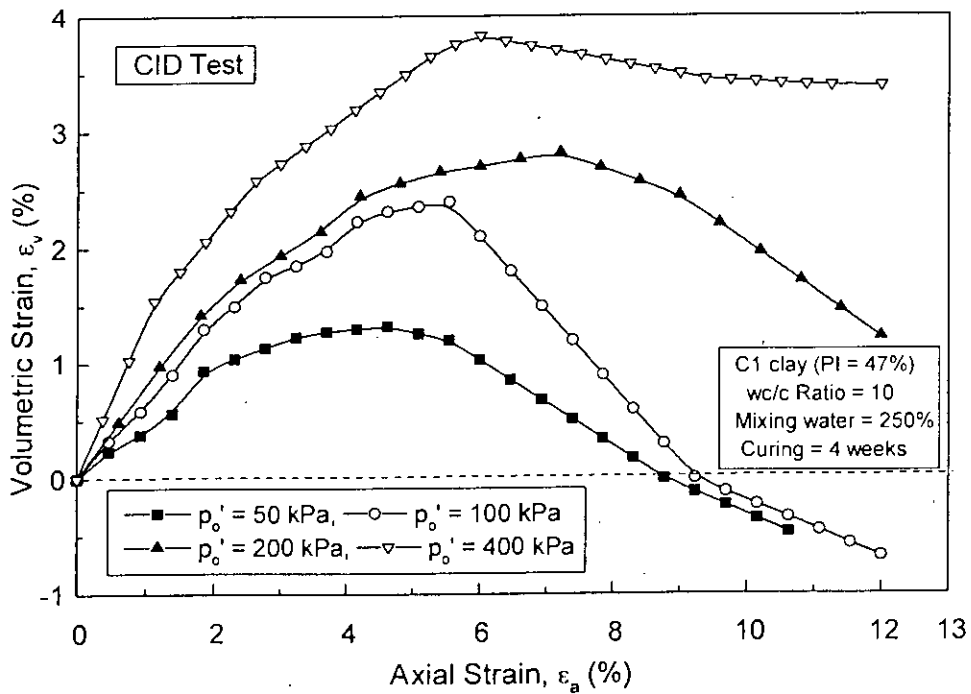
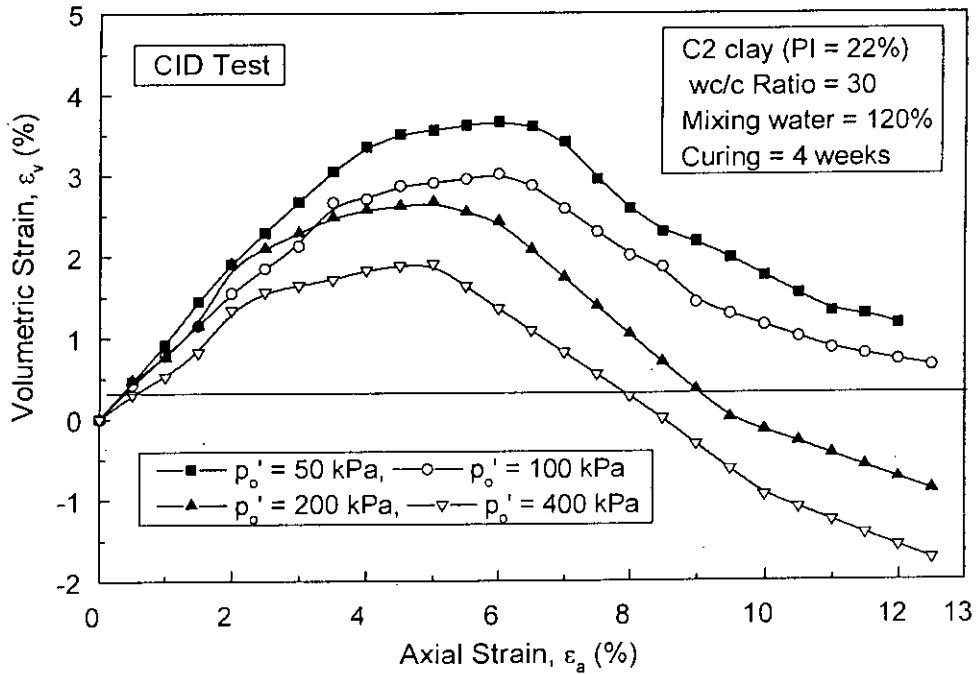
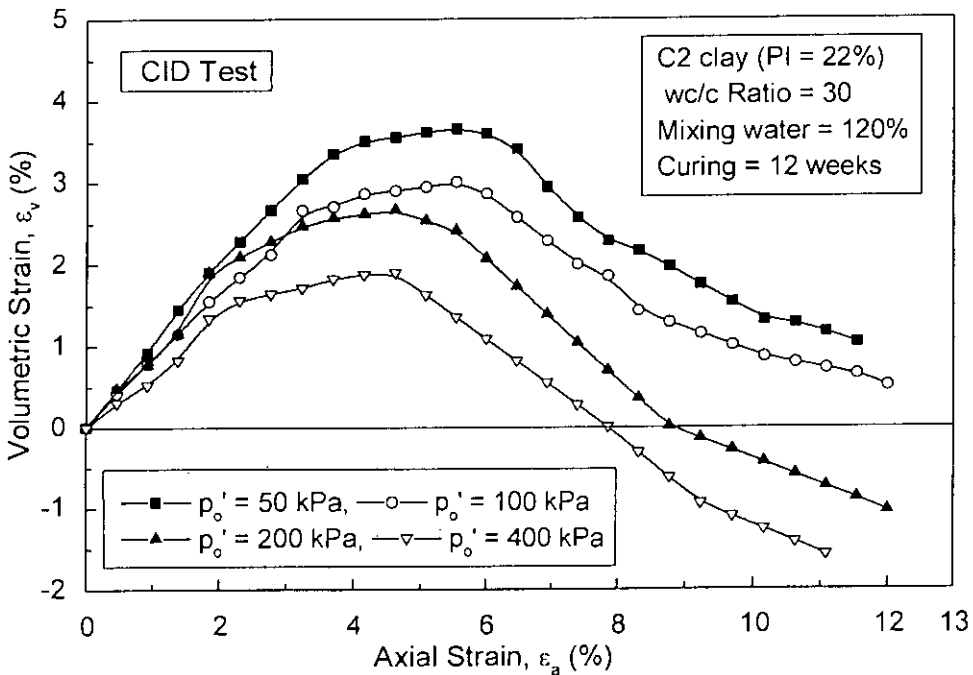


Fig. 5.113 Effect of Pre-Shear Effective Consolidation Pressure on Volumetric Strain Versus Axial Strain Response of C1 Clay





(a)



(b)

Fig. 5.114 Effect of Pre-Shear Effective Pressure on Volumetric Strain Versus Axial Strain of C2 clay at Large wc/c (a) 4 w and (b) 12 w Curing

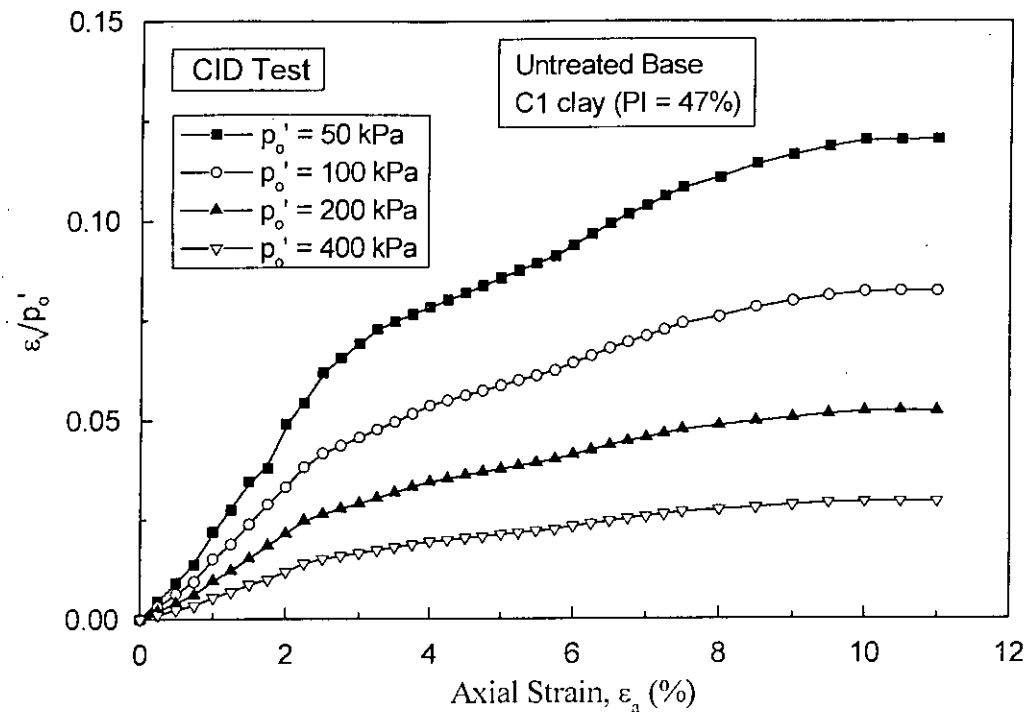


Fig. 5.115 Normalized Relationship Plots  $\epsilon_v/p'_o - \epsilon_a$  for Untreated Base C1 Clay

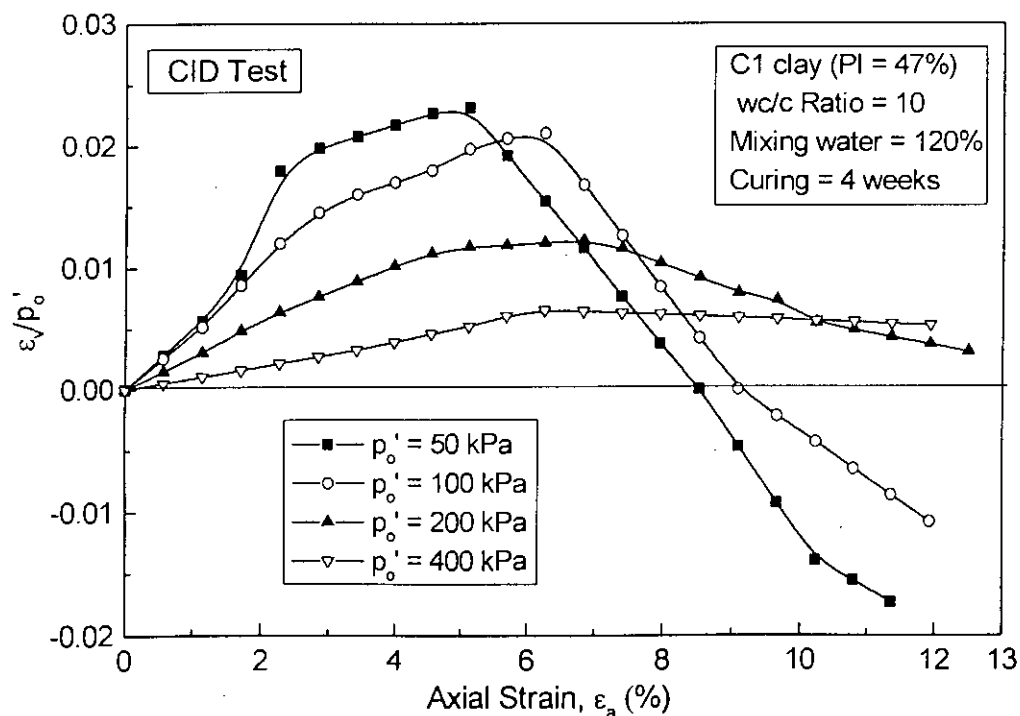
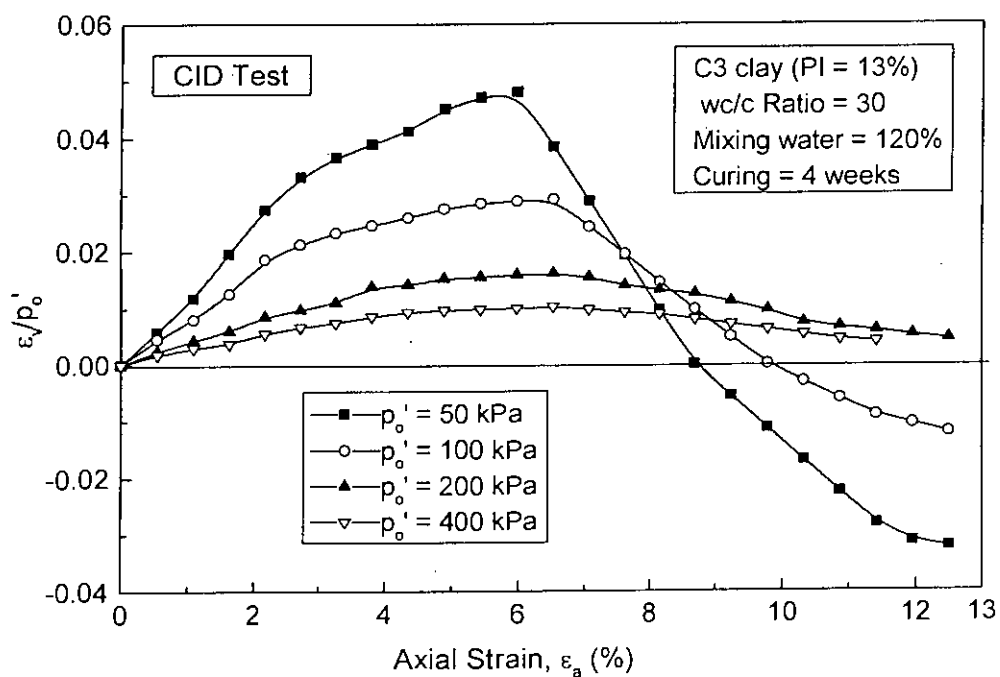
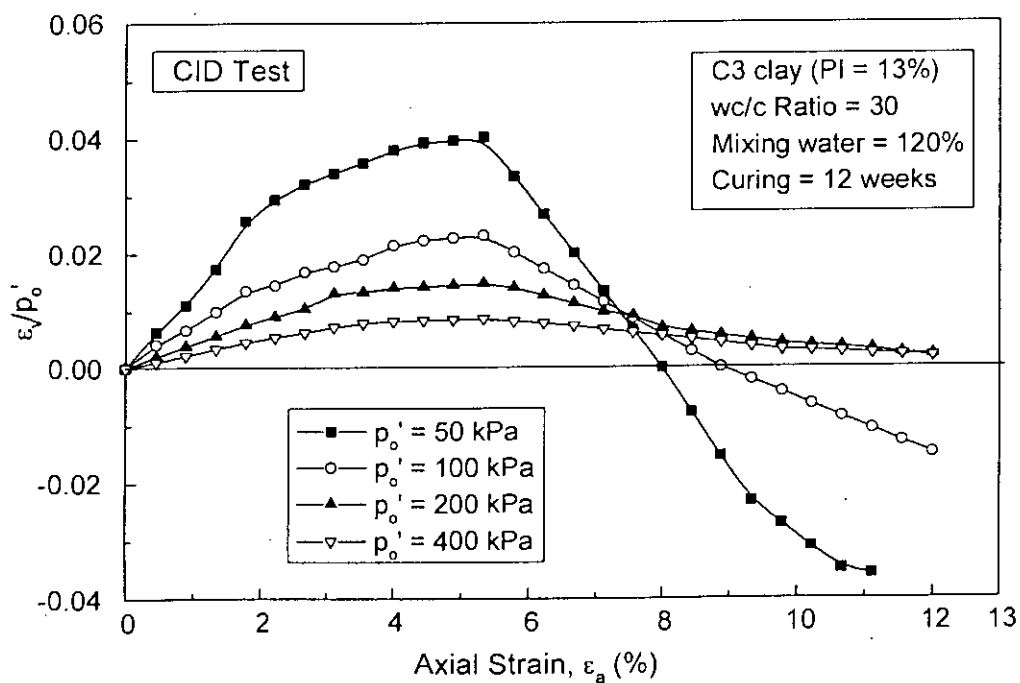


Fig. 5.116 Normalized Relationship Plots  $\epsilon_v/p'_o - \epsilon_a$  for Cement Treated C1 clay

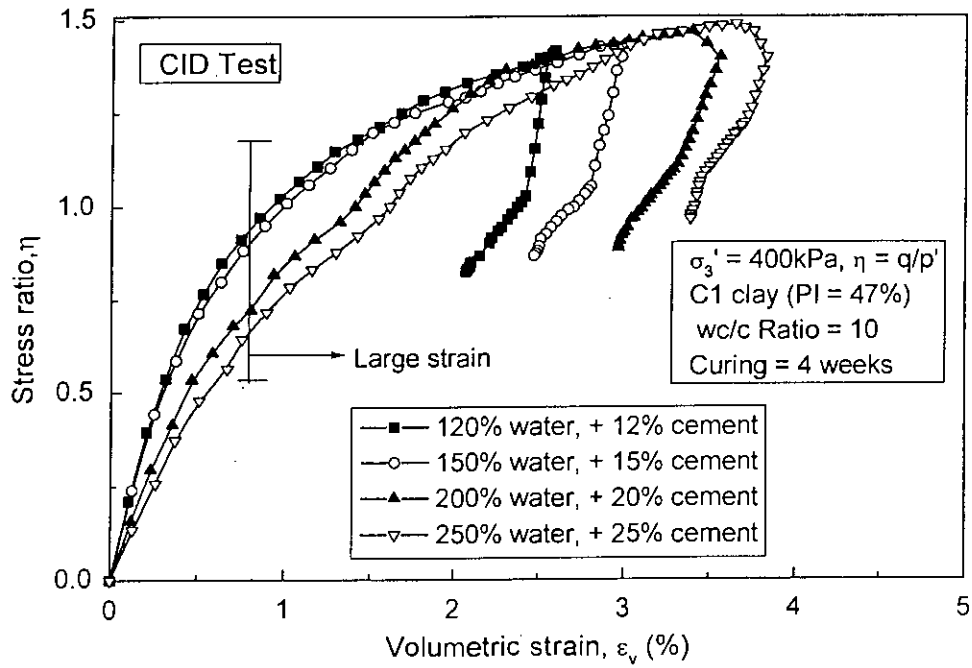


(a)

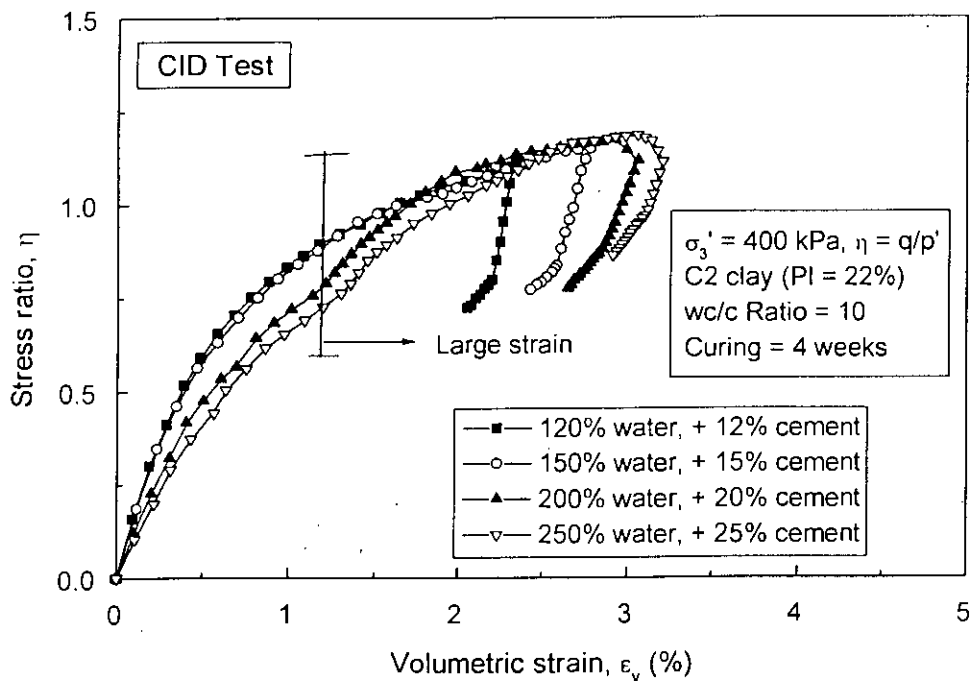


(b)

Fig. 5.117 Normalized Relationship Plots  $\epsilon_v/p_o' - \epsilon_a$  for Treated C3 clay at Curing Time (a) 4 week and (b) 12 week

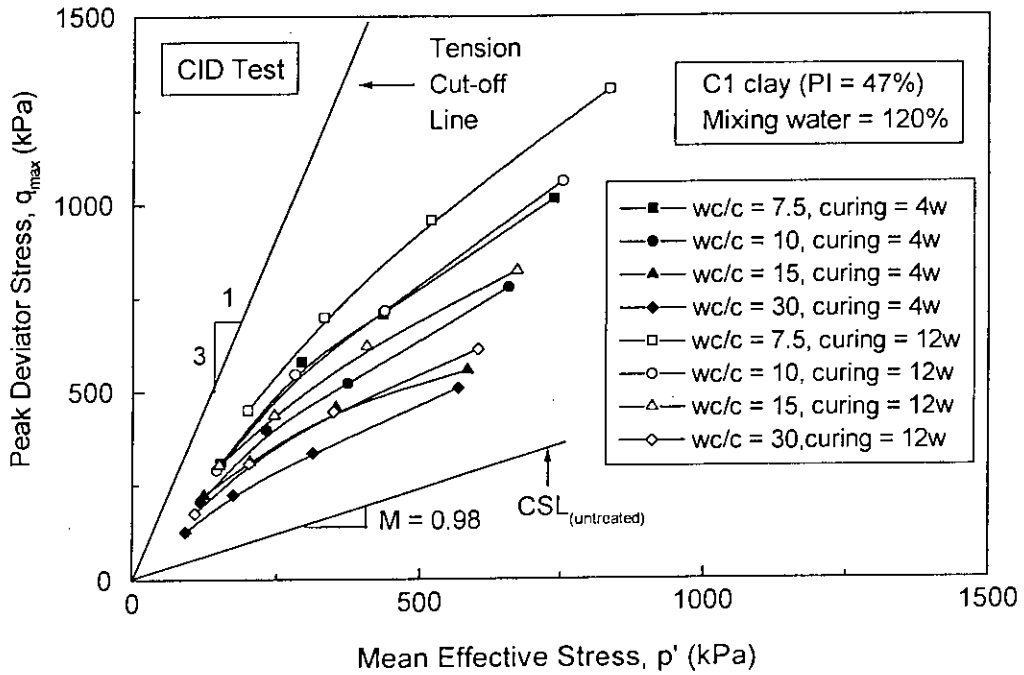


(a)

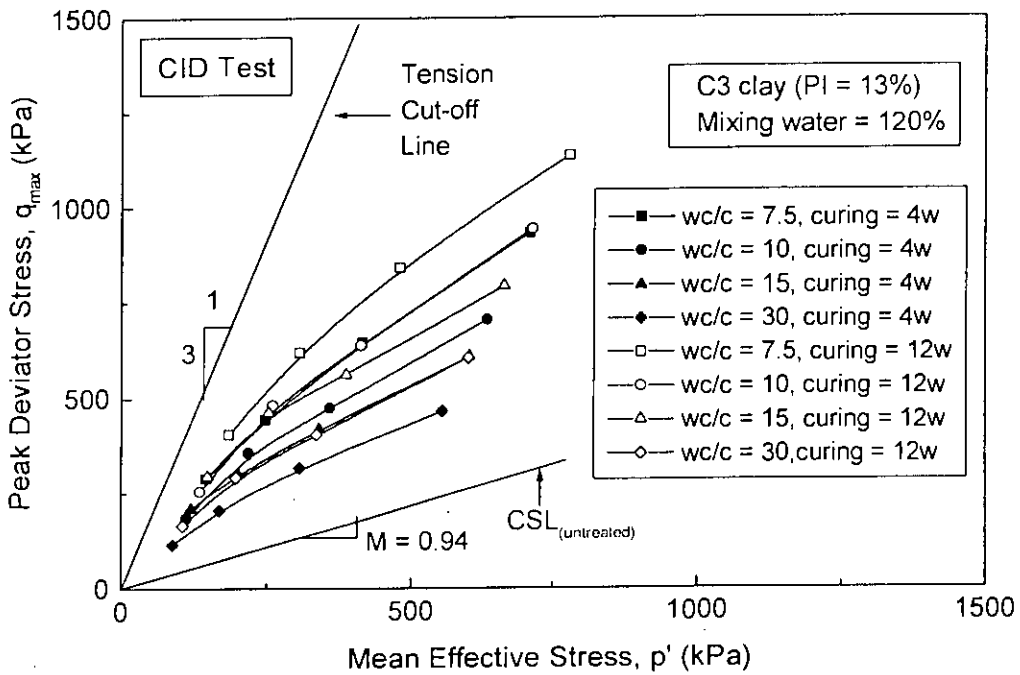


(b)

Fig. 5.118 Stress Ratio Versus Volumetric Strain,  $\eta - \epsilon_v$  Relationships of Cement Treated Clays (a) C1 Clay and (b) C3 Clay

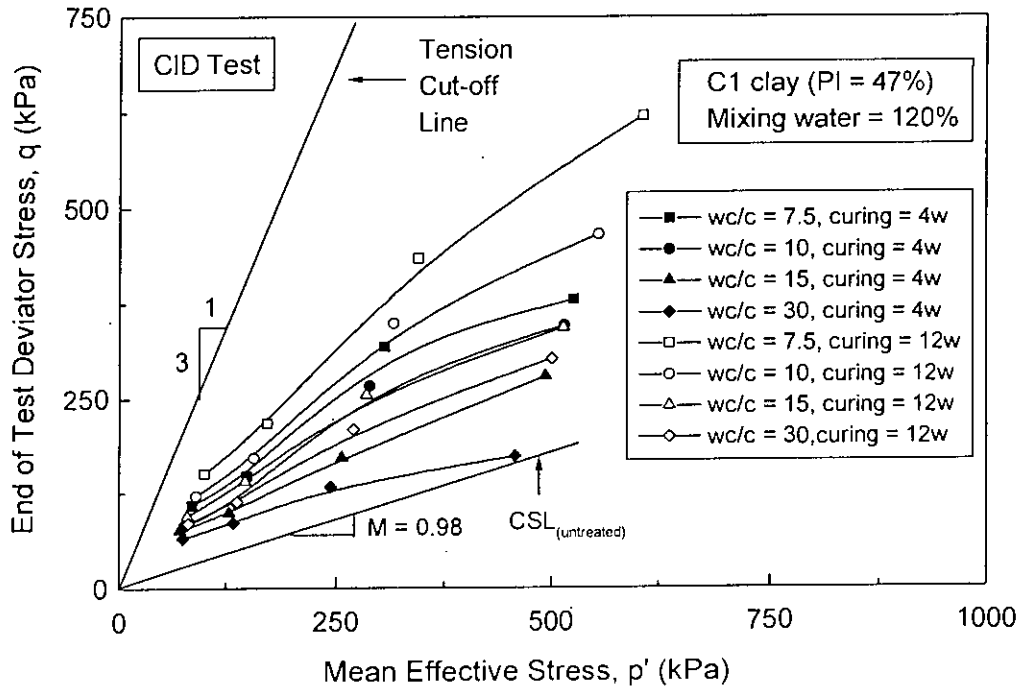


(a)

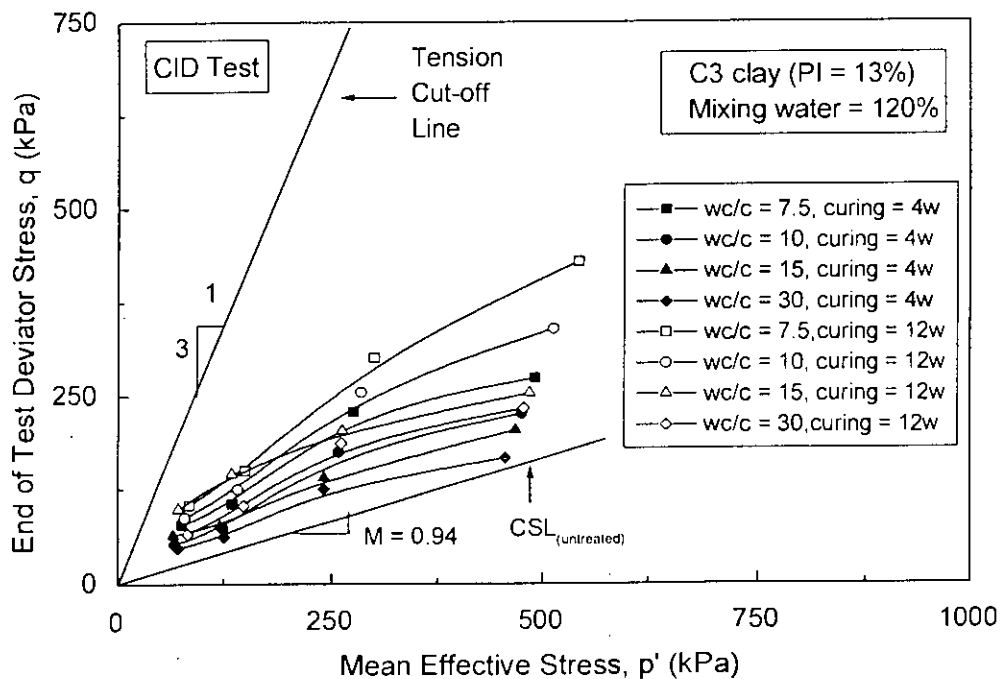


(b)

Fig. 5.119 Peak Deviator Stress Envelopes from CID Test of Cement Treated Clays (a) C1 Clay and (b) C3 Clay



(a)



(b)

Fig. 5.120 End-of-Test Destructured Envelopes from CID Test of Cement Treated Clays (a) C1 Clay and (b) C3 Clay

## CHAPTER 6

### NUMERICAL ANALYSIS OF TREATED CLAYS USING DIFFERENT MODELS

#### 6.1 General

The stress-strain response of cement treated and untreated clays have been numerically simulated using the finite element models and the predictions have been compared with the experimental data obtained in this study. The soil constants, critical state parameters and state boundary surface for untreated and treated clays were also analyzed, compared and discussed in this chapter.

The three finite element constitutive models, namely, Modified Cam Clay (MCC) model (which is defined as modification of cam clay model incorporating volumetric strain hardening parameter), Modified Modified Cam Clay (MMCC) model (which is defined as MCC model incorporating cementation tensile strength parameters) and Extended Modified Modified Cam Clay (EMMCC) model (which is defined as MMCC model incorporating cementation break down parameters) have been used to predict deviator stress, volumetric strain, pore pressure and stress path characteristics. The Cap models (plane and elliptic cap model) have also been applied for prediction soil behaviour. The predictions were compared with experimental data.

For this purpose of using MCC, MMCC and EMMCC models, the finite element program AFENA have been used. Carter and Balaam (1995) developed AFENA, which is a finite element package program for the numerical analysis of problems in geotechnical engineering. An 8-noded axisymmetric, quadrilateral and isoparametric elements with reduced Gaussian integration have been used in AFENA. The Cap model developed by Chen and Mizuno (1990) was used in this study.

#### 6.2 Soil Constants and Critical State Parameters Analysis of Untreated and Treated Clays

Figs. 6.1 to 6.3 show the typical results of isotropic compression and swelling tests in triaxial cell of the untreated and treated samples in  $\ln p-v$  space. In these figures the up sloping line, AB is the isotropic virgin/compression line (often called the isotropic normal consolidation line) and the down sloping line, BC is the average line of swelling and recompression lines. It is evident from Figs. 6.1 to 6.3 that if the soil sample is loaded isotropically from A, the normal consolidation line (NCL) always will follow the path AB and its state may be moved to the left of AB by unloading along a swelling line such as BC, but it is not possible to move the state of the soil to the right of AB. The line AB represents a boundary between possible states to the left and impossible states to the right as indicated in the Figs. 6.1 to 6.3. The

values of soil constants  $\lambda$ ,  $N$  and  $\kappa$  have been determined from the slopes of isotropic normal consolidation and swelling lines. The values of soil constants  $\lambda$ ,  $N$  and  $\kappa$  of the untreated and treated clays are presented in Table 6.1. It can be seen from Table 6.1 that the values of soil constants  $\lambda$  and  $\kappa$  for the treated clays are less than those for the untreated clays while the values of the constant  $N$  are greater for the cement treated clays than those of untreated clays. It is evident from the data presented in Table 6.1 that at a particular curing time, the soil constants  $\lambda$  and  $\kappa$  increased, while the constant  $N$  decreased with increasing  $w/c$  ratio (i.e., decreasing cement content). Table 6.1 also shows that at a particular  $w/c$  ratio, the values of soil constants  $\lambda$  and  $\kappa$  are greater but the constant  $N$  is lower for the curing time of 4 week than those for the samples cured for 12 weeks, i.e. the soil constants  $\lambda$  and  $\kappa$  decreased, while the constant  $N$  increased with increasing curing time for the treated clays. It can also be seen from the data presented in Table 6.1 that the values of the soil constants  $\lambda$ ,  $\kappa$  and  $N$  increased with the increase of plasticity index of the clays. Similar behaviours were observed by Parry et al. (1973), Bashar (2002) and Khalilullah (2007).

### 6.3 Critical State Lines of the Untreated and Treated Clays

Figs. 6.4 to 6.6 present the critical state line (CSL) in  $p'$ ,  $q'$  plot for three untreated and treated clay samples. Though the critical state line is a curved line in three-dimensional ( $p'$ ,  $v$ ,  $q'$ ) space. The projection of the CSL onto the  $q'$ :  $p'$  plane is a straight line and can be represented by the following equation.

$$q' = Mp' \quad (6.1a)$$

where  $M$  is the gradient of the CSL,  $q'$  and  $p'$  are the values of deviator stress and mean effective stress, respectively at the failure point.

In the Fig. 6.4, the lines joining  $AB_3$ ,  $AB_2$  and  $AB_1$  are called the CSL of untreated C1, C2 and C3 clays, respectively. The values of  $M$  thus obtained are 0.98, 0.91 and 0.94 for untreated C1, C2 and C3 clays respectively. Figs. 6.5 and 6.6 present the effect of cement content on the stress paths and CSL of treated clays cured for 4 weeks. The values of  $M$  at 8% cement thus obtained are 1.85, 1.81 and 1.68, while the values of  $M$  at 16% cement have been found to be 2.34, 2.19 and 2.22 for samples of treated C1, C2 and C3 clays, respectively. It has been found that the values of  $M$  for treated clays are greater than those of untreated clays for all soils. It has also been found that at a particular curing time, the values of  $M$  for treated clays increased with increasing cement content as shown in Fig. 6.7.

Figs. 6.8 and 6.9 present the effect of curing time on stress paths and CSL of the samplers of treated clays having 12% cement content. The values of  $M$  at 4 week curing thus obtained are 2.13, 2.03 and 2.09, while the values of  $M$  at 12 week curing have been found to be 2.18, 2.08 and 2.14 for samples of treated C1, C2 and C3 clays, respectively. It has been found that at



particular cement content, the values of  $M$  for treated clays have been found to increase with increasing curing time.

#### 6.4 State Boundary Surfaces of the Untreated and Treated Clays

It has been established the samples of untreated clay are normally consolidated in nature and the samples of treated clay are lightly overconsolidated to heavily overconsolidated in nature depend on the amount of cement content. The overconsolidation ratios of treated clay are increased with increasing the amount of cement content. The typical effective undrained stress paths in  $p'$ - $q'$  space of untreated and treated samples of C1 clay are shown in Fig. 6.10. The behaviour of the heavily overconsolidated samples shown in Fig. 6.10 has been seen to be strongly dilatant because of treating with high percentage of cement with the undrained effective stress paths traveling a long way up to the right before rupture. Since these undrained stress paths are sections of the state boundary surface by constant void ratio planes, it is possible to transform the 3-dimensional state boundary surface ( $p'$ :  $v$  :  $q'$  space) to a 2--dimensional curve by a suitable selection of stress parameters. The parameters selected were  $q'/p'_e$  and  $p'/p'_e$  where the parameter  $p'_e$  is similar to that suggested by Hvorslev (1949).

$$p'_e = p' \exp[(e_0 - e)/\lambda] \quad (6.2)$$

where,  $p'$  and  $e_0$  correspond to the isotropic stress and void ratio respectively on the isotropic consolidation line in an ( $e - \log p'$ ) plot. For undrained test, void ratio is constant throughout the shear test, i.e.,  $e_0 = e$ , then  $p'_e = p'$ .

The normalized typical stress paths obtained from the undrained test on samples of untreated and treated samples of C1 clay are shown in Fig. 6.11. together with points representing the isotropic normal consolidation lines and the critical state lines for compression. Together these define a smooth state boundary surface for treated and untreated clay. The line DE defines the Roscoe surface for the untreated clay while the line BC defines the Hvorslev surface for the treated clay. Since, the natures of the effective stress paths of the treated clay are similar to those of lightly overconsolidated to heavily overconsolidated clays, no definite Roscoe surface could be established for the treated clay. Similar state boundary surface has also been obtained for samples of cement treated C2 and C3 clays.

#### 6.5 Correlation of Soil Constants with Plasticity Index

To specify the some constitutive models such as Cam clay model (Schofield and Wroth, 1968), the following three basic soil parameters are required:  $\lambda$ ,  $\kappa$  and  $N$ . In order to specify the behaviour of the models, three other values are also required to describe the current condition of the soils, namely, initial void ratio (or specific volume), pre-shear consolidation state and current stress state of the soils. The Soil constants,  $\lambda$ ,  $\kappa$  and  $N$  of untreated and treated samples have been used to study whether it is possible to determine parameters

specifying a constitutive soil model simply by using the plasticity index. In this section, the correlation of the three basic parameters with plasticity index has been established.

Figs. 6.12 and 6.13 show the compressibility index,  $\lambda$  data plotted against the plasticity index (PI) to assess the effect of cement and curing time, respectively. As shown in the figures, the nature of correlation for untreated and treated clay samples is same but the values of  $\lambda$  for treated clays are lower than those of untreated clays. Figs. 6.12 and 6.13 also show that for treated clays, the values of  $\lambda$  decreased with increasing cement content and with increasing curing time. As shown in the figures, the compressibility of soils increases with increasing plasticity index. Various researchers have reported this trend. In their experiments, Nakase, et al. (1988) and Bashar (2002) reported the existence of a linear relationship between PI and compressibility. Critical state soil mechanics theory (Schofield and Wroth, 1968) also predicted the following relationship for isotropic stress condition:

$$\lambda = 0.00585 \text{ PI} \quad (6.4a)$$

Bashar (2002) predicted the following relationship between PI and compressibility for untreated coastal soils:

$$\lambda = 0.09405 + 0.0021 \text{ PI} \quad (6.4b)$$

Regression lines (Fig. 6.12) for these relationships obtained from the present data for untreated and treated clays, incorporating the effect of cement content, can be given as for isotropic stress condition.

$$\lambda = 0.2294 + 0.003 \text{ PI} \quad \text{for untreated clays} \quad (6.5a)$$

$$\lambda = 0.126 + 0.0025 \text{ PI} \quad \text{for 8\% cement content (curing = 4w)} \quad (6.5b)$$

$$\lambda = 0.091 + 0.001 \text{ PI} \quad \text{for 16\% cement content (curing = 4w)} \quad (6.5c)$$

The values of the correlation coefficient (R) are high. R = 0.994, 0.996 and 0.998 for the equations respectively.

Regression lines (Fig. 6.13) for these relationships obtained from the present data incorporating the effect of curing time for treated (cement = 12%) clays can be given as for isotropic stress condition.

$$\lambda = 0.115 + 0.002 \text{ PI} \quad \text{for 4 weeks curing} \quad (6.5d)$$

$$\lambda = 0.105 + 0.0015 \text{ PI} \quad \text{for 12 weeks curing} \quad (6.5e)$$

The values of the correlation coefficient (R) are 0.999 and 0.999 for the equations respectively.

Figs. 6.14 and 6.15 show the swelling index,  $\kappa$  data plotted against PI to investigate the effect of cement content and curing time, respectively. As shown in the figures, the natures of correlation for untreated and treated clay samples are same but the values of  $\kappa$  for treated clays are lower than those of untreated clays. It can also be seen from Figs. 6.14 and 6.15 that for treated clays, the values of  $\kappa$  are decreased with increasing cement content and with increasing curing time. The swelling of soils increases with increasing plasticity index. A similar relationship was found between the swelling index and the plasticity index. Similar behaviour was also observed by Schofield and Wroth, (1968), Nakase et al. (1988) and Bashar, (2002). Bashar (2002). predicted the following relationship between  $\kappa$  and PI for untreated coastal soils:

$$\kappa = 0.00766 + 0.0011 \text{ PI} \quad (6.6)$$

Regression lines (Fig. 6.14) for these relationships obtained from the present data for untreated and treated clays can be given as for isotropic stress condition.

$$\kappa = 0.0062 + 0.0006 \text{ PI} \quad \text{for untreated clays} \quad (6.7a)$$

$$\kappa = 0.0112 + 0.0003 \text{ PI} \quad \text{for 8\% cement content (curing = 4w)} \quad (6.7b)$$

$$\kappa = 0.0016 + 0.0002 \text{ PI} \quad \text{for 16\% cement content (curing = 4w)} \quad (6.7c)$$

The values of the correlation coefficient (R) are high. R = 0.999, 0.998 and 1.00 for the equations respectively.

Regression lines (Fig. 6.15) for these relationships obtained from the present data incorporating the effect of curing of treated (cement = 12%) clays can be given as for isotropic stress condition.

$$\kappa = 0.0031 + 0.0003 \text{ PI} \quad \text{for 4 weeks curing} \quad (6.7d)$$

$$\kappa = 0.0025 + 0.0002 \text{ PI} \quad \text{for 12 weeks curing} \quad (6.7e)$$

The values of the correlation coefficient (R) are high. R = 1.00 and 0.995 for the equations respectively.

Figs. 6.16 and 6.17 show the specific volume, N data plotted against PI. As shown in the figures, the nature of correlation for untreated and treated clay samples is same but the values of N for treated clays are greater than those of untreated clays. Figs. 6.16 and 6.17 also show that for treated clays, the values of N are increased with increasing cement content and with increasing curing time. The values of N increase with increasing plasticity index. Similar behaviour was reported by Schofield and Wroth (1968) and Bashar (2002) for isotropic stress condition. Bashar (2002) reported the following relationships between N and PI for untreated coastal soils:

$$N = 2.128 + 0.0158 \text{ PI} \quad (6.8)$$

The resulting constitutive equations (Fig. 6.16) for the present study for untreated and treated clays are as follows:

$$N = 1.5986 + 0.0065 \text{ PI} \quad \text{for untreated clays} \quad (6.9a)$$

$$N = 1.7931 + 0.0074 \text{ PI} \quad \text{for 8\% cement content (curing = 4w)} \quad (6.9b)$$

$$N = 2.0521 + 0.0093 \text{ PI} \quad \text{for 16\% cement content (curing = 4w)} \quad (6.9c)$$

The values of the correlation coefficient (R) are 0.980, 0.985 and 0.999 for the equations respectively.

The resulting constitutive equations (Fig. 6.17) for the present study, incorporating the effect of curing, for treated clay (cement = 12%) clays are as follows:

$$N = 1.949 + 0.0076 \text{ PI} \quad \text{for 4 weeks curing} \quad (6.9d)$$

$$N = 2.176 + 0.0075 \text{ PI} \quad \text{for 12 weeks curing} \quad (6.9e)$$

The values of the correlation coefficient (R) are 1.00 and 0.998 for the equations respectively.

It therefore appears from the above correlations that, the soil constants can be well correlated with plasticity index for the untreated and cement treated clays incorporating both the effects of cement content and curing age.

## 6.6 Prediction of Drained Response Using MCC, MMCC and EMMCC Models

The prediction of triaxial drained response using MCC, MMCC and EMMCC for typical untreated and treated samples of C1 clays are discussed in the following sections:

### 6.6.1 Model Parameters

The parameters used in drained tests for MCC, MMCC and EMMCC models of cement treated and untreated clays are given in Table 6.2. The parameter  $\mu$  is the elastic shear modulus of the soil (G), which is defined as Poisson's ratio of the soil. The parameter, B (BWRAT) is defined as the ratio of the bulk modulus of the pore water to the bulk modulus of the soil. For drained test, the values of B has been considered as zero. The parameter,  $p_{co}$  (PCO) is defined as the preconsolidation pressure for cement treated and untreated clays. The  $p_m$  (PTO) includes the tensile strength parameter computed using the value of unconfined compression strength  $q_u$ , preconsolidation effective cell pressure  $p'_o$  and critical state strength parameter, M. The  $\rho_m$  (RHO) is known as cementation breakdown parameter, as the degradation parameter for increment of consolidation strength of soil due to cementation. For cemented soil,  $\rho_m$  is generally a large positive number greater than 1.0 and  $\rho_m$  is considered

as 60 to 90. The values of  $\rho_m$  is considered zero for uncemented soils. In the undrained test, the parameters,  $\mu$ ,  $B$  and  $p_{co}$  are used in the MCC, MMCC and EMMCC models. The parameters,  $p_{mo}$  and  $p_w$  are used only in the MMCC and EMMCC models and the parameters,  $\rho_m$  are used only in the EMMCC model.

The significance of application for  $\kappa$  (RKAP),  $\lambda$  (RLAM),  $M$  (RMU) and  $N$  (ECS) in the MCC, MMCC and EMMCC models can easily be explained. If the values  $\kappa$  and  $\lambda$  are increased in these models, the predicted strength is decreased and predicted volumetric strain is increased. If the values  $M$  and  $N$  are increased in these models, the predicted strength is increased but predicted volumetric strain is decreased. The drained analysis using these model parameters have been applied in the MCC, MMCC and EMMCC models to compute the stress-strain and volume strain change characteristics of the clays studied in this research with and without cementation.

### 6.6.2 Drained Stress-Strain Behaviour

Fig. 6.18 shows the typical drained stress-strain response of samples of untreated CI clay, using the MCC model for different pre-consolidation effective cell pressures. For the untreated clay, it has been observed that stress at initial axial strain levels (up to 4.5%) stresses predicted using the MCC model appears to be significantly close to experimental values. At large strains, however, the MCC model over estimates the experimental stresses. It therefore can be concluded that MCC model can be used to predict the drained stress-strain response up to certain initial strain level.

Figs. 6.19 to 6.21 show the typical drained stress-strain response of samples of cement treated CI clay (4% and 12% cement content, 4 weeks and 12 weeks curing time), using the MCC model, MMCC model and EMMCC model for different pre-consolidation effective cell pressures i.e., 100, 200 and 400 kPa. It has been observed that, in general, initial stiffness predicted by the MMCC model and EMMCC model are significantly higher than that of experimental results while the MCC model underestimates the experimental values. The predicted deviator stress ultimately attains a constant value with continuous shearing. This implies that critical state has been reached. Other important observations from Figs. 6.19 to 6.21 are as follows:

- (i) MCC model underestimates post-peak stresses at high cement content (12%).
- (ii) MMCC model overestimates post-peak stresses at high cement content (12%).
- (iii) Peak deviator stress predicted using EMMCC agrees well with the experimental value at high cement content (12%).
- (iv) For low curing age (4 weeks) and high cement content (12%), initial stiffness predicted using MCC model compares well with experimental values (Fig. 6.19a).

- (v) For long curing age (12 weeks) and high cement content (12%), initial stiffness predicted using EMMCC model compares very well with experimental values (Fig. 6.19b).
- (vi) For low curing age (4 weeks), low cement content (4%) and low pre-shear effective consolidation pressure, initial stiffness predicted using MCC model compares well with experimental values (Fig. 6.20a).
- (vii) For low curing age (4 weeks), low cement content (4%) and high pre-shear effective consolidation pressure, initial stiffness predicted using EMMCC model compares very well with experimental values (Fig. 6.20b).
- (viii) At low cement content (4%), peak deviator stress predicted using EMMCC agrees well with the experimental value (Fig. 6.21).

From the above observations, it appears that MCC, MMCC and EMMCC models are not so effective to predict the drained stress-strain response and therefore may not be applicable to predict drained stress-strain behaviour of cemented clays. Nevertheless, the EMMCC model predictions compares well in some respects with the observed experimental behaviour. Youwai and Bergado (2003) found satisfactory applicability of constitutive models for stabilized soil while, Islam et al. (2007) and Khalilullah (2007) found that the unsatisfactory applicability of the constitutive models for cement treated clays. There had been a breakdown of stress-strain curves from the prediction of Bergado (2003), while there was a no breakdown of stress-strain curves from the prediction of Khalilullah (2007) where stress became constant with continuous shearing deformation. The predictions obtained in this study agreed reasonably with those reported by Khalilullah (2007) for cement treated clays of Bangladesh.

### 6.6.3 Volume Change Responses

Fig. 6.22 shows the typical volume changes response of samples of untreated C1 clay, using the MCC model for different pre-shear effective consolidation pressure. It has been observed from Fig. 6.22 that volumetric strains at initial axial strain level (up to only 2%) predicted using the MCC model are significantly close to or slightly higher than that of experimental values. Volumetric strains predicted by the MCC model at large axial strains, however, are higher for higher cell pressures and lower for lower cell pressures than that of experimental results. Islam et al. (2007) and Khalilullah (2007) also found that similar predictions of volume change responses for untreated clays of Bangladesh.

Figs. 6.23 to 6.25 show the typical volumetric change responses of samples of cement treated C1 clay (4% and 12% cement content; 4 weeks and 12 weeks curing age), using the MCC model, MMCC model and EMMCC model for different pre-shear effective consolidation pressure i.e., 100, 200 and 400 kPa. Figs. 6.23 to 6.25, in general, shows the following salient features:

- (i) MMCC model and EMMCC model over predicts the initial volumetric strain for large cement content (12%).
- (ii) Initial volumetric strain predicted using MCC model agrees reasonably well with the experimental values.
- (iii) Volumetric strain-axial strain responses predicted by the MMCC model for high cement content, large pre-shear effective consolidation pressure compares reasonably well with the experimental curve.
- (iv) Volumetric strain-axial strain responses (up to peak value) predicted using MMCC model for low cement content and high pre-shear effective consolidation pressure agrees reasonably well with the experimental curve.
- (v) The predicted volumetric strain predicted using all the models ultimately attains a constant value with continuous shearing. This implies that the critical state has been reached.

From the above findings, it can be concluded that the predictions for volumetric changes behaviour using MCC, MMCC and EMMCC model are not effectively applicable for such cement treated clays at high water content, although MCC and MMCC predictions agrees well with the experimental behaviour in some respects. Youwai and Bergado (2003) reported constitutive models can be satisfactorily used for of stabilized soil while, Islam et al. (2007) and Khalilullah (2007) reported that constitutive models may not be applicable for of cement treated clays to predict volumetric strain responses. The prediction in this study agrees well with those reported by Khalilullah (2007) for cement treated clays Bangladesh.

## 6.7 Prediction of Undrained Response Using MCC, MMCC and EMMCC

The predicted undrained response using MCC, MMCC and EMMCC for untreated and treated clays are discussed in the following sections:

### 6.7.1 Model Parameters

The parameters used in undrained tests for MCC, MMCC and EMMCC models of cement treated and untreated clays are given in Table 6.3. The parameters,  $\mu$ ,  $B$ ,  $p_{co}$ ,  $p_w$  and  $\rho_m$  have been defined earlier in section 6.6.1. For undrained test, the range of  $\mu$  has been taken as 0.40 to 0.50. For undrained test, the values of  $B$  (BWRAT) is generally a large positive number greater than 1.0 and considered as 1 to 40. The values of  $B$  has been increased with increasing strength of soil. For cemented soil,  $\rho_m$  is generally a large positive number greater than 1.0,  $\rho_m$  has been considered as 55 to 85. The values of  $\rho_m$  is considered zero for uncemented soils. In the undrained test, the parameters,  $\mu$ ,  $B$  and  $p_{co}$  are used in the MCC, MMCC and EMMCC models. The parameters,  $p_{m0}$  and  $p_w$  are used only in the MMCC and

EMMCC models and the parameters,  $\rho_m$  are used only in the EMMCC model.

The significance of application for  $\kappa$  (RKAP),  $\lambda$  (RLAM),  $M$  (RMU) and  $N$  (ECS) in the MCC, MMCC and EMMCC models can easily be explained. If the values  $\kappa$  and  $\lambda$  are increased in these models, the predicted strength is decreased and predicted excess pore pressure is increased. If the values  $M$  and  $N$  are increased in these models, the predicted strength is increased and predicted excess pore pressure is decreased. The undrained analysis using these model parameters have been used in the MCC, MMCC and EMMCC models to compute the stress-strain, pore pressure response and stress path characteristics of the clays, with and without cementation.

### 6.7.2 Undrained Stress-Strain Behaviour

Fig. 6.26 shows the typical undrained deviator stress-axial strain response of samples of untreated C1 clay using the MCC model for different pre-shear effective consolidation pressures. For untreated clay, it has been observed that the MCC model overestimates the experimental values at both the pre-shear effective consolidation pressures. Siddiquee (2006), Siddique et al. (2003) and Bashar (2002) also reported similar observations.

Figs. 6.27 to 6.29 show typical undrained deviator stress-axial strain response of samples of cement treated C1 clay (4 and 12% cement content; 4 weeks and 12 weeks curing time), using the MCC model, model and EMMCC model for different pre-shear effective consolidation pressures i.e., 100, 200 and 400 kPa. Figs. 6.27 to 6.29, in general, show the following major observations:

- (i) MMCC model and EMMCC model overestimates the initial stiffness at low and high cement contents.
- (ii) Peak deviator stresses predicted using MMCC model compares well with the experimental values at high cement content and moderately high pre-shear effective consolidation pressures (200 kPa and 400 kPa). At low pre-shear effective consolidation pressures (100 kPa), peak deviator stresses predicted using EMMCC model agrees well with the experimental value.
- (iii) At low cement content (4%), peak deviator stresses predicted using EMMCC model compares reasonably good with the experimental values (Fig. 6.29) at pre-shear effective consolidation pressures of 100 kPa and 400 kPa.
- (iv) MCC model highly underestimates the peak deviator stresses irrespective of cement content, curing age and pre-shear effective consolidation pressures.
- (v) Using all the models, the predicted deviator stress ultimately attains a constant value with continuous shearing. This implies that the critical state is reached.



From the above findings, it can be concluded that for the prediction for undrained stress-strain behaviour, MCC, MMCC and EMMCC models are not so effective for cemented clays at high water content, although MMCC and EMMCC predictions compares reasonably well with the experimental values in some respects. Siddiquee (2006) and Khalilullah (2007) also reported that predictions of undrained stress-strain responses using MCC, MMCC and EMMCC models are not satisfactory. The predictions obtained in this study are more or less similar to those reported by Khalilullah (2007) for cement treated clays of Bangladesh.

### 6.7.3 Pore Pressure Change Responses

Fig. 6.30 presents typical excess pore pressure response of samples of untreated C1 clay, using the MCC model for different pre-shear effective consolidation effective pressures. For the untreated clay, it has been observed that although the initial excess pore pressure values compares very well with the experimental values up an axial strain level of only about 1%, at larger axial strains, MCC model significantly overestimates the excess pore pressure values at both the pre-shear effective consolidation effective pressures. Islam et al. (2007) and Khalilullah (2007) also found similar predictions for pore pressure response of untreated clays of Bangladesh.

Figs. 6.31 to 6.33 show typical the pore pressure change responses of samples of cement treated C1 clay (4 and 12% cement content; 4 weeks and 12 weeks curing time), using the MCC model, MMCC model and EMMCC model for different pre-shear effective consolidation effective pressures i.e., 100, 200 and 400 kPa. Figs. 6.31 to 6.33, in general, show the following salient features:

- (i) MCC, MMCC and EMMCC models over predicts the initial pore pressure changes at low and high cement contents.
- (ii) Peak pore pressure change predicted using MMCC model compares well with the experimental values at high cement content and moderately high pre-shear effective consolidation pressures (200 kPa) while EMMCC overestimates peak pore pressure change at high cement content and moderately high pre-shear effective consolidation pressures (200 kPa). At low pre-shear effective consolidation pressures (100 kPa), however, excess pore pressure predicted using EMMCC have been found to be negative at high and low cement content.
- (iii) Peak pore pressure change predicted using EMMCC model compares very well with the experimental value at high pre-shear effective consolidation pressures of 400 kPa (Fig. 6.32b).
- (iv) MCC model highly underestimates the peak pore pressure change at all cement contents, curing ages and moderate to high pre-shear effective consolidation pressures (200 kPa and 400 kPa). At low pre-shear effective consolidation pressure (100 kPa),

experimental peak pore pressure change agrees well with that predicted using MCC model.

- (v) Using all the models, the predicted pore pressure change ultimately attains a constant value with continuous shearing. This implies that the critical state has been reached.

From the findings, it appears that the MCC, MMCC and EMMCC models may not be appropriate for the prediction of pore pressure change responses for such cement treated clays at high water content. Siddiquee (2006) and Khalilullah (2007) reported MCC, MMCC and EMMCC models may not be applicable to predict pore pressure responses of untreated and cement treated clays. There had been no breakdown of pore pressure-axial strain curves where pore pressure became constant with continuous shearing deformation (Siddiquee, 2006; Khalilullah, 2007). The predictions in this study are similar to those reported by Khalilullah (2007) for cement treated clays of Bangladesh.

#### 6.7.4 Undrained Stress Paths

Fig. 6.34 shows typical predicted undrained effective stress paths for samples of untreated C1 clay using the MCC model at different pre-shear effective consolidation pressures. Fig. 6.34 shows that the predicted undrained effective stress paths of untreated clay agree reasonably well with the observed stress paths at lower pre-shear effective consolidation pressures (100 kPa and 200 kPa).

Figs. 6.35 to 6.37 present the predicted undrained effective stress paths of samples of cement treated C1 clay using the MCC, MMCC and EMMCC models at pre-shear effective consolidation pressures of 100 kPa, 200 kPa and 400 kPa, respectively. The predicted undrained effective stress paths have been observed to be vertical in  $p' - q$  space. Increasing deviator stresses at constant mean pressure have been predicted. It can be seen from Figs. 6.35 to 6.37 that, in general show the observed undrained effective stress paths compares reasonably well with those predicted using EMMCC model, particularly at pre-shear effective consolidation pressures of 100 kPa and 400 kPa. From the above observations, it can be concluded that the EMMCC model may be used for the predictions of undrained effective stress paths of cemented clays at high water content. Siddiquee (2006) and Khalilullah (2007), however, found unsatisfactory predictions using MCC, MMCC and EMMCC models for untreated and cement treated clays.

#### 6.8 Prediction of Drained and Undrained Responses using Cap Model

Cap Model has been used for prediction of drained and undrained behaviour. The calculation steps for the Coulomb and Drucker-prager models have been explained in the Flow Chart of Fig. 2.61. The model parameters, which have been used in drained tests for Plane Cap and Elliptic Cap models of cement treated clays are listed in Table 6.4.

### 6.8.1 Drained Stress-Strain Behaviour

Figs. 6.38 to 6.40 show typical deviator stress-axial-strain response of samples of cemented C1 clay using the Plane Cap and Elliptic Cap models for different cement content, curing time and pre-shear effective consolidation pressures. It can be seen from these figures that neither the Plane Cap nor the Elliptic Cap predictions agree with the experimentally observed stress-strain curves irrespective of cement content, curing time and pre-shear effective consolidation pressures. At pre-peak stress levels, Plane Cap and the Elliptic Cap underestimate the observed stresses while at post-peak stress levels, Plane Cap and Elliptic Cap models over predict the observed stresses. It appears from the findings that Cap models cannot be applied for predictions of drained stress-strain behaviour of cemented clays at high water content.

### 6.8.2 Volume Change Response

Figs. 6.41 to 6.43 show typical volume changes response of samples of cemented C1 clay using the Plane Cap and Elliptic Cap models for different cement content, curing time and pre-shear effective consolidation pressures. It can be observed from Figs. 6.41 to 6.43 that both the Plane Cap and Elliptic Cap predictions do not compare at all with the experimentally observed volumetric strain-axial strain curves irrespective of cement content, curing time and pre-shear effective consolidation pressures. At pre-peak volumetric strain levels, Plane Cap and the Elliptic Cap underestimate the observed stresses while at post-peak stress levels, Plane Cap and Elliptic Cap models over predict the observed volumetric strains. It appears from the findings that Cap models cannot be applied for predictions of volumetric strain-axial strain behaviour of cemented clays at high water content.

## 6.9 Prediction of Undrained Response using Cap Model

Cap Model has been used for prediction of undrained behaviour. The model parameters, which, have been used in undrained tests for Plane Cap and Elliptic Cap models of cement treated clays as listed in Table 6.5.

### 6.9.1 Undrained Stress-Strain Behaviour

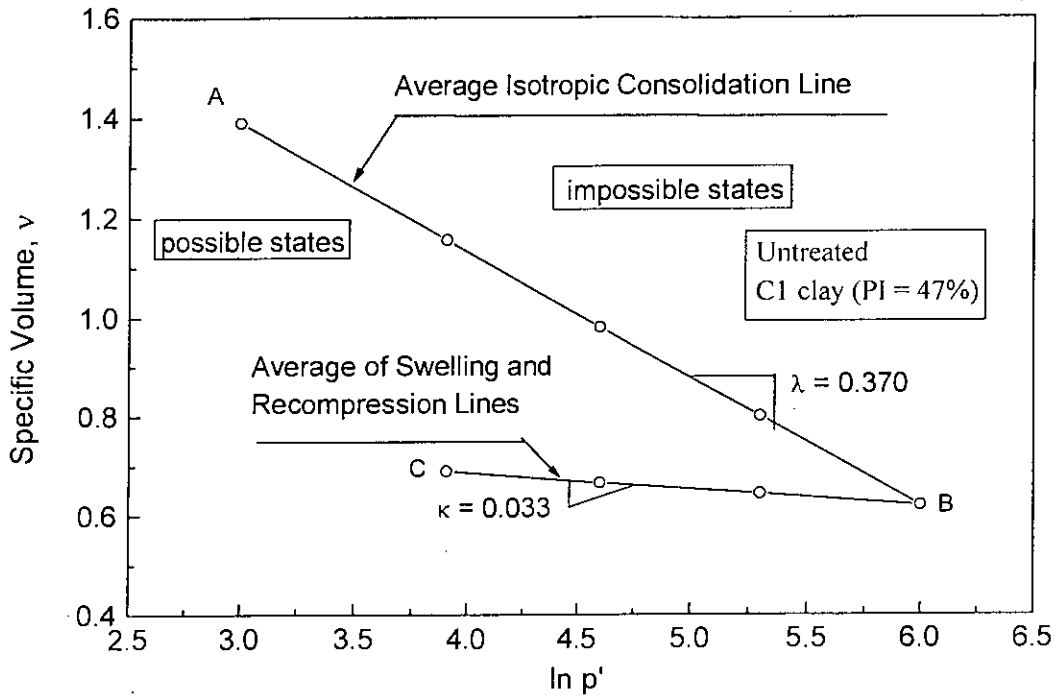
Figs. 6.44 to 6.46 show typical deviator stress-axial strain response of samples of cemented C1 clay using the Plane Cap and Elliptic Cap models for different cement content, curing time and pre-shear effective consolidation pressures. It can be seen from these figures that neither the Plane Cap nor the Elliptic Cap predictions compare well with the experimentally observed stress-strain curves irrespective of cement content, curing time and pre-shear effective consolidation pressures. Similar to the predictions of drained stress-strain behaviour, at pre-peak stress levels, both the Cap models underestimate the observed stresses while at post-peak stress levels, Plane Cap and Elliptic Cap models overestimate the observed stresses. It appears from the findings that Cap models cannot be applied for predictions of undrained stress-strain behaviour of cemented clays at high water content.

### 6.9.2 Pore Pressure Change Response

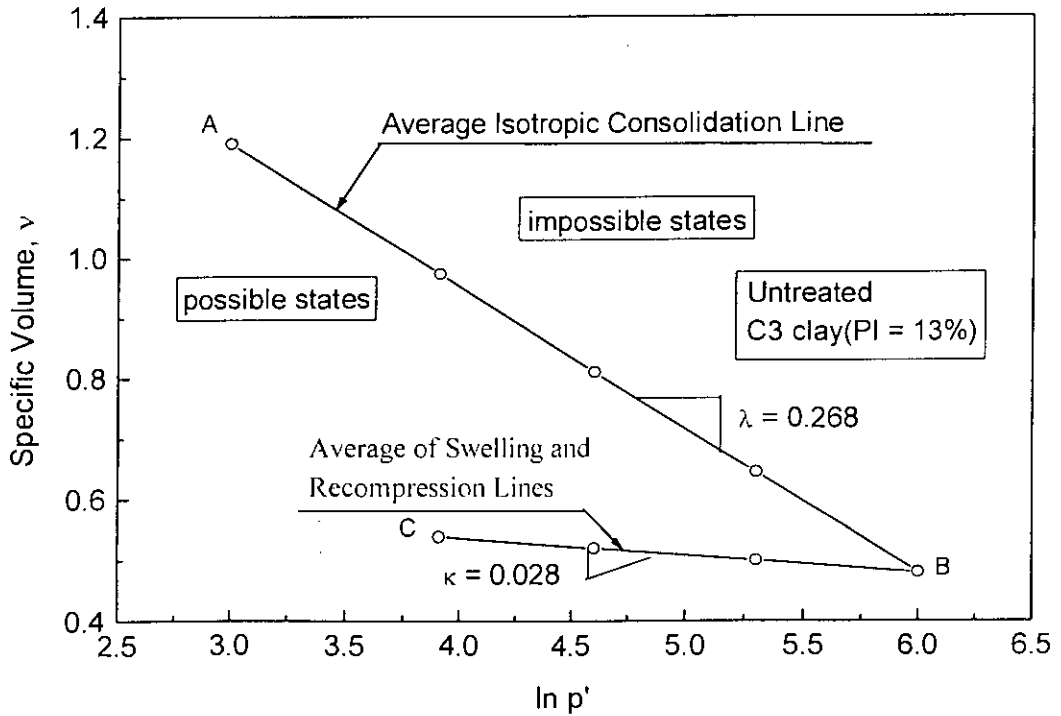
Figs. 6.47 to 6.49 show typical pore pressure change-axial strain response of samples of cemented Cl clay using the Plane Cap and Elliptic Cap models for different cement content, curing time and pre-shear effective consolidation pressures. It can be seen from these figures that neither the Plane Cap nor the Elliptic Cap predictions compare well with the experimentally observed pore pressure change versus axial strain curves, irrespective of cement content, curing time and pre-shear effective consolidation pressures. It appears from Figs. 6.47 to 6.49 that at pre-peak pore pressure change levels, both the Plane Cap and Elliptic Cap models underestimate the observed excess pore pressure while at post-peak pore pressure change levels, Plane Cap and Elliptic Cap models over predict the experimentally observed pore pressure change. It, therefore, can be concluded that from the findings of the present study that Cap models cannot be applied for predictions of pore pressure change responses of cemented clays at high water content.

### 6.9.3 Stress Path in the $I_1 - \sqrt{J_2}$ Space

Similarly, the axial stress-strain curves for the strain - increasing and decreasing paths are presented in Fig. 6.50 with the elliptic cap model. The stress path in the  $I_1 - \sqrt{J_2}$  space during the strain- increasing path is seen to move first within the failure envelope and then later to situate on the elliptic cap surface. A hardening surface coding is therefore employed here. At the axial compressive strain of elliptic cap model, which is smaller than that for the plane cap model. On the other hand, the stress state during the strain-decreasing path moves within the current elastic region while the elliptic cap remains fixed in the stress space. Consequently, the axial stress- strain curve is linearly elastic until the stress state touches the failure surface. Once the stress state reaches the failure envelop, the yield surface coding is utilized to determine the plastic volume expansion or dilatancy. As a result of this dilatancy, the cap contracts toward the origin. The cap contraction stops at the current stress state, and this leads to the development of the corner point between the elliptic cap and failure surface at the current stress state. Consequently, the corner coding is triggered until the stress state reaches the origin. The main difference between the predictions of the plane cap model and the elliptic cap model is that they follow a different stress path during the strain - decreasing path.

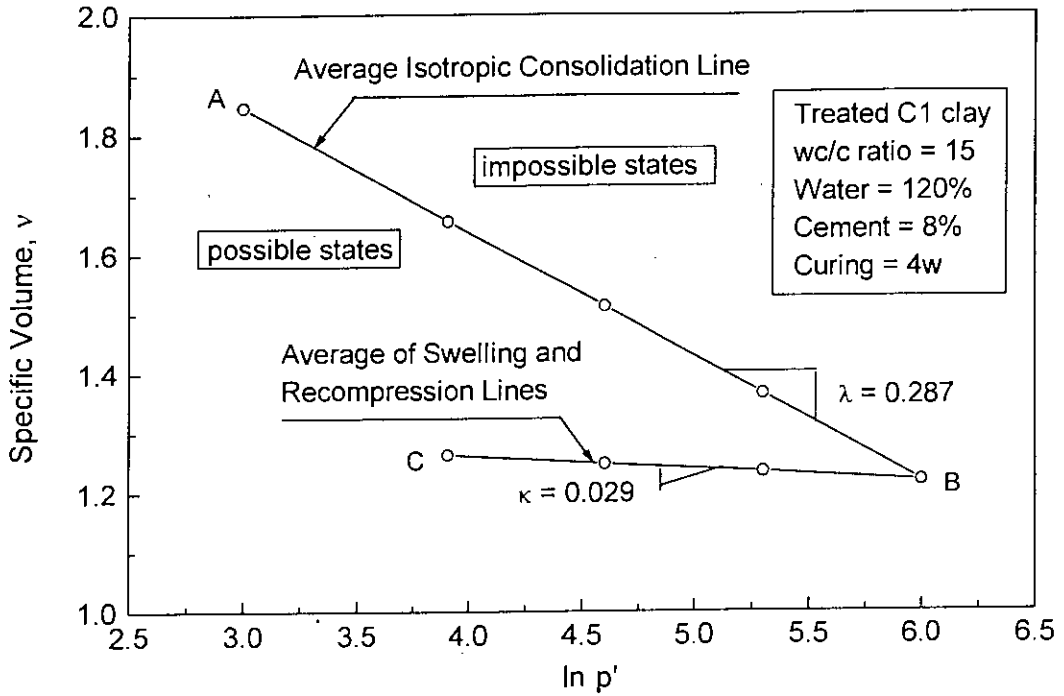


(a)

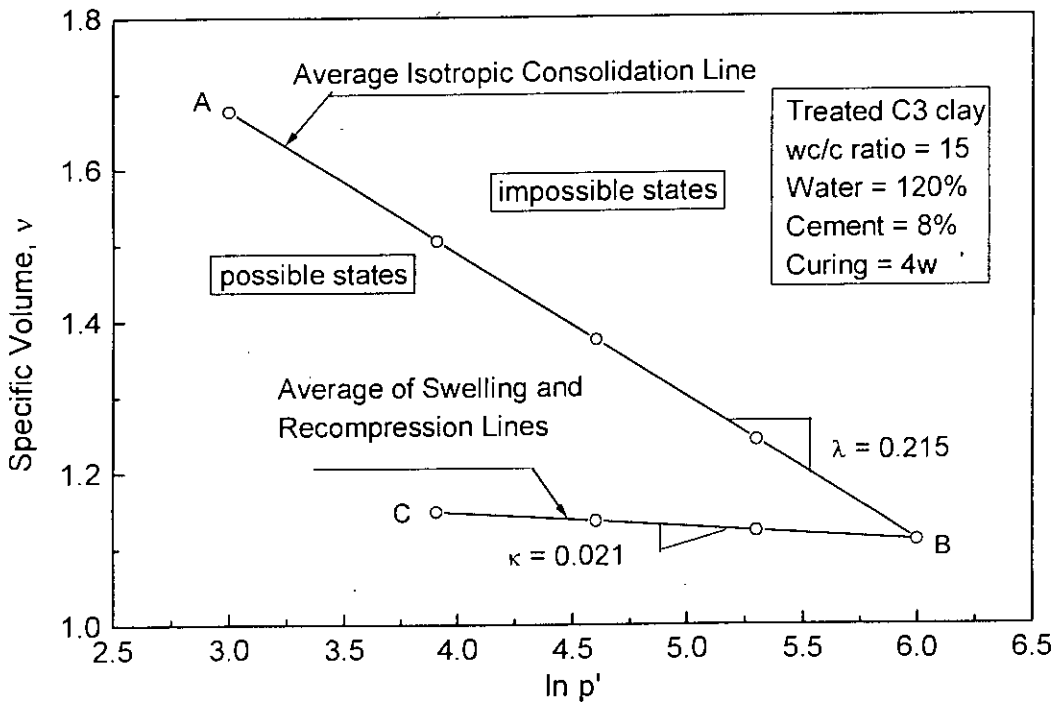


(b)

Fig. 6.1 Isotropic Consolidation and Swelling Curves of Untreated Clays  
(a) C1 clay and (b) C3 clay

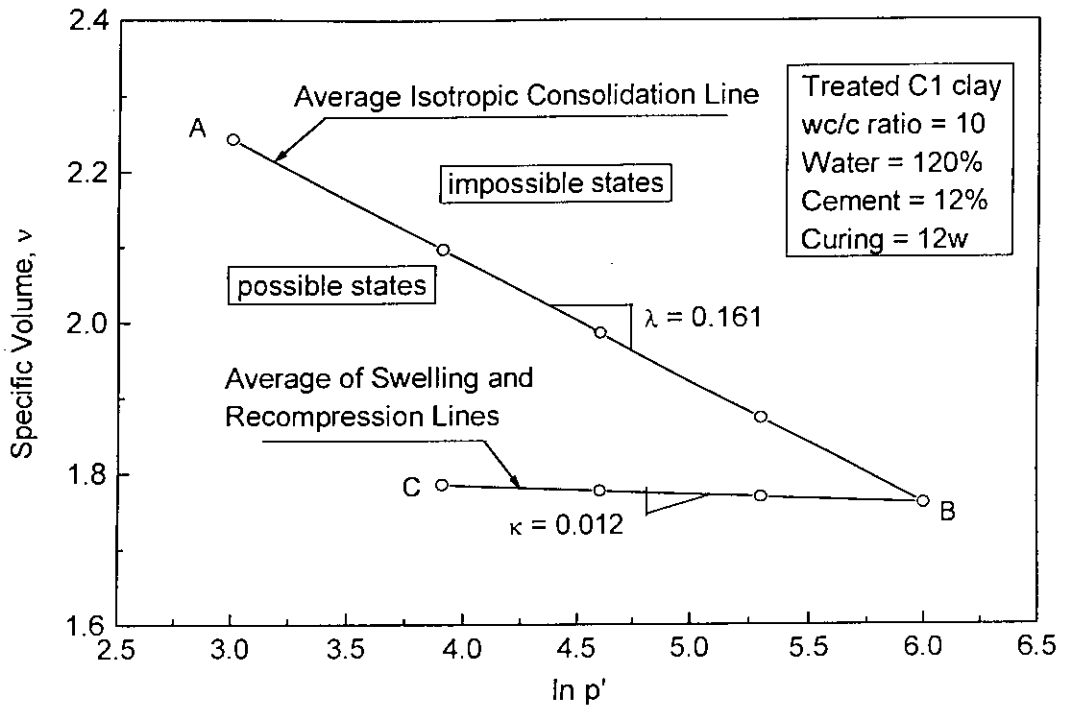


(a)

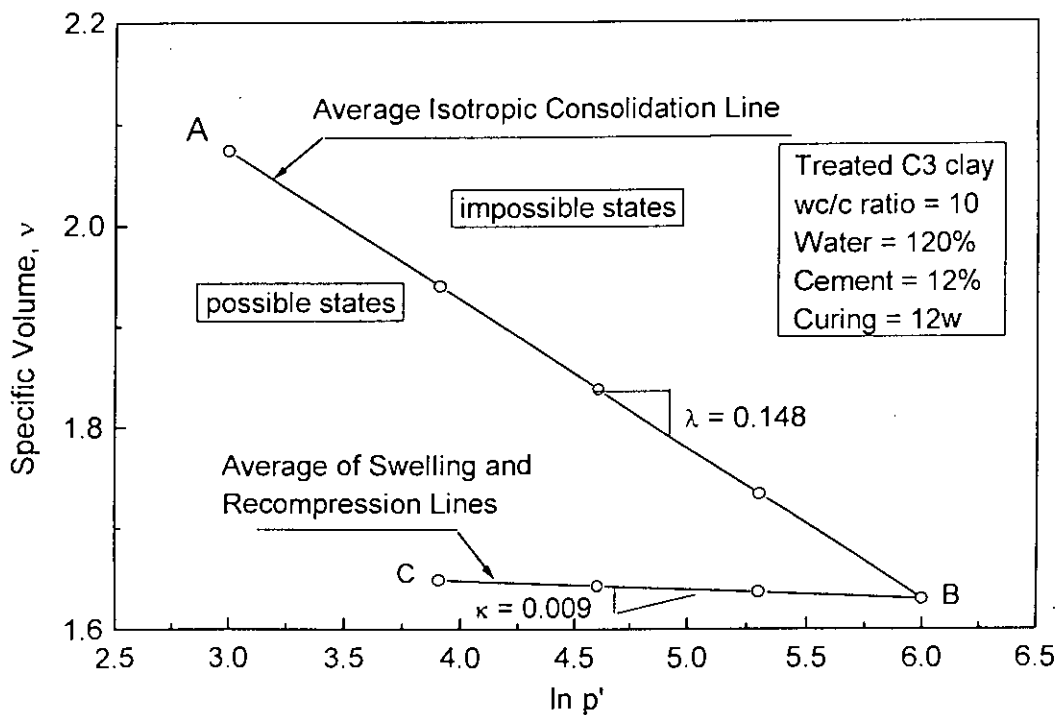


(b)

Fig. 6.2 Isotropic Consolidation and Swelling Curves at Cement = 8% and Curing = 4 w of Cement Treated clays (a) C1 clay and (b) C3 clay



(a)



(b)

Fig. 6.3 Isotropic Consolidation and Swelling Curves at Cement = 12% and Curing = 12 w of Cement Treated clays (a) C1 clay and (b) C2 clay

**Table 6.1 Effect of Cement Content and Curing Time on Soil Constants ( $\lambda$ ,  $\kappa$  and  $N$ ) under Isotropic Condition for Cement Treated Clays**

Curing time in weeks	Type of clays	wc/c ratio	Plasticity index	Soil constants		
			PI (%)	$\lambda$	$\kappa$	$N$
untreated	C1	-	47	0.370	0.033	1.90
	C2	-	22	0.295	0.030	1.76
	C3	-	13	0.268	0.028	1.67
4 weeks	C1	7.5	57	0.151	0.013	2.58
		10	63	0.181	0.017	2.48
		15	65	0.287	0.029	2.27
		30	71	0.331	0.034	1.87
	C2	7.5	37	0.134	0.009	2.58
		10	43	0.170	0.015	2.28
		15	46	0.240	0.024	2.15
		30	51	0.273	0.029	1.72
	C3	7.5	27	0.127	0.008	2.30
		10	33	0.164	0.011	2.20
		15	36	0.215	0.021	2.05
		30	41	0.227	0.025	1.64
12 weeks	C1	10	53	0.161	0.012	2.57
	C2	10	36	0.153	0.010	2.45
	C3	10	25	0.148	0.009	2.36



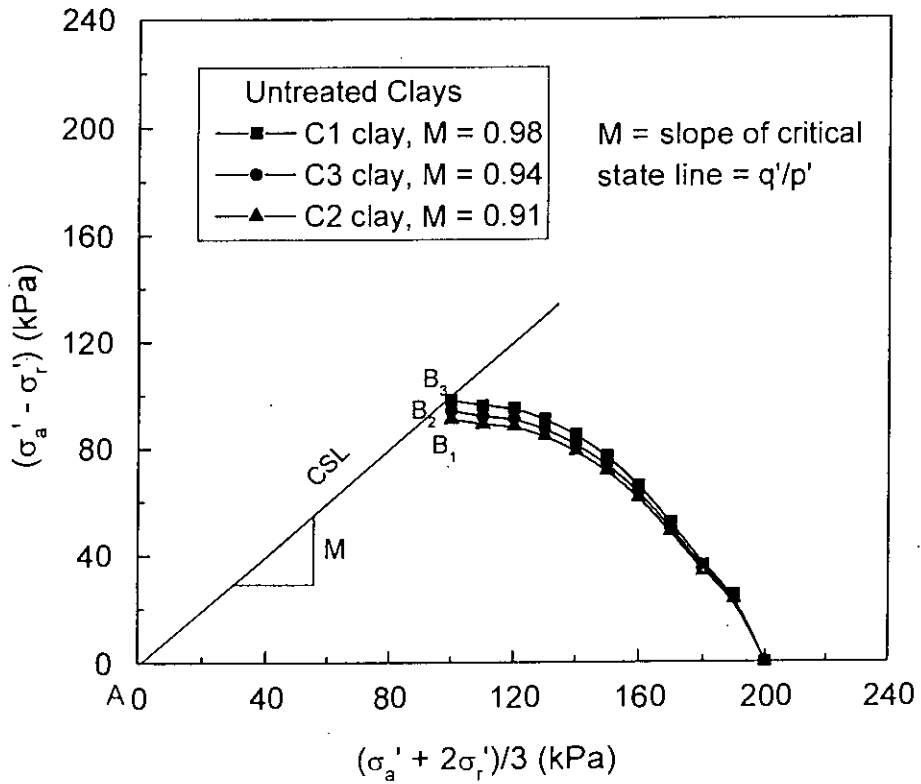


Fig. 6.4 Effective Stress Path for Three Untreated Isotropically Consolidated Clays

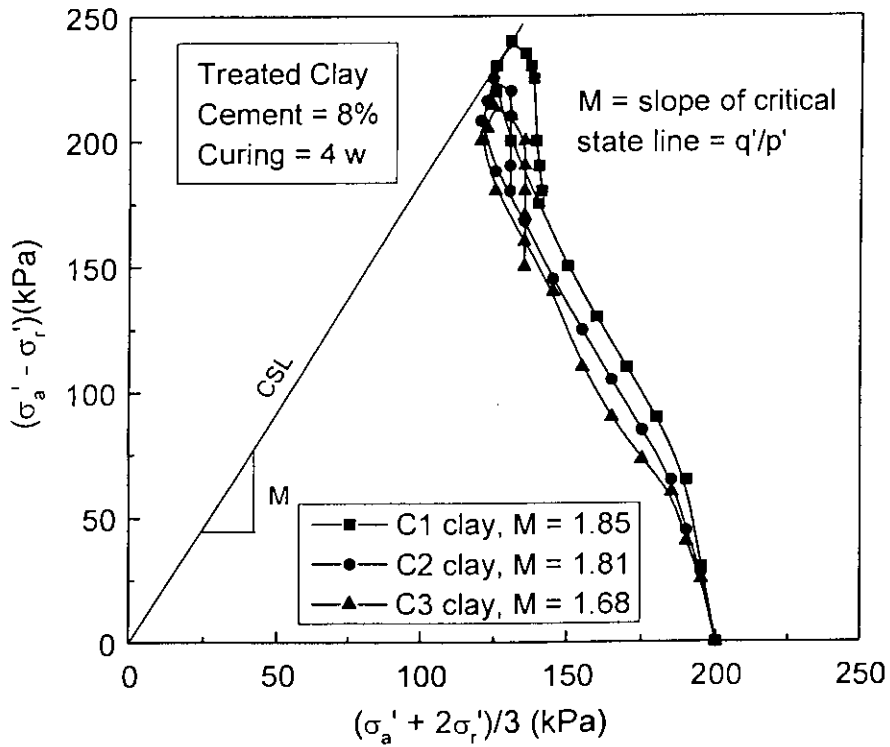


Fig. 6.5 Effective Stress Path for Three Cement Treated Clays at Cement = 8% and Water = 120%

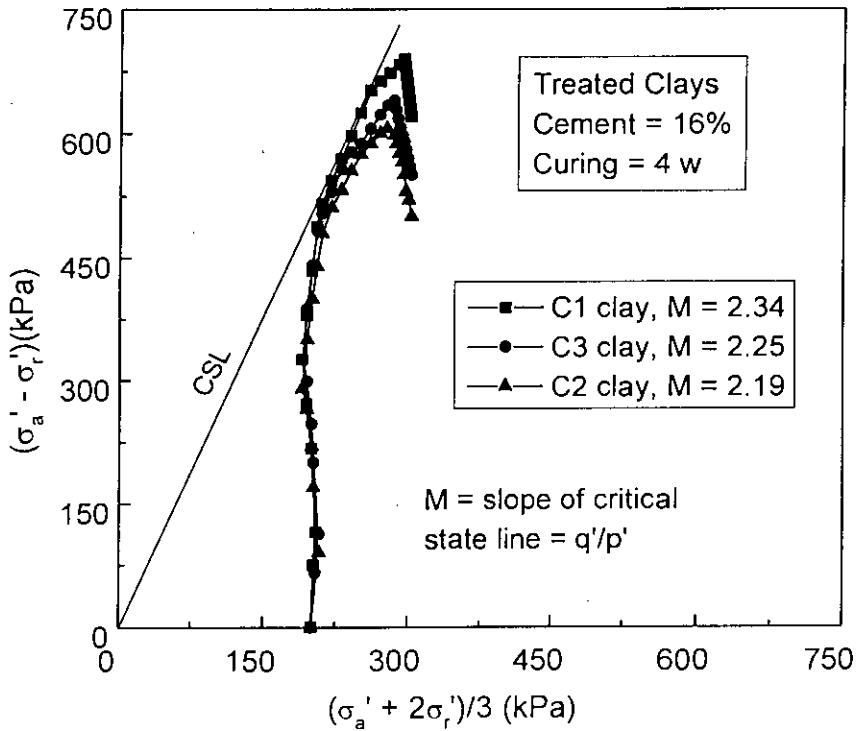


Fig. 6.6 Effective Stress Path for Three Cement Treated Clays at Cement = 16% and Water = 120%

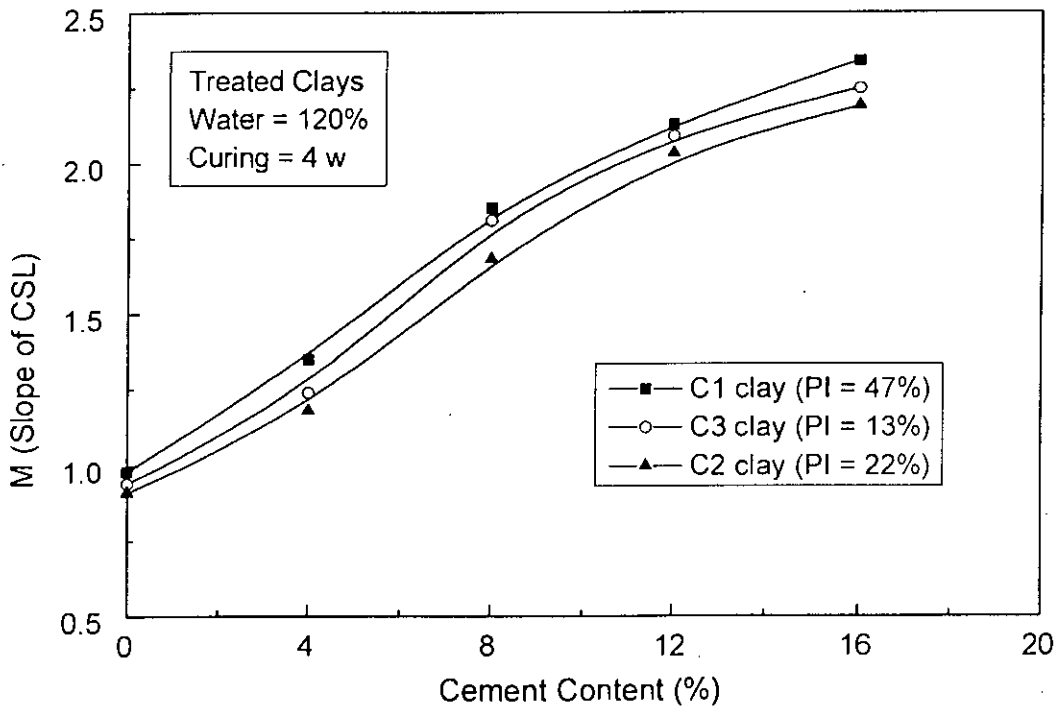


Fig. 6.7 Variation the Values of M with Cement Content for Various Clays

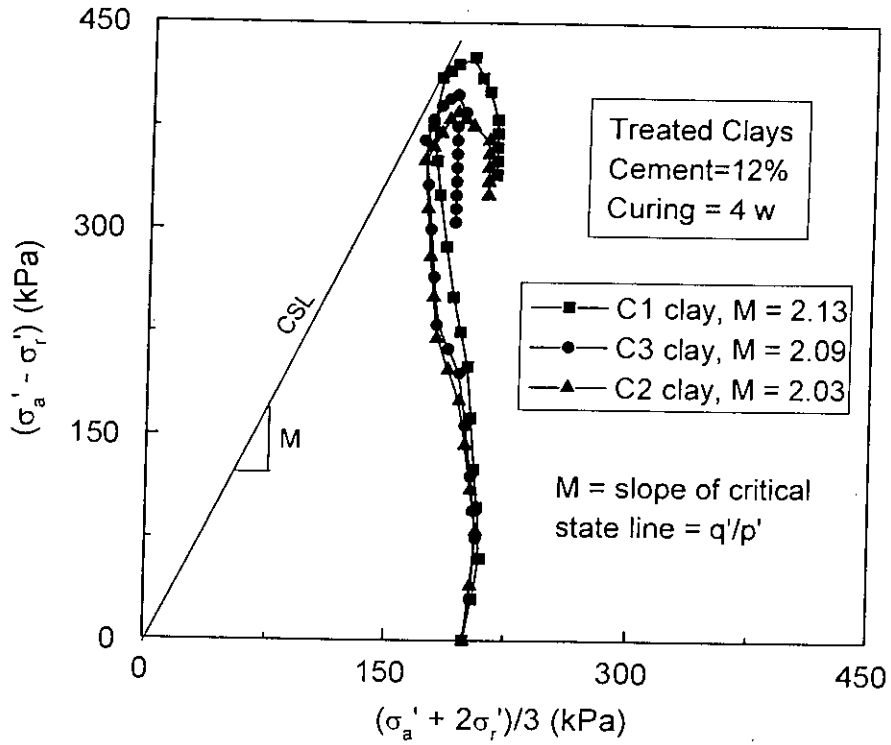


Fig. 6.8 Effective Stress Path for Three Cement Treated Clays at Cement = 12% and Water = 120%

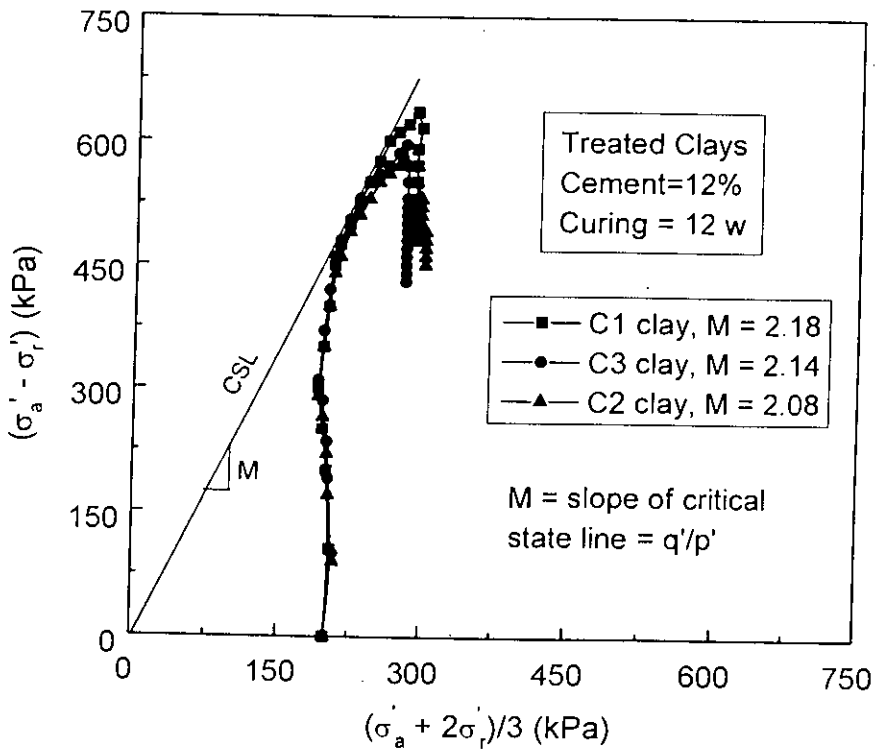


Fig. 6.9 Effective Stress Path for Three Cement Treated Clays at Cement = 12% and Water = 120%

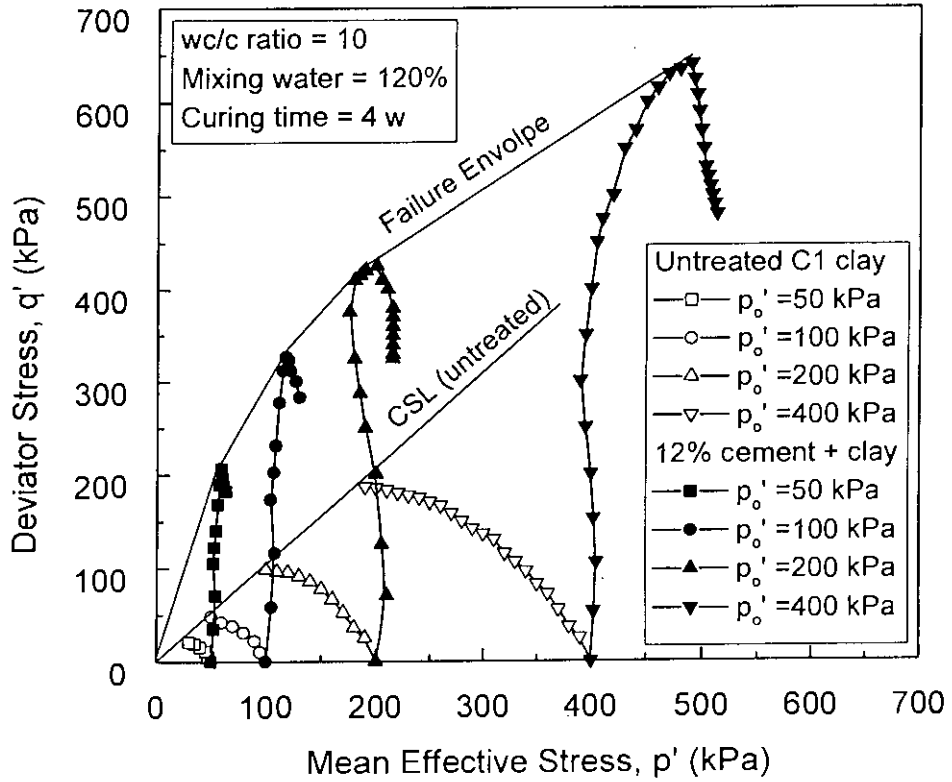


Fig. 6.10 Undrained Effective Stress Paths of Untreated and Cement Treated C1 clay

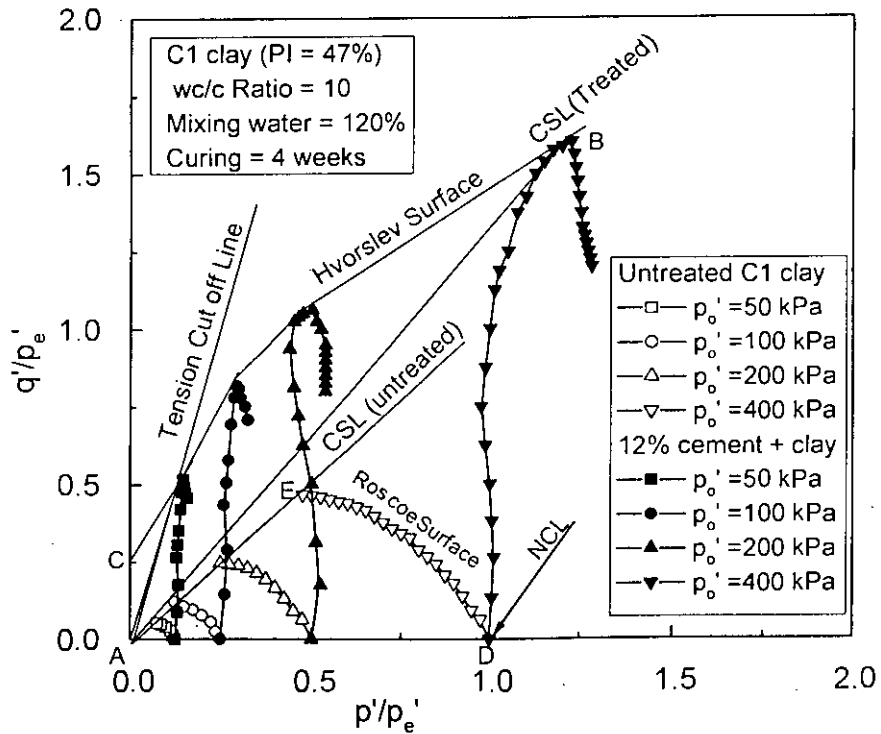


Fig. 6.11 Paths in  $q'/p'_e' : p'/p'_e'$  Space of Untreated and Cement Treated C1 clay

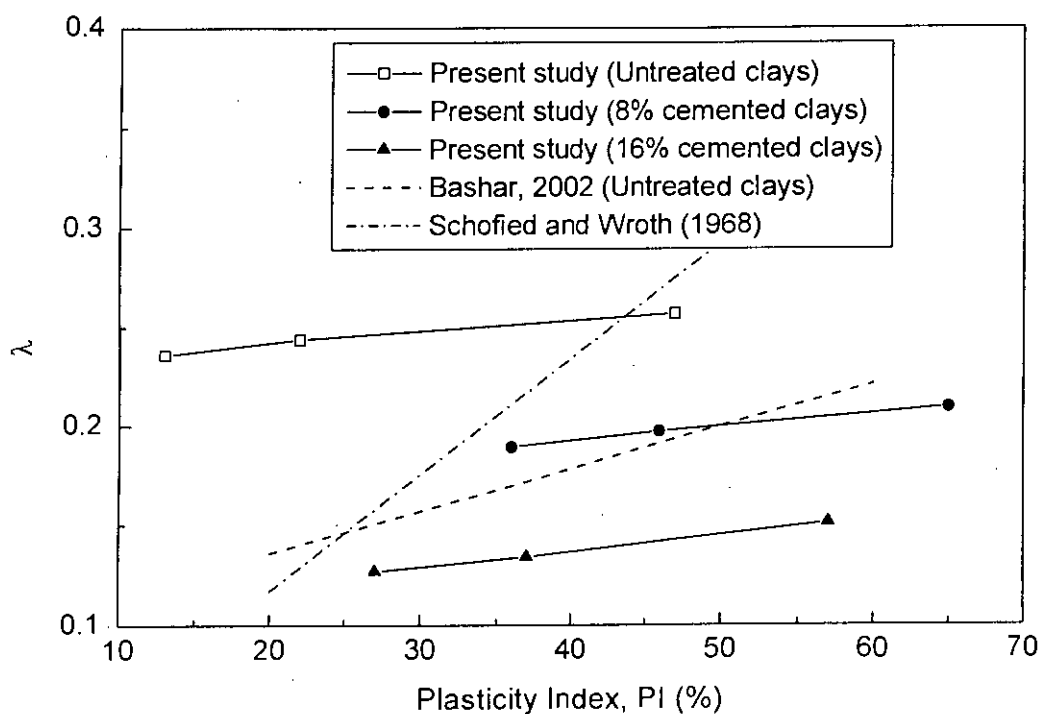


Fig. 6.12 Effect of Cement (curing = 4 w) on Correlation between Critical Compressibility Index ( $\lambda$ ) and Plasticity Index (PI)

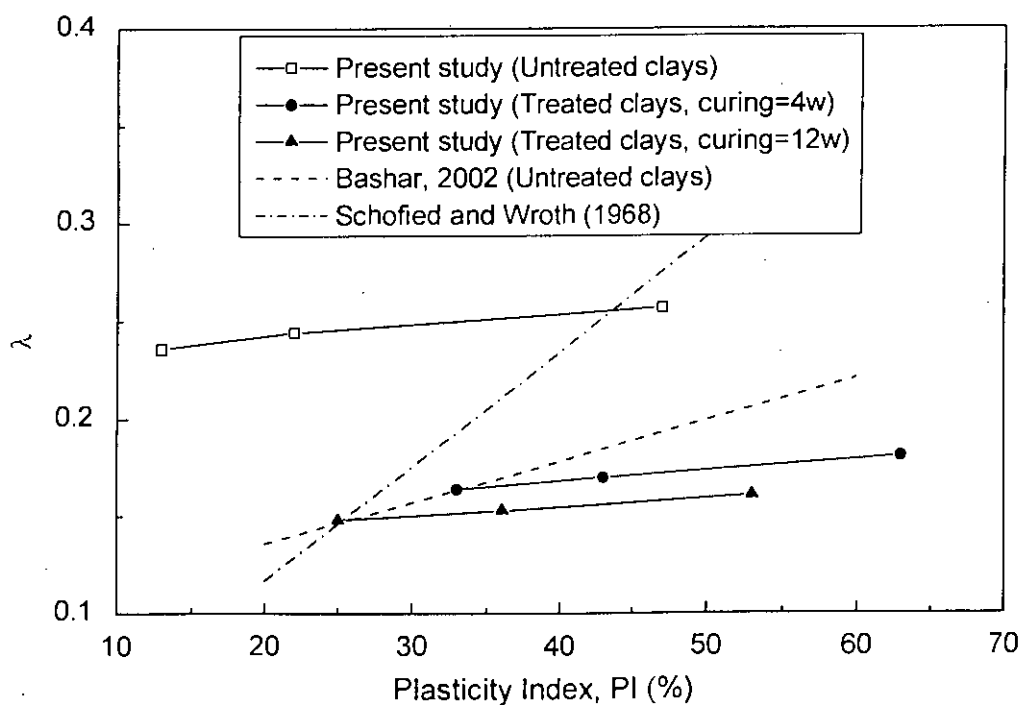


Fig. 6.13 Effect of Curing Time (cement = 12%) on Correlation between Critical Compressibility Index ( $\lambda$ ) and Plasticity Index (PI)

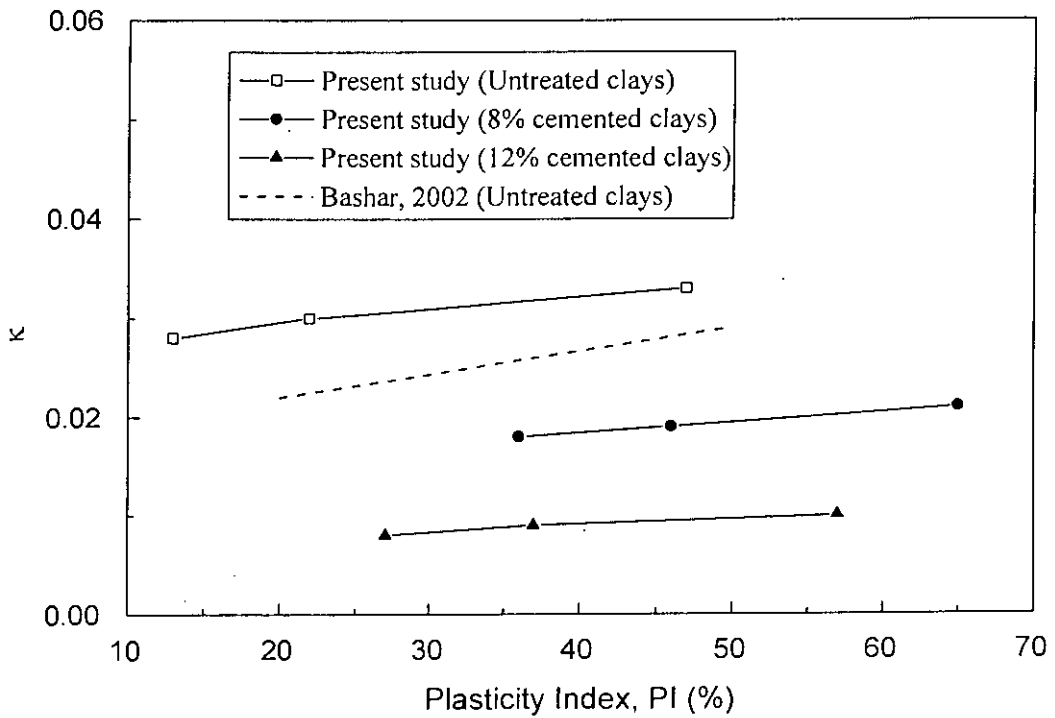


Fig. 6.14 Effect of Cement (curing = 4 w) on Correlation between Critical Swelling Index ( $\kappa$ ) and Plasticity Index (PI)

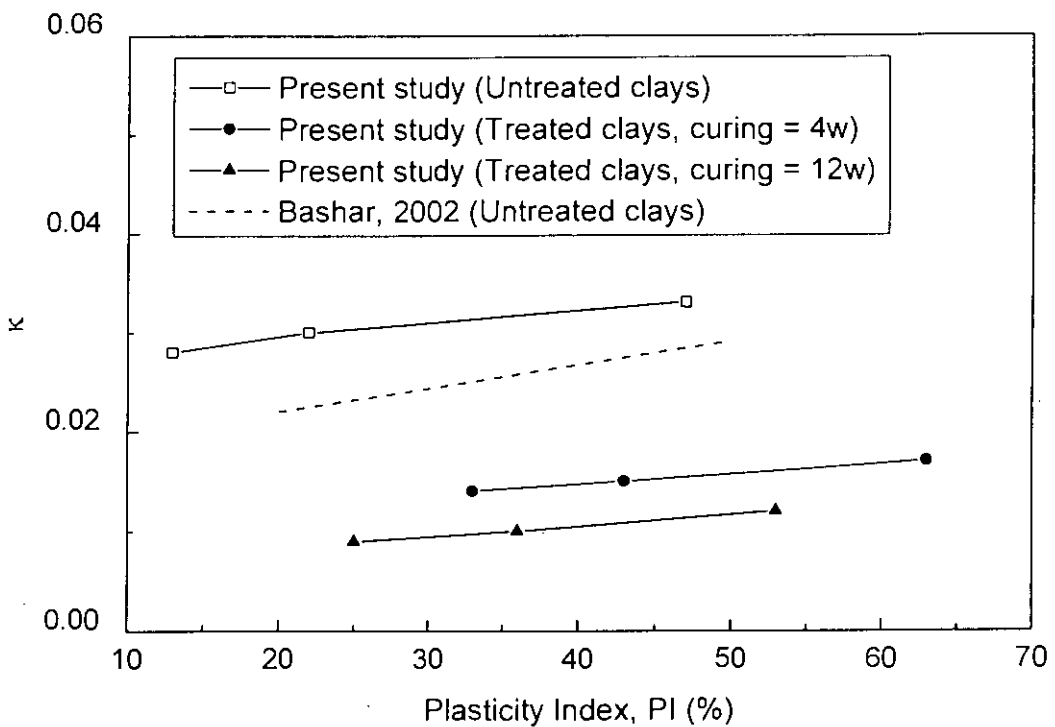


Fig. 6.15 Effect of Curing Time (cement = 12%) on Correlation between Critical Swelling Index ( $\kappa$ ) and Plasticity Index (PI)

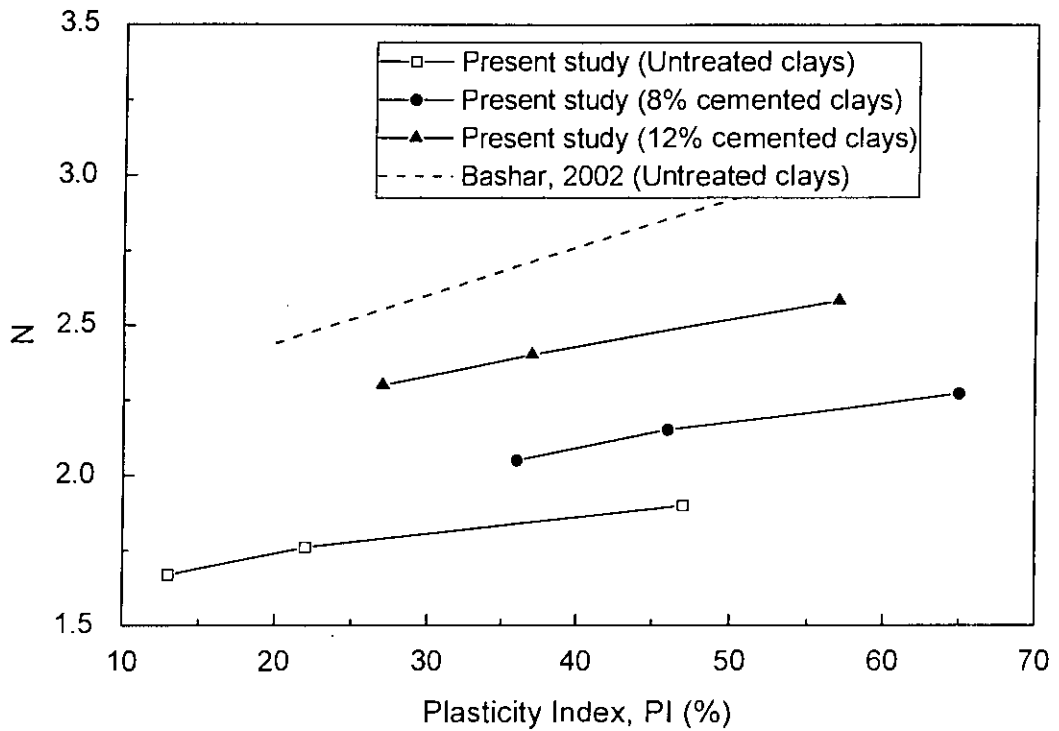


Fig. 6.16 Effect of Cement (curing = 4 w) on Correlation between Critical Specific Volume (N) and Plasticity Index (PI)

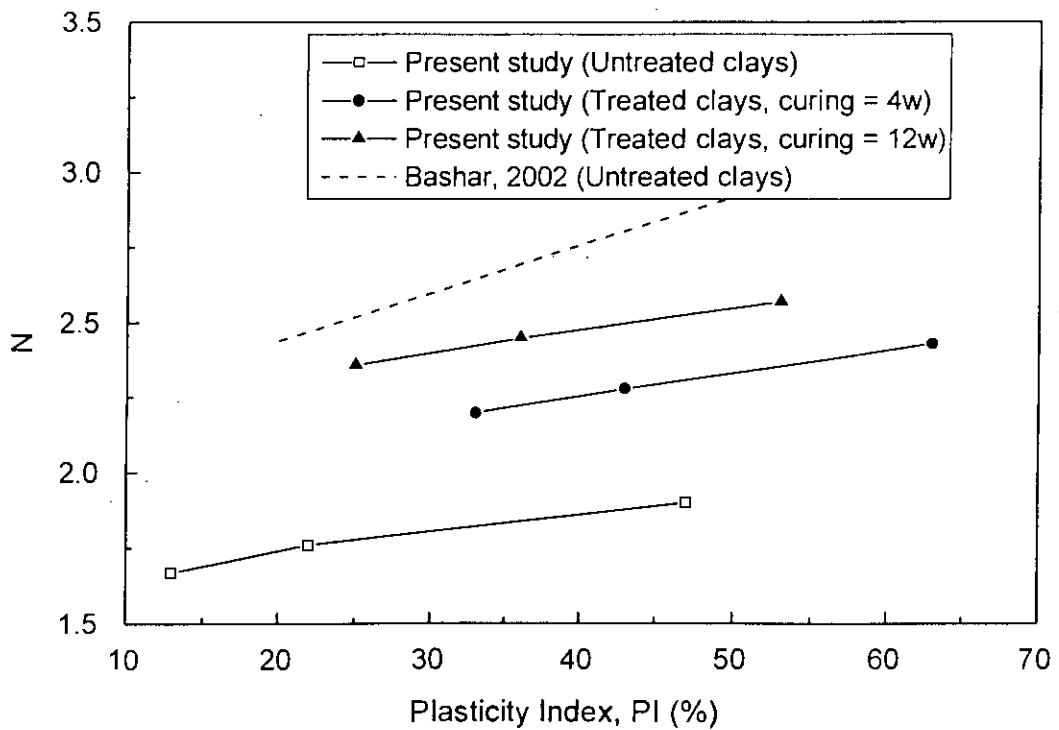


Fig. 6.17 Effect of Curing Time (cement = 12%) on Correlation between Critical Specific Volume (N) and Plasticity Index (PI)

Table 6.2 MCC, MMCC and EMMCC Model Parameters of C1 Clay for Drained Test

Parameters for models	Untreated clays	Cement treated clays ( $w_i = 120\%$ )		
		Curing = 4 w		Curing = 12 w
		wc/c ratio = 30	wc/c ratio = 10	wc/c ratio = 10
$\mu$	0.29	0.27	0.23	0.21
B	0	0	0	0
$\rho_m$	0	60	80	90
$\lambda$	0.370	0.331	0.181	0.161
$\kappa$	0.033	0.034	0.017	0.012
M	0.98	1.35	2.13	2.18
N	1.90	1.87	2.48	2.57
$p_{co}$	70	381	510	534
$p_{to}$	0	110	197	260

**Note:**

1. The same input values  $\mu$ , B,  $\lambda$ ,  $\kappa$ , M, N and  $p_{co}$  for each MCC, MMCC and EMMCC models are same for any cement treated clays.
2. The same input values and  $p_{to}$  for each MMCC and EMMCC models are same for any cement treated clays but values  $p_{to}$  for MCC model are considered zero.
3. The input values  $\rho_m$  for EMMCC model are used only but values  $\rho_m$  for MCC and MMCC models are considered zero.



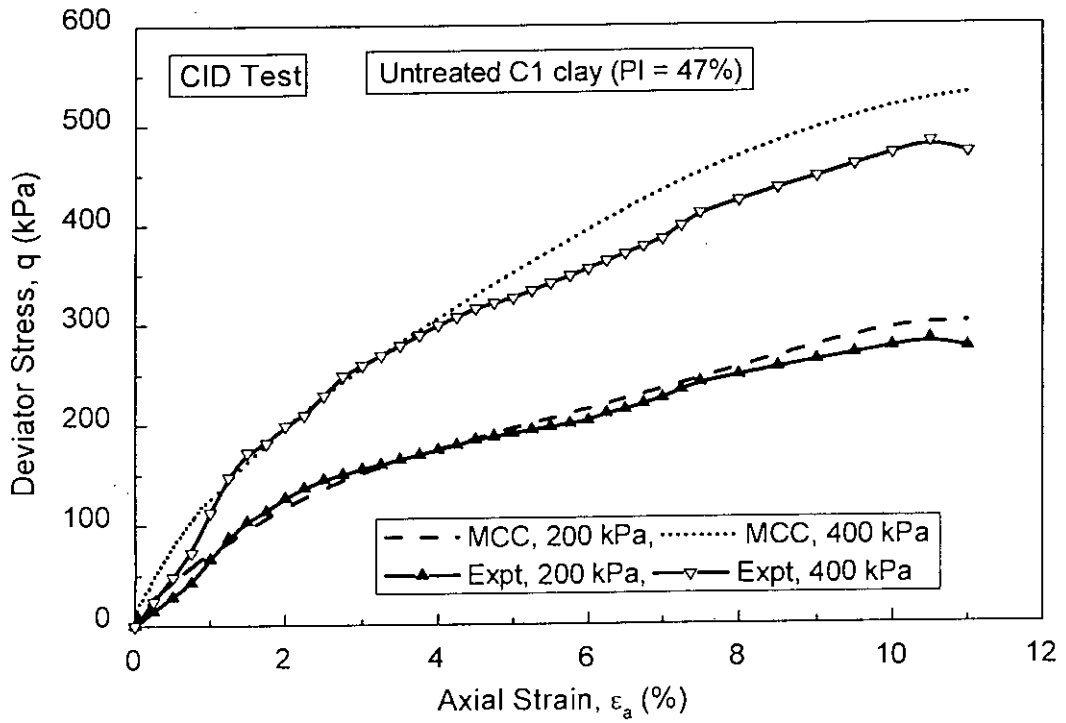
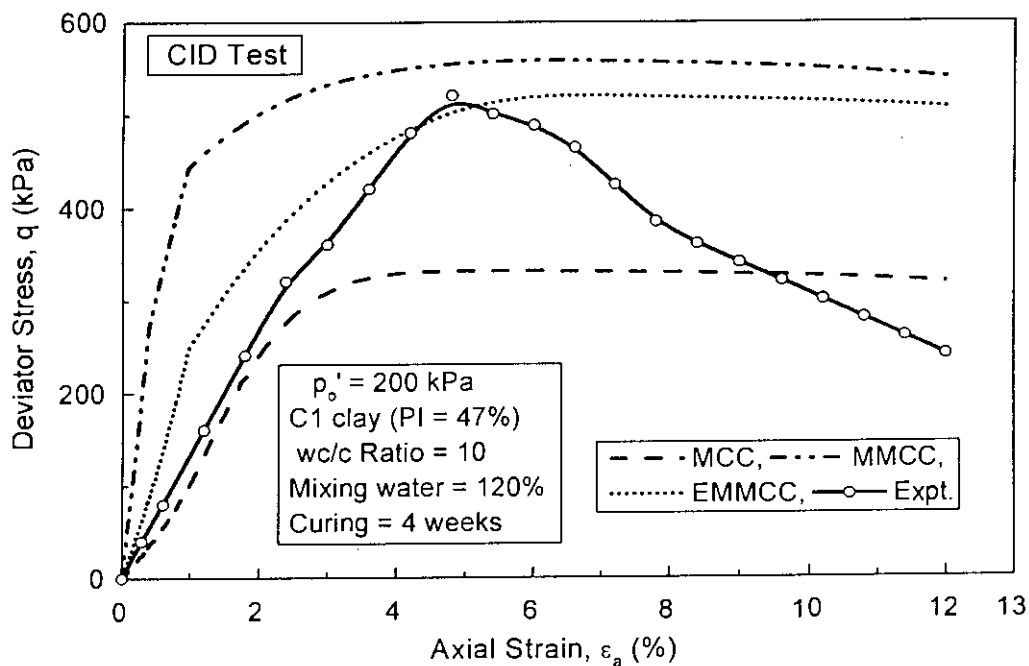
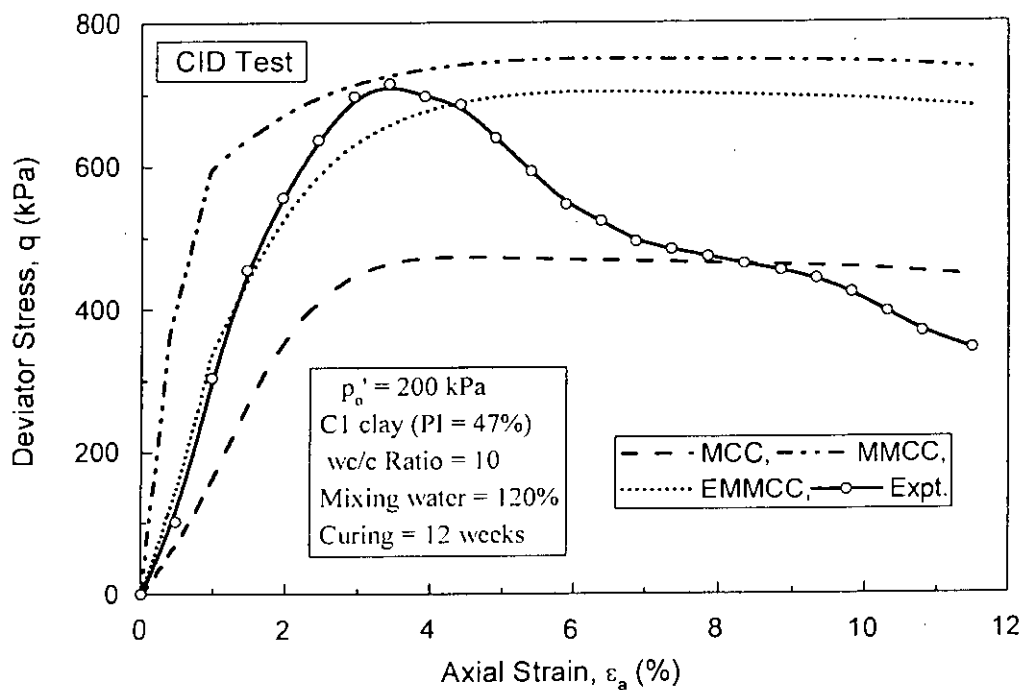


Fig. 6.18 Comparison of MCC Prediction and Observed Deviator Stress-Axial Curves in CID Test for Untreated Base C1 clay

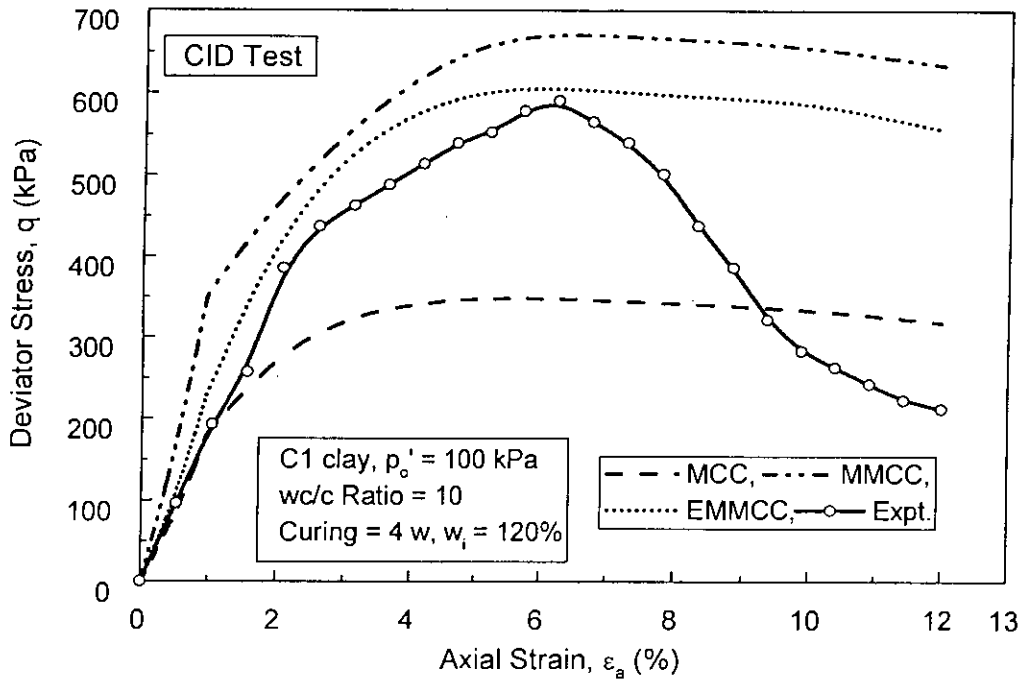


(a)

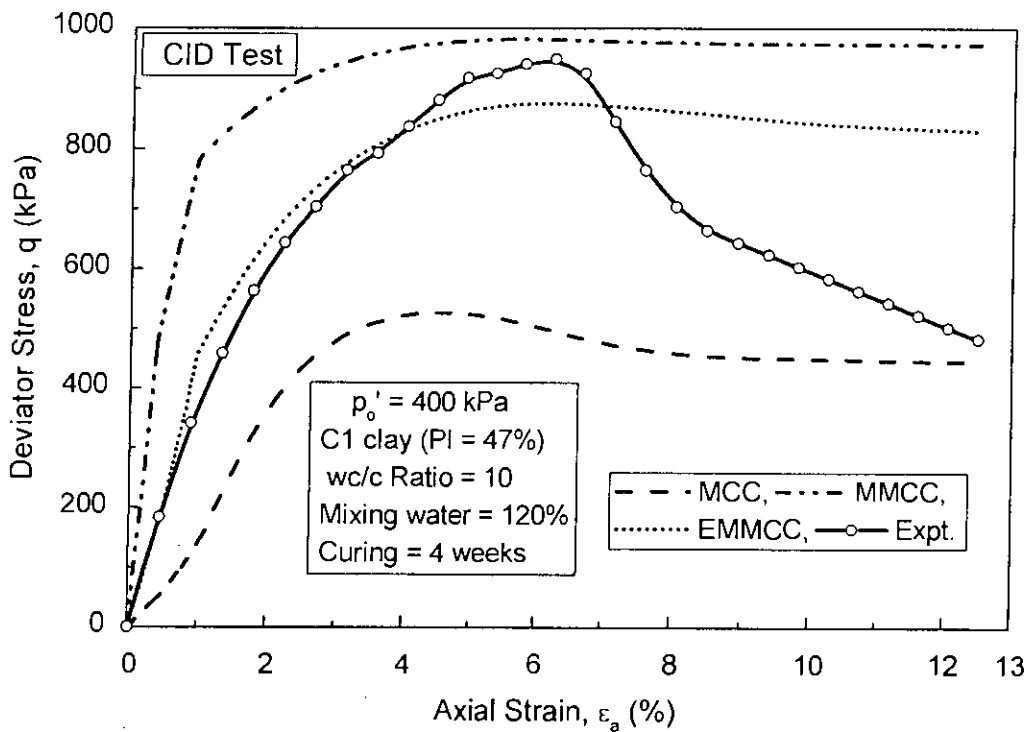


(b)

Fig. 6.19 Comparison of MCC, MMCC and EMMCC Predictions and Observed Deviator Stress-Axial Curves in CID Test for Cement Treated C1 clay (a) 4 w Curing and (b) 12 w Curing

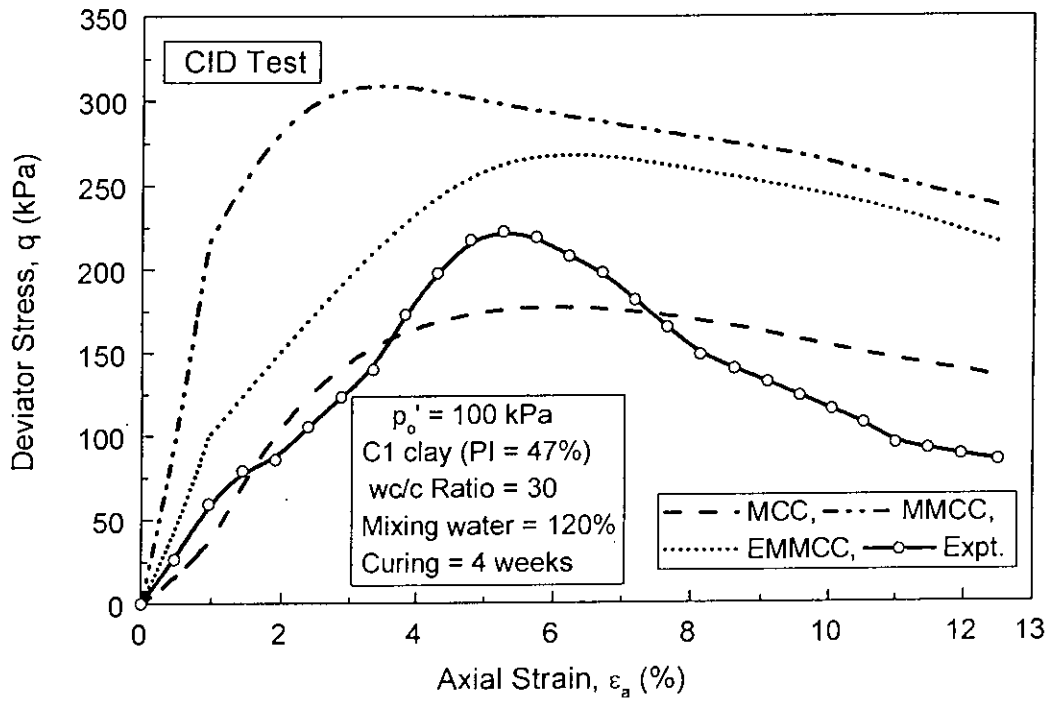


(a)

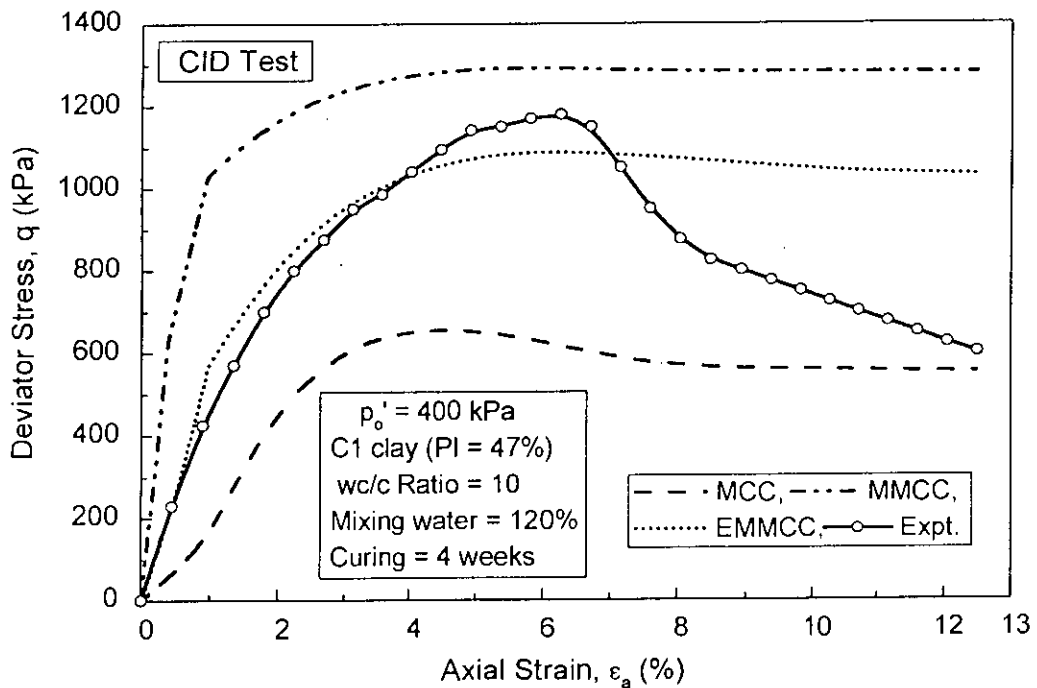


(b)

Fig. 6.20 Comparison of MCC, MMCC and EMMCC Predictions and Observed Deviator Stress-Axial Curves in CID Test for Treated C1 clay ( $w/c = 10$ ) (a)  $p'_o = 100$  kPa and (b)  $p'_o = 400$  kPa



(a)



(b)

Fig. 6.21 Comparison of MCC, MMCC and EMMCC Predictions and Observed Deviator Stress-Axial Curves in CID Test for Treated C1 clay (wc/c = 30) (a)  $p'_o = 100$  kPa and (b)  $p'_o = 400$  kPa

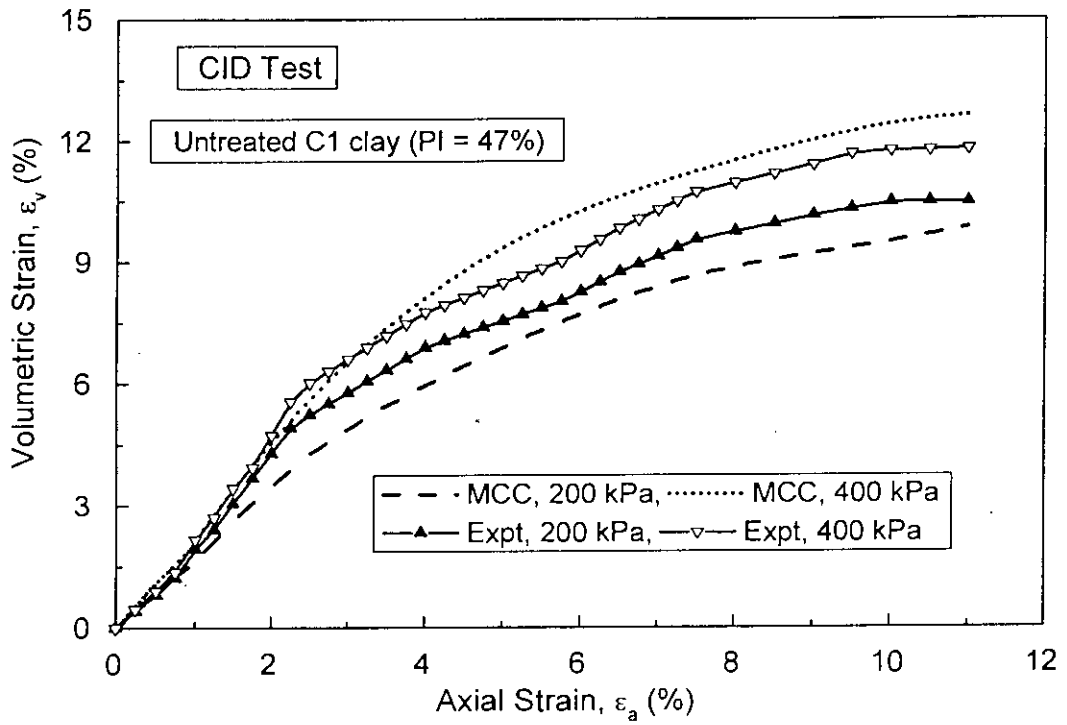
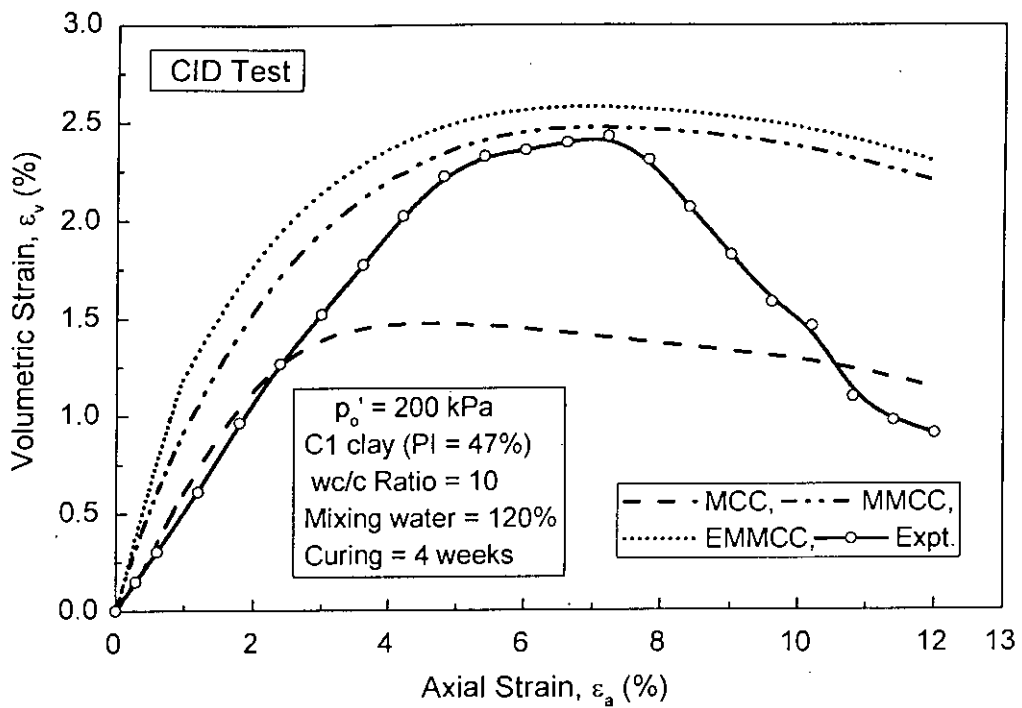
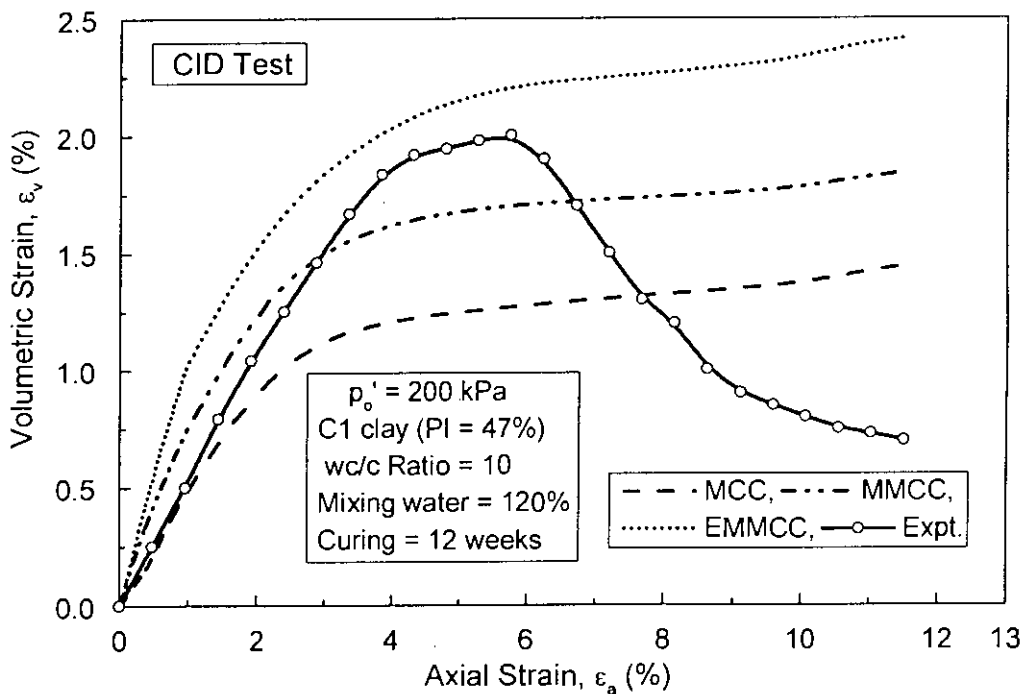


Fig. 6.22 Comparison of MCC Prediction and Observed Volumetric Strain-Axial Curves in CID Test for Untreated Base C1 clay

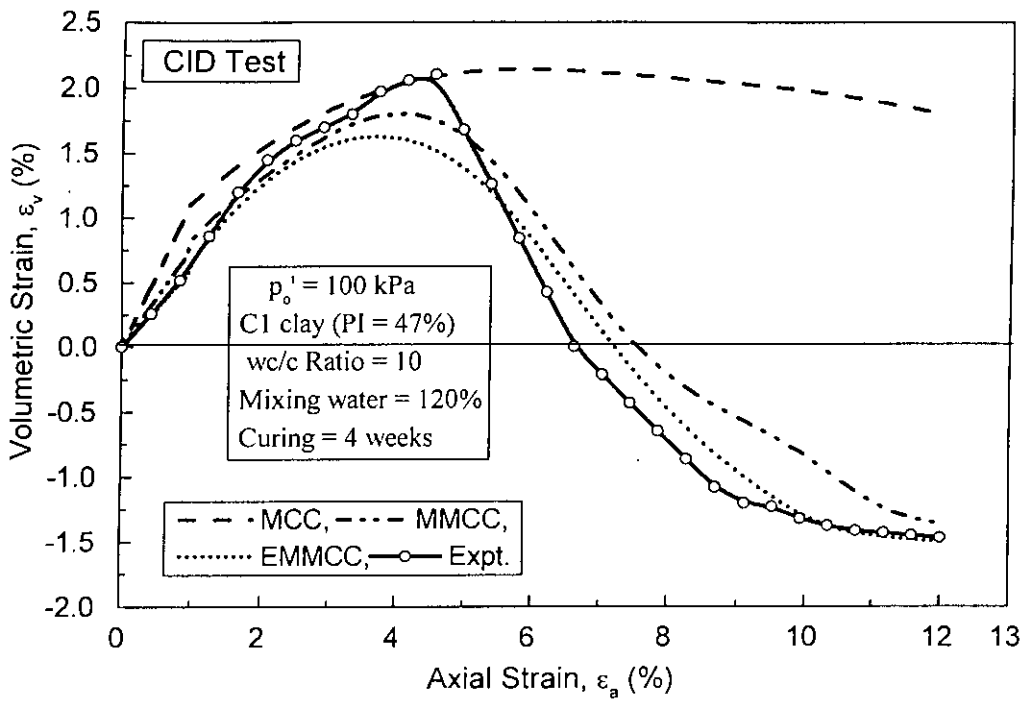


(a)

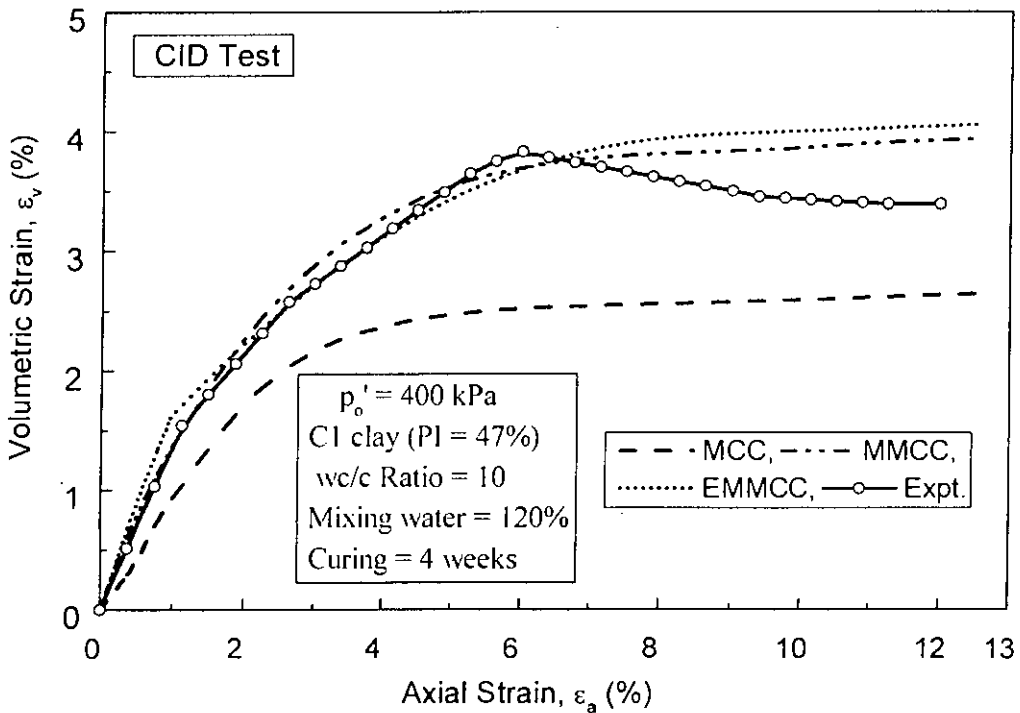


(b)

Fig. 6.23 Comparison of MCC, MMCC and EMMCC Predictions and Observed Volumetric Strain -Axial Curves in CID Test for Cement Treated C1 clay (a) 4 w Curing and (b) 12 w Curing

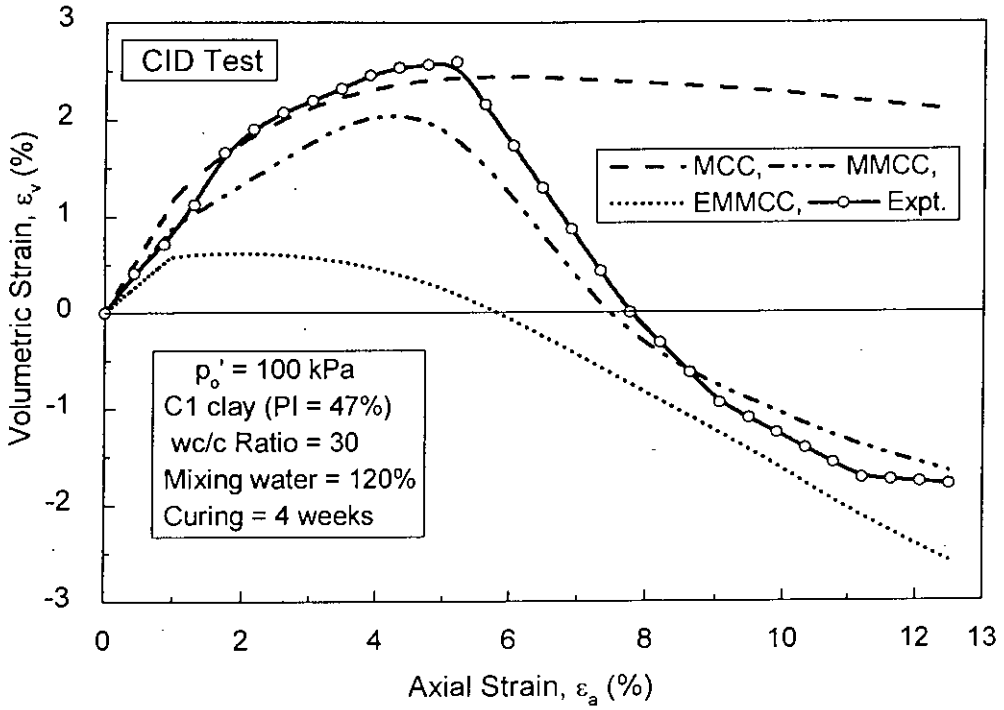


(a)

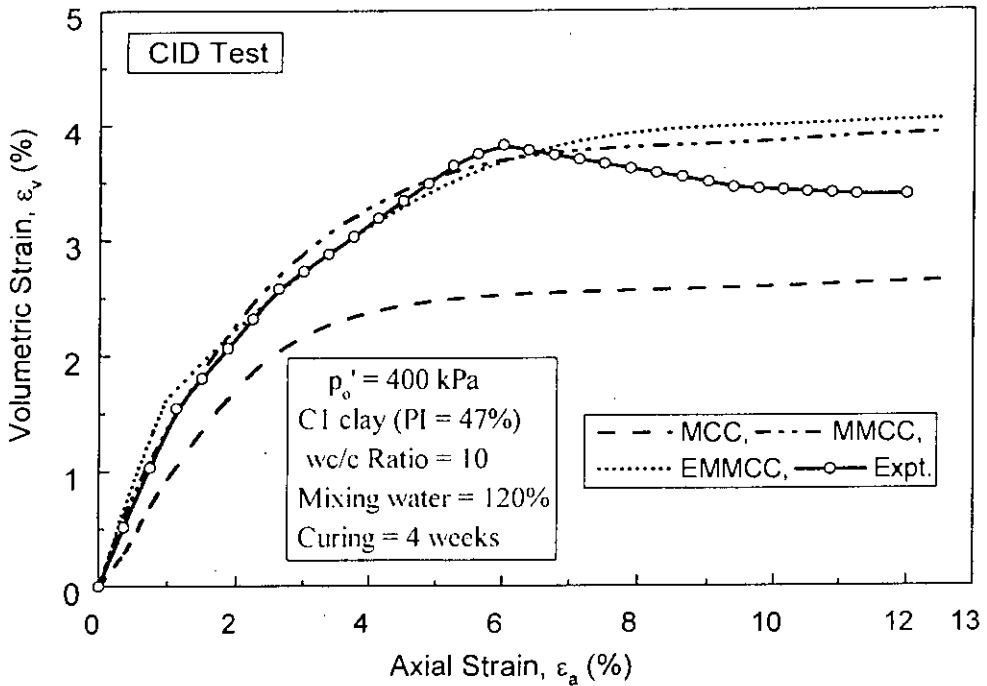


(b)

Fig. 6.24 Comparison of MCC, MMCC and EMMCC Predictions and Observed Volumetric Strain-Axial Curves in CID for Treated C1 clay (wc/c = 10) (a)  $p'_o = 100$  kPa and (b)  $p'_o = 400$  kPa



(a)



(b)

Fig. 6.25 Comparison of MCC, MMCC and EMMCC Predictions and Observed Volumetric Strain-Axial Curves in CID for Treated C1 clay (wc/c = 30) (a)  $p'_o = 100$  kPa and (b)  $p'_o = 400$  kPa



**Table 6.3 MCC, MMCC and EMMCC Model Parameters of C1 Clay for Undrained Test**

Parameters for models	Untreated clays	Cement treated clays ( $w_i = 120\%$ )		
		Curing = 4 w		Curing = 12 w
		wc/c ratio = 30	wc/c ratio = 10	wc/c ratio = 10
$\mu$	0.50	0.48	0.44	0.42
B	1	10	30	40
$\rho_m$	0	55	75	85
$\lambda$	0.370	0.331	0.181	0.161
$\kappa$	0.033	0.034	0.017	0.012
M	0.98	1.35	2.13	2.18
N	1.90	1.87	2.48	2.57
$p_{co}$	70	381	510	534
$p_w$	0	110	197	260

**Note:**

1. The same input values  $\mu$ , B,  $\lambda$ ,  $\kappa$ , M, N and  $p_{co}$  for each MCC, MMCC and EMMCC models are same for any cement treated clays.
2. The same input values and  $p_m$  for each MMCC and EMMCC models are same for any cement treated clays but values  $p_w$  for MCC model are considered zero.
3. The input values  $\rho_m$  for EMMCC model are used only but values  $\rho_m$  for MCC and MMCC models are considered zero.
4. The input values  $\mu$ , B and  $\rho_m$  are different for drained and undrained tests but all others values are same for each MCC, MMCC and EMMCC models for any cement treated clays.

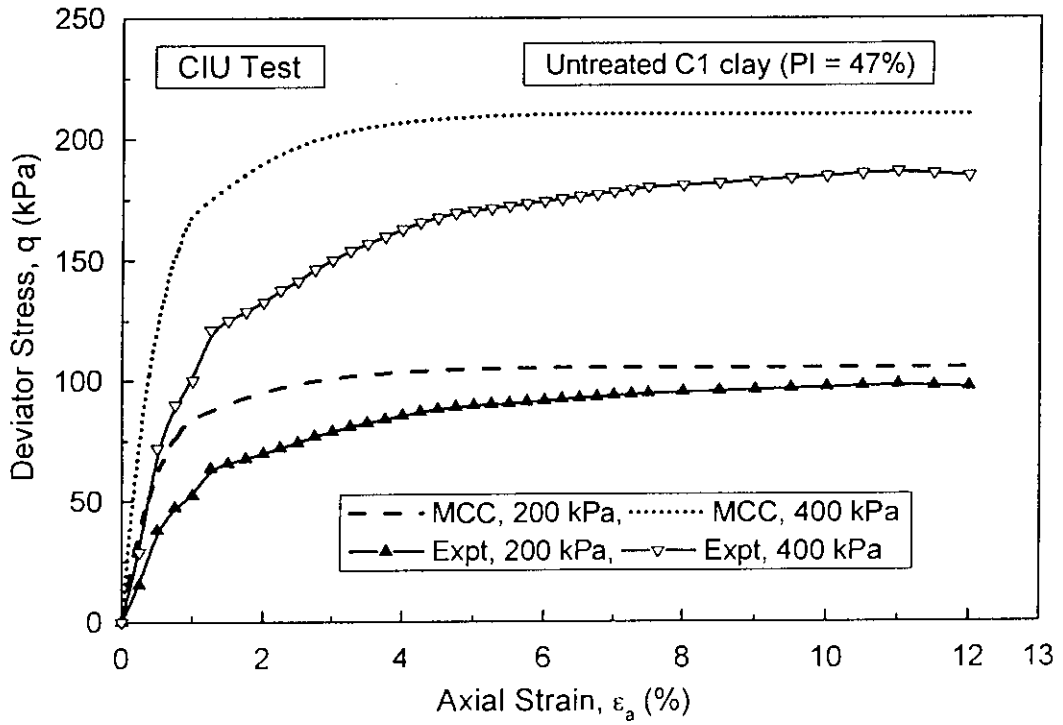
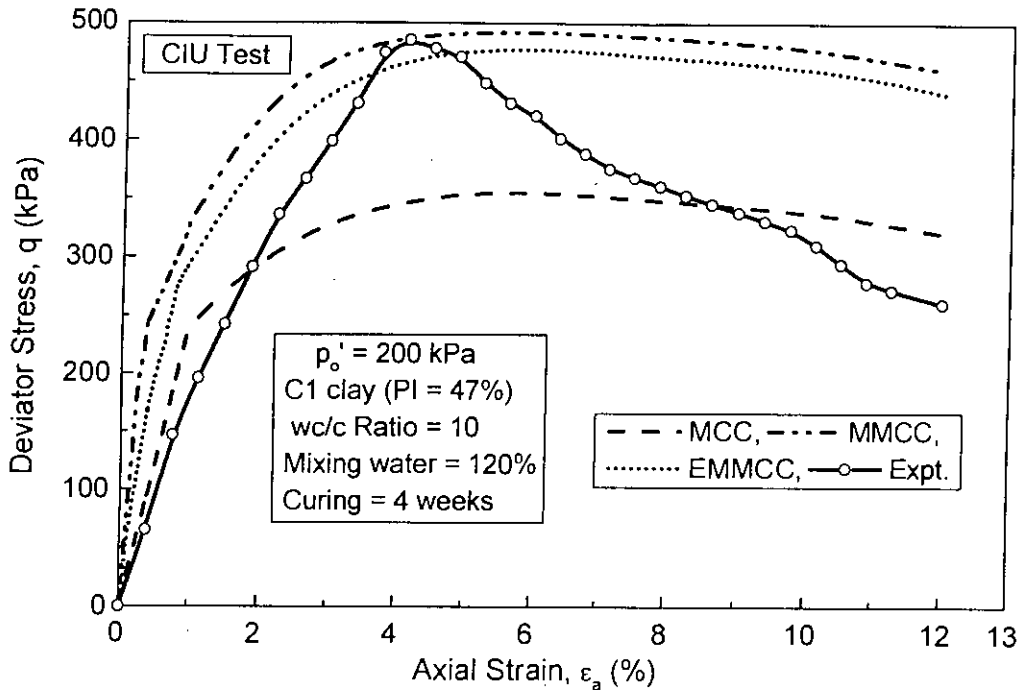
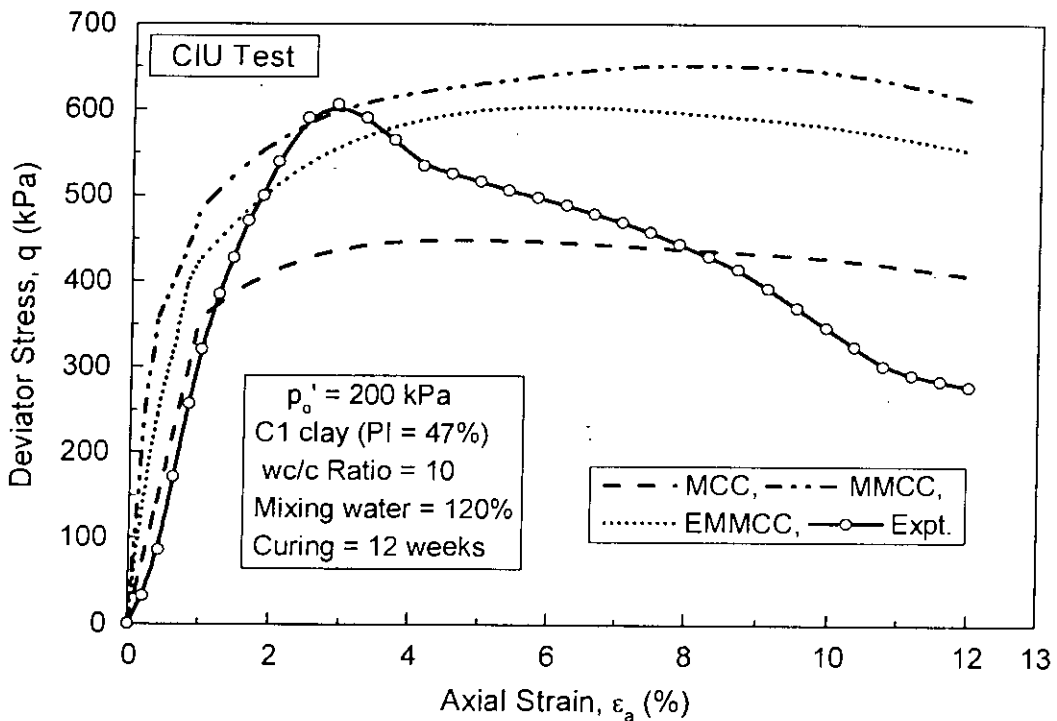


Fig. 6.26 Comparison of MCC Prediction and Observed Deviator Stress-Axial Curves in CIU Test for Untreated Base C1 clay

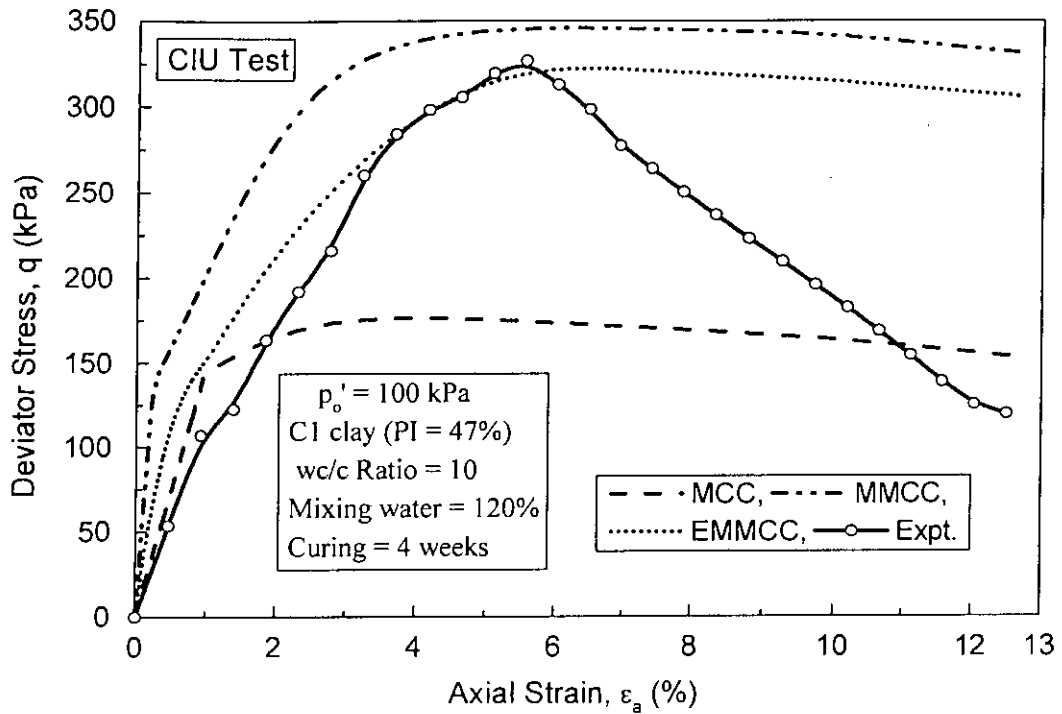


(a)

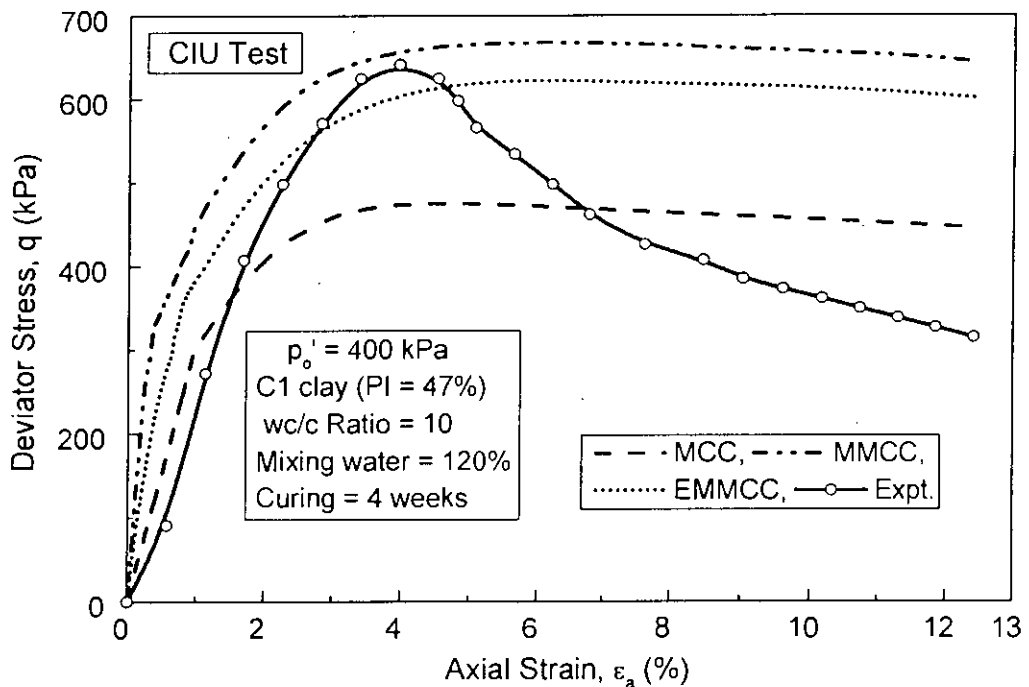


(b)

Fig. 6.27 Comparison of MCC, MMCC and EMMCC Predictions and Observed Deviator Stress-Axial Curves in CIU Test for Cement Treated C1 clay (a) 4 w Curing and (b) 12 w Curing

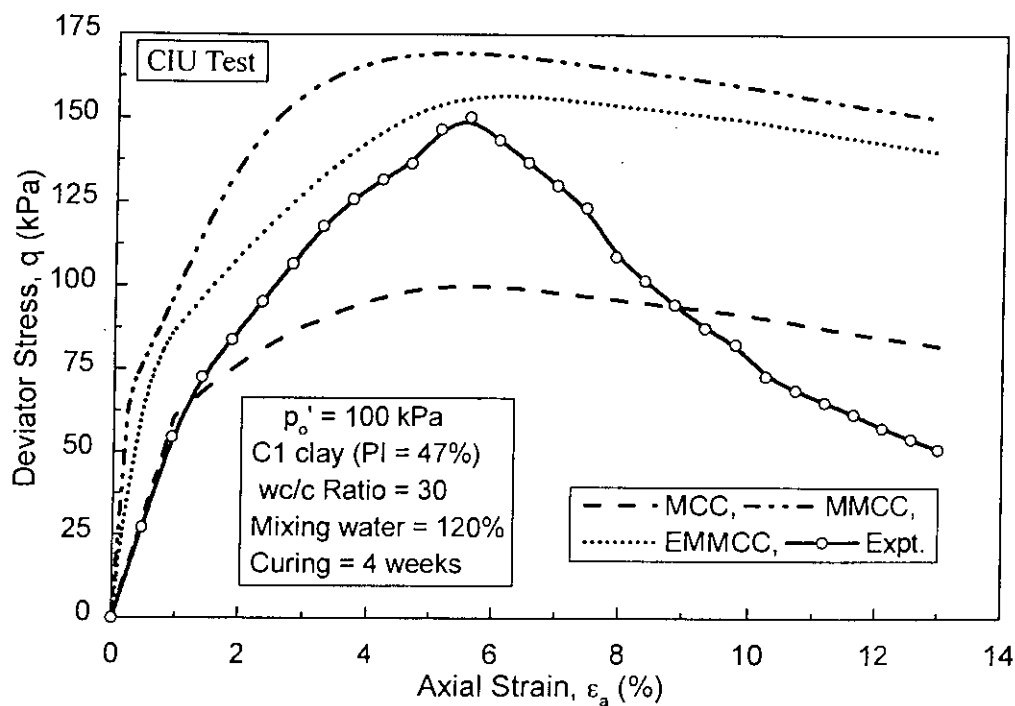


(a)

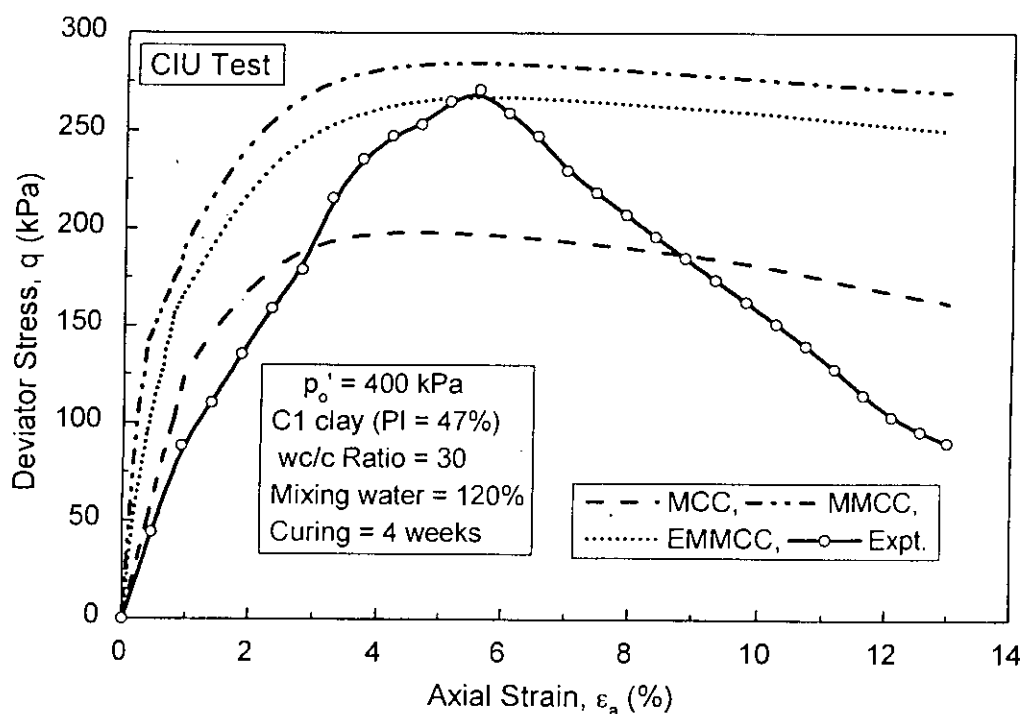


(b)

Fig. 6.28 Comparison of MCC, MMCC and EMMCC Predictions and Observed Deviator Stress-Axial Curves in CIU Test for Treated C1 clay (wc/c = 10) (a)  $p'_o = 100$  kPa and (b)  $p'_o = 400$  kPa



(a)



(b)

Fig. 6.29 Comparison of MCC, MMCC and EMMCC Predictions and Observed Deviator Stress-Axial Curves in CIU Test for Treated C1 clay (wc/c = 30) (a)  $p'_o = 100$  kPa and (b)  $p'_o = 400$  kPa

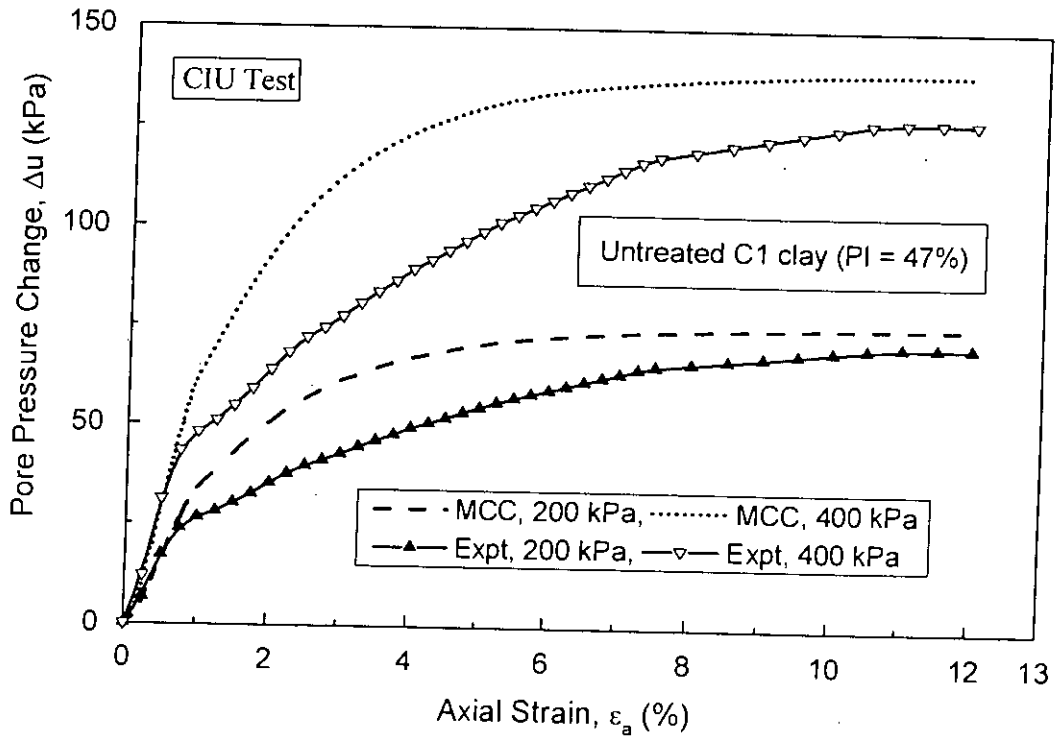
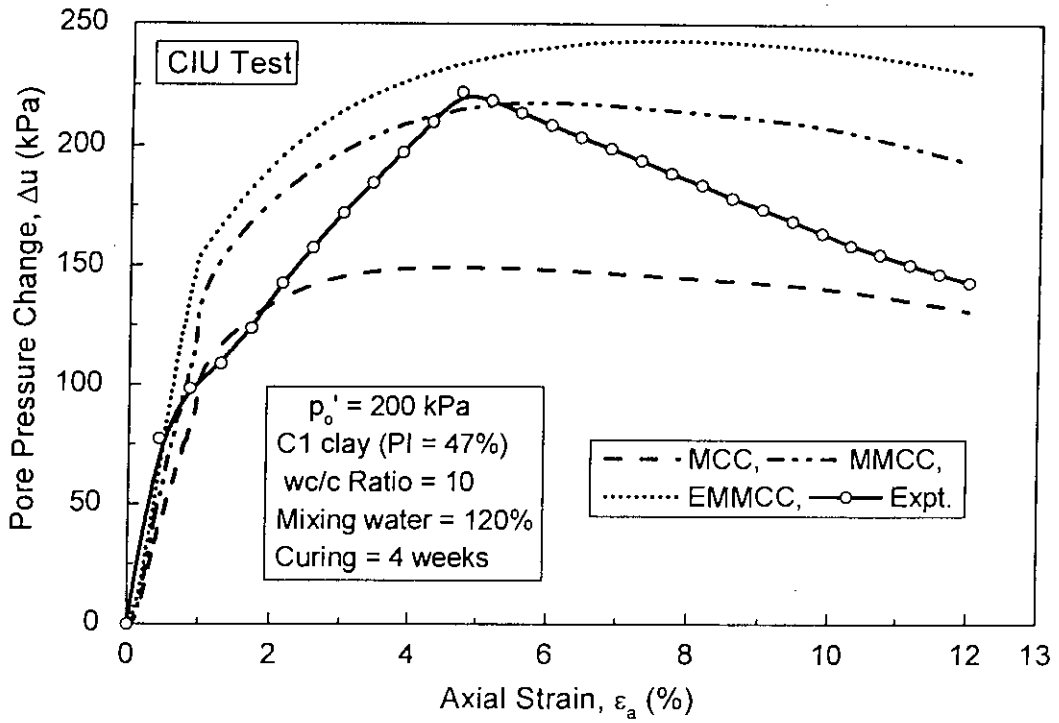
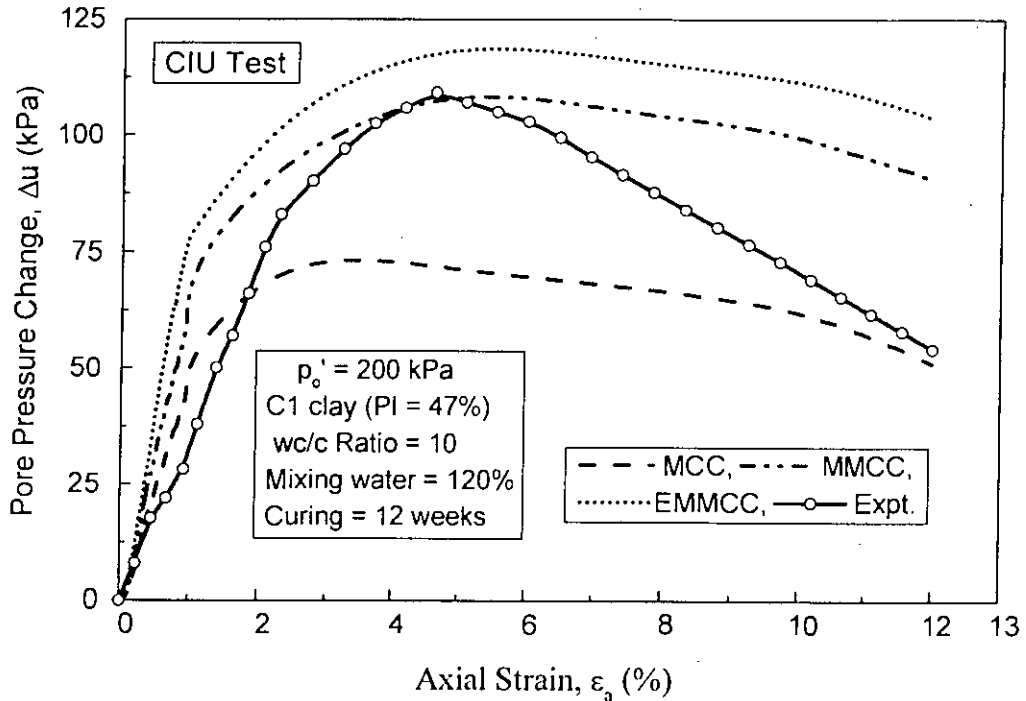


Fig. 6.30 Comparison of MCC Prediction and Observed Pore Pressure Change-Axial Curves in CIU Test for Untreated Base C1 clay

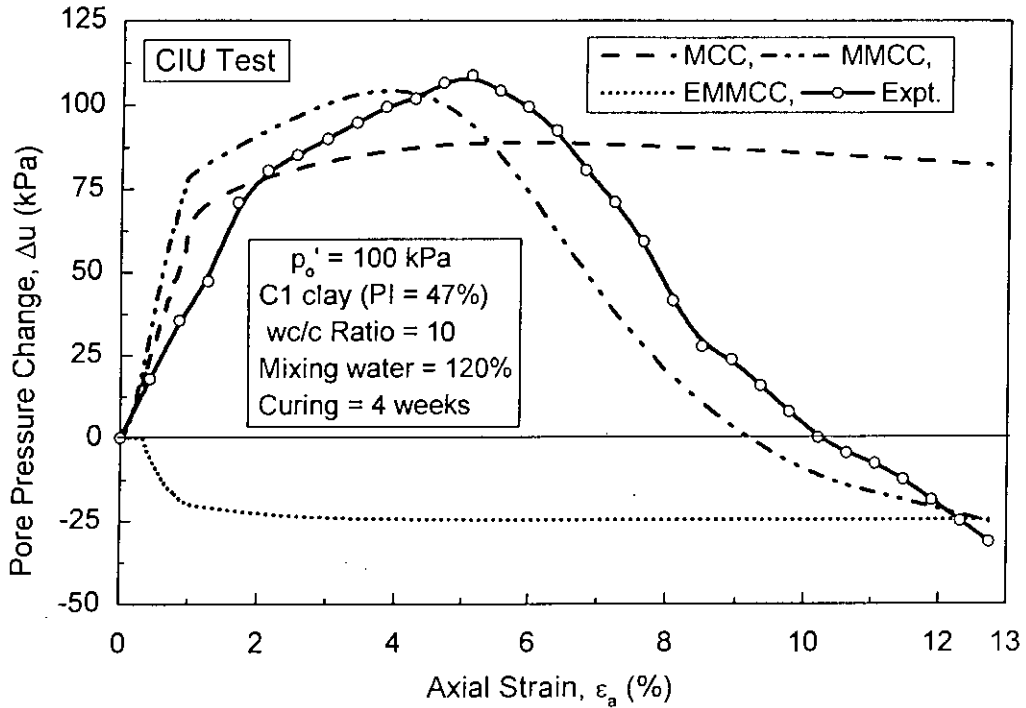


(a)

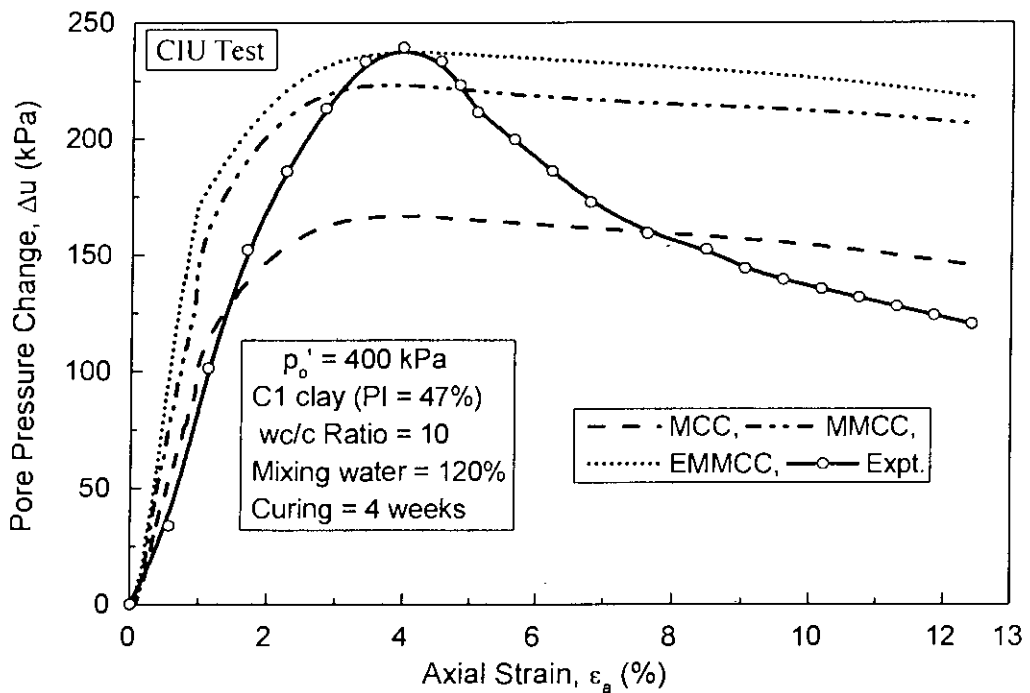


(b)

Fig. 6.31 Comparison of MCC, MMCC and EMMCC Predictions and Observed Pore Pressure Change-Axial Curves in CIU Test for Cement Treated C1 clay (a) 4 w Curing and (b) 12 w Curing



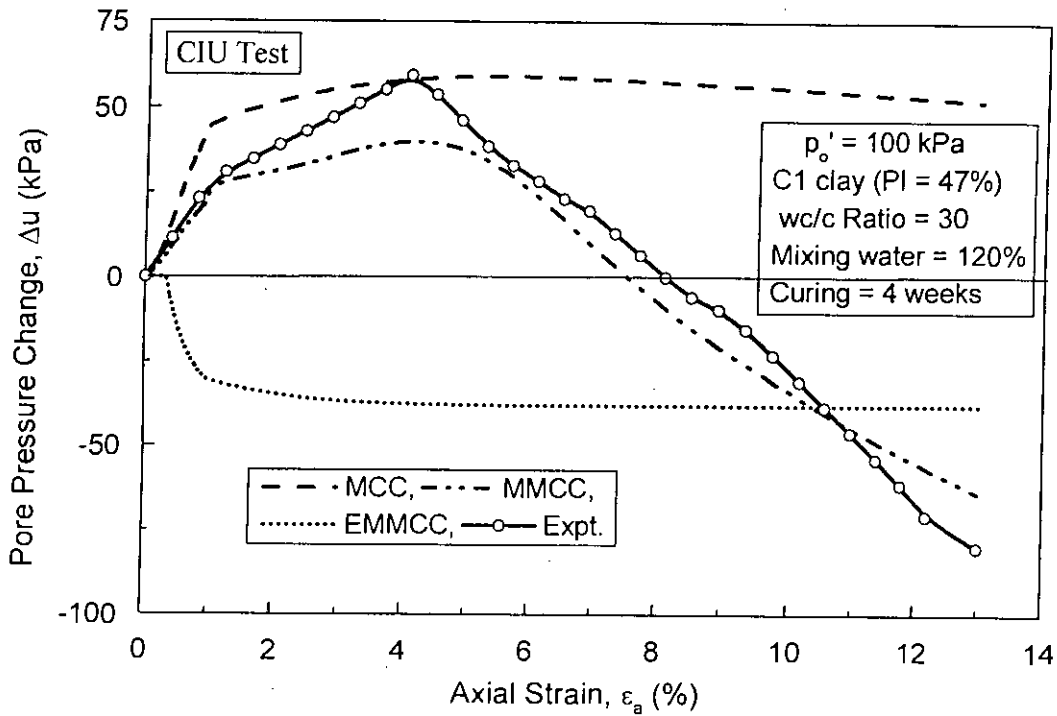
(a)



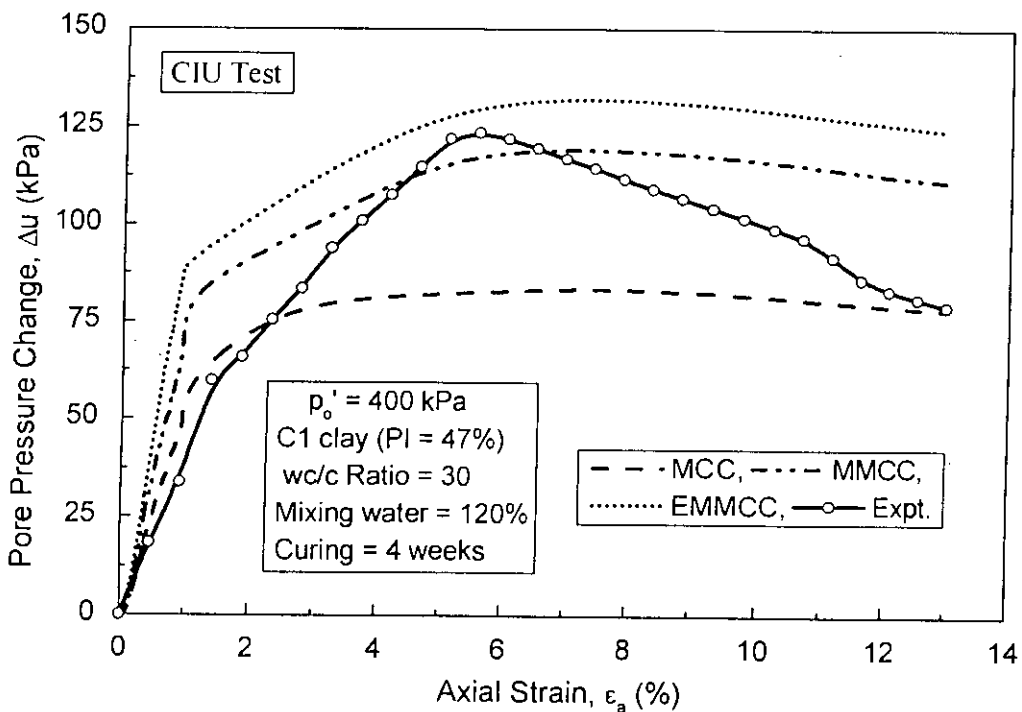
(b)

Fig. 6.32 Comparison of MCC, MMCC and EMMCC Predictions and Observed Pore Pressure Change-Axial Curves in CIU Test for Treated C1 clay (wc/c = 10) (a)  $p'_o = 100 \text{ kPa}$  and (b)  $p'_o = 400 \text{ kPa}$





(a)



(b)

Fig. 6.33 Comparison of MCC, MMCC and EMMCC Predictions and Observed Pore Pressure Change-Axial Curves in CIU Test for Treated C1 clay (wc/c = 30) (a)  $p'_o = 100 \text{ kPa}$  and (b)  $p'_o = 400 \text{ kPa}$

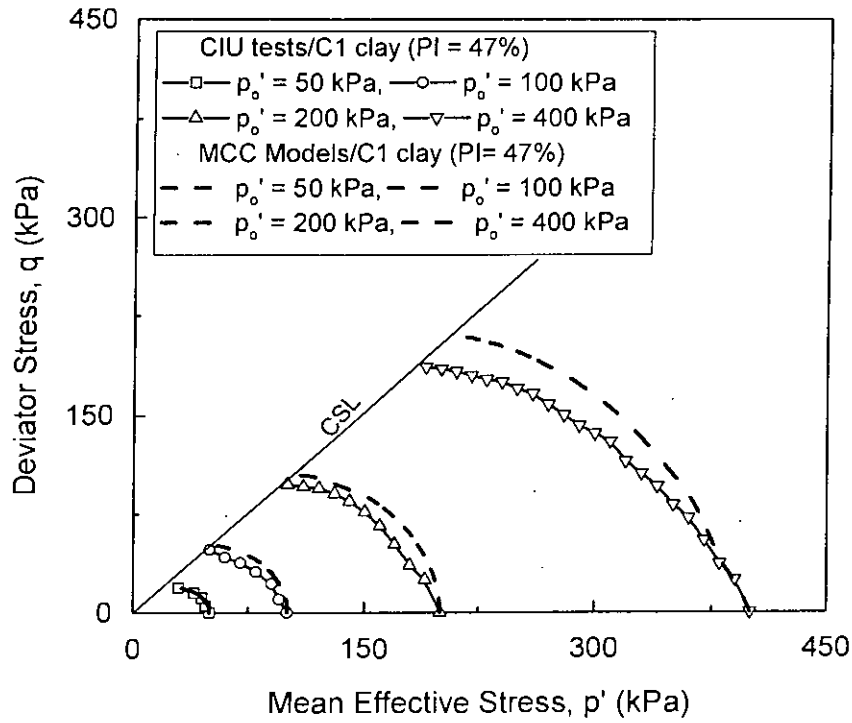


Fig. 6.34 Comparison of MCC Prediction and Observed Undrained Stress Path in CIU Test for Untreated Base C1 clay

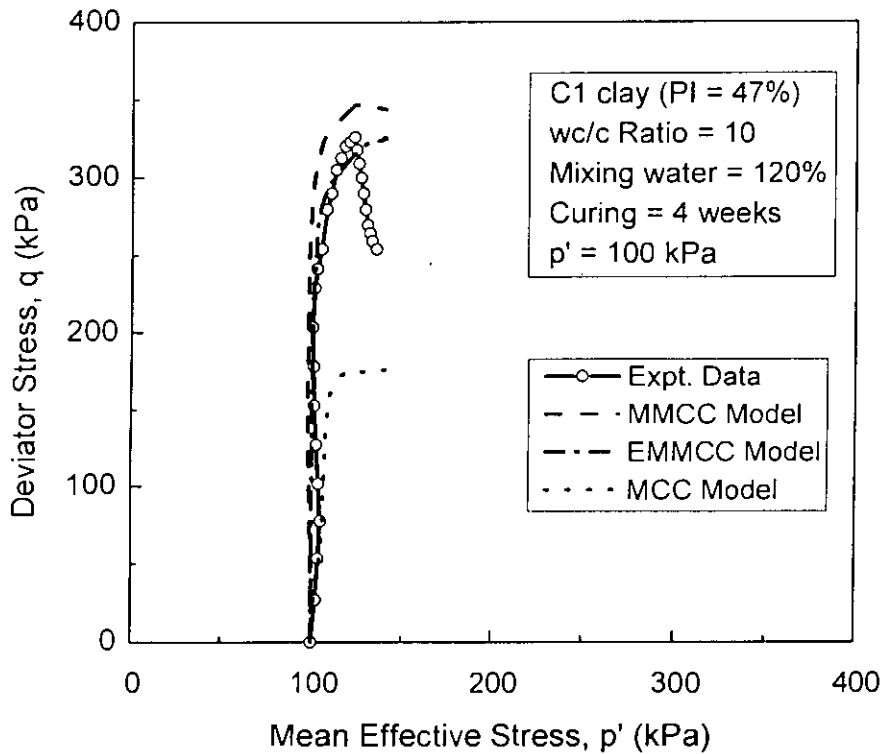


Fig. 6.35 Comparison of MCC, MMCC and EMMCC Prediction and Observed Undrained Stress Path in CIU for Cement Treated C1 clay ( $w_c/c = 10$ ) at  $p_o' = 100$  kPa

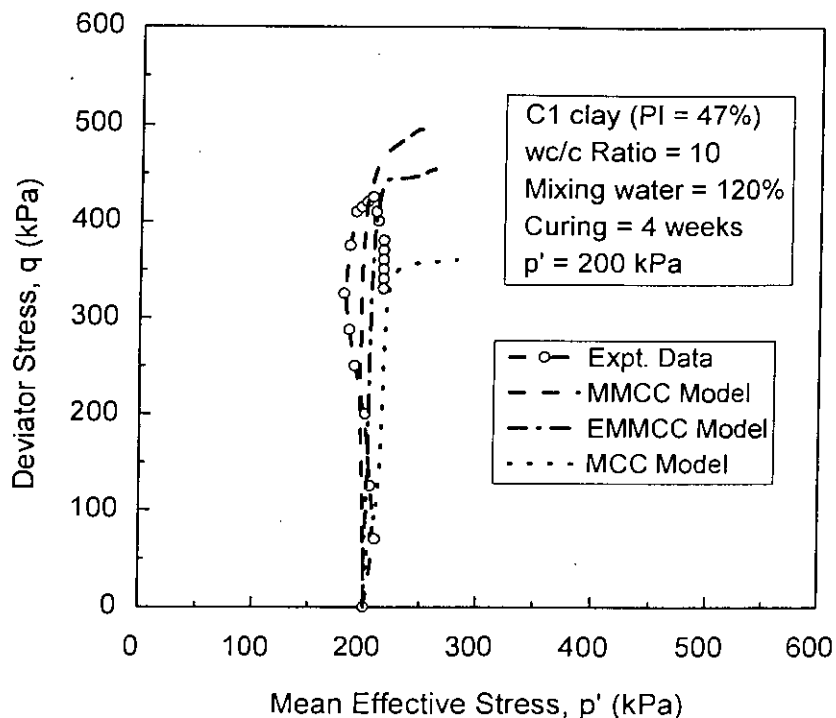


Fig. 6.36 Comparison of MCC, MMCC and EMMCC Prediction and Observed Undrained Stress Path in CIU for Cement Treated C1 clay ( $w_c/c = 10$ ) at  $p'_o = 200$  kPa

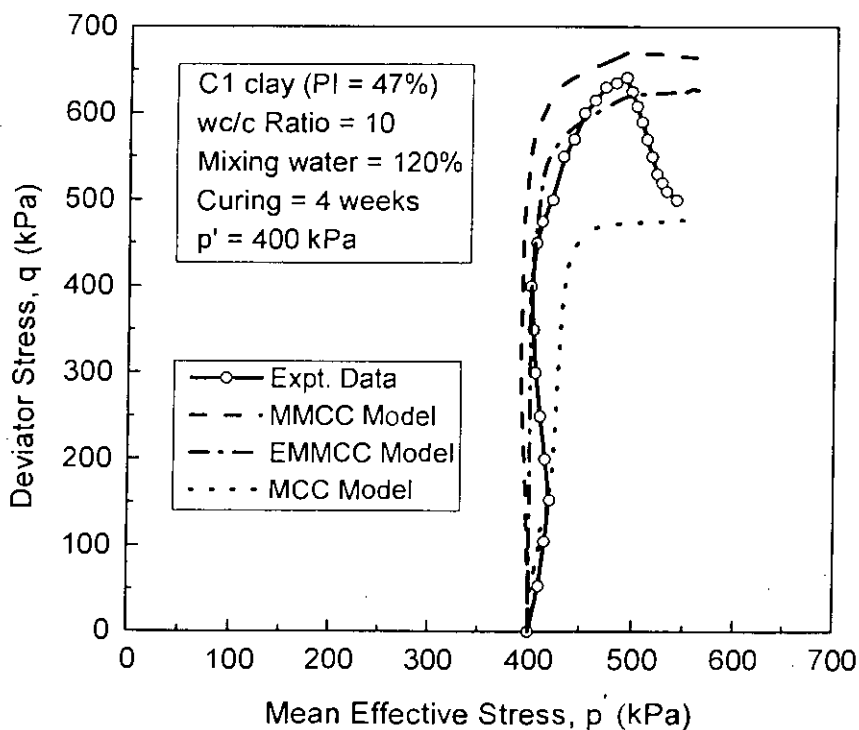


Fig. 6.37 Comparison of MCC, MMCC and EMMCC Predictions and Observed Undrained Stress Path in CIU for Cement Treated C1 clay ( $w_c/c = 10$ ) at  $p'_o = 400$  kPa

**Table 6.4 Cap Model Parameters of C1 Clay for Drained Test**

Parameters for models	Cement treated clays ( $w_i = 120\%$ )		
	Curing = 4 w		Curing = 12 w
	wc/c ratio = 10	wc/c ratio = 7.5	wc/c ratio = 10
E (MPa)	29	34	33
$\mu$	0.25	0.23	0.22
$\alpha$ (plane cap)	0.13	0.16	0.15
k (plane cap)	0.16	0.19	0.18
EL (plane cap)	0	0	0
$\alpha$ (elliptic cap)	0.17	0.22	0.20
k (elliptic cap)	0.18	0.24	0.22
EL (elliptic cap)	0.36	0.39	0.38

**Note:**

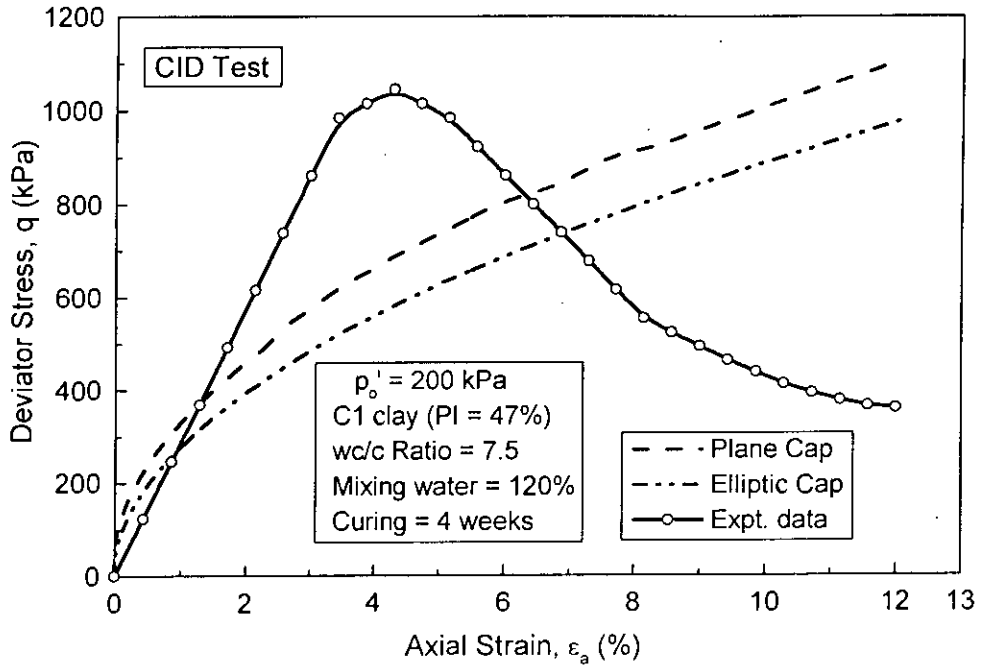
The input values for cement treated clays as follows:

1. Initial stress and strain conditions:  $\sigma_{11} = \sigma_{22} = \sigma_{33} = \sigma_{12} = 0$  and  $\epsilon_{11} = \epsilon_{22} = \epsilon_{33} = \epsilon_{12} = 0$ .
2. Cap materials constant:  $W = 0.0075$  and  $D = 1.42$ .
3. Cap location =  $XL = 0$ .
4. Tension cut-off limit = 3.
5. Material type = 3 for plane cap and = 4 for elliptic cap.
6. Shape ratio = 0 for plane cap and = 4.33 for elliptic cap.
7. Hardening surface L-type = 1 for elastic soft soil and = 2 for non-elastic stiff soil / soft rock
8. For the three-dimensional matching along the compressive meridian:

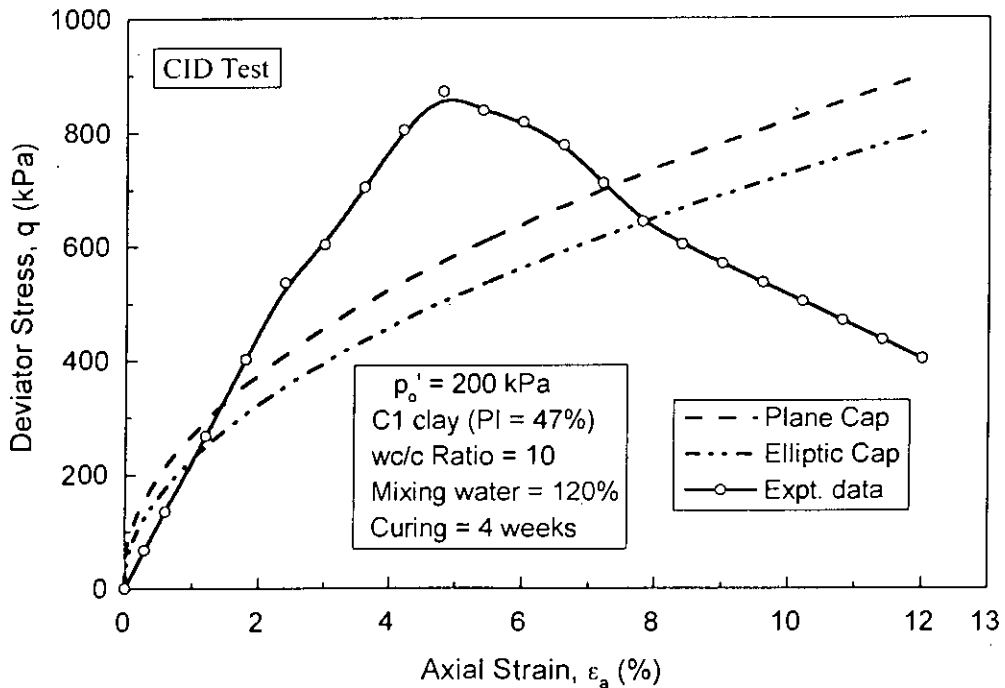
$$\alpha = \frac{2 \sin \phi}{\sqrt{3}(3 - \sin \phi)} \quad \text{and} \quad k = \frac{6c \cos \phi}{\sqrt{3}(3 - \sin \phi)}$$

9. For the plane strain matching with the same limit load:

$$\alpha = \frac{\tan \phi}{\sqrt{9 + 12 \tan^2 \phi}} \quad \text{and} \quad k = \frac{3c}{\sqrt{9 + 12 \tan^2 \phi}}$$



(a)



(b)

Fig. 6.38 Comparison of Plane Cap and Elliptic Cap Predictions and Observed Deviator Stress-Axial Strain Curves in CID Test for Treated C1 clay at Curing = 4 w (a)  $w/c = 7.5$  and (b)  $w/c = 10$

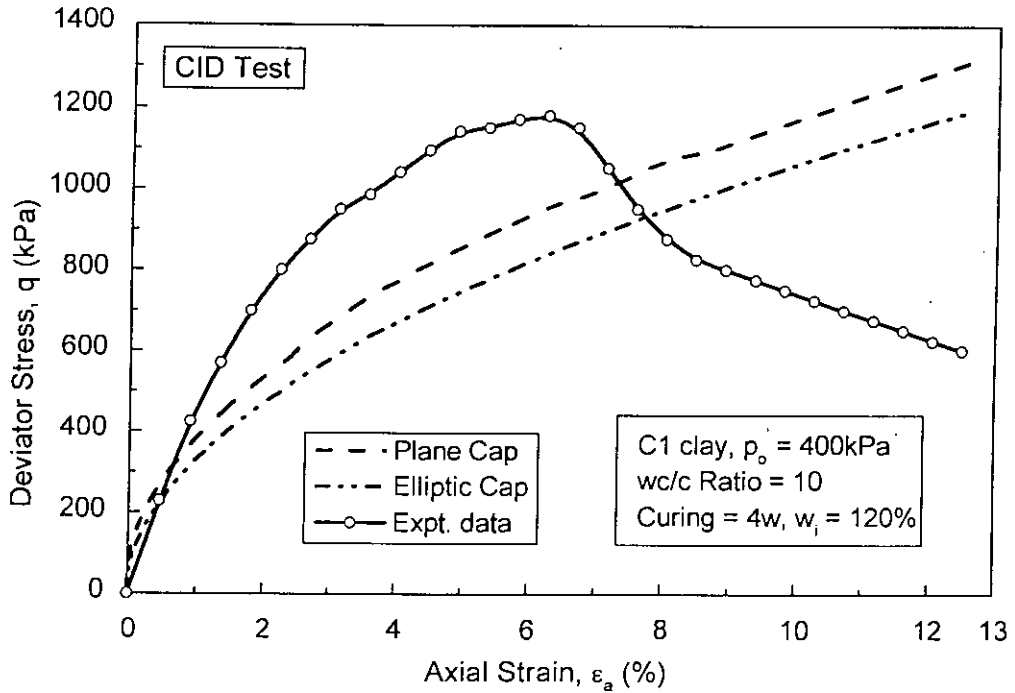


Fig. 6.39 Comparison of Plane Cap and Elliptic Cap Predictions and Observed Deviator Stress-Axial Strain Curves in CID Test for Treated C1 clay at  $p'_o = 400$  kPa,  $w/c = 10$  and Curing = 4 w

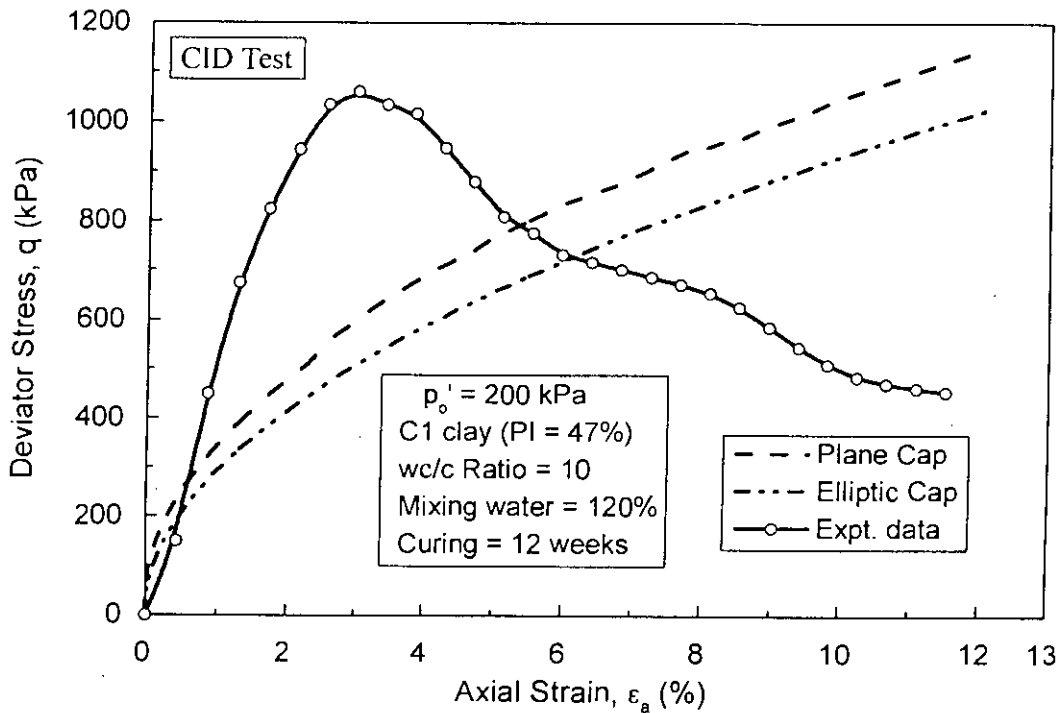
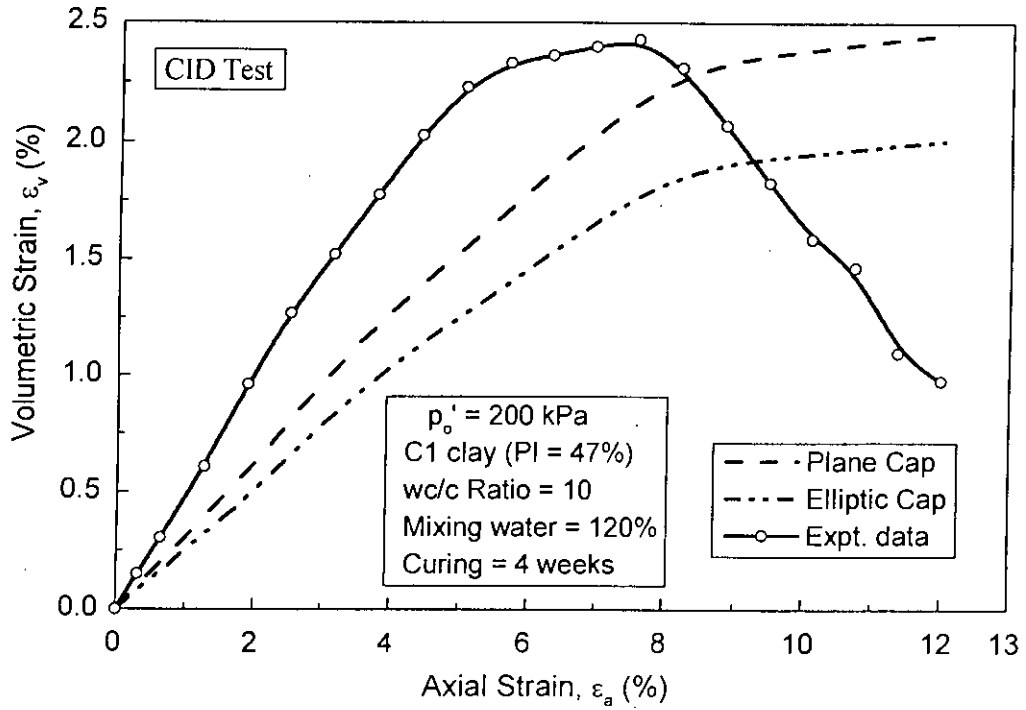
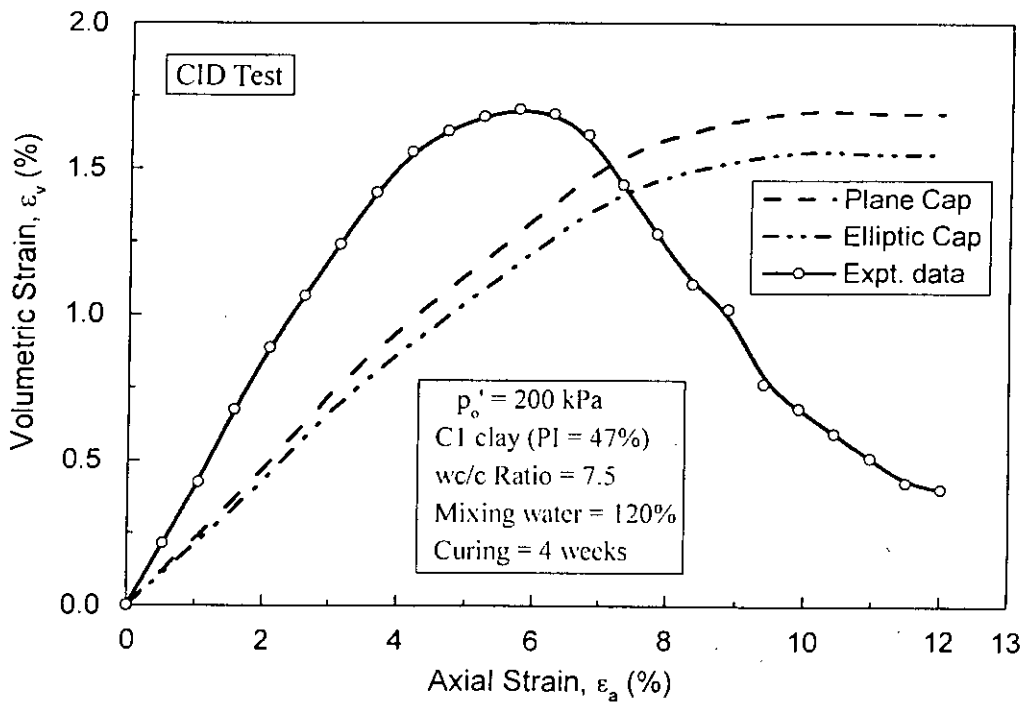


Fig. 6.40 Comparison of Plane Cap and Elliptic Cap Predictions and Observed Deviator Stress -Axial Strain Curves in CID Test for Treated C1 clay at  $p'_o = 200$  kPa,  $w/c = 10$  and Curing = 12 w



(a)



(b)

Fig. 6.41 Comparison of Plane Cap and Elliptic Cap Predictions and Observed Volumetric Strain-Axial Strain Curves in CID Test for Treated C1 clay at Curing = 4 w (a)  $w/c = 7.5$  and (b)  $w/c = 10$

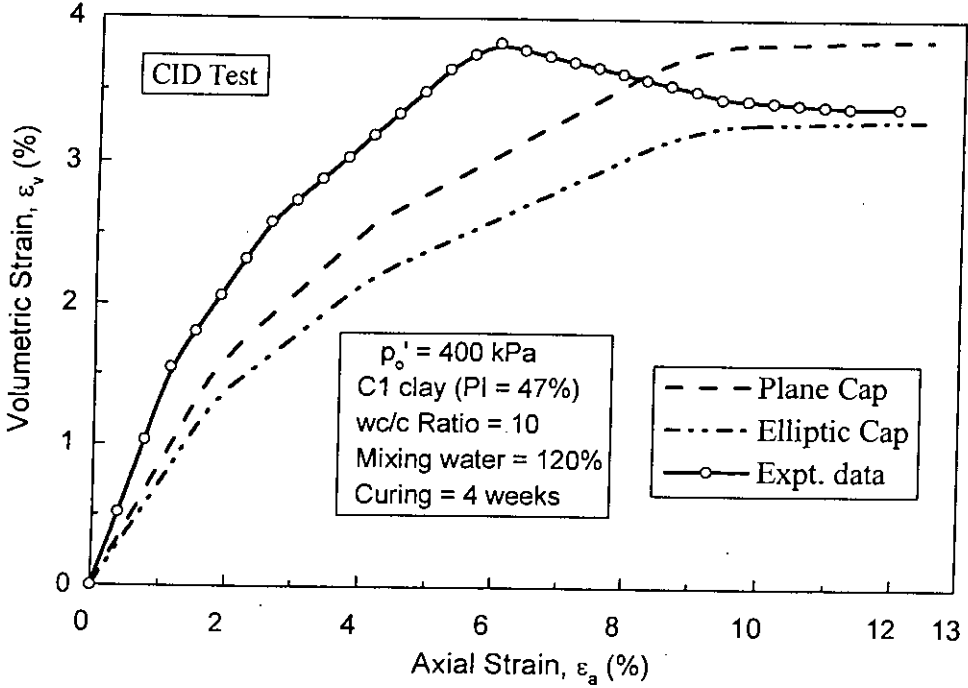


Fig. 6.42 Comparison of Plane Cap and Elliptic Cap Predictions and Observed Volumetric Strain-Axial Strain Curves in CID Test for Treated C1 clay at  $p'_0 = 400 \text{ kPa}$ ,  $wc/c = 10$  and Curing = 4 w

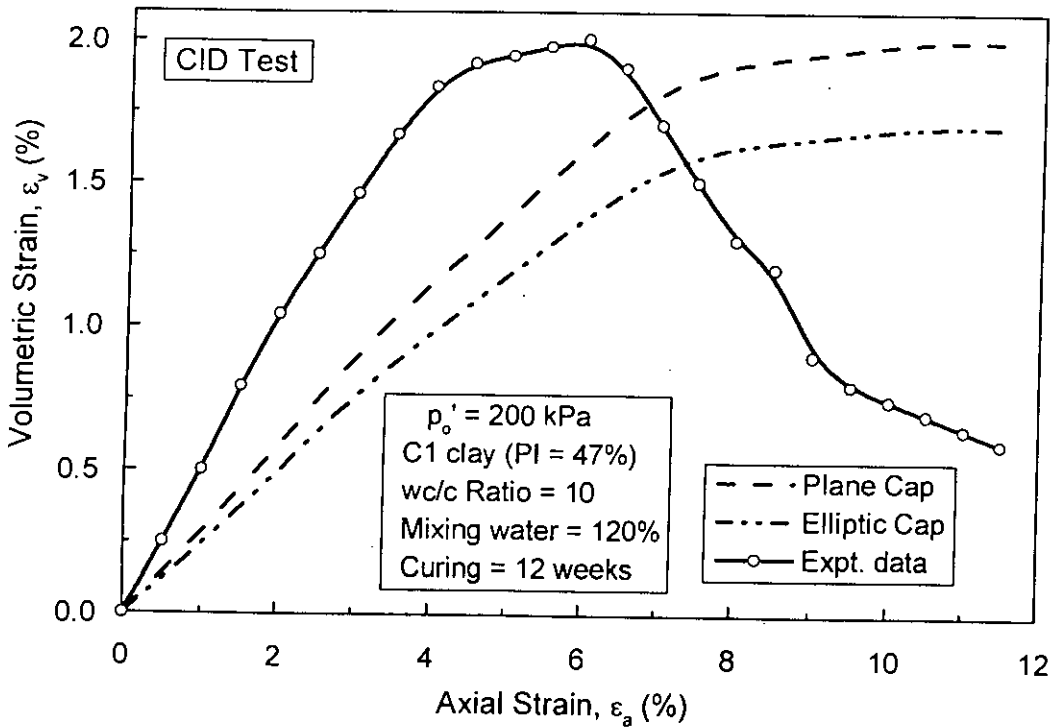


Fig. 6.43 Comparison of Plane Cap and Elliptic Cap Predictions and Observed Volumetric Strain-Axial Strain Curves in CID Test for Treated C1 clay at  $p'_0 = 200 \text{ kPa}$ ,  $wc/c = 10$  and Curing = 12 w



**Table 6.5 Cap Model Parameters of C1 Clay for Undrained Test**

Parameters for models	Cement treated clays ( $w_i = 120\%$ )		
	Curing = 4 w		Curing = 12 w
	wc/c ratio = 10	wc/c ratio = 7.5	wc/c ratio = 10
E (MPa)	27	32	30
$\mu$	0.44	0.41	0.42
$\alpha$ (plane cap)	0.13	0.16	0.15
k (plane cap)	0.16	0.19	0.18
EL (plane cap)	0	0	0
$\alpha$ (elliptic cap)	0.17	0.22	0.20
k (elliptic cap)	0.18	0.24	0.22
EL (elliptic cap)	0.36	0.39	0.38

**Note:**

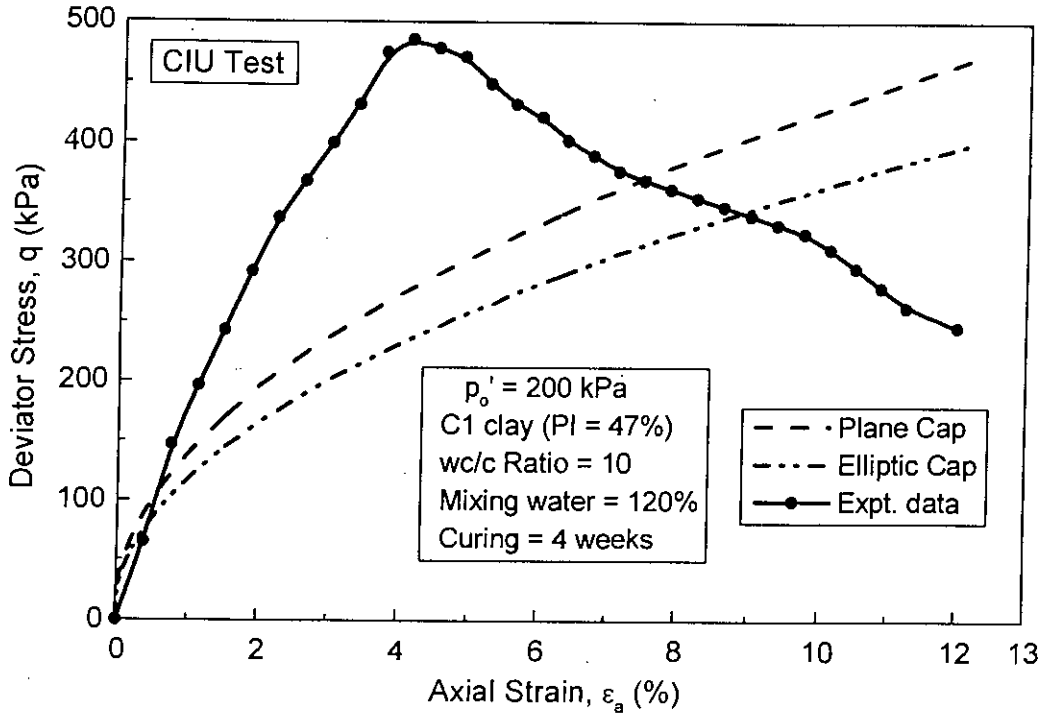
The input values for cement treated clays as follows:

1. Initial stress and strain conditions:  $\sigma_{11} = \sigma_{22} = \sigma_{33} = \sigma_{12} = 0$  and  $\epsilon_{11} = \epsilon_{22} = \epsilon_{33} = \epsilon_{12} = 0$ .
2. Cap materials constant:  $W = 0.0075$  and  $D = 1.42$ .
3. Cap location =  $XL = 0$ .
4. Tension cut-off limit = 3.
5. Material type = 3 for plane cap and = 4 for elliptic cap.
6. Shape ratio = 0 for plane cap and = 4.33 for elliptic cap.
7. Hardening surface L-type = 1 for elastic soft soil and = 2 for non-elastic stiff soil / soft rock.
8. For the three-dimensional matching along the compressive meridian:

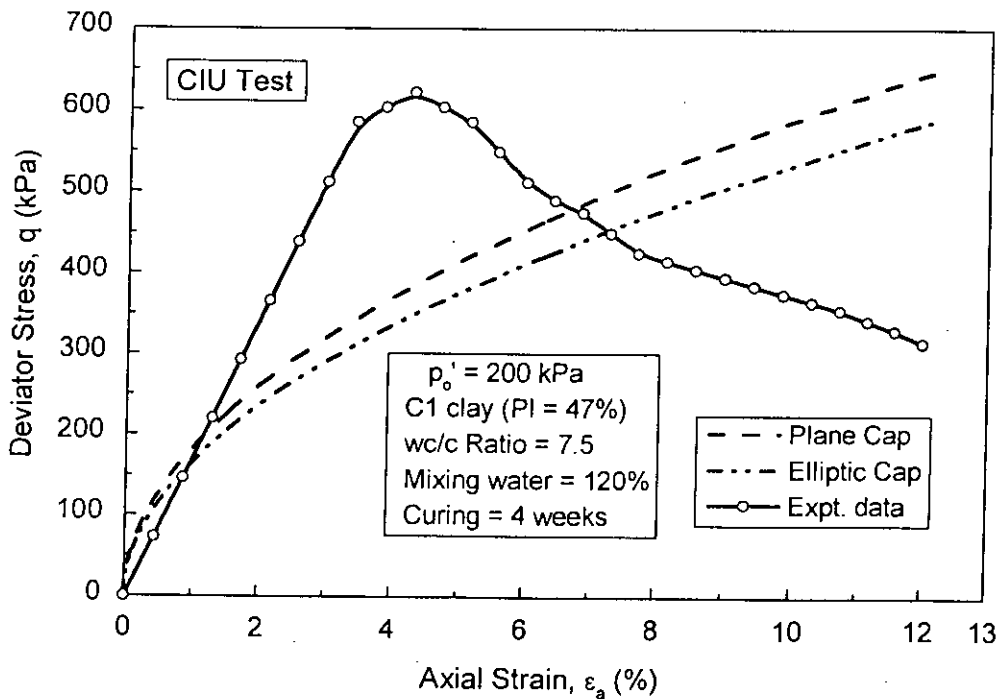
$$\alpha = \frac{2 \sin \phi}{\sqrt{3}(3 - \sin \phi)} \quad \text{and} \quad k = \frac{6c \cos \phi}{\sqrt{3}(3 - \sin \phi)}$$

9. For the plane strain matching with the same limit load:

$$\alpha = \frac{\tan \phi}{\sqrt{9 + 12 \tan^2 \phi}} \quad \text{and} \quad k = \frac{3c}{\sqrt{9 + 12 \tan^2 \phi}}$$



(a)



(b)

Fig. 6.44 Comparison of Plane Cap and Elliptic Cap Predictions and Observed Deviator Stress-Axial Strain Curves in CIU Test for Treated C1 clay at Curing = 4 w (a)  $wc/c = 7.5$  and (b)  $wc/c = 10$

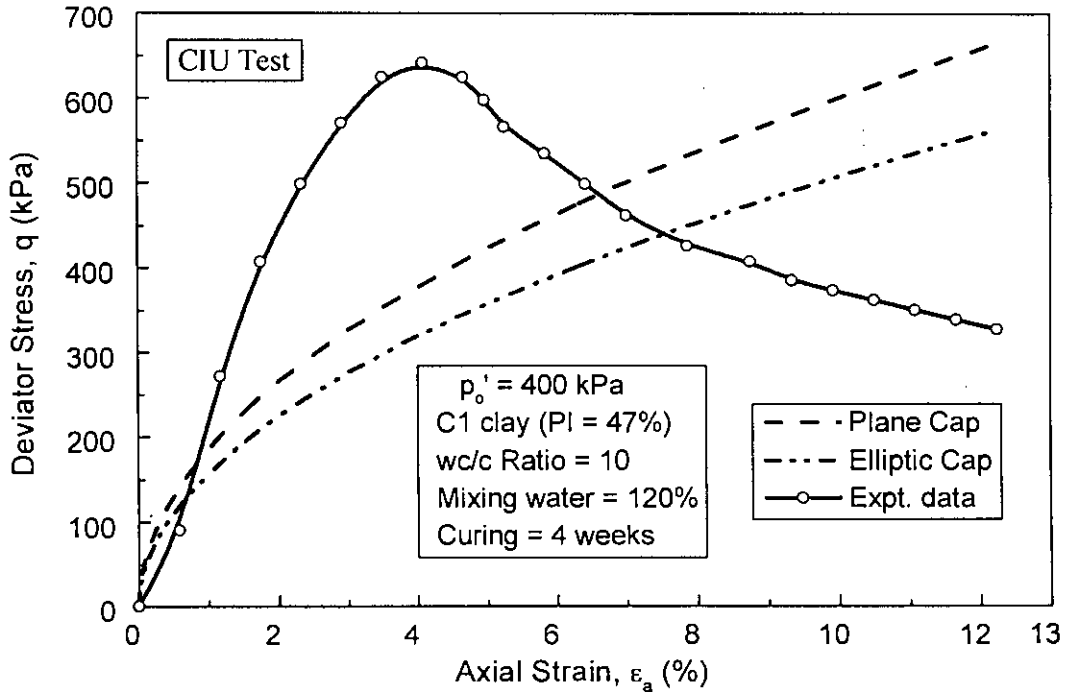


Fig. 6.45 Comparison of Plane Cap and Elliptic Cap Predictions and Observed Deviator Stress -Axial Strain Curves in CIU Test for Treated C1 clay  $p'_o = 400$  kPa,  $wc/c = 10$  and Curing = 4 w

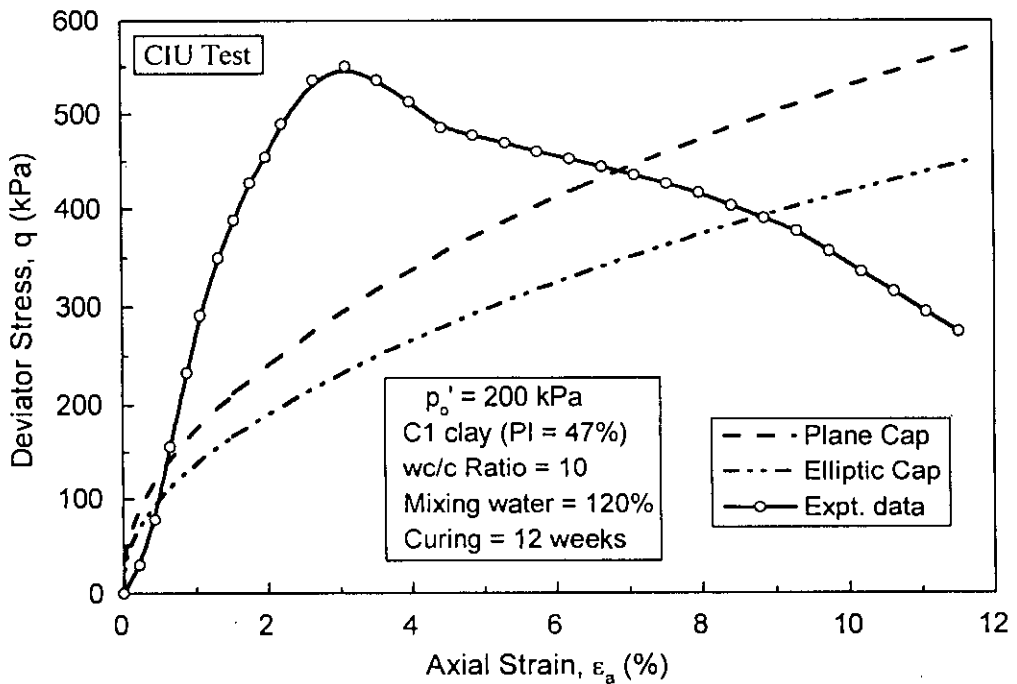
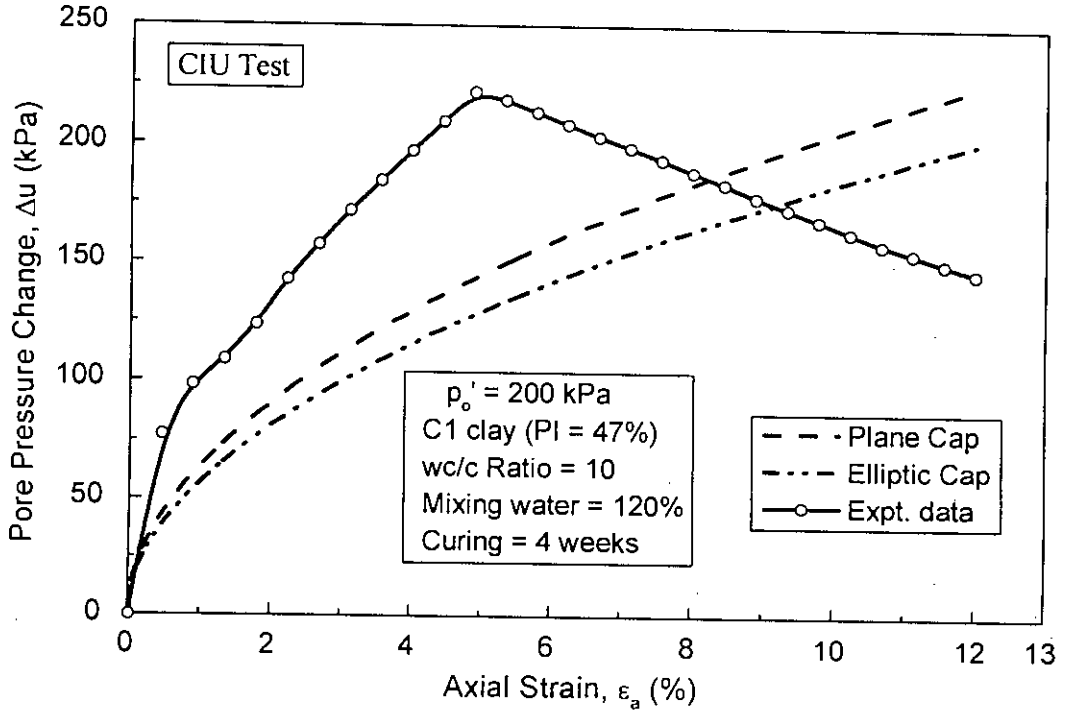
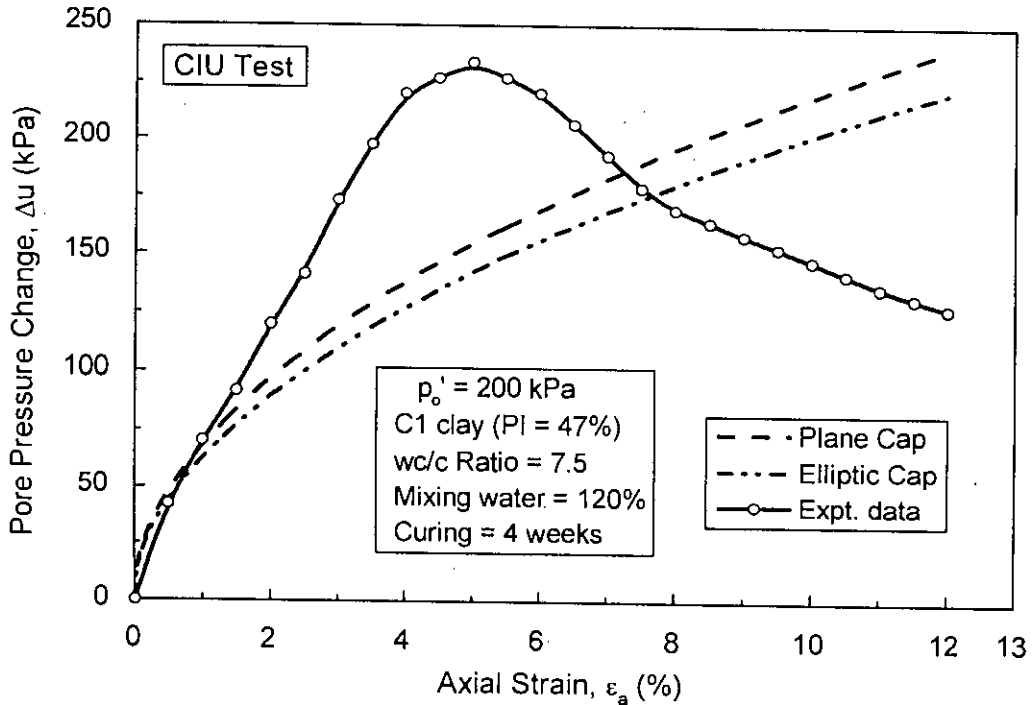


Fig. 6.46 Comparison of Plane Cap and Elliptic Cap Predictions and Observed Deviator Stress -Axial Strain Curves in CIU Test for Treated C1 clay at  $p'_o = 200$  kPa,  $wc/c = 10$  and Curing = 12 w



(a)



(b)

Fig. 6.47 Comparison of Plane Cap and Elliptic Cap Predictions and Observed Pore Pressure Change-Axial Strain Curves in CIU Test for Treated C1 clay at Curing = 4 w (a) wc/c = 7.5 and (b) wc/c = 10

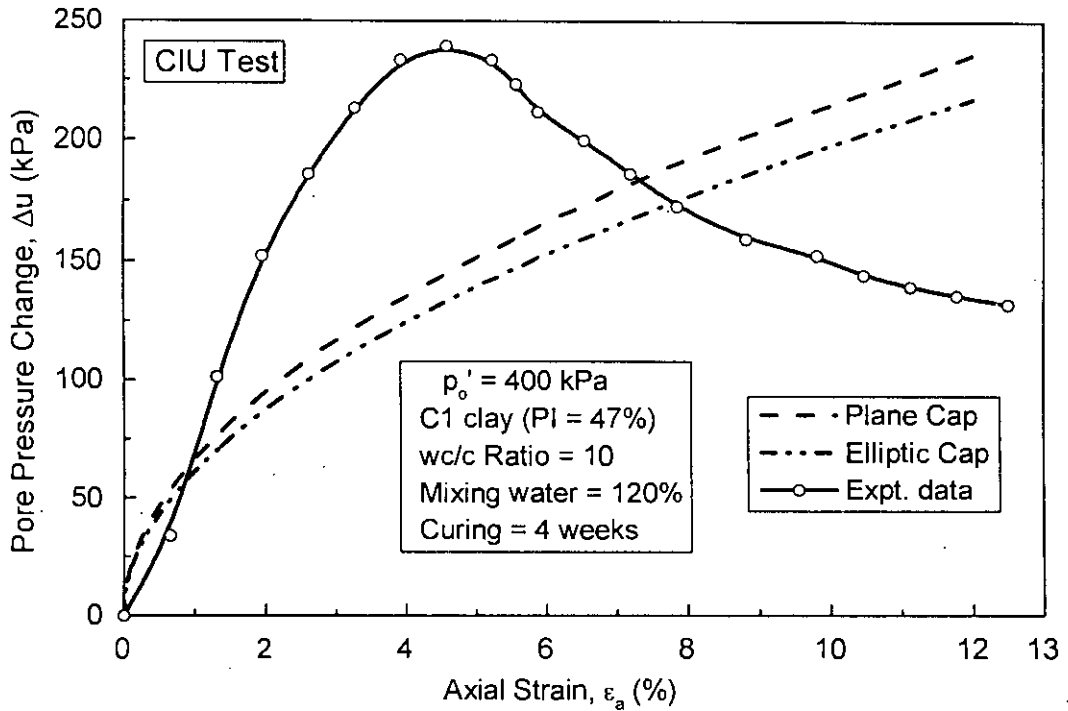


Fig. 6.48 Comparison of Plane Cap and Elliptic Cap Predictions and Observed Pore Pressure Change-Axial Strain Curves in CIU Test for Treated C1 clay at  $p'_o = 400 \text{ kPa}$ ,  $wc/c = 10$  and Curing = 4 w

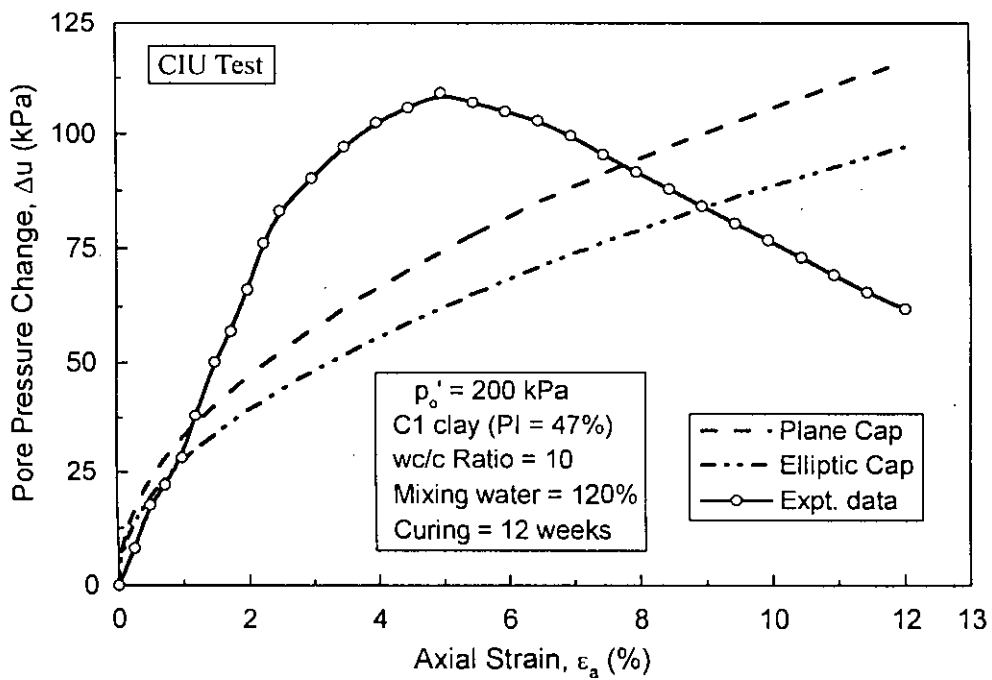
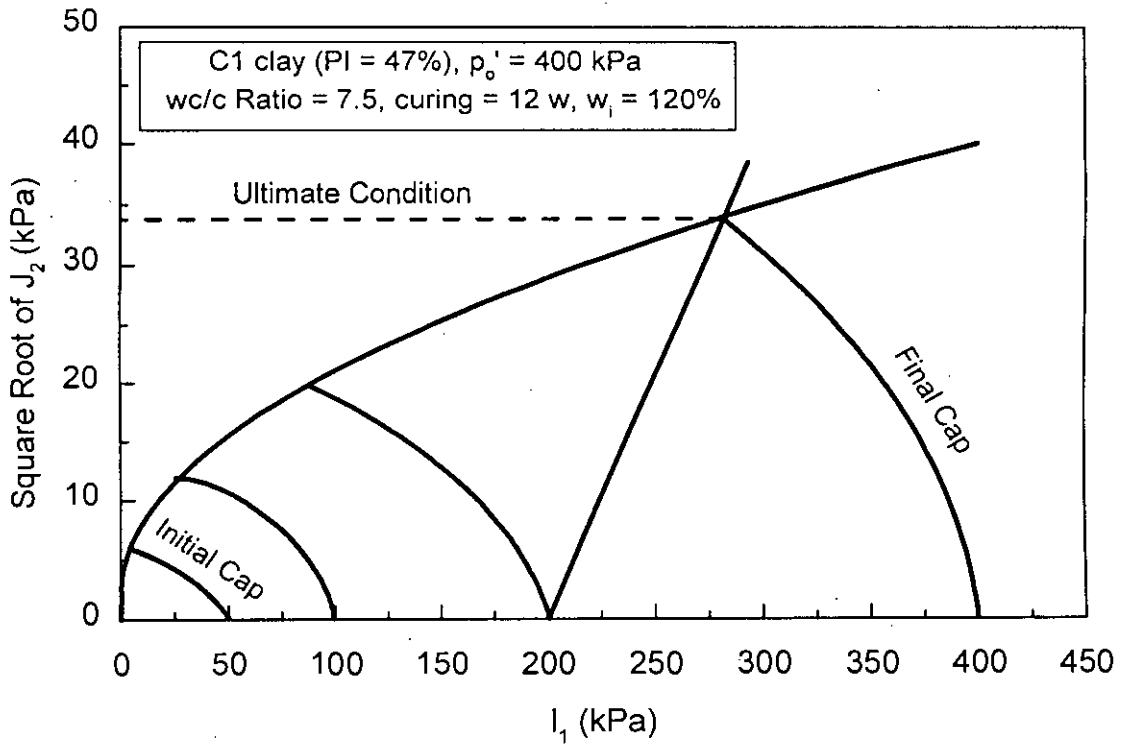


Fig. 6.49 Comparison of Plane Cap and Elliptic Cap Predictions and Observed Pore Pressure Change-Axial Strain Curves in CIU Test for Treated C1 clay at  $p'_o = 200 \text{ kPa}$ ,  $wc/c = 10$  and Curing = 12 w



(a)

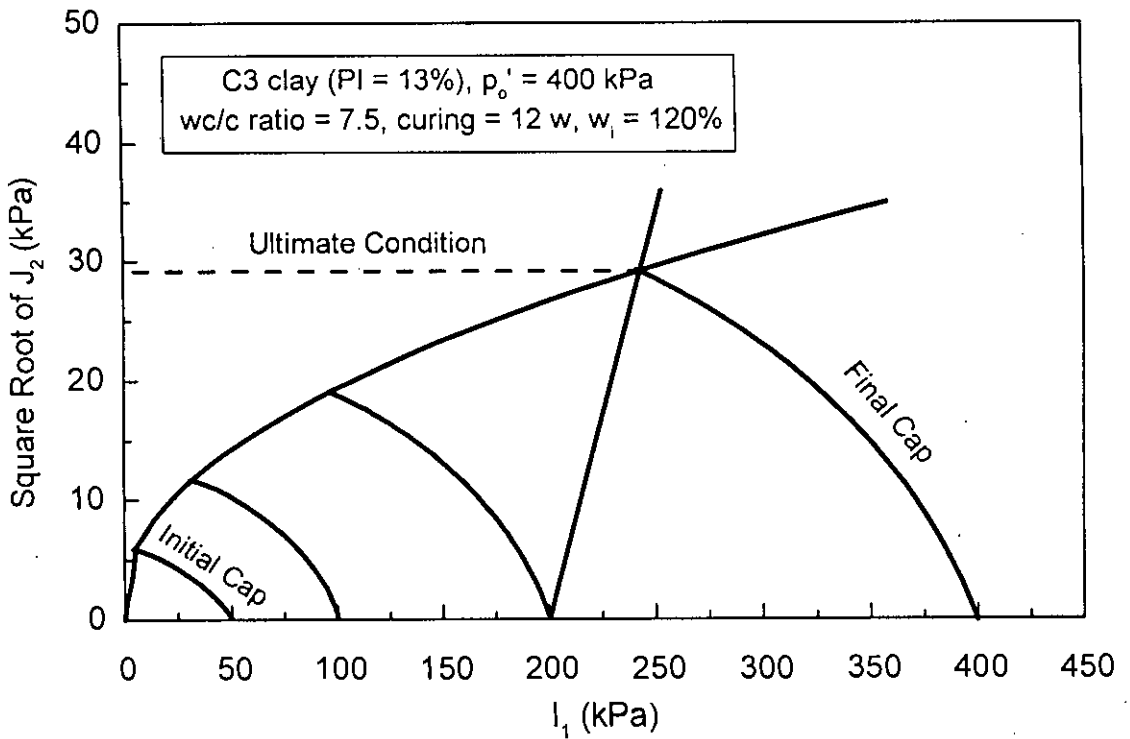


Fig. 6.50 Stress Path in  $I_1 - \sqrt{J_2}$  Space from Cap Model for Cement Treated  
 (a) C1 clay and (b) C3 clay

## CHAPTER 7

### CONCLUSIONS AND RECOMMENDATIONS

#### 7.1 Conclusions

In the present study, physicochemical as well as micro-structural behaviour of three untreated and cement treated soft clays having plasticity index values of 47%, 22% and 13%, have been investigated. The micro-structural and physicochemical properties were investigated by conducting X-ray Diffraction, Scanning Electron Microscopy, particle size distribution, pH measurement, organic content, electrical conductivity, cation exchange capacity, exchangeable cation, water content, unit weight, specific gravity, and Atterberg limits tests. Compressibility and permeability of properties of untreated and, cement and lime treated clays were investigated by performing one-dimensional consolidation tests. Stress-strain, strength and stiffness behaviour of untreated and, cement and lime treated clays were evaluated by performing unconfined compression (UC) tests. Consolidated drained direct shear (DS), unconsolidated undrained (UU), isotropically consolidated undrained (CIU) and isotropically consolidated drained (CID) triaxial compression tests were also carried out to assess the stress, deformation and strength properties of cement treated clays at high water content. Sets of variables considered in the testing program include a wide range for type of clay, type of admixture, clay-water/cement ratio, curing time, mixing water content of the clay slurry and pre-shear consolidation effective pressure.

Finally, the values of soil constants  $\lambda$ ,  $\kappa$ ,  $N$  and  $M$  for the untreated clays and treated were evaluated for different cement contents and curing ages. Deviator stress, volumetric strains, pore pressures and stress paths of cemented clays were predicted using three finite element constitutive models, namely, Modified Cam Clay (MCC) model, Modified Modified Cam Clay (MMCC) model and Extended Modified Modified Cam Clay (EMMCC) model while MCC model has been used for predicting the behaviour of untreated clay. The Cap model has also been applied for prediction behaviour of treated soil. The predictions were compared with experimental data.

The main findings and conclusions of the present study have been separated into four sections relating to the following areas:

- (i) Effects of cement treatment on chemical, mineralogical and physical properties.
- (ii) Effects of cement and lime treatment on compressibility and permeability properties.
- (iii) Effects of cement and lime treatment on stress-strain, strength and stiffness characteristics.

- (iv) Effect of cement treatment on the values of soil constants and applicability of different constitutive models and cap Model for the prediction of deviator stresses, volumetric strains, pore pressures and stress paths of untreated and cemented clays at high water content.

The major findings and conclusions relating to the above mentioned areas are presented in the following sections.

### 7.1.1 Investigation of Physicochemical and Micro-Structural Behaviour of Cement Treated Clays

The major findings and conclusions relating to the effect cement treatment on chemical, mineralogical and physical properties are summarized below:

- (i) pH value increases with decreasing clay-water/cement ratio (i.e. increasing cement content) but pH value decreases with increasing curing time. The pH value increases with increasing initial mixing water content and also the pH value increases with increasing plasticity of soil.
- (ii) Loss on ignition of base clays decreases due to cement treatment and also loss on ignition value decreases with increasing curing time. But the loss on ignition value increases with increasing plasticity of soil.
- (iii) Organic content of base clays decreases due to cement treatment and the organic content decreases with increasing curing time. But the organic content increases with increasing plasticity of soil.
- (iv) Electrical conductivity (EC) value increases with decreasing clay-water/cement ratio (i.e. increasing cement content) but EC value increases with increasing curing time. For cemented clays, the EC value increases with increasing plasticity of soil.
- (v) Cation exchange capacity increases with increasing cement content, increasing curing time and increasing plasticity of soil. Exchangeable cations  $Mg^{2+}$  increases with increasing plasticity index while  $Na^+$  and  $K^+$  decreases with increasing plasticity index.  $Ca^{2+}$ ,  $Na^+$  and  $K^+$  increases with increasing cement content while  $Mg^{2+}$  decreases with increasing cement content. Nitrogen and phosphorus increase with decreasing clay-water/cement ratio (i.e. increasing cement content). Nitrogen increases with increasing curing time and increasing plasticity of soil. Phosphorus, however, decreases with increasing curing time and increasing plasticity of soil.
- (vi) XRD results show that the illite, montmorillonite and kaolinite clay minerals are presented in three untreated base clays studied, of which illite is the dominant clay mineral. X-Ray Diffraction (XRD) analysis of cement treated clay has been confirmed the existence of several pozzolanic reactive products (secondary cementitious products), and they have been identified as calcium silicate hydrate (CSH) and calcium



aluminum silicate hydrate (CASH) and the non-existence of kaolinite mineral instead of illite and monmorillonite. The amount of CSH and CASH products increases with increasing cement content and increasing curing time. The amount of CSH and CASH content increases with increase in plasticity of soil.

- (vii) Dispersed nature of clay particles in untreated base clays has been seen from the Scanning Electron Microscopic (SEM) images. However, the fabric of the treated clay changes to flocculated type, comprising of clay-cement clusters separated by large inter-cluster voids ( $\geq 3 \mu\text{m}$ ) with more smaller intra-cluster pores ( $\leq 2 \mu\text{m}$ ). The flocculation of the clay particles also causes water to be trapped within the cluster. As inter-cluster voids are increased with increasing initial mixing water content. The increase in the effective size of the particles or/and cluster and the presence of entrapped water leads to a rise in the plastic and liquid limits with respect to the untreated clay. The presences of both inter and intra-cluster voids also leads to an increase in the permeability of the treated clays as compared to the untreated clays. The flocculation of clay-cement cluster has been more pronounced with higher cement content and longer curing time. At prolonged curing time, the fabric of the treated clay has been appeared to be platy in nature and at the same time the fabrics are interspersed by large openings (i.e., inter-cluster void). The platy and reticular types of cementitious products have been identified as CASH and CSH respectively (Locat et al., 1990). The continued increase in cluster size leads to an increase in plastic limit over time. Plastic limit was also found to increase with cement content (or decreasing clay-water/cement ratio). The deposition of secondary cementitious products on the clay clusters, on the other hand, leads to a decrease in surface activity of the illite clusters. As a result, the liquid limit decreases over time as well as decreases with increasing cement content (or decreasing clay-water/cement ratio).
- (viii) The plasticity index has been normalized by the final water content of the hardened cemented clays. This normalized plasticity index was found to have a strong correlation with the cement content, and was independent of curing time. Hence, the unique normalized plasticity behaviour can be used to quantify the engineering properties of cement treated clays.
- (ix) The specific gravity reduces while unit weight increases with increasing cement content and curing time. The specific gravity increases while unit weight reduces with increasing mixing water content and plasticity of soil.

### 7.1.2 Investigation of Compressibility and Permeability Properties of Cement and Lime Treated Clays

The major findings and conclusions relating to the effect cement and lime treatment on compressibility and permeability properties of clays at high water content can be summarized as follows:

- (i) At higher stress beyond the apparent pre-consolidation pressure (yield stress), the  $e - \log \sigma'_v$  and  $\epsilon_v - \log \sigma'_v$  curves of the treated clays shift at higher void ratio and volumetric strain respectively than those of the untreated clays with the same consolidation pressure. This shifting is almost parallel with the virgin consolidation line of the untreated clay and is more significant with higher admixture content and longer curing periods.
- (ii) The significant increase in apparent pre-consolidation pressure,  $p_c$  (yield stress,  $\sigma'_y$ ) and reduction in compression index ( $C_c$ ) and swell index ( $C_s$ ) have been observed with increasing admixture (cement/lime) content (or decreasing clay-water/admixture ratio) and increasing curing time. This is due to the structuration (existing of cementation bond) of treated clay particles.  $C_c$  and  $C_s$  for lime treated clays are greater than those of cement treated clays. The swelling behaviour of treated clays has been found to be very stiff resulting in very low  $C_s$ . At a particular  $w/c$  ratio,  $C_c$  and  $C_s$  values resulting due to the hardening effect imposed on the treated soil mass, increase significantly with the increase of mixing clay-water content. At the same mixing water content,  $C_c$  and  $C_s$  values for lime treated clays are higher than those of cement treated clays. The lime-treated clays are gained comparatively more higher void ratio, higher volumetric strain and lower yield stress than those of cement-treated clays.  $C_c$  and  $C_s$  increases with the decrease in plasticity index of clays.
- (iii) The effect of cementation is to increase the values of coefficient of consolidation ( $c_v$ ) and coefficient of volume compressibility ( $m_v$ ), which generally decrease, with increasing effective consolidation pressure similar to those of natural soft untreated clays. The higher the cement / lime content (lower clay-water/admixture ratio) and curing time, the lower is the value of  $c_v$  and  $m_v$ . It also appears that at a particular clay-water admixture ratio and effective vertical pressure,  $c_v$  and  $m_v$  values for lime treated clay are higher than those of cement treated clay. Yield stress (preconsolidation pressure) increases with the decrease of initial mixing water content. A substantial increase in the value of  $c_v$  and  $m_v$  was found to have occurred within higher mixing water content. The values of  $c_v$  and  $m_v$  decreases with increasing plasticity index of clay.
- (iv) At higher stress level, progressive destructuration (breaking down of cementation bond) of the treated clay particles occurred. This has been verified from the SEM images of cement treated clay compressed at different consolidation pressure. At this stage the

fabric of the treated clay plays dominant role on the compressibility of the treated clay. During one-dimensional consolidation, the largest inter-cluster voids are collapsed at the early stage of consolidation pressure and small intra-cluster pores are not compressed until the later stage at pressure exceeding the pre-consolidation pressure.

- (v) The Intrinsic Compression Line (ICL) and Generalized Compression Line (GCL) have been proposed for the untreated and treated clays. The ICL and GCL have been shifted due to cementation and confirmed the overconsolidation effect of the treated clays. It has been found that ICL and GCL for cement clays are also shifted more rightward than those of lime treated clays. From ICL and GCL for treated clays, it can be concluded that cement is more effective and active binding material than those of lime, because in both cases, it has been confirmed that cement treated clays experienced more yield strength and overconsolidated behaviour than those of lime treated clays.
- (vi) An addition of admixture to the clay increases the permeability and void of the soils, due to flocculation of the soil particles, which has been seen from SEM images. The increase in permeability has been linearly correlated to the increase in void ratio. Permeability and void ratio relationships have also been proposed for cement and lime treated clays. The coefficient of permeability ( $k$ ) of the cemented clays has been reduced with increasing cement or lime content (lowering  $w/c$  or  $w/l$  ratio) and curing period. At the same vertical effective stress and curing time,  $k$  values for lime treated clays have been found to be higher than those of cement treated clays. It has been found that the value of  $k$  decreases with increasing plasticity index of clays.

### **7.1.3 Investigation of Stress-Strain, Strength, Stiffness Characteristics of Cement and Lime Treated Clays**

The major findings and conclusions relating to the effect cement and lime treatment on stress-strain, strength and stiffness characteristics are summarized as below:

- (i) Shear types of failures were observed in the unconfined compression (UC) tests and unconsolidated undrained (UU) triaxial compression tests. The stress-strain curves show that the samples exhibit strength that reaches a peak and then reduces gradually as straining continues. In general, stress-strain curves of the treated samples were found to increase abruptly to peak values, then suddenly decreased to low residual values at low clay-water/cement ratio and long curing time. Comparing the undrained shear strength and failure strain obtained from UU triaxial compression and unconfined compression tests, it has been found that undrained shear strengths obtained from UU triaxial compression test are about 1.2 times higher than those obtained in UC test but failure strains for UU triaxial compression test are increased to about 2 times than those obtained from unconfined compression tests.

From the aspect of stress-strain relationships, the overall behaviour has been categorized into brittle, quasi-brittle and ductile. Comparatively, brittle, quasi-brittle and ductile types for the cement treated clays, while quasi-brittle and ductile types for the lime treated clays have been found. Based on the observations, unconfined compressive strength ( $q_u$ ) and admixture content relationships can be divided into 3 zones: Inactive Zone, Active Zone and Inert Zone. The treated clay with cement content up to 4% and at all ranges of curing periods, shows only a very marginal improvement of strength and is termed as Inactive Zone. The end result of the complete cementation is to increase the shear strength and this zone is termed as active zone. The upper limit of this zone is about 34% to 38% of admixture content. Beyond the active zone, the rate of increase of strength reduces and seems to be asymptotic. Such region is referred to as inert zone. Significant increase in strength development index with admixture content and curing time has also been found.

- (ii) The correlation between yield stress, ( $\sigma'_y$ ) and unconfined compressive strength ( $q_u$ ) of cement treated clays (where  $w/c$  are varied from 15 to 7.5) as  $\sigma'_y = (1.34 \text{ to } 2.56) q_u$  for the clays studied has been proposed.
- (iii) The salient effect of clay-water content/cement ratio ( $w/c$ ) on the stabilized clay has been found to be an influential parameter governing the strength and deformation characteristics. Since the behaviour of stabilized clays is remarkably governed by  $w/c$ , the strength assessment in terms of  $w/c$  as well as the interrelationship involving strength,  $w/c$  and curing time have been proposed as follows:

$$\left( \frac{q_{(w/c)1}}{q_{(w/c)2}} \right) = 1.24 \{ (w/c)^2 - (w/c) \} \text{ and}$$

$$\left( \frac{q_{(w/c)1,D}}{q_{(w/c)28}} \right) = 1.24 \{ (w/c)^2 8 - (w/c) \cdot D \} (-0.513 + 1.07 \ln D)$$

- (iv) The axial strain at failure ( $\epsilon_f$ ) of treated clay decreases with the increase of admixture content (or decreasing clay-water/admixture ratio) and curing time. Values of  $\epsilon_f$  for lime treated clays are higher than those of cement treated clays at same mixing ratio. At a particular clay water/admixture ratio,  $\epsilon_f$  increases with the decreasing plasticity index of clays. The correlations between  $\epsilon_f$  and  $q_u$  of cement treated clays have also been proposed.
- (v) Due to the effect of cementation, the initial stiffness ( $E_i$ ) and secant stiffness ( $E_{50}$ ) of treated clay increases significantly with the increase of admixture content (or decreasing clay-water/admixture ratio) and curing time.  $E_i$  and  $E_{50}$  for cement treated clays are higher than those of lime treated clays at same mixing water ratio. The correlations between stiffness ( $E_i$  and  $E_{50}$ ) and  $q_u$  of cement treated clays have also been established.

- (vi) The shear stress-displacement curves in consolidated drained direct shear tests showed that the samples exhibit a shear strength that reaches a peak and then reduces gradually as shear displacement continues. The cement treated clays have gained more shear strength and shear straining than that of untreated clays. For cement treated clays, vertical expansion (dilation) was observed at low normal stress and experienced vertical contractions or settlement throughout the shearing stage at higher normal stress. Relatively, high plastic clay has gained more shear strength, less shear straining, lower vertical settlements and higher dilation.
- (vii) Effective shear strength parameters, ( $c'$ ,  $\phi'$ ) for cement treated clays were determined from direct shear test. It has been found that the effective cohesion ( $c'$ ) and friction angle ( $\phi'$ ) of samples increased with increasing cement content (or decreasing  $w_c/c$  ratio) but  $c'$  increases and  $\phi'$  decreases with increasing curing time. This may be due to the effect of stiffness and more lubricating effect in cement treated condition that prevents soil slippage and frictional movement. At particular cement content and curing time,  $c'$  increases and  $\phi'$  decreases, in general, with increasing plasticity index. At a particular curing time,  $c'$  and  $\phi'$  of treated clays has been found to decrease with increasing clay-water content because the soil slippage and frictional movement are less prevented due to hydration of cementation at high water content.
- (viii) The shear stress ( $\tau_{10}$ ) at zero normal stress, i.e., cohesion of cement treated clay increases with the increase of cement content (or decreasing clay-water/cement ratio) and increasing curing time. The correlation between  $\tau_{10}$  and  $q_u$  of treated clay as  $\tau_{10} = 99.86 - 0.103q_u + 0.0003q_u^2$  for the clays studied has been proposed.
- (ix) The undrained effective stress paths of the cement treated clays have been obtained from CIU triaxial compression tests indicate that the stress paths belong to different category of states such as normally consolidated, lightly, moderately and heavily over-consolidated state. The degree of alteration have been found different for different samples depending on the amount of cement content (or  $w_c/c$  ratio), curing time and pre-shear effective consolidation pressure. The effect of structuration increases with the increase of cement content (or decreasing clay-water/cement ratio) and curing time which have been observed from the outward shifting of undrained stress path. Upon reaching the peak deviator stress for CIU triaxial test, the progressive destructuration takes place and thus the stress path tends to seek the failure state moving either on the Hvorslev envelope or envelope of strain softening behaviour.
- (x) Deviator stress-axial strain ( $q-\epsilon_a$ ) relationships in CIU triaxial compression tests are largely dependent on  $w_c/c$  ratio. After reaching the peak deviator stress, all the  $q-\epsilon_a$  relationships have been found to fall under varying rates depending on the parameter,  $w_c/c$ , revealing that cement is the paramount factor that controls the post-treatment relationships of  $q-\epsilon_a$  relationships. A general trend is that the maximum deviator stress

increases with decreasing clay-water/cement ratio (i.e., increasing value of cement content). It has also been found that generally the axial strain at the maximum deviator stress is reduced when  $w_c/c$  ratio has been decreased (i.e., cement content has been increased).

- (xi) At a particular  $p_o'$ , peak pore pressure change ( $\Delta u$ ) increases with decreasing  $w_c/c$  ratio (increasing cement content). It has been found that after reaching the peak  $\Delta u$ , pore pressures fall under varying rates with an increase in axial strain. The falling characteristics after peak depend very much on the  $w_c/c$  ratio. The rate of increase is greater for lower  $w_c/c$  ratio. A comparative study also shows that 12 weeks samples attain peak pore pressures at lower strains than those of 4 weeks samples. Higher the value of  $p_o'$ , the greater is the pore pressure generation. At low values of  $p_o'$  (e.g., 50 kPa and 100 kPa), large amount negative pore pressure has been generated. An overall characteristic of the treated clay is noticeable that the peak pore pressure has been mobilized always at much lower value of axial strains than those of untreated clay. For natural base clay,  $\Delta u$  keeps on increasing with  $\epsilon_a$  without showing any maximum value, i.e.,  $u_{max}$  is located at the end-of-test condition, which reflects one of the characteristics of the normally consolidated clay
- (xii) SEM results of CIU triaxial sheared samples suggest that complete destructuration only take place on the shear plane at which the clay-cement cluster crushes. Both inter and intra cluster voids have been found to be very negligible in the shear plane as compared to the intact sample. However, the image of the sample outside of the shear plane has been found to be quite different from that within the shear plane. For sample outside the shear plane, the breaking of large clay-cement clusters is apparent but still contain small clusters in the form of reticulation. At this stage, no breakage of treated clay particles has been observed. More inter-cluster voids are visible as compared to the image of sample within the shear plane. It has been concluded that during the isotropic consolidation, the cementation bond in the form of clay-cement cluster did not completely break down, and may affect the subsequent shearing stage. This observation affects the shape of the undrained stress path.
- (xiii) Compared with the results of CIU tests, the stress-strain curves from CID tests increase less sharply with increasing strain, suggesting that the drained stiffness is less than the undrained stiffness. Furthermore, the stress-strain curves show that the axial strains of CID tests are greater than those of CIU tests. A unique type of relationship is evident among the untreated samples. These curves possess certain definite patterns. The usual trend exists, the higher the  $p_o'$ , greater is the value of deviator stress. The overall nature of the curves seems to indicate that the samples are behaving as if they are normally consolidated to lightly overconsolidated.

- (xiv) Similar nature of stress-strain relationships has been realized for all samples having the identical  $w/c$  in CID triaxial compression tests. At a particular mixing water content and curing time, peak volumetric strains increase with increasing  $w/c$  ratio (decreasing cement content). All samples having the same  $w/c$  both made up at low and high clay-water contents exhibit identical volumetric strain versus axial strain response. The engineering behaviour is identical as long as the  $w/c$  is the about same, which have been strengthened by test results of samples with water contents varying from 120% to 250% in CID triaxial compression tests. So, the  $w/c$  is a prime parameter governing the engineering behaviour of cement treated samples having different mixing water content.
- (xv) The fabric has a great influence on the stress-strain behaviour for samples made up at a low  $w/c$  and subjected to high effective cell pressures in CID triaxial tests. Their states of stress lie on the state boundary surface where the samples exhibit elasto-plastic behaviour. It is revealed that samples having the same  $w/c$  develop practically the same peak deviator stress. However, samples with a high clay water content (the initial water content is 200% to 250%) undergo low stiffness and high volumetric strain. The effect of fabric has also been clearly elaborated by the consolidation test results showing that samples having higher clay water contents sustain higher volume change after the yield state.
- (xvi) For cement treated clays, the peak deviator stress ( $q_{max}$ ) criterion of failure envelopes can be used as obtained from CIU and CID triaxial compression tests. The treated clays possess various degrees of over-consolidation depending mainly on cement, curing time and pre-shear consolidation pressure ( $p_o'$ ). The occurrence of  $q_{max}$  depends upon the degree of over-consolidation. For treated soil with high over-consolidation, the peak deviator stress ( $q_{max}$ ) occurs at much lower strain than corresponding failure strain and thus the criterion of peak deviator stress ( $q_{max}$ ) becomes in consistent and valid to refine the residual states of the treated soil mass. Thus in this study, the maximum deviator stress criterion has been considered to define the failure condition. One noticeable aspect is that the parameter of  $w/c$  ratio renders greater impact on hardening potential than the curing time. The degree of overall curvature of the failure envelope for each type of clay depends on the range of consolidation stresses and hence increases with increasing cement content and curing time.

#### **7.1.4 Evaluation of Soil Constants and Applicability of Constitutive Models and Cap Models for the Prediction of Drained and Undrained Behaviour of Untreated and Cement Treated Clays**

The major findings and conclusions regarding the effect of cement treatment on soil constants and the applicability of different constitutive models and cap Model for the

prediction of deviator stresses, volumetric strains, pore pressures and stress paths of untreated and cemented clays at high water content are summarized as below:

- (i) The values of soil constants  $\lambda$  and  $\kappa$  for the treated clays have been found to be less than those for the untreated clays while the values of the constant M and N are greater for the cement treated clays than those of untreated clays. At a particular curing time, the soil constants  $\lambda$  and  $\kappa$  decreased, while the constant M and N increased with increasing cement content (i.e., decreasing wc/c ratio). The values of the soil constants  $\lambda$ ,  $\kappa$  and N have also been found to increase with the increase of plasticity index of the clays. Correlations between the soil constants  $\lambda$ ,  $\kappa$  and N with plasticity index have been proposed.
- (ii) The shape of normalized effective stress paths of samples of untreated base clays are normally consolidated in nature. These have been seen to be non-dilatant, traveling a way up to the left before rupture and thereby generated Roscoe surface. The shape of the normalized undrained effective stress paths for cement treated clays has been seen to be lightly overconsolidated to heavily overconsolidated in nature. These have been seen to be strongly dilatant, traveling a long way up to the right before rupture and thereby Hvorslev surface can be established for the cemented clays. No definite Roscoe surface could be established for cemented clays.
- (iii) For the untreated clay, it has been observed that at small strain levels deviator stresses and volumetric strains predicted using the MCC model appears to be significantly close to experimental values obtained in CID triaxial compression tests. It has been observed that the MCC model overestimates the experimental values of deviator stresses obtained in the CIU triaxial compression tests although the initial excess pore pressure values compares very well with the experimental values at very low strain levels. The predicted undrained effective stress paths of untreated clay agree reasonably well with the observed stress paths at lower pre-shear effective consolidation pressures (100 and 200 kPa).
- (iv) It appears from the present study that MCC, MMCC and EMMCC models are not so effective to predict the drained stress-strain response and volumetric changes, and, therefore may not be applicable to predict drained behaviour of cemented clays. It has also been observed that for the prediction for undrained stress-strain behaviour and pore pressure change responses, MCC, MMCC and EMMCC models may not be applicable for cemented clays at high water content. Nevertheless, the MMCC and EMMCC model predictions compares reasonably well in some respects with the observed experimental drained and undrained behaviours. Particularly, EMMCC model may be used for the predictions of undrained effective stress paths of cemented clays at high water content.



- (v) It appears from the present investigation that Cap models (Plane Cap and Elliptic Cap) cannot be applied for predictions of drained and undrained behaviour of cemented clays at high water content.

## 7.2 Recommendations for Future Study

- (i) In the present research study, physicochemical as well as micro-structural behaviour of cement treated clay has been investigated at different cement content and curing periods with different initial high water content without compaction blows. Thus, further study can be performed on the micro-structural behaviour of cement/lime treated clay at various low water content with compaction blows and relate them with the observed engineering behaviour in both short term as well as prolonged curing condition.
- (ii) The strength, stiffness and compressibility of cement treated expansive and organic soils improved significantly if the treated samples are cured under preloading. Thus, further research can be conducted to assess the physicochemical as well as micro-structural behaviour with swelling measurement of cement treated expansive and organic clay incorporating the effect of curing under preloading and integrate these results with the observed engineering behaviour.
- (iii) Consoli et al. (2000) reported that the strength and stiffness of cement treated sandy soil improved significantly if the treated samples are cured under stress rather than cured in humid chamber/water. Thus, further research can be carried out on micro-structural behaviour of cement treated clay incorporating the effect of curing under stress and integrate the results with the observed engineering behaviour at high water content.
- (iv) In the present study, due to the bedding error in conventional method of strain measurement, the stiffness measured from local strain measurement is much larger. It is found that performing proper unloading-reloading cycle at the initial elastic zone of the stress-strain curve can eliminate the bedding error. The effect of destructuration on the stiffness of treated clay suggests that the stiffness at destructured state reduces significantly. It may be recommended that local small strain measurements enables the accurate determination of the true stiffness of the cemented clay, especially at small strain level.
- (v) There are so many test variables used in the present study on which the evaluation of strength and deformation characteristics of cement treated clay has been done. There is no software known available, which uses test variables for calculating engineering parameters. Thus, further research can be done on software development where solution can be given of the geotechnical problems by using test variables of this study for determining engineering parameters (especially, strength and deformation).

## REFERENCES

- Ahnberg, H., Ljungkrantz, C. and Holmqvist, L. (1995): "Deep stabilization of different types of soft soils", Proceedings of the 11<sup>th</sup> European Conference on Soil Mechanics and Foundation Engineering, Vol. 3, No. 7, pp. 167-172.
- Ahmed, N.U. (1984), "Geotechnical Properties of Selected Local Soils Stabilized With Lime and Cement", M.Sc. Engineering Thesis, Department of Civil Engineering, Bangladesh University of Engineering and Technology, Dhaka.
- Alam, M.K.A., Hasan, A.K.M.S., Khan, M.R., and Whitney J.W., (1990): "Geological Map of Bangladesh", Scientific Publication, U. S. Geological Survey, pp. 1-12.
- Allman, M. A. and Atkinson, J. H. (1992): "Mechanical properties of reconstituted Bothkennar soil", Journal of Geotechnique, Japan, Vol. 42, No.-2, pp. 289-301.
- Ameen, S.F. and Safiullah, A.M.M. (1986): "Undrained shear strength characteristics of Dhaka clay, Journal of IEB, Bangladesh", Vol. 14, No. 4, pp. 1-8.
- Amin, M.N., Kabir, M.H., Saha, G.P. and Ahmed, M. (1987): "Geotechnical behaviour of soils from coastal regions of Bangladesh", 9<sup>th</sup> SEAGC, Bangkok, pp. 5.1-5.12.
- Ansary, M. A. and Daulah, I. U, (1993): "Ground improvement state of the art report and application prospect in Bangladesh", Proc., First Bangladesh-Japan Joint Geotechnical seminar on ground Improvement, pp. 1-25.
- Ansary, M.A., Siddique, A. and Safiullah, A.M.M, (1999): "Compressibility and permeability characteristics of selected coastal soils of Bangladesh", Indian Geotechnical Journal, Vol. 29, No. 2, pp. 162-185.
- Ansary, M.A., Siddique, A. and Hasan, K. A. (2003): "A study of lime stabilization on soil of a selected reclaimed site of Dhaka clays." Proceedings of 12<sup>th</sup> Asian Regional conference on Soil Mechanics and Geotechnical Engineering, Singapore, Volume 1, pp. 439-442.
- Arora, K.R. (2000): "Soil mechanics and foundation engineering", Standard Publishers, Delhi, India, pp. 132-181.
- Atkinson, J.H. and Bransby, P.L. (1978): "The mechanics of soils - An introduction to critical state soil mechanics", McGraw-Hill, New York, England, pp. 15-85.
- Assarson, K., Broms, B., Granholm, S. and Paus, K. (1974): "Deep stabilization of soft cohesive soils", Linden Alimark, Sweden, pp. 118-138.
- Balasubramaniam, A. S. (1973): "Stress history effects on stress-strain behaviour of saturated clay", Geotech. Engrg. J., ASCE, Vol. 4, pp. 91-111.
- Balasubramaniam, A.S., Kamruzzaman, A.H.M., Uddin, K., Un, D.G., Phienwij, N. and Bergado, D.T. (1998): "Chemical stabilization of Bangkok clay with cement, lime and fly ash additives", Proceedings of the 13<sup>th</sup> Southeast Asian Geotechnical Conference, Taipei, pp. 253-258.
- Balasubramaniam, A.S., Un, D.G., Sharma, S.S., Kamruzzaman, A.H.M., Uddin, K., and Bergado, D.T. (1999): "Behaviour of soft Bangkok clay treated with additives",

- Proceedings of the 11<sup>th</sup> Asian Regional Conference on Soil Mechanics and Geotechnical Engineering, Seoul, pp. 11-14.
- Bashar, M. A. (2002): "Stress-deformation characteristics of selected coastal soils of Bangladesh and their sampling effects", Ph. D. Thesis, Dept. of Civil Engg., BUET, Dhaka.
- Bell F. G. (1993) "Engineering Treatment of Soil", Spon, New York, London.
- Bergado, D.T., Lorenzo G.A. and Balasubramaniam, A.S. (2003), "Engineering behaviour of cement and lime treated soft Bangkok clay", Journal of Geotechnical Engineering, School of civil Engg., AIT, Bangkok.
- Bergado, D.T., Anderson, L.R., Miura, N. and Balasubramaniam, A.S. (1996): "Soft ground improvement in lowland and other environments", New York, ASCE Press, England, pp. 1-9.
- Berube, M.A., Choquette, M. and Locat, J (1990): "Effects of lime on common soil and rock forming minerals", Applied Clay Science, Vol. 5, pp. 145-163.
- Bowles, J. E. (1982): "Engineering properties of soils and their measurement", International student edition, McGraw-Hill international book company, New York, London, England, pp. 11-175.
- Brandl, H. (1981): "Alteration of soil parameters by stabilization with lime", Proceedings of the 10<sup>th</sup> International Conference on Soil Mechanics and Foundation Engineering, Stockholm, Vol. 3, pp. 587-594.
- Broderic, G.P. and Daniel, D.E. (1990): "Stabilizing compacted clays against chemical attack", Journal of Geotechnical Engineering, ASCE, Vol. 116(10), pp. 1549-1567.
- Broms, B. (1986): "Stabilization of soft clay with lime and cement columns in Southeast Asia", Applied Research Pro., Nanyang Technical Institute, Singapore, pp. 1-8.
- Broms, B., Boman, P. and Paus, K. (1980): "The lime column method". Swedish Council for Building Research, Translated by Guber, Sweden, pp. 112-123.
- Brown, G. (1961): "The x-ray identification and crystal structures of clay mineral", Mineralogical Society (Clay Minerals Group), London, pp. 102-124.
- BS 1377 (1990): "British standard methods of test for soils for civil engineering purposes", British Standard Institution, London.
- Burland, J. B. (1965): "The yielding and dilation of clay correspondence", Journal of Geotechnique, Japan, Vol. 15, No. 2, pp. 211-214.
- Burland, J.B. (1990): "On the compressibility and shear strength of natural soils", Journal of Geotechnique, Japan, Vol. 40 (3), pp. 329-378.
- Carter, J.P. and Balaam, N.P. (1995): "AFENA-A finite element numerical algorithm, users' manual", Version 5.0, Centre for Geotechnical Research, University of Sydney, Australia, pp. 1-22.
- Chew, S.H., Lee, F.H. and Lee, Y. (1997): "Jet grouting in Singapore marine clay", Proceedings of the 3<sup>rd</sup> Asian Young Geotechnical Engineering Conference, Singapore, pp. 231-238.

- Chew, S. H., Kamruzzaman, A. H. M. and Lee, F. H. (2001): "Strength and deformation characteristics of cement treated marine clay", Proceedings of the 14<sup>th</sup> Southeast Asian Geotechnical Conference, Hong Kong, pp. 285-290.
- Chew, S. H., Kamruzzaman, A. H. M. and Lee, F. H. (2002): "Structuration and destructuration behaviour of cemented clays", Journal of Geotechnique, Japan, pp.1-9.
- Chew, S. H., Kamruzzaman, A. H. M. and Lee, F. H. (2004): "Physicochemical and engineering behaviour of cement treated clays", Journal of Geotechnical and Geoenvironmental Engineering, ASCE, pp. 696-706.
- Cokca, E. (2001): "Use of class C flyashes for the stabilization of an expansive soil" Journal of Geotechnical and Geoenvironmental Engg., ASCE, Vol. 7 pp. 568-573.
- Consoli, N.C., Rotta, G.V. and Prietto, P.D.M. (2000): "Influence of curing under stress on the triaxial response of cemented soils", Geotechnique, Vol. 50(1), pp. 99-105.
- Das, B.M. (1999): "Advanced soil mechanics", McGraw-Hill Book Company, Hemisphere Publishing Corporation, Washington New York, London, pp.15-63.
- Davidson, L.K., Demirel, T. and Handy, R.L. (1965): "Soil pulverization and lime migration in soil lime stabilization". Highway Research Record no. 92, Highway Research Board, pp.103-126.
- Desai and Siriwardane (1984): "Constitutive laws for engineering materials with emphasis on geologic materials", Prentice-Hall, Inc., Englewood Cliffs, USA.
- Diamond, S. and Kinter, E. B. (1965): "Mechanisms of soil-lime stabilization", An Interpretative Review Public Roads, Vol. 33, No. 12, pp. 260-265.
- Eades, J.L. and Grim, R.E. (1960): "Reactions of hydrated lime with pure clay minerals in soil stabilization", Highway Research Bulletin, Washington, Vol. 262, pp. 51-63.
- Ghee, C. K., Hou, L. F. and Dasari, G. K. (2004): "Effect, of curing stress on mechanical properties of cement treated soft marine clay", Engineering practice and performance of soft Deposits, Japan, IS-OSAKA, ISBN-4-88644-812-7, pp. 217-222.
- Grim, R.E. (1981): "Clay mineralogy", 3<sup>rd</sup> edition, McGraw-Hill international book company, New York, London, England, pp. 126-184.
- Handy R.L. Demirel, T., Ho, C., Nady, R.M. and Ruff C.G., (1965): "Discussion on mechanism of soil lime stabilization" An Interpretative Review, by Diamond. S. and Kinter, E. B., pp. 96-99.
- Harada, K., Tsuboi, H., Fukada H., Ideno, T. and Matsni T. (2004): "Development and application of and advanced deep mixing method meeting large-Pile-diameter and high-speed execution", Engineering practice and performance of soft deposits, Japan, IS-OSAKA, ISBN-4-88644-812-7, pp. 251-256.
- Hasan, K.A. (2002): "A study on cement and lime stabilization on soil of selected reclaimed sites of Dhaka clay", M. Sc. Engg. Thesis, Civil Engg. Dept., BUET, Dhaka.
- Head, K.H. (1990): "Manual of Soil Laboratory Testing", Vol.- 3, 3<sup>rd</sup> Edition, ELE International Ltd., Pentech Press, London, pp. 971-1119.

- Herrin M. and Mitchell, H. (1961): "Lime soil mixture", Bulletin No. 304, Highway Research Board, pp. 99-138.
- Herzog, A. (1967): "Evidence for a skeleton-matrix structure in clays stabilized with Portland cement", 5<sup>th</sup> Australia-New Zealand Conf. on SMFE, pp. 64-72.
- Horpibulsuk, S. (2002): "Analysis of compressibility of cement admixed clays", Proc. Int. Symposium on Lowland Technology, Saga University, Saga, Japan, pp. 175-180.
- Horpibulsuk; S., Miura, N. and Nagaraj. T.S. (1999): "Prediction of strength and consolidation parameters of cement stabilized clays", Report of the Faculty of Science and Engineering, Saga University, Japan Vol. 28, No. 2, pp. 27-38.
- Horpibulsuk, S., Miura, N. and Nagaraj. T.S. (2000): "A new method for predicting strength of cement stabilized clays", Coastal Geotechnical Engineering in practice, Nakase and Tsuchida, BALKEMA, Rotterdam, ISBN 50 5809 1511, pp. 605-610.
- Horpibulsuk, S., and Miura, N. and Nagaraj, T.S. (2001): "Analysis and assessment of strength development in cement admixed clays", Proc. Int. Conf. on Civil Engg., Indian Institute of Science, India, Vol. 2, pp. 156-163.
- Hossain, M. A. (2001), "Geotechnical Behaviour of a Lime Treated Expansive Soil." M. Sc. Engineering thesis, Department of Civil Engineering, Bangladesh University of Engineering and Technology, Dhaka, Bangladesh.
- Hvorslev, M. J. (1949): "Subsurface exploration and sampling of soils for civil engineering purposes" Waterways Experimental Station, Vicksburg, Mississippi.
- Ingles, O.G. and Metcalf, J. B. (1972): "Soil stabilization principles and practice", Butter Worths Pty Ltd., Melbourne, pp. 1-8.
- Islam, M.S., Siddique, A. and Muktedir, A. (2004): "Mechanical properties of soft organic Dhaka clay", Journal of Civil Engineering, The Institution of Engineers Bangladesh, Vol. CE 32, No. 2, pp. 143-161.
- Islam. M. K., Siddique, A., and Khalilullah M. I., (2007): "Modelling the stress-strain response of cemented regional clay", 10<sup>th</sup> Australia New Zealand conference on Geomechanics, Brinsbane, Australia.
- Jackson, M.L. (1985): "Soil chemical analysis", Englewood Cliffs, N.J., Prentice-Hall.
- JCPDS (1995): "Index to the powder diffraction file", International Center for Diffraction Data, U.S.A.
- Kamaluddin, M. (1995): "Strength and deformation behaviour of cement-treated Bangkok clay", Ph. D. Thesis, AIT, Bangkok, Thailand.
- Kamaluddin, M., (2001): "Intrinsic compressibility, shear properties and some strength models for Dhaka clay", The Journal of Civil Engineering, The Institution of Engineers, Bangladesh (IEB), Dhaka, Bangladesh, Vol. CE 27, No. 2., 87-99
- Kamaluddin, M., (2004): "Advanced ground improvement technique by cement and lime treatment", Institute of Appropriate Technology, BUET, Dhaka, Vol. 1, pp. 1-117.
- Kamaluddin, M., Balasubramaniam, A.S. and Bergado, D.T. (1997): "Engineering behaviour of cement treated Bangkok soft clay", Geotechnical Eng., SEAGS, Vol. 28(1), 89-119

- Kamaluddin, M. and Buensuceso, B. R., (2001): "Engineering properties and a conceptual model for lime treated clay", *The Journal of Civil Engineering, The Institution of Engineers, Bangladesh.*, Vol. CE 28, No. 2, pp. 119-129
- Kamaluddin, M. and Buensuceso, B. R., (2002): "Lime treated clay: salient engineering properties and a conceptual model", *Journal of Soils and Foundations, The Japanese Geotechnical Society, Tokyo Japan*, Vol. 42, No. 5, pp. 79-89.
- Kamruzzaman, A. H. M. (2002): "Physicochemical and engineering behaviour of cement treated Singapore marine clay", Ph. D. thesis, National University of Singapore.
- Kamruzzaman, A. H. M., Chew, S. H., and Lee, F. H. (2001): "Behaviour of soft Singapore marine clay treated with cement", *ASCE Geotech. Special Publication, GSP*, Vol. 113, pp. 472-485.
- Kamruzzaman, A. H. M., Chew, S. H. and Lee, F. H. (2002): "Microstructure of cement treated Singapore marine clay", *Soils and Foundations, JGS, Japan*, pp. 48-60.
- Kaushinger, J.L. Perry, E. B. and Hankour, R. (1992). "Jet Grouting: State of the practice", *Proceedings of the Conference of Grouting, Soil Improvement and Geosynthetics, ASCE*, Vol. 1, pp. 169-181.
- Kawasaki, T., Niina, A., Saitoh, S., Suzuki, Y. and Honjyo, Y. (1981): "Deep mixing method using cement hardening agent", *Proceedings of the 10th International Conference on Soil Mechanics and Foundation Engineering, Stockholm*, pp. 721-724.
- Kezdi (1979): "Stabilized Earth Roads", *Development in Geotechnical Engineering, Elsevier Scientific Publishing Company, London, England*, pp. 18-27.
- Khalilullah M. I., (2007): "Experimental and numerical study of cemented clays", M. Sc.Engg. Thesis, Dept. of Civil, BUET, Dhaka, Bangladesh.
- Kinuthia, J.M., Wild, S. and Jones, G.I. (1999): "Effects of monovalent and divalent metal sulphates on consistency and compaction of lime stabilized kaolinite", *Applied Clay Science*, Vol. 14, pp. 27-45.
- Lambe, T.W. (1977): "Soil Testing for Engineers", *Wiley, New York, Landon*, pp.13-165.
- Lambe, T. W., and Z. C. (1957): "Improvement of strength of soil-cement with additives", *Bulletin 183, Highway Research Board*, pp. 33-47.
- Lea, F.M. (1956): "The chemistry of cement and concrete", *Edward Arnold Publishers, London*
- Lee, S. L., Ramaswamy S. D. and Aziz, M. A. (1982): "A Study of the soil type suitable for stabilization with lime" *Proc. 7<sup>th</sup> SEAGC, Hongkong*, pp. 615-629.
- Lerouiel, S. and Vaughan, P.R. (1990): "The general and congruent effects of structure in natural soils and weak rock", *Geotechnique*, 40(3), pp. 467-488.
- Liu, M.D. and Carter, J.P. (1999): "Virgin compression of structured soils", *Journal of Geotechnique, Japan*, Vol. 49(1), pp. 43-57.
- Locat, J., Berube, M.A. and Choquette, M. (1990): "Laboratory investigations on the lime stabilization of sensitive clays: shear strength development", *Canadian Geotechnical Journal, Canada*, Vol. 27, pp. 294-304.

- Locat, J., Tremblay, H. and Leroueil, S. (1996): "Mechanical and hydraulic behaviour of soft inorganic clay treated with lime", Canadian Geotechnical Journal, Vol. 33, pp. 654-669.
- Mitchell, J.K. (1981): "Soil Improvement-State of the Art Report", Proceedings of the 10<sup>th</sup> International Conference on Soil Mechanics and Foundation Engineering, Stockholm, Vol. 4, pp. 509-565.
- Mitchell, R.J. (1993): "On the yielding and mechanical strength of Leda clays", Canadian Geotechnical Journal, Canada, Vol. 7, pp. 297-312
- Miura, N., Horpibulsuk, S. and Nagaraj, T.S. (2001): "Engineering behaviour of cement stabilized clay at high water content", Soils and Foundations, JGS, Vol. 41, pp. 33-45.
- Miura, N., Koga, Y. and Nishida, K. (1986): "Application of a Deep Mixing Method with Quicklime for the Ariake Clay Ground", Soils and Foundations, Japan, Vol. 39(4), pp. 5-11.
- Molla, M. A. (1993): "Geotechnical conditions of the deltaic alluvial plains of Bangladesh and associated problems", Engineering Geology, Vol. 36, pp. 125-140.
- Molla, M.A.A. (1997), "Effect of Compaction Conditions and State Variables on Engineering Properties of the Lime Stabilized Soil", M.Sc. Engineering Thesis, Department of Civil Engineering, BUET, Dhaka, Bangladesh.
- Morgan, J. P. and McIntire W. G. (1959): "Quaternary Geology of Bengal Basin, Bangladesh and India" Bulletin of Geotechnique Society, America, Vol. 70. pp. 319-336.
- Mayne, P. W. and Asce A. M. (1981): "Cam-clay Prediction, of Undrained strength", Geotechnical Engg. J., law Engineering Testing co., Washington D. C. pp. 1218-1238.
- Nagaraj, T.S., Pandian, N.S. and Narasimha Raju, P.S.R. (1998): "Compressibility behaviour of soft cemented soils", Journal of Geotechnique, Japan, Vol. 48(2), PP. 281-287.
- Nagaraj, T.S., Miura, N., Yaligar, P.P. and Yamadera, A. (1996): "Prediction Strength Development by Cement Admixture Based on Water Content", Proceedings of the 2<sup>nd</sup> International Conference on Ground Improvement Geosystems. Grouting and Deep Mixing, Tokyo, 431-436.
- Nakase, A, Kamei, T and Kusakabe, O (1988): "Constitutive parameters estimated by plasticity index, Journal of Geotechnical Engineering", ASCE, Vol. 114, No. 7, pp. 844-858
- NASSRA (1970), "Guide to Stabilization to in Roadwork", National Association of Australia State Road Authorities.
- Rajbongshi, B. (1997), "A Study on Cement and Lime Stabilized Chittagong Coastal Soils for Use in Road Construction", M.Sc. Engineering Thesis, Department of Civil Engineering, Bangladesh University of Engineering and Technology, Dhaka.
- Onitsuka, K. Modmoltin, C. and Kouno, M. (2001): "Investigation on microstructure and strength of lime and cement stabilized Ariake clay", Repots of the Faculty of science and Engineering, Saga University, Japan, vol. 40, No. 1, pp. 111-118.
- Parry, R.H.G. and Nadarajah, V. (1973): "A volumetric yield locus for lightly overconsolidated clay", Journal of Geotechnique, Japan, Vol. 23, pp. 450-453.

- Petchgate, K, Voottipruex, p. and Pongsiwasatit, S. (2002): "Assessment of Engineering Behaviours of cement lime treated soft Bangkok clay", Proceeding of the international symposium on lowland Technology, Saga University, Japan, pp. 199-204.
- Pierce, J. W., and Siegel, F. R. (1969): "Quantification in clay mineral studies of sediments and sedimentary rocks", *J. of Sedimentary Petrology*, Vol. 39, pp. 187-193.
- Porbaha, A., Shibuya, S. and Kishida, T. (2000): "State of the art in deep mixing technology. Part III: geo-material characterization", *Ground Improvement*, Technical Research Institute, TOA corporation, Yokohama, Japan, 4 (3), pp. 91-110.
- Radwan, A.M. (1988): "Properties of granite soil in Aswan, Egypt", In proc. 3<sup>rd</sup> Int'l Conf. on Geo-mechanics in Tropical Soils, Singapore, pp. 203-209.
- Rajasekaran, G. and Rao, S.N. (1998): "X-Ray diffraction and microstructural studies of lime-marine clay reaction products", *Geotech. Engineering*, SEAGS, 29(1), pp. 1-27.
- Rajbongshi, B (1997): "A study on Cement and Lime Stabilized Chittagong Coastal Soils for use in road Construction", M. Sc Engg. Thesis, Civil Engg. Deptt., BUET, Dhaka.
- Rao, S.N. and Rajasekaran, G. (1996). "Reaction products formed in lime-stabilized marine clays", *Journal of Geotechnical Engineering*, ASCE, 122 (5), pp. 329-336.
- Rendulic, L. (1937): "Relation between void ratio and effective stress for a remoulded silty clay", *Proc. 1st Int Conf SMFE*, Harvard, 3, pp. 48-51
- Roscoe, K.H. and Burland, J.B., (1968): "On the generalized stress-strain behaviour of 'wet' clay in Engineering Plasticity", Ed. J. Heyman and F.A. Leckie, Cambridge University Press, London, pp. 535-609.
- Roscoe, K.H., Schofield, A.N. and Wroth, C.P. (1958): "On the yielding of soils", *Journal of Geotechnique*, Japan, 8, pp. 22-53
- Safiullah, A.M.M.(1984): "Freezing soil specimen for fabric observation by Scanning Microscope", *Journal of Civil Engineering*, The Institution of Engineers Bangladesh, Vol. CE 12, No. 4, 113-119.
- Safiullah, A. M. M. (1991): "Some geotechnical aspects of Bangladesh soils", 9<sup>th</sup> Asian Regional conferences on soil and foundations Engineering, Thailand, Vol. 2, pp. 5-13.
- Saitoh, S., Suzuki, Y. and Shirai, K. (1985): "Hardening of soil improved by deep mixing using cementitious agents", *Proceedings of the 11<sup>th</sup> International Conference on Soil Mechanics and Foundation Engineering*, San Francisco, 3, pp. 1745-1748.
- Santamariana, J. C., Klein, K. and Fam, M. (2001): "Sails and waves", Wiley, New York, London, pp. 111-131.
- Schaefer, V.R., Abramson, L. W., Drumheller, J.C. and Sharp, K.D. (1997): "Ground Improvement, ground reinforcement and ground treatment", *Developments 1987-1997*, *Geotechnical Special Publication*, ASCE, pp. 69-78.
- Schofield, A. N. and Wroth, C. P. (1968): "Critical state soil mechanics", McGraw-Hill Ltd. London, England, pp. 118-148.



- Serajuddin, M. and Azmal, M. (1991), "Fine-Grained Soils of Bangladesh for Road Construction", Proc., Ninth Asian Regional Conference on Soil Mechanics and Foundation Engineering, Vol. 1, Bangkok, Thailand, pp. 175-178.
- Serajuddin (1992): "Chemical Stabilization of Bangladesh fine grained Soils for Improvement of road Sub-grade", Proceeding of the Indian Geotechnical Conference Vol. 1, pp. 223-226.
- Shahjahan, A.B.M (2001): "Long term strength development of lime stabilized soils", M.Sc. Engg. Thesis, Deptt. of Civil Engg., BUET, Dhaka, Bangladesh.
- Shen, S.L. (1998): "Behaviour of deep mixing columns in composite clay ground.", Ph. D. Thesis, Saga University, Japan.
- Shibuya, S. and Ozawa, H. (1992): "Extension of spatially mobilized plane (SPM) to friction and cohesive materials and its application to cemented sand", Soils and Foundations, JGS, Japan, 36(4), pp. 137-138.
- Siddique, A., Islam. M. K., and Siddiquee, A.K.M.A.R., (2007): "Modeling the stress-strain response of Coastal clays of Bangladesh", 10<sup>th</sup> Australia New Zealand conference on Geomechanics, Brinsbane, Australia.
- Siddique, A., Safiullah A.M.M., and Ansary M.A., (2002): "Characteristic features of soft ground engineering in Bangladesh", Proceedings of International Symposium- ISYokomama 2000 on Coastal Geotechnical Engineering in Practice, Yokohama, Japan, Vol. 2, pp. 231-248.
- Siddique, A. and Safiullah, A.M.M., (1995): "Permeability characteristics of Dhaka clay", Journal of the Civil Engineering Division, The Institution of Engineers, Bangladesh, Vol. CE 23, No. 1, pp. 103-115.
- Siddique, A. and Rajbongshi. B. (2001): "Mechanical properties of a cement stabilized coastal soil for use in road construction." Proceedings of GEOTROPIKA 2001 Conference on Geotechnical Engineering, Kuching, Sarawak, Malaysia.
- Siddique, A. and Rajbongshi. B. (2002): "Engineering properties of a cement stabilized coastal soil", Journal of the Civil Engineering Division, The Institution of Engineers, Bangladesh, Vol. CE 30, No. 1, pp. 51-67.
- Siddique, A., Safiullah, A.M.M. and Bashar, M. A. (2003): "Critical state parameters and State boundary surface of selected coastal soils of Bangladesh", Proceedings of 12<sup>th</sup> Asian Regional conference on Soil Mechanics and Geotechnical Engineering, Singapore, Vol. 1, pp. 89-92.
- Siddique, A. and Hossain, M. A. (2003): "Effect of lime stabilization on swelling and strength properties of an expansive soil." Proceedings of 12<sup>th</sup> Asian Regional conference on Soil Mechanics and Geotechnical Engineering, Singapore, Vol. 1, pp. 537-540.
- Siddique, A. and Hossain, M. A. (2003): " Effect of lime stabilization on swelling and strength properties of an expansive soil." Proceedings of 12<sup>th</sup> Asian Regional conference on Soil Mechanics and Geotechnical Engineering, Singapore, Volume 1, pp. 537-540.

- Siddiquee, A.K.M.A.R. (2006): "Experimental and numerical study of coastal clays of Bangladesh ", M. Sc. Engg. Thesis, Dept. of Civil, BUET, Dhaka, Bangladesh.
- Singh, A.(1988): "Field identification and classification of soils", Geotechnical Testing and Instrumentation, Soil Engineering in theory and practice, Delhi, India, pp. 54-74.
- Sivapullaiah, P.Y., Sridharan, A. and Bhaskar Raju, K.Y. (2000): "Role of amount and type of clay in the lime stabilization of soil", Ground Improvement, 4(1), pp. 37-45.
- Sridaran, A., Abraham, B.M. and Jose, B.T. (1991): "Improved technique for estimation of preconsolidation pressure", Jour. of Geotechnique, Japan, Vol. 41 (2), pp. 263-268.
- Taha, M.R., Hossain, M.K., Chik, Z., and Nayan, K.A.M. (1998): "Geotechnical behaviour of a Malaysian granite soil", Pertanika J. Society and Technol, University Putra Malaysia, 7(2), pp. 151-169.
- Taylor, W. H. and Arman, A., (1960): "Lime stabilization using preconditioned soils", Bulletin No. 262, Highway Research Board, pp. 1-11.
- Taiyab, M.A., (2006): "A study on the effect of overburden pressure on engineering properties of stabilized Khulna clay", M. Sc, Engg. Thesis, Dept. of Civil Engg., Dhaka University of Engineering and Technology (DUET), Gazipur, Bangladesh.
- Takahashi, H. and Kitazume, M (2004): "Consolidation and permeability characteristics on cement treated clays from laboratory tests", Engineering practice and performance of soft deposits, Japan, IS-OSAKA, ISBN-4-88644-812-7, pp. 187-192.
- Taki, O. and Yang, D. (1991): "Soil cement mixed wall technique", Geotechnical Engineering Congress, ASCE, New York, Special Publication, 27, pp. 298-203.
- Tovey, N. K., and Wong. K. Y. (1973): "The preparation of soils and other geological materials for the SEM." Proc. Int. Symp. on Soil Structure, pp. 59-67.
- Winterkorn, H. F. (1975): "Soil Stabilization", Foundation Engineering Handbook, Van Nostrand Reinhold Company, New York, London, pp. 312-336.
- Wissa, A.E.Z., Ladd, C.C. and Lambe, T. W. (1965): "Effective stress strength parameters of stabilized soil", Proceedings of the 61h International Conference on Soil Mechanics and Foundation Engineering, Montreal, Vol. 1, pp. 412-416.
- Yamadera, A., Nagaraj, T. S. and Miura, N. (1997): "Prediction of strength development in cement stabilized marine clay", Proc. G. Engg. Conf., AIT, Bangkok, pp. 18-24.
- Youwai, S. and Bergado, D. T. (2003): "Strength and deformation characteristics of shredded rubber tire-sand mixtures", Canadian Geotechnical Journal Vol. 40; pp.54-64.
- Yu, Y., Pu, J., Ugai, K. and Takashi, H. (1999): "A study of the permeability of soil-cement mixture", Soils and Foundations, JGS, Japan, Vol. 39 (5), pp. 145-149.
- Verastegui R.D., Impe, W.V. and Afsehrift, P. (2004): "Limc-cement mixing for improvement of alluvial soft Belgian soil", Engineering practice and performance of soft deposits, Japan, IS-OSAKA, ISBN-4-88644-812-7, pp. 241-246.